Diapsid Phylogeny and the Origin and Early Evolution of Squamates

by

Tiago Rodrigues Simões

A thesis submitted in partial fulfillment of the requirements for the degree of

Doctor of Philosophy

in

SYSTEMATICS AND EVOLUTION

Department of Biological Sciences
University of Alberta

ABSTRACT

Squamate reptiles comprise over 10,000 living species and hundreds of fossil species of lizards, snakes and amphisbaenians, with their origins dating back at least as far back as the Middle Jurassic. Despite this enormous diversity and a long evolutionary history, numerous fundamental questions remain to be answered regarding the early evolution and origin of this major clade of tetrapods. Such long-standing issues include identifying the oldest fossil squamate, when exactly did squamates originate, and why morphological and molecular analyses of squamate evolution have strong disagreements on fundamental aspects of the squamate tree of life. Additionally, despite much debate, there is no existing consensus over the composition of the Lepidosauromorpha (the clade that includes squamates and their sister taxon, the Rhynchocephalia), making the squamate origin problem part of a broader and more complex reptile phylogeny issue. In this thesis, I provide a series of taxonomic, phylogenetic, biogeographic and morpho-functional contributions to shed light on these problems. I describe a new taxon that overwhelms previous hypothesis of iguanian biogeography and evolution in Gondwana (*Gueragama sulamericana*). I re-describe and assess the functional morphology of some of the oldest known articulated lizards in the world (*Eichstaettisaurus schroederi* and *Ardeosaurus digitatellus*), providing clues to the ancestry of geckoes, and the early evolution of their scansorial behaviour. I also provide a re-description and considerations on ontogeny and sexual dimorphism in the most complete Cretaceous lizard from North America (*Polyglyphanodon sternbergi*), followed by a biomechanical study on the function of the lower temporal bar in squamates, and a case of non-adaptive reacquisition of this structure in borioteiioids. As the groundwork for my phylogenetic dataset, I provide a thorough discussion on morphological dataset construction for phylogenetic analysis, including a set of basic criteria

to be followed in order to avoid logical and biological biases in morphological characters. This is followed by a detailed revision of nearly 1,000 characters previously proposed for squamate phylogenies. In my final chapter, I introduce data personally collected by me over the course of 400 days of collection visits on all major lineages of diapsid reptiles and squamates. I analyse these morphological data along with molecular data obtained from online repositories and provide a new diapsid reptile phylogeny tested under distinct optimality criteria, also being the first with a deep sampling of squamates lineages. I find the first ever agreement between morphological and molecular data regarding the early evolution of squamates, and evidence that the Middle Triassic reptile *Megachirella wachtleri* represents the oldest known fossil squamate in the world. I implement the latest developments in divergence time estimation under relaxed clock Bayesian inference upon this dataset, and I find that the origin of the major diapsid clades, including lepidosaurs, lies prior to the Permian-Triassic extinction event. This revises previous ideas that the origin of lepidosaurs, archosaurs, and other important diapsid lineages happened in the Triassic, and indicates that, rather than triggering their origin, the Permian-Triassic Mass extinction triggered the diversification of already existing diapsid lineages.

PREFACE

The contents of this thesis include only works that have been led by myself, with contributions from my supervisor (Dr. Michael Caldwell), our main collaborator (Dr. Randall Nydam), additional collaborators from the University of Alberta and from notable other locations around the world. However, I have performed the majority of the work in all of the components of this thesis, including published chapters, to justify their inclusion herein.

Chapters 1 and 7 were entirely written by myself, but includes short pieces of text that I have previously published in review studies: Simões, T. R., Apesteguía, S., Hsiou, A. S. & Daza, J. D. 2017. Lepidosaurs from Gondwana: An Introduction. Journal of Herpetology, 51(3), 297-299; and Simões, T. R., Caldwell, M. W., Weinschütz, L. C., Wilner, E. & Kellner, A. W. A. 2017. Mesozoic Lizards from Brazil and Their Role in Early Squamate Evolution in South America. Journal of Herpetology, 51(3), 307-315.

Chapter 2 has been published as Simões, T. R., E. Wilner, M. W. Caldwell, L. C. Weinschütz and A. W. A. Kellner. 2015. A stem acrodontan lizard in the cretaceous of brazil revises early lizard evolution in gondwana. Nature Communications 6: 9149. I contributed with the description of the new taxon, the phylogenetic analysis, biogeographic considerations, and most of the manuscript writing. Dr. Kellner, Dr. Wilner and Dr. Weinschütz contributed with the fieldwork, Dr. Caldwell contributed with the discussions and editing of the manuscript.

Chapter 3 has been published as in Simões, T. R., M. W. Caldwell, R. L. Nydam and P. Jiménez-Huidobro. 2017. Osteology, phylogeny, and functional morphology of two Jurassic lizard species and the early evolution of scansoriality in geckoes. Zoological Journal of the Linnean Society 180: 216-241. I contributed with the redescription of the specimens studying in this work, the phylogenetic analysis, morpho-functional considerations, and most of the

manuscript writing. Dr. Jiménez-Huidobro contributed with image editing, and all my co-authors contributed with discussions and text editing.

Chapter 4 has been published as Simões, T. R., G. F. Funston, B. Vafaeian, R. L. Nydam, M. R. Doschak and M. W. Caldwell. 2016. Reacquisition of the lower temporal bar in sexually dimorphic fossil lizards provides a rare case of convergent evolution. Scientific Reports 6: 24087. In this study, I was responsible for the specimens` redescription, phylogenetic analysis, ontogenetic and sexual dimorphism discussions, providing anatomical dissections and muscle load values for biomechanical analysis, and manuscript writing. G.F. Funston and B. Vafaeian conducted the finite element analysis, Dr. Doschak helped with the CT scans, and Dr. Caldwell and Dr. Nydam helped with discussions and manuscript editing.

Chapter 5 has been published as Simões, T. R., M. W. Caldwell, A. Palci and R. L. Nydam. 2017. Giant taxon-character matrices: Quality of character constructions remains critical regardless of size. Cladistics 33: 198-219. I contributed with the development of the theoretical background, the phylogenetic character revisions, the phylogenetic analysis and the manuscript writing. My co-authors equally contributed to the discussions, expanding the theoretical concepts and manuscript editing.

Chapter 6 is currently accepted for publication as Simões, Caldwell, Tałanda, Bernardi, Palci, Vernygora, Bernardini, Mancini & Nydam. The Origin of Squamates Revealed by a Middle Triassic Lizard from the Italian Alps. Nature. I contributed with the data collection, dataset construction, specimen redescription and phylogenetic analysis, and also wrote most of the manuscript. Dr. Bernardi, Mancini and Bernardini perform the synchrotron CT scan of the specimen, Dr. Palci helped with the CT scan segmentation of the skull of the specimen, O.

Vernygora helped with molecular alignments and figure editing, and Dr. Caldwell and Dr. Nydam supervised the project, helped with anatomical interpretations and discussions.

DEDICATION

To my wife, Fernanda. My greatest source of intellectual inspiration.

ACKNOWLEDGEMENTS

I am greatly thankful for the support provided to me since the very first stages of this project by my supervisor, Dr. Michael Caldwell and our collaborator Dr. Randall Nydam. Dr. Caldwell conceptualized this project several years ago, and I was given the great honour and satisfaction of executing it. I am also grateful for the numerous inspiring discussions on homology and the evolution of lizards and snakes with both Dr. Caldwell and Dr. Nydam. I also thank the financial support provided to me by the two PhD scholarships I received during the last five years: the Vanier Canada Graduate Scholarship and the Izaak Walton Killam Memorial Scholarship.

I like to thank the numerous discussions I have had with several people during the course of my PhD, including Alexander Kellner, Sebastián Apesteguía, Julia Desojo, Marisol Montellano-Balesteros, Jacques Gauthier, Gabriela Sobral, Aaron LeBlanc, Oksana Vernygora, Rodrigo Figueiredo, Taissa Rodrigues, Mateusz Talanda, Ilaria Papparella, Paulina Jimenez-Huidobro, Alessandro Palci, Takuya Konishi, Angelica Torrices, and Javier Luque.

Finally, I am greatly that to all the curators who have hosted me during the last 5 ½ years of data collection in numerous museums and universities across several countries, in the following institutions: AM: Rose Prevec; AMNH (Paleontology): Mark Norell, Carl Mehling; AMNH (Herpetology): Lauren Vonnahme, Margareth Arnold, David Kizirian, Christopher Raxworthy; AUP: Gordon Walkden, Colin Taylor; BPI: Bruce Rubidge, Sifelani Jirah, Bernhard Zipfel; BSPG: Oliver Rauhut; BU: Michael Benton; CJB: Chris Bell; CM (Paleontology): Amy Henrici; CM (Herpetology): Steve Rogers; FMNH (Paleontology): Olivier Rieppel, William Simpson; FMNH (Herpetology): Alan Resetar; GMPKU: Dayong Jiang, Zuoyu Sun; IGM: Maria del Carmen Perrilliat, Marisol Montellano; IVPP: Yuan Wang, Chun Li; KUVP: Desui Miao; LH: Angela Buscalioni, Francisco Ortega; MACN: Stella Alvarez; MB: Johannes Müller, Daniela

Schwarz-Wings; MBSN: Anna Paganoni; MCZ (Paleontology): Jessica Cundiff, Stephanie Pierce; MCZ (Herpetology): Jonathan Losos, José Rosado; MFSN: Giuseppe Muscio; MGB: Vincent Vicedo, Jaume Gallemí; MGM: David Morris; MLP: Marcelo Reguero; MN: Alexander W. A. Kellner, Deise Henriques, Luciana Carvalho Sérgio Alex K. Azevedo; MNHN: Nour-Eddine Jalil; MPCA: Ignacio Cerda,; MPSC: Álamo Feitosa Saraiva, João Kerensky; MSNM: Cristiano dal Sasso; NHMUK: Sandra Chapman, Lorna Steel; NMNH: Amanda Millhouse, Matthew Carrano; NMOK: Cornelia Kurz; NMQR: Elize Butler; NMS: Nicholas Fraser; NSM: Makoto Manabe; PIMUZ: Christian Klug, Thodoris Argyriou; PKU: Jiang Da-yong, Sunzuoyu Zuoyu; PZ: Evelyn Kustatscher; SAM: Zaituna Erasmus, Roger Smith; SMF: Rainer Brocke, Gunnar Riegel; SMNS: Erin Maxwell, Rainer Schoch; SSWG: Stefan Meng, Sebastian Stumpf; TM: Heidi Fourie; TMM: Brandon Strilisky; TMP: Brandon Strilisky ; UFRGS: Cesar Schultz, Marina Bento Soares; UFSM: Atila da Rosa.; UHR: Yoshitsugu Kobayashi; UMO BT: Joachim Rabold; UMZC: Jason Head, Tom White; UofT: Robert Reisz; WMsN: Lothar Schöllmann; YPM: Jacques Gauthier, Daniel Brinkman; ZPAL: Magdalena Borsuk-Białynicka, Adam Halamski.

INSTITUTIONAL ABBREVIATIONS

AM – Grahamstown, South Africa
AMNH – American Museum of Natural History, New York-NY, USA.
AUP – University of Aberdeen Paleontology collection
BPI – Evolutionary Studies (former Bernard Price) Institute for Palaeontological Research, University of the Witwatersrand, Johannesburg.
BSPG - Bayerische Staatssammlung für Paläontologie und historische Geologie, Munich, Germany
BU – University of Bristol, Bristol, UK.
CJB – Chris J. Bell personal collection
CM – Carnegie Museum of Natural History, Pittsburgh, PA, USA.
DGM - Departamento Nacional de Producão Mineral, Rio de Janeiro, Brazil.
DNM – Dinosaur Natinal Monument, Utah, USA.
FMNH – Field Museum of Natural History, Chicago, IL, USA.
GMPKU - Geological Museum of Peking University, Beijing, China.
GMV - Geological Museum of China, Beijing, China.
HUJ-PAL - Hebrew University of Jerusalem, Palaeontology Collections, Jerusalem, Israel.
IGM - Instituto de Geología, Universidad Nacional Autónoma de México
IVPP – Institute of Vertebrate Paleontology and Paleoanthropology, Beijing, China.
KUVP – Museum of Natural History, University of Kansas, Lawrence, KA, USA.
LH - Museo de Cuenca (Las Hoyas material), Cuenca, Spain.
MACN - Museo Argentino de Ciencias Naturales "Bernardino Rivadavia," Buenos Aires, Argentina
MB – Museum fur Naturkunde, Berlin, Germany
MBSN – Museo Brembano di Scienzi Naturali, San Pelegrino, Bergamo, Italy.
MCZ – Museum of Comparative Zoology, Harvard University, Cambridge, MA, USA.
MFSN – Museo Friulano di Storia Naturale, Udine, Italy.
MGB, Museu de Geologia de Barcelona, Barcelona, Spain
MGM - McGregor Museum – Kimberely, South Africa
MLP – Museu de La Plata, La Plata, Argentina
MN – Museu Nacional/UFRJ, Rio de Janeiro, Rio de Janeiro, Brazil.
MNHN – Muséum National d'Histoire Naturelle, Paris, France.
MPCA - Museo Carlos Ameghino, Cipolletti, Río Negro Province, Argentina
MPSC – Museu de Paleontologia de Santana do Cariri, Santana do Cariri, Ceará, Brazil.
MSNM – Museo Civico di Storia Naturale di Milano, Milano, Italy.
NHMUK – Natural History Museum, London, UK.
NHMW – Naturhistorisches Museum Wien
NMMNH - New Mexico Museum of Natural History and Science, Albuquerque
NMNH – National Museum of Natural History, Washington, D.C., USA.
NMOK - Naturkundemuseum im Ottoneum Kassel, Kassel, Germany.
NMQR – National Museum, Bloemfontein, South Africa.
NMS – National Museum of Scotland, Edinburgh, United Kingdom
NSM - National Science Museum, Tokyo, Japan
PIN - Paleontological Institute, Academia Nauk, Moscow, Russia

PIMUZ - Paläontologisches Institut und Museum der Universität Zürich, Switzerland
PKU – Peking University, Beijing, China.
PMU – Paleontological Museum, Uppsala.
PZ – Museo Archeologico dell'Alto Adige, Bolzano (Bozen), Italy.
SAM – South Africa Museum (Iziko Museums), Cape Town, South Africa.
SMF - Senckenberg Museum, Frankfurt, Germany
SMNS – Staatliches Museum fur Naturkunde, Stuttgart, Germany.
SSWG - Sektion Geologie, Ernst-Moritz-Arndt Universitat, Greifswald, Germany
TM – Ditsong (former Transvaal) Museum, Pretoria, South Africa
TMM – Texas Memorial Museum, Austin, Texas, USA.
TMP – Royal Tyrrell Museum, Drumheller, Alberta, Canada
UALVP – University of Alberta Laboratory for Vertebrate Paleontology (Department of Biological Sciences), Edmonton, Canada.
UAMZ – University of Alberta Museum of Zoology, Edmonton, Alberta, Canada.
UFRGS – Universidade Federal do Rio Grande do Sul, Porto Alegre, Rio Grande do Sul, Brazil.
UFSM – Universidade Federal de Santa Maria, Santa Maria-RS, Brazil.
UHR - Hokkaido University, Sapporo, Japan
UMO BT – Urwelt-Museum Oberfranken, Bayreuth, Germany.
UMZC –Cambridge University Museum of Zoology, Cambridge, UK.
WMsN – Westfalisches Museum fur Naturkunde, Munster, Germany.
YPM – Yale Peabody Museum, Yale University, New Haven, CO, USA.
ZPAL - Institute of Paleobiology Polish Academy of Sciences, Warsaw, Poland

TABLE OF CONTENTS

LIST OF TABLES

LIST OF FIGURES

CHAPTER ONE: GENERAL INTRODUCTION

Lepidosaurian reptiles (tuataras, lizards, snakes and amphisbaenians) comprise about half the extant world species richness of sauropsid reptiles (the other half being comprised of mostly birds) with little more than 10,000 species (Lepage 2017; Uetz & Hošek 2017). They inhabit a wide diversity of environments and lifestyles, from desert to tropical islands, from burrowing to gliding morphotypes (Pianka & Vitt 2003). Interestingly, a significant part of this diversity has been discovered recently, since during the last decades the number of annually described species of extant squamates has increased dramatically (Pincheira-Donoso *et al.* 2013), with nearly 160 new species being described in some years.

The increased interest in the study of lepidosaurian reptiles is not only confined to taxonomic studies, but it has also expanded to other fields of biological sciences, including evolutionary biology, ecology, and paleontology. To quantitatively evaluate the changes in the volume of research on lepidosaurs, I searched for scholarly articles in the Web of Science core database. I investigated the number of papers published during the last two decades mentioning lepidosaurs (keywords: Lepidosauria, Squamata, Rhynchocephalia, *Sphenodon*, lizards, snakes, and amphisbaenians), carried out in different geographic regions (Gondwanan vs Laurasian regions) and mentioning keywords related to evolutionary research (e.g. evolution, biogeography, macroevolution, phylogeny, and fossils). I subsequently filtered the evolutionary research papers for those that focused on the study of fossil organisms only to assess how many of those were produced with the aid of paleontological data.

The results (Table 1) indicate general studies on the evolution of lepidosaurs in Gondwana dramatically increased between 2006 and 2015 compared to the preceding 10 years. Whereas evolutionary studies on lepidosaurs from Laurasian regions increased by 298%, there was an increase of 340% on lepidosaurs from Gondwana. Out of these, there was an increase of 432% of research papers on lepidosaurs that used or mentioned fossil specimens from Gondwana between 2006 and 2015 compared to the 10 previous years; while there was an increase of 312% of equivalent papers from Laurasian regions. Therefore, there was a substantial increase in the study of lepidosaurs worldwide (primarily squamates) between 2006 and 2015, mostly marked by an increase in the study on lepidosaurs from Gondwanan regions. This increase was even more substantial in studies using fossil lepidosaurs from Gondwana.

Despite the importance of lepidosaurian reptiles regarding their large taxonomic and ecological diversity among extant tetrapods, and the recent increase in interest of scientific

research on lepidosaurian reptiles, numerous important and fundamental aspects of their deep time evolutionary history remain unsolved. This includes the basic patterns and processes of early lepidosaurian evolution and the origin of squamates. In the present thesis, I intend to shed light on several aspects of early squamate evolution. Below, I introduce some of the greatest challenges to understanding early squamates and early lepidosaurian evolution, and the approaches I took to solve them, respectively.

The oldest known squamates

Perhaps the greatest challenge in identifying the major patterns of morphological evolution during the initial stages of squamate evolution is the lack of sufficient fossa data from that time frame. The widely accepted sister-group relationship between squamates and rhynchocephalians, and the fact that the oldest known rhynchocephalians are from the Middle Triassic (Jones *et al.* 2013), indicate that squamates should be at least as old as the Middle Triassic. On top of that, molecular and combined evidence divergence time estimates have systematically placed the origin of crown squamates in the Triassic or Early Jurassic, and the squamate root back in the Permian or Triassic (Vidal & Hedges 2005; Jones *et al.* 2013; Zheng & Wiens 2016; Irisarri *et al.* 2017; Pyron 2017). However, the oldest known squamates come from the Middle Jurassic of Britain, Morocco and Kyrgyzstan in central Asia (Evans & Jones 2010; Rage 2013; Haddoumi *et al.* 2016; Conrad 2017; Simões *et al.* 2017b). This is initially creates a gap of at least 70 million years between the oldest known squamates and the inferred divergence time for the entire Squamata.

The oldest known fossil squamates include *Bellairsia graclis, Balnealacerta silvestris, Oxiela tenuis, Saurillodon marmorensis*, *Paramacellodus* sp., possible gekkotan vertebrae and *Eophis underwoodi* from the Bathonian of Oxfordshire (Evans & Milner 1994; Waldman & Evans 1994; Evans 1998; Caldwell *et al.* 2015); *Changetisaurus estesi* (Callovian) and other very fragmentary remains (Bathonian) from Kyrgyzstan (Nessov 1985; 1988; Fedorov & Nessov 1992); and fragmentary squamate remains, regarded as Scincomorpha indet., cf. *Parviraptor*, and a non-ophidian anguimorph, from the Bathonian of Morocco (Haddoumi *et al.* 2016). *Bharatagama*, from the Middle Jurassic of India (Evans *et al.* 2002), is another potential Middle Jurassic squamate. However, it has recently been suggested that it represents a sphenodontian (Jones *et al.* 2013; Conrad 2017). *Tikiguana*, an acrodont jaw initially published as from the

Triassic of India, was eventually found to be re-worked material from recent deposits (Hutchinson *et al.* 2012). Therefore, prior to this study, the oldest unquestionable squamates were from the Middle Jurassic, ranging from the Callovian to the Bathonian (168.3 – 166.1 million years ago) (Ogg *et al.* 2016). This was already a relatively diverse assemblage (Rage 2013) that included distinct lizard morphotypes, possible geckoes, and snakes, distributed across two quite distant areas of the world.

Despite the oldest known squamate fossils coming from the Middle Jurassic, it is only from the Tithonian (Late Jurassic) deposits of Solnhofen, Germany, that the oldest known well-preserved and articulated squamates come from (Hoffstetter 1964; 1966; Mateer 1982; Evans 1994b). There is one articulated squamate from the Middle Jurassic, named *Sharovisaurus* (Hecht & Hecht 1984), but it is not as well preserved as the Solnhofen specimens, and it has only been very briefly described. Therefore, there is a gap of at least 85 million years between the oldest known well-preserved and articulated squamates and the inferred divergence time for all squamates. To complicate matters even further, those Late Jurassic articulated squamates have only been briefly described, with the exception of *Ardeosaurus brevipes* (Mateer 1982).

The lack of good squamate data from the Jurassic and the complete absence of definitive squamate material from the Triassic greatly hamper our current knowledge regarding the patterns of early squamates morphological evolution, also creating significant problems for assessing the phylogenetic relationships among early lepidosauromorphs, and estimating the divergence time for squamates and lepidosaurs with greater precision.

Assessing the composition of the Lepidosauromorpha and early squamates evolution

Broad level relationships among the major groups of reptiles remain unresolved, with many conflicting hypotheses proposed during the last decades, and quite disparate proposals for the internal composition of the Lepidosauromorpha (Benton 1985; Evans 1988; Laurin 1991; Caldwell 1996; Gower 1996; Rieppel & de Braga 1996; Motani *et al.* 1998; Lee 2001; Müller 2004; Hill 2005; Scheyer *et al.* 2017; Turner *et al.* 2017). Therefore, any assumptions regarding the internal composition of the Lepidosauromorpha would be necessarily based on a preference over one of these competing hypothesis.

Additionally, all of the diapsid datasets mentioned above suffer from the following caveats. Firstly, squamates, which include over 10,000 extant lineages and hundreds of fossil ones over the past 250 million years are usually, are almost invariably represented as a single terminal taxon (Squamata). This extreme oversimplification on the diversity of morphotypes and genotypes within squamates is likely to affect what other diapsid lineages fall closer to squamates within lepidosauromorpha, and the overall composition of lepidosauromophs. The only exception to this case that is known to me is the study of Hill (2005), which includes some squamate taxa at the species level. However, most of the taxa used in that study are from the same clades (mostly scincids, anguids and cordylids), thus still lacking many important lineages, including the putative earliest evolving crown squamates (iguanians, geckoes and dibamids—see more below), as well as snakes and amphisbaenians.

Secondly, there is no consensus on which squamate clade represents the earliest evolving squamate lineage. Thus far, all broad level analyses of squamate relationships using only morphological data have suggested iguanians are the earliest evolving crown group squamates [e.g. (Estes *et al.* 1988; Lee 1998; Lee & Caldwell 2000; Evans *et al.* 2005; Conrad 2008; Gauthier *et al.* 2012; Simões *et al.* 2015a)]. However, the molecular signal has always indicated geckoes and dibamids to represent the earliest evolving forms (Townsend *et al.* 2004; Vidal & Hedges 2005; Hugall *et al.* 2007; Kumazawa 2007; Vidal & Hedges 2009; Wiens *et al.* 2010; Wiens *et al.* 2012; Pyron *et al.* 2013). Combined evidence studies have also suggested the earliest squamates to be geckoes and dibamids, likely because of the overwhelming influence of molecular characters, which are usually far greater in number than morphological characters (Wiens *et al.* 2010; Reeder *et al.* 2015; Pyron 2017), apart from one study known to me (Lee 2005a), which yields a similar result to morphological data, but also has far less molecular loci than more recent combined evidence studies. Therefore, selecting a single crown group to represent the entire Squamata is also not trivial for large scale reptile datasets.

My approach to solve the issues above

As stated above, there are several important issues that prevent a clear picture concerning the early evolution of squamates, and as a consequence, of early lepidosaur evolution. Summarizing the above issues, I have: (1) A fossil gap of at least 70 million years between the minimum age for the origin of squamates and the oldest known squamates fossils; (2) A fossil gap of at least 85

million years between the oldest phylogenetic informative fossa squamates and the origin of squamates; (3) A relatively poor description of most of the oldest known articulated squamates, especially the extremely well-preserved *Eichstaettisaurus* and *Ardeosaurus*; (4) Great uncertainty concerning the composition of the early members of the Lepidosauromorpha; (5) Lack of agreement between morphological data and molecular data concerning important aspects of the squamate tree of life, including the earliest crown squamates group to evolve (iguanians, according to morphological data and geckoes + dibamids according to molecular data).

In the present study, I aimed to shed light on all of the aspects above by visiting numerous museum and university collections around the world in order to re-assess numerous fossil reptiles that have been proposed at some point or another to be close relatives to squamates and rhynchocephalians, provide the first detailed description of some of the oldest known articulated squamates, and describe new Mesozoic squamate taxa, to tackle issues 1-3. I will also provide the first diapsid phylogenetic dataset with a deep sampling of squamates and rhynchocephalians, which will allow me to tackle issues 4 and 5.

The phylogenetic component of my thesis is perhaps the most likely to overcome some of those important issues from previous assessments of early squamates evolution. Not only the data sampling will allow me to re-assess the morphology of some key taxa, but it also is not dependent on new fossil findings, therefore making it feasible to answer some of the most contending questions regarding early lepidosaur and squamates evolution, at least from a phylogenetic perspective.

Thesis chapters

Chapter one, presents a general introduction.

Chapter two consists of the description, phylogenetic analysis and biogeographic considerations concerning a new species of squamates from the Late Cretaceous of Brazil. This new taxon (*Gueragama sulamericana*) represents the first acrodontan lizard from South America, either living or extinct. I indicate how this taxon revises the early history of iguanian evolution in South America, and in Gondwana as a whole.

Chapter three offers the first detailed description of the Late Jurassic taxa *Eichstaettisaurus schroederi* and *Ardeosaurus digitatellus*, two of the oldest and best preserved squamates in the world. I also provide evidence that those taxa, especially *Eichstaettisaurus*, possessed features

only found among geckoes, and that *Eichstaettisaurus* represents the oldest known gecko. Finally, I provide an assessment of the functional morphology of both taxa, indicating their adaptations to scansoriality. I conclude, indicating that the adaptations to scansoriality evolved prior to the evolution of the adhesive toe pads in geckoes.

Chapter four presents a paleobiological reinterpretation of the most complete lizard specimens from the Cretaceous of North America, all belonging to the taxon *Polyglyphanodon sternbergi*. I indicate evidence for sexual dimorphism and a previously unnoticed complete lower temporal bar in *Polyglyphanodon*. The lower temporal bar is generally considered to be absent in all squamates, but it had been previously found in another fossil lizard from the same clade as *Polyglyphanodon*. Therefore, I performed a phylogenetic analysis that indicates that the reacquisition of the lower temporal bar occurred at least twice independently within squamates. Additionally, a biomechanical analysis utilizing finite elements analysis allow the functional assessment for the evolution of this feature in squamates. I conclude that while adaptively relevant to some lepidosaurs, the lower temporal bar in *Polyglyphanodon* is better explained as a result of release of functional constraint, and not adaptive evolution.

Chapter five includes a large-scale compilation, as well as newly conceptualized, criteria for improved practices for morphological phylogenetic character construction. This chapter, I review and expand upon a large set of character types that violate those basic principles of morphological character construction using examples from the squamate literature. I review over 1000 squamates morphological characters, providing individual comments upon the ones that fail the basic premises of character construction that I propose. I also re-analyse the original datasets by either removing or re-coding those problematic characters, thus demonstrating how they impact sister-group relationships and overall character agreement in the two largest morphological squamates datasets available. This chapter serves as the steppingstone to avoid logical and biological biases in morphological datasets, that I implement in my own dataset in the following chapters.

Chapter six provides the results of the first set of phylogenetic analyses of my thesis. It represents a diapsid phylogeny, with deep sampling of both squamates and non-squamatan diapsids. This dataset is the first reptile phylogenetic dataset that applies a strong control in morphological character construction to avoid logical and biological biases presented in chapter five. It also provides more intensive taxon sampling of all major diapsid lineages than any

previous diapsid phylogenetic dataset available. I also combined the morphological data I compiled with molecular sequences for the extant taxa represented in my dataset retrieved from sequences available in GenBank. Finally, I provide a re-description of *Megachirella wachtleri*, a taxon previously regarded as a non-squamatan lepidosauromorph from the Middle Triassic of the Italian Alps based on high resolution CT scan data. My phylogenetic dataset, along with the new data provided by the CT scans reveal that *Megachirella* is the oldest known fossil squamates, and not an early lepidosauromorph. Additionally, my morphological analysis indicates geckoes to be the earliest evolving crown clade squamates, with iguanians always nested crownward on the tree, either nested with anguimorphs, mosasaurs and snakes (resembling the clade Toxicofera), or the nest with teiioids. This result is obtained under all optimality criteria tested herein (equal weight and implied weighting maximum parsimony, and Bayesian inference). This offers the first ever agreement between morphological and molecular data concerning the early evolution of squamates, with divergence time estimates based on relaxed clock Bayesian inference indicating the origin of squamates and other major lineages of diapsid reptiles to have occurred prior to the Permian-Triassic extinction event.

Table 1.1. Record of studies on lepidosaurian reptiles extracted from the Web of Science database.

	[1]Le+La	Le+La+Evo	Le+La+Pal	Le+Go	Le+Go+Evo	Le+Go+Pal
1995-2005	1083	300	51	1131	301	28
2006-2015	2458	893	159	2653	1025	121

[1] Le+La = Studies on lepidosaurs from Laurasian derived regions

Le+Go = studies on lepidosaurs from Gondwanan derived regions

Pal = studies focused on fossils.

Evo = studies focused on multiple areas of evolutionary biology

CHAPTER TWO: A STEM ACRODONTAN LIZARD IN THE CRETACEOUS OF BRAZIL REVISES EARLY LIZARD EVOLUTION IN GONDWANA

[The contents of this chapter have been published in Simões, T. R., E. Wilner, M. W. Caldwell, L. C. Weinschütz and A. W. A. Kellner. 2015. A stem acrodontan lizard in the cretaceous of brazil revises early lizard evolution in gondwana. *Nature Communications* 6: 9149.]

Introduction

Squamates (lizards, snakes and amphisbaenians) are the most speciose extant group of reptiles, represented by more than 9,000 living species, and iguanians are one of the most diverse group of lizards globally, with more than 1700 species (Uetz & Hošek 2016). Acrodontan iguanians are characterized by unique jaw features among lizards, as well as an evolutionary trend towards tooth placement at the apex of the jaws and fusion to it (acrodonty and pleuroacrodonty) whereas non-acrodontans (iguanids, tropidurids, among others) are pleurodont, with teeth attached to the lingual wall of the jaws. Amongst extant taxa, while acrodontans have an Old World distribution, non-acrodontan iguanians dominate the New World, as well as Madagascar and a few Pacific islands (Pianka & Vitt 2003). The origins of these two groups, with their almost disjunct distributions, and the dominance of non-acrodontans in the Americas have been the subject of great conjectures and debate (Moody 1980; Estes 1983a; Honda *et al.* 2000; Macey *et al.* 2000; Raxworthy *et al.* 2002; Evans 2003a). The difficulty in providing answers to these questions is due to a poor fossil record worldwide during the time of origin of squamates (Early-Mid Mesozoic), and during the entire Mesozoic of Gondwana—nine species of lizards (Simões *et al.* 2015a), versus ~150 species in Laurasia (data compiled from (Evans 2003a) and several subsequent publications).

Here I report on the first known acrodontan iguanian lizard from South America, the New World component of ancient Gondwana, recovered from a new locality in Brazil dated as Late Cretaceous. This discovery overturns long held hypotheses of the evolution and palaeobiogeography of modern iguanian lizards, and provides important insights into the early evolution of lizards in South America.

Materials and Methods

Anatomical nomenclature. Nomenclature throughout the text follows two main sources (Klembara *et al.* 2010; Rage & Augé 2010)

Phylogenetic analysis. To phylogenetically infer the systematic position of *Gueragama sulamericana* amongst squamates, I included it into the data matrix of Gauthier *et al.* (2012) with the taxon scoring corrections performed by Simões *et al.* (2015a). The search parameters involved the New Technology algorithms implemented in T.N.T. (Goloboff *et al.* 2008b), as these are the more appropriate ones for retrieving trees from the largest number of possible local optima for data matrices larger than 100 taxa. The algorithms used were Sectorial Search, Ratchet and Tree Fusing, followed by a traditional heuristic search using the protocol performed by Simões *et al.* (2015a). This method allowed me to obtain shorter most parsimonious-trees and in larger numbers than the original run by Gauthier *et al.* (2012). During this process, additional incorrect character state scores were identified for some taxa, and corrections were made (see Supplementary Information 3.1).

Results

Systematic palaeontology

Squamata Oppel, 1811

Acrodonta Cope, 1864

Gueragama sulamericana gen. et sp. nov.

*Etymology***.** "Guera", meaning "ancient" (native Brazilian Tupi-Guarani); "agama" (gender feminine) in reference to agamid lizards; "sulamericana", meaning "from South America" (Portuguese).

Holotype. CP.V 2187, partial lower jaw (Fig. 1), CENPALEO – Universidade do Contestado, Santa Catarina, Brazil.

Additional material. CP.V 2188 (unprepared fragments of possible maxillary and teeth)

Type locality and horizon. Cruzeiro do Oeste, Paraná State, Brazil; Goio-Erê Formation, Caiuá Group, Bauru Basin; Turonian-Campanian, Late Cretaceous(Manzig *et al.* 2014).

Diagnosis. Stem acrodontan species separated from all other squamates by following combination of characters: coronoid process of dentary with dorsal and posteriorly elongate component; posterior process of dentary undivided and extending well beyond level of coronoid process; presence of subdental shelf; dental sulcus present anteriorly; no splenial articulatory facet on dentary (splenial either small or absent); large facet for anteromedial process of coronoid on dentary; angular extending anterior to posteriormost tooth; anterior teeth pleurodont, peg-like, with pointed and laterally compressed apices; posterior marginal teeth: pleuroacrodont, straight, posteriorly increasing in size (except for the last tooth) and labiolingually expanded, increasing degree of ankylosis with subdental shelf and labial wall of dentary posteriorly, and with apical wear creating labial and lingual shearing crests; replacement pits lingual to functional tooth.

Description

The preserved dentary has a convex ventral border that is partially broken in its midsection and bears six mental foramina laterally. The coronoid process would have covered the coronoid eminence laterally, probably reaching to or beyond its posterior margin. In medial view, the anterior tip of the dentary has a horizontally elongate symphysial flat surface that would have butted against its right counterpart and is barely indented ventrally by the Meckelian canal. The subdental shelf has a medial ridge that diminishes in height posteriorly, and which delimits a dental sulcus anteriorly that is not filled with cementum (as opposed to teiids) and is mostly empty. Despite the ventral border of the dentary being broken in its midsection, the ventral crest of the dentary is preserved and visible in medial view ventral to the subdental shelf, anteriorly and posteriorly. It does not extend medially, and does not contact the subdental ridge, even in its deepest part on the anteriormost section of the dentary. This indicates that the Meckelian canal was fully open medially, even in the region where the subdental shelf was deepest. Posterior to the last tooth position there is a large facet for the coronoid anteriomedial process, and posterior and laterally to this, facets for the surangular and angular bones (Fig. 1). Inside the Meckelian canal, the intramandibular septum is not seen posteriorly. There is an excavation on the dorsolateral surface of the dentary, which creates a posterodorsal crest that extends onto the coronoid process, as observed in the extant agamid *Uromastyx.* There is no facet for the splenial medially on the subdental shelf.

There are 18 tooth positions, with most teeth preserved in situ and displaying moderate heterodonty. The anteriormost 5 teeth display no obvious ankylosis to the labial wall. However, there is an increasing degree of ankylosis to the labial wall of the dentary and the subdental shelf after the 8th tooth, with the dorsal crest of the dentary eventually becoming indistinguishable from the teeth (Fig 2d). Posterior teeth are also positioned more dorsally on the jaw relative to anterior teeth, with the labial wall of the dentary (and its dorsal crest) not being visible in dorsal view. Thus, the anteriormost teeth can be classified as pleurodont, and the posterior series as pleuroacrodont. The resorption pits are elliptical, having a wider diameter in the apicobasal axis.

The teeth in the middle and posterior sections of the jaw are straight and closely spaced, whereas the three anteriormost teeth are slightly inclined anteriorly. Resorption pits are observed throughout the dentary, indicating replacement was active. The anterior teeth also have pointed apices that are laterally compressed, forming relatively sharp anterior and posterior ridges. The teeth posterior to the eighth tooth position become gradually different, bearing a sagittaly-oriented wear facet at their apices, leaving a labial and a lingual shearing crest, and forming a molariform series.

Systematic comparisons to other lepidosaurs

Some features of the jaw of *Gueragama*, such as a posteriorly elongated coronoid process of the dentary, and an undivided and elongate posterior process, are similar to those found in most rhynchocephalians. However, rhynchocephalians usually have a fully acrodont dentition and show no tooth replacement, making them very distinct from *Gueragama*. The early rhynchocephalians *Gephyrosaurus* (Evans 1980) and *Diphyodontosaurus* (Whiteside 1986) from the Late Triassic and Early Jurassic of Britain, nevertheless, show pleurodont tooth attachment and pleurodont+acrodont attachment, respectively. Yet, these and all other rhynchocephalians differ from *Gueragama* and crown acrodontans by having a closed Meckelian fossa, or nearly closed in *Gephyrosaurus*. Even in the latter condition, the ventral crest of the dentary is curved medially and deep anteriorly, as in other rhynchocephalians, unlike *Gueragama* and crown acrodontans. *Gephyrosaurus* and *Diphyodontosaurus* also show the primitive lepidosaurian condition of an elongate jaw with a high tooth count (Evans 1980; Whiteside 1986) (reaching up to 40 dentary teeth in *Gephyrosaurus* (Evans 1985), whereas the jaw in *Gueragama* and crown

acrodontans is much shorter with a lower tooth count. The anterior inferior alveolar foramen (AIAF) is usually located at the level of the coronoid process in rhynchocephalians (or slightly anteriorly in other cases), but it is more anterior in acrodontans (Evans *et al.* 2002). *Gueragama* does not have the AIAF at the level of the coronoid, and it is inferred to be located well anteriorly (its probable location is covered by matrix and is too fragile for preparation). Finally, *Gephyrosaurus* and *Diphyodontosaurus* have an oval symphysis split by the Meckelian canal, and later rhynchocephalians have a vertically elongate symphysis. *Gueragama*, as in acrodontans (except chamaeleonids), has the symphysis elongated and nearly horizontal, differing from the conditions observed in rhynchocephalians. All these factors indicate *Gueragama* is not a rhynchocephalian, and is instead, an acrodontan.

Within Squamata, the lack of plicidentine infolding coupled with straight teeth, and the long and undivided posterior process of the dentary, makes *Gueragama* different from all members of the Anguimorpha. The medially open Meckelian canal also indicates *Gueragama* is neither a gekkotan nor a xantusiid, which possess a medially closed Meckelian canal via fusion of the dentary subdental shelf to the ventral border of the dentary. An open Meckelian canal is a common feature amongst most lizards classically classified in the "Scincomorpha". However, among scincomorphs, *Gueragama* differs from teiioids by having a long undivided posterior process of the dentary, a well-developed and dorsally oriented component of the coronoid process, and by having an elliptical (wider diameter in the apicobasal axis) rather than semi-circular resorption pits and lacking deep deposits of cementum. From lacertids, it differs by its long posterior and coronoid processes of the dentary. Xantusiids, cordyloids, scincids (including the fossil contogenoids from the Late Cretaceous of North America), as well as some other fossil taxa possibly closely related to them, such as *Globaura* and *Carusia* from the Late Cretaceous of East Asia, do have an elongate posterior process of the dentary that is undivided. However, in these groups the posterior process usually differs from the condition observed in *Gueragama* by being located on the ventral margin of the jaw, at some distance from the coronoid process and the anterior surangular foramen and separated from them by the surangular. In some forms in these families, this process can be straight (e.g. the scincid *Tiliqua* and contogenoids, as well as the xantusiid *Palaeoxantusia* from the Eocene of Wyoming and North Dakota). Yet, and most importantly, all these groups differ from *Gueragama*, by possessing a Meckelian canal that is closed anteriorly (with subdental shelf and ventral crests in contact medially), or totally closed,

as in xantusiids; a coronoid process of the dentary that extends mostly dorsally, exposing the coronoid labial process posteriorly to it; anterior and posterior ridges on the lingual side of marginal teeth (for contogenoids); an elongate splenial (apart from xantusiids); and having tall chisel-like teeth, usually with crown striations (mostly in scincids). *Gueragama* also differs from the Late Cretaceous borioteiioids by having a posteriorly elongate coronoid process (much shorter in borioteiioids), the elongate posterior process of the dentary (very reduced in borioteiioids), and a reduced/absent splenial (elongate in borioteiioids).

Gueragama sulamericana shares with iguanian lizards a subdental shelf, closely spaced teeth, and the replacement teeth positioned lingually. Whereas some families of iguanians have a closed Meckelian canal, the new species possesses an open Meckelian canal, which is also the case for acrodontans, and some species of *Oplurus*, and *Phrynosoma*, for instance. The new species shares with acrodontan lizards numerous other features (see Table 2.1) such as an undivided and straight posterior process of the dentary, separated from the coronoid process by a small gap through which the anterior surangular foramen opened; a coronoid process with an elongate posterior component, which covers the lateral surface of the coronoid bone; a dorsolateral excavation on the labial margin of the dentary, producing a posterodorsal crest connecting it to the coronoid process; splenial either small or absent; an anteriorly elongate angular facet on the dentary, indicating that element extended anteriorly to the posteriormost teeth. When compared to all fossil and extant squamates, the combination of these features is observed only in acrodontan lizards (Figs. 2.1 and 2.2). The new taxon is most similar to the basal acrodontan group Leiolepidinae, especially *Uromastyx,* including the morphology of the coronoid process which is subdivided into a dorsal and a posterior elongate component in *Uromastyx* (Fig. 2.2; Table 2.1).

Comparative anatomy of acrodontans and priscagamids

Crown acrodontans and the Priscagamidae, from the Late Cretaceous of Mongolia (Borsuk-Białynicka & Moody 1984), form a monophyletic group according to most authors (Borsuk-Białynicka & Moody 1984; Alifanov 1989; Frost & Etheridge 1989; Conrad 2008; Gauthier *et al.* 2012). The dentition of *G. sulamericana* is more similar to primitive priscagamids by having its posterior teeth predominantly placed on the medial side of the jaw. For instance,

Pleurodontagama (Borsuk-Białynicka & Moody 1984; Borsuk-Białynicka 1996), *Flaviagama* and *Mimeosaurus tugrikinesis* (Alifanov 1989) have an exclusively pleurodont dentition, as does *Ctenomastax* (Gao & Norell 2000), a putative sister taxon to priscagamids+acrodontans (Gauthier *et al.* 2012). *Priscagama* had both pleurodont and acrodont teeth posteriorly. Among acrodontans, transitional dentitions that are still not fully acrodont occur in Eocene species from Mongolia, such as *Khaichinsaurus* and *Lentisaurus* (Alifanov 2009), as well as a few modern forms (e.g. *Uromastyx* and *Calotes* (Budney 2004)). The tooth attachment modes in these taxa suggest acrodonty could have evolved as a derived condition within Iguania, and that the priscagamids (and some acrodontans) represent transitional forms evolving towards that dental condition (Borsuk-Białynicka 1996). In the priscagamids *Pleurodontagama* and *Morunasius*, some resorption pits indicating tooth replacement are also retained (Borsuk-Białynicka 1996).

Gueragama sulamericana displays an increasing degree of dental ankylosis of the posterior teeth, the lack of it in the anteriormost teeth, and the presence of a dental sulcus as in *Priscagama* and *Pleurodontagama* (Borsuk-Białynicka & Moody 1984; Borsuk-Białynicka 1996). Tooth replacement is still present, as in *Pleurodontagama* and *Morunasius.* Furthermore, the variation in tooth placement on the jaw of *G. sulamericana* is also seen in priscagamids and acrodontans. *Gueragama sulamericana* also displays close packing of the teeth, which resembles the primitive iguanian condition, as observed in *Ctenomastax*. However, *G. sulamericana* preserves 18 teeth, differing from the higher number of teeth in non-acrodontan iguanian dentaries (20-35), and matching the tooth count of acrodontans and some priscagamids, which varies between 15-20(Edmund 1969). Thus, *Gueragama* displays unique lower jaw features of acrodontans as well as their tooth count, but still bears dental characteristics of other iguanians that are also retained in priscagamids.

Phylogeny

I inferred the phylogenetic position of *Gueragama sulamericana* in a dataset representative of all major squamate groups (Gauthier *et al.* 2012), and obtained a well resolved strict consensus tree topology and an unambiguous placement for the new taxon (Fig. 3a). *Gueragama* was found as a stem acrodontan, being more closely related to crown acrodontans than to the Priscagamidae and *Ctenomastax*. *Gueragama* breaks the long branch between priscagamids and

acrodontans found a previous analysis (Gauthier *et al.* 2012), providing clues for character evolution along the stem lineage of Acrodonta.

Despite the limited number of characters that could be scored for *Gueragama* in this character matrix, taxon incompleteness should not be an *a priori* criterion for not including a taxon in a phylogenetic analysis. Retrieving an unambiguous positioning for a taxon with few scorable characters, and good resolution for the entire tree, depends on the taxon possessing the key synapomorphies that are necessary for its correct placement (Wiens 2003; 2006), and this cannot be predicted before the analysis (Kearney 2002). The inclusion of *Gueragama* in the matrix of Gauthier *et al.* (2012) supports this hypothesis. *Gueragama* was found within the clade formed by *Ctenomastax*, along with priscagamids and acrodonts, within the acrodontan clade, but outside of the crown, supporting the transitional position for this taxon.

In a preliminary analysis without the inclusion of *Gueragama*, the branch between priscagamids and extant acrodontans was 18 steps long. The inclusion of *Gueragama* broke this relatively long branch leading to the acrodontan crown clade into two shorter branches: one of four steps (subtending *Gueragama* and crown acrodontans) and another of three steps (subtending the crown clade). The inclusion of this fossil form does not change the relationship between major clades of squamates obtained before its inclusion, but helps to understand the sequence of character evolution leading to the evolution of the peculiar jaw and teeth features that characterize acrodontans amongst all other squamates. Furthermore, breaking long branches makes the overall analysis more accurate, as biases due to long-branch attraction are diminished. The long branch obtained by Gauthier *et al.* (2012) for the chamaeleonids (*Chamaeleo* and *Brookesia*) was also inferred from the present analysis. This configuration is expected given the high degree of morphological specialization of the members of this clade in relation to its sister taxa, and the absence of intermediate fossil forms representing the transition to that morphotype. It is likely, given the ancestry of the clade Acrodonta (back into the Jurassic (Evans *et al.* 2002)), the lack of intermediate fossils leading to crown chamaeleonids, and the paucity of African and Malagasy fossils, that this long branch will be broken by the discovery of stem chamaeleonids, as has occurred for acrodontans after the inclusion of *Gueragama*. Whether stem chamaeleonids first diversified in Madagascar, Africa or other regions may not affect current ideas on the origin of the modern fauna. Crown chamaeleonids (which have been estimated to have originated in

Madagascar (Raxworthy *et al.* 2002) may be the last survivors of a previously more diverse chamaeleonid total clade, the origin of which is still unknown.

Palaeohabitat

Gueragama sulamericana lived in an arid to desert environment, the Caiuá desert belonging to the Bauru Group in Southeastern/Southern Brazil during the Late Cretaceous. Ichnofossils of large dinosaurs are known from the central areas of that desert, indicating that large animals were able to survive there. This was probably due to seasonal water availability and the interdune wetland characteristics of the Goio-Erê Formation (Fernandes *et al.* 2009). The Goio-Erê oasis probably supported some plant life, though plant fossils are still unknown. Pterosaurs were also abundant in that region, represented by hundreds of bones of the tapejarid *Caiuajara dobruskii* that have been found in the same locality as *Gueragama* (Manzig *et al.* 2014). Like modern agamid lizards living in arid regions, *Gueragama* probably lived in burrows to avoid extreme temperatures during at least part of the day

Discussion

Gueragama sulamericana provides fundamental insights on the acquisition of the peculiar lower jaw and tooth morphologies of modern acrodontans. Tooth ankylosis in the early branching priscagamids with pleurodont tooth attachment, and in *Gueragama sulamericana* with pleurodont and pleuroacrodont attachment, indicates that ankylosis evolved before the dorsal placement of the posterior teeth that is characteristic of the dentition of modern agamids and chamaeleonids. In fact, *Uromastyx* and some other agamids also have a dorsomedial, rather than a strictly dorsal (e.g. chamaeleonids), placement of the posterior teeth on the lower jaw, despite full ankylosis of the posterior adult teeth. The position of *Priscagama* as an early branching priscagamid in previous works (Conrad 2008; Gauthier *et al.* 2012) also suggests that fully acrodont attachment evolved independently within the priscagamids and acrodontans, now further supported by *G. sulamericana*. Furthermore, *Uromastyx*, later branching agamids, possesses an anteromedial projection of the dentary, which seems to be the remnant of a subdental shelf (Fig. 2.2), still present in *G. sulamericana.* The strong apical wear facets that

create a sagittal groove in *G. sulamericana* are unusual for extant acrodontans, which usually possess this feature on the labial surface of the dentary (Cooper & Poole 1973). A similar wear pattern has recently been identified in an Oligocene specimen that represents the oldest known acrodontan from Africa and also shares many features with *Uromastyx* (Holmes *et al.* 2010).

The oldest known acrodontans are from the Early-Middle Jurassic of India (Evans *et al.* 2002). Furthermore, morphological phylogenetic data suggests Iguania (including acrodontans) and Scleroglossa separated before the break-up of Pangea (Evans 2003a), which would explain the worldwide distribution reported for non-acrodontan iguanians by the Late Cretaceous (Gao & Fox 1996; Gao & Norell 2000; Evans 2003a). *Gueragama* indicates that a worldwide distribution was also achieved by acrodontan lizards by the Late Cretaceous, occurring not only in East Gondwana and East Laurasia, but also reaching West Gondwana during the Mesozoic. This reinforces the idea of an early radiation and wide distribution for all iguanians, and also implies that the acrodontan presence in Africa could be much older than the current oldest record (Holmes *et al.* 2010). Finally, *Gueragama* indicates that acrodontan dispersal through Gondwanan continents first occurred before the final break-up of Gondwana, and not by later dispersal events, thus contradicting previous hypotheses (Moody 1980; Honda *et al.* 2000). Therefore, it becomes clear that iguanians underwent a worldwide radiation in the Mesozoic. Whether the modern distribution of these faunas is a result of this early radiation, with subsequent extinction in some areas (e.g. acrodontans in South America), or the result of subsequent Cenozoic dispersal, remains to be established. However, my findings, along with previous ones (Macey *et al.* 2000; Raxworthy *et al.* 2002), suggest both factors were important.

It is clear that at some point in time, a diverse non-acrodontan iguanian fauna eventually replaced *Gueragama* and other potential acrodontans in South America. These two large groups of iguanians may well have come into contact during the Late Cretaceous in South America (Estes & Price 1973; Nava & Martinelli 2011), similar to what occurred in East Asia for non-acrodontans and priscagamids during this same time period (Borsuk-Białynicka & Moody 1984; Gao & Norell 2000). Acrodontan and non-acrodontan iguanians share very similar ecologies (Pianka & Vitt 2003) and their current almost exclusively non-overlapping distributions worldwide suggest competitive exclusion as a possible explanation for their current distributions. Alternatively, the Late Cretaceous extinction event could have paved the way for non-acrodontan iguanian dominance in South America.

Gueragama also suggests a new scenario for early acrodontan radiation, never considered before: that the stem acrodontan lineage could have evolved in West Gondwana, rather than in East Gondwana. Whether acrodontans originated in, or radiated into South America during the Mesozoic, is still unclear. Further sampling from both South America and other Gondwanan localities are necessary to appropriately address this question. Yet, *Gueragama* does indicate that at least some of the oldest known lizards in South America include species that are more closely related to the extant fauna of Old World continents, rather than to the modern fauna of South America.

In spite of limited knowledge of the squamate fossil record in South America, new finds are continuing to expand my understanding of squamate evolution in South America, especially in Brazil (Nava & Martinelli 2011; Hsiou *et al.* 2014; Simões *et al.* 2015a) and Argentina (Apesteguía & Zaher 2006; Brizuela & Albino 2011). The diversity of lizards in the Cretaceous of South America is higher than previously thought, and is not dominated by sphenodontians as was previously suggested for that time period (Apesteguia & Novas 2003). Rather, the previous lack of lizard records seems to have been a collection bias from southern latitudes in South America. The current pattern of distribution suggests that different major lizard groups were already present in Northeastern and Southern Brazil (this work and (Estes & Price 1973; Nava & Martinelli 2011; Simões *et al.* 2015a), where no sphenodontians are currently known (Fig. 2.3b), while sphenodontians were still abundant, but apparently restricted to more southern latitudes (Southernmost Brazil and Argentina).

Supplementary Information 2.1

Supplementary Information 2.1 is available online as part of the publish contents of this chapter through the following link:
https://www.nature.com/articles/ncomms9149#supplementary-information

Figures and Tables

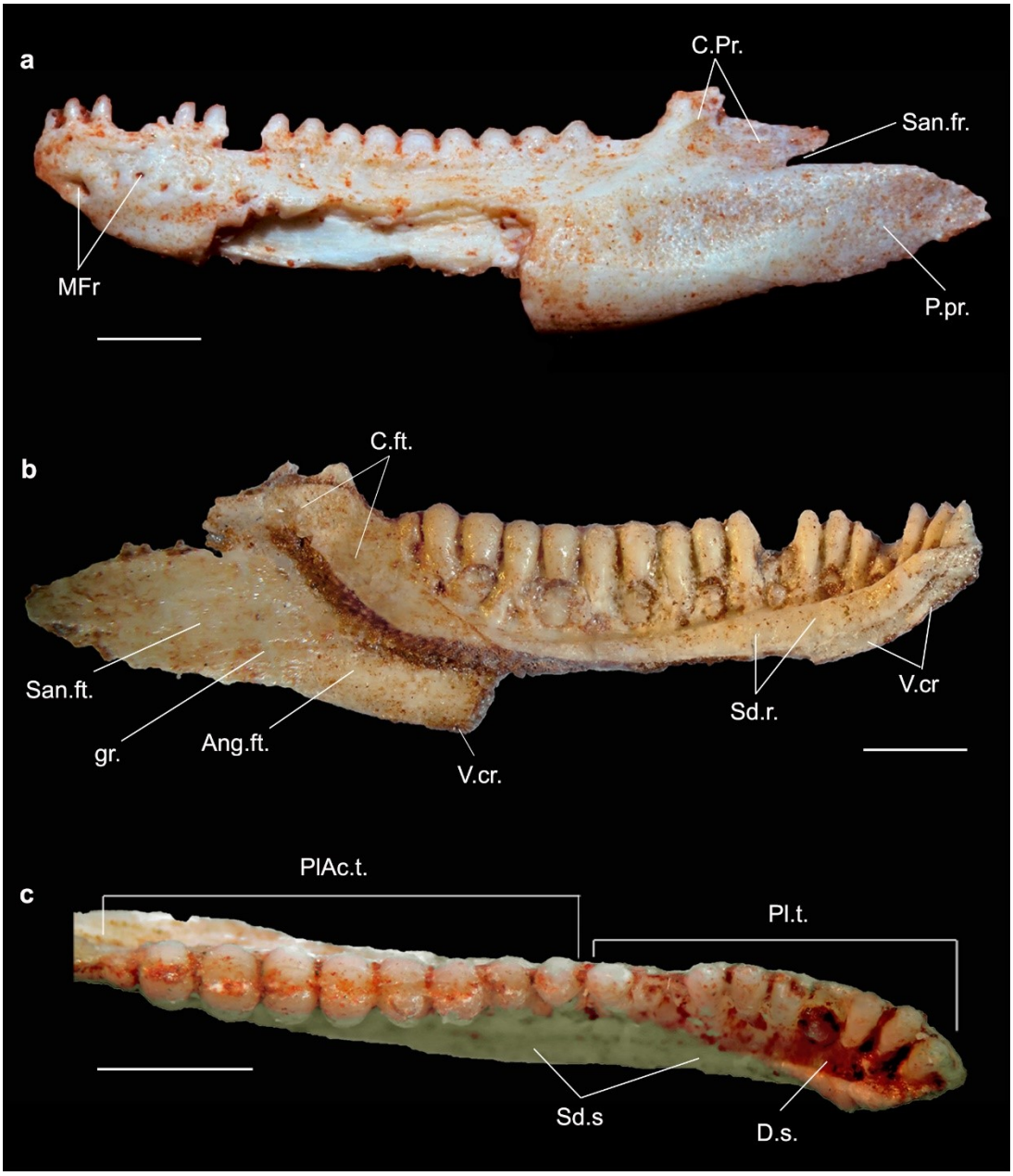

Figure 2.1. Holotype of *Gueragama sulamericana.* CP.V 2187 in (a) labial, (b) lingual, and (c) occlusal views. Ang.ft., angular facet; C.ft., coronoid facet; C.Pr., coronoid process; D.s., dental sulcus; gr., groove; M.fr., mental foramina; P.pr., posterior process; Pl.t., pleurodont teeth; PlAc.t., pleuroacrodontan teeth; San.fr., surangular foramen; San.ft. surangular facet; Sd.r., subdental ridge; Sd.s., subdental shelf; V.cr., ventral crest of dentary. Scale bars = 2mm.

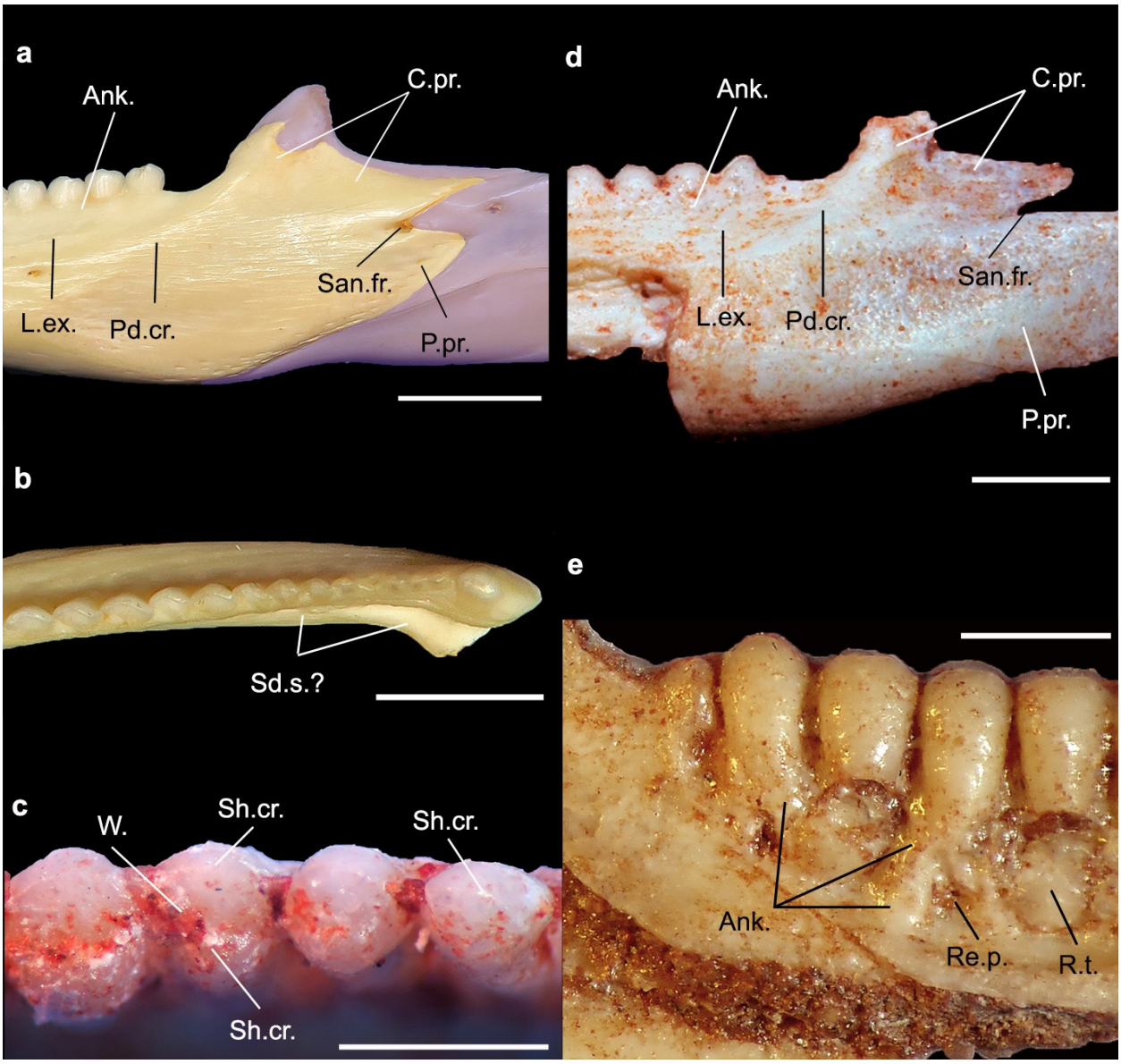

Figure 2.2. Details of *Gueragama sulamericana* and comparisons. Details of the lower jaw of *Uromastyx acanthinurus* (modern acrodontan – MCZ 27382) in labial (a) and occlusal (b) views. Scale bars = 5mm. Details on the dentition and dentary of *Gueragama sulamericana* (CP.V 2187) in occlusal (c), labial (d) and lingual (e) views. Scale bars = 1mm. Abbreviations: Ank., tooth ankylosis to dentary bone; L.ex., labial excavation on dentary; Pd.cr., posterodorsally ascending crest; Re.p., resorption pits; Re.t., replacement tooth; Sd.s., subdental shelf; Sh.cr., shearing crest; W., mediodistal wear facet.

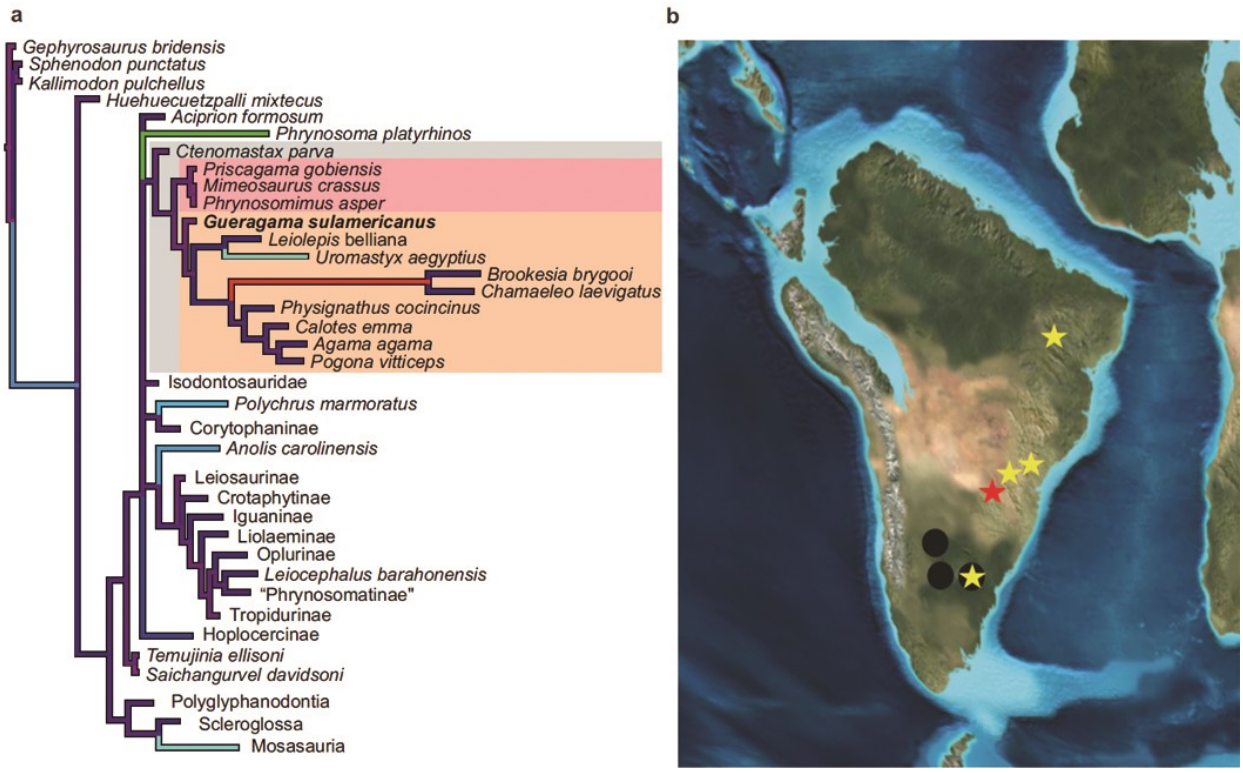

Figure. 2.3. Phylogenetic position of *Gueragama sulamericana* among other squamates, and lepidosaur distribution in the Cretaceous of South America. (a) Strict consensus tree of 373 most parsimonious trees of 5,287 steps each (consistency index = 0.2012; retention index = 0.7714). Branches are proportional to lengths, and emphasized by a color gradient of increasing branch length as follows: pink, purple, blue, cyan, green, yellow and red. The following clades are denoted: Priscagamidae (pink box), Acrodonta (light orange box), Priscagamidae+Acrodonta+*Ctenomastax* (gray box). The extremely long branch leading to chamaeleons (*Brookesia* and *Chamaeleo*) suggests either the absence of basal fossil forms, or rapid evolutionary rates. (b) Between the Aptian/Albian (112mya) and the Campanian (83mya), sphenodontians were present in northern Patagonia, in the provinces of Chubut (Queso Rallado), Río Negro (Los Alamitos, Cerro Tortuga, Cerro Bonaparte and La Buitrera) and Neuquén (El Chocón), represented by black circles. Lizards were present in the state of Ceará in northeastern Brazil (Araripe Basin), as well as in the southeastern/southern states of Minas Gerais (Peirópolis), São Paulo (Marília and Presidente Prudente) and Paraná (Cruzeiro do Oeste), and in the province of Río Negro (Cinco Saltos and La Buitrera), Argentina, represented by stars. The red star indicates the type locality of *Gueragama sulamericana*.

Table 2.1 Distribution of diagnostic features present in *Gueragama sulamericana* sp. nov. and other acrodontans+priscagamids

	Anatomical traits	Priscagamids	*Gueragama sulamericana*	Leiolepidinae*	Other acrodontans
1.	Fully open Meckelian canal	Present	Present	Present	Present
2.	Elongate angular facet on dentary (angular anterior to posteriormost tooth)	Present	Present	Present	Present
3.	Heterodonty (disconsidering the extreme wear that erodes the anterior teeth in some acrodontans during ontogeny)	Present	Present	Present	Present
4.	Posterior teeth ankylosis to dentary lingual wall	Present	Present	Present	Present
5.	Posterior teeth positioned apicolingually on the jaw	Present	Present	Present	Variably present
6.	Number of teeth ranging between 15-20 on the lower jaw	Variably present	Present	Present	Present
7.	Close packing of teeth	Variably present	Present	Variably present	Variably present
8.	Undivided and straight posterior process of the dentary	Absent	Present	Present	Present
9.	Posterior process separated by a small gap from coronoid process (aperture for surangular foramen)	Absent	Present	Present	Present
10.	Coronoid process with an elongate posterior component	Absent	Present	Present	Present
11.	Dorsolateral excavation on the labial margin of the lower jaw, producing osterodorsally ascending crest on coronoid process anterior margin	Absent	Present	Present	Variably present
12.	No articulatory facet for the splenial on the medial margin of the dentary (splenial small or absent)	Absent	Present	Present	Present

*Leiolepidinae (*Uromastyx* and *Leiolepis*) is taken separately from other acrodontans, due to its key position, generally taken as an early branching acrodontan. Leiolepidines have important features peculiar to them amongst extant forms, which are variably present in other acrodontans, and are also retained in *G. sulamericana* and other fossil acrodontans.

CHAPTER THREE: OSTEOLOGY, PHYLOGENY AND FUNCTIONAL MORPHOLOGY OF TWO JURASSIC LIZARD SPECIES AND THE EARLY EVOLUTION OF SCANSORIALITY IN GECKOES

[The contents of this chapter have been published in Simões, T. R., M. W. Caldwell, R. L. Nydam and P. Jiménez-Huidobro. 2017. Osteology, phylogeny, and functional morphology of two Jurassic lizard species and the early evolution of scansoriality in geckoes. Zoological Journal of the Linnean Society 180: 216-241.]

Introduction

The early evolution of squamates remains enigmatic, due to three main factors. The first, is the temporal gap between the expected origin of the group in the Middle Triassic (inferred from the sister-group relationship between squamates and rhynchocephalians—see Jones *et al.* (2013) for an update), and the first known squamate assemblages from the Middle Jurassic of Britain (Waldman & Evans 1994; Evans 1998; Caldwell *et al.* 2015), India (Evans *et al.* 2002) and Central Asia (Nessov 1988). The second is that these oldest known squamates are represented by poorly preserved materials. Despite providing important clues to the age of origin of some squamate clades, such as snakes (Caldwell *et al.* 2015) and acrodontans (Evans *et al.* 2002), these fragmentary materials are limited in terms of quantity and quality of data. Thirdly, though relatively complete specimens can provide more phylogenetically informative data for cladistic analyses, influencing my understanding of the relationships amongst crown-groups, as well as providing fundamental information on character evolution, some of the oldest known articulated squamates have never been fully analysed. In the present study, I aim to address the latter issue.

Eichstaettisaurus schroederi Broili, 1938; *Ardeosaurus brevipes* (Meyer 1855), *Ardeosaurus digitatellus* (Grier 1914), *Bavarisaurus macrodactylus* (Wagner 1852) and *Palaeolacerta bavarica* Cocude-Michel, 1961 from the Tithonian of Solnhofen, Germany, represent some of the oldest known articulated squamate remains. Amongst these, *Palaeolacerta* preserves very little detail of its cranial morphology (Estes 1983b). *Bavarisaurus macrodactylus* and *A. brevipes* are represented by better preserved specimens (especially the latter), and have received more detailed re-descriptions (Mateer 1982; Evans 1994b). The osteology of *E. schroederi* and *A. digitatellus* has never been thoroughly re-described beyond some very brief descriptions—e.g. Grier (1914), Broili (1938), Cocude-Michel (1963a), and Hoffstetter (1966); as a result, there has been little or no rigorous analysis of the functional morphology of either species, and they have never been analyzed together in a broadly sampled species-level data matrix of squamate phylogeny.

Eichstaettisaurus schroederi is a very important taxon as it is the most complete Jurassic squamate currently known, and is therefore a potential source of key data on early squamate evolution and phylogenetic relationships. Furthermore, the holotype of *A. digitatellus* represents the only specimen with significant osteological material directly preserved attributable to the *A.*

digitatellus of which the present location is known to us, whereas all previously published materials referable to *A. brevipes* are now considered to be lost—Estes (1983b) and B. Kear (pers. comm.). Here, I provide the first detailed osteological description of the holotypes of *Eichstaettisaurus schroederi* and *Ardeosaurus digitatellus*, along with a taxonomic revision of both genera. Furthermore, I provide a thorough discussion of their functional morphology, and place them within a species level analysis of squamate phylogenetic relationships. Despite previous disputes about their phylogenetic position, my comparisons and cladistic analysis confirms their assignment to the Gekkota, and indicate that the scansorial locomotion of geckoes might be an ancestral trait in the early evolution of the group, dating as far back as the Jurassic.

Geological Settings

The specimens studied here came from Wintershof, near Eichstätt, Germany, and are from rock units of the Solnhofen Group quarried near Solnhofen and Eichstätt in Bavaria, southeast Germany. During the Upper Jurassic this area corresponded to an archipelago in the Tethys Sea, forming a system of lagoons with restricted exchange with the main Tethys (Barthel *et al.* 1990). The sediments are derived from sponge and algal reef fragments mixed with bioclastic carbonate muds to form very finely laminated limestones marked by thin micritic layers and notable for the absence of bioturbation (Schmid *et al.* 2005).

The Tithonian age is based on ammonite faunal associations. Traditionally, the Eichstätt locality was considered to correspond to the same lithological member and chronostratigraphic age as the Solnhofen area (i.e., early Tithonian) based on the ammonite biozone of *Hybonoticeras hybonotum, Neochetoceras steraspis,*and *Paralingulaticeras lithographicum* (Zeiss 1968). This age was also supported based on the presence of the ammonites *Sutneria eugyra* and *S. bracheri* (Geyer 1969). However, Schweigert (2007) recently considered the correlation of the Eichstätt limestones to be problematic, and thus suggested a broader age spectrum: the Kimmeridgian to the Tithonian.

Materials and Methods

Digital photographs of the holotype of *Eichstaettisaurus schroederi* BSPG 1937 I 1 a & b, were taken using a Nikon Cool Pix 4500. Illustrations were made using Adobe Photoshop CC. Measurements were made digitally using the measurement tool in Photoshop CC, and calibrated using the embedded scale bar in the high resolution digital images taken under a dissecting microscope. Forelimb and hindlimb lengths were calculated based on the average of humeral-ulnar lengths and femoral-tibial lengths, respectively. This provides a better comparison across multiple species, as it is independent of variation in phalangeal number. The estimated snout-vent length (SVL) is provided for comparison with extant lizards in the literature, and calculated using the boundary between the first and second caudals as a proxy (Blob 1998). Measurements were taken from the skeletal remains of *E. schroederi*, and skeletal remains, as well as impressions on the matrix, for *A. digitatellus*.

The new data gathered herein was analyzed using the morphological data matrix of Gauthier *et al.* (2012), as recently updated by Simões *et al.* (2015b) with the characters made unordered (see "Supplementary Information 3.1"). The data was analyzed under maximum parsimony using the software T.N.T. (Goloboff *et al.* 2008b), with multiple runs of the 'New Technology Search' algorithm 'Ratchet' (1,000 initial trees by RAS + 100 iterations, followed by runs of 1,000 iterations each) and 'Sectorial Search' (1,000 initial trees by RAS + 100 rounds, followed by runs of 1,000 rounds each). Both 'Ratchet' and 'Sectorial Search' runs were always complemented by 'Tree Fusing' (1,000 rounds in each run). The most parsimonious trees (MPTs) found by both set of analyses (2,041 MPTs) were used in a subsequent run as the initial trees for a traditional TBR (heuristic) search, recovering a total of 3,174 MPTs. The usage of the New Technology algorithms in T.N.T. provides a more extensive search for all possible local optima of MPTs and also obtaining shorter MPTs, as recently demonstrated for another version of this same data matrix (Simões *et al.* 2015a).

Systematic terminology used. I have used some clade names such as Scincomorpha or Scleroglossa where necessary, such as when discussing the results of phylogenies in which those clades are monophyletic—e.g. Conrad (2008) and Gauthier *et al.* (2012). However, it is important to note that in analyses which utilize molecular data both clades are not monophyletic—e.g. Pyron *et al.* (2013) and Reeder *et al.* (2015)—, and scincomorphs are also

paraphyletic according to some morphological analyses—e.g. Lee & Caldwell (2000) and Lee (2005b).

Institutional Abbreviations: AMNH, American Museum of Natural History, New York, USA; BSPG, Bayerische Staatssammlung für Paläontologie und Historische Geologie, München, Germany; CM, Carnegie Museum of Natural History, Pittsburgh, Pennsylvania, USA; MPN, Museo di Paleontologia, Università di Napoli, Italy; NHMUK, Natural History Museum, London, UK; PMU, Paleontological Museum, Uppsala, Sweden; TMP, Royal Tyrrell Museum, Drumheller, Alberta, Canada .

Results

Systematic Palaeontology

Lepidosauria Haeckel, 1866

Squamata Oppel, 1811

Gekkonomorpha Fürbringer, 1900

Eichstaettisaurus Kuhn, 1958

Ardeosaurus? Broili, 1938: P. 97, Taf. 1-4

Broilisaurus Hoffstetter, 1953: P. 347, Fig. 1a

Type species: *Eichstaettisaurus schroederi*

Revised diagnosis: *Eichstaettisaurus* can be distinguished from other genera of squamates by the following combination of characters: skull depressed; short blunt snout; parietals paired; wide posterior parietal margin between supratemporal processes; parietals supratemporal processes short and with medial fossa; parietals without posteromedial process, or nuchal fossa; frontals fused; frontals widen anteriorly; frontal interorbital/frontoparietal width ratio between 0.2-0.3; frontal subolfactory processes well-developed; short supratemporal present; lacrimals absent; postorbital and postfrontal are separate elements; postorbital with wide posterior process dorsal to anterior end of squamosal; jugals without posteroventral process; premaxillae paired; zygosphene accessory articulations present; scapula with well-developed acromion process;

pubis without pubic tubercle; penultimate phalanges of hands and feet more elongate than preceding one.

Eichstaettisaurus schroederi (Broili, 1938)

Ardeosaurus? *schröderi* Broili, 1938: p. 97, Taf. 1-4
Broilisaurus schroederi Hoffstetter, 1953: p. 347, Fig. 1A
Eichstaettisaurus schroederi Kuhn, 1958: p. 380
Eichstaettisaurus digitatellus Cocude-Michel, 1963: p. 150, plate XXX, B
Eichstaettisaurus schroederi Hoffstetter, 1964: p. 287, plate 6 (Fig. 5)

Holotype: BSPG 1937 I 1a & b (Fig. 3.1), complete skeleton preserved in dorsal view and counterpart.
Locality and horizon: Solnhofen Limestone, Tithonian, Late Jurassic; Wintershof wei Eichstätt, Germany.
Revised diagnosis: *Eichstaettisaurus schroederi* can be distinguished from *E. gouldi* in having the parietals paired; frontal subolfactory processes in contact medially; a frontoparietal suture smooth and slightly convex anteriorly; frontal and parietals of equal width at their suture and in contact laterally; straight and laterally projecting caudal transverse processes; autotomy septa at the level of the fifth caudal.
Remarks: *Eichstaettisaurus schroederi* differs from both *Ardeosaurus* species in having strongly laterally emarginated paired parietals; frontals totally fused in dorsal aspect; parietals with shorter supratemporal processes; frontoparietal suture slightly convex anteriorly; postorbital and postfrontal as separate elements; 7 cervical vertebrae; and more than 30 presacral vertebrae. *Eichstaettisaurus schroederi* differs further from *A. digitatellus* in having a wide posterior parietal margin between supratemporal processes. *Eichstaettisaurus schroederi* further differs from *A. brevipes* in the absence of skull roof ornamentation and cephalic osteoderms, as well as pedal phalangeal formula of 2-3-4-5-4. The difference in the degree of frontal interorbital constriction between *E. schroederi* and *E. gouldi* used by Evans *et al.* (2004) to differentiate both species does not correspond to my measurements. The authors ratio for the frontal interorbital/frontoparietal widths for *E. gouldi* (0.2) seems to be accurate based on my analysis of

the published picture of the holotype. However, my personal measurement of *E. schroederi* indicates the interorbital/frontoparietal ratio is 0.25, not 0.32 as reported by Evans *et al.* (2004)—see Table 3.1, below, as well as the Material and Methods section, above.

Eichstaettisaurus gouldi Evans, Raia & Barbera, 2004

Holotype: MPN 19457, articulated partial skeleton preserved in ventral view.
Locality and horizon: La Cavere outcrop, Pietraroia, Mount Matese, southern Italy. The horizon is Albian (Upper Plattenkalk), Early Cretaceous.
Revised diagnosis: *Eichstaettisaurus gouldi* can be distinguished from *E. schroederi* in having the parietals fused; subolfactory processes of frontals well-developed, but not in contact medially; frontoparietal suture with the parietal slightly concave medially, receiving a posterior convexity of the frontal; the frontal being slightly wider than the parietals at their suture; at least one posteriorly oriented anterior caudal transverse process; autotomy septa, if present, begin beyond the level of the sixth caudal.
Remarks: *Eichstaettisaurus gouldi* shares with *E. schroederi* a depressed skull; short and blunt snout; absence of lacrimals; paired premaxillae; postorbital and postfrontal as separate elements; frontals fused; frontals widen anteriorly; frontal interorbital/frontoparietal width ratio between 0.2-0.3.

Osteology of *Eichstaettisaurus schroederi*

The holotype of *Eichstaettisaurus schroederi* (BSPG 1937 I 1 a & b) consists of two slabs representing part and counterpart. One slab includes all the preserved bone elements in dorsal view, and has been partially prepared on the opposite side, revealing portions of the ventral side of the skull. The counterpart preserves only the impression of those elements in the soft calcareous matrix, but provides some good morphological detail.

Cranium

The skull is depressed (Fig. 3.2a & b), and the bones are unsculptured. The snout is short, broad, and rounded anteriorly. The premaxillae are paired, possess a short nasal process that contacts the anterior end of the nasals, and forms the anteromedial border of the external nares. The

maxillary process in each premaxilla is short and has a smoothly rounded posterior end that contacts the maxilla (Fig. 3.3). The anterior end of the premaxillary process of each maxilla has a similar shape, and it is likely that a soft tissue connection existed between both elements. No anterior ethmoidal foramina are visible on the premaxillae, indicating the medial ethmoidal nerves likely exited through the large external nares.

The nasals are paired and their anterior halves form the medial-posteromedial borders of the external nares. No nasal foramina are observable dorsally, and there are no ventrolateral projections. On the ventral side, the straight suture between both nasals is visible and there is no midline crest. The septomaxillae can be seen within the nasal capsule on both sides. They seem to be flattened anteriorly, although this could be due to the deformation of the specimen.

Each maxilla bears a short premaxillary process, which forms a steep angle with the maxillary nasal process. The nasal process on each side contacts the nasal dorsomedially, and the prefrontal posteriorly. Small alveolar foramina for the cutaneous branches of the superior alveolar nerve and artery are visible close to the margin of the tooth row, but the anterior superior alveolar foramen is not visible externally, and is probably present close to the base of the medial margin of the nasal process, thus not visible in lateral aspect. The suborbital process of each maxilla extends to the mid-point of the orbit with its posterior tip lying ventral to the anterior end of the jugal.

A lacrimal bone is absent, and the anterior border of the orbit is formed mostly by the prefrontals, which lack any surface ornamentation, and possess a faint ridge projecting posterodorsally. This ridge does not form a prefrontal boss, as seen amongst many iguanians. The lacrimal foramen is not visible laterally, and it was probably present posteriorly, with the lacrimal duct opening into the orbital cavity, as observed in most lizards.

Both jugals are preserved. Whereas the left element is apparently complete, the right one is broken, preserving only its postorbital process. Each jugal is a semi-lunate element extending far anteriorly, approaching the prefrontal. It lacks a posteroventral process, and ascends posteriorly in a smooth curve contacting the postorbital on its posterior margin. The posterior end of the postorbital process of the jugal approaches the anterior end of the squamosal, but does not contact it.

The postorbitals and postfrontals are evident on both sides of the skull, but the right elements are better preserved, and in articulation. The postfrontals are forked medially, lying lateral to the

fronto-parietal articulation, and each possesses a single distal process that clasps the postorbital posteriorly.

Each postorbital is a triradiate element that is separate from the postfrontal and forms most of the posterior margin of the orbit. This differs from previous interpretations, in which the postorbitals are considered to be fused to the postfrontals (Cocude-Michel 1963a; Hoffstetter 1966; Estes 1983b). The ventral process of the postorbital contacts the orbital margin of the jugal, whereas its dorsal process contacts the postfrontal also on the orbital margin. The latter feature is uncommon among lizards, because the dorsal process of the postorbital usually contacts the posterior margin of the distal process of the postfrontal. The posterior process of the postorbital is relatively elongate, extending more than half the length of the upper temporal fenestra, and lying dorsal to the squamosal.

The squamosals are similar to those of most other lizards in being relatively slender and each having a posteroventral process contacting the cephalic condyle of the quadrate. Both squamosals lack a dorsal process, a feature that is usually present in iguanians and teiids. A relatively short supratemporal bone is present between the posterior end of the squamosal and the parietal, being short in length and butting against the lateral margin of the supratemporal process of the parietal.

The frontals are fused to each other, and form most of the dorsomedial margin of the orbits. They are widely expanded posteriorly, but are constricted at their midpoint and are slightly expanded anteriorly. The anterolateral processes of the frontal are elongate, but do not reach the maxillae, allowing for a short contact between the nasal and prefrontal. A much shorter anteromedial process intrudes between the nasals. In ventral view (Fig. 3.2c), the frontals bear subolfactory processes (best seen posteriorly) which seem to never touch medially at any point, but matrix partially obscures their central portion. There is seemingly no midventral crest of the frontals. Posteriorly, the frontals contact the parietals along a weakly anteriorly convex suture. There is no evidence of parietals tabs of the frontal either dorsally or ventrally.

The parietals are paired elements, which is uncommon to most squamates, but seen in some extant geckoes [e.g., *Nephrurus* (Evans 2003b), *Sphaerodactylus* (Daza *et al.* 2008), and *Pygopus* (AMNH R 140843)], and *Xantusia* (AMNH R 150172 and AMNH R 150174). The pineal foramen is present close to the centre of the parietal table, the lateral margins of the parietals are emarginated, and form most of the medial border of the upper temporal fenestrae.

The supratemporal processes are relatively short and bear a medial excavation. A posteromedial process is absent, as is also seems to be the case for the nuchal fossa. No frontal tabs are present either dorsally or ventrally.

The palatines do not contact in the midline, being widely separated from each other, and are relatively short anteroposteriorly (Fig. 3.2a and b). Their anterior margins are almost entirely visible in dorsal aspect, contacting the posteroventral margin of the prefrontals, thus the palatines make little or no contact with the frontals anterodorsomedially. Most of their posterior ends form a wide and nearly straight contact with the anteromedial processes of the pterygoids.

The pterygoids are widely separated from each other. Each pterygoid has a relatively wide undivided anteromedial process and, based on the right side of the skull (which is better preserved than the left side), seems to be inclined medially. The transverse process of the pterygoid is short and directed anterolaterally, contacting the ectopterygoid on the left side (but see below). The quadrate process of the pterygoid is slender and extends far posteriorly, though disarticulated from the quadrates as preserved in BSPG 1937 I a,b. As the slab with the bone elements in the holotype is preserved in dorsal aspect, and the palate is not clearly visible in ventral view, it cannot be determined whether a ventral flange was present on the transverse process of each pterygoid, nor whether or not teeth are absent or present on the palate.

The left ectopterygoid is visible and a small broken element lateral to the transverse process of the right pterygoid might represent its right counterpart, although it may also represent part of the anterior extension of the right jugal. The left ectopterygoid is semi-lunate and has no lateral process. Its posterior end lies dorsal to the pterygoids, as is the case in some geckoes (e.g., *Coleonyx*—AMNH R 89271) and anguids (e.g., *Diploglossus*—AMNH R 154690).

The supraoccipital is visible in dorsal view, bearing an ossified processus ascendens tecti synocti that contacts the parietal posteriorly. It cannot be determined whether anterolateral processes of the supraoccipital are present. A pair of posterolaterally oriented crests are present on the supraoccipital. These are similar to the "crests" formed on the supraoccipital by the posterior semicircular canal in some geckoes (e.g. *Hoplodactylus pacificus*—MCZ R-141790 and *Coleonyx variegatus*—AMNH R 89271) and some other lizards of reduced size (e.g. *Feylinia corrori*—MCZ R-42886 and MCZ R-106990). The latter feature is thus considered herein as a consequence of a reduced degree of ossification.

On the ventral side of the slab containing skeletal elements (Fig. 3.2c), parts of the basioccipital and basisphenoid are visible. These elements are not fused to each other, and the basisphenoid is flat on its ventral surface. The basipterygoid processes are stout, have slightly expanded distal ends, but are no longer in articulation with the pterygoids.

The quadrates have been tilted posteriorly and their anterior surfaces face dorsally (Fig. 3.1a & b). They each have a shallow anterior concavity, and the two articular condyles are of similar size.

Mandibles

The dentaries are visible on both sides of the slab containing the skeletal elements, but they are more readily observed on the ventral side of the specimen (Fig. 3.2d). The Meckel's canal is closed medially by the fusion of the subdental ridge to the ventral crest of the dentary in its anterior half, as is also observed in extant geckoes and xantusiids (Evans 2008). The splenial is not visible, and it cannot be determined whether it is overlain by the matrix, not preserved, or perhaps fused with the dentary as in xantusiids (Estes *et al.* 1988). In dorsal aspect, most of each mandible is obscured beneath the skull. However, part of the posterior end of each dentary can be observed, open medially (contrasting with the anterior and middle portions of the dentary), where the splenial usually articulates. The splenial is not visible, however, and it may have been detached from the mandible, as commonly occurs with fossil squamates.

The coronoids are partially visible on both sides. The left one bears a relatively elongate posteroventral process, but no posterior process. The right counterpart is mostly overlain by the pterygoid transverse process, and a broken element that might represent either the jugal or the ectopterygoid. The coronoid bears a very short anteromedial process that is directed ventrally.

Both surangulars are visible dorsally and each has a thickened dorsal border, forming the labial margin of the adductor fossa. The latter is relatively deep, but narrow, and faces dorsomedially. A short posteriorly directed retroarticular process is present posterior to the glenoid, and lacks any lateral notching.

Dentition

The dentary teeth are not visible in the holotype, but the maxillary teeth are visible on both sides (Fig. 3.3), along with some of the premaxillary teeth. The teeth are small, narrow, conical

and appear to be unicuspid, with no differentiation between the premaxillary and maxillary regions. The tooth count cannot be established with precision for the premaxillae, but there are ca. 22 teeth preserved *in situ* on the right maxilla, and the total tooth count in each jaw half is estimated to be at least 30. Variation in tooth height throughout the dental arcade indicates tooth replacement was present and was still active at the time of death. The teeth are positioned medially on the jaw labial margin (or parapet), and are unfused to the jaw margins, suggesting pleurodonty.

Postcranium

The preserved vertebral column includes the axis, the remaining cervical vertebrae, the dorsals, sacrals, and anterior caudals. The number of cervicals is estimated to be seven, because the eighth presacral vertebra seems to be the first one bearing ribs long enough to reach the sternum (Fig. 3.4a). Only the neural arches and neural spine of the axis are visible, with its intercentrum, and the atlas, being hidden from view. The postaxial cervicals bear very low neural spines, and most bear no ribs. The first ribs appear at the level of the sixth or seventh cervical.

Based on the identification of the eighth presacral as the first dorsal, the total number of dorsals is estimated to be 24, giving a total of 31 presacrals. This is a higher presacral vertebral count in comparison to that of most iguanians (with 24 presacrals), a number of scincomorphans (e.g. cordylids, gerrhosaurids, lacertids and teiioids), and gekkotans, many of which bear 26 presacrals. Yet, a slight increase in the presacral count as ocurring in *Eichstaettisaurus schroederi* (around 30 presacrals) is observed in a variety of taxa, including xantusiids and some gekkotans, as well as scincids , xenosaurids, anguids and varanids (Hoffstetter & Gasc 1969). The neural spines in the dorsal region are also small, and the last presacrals seem to lack any ribs (thus characterizing lumbar vertebrae). One striking feature of the vertebral morphology is the presence of accessory intervertebral articulations (zygosphenes and zygantra; Fig. 3.4b). The zygosphenes face dorsolaterally as in many iguanians, cordylids, gerrhosaurids, lacertids and gekkotans (although they are absent in pygopodids), and are notched anteriorly, as is the case in all aforementioned groups, as well as in teiids. Estes (1983b), following Broili (1938), reported a procoelic condition for the intervertebral articulations. However, as previously noted by Hoffstetter (1964) and Evans *et al.* (2004), it is not possible to determine the structure of centra with any confidence in this specimen since it is preserved in dorsal view.

Two sacral vertebrae can be identified just medial to the anterior half of the ilia and anterior to the first caudal that bears short transverse processes (Fig. 3.4c). Five anterior caudals are preserved, the remaining part of the tail having been autotomized (Figs. 3.1 & 3.4c). The soft tissue impression of the cartilaginous rod that developed subsequently to the loss of the tail can be seen on both slabs, and was previously illustrated under UV-light by Tischlinger & Wild (2009).

The ribs are holocephalous with circular articular surfaces. There are 21 or 22 pairs of presacral ribs. The posteriormost presacral vertebrae do not bear any ribs, therefore constituting a "lumbar" region. There are no accessory tuberculi anteriorly or posteriorly to the rib heads, and the ribs lack any degree of pachyostosis. Gastralia are absent, as is the case for all other squamates, but inscriptional ribs are visible attached to the distal ends of most of the dorsal ribs, but absent from the posteriormost four.

Of the pectoral girdle, the clavicles, left scapula and part of both coracoids are preserved (Fig. 3.4a & d). The clavicles lack the dorsally located cranial curvature observed in most autarchoglossans (Estes *et al.* 1988), as well as the posterior process that is seen in some scincids and cordyloids (e.g. *Mabuya mabouia*—AMNH 141128 and *Gerrhosaurus major*—AMNH 173621). It is not possible to determine whether the clavicles have a proximoventral fenestra, but they are expanded in this region.

The left scapulacoracoid exhibits no suture between the scapula and coracoid. The scapula is short, has an expanded acromion process dorsally, and lacks a scapular ray defining a separate scapular emargination dorsal to the scapulocoracoid fenestra (Fig. 3.4d). The supracoracoid foramen is visible medially on the scapulacoracoid (Fig. 3.4d), located at the level of, and just posterior to, the anterior coracoid ray and anterior (or primary) coracoid emargination of most lizards. The anterior (or primary) coracoid ray, delimiting the anterior coracoid emargination ventrally, is partially overlain by one of the left dorsal ribs. The left coracoid is mostly obscured beneath the vertebral column, and the right coracoid is preserved mostly as an impression in the calcareous matrix. The coracoids are relatively small when compared to most other lizards studied by us, being similar in dimension to the scapula.

Both forelimbs are preserved in articulation (Figs. 3.1 & 3.4a). Details of the proximal surface of the humerus are better seen on the left element (Fig. 3.4a), in which the bicipital fossa faces dorsally. The distal end of the humerus is twisted posteriorly relative to the longitudinal axis of

the humeral shaft, and the state of preservation hampers identification of either an ectepicondylar or an entepicondylar foramen (Figs. 3.4e & f). The ulna has a well-developed olecranon process as well as an expanded distal epiphysis. The radius is present, but its distal epiphysis has suffered some degree of weathering, so the styloid process cannot is not preserved (Figs. 3.4g & h).

The right manual carpus (Fig. 3.4g) preserves the fourth distal carpal proximal to the fourth metacarpal, but no other distal carpals are distinguishable due to poor preservation of this region. The metacarpals increase in length from the first to the fourth metacarpal, with the fifth being approximately half the length of the fourth. The phalangeal formula is 2-3-4-5-3, and the penultimate phalanges are elongated in comparison to the intermediate ones between the first and the penultimate ones (Tables 3.2 & 3.4).

For the pelvic girdle, the pubes, ischia, and the impressions of both ilia are preserved. The pubes have relatively narrow pubic aprons, which are directed anteromedially, and lack pubic tubercles. The obturator foramen is not visible, probably due to the crushing present on the acetabular margin of the pubes. The ischia possessed enlarged plates, which seemingly contributed to a long symphysial contact between both elements. Each ilium contained a long posteriorly directed blade, but it cannot be determined if a preacetabular process (Russell & Bauer 2008) is present.

Both hindlimbs are preserved in articulation and in posterior aspect. The shaft of the femur is almost straight, diverging from the more common sigmoidal shape observed in lizards. The femoral heads are badly crushed along with the other elements in the acetabular region, and the distal ends of the femora have only their posterior margin exposed. The tibiae and fibulae lay in close apposition to each other, and their distal epiphyses were not totally ossified.

The astragulus and calcaneum were not totally fused to each other, and the tibial facet on the astragulus is almost flat, lacking a crest for articulation with the tibia (Figs. 3.8 a, b & d). The distal tarsals are crushed against the metatarsals, and their morphology cannot be described in detail. However, it seems that both distal tarsals three and four are present. The first metatarsal is slightly shorter than metatarsals II-IV, the latter being subequal in length. The fifth metatarsal has its proximal head hooked medially, contacting the fourth distal tarsal, and is significantly shorter than the other metatarsals. The phalangeal formula is 2-3-4-5-4, and the penultimate phalanges are elongated compared to the intermediate ones, being between 30% and 56% longer than the antepenultimate phalanx (Figs. 3.8 a, b & d; Tables 3.3 & 3.4). Phalanges II (digit III)

and I and III (digit IV) of the right pes, as well as phalanges I and II (digit III), and I (digit V) of the left pes have better preserved articulatory surfaces. Distally, these phalanges have a hemispherical (convex) shape and, at least some phalanges (e.g. phalanx II, digit III, right pes) articulate with a concave proximal surface of the phalanx distally to it. This condition is different from the typical ginglymoid bicondylar articulation of the intermediate phalanges of most lizards, and would have allowed a greater range of horizontal movement. Horizontal movement also occurs in the crescentic/cup-shaped articulation in the intermediate phalanges of *Gekko gecko* (Russell 1975), but in the latter it is probably greater than in *E. schroederi* due to its expanded distal phalangeal articulations.

The unguals form claws that are slightly curved and dorsoventrally deepened (Russell 1975), or tall, at their bases—claw height defined as the distance measured from dorsal to ventral at the base of the claw (Zani 2000; Tulli *et al.* 2009; Crandell *et al.* 2014). Higher (or deeper) claws in *E. schroederi*, as well as in *Gekko gecko* (Fig. 3.9), bear a ventral expansion in lateral view, below the level of the contact with the penultimate phalanx, the functional consequences of which are further discussed below (see Functional Morphology). In *E. schroederi*, average pedal claw height (measured from those claws visible in lateral aspect) equals 0.70mm. The ratio between claw height/area of contact between the claw and the penultimate phalanx equals 1.707, indicating the claw is about 70% higher than the area of contact with the penultimate phalanx.

Systematic Palaeontology

Lepidosauria Haeckel, 1866

Squamata Oppel, 1811

Gekkonomorpha Fürbringer, 1900

Ardeosaurus Meyer, 1860

Homeosaurus, Meyer, 1855: p. 335

Type species: *Ardeosaurus brevipes*

Revised diagnosis: *Ardeosaurus* can be distinguished from other genera of squamates by the following combination of characters: paired premaxillae; the parietals fused and with weak lateral emargination (creating a narrow upper temporal fenestra); parietals with long

supratemporal processes; posteromedial process of parietal present; pineal foramen present; frontoparietal suture straight; frontals paired; frontals expand posteriorly, but do not expand anteriorly; frontals interorbital/frontoparietal width ratio ca. 0.5; postfrontal (or postorbitofrontal) forked medially; jugal without posteroventral process.

Ardeosaurus digitatellus (Grier 1914)

Homeosaurus digitatellus Grier, 1914: p. 86, plate XXII
Eichstaettisaurus digitatellus Cocude-Michel, 1963: p. 150, plate XXX, A
Ardeosaurus digitatellus Hoffstetter, 1964: p. 284, plates 4 (Fig. 2) and 5 (Fig. 3)

Holotype: CM 4026 (Fig. 3.6), partial skeleton including skull and parts of the postcranium preserved in dorsal view.
Locality and horizon: Solnhofen Limestone, Tithonian, Late Jurassic; Wintershof wei Eichstaett, Germany.
Revised diagnosis: *Ardeosaurus digitatellus* can be distinguished from *A. brevipes* by the absence of skull roof ornamentation and cephalic osteoderms; narrow parietal posterior margin between supratemporal processes; parietal posteromedial process absent; postorbital and postfrontal fused into a postorbitofrontal; 27 presacral vertebrae; pedal phalangeal formula ?-3-4-5-4.

Ardeosaurus brevipes (Meyer, 1855)

Homeosaurus brevipes Meyer, 1855: p. 335, Fig. IB.
Ardeosaurus brevipes Meyer, 1860: p. 106, Taf. 12, Figs. 4-5
Homeosaurus brevipes Broili, 1925: p. 108
Ardeosaurus brevipes Hoffstetter, 1953: p. 347, Fig. 1B

Holotype: Collection Hetzell, now lost (Mateer 1982; Estes 1983b). Represented solely by a cast (NHMUK 38006).
*Referred material***:** PMU.R58, described by Mateer (1982), but now also lost.

Locality and horizon: Solnhofen Limestone, Tithonian, Late Jurassic; Wintershof wei Eichstaett, Germany.

Revised diagnosis: *Ardeosaurus brevipes* can be distinguished from *A. digitatellus* by the presence of skull roof ornamentation and cephalic osteoderms; wider parietal posterior margin between supratemporal processes; parietal posteromedial process present; postorbital and postfrontal separate elements; 23 presacral vertebrae; foot phalangeal formula 2-3-4-5-3.

Remarks: the above diagnosis is based on comparisons between the holotype of *A. digitatellus* and the description provided by Mateer (1982) of *A. brevipes.*

Osteology of *Ardeosaurus digitatellus*

Cranium

The holotype of *Ardeosaurus digitatellus* is represented by a one slab containing a single individual in dorsal view (Fig. 3.5a). Osteological material is preserved in the skull and postcranium, along with impressions of some of the missing elements in the surrounding matrix.

The snout elements are not preserved in the holotype of *A. digitatellus*, but some impressions indicate their outline. The anteriormost elements preserved are the prefrontals, which are quite large compared to the prefrontals of most lizards known to us, also suggesting the absence of lacrimals (Fig. 3.5b and c). They do not bear surface ornamentation or a prefrontal boss. They are connected posteromedially to the frontals. The frontals are fused anteriorly, but still preserve a sutural line in their posterior half. It is not possible to determine if they became completely fused later in ontogeny. The frontals are expanded at the frontoparietal contact, and become constricted between the orbits. As in *A. brevipes*, the frontals do not expand anteriorly (Mateer 1982) and are less constricted between the orbits than they are in *E. schroederi* (Table 3.1).

The frontoparietal suture is straight in *A. digitatellus*, and the parietals are completely fused (Figs. 3.5a & b), bearing no remnants of the sutural line between them. The pineal foramen is present and located in the centre of the parietal table. The parietal is weakly emarginated on both lateral margins. This weak emargination, along with the orientation of the right squamosal (which had less displaced than its left counterpart), indicates the upper temporal fenestra is narrower than the one observed in *E. schroederi*. The supratemporal processes are present, elongate, and also possess a medial excavation (Fig. 3.6a). The posterior margin of the parietal

between the supratemporal processes is reduced, forming a V-shaped posterior margin. A small protuberance observed posteromedially to the parietal table may represent a posteromedial process, or part of the processus ascendens of the supraoccipital, but I could not determine either because most of this element was eroded away. The supratemporal bone is short and is located between the posterior end of the supratemporal process of the parietal medially, and the squamosal laterally.

The jugals are not entirely preserved, but their postorbital process is evident on both sides of the skull, the left element still contacting the ventral margin of the posterior process of the postorbitofrontal. The postorbital and postfrontal on the right side of the skull are fused into a postorbitofrontal (Fig. 3.6b). Medially, the postorbitofrontal has one parietal and one comparatively longer frontal process, both processes contributing to an extensive contact with the frontal and parietal. The posterior process of the postorbitofrontal extends far posteriorly, beyond the midpoint of the upper temporal fenestra.

The right squamosal is preserved lateral to the postorbitofrontal, indicating that the jugal extended far posteriorly, intervening between the postorbitofrontal and the squamosal. The posterior end of the left jugal is placed more anteriorly and did not reach beyond the posterior end of the postorbitofrontal. Whether the left jugal was displaced more anteriorly or the right one more posteriorly cannot be determined, but the impression of the anterior end of the left squamosal is located lateral to the posterior end of the left jugal, as observed on the right side. Therefore, it is concluded that the jugal prevented the postorbitofrontal from contacting the squamosal.

The squamosal is a moderately stout element, bearing a posteroventral process contacting the cephalic condyle of the quadrate. The posterodorsal process contacting the supratemporal process of the parietal is absent. Parts of both quadrates are preserved in articulation with the squamosal, supratemporal, and likely, the supratemporal process of the parietal. The ventral margin of both quadrates has been displaced anteriorly, so that they lie with their anterior surfaces facing dorsally. The right element is better preserved and still preserves a quadrate conch posterolaterally, as well as a distinct tympanic crest.

Postcranium

The holotype of *Ardeosaurus digitatellus* has the postcranium preserved mostly as impressions in the calcareous matrix, with a few cervical and dorsal vertebrae, as well as parts of the pelvic girdle preserved as osteological material. Yet, the quality of preservation allows many details of the vertebral, and especially, fore- and hindlimb anatomy to be discerned.

There are five or six cervical vertebrae (Fig. 3.5b), a relatively low cervical vertebral count among lizards, and only the posteriormost one or two cervicals bore ribs, as also observed in the holotype of *E. schroederi*. The total presacral vertebral count is estimated to be 27, followed by two sacrals and six caudals. The anterior cervicals are preserved in dorsal aspect, and had very low neural spines. The cervical pleurocentra are very fragmented, preventing a detailed description, but they are similar in length to the anterior dorsal pleurocentra. The dorsal vertebrae are preserved in lateral aspect, revealing some information about the morphology of their centra, despite some limitations due to deformation and some degree of shattering. The dorsal centra show no indication of bearing a posterior condyle. A structure resembling a condyle is observed anteriorly on the dorsal vertebrae however, as seen in lateral aspect (Fig. 3.7a). In the caudal region, impressions of the anterior caudals also show the anterior border of the vertebrae to be convex, and the posterior border to be concave (Figs. 3.7b-d), indicative of opisthocoely, a condition currently unknown for any extant or fossil squamate. However, it could also represent amphicoely with a sediment mould forming in the space between them. Therefore, the form of articulation cannot be determined with confidence, but it certainly is not procoelic as in most squamates. The neural arches are partially preserved and are as tall as the centra.

The ribs are single headed and articulated on circular synapophyses of the centra. The dorsal ribs are present up to the level of the penultimate presacral, but the condition in the last presacral cannot be determined due to poor preservation. The sacral ribs, as well as the anterior caudal ribs are preserved only as impressions, being laterally oriented and not forked.

No elements of the pectoral girdle are preserved, but parts of both fore limbs are preserved as impressions (Fig. 3.5a). The humeri, radii and ulnae do not reveal finer details of their anatomy, but it is possible to detect that the fore limbs were relatively small in relation to snout-vent length (Table 3.5). The left manus (Fig. 3.7e) has digits 3, 4 and 5 preserved, indicating a phalangeal formula of: ?-?-4-5-3. The penultimate phalanges of those digits are elongate compared to the

intermediate phalanges (Tables 3.2 and 3.4), and are followed by unguals that are curved and tall at their bases.

Both ilia are preserved in dorsal view, revealing elongate posterior blades. The impression of the right pubis indicates this element was narrow and strongly angled anteromedially. No impressions of the pubic tubercle are evident, suggesting it was very small or absent. The ilia are not preserved either as bony elements or impressions.

The hind limbs are also proportionally short compared to snout-vent length, and similar in length to the forelimbs (Table 3.5). The femora are relatively slender and not sigmoidal, as was also observed for *E. schroederi*. The tibia and fibula on both sides are of similar width to each other and diverge distally. The left pes is better preserved than the right, with parts of all digits in articulation, indicating a phalangeal formula of: ?-3-4-5-4. As in the forelimbs, the penultimate phalanges are elongate compared to the intermediate ones, being ca. 40% longer than the phalanx immediately preceding it in the third digit (Fig. 3.8c; Table 3.3 & 3.4). Most articulatory surfaces are not well preserved, but in the left pes, articulation between phalanges I and II in digit II is concave-convex, as reported for *E. schroederi* above.

The unguals are recurved and relatively tall at their bases due to a ventral expansion beyond the level of contact with the penultimate phalanx, as in *Gekko gecko* (Fig. 3.9) and *E. schroederi* (see above): pedal claw height equals 0.65mm. The ratio between claw height/area of contact between the claw and the penultimate phalanx equals 1.625.

Functional Morphology

The functional morphology of *Eichstaettisaurus* and *Ardeosaurus* has never been given extensive attention, despite some particularly interesting aspects of their limb morphology. Russell *et al.* (1997) briefly mentioned some gecko-like aspects of the feet of *Eichstaettisaurus schroederi*, suggesting a reduction in length of the fourth metatarsal and a slight divergence between metatarsals III and IV, but did not go further.

Relatively short fore- and hind limbs: One of the most apparent aspects of the body form of both *E. schroederi* and *A. digitatellus* is the relatively short fore- and hindlimbs (Figs. 3.1a&b, 3.5a), which are also similar in length to each other (see Table 3.5 and 3.6). Short fore- and hindlimbs have been proposed to be functionally advantageous for scansoriality (the capacity to climb) as shorter limbs bring the center of gravity closer to the substrate and reduce the rotatory

moment of its body in relation to the inclined plane (Cartmill 1985). This is further enhanced by the overall body depression observed in *E. schroederi* and *A. digitatellus*, a feature also observed among gekkotans, and previously suggested to enhance climbing performance in *Gekko gecko* (Russell 1975). However, recent studies have contested the correlation of short fore and hind limbs with scansoriality for lacertids and geckoes (Vanhooydonck & Van Damme 1999; Zaaf & Van Damme 2001) and this particular feature may instead be related to phylogeny (see below).

*Fore- and hindlimbs of similar length*s: Fore and hind limbs of similar lengths to each other may also contribute to stable climbing, as limbs of very distinct lengths would result in different stride lengths, and in the tendency to have fewer limbs maintaining contact with the substrate during fast locomotion. It is important to maintain grip in some climbing lizards, as documented for *Lacerta oxycephala*, which maintains three or four limbs in contact with the substrate most of the time during fast locomotion (Arnold 1973). Yet, the latter may not be applicable to geckoes with highly developed adhesive toepads, such as *Gekko gecko*, as the latter keeps only two limbs (and occasionally only one) in contact with the substrate most of the time (Russell 1975). This latter attribute, as displayed by pad-bearing geckoes, may be limited to those climbing lizards with adhesive toepads, due to their greater clinging capacity in relation to frictional grip relative to other lizards.

The correlation between fore to hind limb ratio and habitat preference has been tested for lacertid lizards, and no significant correlation has been found (Vanhooydonck & Van Damme 1999). However, as acknowledged by the latter authors, lacertids may use several other habitats, thus not usually being specialized in that regard. Therefore, the relevance of fore to hind limb ratios is dependent on particular clades due to phylogenetic signal, the level of specialization for a particular habitat, as well as the influence of functionally related structures (e.g. adhesive toepads). Therefore, fore to hind limb ratios, when taken alone, have to be interpreted with caution when trying to differentiate between scansorial and ground-dwelling habits for lizards.

Claws tall at their bases: Despite some ambiguity regarding the relevance of fore and hind limb lengths as adaptations to scansoriality, both the manus and pedes of *E. schroederi* and *A. digitatellus* bear claws that are relatively tall at their bases (Figs. 3.4e, 3.7e, 3.8 a-d, and descriptions with ratios above). This feature has been positively correlated with climbing in lizards, and advocated to be a functional adaptation, even when phylogenetic history is taken into consideration (Zani 2000; Tulli *et al.* 2009; Crandell *et al.* 2014). A possible explanation for this

correlation is that higher claws exhibit a ventral expansion relative to the level of contact with the penultimate phalanx, when compared to terrestrial non-scansorial lizards (Fig. 3.9). The flexor tendon, which runs ventrally and inserts proximally in each phalanx (including the claw), would have a greater lever arm and increase holding strength against the substrate, thus aiding lizards in climbing (Russell 1975). In addition to height, the claws of *A. digitatellus* are more elongate and curved relative to those of *E. digitatellus*. However, the relevance of claw length to clinging performance is debatable, due to contrasting conclusions (Zani 2000; Tulli *et al.* 2009; Crandell *et al.* 2014), especially when gekkotans (typically with short claws) are considered.

Elongate penultimate phalanges: *Eichstaettisaurus schroederi* and *A. digitatellus* also bear elongate penultimate phalanges in both their fore- and hindlimbs (Fig. 3.8 a-d). This feature has been strongly correlated with climbing habits in a variety of reptiles, including lizards (Kavanagh *et al.* 2013). It has also been observed in other fossil lizards that have been interpreted as having had a scansorial lifestyle, such as *Scandensia* from the Early Cretaceous of Spain (Evans & Barbadillo 1998; Bolet & Evans 2011) and *Calanguban* from the Early Cretaceous of Brazil (Simões *et al.* 2015a).

Foot symmetry: Geckoes bear radiating digits, instead of the sub-parallel digits evident in most lizards, creating a symmetrical foot in relation to the typical lizard condition (Figs. 3.8e & f). This feature is associated with the adhesive toepad climbing mechanism of geckoes, as this facilitates the spreading of the seta-bearing surfaces about a broad arc (Russell 1975). The latter allows for various combinations of digital orientation that maximize their potential in passive loading, thus aiding in the maintenance of grip in a variety of body orientations (Russell 1986; Russell *et al.* 1997; Russell & Oetelaar 2015). Also, a symmetrical foot with digits that radiate distally helps in providing grip, as it allows the first and fifth digits to develop opposability (Robinson 1975; Rewcastle 1983). Foot symmetry is achieved by a variety of factors.

Whereas most lizards have a first metatarsal (MT I) of about half the length of MT II and III—MT III/MT I length ratio of 2:1—geckoes have a proportionally longer MT I in relation to MT III, with a MT III/MT I ratio between 1.3 and 1.5, with the greatest average amongst geckoes (1.47) being found in padless diplodactylines (Russell *et al.* 1997). *Eichstaettisaurus schroederi* and *Ardeosaurus digitatellus* display a MT III/MT I ratio of 1.41 and 1.48 respectively (Table 3.5), falling within the range reported by Russell *et al.* (1997) for extant geckoes.

Another factor contributing to foot symmetry is the reduction in length of MT IV. Whereas most lizards have a MT IV that is longer than MT III, geckoes have an MT IV shorter than MT III (Russell *et al.* 1997; Russell & Bauer 2008). Some varanids have similar lengths for metatarsals MT III and IV (Russell *et al.* 1997). This is also seen in *Heloderma*, but in both cases they are usually never shorter than MT III (TRS, pers. obs.). Reduction in length of MT IV is observed in *E. schroederi* (Figs. 3.8a, b & c), and may be the case for *A. digitatellus* (Fig. 3.8c) as well, although this cannot be confirmed.

Other features related to foot symmetry are the broadened proximal head of MT IV, which greatly increases the angle between the shafts of MT III and MT V, as well as the reduction of imbrication among the metatarsals proximally. Both features help to create an expanded digital arc, and contribute to foot symmetry (Russell *et al.* 1997). These features, however, are not observable for either *E. schroederi* or *A. digitatellus*. *Eichstaettisaurus* has a somewhat broadened proximal head of MT IV, but it does not seem to be proportionally larger than the condition seen in *Iguana iguana* and most other lizards. Therefore, both species display partial development of foot symmetry, this being more developed in *E. schroederi*.

A few conspicuous features of the foot of *E. schroederi* and *A. digitatellus* are applicable to understanding their consequence for the locomotion of these lizards, even though they are not necessarily linked to scansorial habits.

Metatarsals of quite distinct lengths contribute to the highly asymmetrical feet of most lizards. The distal tips of the metatarsals form a straight metatarsophalangeal line (Fig. 3.8e), which is directed perpendicular to the parasagittal plane at rest. During limb retraction in sprawling locomotion, this aids in maintaining the first three digits in contact with the substrate and provides even support amongst these digits for bearing the animal's body weight (Brinkman 1980; Rewcastle 1983). If they were of equal length, most of the weight would be concentrated on the first digit only, as a consequence of the lateral orientation of the femur. Metatarsals of similar length are usually observed only in lizards with more anteriorly oriented feet (Brinkman 1980). Therefore, the highly symmetrical metatarsals of *E. schroederi* and *A. digitatellus* indicate their feet were likely more anteriorly, rather than laterally, oriented.

Another character of laterally oriented feet is the development of the ginglymoid bicondylar articulation observed with greater development on the first three pedal digits of most lizards. These joints, along with tendinous bands that lie along the lateral sides of the fingers, contribute

to resisting lateral displacement while enabling dorsoventral flexion of the phalanges (Russell 1975; Landsmeer 1981). This is important considering that the posteriorly-directed thrust during limb retraction has a perpendicular orientation relative to the laterally-oriented phalanges (Rewcastle 1983)—see Figs. 3.8e & f—thus an interlocking mechanism represented by the bicondylar articulations provides greater stability. In lizards with more anteriorly oriented feet, this morphology would be less effective. Bicondylar articulations are not observed in *E. schroederi* or *A. digitatellus*, which have convex-concave joints in the intermediate phalanges where articulatory surfaces were well preserved. This is another indication that *E. schroederi* and *A. digitatellus* had more anteriorly oriented feet than most lizards, which bear bicondylar articulations. Finally, in *E. schroederi* and *A. digitatellus* the long axis of the first metatarsal makes a right angle with that of the tibia, a condition observed in *Gecko gecko*. This is compatible with anteriorly oriented feet. While it is possible that this latter anatomy is an artifact of post-mortem changes in orientation, the metatarsal proportions and shape of interphalangeal articulations do support interpretation of the pedes of *E. schroederi* and *A. digitatellus* as having an anteromedial orientation similar to that found in geckoes and at least some platynotans.

There are limitations in differentiating ground-dwelling from scansorial lizard species based on limb to snout-vent length ratios, as well as fore to hind limb length ratios, as indicated above. However, a dorsoventrally expanded claw and elongate penultimate phalanges have a significant correlation to habitat usage in lizards and other reptiles (Zani 2000; Tulli *et al.* 2009; Kavanagh *et al.* 2013; Crandell *et al.* 2014). Therefore, the combination of the latter, along with a depressed body and skull in *E. schroederi* and *A. digitatellus*, provide a suit of features that are usually found together only in species specialized to climbing.

DISCUSSION

Ardeosaurus brevipes and *A. digitatellus* were both initially classified as rhynchocephalians, within *Homeosaurus*, and were later classified as lizards (Grier 1914; Camp 1923; Cocude-Michel 1963a; Hoffstetter 1964). Camp (1923) was the first to identify *Ardeosaurus brevipes* as a gekkotan, erecting the family Ardeosauridae. Cocude-Michel (1963a) later synonymized *H. digitatellus* with *Eichstaettisaurus*, within the family Eichstaettisauridae Kuhn 1958, and

maintained *Ardeosaurus* (represented solely by *A. brevipes*) within the family Ardeosauridae; he also maintained Eichstaettisauridae and Ardeosauridae within Gekkonoidea, recognizing their gekkotan affinities. Hoffstetter (1964) placed *H. digitatellus* within the genus *Ardeosaurus*, along with *A. brevipes*, and further supported their designation as geckoes, subsequently placing all three species (*A. brevipes*, *A. digitatellus,* and *E. schroederi*) within Ardeosauridae (Gekkonoidea) (Hoffstetter 1966). The position of *Ardeosaurus* as a gekkotan was maintained by Mateer (1982) and Estes (1983b). The attribution of *Ardeosaurus* to gekkotans was later contested by Evans (1994b).

Eichstaettisaurus schroederi was initially suggested to belong to the genus *Ardeosaurus*, within Xantusiidae (Broili 1938). Later, this species was placed in its own genus, *Broilisaurus*, but still maintained within the Xantusiidae (Hoffstetter 1953). Kuhn (1958) noted that the name *Broilisaurus* was pre-occupied and erected the genus *Eichstaettisaurus*, simultaneously erecting the family Eichstaettisauridae to replace the previous Broilisauridae. Cocude-Michel (1961) was the first to propose that *Eichstaettisaurus* was a gecko, and soon afterwards (Cocude-Michel 1963a) placed Eichstaettisauridae and Ardeosauridae within Gekkota (see also above). This association with geckoes was accepted by Hoffstetter (1964; 1966), Estes (1983b) and Evans (1993).

Later, both *Ardeosaurus* and *Eichstaettisaurus* were considered to be an early branch of the squamate stem, and not crown-group squamates (Evans & Barbadillo 1998; Evans & Chure 1998; Evans & Barbadillo 1999; Evans *et al.* 2000; Evans *et al.* 2004). Their position became even more controversial when *Eichstaettisaurus* was retrieved within the monophyletic group formed by *Dalinghosaurus* and xenosaurids, whereas *Ardeosaurus* was retrieved as the sister taxon to iguanians (Evans & Wang 2005). Subsequently, *Eichstaettisaurus* was retrieved with *Hoyalacerta*, *Scandensia* and *Parviraptor—sensu* Evans (1994a), but see Caldwell *et al.* (2015)—forming the sister-group to anguimorphs, and *Ardeosaurus* was placed once again in the stem of Squamata (Evans *et al.* 2005).

The more recent analyses of squamate relationships that have included a large number of fossils have not found consensus either. Conrad (2008) recovered *Eichstaettisaurus* and *Ardeosaurus* as stem scleroglossans and the sister taxon to geckoes. However, subsequent reanalyses of that data same matrix placed both species either in the scleroglossan stem or in a polytomy with members of the squamate crown (Bolet & Evans 2010; Bolet & Evans 2011;

Bolet & Evans 2012). Gauthier *et al.* (2012) recovered *Eichstaettisaurus* as a stem gekkotan, an outcome similar to the first systematic classifications of the species, but they did not include *Ardeosaurus* in their analysis.

Despite all these previous efforts attempting to identify the phylogenetic position of *Eichstaettisaurus* and *Ardeosaurus*, the authors were hampered by limited knowledge available on the osteology of these two taxa, as well as on methods of their inclusion in data matrices. For example, neither species was ever included in a species level analysis of squamate relationships in association with first hand observation of the holotypes. The more recent dataset of Gauthier *et al.* (2012), includes personal observations of the specimens, but the scorings for the *Eichstaettisaurus* OTU (operational taxonomic unit) was at the generic (based on a combination of information from different species) not species level. Scoring both species as a single OTU may be problematic because important differences exist between them. Such a practice may have the undesirable consequence of scoring putative key character states from both species as polymorphisms.

In order to evaluate the systematic placement of these species in light of the criticisms given above, I rescored *Eichstaettisaurus* in the matrix of Gauthier *et al.* (2012), with the additional taxon-scoring corrections presented by Simões *et al.* (2015b) (see "MATERIAL AND METHODS" and "Supplementary Information 3.1" for details). I scored only those character states that can be observed for *E. schroederi*, following personal observation of the holotype (and only known specimen attributable to that species). Even after re-scoring characters that were based on *E. gouldi* only, a number of other characters were scored that were previously treated as missing data. I also included scorings for *A. digitatellus* in that matrix. I tested three different scorings for the vertebral morphology of *A. digitatellus* (see above for my observations and interpretations): amphicoelous, opisthocoelous, and missing data (?).

In all of my results (Fig. 3.10), I found that *E. schroederi* and *A. digitatellus* fall along the gekkotan stem, along with AMNH FR 21444, regardless of the scoring of vertebral morphology for *A. digitatellus*. I found that *E. schroederi*, *A. digitatellus*, AMNH FR 21444 and crown gekkotans are united by the following eight synapomorphies: 38(1), frontal subolfactory processes arch beneath the brain (but do not contact at the midline); 39 (3), frontal subolfactory process depth between 75-85%; 88(0), parietals paired; 95(1), parietal postparietal (posteromedial) projection near midline; 135(1), prefrontal has a broad articulation with

supradental shelf of maxilla lateral to palatine; 137(1), lacrimal absent; 420(4), 31 or more maxillary teeth; and 470(2), caudal autotomic septum posterior to the caudal rib—characters referred to as described by Gauthier *et al.* (2012).

Compared to previous analyses of this dataset, including results from Gauthier *et al.* (2012), Simões *et al.* (2015a) and Simões *et al.* (2015b), major differences lie in the level of resolution within Scincomorpha, and most importantly, in the placement of snakes. Snakes are still recovered in a clade with amphisbaenians, dibamids, *Sineoamphisbaena* and *Anniella* (with *Anniella* falling closer to snakes), but all these taxa now are nested within scincomorphans, forming a clade (with the addition of *Feylinia* and *Acontias*) that lies as a sister clade to Xantusiidae+*Tepexisaurus*.

Eichstaettisaurus schroederi exhibits a greater amount of morphological similarity to geckoes than does *A. digitatellus,* even though the latter lacks preservation sufficient to evaluate some of its features. Previous considerations suggested the similarities between *Eichstaettisaurus* and geckoes were not exclusive to geckoes (Evans *et al.* 2004; Daza *et al.* 2014). However, the overall character agreement presented by the phylogenetic analysis herein indicates otherwise. Additionally, I note here for the first time an important combination of features that support gekkotan affinities (particularly for *E. schroederi*). These include: paired parietals; Meckelian canal closed medially; small conical maxillary teeth with high tooth counts; short and blunt snout; depressed skull; ectopterygoid lying dorsal to transverse process of pterygoid; wide separation between both pterygoids and both palatines; wide suture between the pterygoid and the adjacent palatine on each side of the skull; and the presence of a "lumbar" region. It is also interesting to note that, at least in *E. schroederi*, the symmetry observed in the metatarsals is observed in combination with convex-concave interphalangeal joints, which is not seen in platynotans that bear some degree of symmetry in their feet, or any other lizards studied by us, apart from gekkotans. This indicates that the kind of foot symmetry observed in *E. schroederi* (and maybe also in *A. digitatellus*) is more similar to that observed in geckoes.

Eichstaettisaurus schroederi possesses a postorbital, squamosal, as well as a long jugal, which are not present in extant geckoes. The presence of these elements is plesiomorphic for Lepidosauria and if geckoes are nested anywhere within lepidosaurs, their stem taxa or sister-taxa can be expected to have also possessed these. As such, the presence of a postorbital, squamosal, and long jugal in *E. schroederi* and *A. digitatellus* is not contradictory— *contra*

Evans *et al.* (2004)—with their position as gekkotans broadly speaking. Other features that are seen in *E. schroederi* and that differ from most extant geckoes are the presence of a processus ascendens of the synotic tectum, and the subolfactory processes of the frontal not touching medially. Yet, the latter condition is also seen in AMNH FR 21444. These features might simply be due to the stem position recovered for *E. schroederi*, and is in agreement with the result of the phylogenetic analysis.

Ardeosaurus digitatellus, despite having some important similarities with *E. schroederi*, and with geckoes, does not share an equally large number of derived features with gekkonomorphs, especially because of non-preserved features. Overall character agreement does, however, place it within gekkonomorphs, and further information on the species (or on *A. brevipes*) will be important for evaluation of whether the features observed in both *E. schroederi* and crown gekkotans, but currently unknown for *A. digitatellus*, are also present in *Ardeosaurus*.

CONCLUSIONS

Morphological comparisons arising from my detailed redescription of *Eichstaettisaurus schroederi* and *Ardeosaurus digitatellus* shows a closest resemblance to geckoes, especially so for *E. schroederi*. This is supported by my revision of the scoring for *Eichstaettisaurus,* and the placement of and scoring for *A. digitatellus* in the dataset of Gauthier *et al.* (2012). This is of fundamental importance to the early evolution of squamates, as it demonstrates the existence of yet another major squamate clade—gekkonomorphs—in the Jurassic, along with snakes (Caldwell *et al.* 2015) and acrodontan lizards (Evans *et al.* 2002).

If geckoes are, along with dibamids, an early evolving clade within squamates, as inferred from all molecular and combined evidence studies— e.g. Vidal & Hedges (2005); Reeder *et al.* (2015); Zheng & Wiens (2016)—then *Eichstaettisaurus* and *Ardeosaurus* should be just part of a wider fauna of Jurassic gekkonomorphs. In fact, estimations of the origin of most of the major clades of squamates (e.g. gekkonomorphs, scincoids, lacertoids, iguanians and anguimorphs) usually place divergence times for their stem back in the Jurassic or the Triassic (Vidal & Hedges 2005; Mulcahy *et al.* 2012; Pyron & Burbrink 2014; Zheng & Wiens 2016). Furthermore, geckoes, acrodontans and snakes represent very distinct points (early and later

deriving clades) in the phylogenetic tree of squamates, given most tree topologies as inferred from either morphological or molecular studies—e.g. Gauthier *et al.* (2012) and Pyron *et al.* (2013). Yet, fossil evidence indicates those different branches of the squamate tree were already present in the Jurassic, some of which have representatives in geographically distant areas. Therefore, the currently available molecular and fossil evidence indicate that other major squamate clades must also have originated in the Jurassic. Given the paucity of information concerning Jurassic squamates, it is not surprising that most of these have yet to be found or identified.

In geckoes, the interphalangeal articulations form a crescentic/cup-shaped system, allowing greater mobility, and are believed to be an adaptation to digital hyperextension. Digital hyperextension is used in geckoes and anoline iguanians during digital release from the substrate in their adhesive toepads clinging mechanism (Russell & Bels 2001; Russell 2002). Neither *E. schroederi* nor *A. digitatellus* show adaptations towards the active digital hyperextension seen in geckoes (e.g. depressed and reduced intermediate phalanges, and arcuate penultimate phalanges). Yet, both species show a combination of features in their claw morphology, penultimate phalanges, head depression and limb ratios that indicate a scansorial habit. This suggests the scansorial lifestyle arose earlier in the evolution of geckoes than previously known. It remains to be investigated if the partial development of foot symmetry in *E. schroederi* or *A. digitatellus* was an initial stage towards the establishment of foot symmetry as seen in later evolving geckoes, or if it is an independent acquisition. This would have important consequences to understanding if gecko foot symmetry—which is highly correlated with the function of adhesive toepads and scansoriality in extant geckoes (see above)—evolved prior to the first appearance of toepads in the group.

Fig. 3.1. Holotype of *Eichstaettisaurus schroederi* BSPG 1937 I 1a & b. Slab (A), and counterslab (B). Scale bars equal to 20mm.

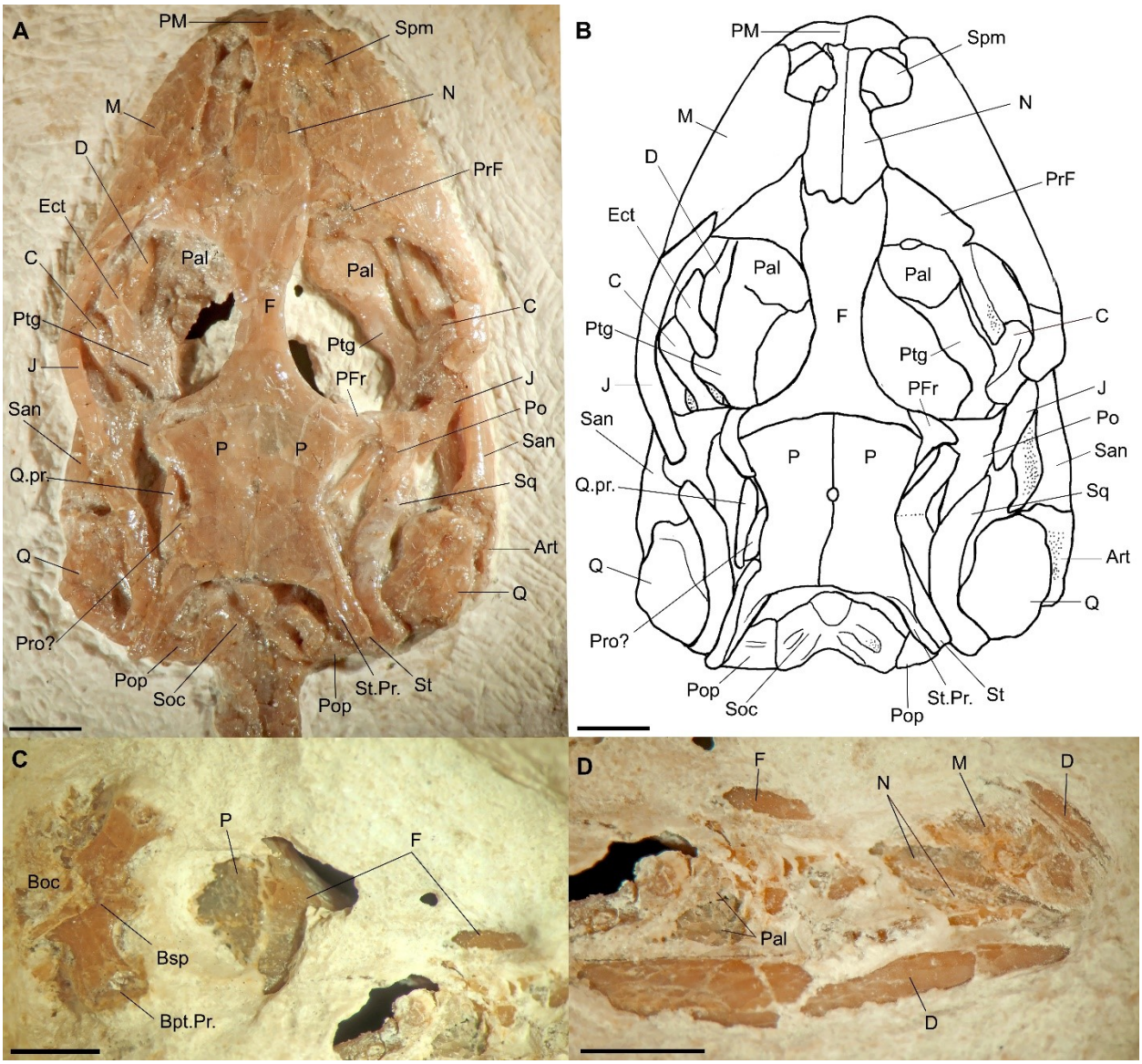

Fig. 3.2. Skull of the holotype of *Eichstaettisaurus schroederi*. (A) specimen in dorsal view, and drawing (B) in dorsal view. Ventral aspect of the skull, depicting parts of the braincase and skull roof (C), and mandibles (D). Abbreviations: Art, articular; Boc, basioccipital; Bpt.Pr., basipterygoid process; Bsp, basiphenoid; C, coronoid; D, dentary; Ect, ectopterygoid; F, frontal; J, jugal, M, maxilla; N, nasal; P, parietal; Pal, palatine; PFr, postfrontal; PM, premaxilla; Po, postorbital; Pop, paroccipital process; PrF; prefrontal; Pro, prootic; Ptg, pterygoid; Q, quadrate; Q.Pr., quadrate process of pterygoid; San, surangular; Spm, septomaxilla; Soc, supraoccipital; Sq, squamosal; St, supratemporal; St.Pr., supratemporal process. Scale bars equal to 2mm.

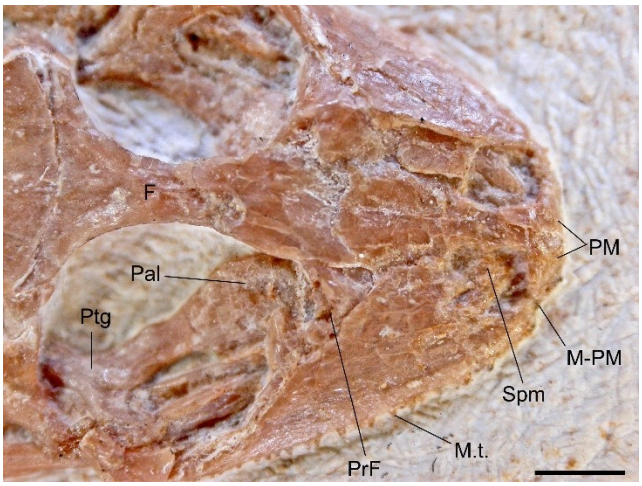

Fig. 3.3. Detail of the antorbital region of the Skull of the holotype of *Eichstaettisaurus schroederi*. Abbreviations: F, frontal; M-PM, contact between maxilla and premaxilla; M.t., maxillary teeth; Pal, palatine; PM, premaxilla; PrF; prefrontal; Ptg, pterygoid; Spm, septomaxilla. Scale bar equal to 2mm.

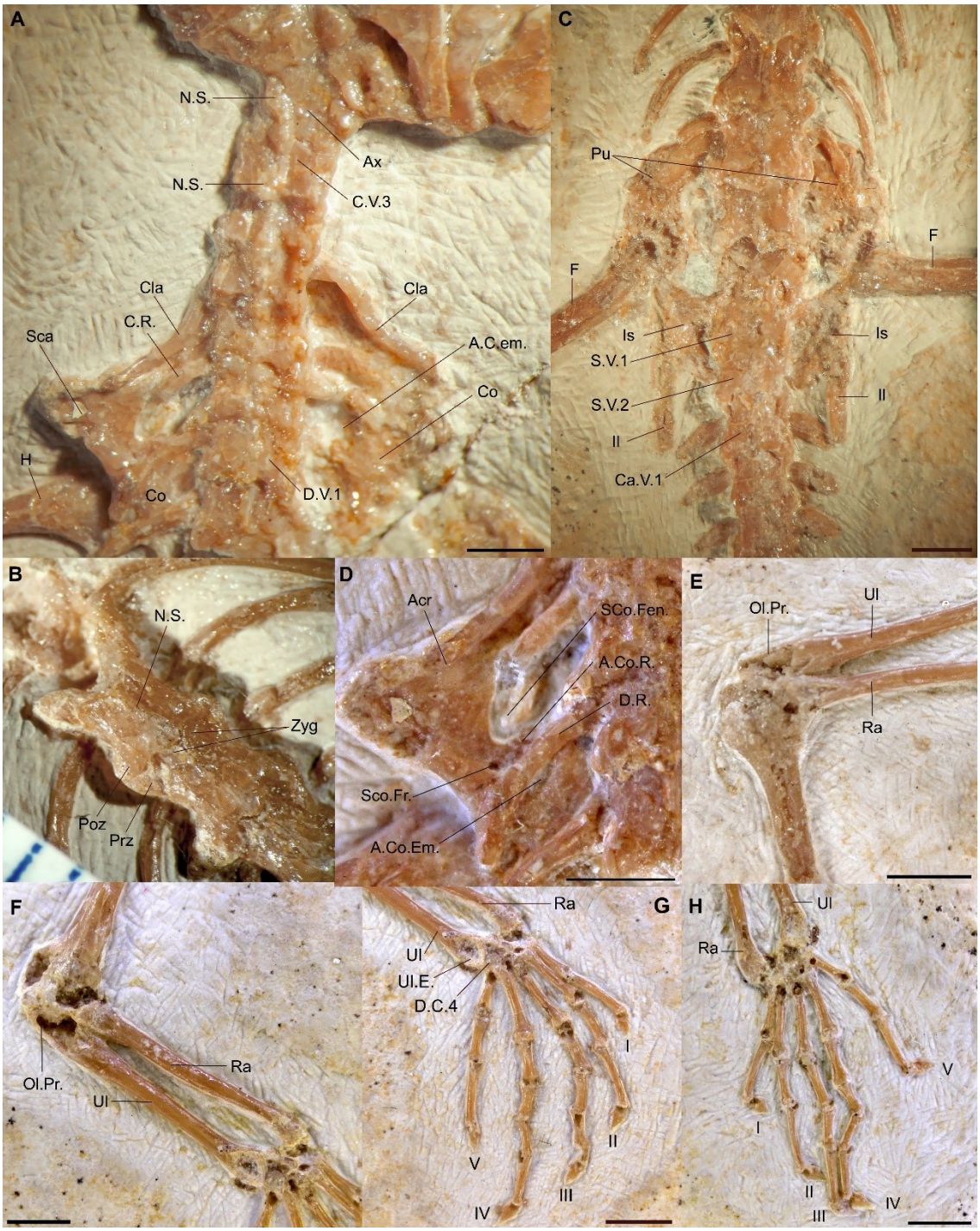

Fig. 3.4. Postcranium of the holotype of *Eichstaettisaurus schroederi*. (A) cervical region and pectoral girdle, (B) detail of dorsal vertebrae, (C) sacrals, anterior caudals and pelvic girdle, (D) detail of pectoral girdle, (E) left forearm, (F) right forearm, (G) right manus, (H) left manus. Abbreviations: A.Co.Em., anterior coracoid emargination; A.Co.R., anterior coracoid ray; Acr, acromion process; Ax, axis, Ca.V., caudal vertebra; Cla, clavicle; Co, coracoid, C.R., cervical rib; C.V. cervical vertebra; D.C. 4, distal carpal 4; D.R., dorsal rib, F, femur; H, humerus;; Il, ilium, Is, isquium; N.S., neural spine; Ol.Pr., olecranon process; Poz, postzygapophysis; Prz, prezygapophysis; Pu, pubis; Sca, scapula; SCo.Fen., scapulocoracoid fenestra; Sco.Fr., supracoracoid foramen; S.V., sacral vertebra; Ra, radius, Ul, ulna; Ul.e., ulnar epiphysis; Zyg, zygosphene; I-V, digit number. Scale bars equal to 2mm (A, C-H) and 1mm (B).

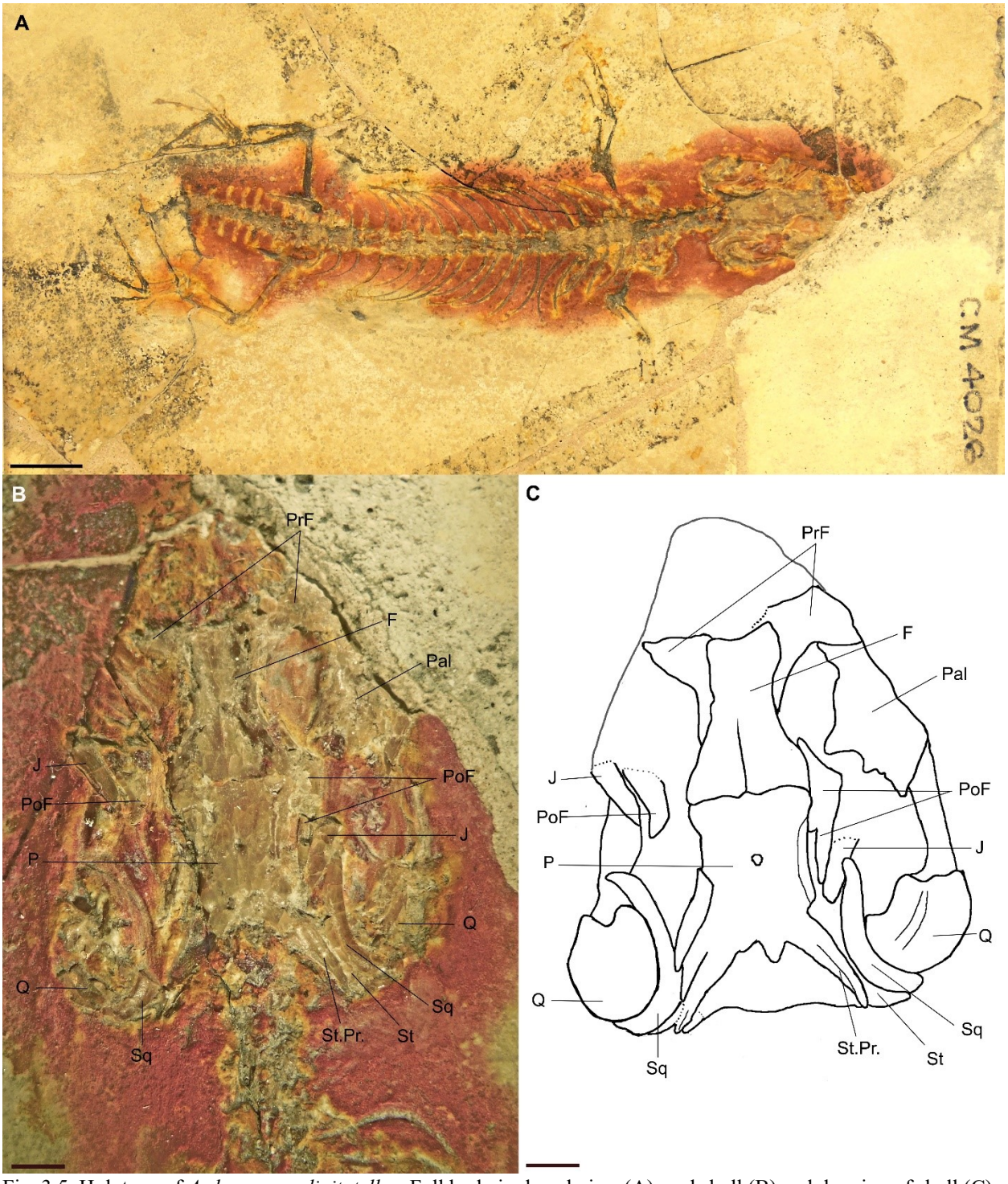

Fig. 3.5. Holotype of *Ardeosaurus digitatellus*. Full body in dorsal view (A), and skull (B) and drawing of skull (C) in dorsal view. Abbreviations: F, frontal; J, jugal, P, parietal; Pal, palatine; PoF, postorbitofrontal; PrF; prefrontal; Q, quadrate; Sq, squamosal; St, supratemporal; St.Pr., supratemporal process. Scale bars equal to 10mm (A) and 2mm (B & C).

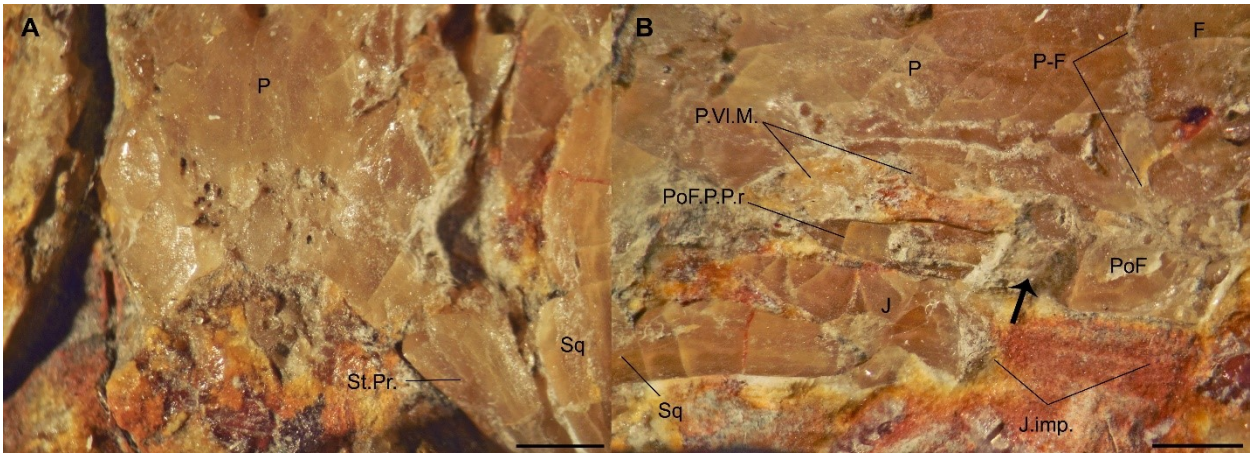

Fig. 3.6. Holotype of *Ardeosaurus digitatellus*, skull details. Parietal (A) and right temporal region (B). Abbreviations: F, frontal; J, jugal; J.imp., impression of jugal bone; P, parietal; P-F, frontoparietal suture; P.Vl.M., parietal ventrolateral margin; PoF, postorbitofrontal; PoF.P.Pr., postorbitofrontal parietal process; Sq, squamosal; St.Pr, supratemporal process. Back arrow indicates point of breakage of the postorbitofrontal. Scale bars equal to 10mm (A) and 2mm (B & C).

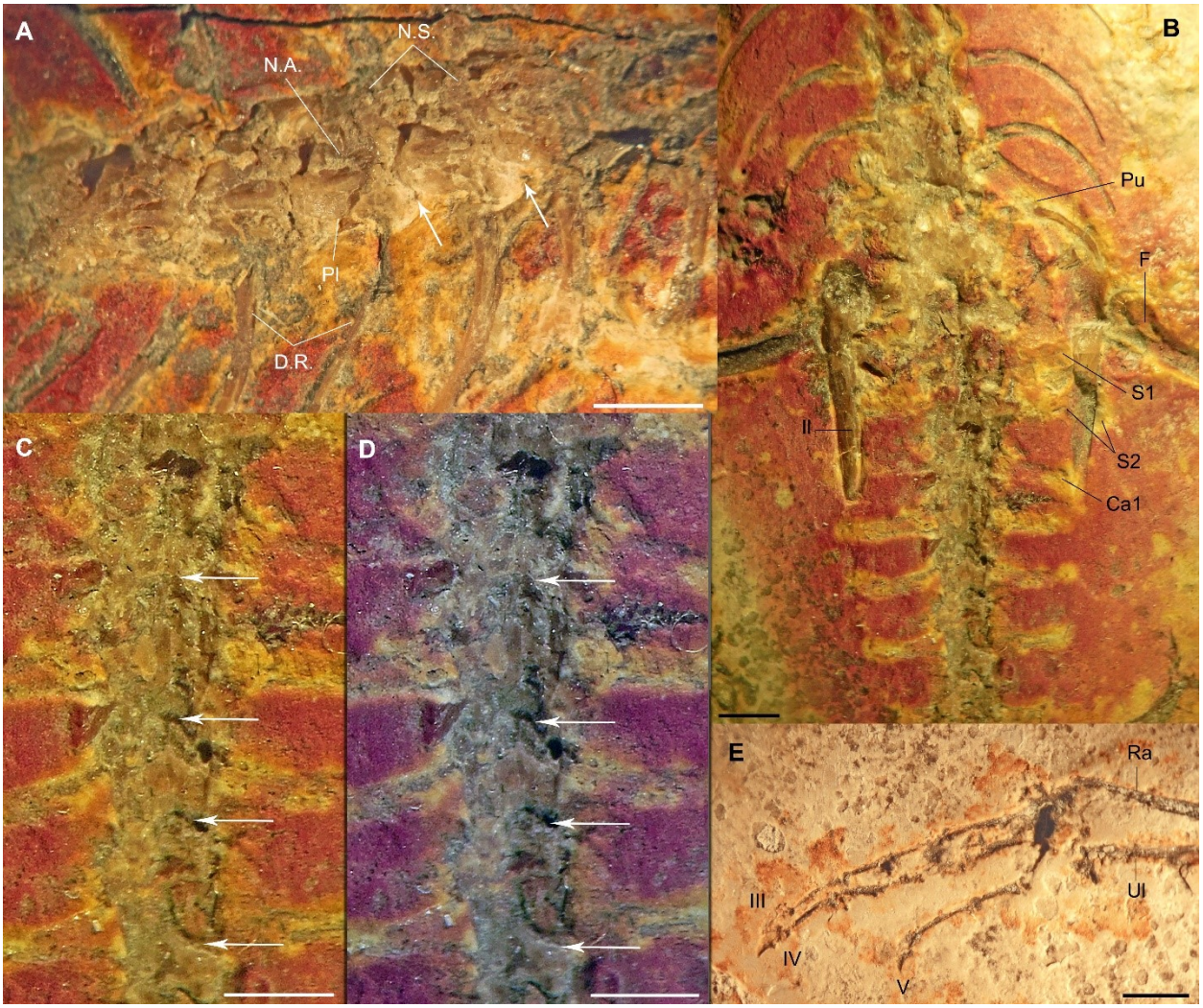

Fig. 3.7. Holotype of *Ardeosaurus digitatellus* postcranium in dorsal view. (A) anterior dorsal vertebrae, (B), posterior dorsals, sacrals, caudals and pelvic girdle, (C & D) detail of anterior caudals, (E) left manus. Abbreviations: Ca, caudal vertebra; D.R., dorsal rib; F, femur; Il, ilium; N.A., neural arch; N.S. neural spine; Pl, pleurocentrum; Pu, pubis; S, sacral rib; Ra, radius; Ul, ulna; III-V, digits;. White arrows indicate the anterior and posterior limits of vertebral pleurocentra. Scale bars equal to 2mm.

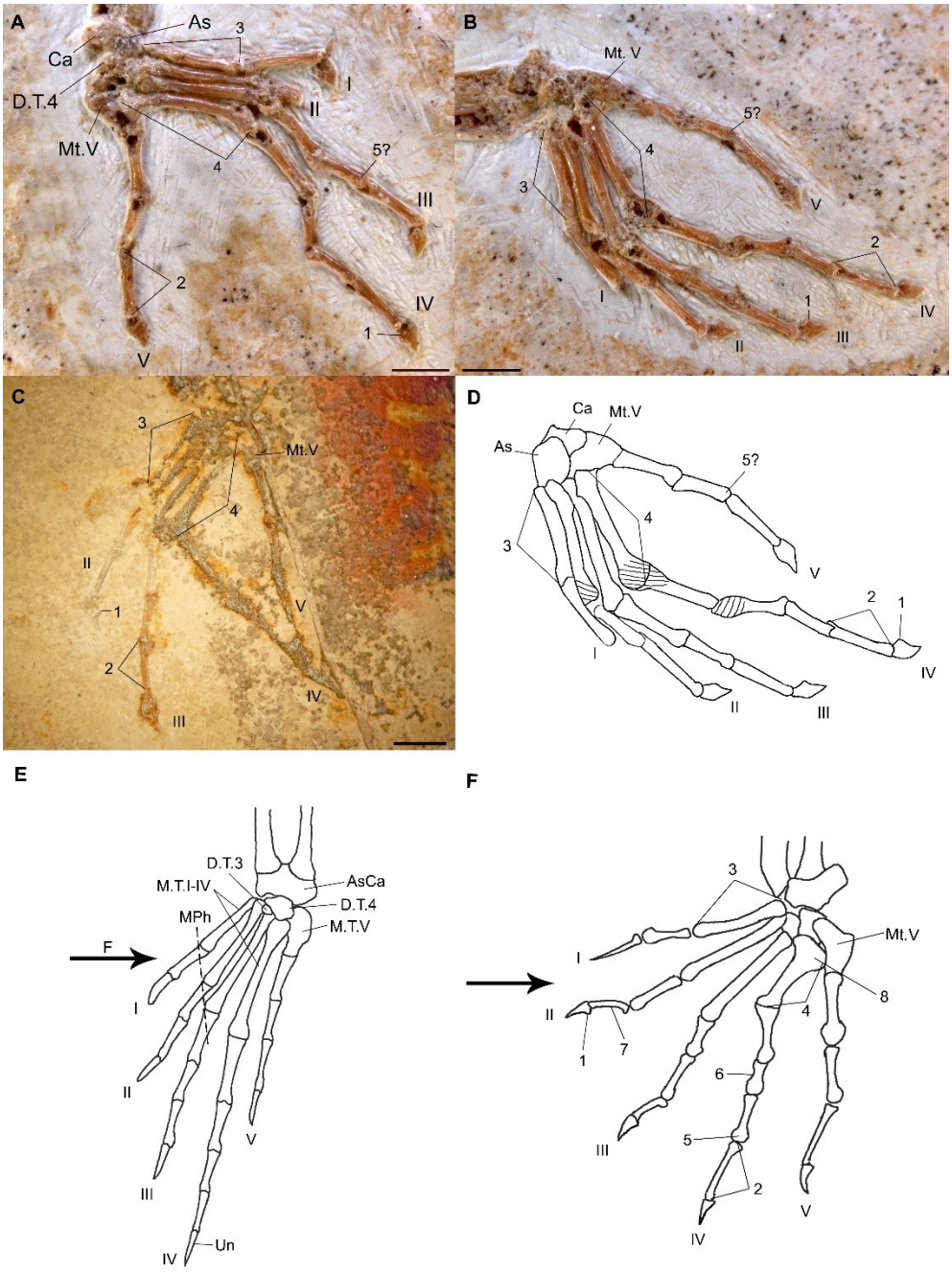

Fig. 3.8. Comparison of pedal morphology across taxa and implications for functional morphology. Right (A) and left (B) pedes of *Eichstaettisaurus schroederi*, (C) left pes of *Ardeosaurus digitatellus*, (D) drawing of left pes of *Eichstaettisaurus schroederi*, (E) left pes of *Iguana iguana*, (F) left pes of *Gekko gecko*. Abbreviations: As, astragalus; AsCa, fused astragalocalcaneum; Ca, calcaneum; D.T.3; third distal tarsal; D.T.4; fourth distal tarsal; MPh, metatarsophalangeal line; Mt. I-IV,first to fourth metatarsals; Mt.V, fifth metatarsal; I-V, digit number. Arabic numerals indicate functional adaptations: 1,unguals tall at their base; 2, elongate penultimate pahalnges; 3, first metatarsal proportionally longer relative to third metatarsal; 4, fourth metatarsal shorter than third metatarsal; 5, convex-concave phalangeal articulations; 6, depressed intermediate phalanges; 7, arcuate penultimate phalanges; 8, expanded head of fourth metatarsal. Black arrow indicates direction of parasagittal plane to the body axis. Scale bars equal to 2mm. Images E and F redrawn after Russell et al. (1997), and also based on TMP 1990.007.0021 and CM 114410.

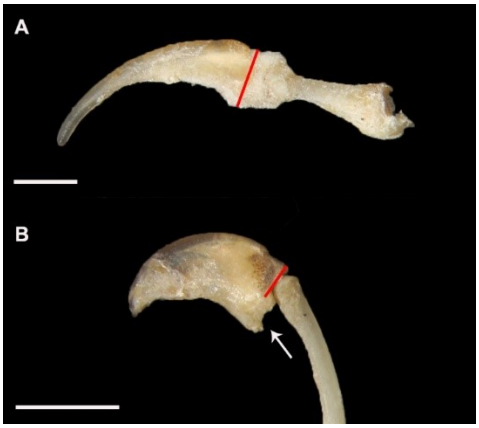

Fig. 3.9. Claw morphology among lizards of different life habits. (A) pedal claw of *Heloderma suspectum* (TMP 1990.07.357), exhibiting a common claw shape among terrestrial non-scansorial lizards—see also Tulli *et al.* (2009). (B) pedal claw of *Gekko gecko* (TMP 1990.007.0021). The white arrow indicates the ventral expansion of the proximal end of the claw, beyond the area of contact with the penultimate phalanx (red line).

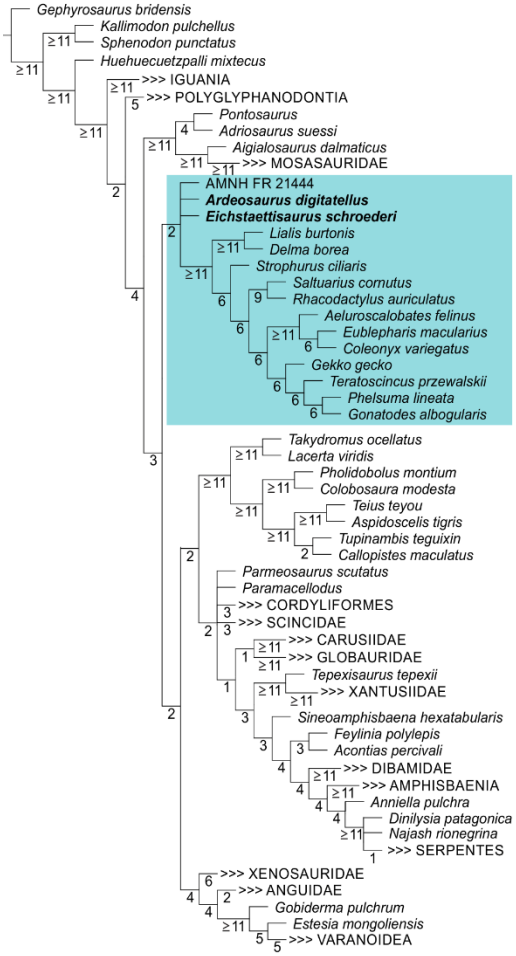

Fig. 3.10. Species level phylogenetic analysis inclusive of *E. schroederi* and *A. digitatellus*. Strict consensus tree of 4,951 steps obtained from 3,174 most parsimonious trees of 4,843 steps each (consistency index = 0.201; retention index = 0.772) after correcting character state scoring for *Eichstaettisaurus schroederi* and including *Ardeosaurus digitatellus* in the dataset. Numbers under branches indicate Bremer support (decay indices). Light blue box delimits the clade composed by crown and stem gekkonomorphs.

Table 3.1. Comparison of diagnostic features across *E. schroederi*, *E. gouldi*, *A. brevipes* and *A. digitatellus*.

	E. schroederi	*E. gouldi*	*A. brevipes*	*A. digitatellus*
1. Parietals paired	X	Y	Y	Y
2. Parietals with strong lateral emargination	X	?	Y	Y
3. Wide parietal posterior margin between supratemporal processes	X	?	X	Y
4. Pairetal supratemporal process with medial fossa	X	?	X	X
5. Pairetals with short supratemporal processes	X	?	Y	Y
6. Fused frontals	X	X	Y	Y
7. Frontals widen anteriorly	X	X	Y	Y
8. Frontoparietal suture slightly bowed anteriorly	X	Z	Y	Y
9. Skull roof ornamentation	X	?	Y	X
10. Cephalic osteoderms	X	?	Y	X
11. Postorbital and postfrontal as separate elements	X	?	X	Y
12. Postorbital with wide posterior process dorsal to the squamosal anterior end	X	?	X	X
13. Lacrimals absent	X	?	X	X
14. Hands and feet penultimate phalanges elongate	X	?	?	X
15. Foot phalangeal formula 2-3-4-5-4	X	?	Y	X
16. Presacral vertebrae number	31	?	23	27
17. Frontal interorbital/frontoparietal width ratio	0.25	0.2	0.46	0.51

The condition seen in *E. schroederi* is marked as "X", and the opposite condition is marked as "Y". For feature number 8, a third condition is added "Z", which is exclusive of *E. gouldi*. Shared features across *Eichstaettisaurus* and *Ardeosaurus* = 3; between *E. schroederi* and *A. brevipes* only = 1; between *E. schroederi* and *A. digitatellus* only = 4; and between *A. brevipes and A. digitatellus* only = 7.

Table 3.2. Individual measurements of manual phalanges in digits II-V for *E. schroederi* and *A. digitatellus* (mm).

	M2I	M2II	M3I	M3II	M3III	M4I	M4II	M4III	M4IV	M5I	M5II
E. schroederi	1.51	2.16	1.31	1.35	1.70	1.43	1.03	1.13	1.60	1.32	2.06
A. digitatellus	?	?	1.58	1.64	1.82	1.40	1.26	1.32	1.90	1.54	2.00

Abbreviations: M1-5, manual digits 1 to 5; I-IV, phalanges I to IV in each corresponding digit. The phalangeal measurements on *E. schroederi* represent the mean values for the right and left manus, whereas on *A. digitatellus* measurements were taken from the left manus only, as the limits between phalanges are mostly non-discernable on the right counterpart.

Table 3.3. Individual measurements of pedal phalanges in digits II-V for *E. schroederi* and *A. digitatellus* (mm).

	P2I	P2II	P3I	P3II	P3III	P4I	P4II	P4III	P4IV	P5I	P5II	P5III
E. schroederi	1.39	2.17	2.59	1.70	2.47	3.17	1.96	1.63	2.46	2.28	1.82	2.38
A. digitatellus	?	2.33	2.79	1.84	2.58	3.01	?	?	?	2.11	1.96	?

Abbreviations: P1-5, pedal digits 1 to 5; I-IV, phalanges I to IV in each corresponding digit. The phalangeal measurements on *E. schroederi* represent the mean values for the right and left pedes (apart from digit II), whereas on *A. digitatellus* measurements were taken from the left pes only, as the limits between phalanges are mostly non-discernable on the right counterpart.

Table 3.4. Ratios between penultimate/immediately preceding phalanx on manus and pedes.

	M2II/2I	M3III/3II	M4IV/4III	M5II/5I	P2II/2I	P3III/3II	P4IV/4III	P5III/5II
E. schroederi	1.430	1.260	1.416	1.561	1.561	1.453	1.509	1.308
A. digitatellus	?	1.110	1.439	1.299	?	1.402	?	?

Abbreviations: M1-5, manual digits 1 to 5; I-IV; P1-5, pedal digits 1 to 5; I-IV, phalanges I to IV in each corresponding digit.

Table 3.5. Comparative measurements between *E. schroederi* and *A. digitatellus* (mm).

	SVL	H+R	F+T	FL	HL	FL/HL	FL/SVL	HL/SVL	MTIII/MTI
E. schroederi	94.4	18.2	21	27.2	34.7	0.784	0.288	0.368	1.41
A. digitatellus	79.4	15.3	18.6	25.4	34.3	0.741	0.319	0.432	1.48

Abbreviations: FL, Forelimb length; F+T, femoro-tibial length; HL, hind limb length; H+R, humero-radial length; MT, metatarsal; SVL, estimated snout-vent length. Absolute values represent means calculated from the right and left sides of the holotype.

Table 3.6. Body and limb lengths and ratios for a selection of extant lizard taxa.

	SVL	FL	HL	FL/ HL	FL/ SVL	HL/ SVL	Habit	Source
Gekko gecko	121.75	44.08	54.22	0.813	0.362	0.445	Scansorial (Arboreal+Saxicolous)	Zaaf & Van Damme (2001)
Tropidurus flaviceps	98.69	46.3	58.8	0.787	0.469	0.596	Scansorial (Arboreal)	Vitt & Zani (1996)
Anolis stratulus	50	20	30.35	0.659	0.4	0.607	Scansorial (Arboreal)	Butler & Losos (2002)
Dinarolacerta mosorensis	64.65	21.5	33.7	0.638	0.333	0.521	Scansorial (saxicolous)	Ljubisavljević *et al.* (2008)
Anolis sagrei	42.95	18.8	32.15	0.585	0.438	0.749	Arboreal/ Ground-dwelling	Butler & Losos (2002)
Podarcis bocagei	55.1	17.2	27.4	0.628	0.312	0.497	Ground-dwelling	Kaliontzopoulou *et al.* (2007)
Cnemidophorus tigris	85	32	62	0.516	0.376	0.729	Ground-dwelling	Irschick & Jayne (1999)
Varanus eremius	157	41.5	58.2	0.713	0.264	0.371	Ground-dwelling	Christian & Garland (1996)
Dipsosaurus dorsalis	87	33	64	0.516	0.379	0.736	Ground-dwelling	Irschick & Jayne (1999)

Abbreviations: FL, Forelimb length; HL, hind limb length; SVL, estimated snout-vent length. Source references indicate studies where measurements were obtained, or calculated from.

Supplementary Information 3.1

Character state scorings for *Eichstaettisaurus schroederi* and *Ardeosaurus digitatellus*

Eichstaettisaurus schroederi

0?0???0?10?0?0??020001???000?0000??101?00???0??20000??01?10??0300000000?0?0001?00
?1?0?00?2??0?0?000?01100000??0??301?0?00000000?00?0?0??1????001?00?2000012?000?01
0010010?0?00001?0?12?0?0?????????000??1??????????????????????????????0????????03????0
??0???????131??0?0?0???001??????????2?2?000???????100000??????????????????????????????
00101??????0?????????0?????0????????????3?????????????01?0???1????000??000???0??00?0
000?4?000??0??0???0?00??????????????????0400001?0?????1020??????0?????????00??01?1?1?
0?10???????000???00??0?000??001??01??0???0?00001?000????01100???00?000???0??0?0000
?0??????????????????????????????

Ardeosaurus digitatellus

??200???01110??21?0?00????0?000?????0??
?01?2??001?000?01100000??????????????????00?00?0????1????0?????????002????0?010010[1
2]00?0?0000??001????0??0????????????????????
??
??
??
??????????????????????????03000?0?0??????0?0??????0????????????????????????????????00
0???????0?00???001??????????0?00001?000???????0????00?000???0??0?0000?0?????????????
???????????????

Autapomorphies recovered for *Eichstaettisaurus schroederi* and *Ardeosaurus digitatellus*

Eichstaettisaurus_schroederi :

Char. 1: 1 --> 0, Char. 9: 0 --> 1, Char. 18: 0 --> 2, Char. 48: 3 --> 2, Char. 57: 1 --> 5, Char. 63: 0 --> 3, Char. 83: 2 --> 1, Char. 95: 1 --> 0, Char. 168: 0 --> 1, Char. 460: 0 --> 1, Char. 497: 0 --> 1, Char. 555: 1 --> 0, Char. 557: 0 --> 1.

Ardeosaurus_digitatellus :

Char. 49: 0 --> 2, Char. 62: 0 --> 2, Char. 63: 0 --> 1, Char. 83: 2 --> 0, Char. 88: 0 --> 1, Char. 154: 1 --> 2, Char. 167: 0 --> 12, Char. 455: 4 --> 3.

CHAPTER FOUR: REACQUISITION OF THE LOWER TEMPORAL BAR IN SEXUALLY DIMORPHIC FOSSIL LIZARDS PROVIDES A RARE CASE OF CONVERGENT EVOLUTION

[The contents of this chapter have been published in Simões, T. R., G. F. Funston, B. Vafaeian, R. L. Nydam, M. R. Doschak and M. W. Caldwell. 2016. Reacquisition of the lower temporal bar in sexually dimorphic fossil lizards provides a rare case of convergent evolution. Scientific Reports 6: 24087.]

Introduction

The repeated independent evolution of similar characteristics (homoplasies) is an extremely important and under-investigated phenomenon (Currie 2012). Homoplasies, such as evolutionary convergences, are often seen as strong evidence for adaptative evolution (Wake 1991; Currie 2013) because similar environmental pressures are expected to elicit similar adaptive morphologies, suggesting that phenotypic homoplasy is often a consequence of natural selection (Wake *et al.* 2011). This is reinforced by the theory of historical contingency (Gould 1989), which suggests that the repeated evolution of very similar structures is rather rare in the history of life.

Possible convergences on the loss, or gain, of temporal fenestration, have been a major issue in the study of reptile evolution in recent years, such as the loss of such fenestration in the evolution of the turtle skull (Rieppel & de Braga 1996; Lyson *et al.* 2010; Bever *et al.* 2015b; Schoch & Sues 2015). The lower temporal bar (LTB) contributes to the formation of a lower temporal fenestra in diapsid reptiles, and is thought to have been absent in the early evolution of lepidosaurs (Wu 2003; Moazen *et al.* 2009a; Evans & Jones 2010), a group that includes *Sphenodon* and squamates, and later reacquired in some rhynchocephalians (*Sphenodon* and its extinct relatives (Whiteside 1986; Fraser 1988; Schaerlaeken *et al.* 2008; Evans & Jones 2010)). Squamates have long been thought to lack a complete LTB, and this feature has been used numerous times as a defining character of the group (Broom 1925; Romer 1956; Carroll 1975; Benton 2005). Recently, this notion was challenged by the discovery of *Tyaniusaurus zhengi*, a borioteiioid lizard from the Late Cretaceous of Asia with a complete bony LTB (Lü *et al.* 2008). Understanding the evolution of temporal fenestration is thus fundamental to understand broad level relationships amongst living and extinct groups of reptiles, as well the phenomenon of evolutionary convergence. In that regard, only a limited number of studies have been dedicated to the evolution (including evolutionary convergence) of the lower temporal bar in lepidosaurian reptiles using modern analytical tools [e.g. (Rieppel & Gronowski 1981; Schaerlaeken *et al.* 2008; Moazen *et al.* 2009a)].

Here I report the discovery of a complete LTB forming an enclosed lower temporal fenestra in another borioteiioid lizard, *Polyglyphanodon sternbergi,* the most complete lizard known to date from the Mesozoic of North America. Even with such a rich osteological record, I noted several

discrepancies between the original description and the morphology as observed by me (including the presence of a complete LTB). These materials include an ontogenetic series, as well as variation in skull shape that can be linked to sexual dimorphism, which provides a rare insight into the paleobiology of an entirely extinct clade of lizards, the borioteiioids. Furthermore, the repeated occurrence of a complete LTB served as the basis for a broader analysis on the evolution of this structure in lepidosaurs, with emphasis on squamate reptiles.

Materials and Methods

Referred specimens

Polyglyphanodon sternbergi: NMNH (National Museum of Natural History – Smithsonian Institute) 15477 (holotype); 15816 (paratype); 15559; 15566; 15567; 15568; 15573; 15817; 15818; 15819; 16367; 16368; 16369; 16374; 16584; 16585; 16586; 16587; 16588; 16724; 427672; 427678; 427682; 427683; 427777 and CM (Carnegie Museum of Natural History) 9188. *Tupinambis teguixin*: FMNH (Field Museum of Natural History) 140193, TMP (Royal Tyrrell Museum) 1990.007.0352; *Iguana iguana* UAMZ (University of Alberta Museum of Zoology) uncatalogued frozen specimen; CM 38489; CM 114409; 92303; CM 125934; *Agama agama* (Midwestern University uncatalogued).

Measurements

Skull height (SH), straight line in lateral aspect from contact of prefrontal with frontal dorsally, to dentigerous border of maxilla ventrally; skull width (SW), distance between lateral border of both postorbitals as seen in dorsal aspect; skull length 1 (SL1), anterior tip of premaxilla to posterior border of parietal table; skull length 2 (SL2), anterior tip of premaxilla to occipital condyle; parietal width (PW), straight line between parietal suture with postfrontals in dorsal aspect; parietal body length (PBL), midline of fronto-parietal suture to midline of posterior border of parietal in dorsal aspect.

Different measurements (e.g. SL1 and SL2) were taken in order to have a larger amount of comparable data across specimens that have differential degrees of preservation (e.g. the

occipital condyle region is not preserved in NMNH 15477, so only SL1 allows some measure of skull length for that specimen). When the skull suffered some deformation, but one of the sides still had the elements in articulation, only that side was measured (e.g. only the left side in 16588 for SW), and the obtained value was doubled in order to estimate the value for the opposite side. Because the lower jaws were usually disarticulated from the skull, and occasionally laterally displaced, head height (including the lower jaws) was not measured, but skull height was used instead (see above).

Phylogenetic analysis

I investigated the phylogenetic position of *Polyglyphanodon sternbergi* using an existing matrix (Conrad 2008), plus the addition of other borioteiioids from east Asia. These include *Aprisaurus, Tuberocephalosaurus,* an unnamed taxon from Jiangxi (Jiangxi_2), and published scorings for *Tianyusaurus* (Mo *et al.* 2010). Other character scorings were corrected for some other borioteiioid taxa (*Erdenetesaurus*, *Adamisaurus*, *Cherminsaurus*, *Gobinatus*, *Darchansaurus*, *Gilmoreteius* and *Chamops*) in the present matrix, but not to the same extent as performed for *P. sternbergi* (scorings available in Supplementary Information Online). Also, one character state was rescored for Jiangxi_2 (character 96) and two were rescored for *Aprisaurus* (characters 30 and 96 were scored A and B, which I considered to be typeset errors and scored "?" for both).

These changes resulted in matrix of 229 taxa and 363 characters that was run using the software T.N.T., with *"*Rhynchocephalia*"* designated as the outgroup. The new interpretation for the morphology of *P. sternbergi* along with data that was not originally scored (Conrad 2008) resulted in 83 characters out of the 363 in total that were modified by us, representing a change in 27% of all the osteological characters of *P. sternbergi* (and 22% overall) in this matrix. In all the analyses performed, searches were initially run using the 'New Technology Search' options followed by a "Traditional Search" following the protocol in (Simões *et al.* 2015a).

Model choice

Despite the existence of relatively complete skulls of *P. sternbergi*, their distortion and lack of a fully intact skull makes the usage of a modern analogue a better structural candidate for a

biomechanical assessment. I used the skull of *Iguana iguana* as a proxy because it has skull dimensions for adults that are very similar to adults of *P. sternbergi*, both in width/length proportions, as well as absolute length. Furthermore, *Iguana iguana* has a naturally non-streptostylic quadrate, which is also the case for *P. sternbergi*. I utilized the skeletally mature skull of an adult *I. iguana* (UAMZ uncatalogued, obtained from the pet trade), with SL1 = 70.79mm; SW = 41.69mm. The specimen was kept frozen since its death, which reduces the chances of having bone articulations being modified, such as being drawn closer together, due to dehydration or physical removal of soft tissue during dry skeleton preparations.

Ex vivo Micro-Computed Tomography

The skeletally mature skull of an adult *Iguana iguana* was secured in the gantry bed of a Skyscan 1076 micro-Computed Tomograph (Bruker-Skyscan, Kontich, BE). The sample was scanned in entirety at 35 μm pixel size, using 6 overlapping unit sub-scan scan lengths, with tube voltage at 100 kV, and a current of 100 μA. Low energy X-rays were removed using a 0.5 mm aluminum filter, and three scan projections were averaged per step, through 180° of rotation at 0.7° step increments with 474 ms exposure time. Using a modified Feldkamp back-projection algorithm, the raw image data were reconstructed at a cross-sectional threshold of 0.0-0.04 using NRecon reconstruction software (version 1.4.4, Skyscan NV, Belgium).

Mesh creation and properties

Reconstructed micro-CT scan data were imported in bitmap format into Mimics x64 and thresholded to produce a surface mesh. The surface mesh was cleaned and repaired in Mimics x64 and Geomagic Studio 12. The cleaned mesh was modified in Geomagic Studio 12 to produce two hypothetical models: one with a complete lower temporal bar, and one with an incomplete lower temporal bar attached by a ligament to the quadrate. The ligaments in all models were represented by sets of tension-only springs with a total stiffness of 50N/mm (Moazen *et al.* 2009a). Number of finite elements (tetrahedral solid): 1,427,173 (models A and B); 1,443,351 (model C); and 1,466,414 (model D). Bone was modeled as an isotropic material, with Young's modulus = 10Gpa, and Poisson's ratio = 0.4 (Reilly & Burstein 1975; Rayfield *et al.* 2001; Kupczik *et al.* 2007). Biting force was applied at an angle of 90º to the tooth row, as

would be expected in *P. sternbergi* given the precise tooth interdigitating observed in that species.

Muscle forces

Muscle forces for FEA analyses which aim to test stress levels on rigid bodies are dependent on a series of distinct variables, such as each muscles' physiological cross-section, fiber length and gape angle (van Ruijven & Weijs 1990; Moazen *et al.* 2008b), which cannot be precisely estimated from fossil species. Therefore, a range of force input values was used to test for possible variations, especially due to head dimensions. Data from published values for the extant lizard species *Uromastyx hardwickii* were used (Moazen *et al.* 2009a), and scaled to the skull length of *Iguana iguana* , which is equivalent to *P. sternbergi* (Table 4.1). *Uromastyx hardwickii*, is a herbivore that displays hard-biting, which is the anatomical/ecological model to be tested (Moazen *et al.* 2009a). Force values are expected to scale to the square of linear measurements of the body (slope = 2.0) if both grow isometrically to each other (Erickson *et al.* 2003). However, data collected by Herrel (2007) indicates positive allometry for muscle forces against skull length among different species of lizards: for herbivorous adult males, bite force vs. head length (measured equally to my SL1 values for *I. iguana* and *P. sternbergi*) slope = 2.7489. I therefore used the latter slope to calculate the scaled forces. The same forces were then scaled again for subsequent analyses (2x and 4x the initial scaled values) to observe if variations in muscle force values would affect the result of stress level.

Application of FEA

Origins of twenty four adductor muscles were mapped on the meshed geometry of all models (using Geomagic Studio 12), and finite element nodes corresponding to each muscle origin were marked using published data on the myology of *Iguana iguana* (Haas 1973; Throckmorton 1976) and from my own dissections. The load of each muscle was then evenly distributed over the nodes corresponding to each muscle origin. This provided a more precise application of muscle loads and stress distribution on areas of attachment than previous applications that used only single or a few nodes for the application of muscle loading conditions (Moazen *et al.* 2008a; Moazen *et al.* 2009a), which created an excessive concentration of stress around those nodes.

Bite forces were applied—one per side—on nodes posteriorly on the tooth row (fifth tooth from posteriormost tooth). This is the position where *P. sternbergi* and *Iguana iguana* have specialized teeth for cropping, and where bite forces are greater along the tooth row (Moazen *et al.* 2008a). Because forces were scaled from a previous study (Moazen *et al.* 2009a) , rather than derived *de novo* in an MDA, equilibrating joint forces from the same studies were inapplicable. Therefore, to ensure equilibrium in the system, the mandibular condyles of the quadrate were fixed, to approximate the near-frictionless joint with the mandible and account for resulting joint forces. Forces, directions, and node selection were controlled between all models. Each of the three skull models—unmodified, complete lower temporal bar, and incomplete temporal bar—was tested identically using the same muscular origins and insertions. Preparation of the FE models, i.e meshing and applying boundary conditions and forces, were performed using Hypermesh v13.0. Linear static finite element analyses were then performed on each model using ABAQUS v6.1.12.

Results

Morphology, ontogeny and sexual dimorphism

From the examination of almost 30 specimens of *Polyglyphanodon sternbergi*, including almost complete skeletons, I obtained new information on the morphology of that species, especially regarding the skull (Fig. 4. 1a-f). Individuals of different size classes present variation that is concentrated on the shape of the frontoparietal suture and the length of the posteroventral process of the jugal (Fig. 4.1g-i). Great variation in the shape of the frontoparietal suture has been reported during the post-embryonic ontogeny of extant lizards (Barahona & Barbadillo 1998; Bell *et al.* 2003) and variation on the length of the jugal process has also been reported during the ontogeny of fossil sphenodontian reptiles (Fraser 1982; Whiteside 1986; Fraser 1988) (see also Table 4.1 and Supplementary Information 4.1). To my knowledge, neither have ever been detected before in fossil lizards. Furthermore, specimens of similar sizes present variations in skull shape. Overall, some individuals possess relatively taller skulls (morphotype A—Fig. 4.1 j) while others have more depressed skulls (morphotype B—Fig. 4.1k). Such variation happens across individuals of all size classes (Table 4.1) and thus cannot be related to ontogeny. Sexual

dimorphism in lizards commonly affects body proportions, with male lizards tending to have proportionally bigger heads—either taller, longer, or wider, or a combination of these (Vitt 1982; Herrel *et al.* 1999; Kaliontzopoulou *et al.* 2007)—for male-male combat or holding females during copulation (see also Supplementary Information 4.1). Therefore, the variation in relative skull height between both morphotypes is suggestive of sexual dimorphism, with morphotype A (proportionally taller skulls) being more likely to represent the male morphotype. All *Polyglyphanodon* individuals come from the same mudstone horizon, in what is considered as the flood basin of a fluvial system (RN, personal observation), being totally or partially articulated. This is indicative that they represent a local population that was caught in a flood, or another similarly catastrophic event, and thus finding individuals of different age and sex classes should be expected.

In all specimens, the jugal bone (when preserved) was usually broken posteriorly. One exception was the paratype (NMNH 15816), which has a complete posteroventral process of the jugal extending posteriorly to the quadrate, forming a complete LTB (Fig. 4.1). In a second specimen (NMNH 16588), despite the posteriormost tip of the jugal being broken, the preserved portion also extended to the level of the quadrate articulation with the mandibles. In both *P. sternbergi* and *T. zhengi*, the LTB differs from the condition observed in other reptiles. Whereas in archosaur reptiles (e.g. crocodilians, dinosaurs and pterosaurs) and *Sphenodon*, the LTB is formed by the jugal and also the quadratojugal, the LTB in the two fossil lizard species is formed exclusively by the jugal, as the quadratojugal is absent in all squamates known so far. Furthermore, juvenile skulls of *P. sternbergi* with a complete jugal have the LTB shorter than in adults and not reaching the quadrate, differing from archosaurs and *Sphenodon*, but similar to the condition reported for other rhynchocephalians: *Clevosaurus* and *Planocephalosaurus* (Fraser 1982; Fraser 1988).

Despite the similarities noted above, the structure of the LTB in *P. sternbergi* differs from the one in *T. zhengi*, as in the latter the bar is firmly sutured to the quadrate, whereas in *P. sternbergi*, there is no discernable articulatory facet on the quadrate. Additionally, on the ventrolateral face of the quadrate tympanic crest there is a rugose surface similar to the one on the cephalic condyle, at the level with the posteroventral process of the jugal (Fig. 4.6). This suggests there was a soft tissue connection between the jugal and the quadrate, likely formed by a reduced quadratojugal ligament, which also connects the jugal to the quadrate in some extant

lizard species, such as *Corucia zebrata* (Herrel *et al.* 1998a). In a large number of lizards and snakes, however, this temporal ligament does not contact the quadrate, but rather the mandible (Herrel *et al.* 1998a; Palci & Caldwell 2013), and it is termed a jugomandibular ligament; in such cases there are no rugose surfaces on the quadrate anteroventral margin. I exclude the possibility of this being an attachment site for the *Musculus adductor mandibulae externus superficialis* (MAMES—Fig. 4.2) because of the similarity in texture between this surface and the one on the cephalic condyle, as well as the absence of such rugosity on the tympanic crest of observed specimens of *Tupinambis teguixin*, a taxon in which the MAMES is extremely well developed.

Another peculiar feature is that the LTB in *P. sternbergi* is straight, rather than bowed laterally (the latter being the condition in *Sphenodon*), indicating that the posterior portion of the MAMES (MAMESP) was relatively modest with respect to its' maximum width (cross-sectional area), unlike the condition usually observed in squamates (Oelrich 1956; Haas 1973; Rieppel & Gronowski 1981) (Fig. 4.2c and Fig. 4.7). However, the ventrally located adductor crest in the lower jaw of *P. sternbergi* indicates that the MAMES extended some distance ventrally on the lateral side of the lower jaw. This ventral expansion is greater than the one seen in *Iguana iguana*, for instance, and would more closely resembles the ventral expansion observed in *Tupinambis* (Rieppel & Gronowski 1981).

Phylogeny

After a revision of the scorings for *P. sternbergi* in a data matrix inclusive of all major clades of squamates, which also contained *T. zhengi* and other borioteiioids (Mo *et al.* 2010), more than a quarter (27%) of the osteological characters for *P. sternbergi* were altered or scored for the first time (see Methods). The results obtained indicate *T. zhengi* groups with other Chinese borioteiioids (clade A—Fig. 4.3), whereas *P. sternbergi* belongs to a separate clade (clade B—Fig. 4.3), indicating the lower temporal bar evolved convergently in *P. sternbergi* and *T. zhengi*. As a consequence, the lower temporal bar not only redeveloped amongst squamates, as recently demonstrated by the discovery of *Tianyusaurus*, but it actually happened twice within the same group of squamates—the Borioteiioidea.

The evolution of the LTB as a functional adaptation

Squamates have a posterior portion—or 1b layer (Haas 1973)—of the MAMES (or MAMESP) that is differentiated from the anterior portion of the same muscle, becoming wider and more expanded ventrally and posteriorly on the lateral side of the lower jaw (Oelrich 1956; Haas 1973; Rieppel & Gronowski 1981) than the MAMES in other reptiles in which the LTB is present (Rieppel & Gronowski 1981). In some instances, however (e.g. *Iguana iguana*) that portion is wider and expanded posteriorly, but it does not extend far ventrally in comparison to the MAMES of *Sphenodon* (Jones & Lappin 2009). The configuration of the squamate skull provides this muscle with a more efficient adductor function than the *M. pterygoideus typicus* (MPTT—Fig. 4.2) and *atypicus* (MPTAT—absent in squamates) of other reptiles, and thus, the loss of the LTB has been considered a selective advantage for allowing more room for an expanded MAMES and a more efficient mandible adductor system (Rieppel & Gronowski 1981). Measurements of the cross-sectional area of the MAMES in *Sphenodon*, along with *in vivo* bite forces, have confirmed *Sphendon* has a smaller adductor muscle mass and bite forces than similar sized agamid lizards (Schaerlaeken *et al.* 2008). These changes provided squamates with a relatively greater bite force in comparison to other reptiles, to the point that a lizard scaled up to the size of a *Tyrannosaurus rex* would be capable of biting ten times harder than *T. rex* (Herrel *et al.* 2012).

The loss of the lower temporal bar may lead to functional disadvantages, however. In crocodilians, for instance, this bar promotes stabilization of the quadrate bone, without which, would tend to rotate anteriorly due to the resultant force of action of the temporal muscles. The same has been described for *Sphenodon* (Wu 2003; Schaerlaeken *et al.* 2008). This would cause interference of the quadrate upon the proper functioning of the temporal muscles just anterior to it (including the MAMES). Lizards and other squamates do not face this problem because of differences in the skeletomuscular configuration of the temporal region, creating a resultant force of the temporal musculature that is directed posterodorsally during jaw closure, and not anterodorsally. For this reason, the quadrate in squamates usually tends to rotate posteriorly (Herrel *et al.* 1998a). Therefore, a jugomandibular ligament (or quadratojugal ligament in some species, such as *Corucia* (Herrel *et al.* 1998a) and *Agama*—Fig. 4.2d) provides stabilization of the quadrate as tension is applied to this ligament. Furthermore, the elastic nature of the ligament allows for a large sized posteroventral portion of the MAMES. In this way, squamates were able

to maintain a stable quadrate while also increasing the size of the temporal musculature (Rieppel & Gronowski 1981; Herrel *et al.* 1998a; Herrel *et al.* 1998b).

This indicates that the reacquisition of the lower temporal bar could be a consequence of either one of the following factors: I) a change in orientation of the temporal bones and muscles creating resultant forces at the quadrato-mandibular joint during biting that would tend to rotate the quadrate anteriorly, similar to archosaurs and thus interfering with proper adductor musculature functioning (Herrel *et al.* 1998a). In this situation, a ligament would not be enough to stabilize the quadrate, as it can only work properly for such a function when the force of action tends to strain the ligament, applying tension to it (Herrel *et al.* 1998a; Moazen *et al.* 2009a); II) the stabilization of the quadrate by the suspensorium (dorsally) and pterygoids (ventrally), such as observed in rhynchocephalians and archosaurs, may provide only limited distribution of stress and/or compressive-tensional forces during hard biting for some species. In some instances, the re-development of a complete LTB could reduce stress and/or strain in the skull (Jones & Lappin 2009; Moazen *et al.* 2009a).

Reacquisition of the LTB in lepidosaurian reptiles—rejected hypotheses

Some of the first hypotheses for the re-development of the LTB in lepidosaurs tried to suggest it as a bracing mechanism to maintain a stable quadrate for precise shearing action (Whiteside 1986; Fraser 1988; Wu 2003). However, in rhynchocephalians (e.g. *Diphyodontosaurus* and *Planocephalosaurus*) in which the quadrate is fixed, the latter is stable enough and able to maintain precise shearing even in earlier ontogenetic stages that lack a complete LTB. The same applies to squamates with precise shearing actions despite lacking a complete LTB, such as *Iguana iguana* (Throckmorton 1976). Even in forms with a mobile quadrate (e.g. *Uromastyx acanthinurus*) precise shearing takes place (Throckmorton 1976; Herrel & Vree 1999).

It has also been suggested that the role of the LTB was to stabilize the quadrate in order to develop translational movements of the jaw observed during proal shearing in *Sphenodon* (Schaerlaeken *et al.* 2008). This suggestion has been discarded in previous studies based on similar comparisons to fossil rhynchocephalians. For instance, *Gephyrosaurus* and *Priosphenodon* display morphological features indicative of translational movement of the jaw,

despite the lack a complete LTB in those species (Jones & Lappin 2009). Therefore, I reject such hypotheses as likely functional explanations for the re-acquisition of the LTB (see more in Supplementary Information 4.1).

Rejection of functional explanations in *P. sternbergi*

Polyglyphanodon sternbergi has an anteriorly arched frontoparietal suture in dorsal aspect that would be likely to prevent mesokinesis in adults (Fig. 4.1 and Fig. 4.8). It also has an enlarged articulation surface between the parietal and the supraoccipital, which would prevent metakinesis—Fig. 4.1, and also illustrated by Gauthier *et al.* (2012). The increased contact between the quadrate, the squamosal and the jugal anterodorsally, as well as the pterygoids ventromedially (Fig. 4.1 and Fig. 4.9), also prevented streptostyly. Therefore, osteological information indicates *P. sternbergi* likely lacked any form of detectable cranial kinesis. The lack of streptostyly prevented quadrate rotation, and thus it could not have rotated anteriorly and interfere with the proper functioning of the MAMES. Furthermore, if the configuration of the temporal skeletomuscular system in *P. stermbergi* was similar to that of most lizards, its quadrate would usually tend to rotate posteriorly (Herrel *et al.* 1998a).

Therefore, the only remaining and plausible hypothesis left to test, is the reduction of mechanical stress during forceful biting, as previously proposed for *T. zhengi* and other reptiles with a fixed quadrate (Moazen *et al.* 2009a). To empirically test whether or not the complete LTB in *P. sternbergi* is an adaptation for reduction of mechanical stress, I tested the biomechanical significance of a complete LTB in a lizard skull. A previous study had been performed to test this issue (Moazen *et al.* 2009a), but in that case the LTB was always inferred to be sutured to the quadrate. In my analysis I included a model with a complete LTB connected to the quadrate by soft tissues (as seen in *P. sternbergi*)—a model that has never been investigated so far for squamate skulls.

Biomechanics

I performed a FEA on a skull of *Iguana iguana* which was used as a proxy to evaluate the stress on the skull of *Polyglyphanodon sternbergi* (see Methods). I tested hard-biting in the *Iguana* skull using 3D muscle attachment maps based on my own dissection (Fig. 4.4) for four

distinct models: (A) the unmodified skull, as obtained from the micro-CT-scan geometry, with a tension-only spring between the jugal and quadrate representing a quadratojugal ligament; (B) the unmodified skull, but with two force vectors applied to the jugal bone and directed towards the lower jaw, representing a jugomandibular ligament. These two different ligament models were tested as both conditions are observed in lizards (Herrel *et al.* 1998a) (see above); (C): the *Iguana* skull recreated with the addition of a complete LTB that was sutured to the quadrate, as previously performed for a similar analysis (Moazen *et al.* 2009a); and (D), the *Iguana* skull with a complete LTB, but connected to the quadrate by a tension only spring (representing a ligament connection), which replicates the condition inferred for *P. sternbergi*. These models were tested for a range of muscle bite forces (see Table 4.2 and 4.3), providing a total of 12 different analyses (see Supplementary Information 4.1s on further considerations and limitations of the analysis).

In all models, variations in the magnitude of bite forces did not change the pattern of distribution of stress or strain in the skull. The resultant joint reaction forces acting on the quadrato-mandibular joint were found in the FEA to be always directed posterodorsally (Fig. 4.10 and Table 4.4), and the ligaments to be under tension, which is in agreement with previous studies (Herrel *et al.* 1998a; Herrel *et al.* 1998b; Moazen *et al.* 2009a).

Among the four models, model B was the best suited for forceful biting. Different regions of the skull showed reduced stress compared with the other models (Fig. 4.5 and 4.11-4.12), apart from a minor increased stress in the nasal process of the maxilla. Model A had comparable areas of the skull with increased stress, such as: the ventral margin of the orbit, parts of the upper temporal bar, the ventral side of the basisphenoid, and especially on the posterior crest of the quadrate, as well as the quadrate process of the pterygoid. The pressure maps also indicate greater compression in the upper temporal and postorbital bars, and greater compression and tension in the pterygoids for model A when compared to B. Von Mises stress values were particularly higher on the quadrate, and especially on the pterygoid (43.2% higher—Table 4.5). My results thus suggest that the jugomandibular ligament represents a derived condition in squamates, emerging in forms with robust akinetic skulls, built for strenuous biting, as previously hypothesized (Herrel *et al.* 1998a).

In the two hypothetical models, which possess different kinds of LTBs (C and D), both models show results that are more similar to model A. Model C has greater stress compared to B,

and similar patterns of compression and tension, in similar regions as model A. Despite the addition of the fused LTB creating a point of increased stress upon it posteriorly, the stress in the quadrate posterior crest and pterygoid close to the junction with the quadrate (regions under highest stress in model A), was reduced—21% less than model A in the pterygoid (although still 28% higher than model B). Therefore, model C (a lizard with a fused lower temporal bar, analogous to *T. zheng*) has reduction of stress compared to a model with a quadratojugal ligament, but still with more areas of increased and higher stress values than model B. Although the patterns of stress distribution by the addition of a LTB were generally the same as the ones using a *Uromastyx* model (Moazen *et al.* 2009a), in the latter a fused LTB performed better for forceful biting than a model with jugomandibular ligaments. It remains to be assessed if these differences relate to the shape of the model under use, the difference in the application and distribution of load values, or another unknown variable. However, if other borioteiioids (including *T. zhengi*) also had the temporal ligaments connecting to the quadrate (my model A, and as inferred for *P. stermbergi*), than the development of a fused LTB in *T. zhengi* could indeed represent a functional advantage, as previously suggested (Moazen *et al.* 2009a).

Model D (replicating the LTB as seen in *P. sternbergi*), has increased stress and strain values relative to model B, in the same areas as models A and C. Differently from C, however, model D does not have any areas of significant reduction of stress in comparison to model A. In fact, there is a slight increase in stress in the skull roof. In the main areas under stress, Von Mises values on the quadrate are 351 Mpa (8.547% higher than model B, and ca. 3% higher than model A). In the pterygoid, there was a slight decrease of stress, but values are still similar to model A (273 Mpa, or 40.659% higher than model B, and ca. 3% less than model A). Generally speaking, model D is very similar in terms of patterns of stress and strain to model A, and with no significant overall difference in stress values in the areas of highest stress. Therefore, model D is not better suited to forceful biting than the two patterns without a LTB.

Discussion

Once it is acknowledged that the redevelopment of the LTB does not have a clear selective advantage (as discussed above) for *Polyglyphanodon sternbergi*, then a less functionalist

explanation should be considered (Gould & Lewontin 1979; Gould 2002). It seems further unlikely that the complete LTB would have developed in this species due to a selective functional advantage that would be restricted only to very old individuals, being absent in juveniles and possibly sub-adults. This would account for one of the examples discussed by Gould & Lewontin (1979) regarding non-adaptive morphological structures: excessive variability (e.g. length and connectivity of the LTB throughout ontogeny in *P. sternbergi*) compared with much reduced variability (e.g. a complete LTB since the hatchling stage in *Sphenodon*) when the same general structure assumes a form judged functional on engineering grounds (reduction of stress during forceful biting, or proal shearing, in *Sphenodon*). Therefore, at least in *Polyglyphanodon*, the complete LTB fails explicit tests of adaptationist causes for its reacquisition and unlikely explanations must arise in order to maintain the functionalist point of view.

Some factors need to be considered in order to evaluate the possible causes for the re-development of the LTB in *P. sternbergi*. First, despite the much reduced oral food processing in some leaf cropping lizards (including *Iguana* and, most likely in *P. sternbergi*—see Supplementary Information 4.1), published data from multiple species indicate that most herbivores (and also omnivores), including species with a variety of food processing strategies, consistently have relatively higher bite force when compared to insectivores (Herrel *et al.* 1998a; Metzger & Herrel 2005; Herrel 2007). Therefore, the presence of a complete LTB in *P. sternbergi*, which implies a reduced cross-section area of the MAMESP compared to most squamates (Rieppel & Gronowski 1981; Herrel *et al.* 1998a) (also observed in the extant *Sphenodon* (Schaerlaeken *et al.* 2008)), seems inconsistent with a dietary habit that usually requires higher bite forces.

One possible explanation for this apparent paradox could reside in the large size of species like *Iguana* and *Polyglyphanodon*. After a certain critical size, some lizards may have a proportionally smaller adductor musculature due to an absolute increase in body and muscle size, which would already provide enough bite force sufficient to break food items without further investment in energetically expensive muscle tissues (Herrel *et al.* 2014). This idea has been tested for *Uromastyx* (Herrel *et al.* 2014), and such a correlation was not detected. However, the authors tested for only two species of *Uromastyx*, both of which attain adult sizes much smaller than adult *Iguana* or *Polyglyphanodon* (close to 50% of the skull length of the specimens I

studied). It is thus possible that, after a certain size, there is a proportionally smaller increase of the adductor musculature at least in some clades. More sampling of *in vivo* bite forces from adults of larger-sized lizards may further elucidate this problem.

Secondly, another interesting factor in *P. sternbergi* is the extremely developed medial process of the ectopterygoid that, along with the transverse flange of the pterygoid, extends ventrally for quite some distance (as also seen in other borioteiioids, such as *Gilmoreteius, Adamisaurus* and *Erdenetesaurus*, but uncommon to most lizards (Mo *et al.* 2010)—and TRS and RN pers. obs.). These structures may have acted as a medial bracing element for the coronoid dorsal process of the mandibles, guiding the jaws for a precise shearing/cropping. The ventral expansion of the ectopterygoids/pterygoid might also have provided a larger area of attachment for the pterygoidal adductor muscle masses (represented by the MPTT in squamates), which would have contributed towards greater adductor power compared to lizards with a reduced MPTT.

Therefore, reduction of relative adductor size, due to a big absolute size of *P. sternbergi*, along with a likely increase in the size of the MPTT, may have enabled sufficient reduction in size of the MAMESP in *P. sternbergi* that allowed the re-development of the LTB without interfering with the insertion of the MAMESP on the lateral side of the lower jaw (as indicated by the position of the adductor crest). Even if other factors currently unknown to me may also have played a role in producing a relatively smaller MAMESP in *P. sternbergi*, reduction in the relative width of that muscle mass was certainly critical for the re-development of the LTB in *P. sternbergi*, and possibly also in *T. zhengi.* Reduction in size (width, insertion area, or both) of the MAMES was thus a likely factor in removing a physical constraint against the complete LTB and allowing its re-development.

In squamates, the positive directional selection for an expanded and laterally inserting posterior portion of the MAMES, which provides greater adductor power (Rieppel & Gronowski 1981) (see above), seems to have created a structural constraint against the development of a complete LTB. In all known squamates, the LTB is virtually non-existent, being always absent or limited to a short and blunt posteroventral process of the jugal, never reaching the degree of development observed within borioteiioids *T. zhengi* and *P. sternbergi*. The observed phenotypic stasis in this feature, despite numerous variations in the surrounding environmental conditions

and dietary habits amongst the numerous squamate families, indicates a case of morphological canalization (Waddington 1942).

All the factors presented above indicate why the reacquisition of a complete LTB within squamates is such a rare event, further illustrating the unexpectedness of observing independent reacquisitions of this trait within borioteiioids lizards. Evolutionary homoplasies (convergences, parallelisms and reversals) are usually expected to represent similar structural morphologies, functions, or behaviours, as a consequence of different species living under similar conditions (Hall & Hallgrimson 2008), thus being strong evidence of adaptative evolution (Wake 1991; Currie 2013). Examples include similar feeding habits (Friedman 2012) or body shape in aquatic vertebrates (Motani 2005). In other cases, convergent evolution may occur due to similar constraints, rather than adaptations, such as the ones driven by structural or phylogenetic constraints—e.g. similar sequences of digit loss in salamanders (Wake *et al.* 2011). However, the convergent evolution of a complete LTB in squamates as represented by *Polyglyphanodon* and *Tyaniusaurus*, is an unexpected example of neither. Their similar morphologies are not convergent solutions to the same pressures, as the LTB in *P. sternbergi* is not adapted for reducing mechanical stress during hard biting, as it might be the case for *T. zhengi*. In fact, the empirical evidence indicates the complete LTB in *P. sternbergi* is not a functional adaptation at all but might be the result of a release of constraint induced by a reduction in width of part of the adductor musculature. Therefore, while the re-acquisition of the LTB in *T. zhengi* would represent the result of adaptative evolution (Moazen *et al.* 2009a), in *P. sternbergi* it seems to be the result of constraint release, thus making a case of "mixed" convergence. This opposes most reported cases of homoplastic evolution, which are driven by either similar functionalist or similar structuralist causes in distinct lineages—e.g. (Losos *et al.* 1998; Motani 2005; Friedman 2012).

The question remains on how borioteiioids were able to break the constraint observed in squamates against a complete LTB, and what factors may have driven it more than once. It is not possible to assess whether the homoplasy of this particular feature is the result of reoccurring genetic mutation in either species (Chan *et al.* 2010), or the unmasking ("de-canalization") of hidden cryptic genetic variation (Colosimo *et al.* 2005), as borioteiioids form an entirely extinct clade of lizards. However, the fact that amongst all living and fossil squamates—extant forms alone representing over 9,000 species (Uetz & Hošek 2016)—the only two taxa in which a

complete LTB is known to have developed belong to the same, relatively small clade (in terms of species richness), may favour the latter hypothesis of "de-canalization". *Polyglyphanodon* and *Tyaniusaurus* indicate that the genetic and developmental framework necessary for the production of a complete LTB was present in geographically and phylogenetically distinct sub-groups of borioteiioids, and the same potentiality does not occur in other clades of squamates. If reoccurring mutations were enough to redevelop a complete LTB when favourable conditions occurred (i.e., in other hard biting lizards, such as *Uromastyx*), then it would be expected to find that variety in other clades as well. Taxa that are more closely related to each other have more similar genetic and developmental backgrounds due to phylogenetic constraints, and thus should have a more similar range of phenotypic responses to variations in surrounding conditions as compared to more distantly related species. Therefore, I conclude that their convergent evolution may actually reflect a genetic/developmental predisposition, allowing for the re-development of a complete LTB. That predisposition seems to have been reacquired at some point in the early evolution of borioteiioid lizards but does not seem to have developed (or reacquired) in other squamate clades.

Supplementary Information 4.1

Supplementary information that is relevant to this chapter and provided as supplementary information to its published version are provided below. However, because of its size, the updates on the data matrix obtained from other authors that was used for the phylogenetic analysis performed herein, are referred to here as **supplementary information online,** available at: https://www.nature.com/articles/srep24087#supplementary-information

Sexual dimorphism

In the observed specimens of *Polyglyphanodon sternbergi* there are two different skull morphotypes: one represented by proportionally taller skulls (Fig. 4.1b,j), and the other by proportionally more depressed skulls (Fig. 4.1i,k), when height is compared against skull length. The snout-vent length is commonly used as an independent variable to determine whether these differences among morphotypes are due to changes in relative height or another dimension of the skulls (width or length). However, considering there are few and mostly disarticulated postcranial materials associated with the skulls, it is difficult to determine the snout-vent length in most of the available specimens. Yet, specimens NMNH 16588 and NMNH 15816 have skulls of fairly similar length and width, but specimen NMNH 16588 is taller than NMNH 15816 (see Table 4.1), indicating these morphotypes differ mostly in relative height. Skull height vs. length ratios for specimens NMNH 16588 and 15477 indicate they are more similar in relative skull height to each other (morphotype A) than to the more depressed skull condition observed in NMNH 15816 and CM 9188 (morphotype B). Despite NMNH 16587 not being directly comparable to NMNH 16588 and NMNH 15477 using the measured data, the SH/SL2 ratio indicates this specimen also has a much taller skull in relation to NMNH 15816 and CM 9188, thus belonging to morphotype A. Somewhat larger skulls are also observed in morphotype A in relation to morphotype B, but not to the same extent as the difference in height. Furthermore, CM 9188 has a slightly longer skull profile in relation to NMNH 15816, but the former is a juvenile and it probably attained a somewhat proportionally shorter skull with age, as indicated by the SW/SL2 and SH/SL2 ratios.

Sexual dimorphism in lizards commonly affects body proportions. For instance, females tend to have longer interlimb lengths, which is usually associated with providing greater fertility (more space for a bigger clutch)(Olsson *et al.* 2002; Ljubisavljević *et al.* 2008). Males, on the other hand, usually have bigger heads due to male-male combat for territory, male-female interaction during mating, or different food niche partitioning between males and females (Vitt 1982; Carothers 1984; Herrel *et al.* 1999; Kratochvíl & Frynta 2002; Olsson *et al.* 2002; Schwarzkopf 2005).

Changes in relative size of the head in male lizards may also be followed by changes in shape, such as when variations in head length, width, and height dimensions are allometric. For instance, males of *Gallotia galloti* have greater relative increase in the length of their skulls, creating greater gape size and a proportional increase in the length (and power) of the MPTT used for male-male combat (Herrel *et al.* 1999). Males may also have relatively wider skulls, as in *Gymnophtalmus multicustatus* (Vitt 1982) and both wider and longer in *Cnemidophorus ocellifer* (Vitt 1983). Taller skulls occur in males of different species of *Podarcis* (Kaliontzopoulou *et al.* 2007) and *Dinarolacerta* (Ljubisavljević *et al.* 2008). Relatively taller skulls are advantageous for male herbivorous lizards that engage on male-male combat or that use the jaws to hold females during copulation. Food niche partitioning between both sexes could also be a possibility, but this is usually restricted to insectivorous lizards (Carothers 1984). Following this reasoning, it is suggested that morphotype A, with taller and, to a lesser degree, wider skulls, might represent males of *P. sternbergi*, whereas morphotype B represents females. It is plausible that, as in extant lizards from different families, males suffered natural or sexual selection for a taller and wider skull due to dispute for females, or territories.

Ontogeny

The ontogenetic status of the studied specimens is based on both the relative size among the many available materials (see Table 4.1), and ontogenetic markers for post-embryonic development of extant squamates. The latter markers include: full ossification of mesopodial elements; fusion of elements of the pelvic girdle; fusion of neurocentral sutures; a great degree of ossification of dermal skull bones; and great development of the parietal supratemporal processes, which are small during early ontogenetic stages (Rieppel 1994c; Barahona &

Barbadillo 1998; Maisano 2002; Evans 2008). Most importantly, the fusion of humeral and femoral proximal epiphyses (as seen in the holotype and the paratype, NMNH 15477 and NMNH 15816, for instance) indicate that NMNH 15477 and NMNH 15816 had reached skeletal maturity, which in many extant squamates occurs only very late during ontogeny, and after sexual maturity in many instances (Maisano 2002).

There are important morphological differences between adult-sized specimens of *P. sternbergi* and smaller (and younger) ones (see Table 4.1). Younger specimens, have a straighter frontoparietal suture (Fig. 4.8), whereas this suture is anteriorly curved in larger individuals (Fig. 4.6b) of both morphotypes. The only apparent exception to this pattern seems to occur between specimens CM 9188 and NMNH 16368, as specimen CM 9188 already has a clearly curved suture, despite being slightly smaller than NMNH 16368. However, both belong to different morphotypes, indicating that the exact timing of change in the shape of the suture could be different between sexes. Another ontogenetic change occurs in the parietal, which becomes relatively larger anteriorly in both skull morphotypes in later ontogenetic stages. This change is better expressed in morphotype A than B, following the trend of larger skull sizes in morphotype A. In extant lizards, such as *Iguana iguana* (Fig. 4.8c) drastic ontogenetic changes can be seen in the shape of the parietal, including variation on the shape of the frontoparietal suture, as previously described in the lacertid *Gallotia galloti* (Barahona & Barbadillo 1998), and to a smaller extent in the gymnophthalmid *Neusticurus ecpleopus* (Bell *et al.* 2003).

Another feature that changes during the ontogeny of *Polyglyphanodon sternbergi* is the relative length of the posteroventral process of the jugal. This process is relatively shorter in juveniles in which it is unbroken (NMNH 16586, NMNH 427672) and does not reach the level of the quadrate (Fig. 4.1g,h). In the two adults in which the posteroventral process of the jugal is relatively complete (NMNH 16588 and NMNH 15816), it reaches the level of the quadrate, forming a complete lower temporal bar (Fig. 4.1i).

Ontogenetic variation in the formation of the lower temporal bar (LTB) is not exclusive for *P. sternbergi* among lepidosaurs possessing a LTB. Although hatchling *Sphenodon* already possess a complete LTB, fossil rhynchocephalians that usually possessed an incomplete lower temporal bar in early ontogenetic stages, such as *Planocephalosaurus* (Fraser 1982), *Clevosaurus* (Fraser 1988)—and possibly, *Diphyodontosaurus*(Whiteside 1986)—have a complete lower temporal bar in older individuals. *Polyglyphanodon sternbergi* lacks replacement teeth, at least in the adult

stage. However, it has a series of posterior teeth that increase in size posteriorly. This indicates that teeth were added posteriorly and increased in size following the increasing size of the jaws throughout ontogeny, as observed in the posterior teeth of agamid lizards and additional teeth of rhynchocephalians (Edmund 1960; 1969; Cooper *et al.* 1970; Cooper & Poole 1973; Robinson 1976; Fraser 1988).

Dietary habit in Polyglyphanodon sternbergi

There is a diversity of feeding habits among herbivorous lizards. For instance, *Corucia zebrata* processes most of the consumed plant material in its mouth, engaging in a significant number of intraoral bites (Herrel & Vree 1999). Conversely, *Uromastyx* processes tough leaves by reducing them into small pieces, but has a low number of intraoral bites (Herrel & Vree 1999). Finally, *Iguana iguana,* mostly crops leaves, with very little food processing in the mouth, swallowing most of the plant contents whole (Throckmorton 1976; Nydam & Cifelli 2005). *Polyglyphanodon sternbergi*, has been proposed to be herbivorous on the basis of its highly specialized cropping dentition(Nydam & Cifelli 2005) and large body size, the latter being correlated with herbivory in many lizards (Metzger & Herrel 2005; Herrel 2007). The apices of the teeth of *P. sternbergi* bear multiple denticles that are similar to those of iguanine lizards, which are adapted for feeding on plant material, especially shearing/cropping leaves (Nydam & Cifelli 2005). The lack of wear facets in the teeth of *P. sternbergi*, even in the absence of tooth replacement, suggests that there was a limited degree of food processing in the mouth before swallowing.

Detailed discussion on rejected hypotheses for the reacquisition of the LTB in lepidosaurian reptiles

One of the earliest theories for the reacquisition of the lower temporal bar in lepidosaurs suggested that the LTB is an important feature for precise shearing action. According to Whiteside (1986) and Fraser (1988), during jaw opening the action of the *M. depressor mandibulae* upon a quadrate that is fixed both dorsally (to the squamosal) and medioventrally (to the pterygoids), but not laterally, would create torque upon the quadrate, twisting it posteriorly. This would interfere with the precise shearing that was important for the feeding mechanism of

some early rhynchocephalians, such as *Diphydontosaurus*. Wu (2003) suggested that the jugomandibular ligament was already present amongst these early rhynchocephalians, and therefore it would have prevented the posterior twisting proposed by Whiteside (1986). According to Wu (2003), the bar would be a functional advantage as a lateral bracing mechanism to prevent anterior twisting of the quadrate during jaw closing. The resultant force of the temporal muscles in these taxa is directed anterodorsally and therefore would tend to twist the quadrate in that direction (Wu 2003).

Nevertheless, this proposed lateral bracing of the quadrate is unnecessary for the proper functioning of a precise shearing system in lepidosaurs. The quadrate in rhynchocephalians has an extensive immobile contact both dorsally (with the suspensorium) and ventrally (with the pterygoid), which hold the quadrate in place against the action of the joint reaction forces acting upon it during biting. Early rhynchocephalians, such as *Gephtrosaurus, Diphyodontosaurus* and *Planocephalosaurus*, which had a fixed quadrate as just described, but also possessed a precise shearing mechanism despite the lack a complete LTB (at least during most of their life) (Evans 1980; Fraser 1982; Whiteside 1986), indicate that a lateral bracing system was not necessary to maintain the proper functioning of the shearing mechanism. If any twisting of the quadrate took place in these taxa, that would have caused damage to the large articulation surface the quadrate has with the squamosal and the quadrate process of the pterygoid. This same inference can be applied to the opisthodontian rhynchocephalian *Priosphenodon* (Apesteguia & Novas 2003; Apesteguia & Carballido 2014), which has a precise shearing mechanism and also lacks a complete LTB. Even in the extant *Iguana iguana*, in which the contact between the quadrate and the other skull elements is far less extensive than in rhynchocephalians, it suffices to prevent any rotation or twisting (Throckmorton 1976), therefore not affecting the precise shearing action of the teeth in this taxon. In some cases, such as in *Iguana iguana* and many borioteiioids, the ventrally expanded pterygoid flanges/ectopterygoids butting against the coronoid bone in the lower jaws must have aided in avoiding lateral displacement of the jaws, thus further contributing to precise shearing(Mo *et al.* 2010). The latter system was proposed to operate in *Tianyusaurus*, and also applies to *Polyglyphanodon sternbergi*, which has similar ventral expansions of the pterygoid flange and ectopterygoids. Juveniles of *P. sternbegi* already present a perfect tooth interlocking system despite having an incomplete LTB, indicating the LTB was

not necessary for such mechanism to operate, and being more likely to depend on the fixation of the quadrate, as well as the ventral expansion of the pterygoids and ectopterygoids.

Previous suggestions that the role of the LTB was to develop the translational movements of the jaw, observed during pro-oral shearing in *Sphenodon*(Schaerlaeken *et al.* 2008), have also been discarded on similar bases. Fossil sphenodontians that display morphological features indicative of translational movement of the jaw (e.g. *Gephyrosaurus* and *Priosphenodon*) lack a complete LTB, rejecting that as an explanation for its re-development in *Sphenodon*(Jones & Lappin 2009). Even if that was a valid explanation for species with pro-oral shearing, the morphology of the glenoid fossa in *P. sternbergi* (compressed antero-posteriorly), along with its interdigitating teeth, indicate *P. sternbergi* did not possess pro-oral shearing.

Despite contributing to the maintenance of precise shearing, the fixation of the quadrate by the suspensorium (dorsally) and pterygoids (ventrally) may not provide enough distribution of stress and/or compressive-tensional forces during hard biting for some species, as previously suggested(Jones & Lappin 2009; Moazen *et al.* 2009a). This is likely to be a valid functional explanation for the re-development of the LTB, and I further discussed that in the main text.

Finally, it has also been previously suggested(Mo *et al.* 2010) that a cropping action involving a backward movement of the head would also induce the development of a lower temporal bar. According to this idea, the movement of the head would create a strong anteriorly directed food resistance force, which would tend to move the quadrate anteriorly. However, *Varanus komodoensis* uses backward movements of the head to rip off chunks of meat from its prey, even though a lower temporal bar is not present and the quadrate is fully streptostylic. This indicates there seems to exist no functional need for the presence of this bar due to backward movements of the head as utilized by squamate reptiles.

Consideration for other possible sequences of evolution

Another suggested sequence of evolution (as proposed by one of my reviewers) towards the condition observed in *Polyglyphanodon sternbergi*, would be the acquisition of a complete LTB before the acquisition of a fixed quadrate (a model with a complete LTB, but with streptostylyc, or movable, quadrate) in an ancestor of *P. sternbergi*. However, a complete LTB would naturally impose a natural restriction on the capacity of the quadrate to swing anteroposteriorly or mediolaterally (streptostyly). Therefore, the quadrate in such a condition would not be

streptostylic by definition. Even in cases in which the LTB would be connected by soft tissues to the quadrate (and the quadrate was also connected to the suspensorium by a movable articulation), it is expected this connection would still restrict the quadrate movement. This restriction in movement can be seen, for instance, in the connection between the quadrate and the pterygoid in lizards with a streptostylyc quadrates. In such cases, the quadrate has a soft tissue contact with the pterygoid, and this connection is strong enough to avoid an independent displacement between the quadrate and the pterygoids. Thus, in typical streptostyly, both elements are displaced together (Frazzetta 1962; Iordansky 1990). In an extreme case, known as hyperstreptostyly, the quadrate does move independently from the pterygoid in some acrodontan taxa such as *Chamaeleo (Iordansky 1990)*. However, that is caused by an even further degree of reduction of contact and connection between both elements. The quadrate in *Chamaeleo* does not have a pterygoid lappet for articulation with the pterygoid and has no rugose surface which could represent a region of soft tissue contact with the pterygoid (TRS pers. obs.). Therefore, it becomes clear that, for an independent movement of the quadrate in the presence of a complete LTB, the quadrate connection to the LTB would have to be by means of a relatively loose connection between both elements, which is unknown in any living or fossil reptile (in *P. sternbergi*, it is clear that this soft tissue connection was extensive by the very rugose surface on the tympanic crest of the quadrate, as illustrated above and in the main text). This would be further hampered by the fact that the quadrate would be connected to the LTB and the pterygoid simultaneously.

Even if the complete LTB of *P. sternbergi* represents a condition acquired previously in the phylogenetic history of North American borioteiioids, the first species to develop that condition would have to have an unrealistic set of conditions to allow a complete LTB to develop in conjunction with a quadrate that was still capable of swinging relative to the dermatocranium. First, the complete LTB would have to have developed before the strong contact of the quadrate to the pterygoid medially and the suspensorium dorsally, as seen in *P sternbergi*. Secondly, the quadrate would need to have a loose soft tissue connection to both the pterygoid and the complete LTB. Thirdly, this connection would have to be so loose as to compensate for the double contact of the quadrate (medially to the pterygoid and laterally to the LTB), and thus allow the quadrate to swing freely between the pterygoid and the LTB. Such a condition is unknown in the entire evolutionary history of reptiles. That may explain why all reptiles with a

complete LTB, also have a non-movable quadrate (including rhynchocephalians, crocodyles, stem archosauriforms, and stem diapsids such as *Petrolacosaurus*).

Considering the relatively enlarged contact between the quadrate and the pterygoid, as well as between the quadrate and the suspensorium, among Mongolian borioteiioids (e.g. *Gilmoreteius* and *Darchansaurus*, TRS pers.obs.), the concept of phylogenetic bracket would suggest that the condition in the lineage leading to *P. sternbergi* already had a quadrate with little or no streptostyly.

Therefore, I consider my model tested herein (a complete LTB with a fixed quadrate) a reasonable test not only for the actually known condition and evidence at hand (observed in *Polyglyphanodon*), but also as the most likely sequence of evolution leading to *Polyglyphanodon*.

FEA—additional notes and limitations

Bite forces

Bite, joint and muscle force input values are the most difficult aspects to estimate in FEAs designed to study the functional morphology of fossil taxa, such as *P. sternbergi*. Such difficulty arises due to a number of factors including the inability to observe the muscles directly (see Methods). Furthermore, multi-body computer model predictions of maximum bite force in lizards and in *Sphenodon* usually underestimate the real maximum bite force (Curtis *et al.* 2010). This is confounded by sexual variation in bite force: males may have bite forces up to four times to that of females, as in *Sauromalus* (Lappin *et al*. 2006).

In order to address these issues, I used a range of values produced by scaling published values for the herbivorous lizards *Uromastyx hardwickii*(Moazen *et al.* 2009b) (see Methods) to the skull length of the models used in the FEA. Published bite force values for *U. hardwickii* seem to be lower than *in vivo* bite force values for similar sized specimens of another species of *Uromastyx* (Herrel *et al.* 2014). Therefore, additional values were used, 2x and 4x the initial scaled values, to observe whether they would affect my results.

Previously published *in vivo* bite force measurements indicate that adult male herbivorous lizards have stronger bite than insectivores, but do not differ significantly from omnivores (Herrel 2007). Unfortunately, there are no published bite force values for adult male herbivorous lizards similar in size to *P. sternbergi* or *I. iguana* to provide estimates of bite force. Despite this,

multiplying the scaled muscle forces for *P. sternbergi* by a factor of 4 seems to represent the best approximation of bite forces for an adult male of this species, as they are higher than the values obtained for males of the herbivorous lizard *Corucia zebrata* (SL = 50mm; bite force posteriorly on tooth row = 206N)(Herrel 2007), and similar to adult females of *Tupinambis merianae* (SL = 88m; bite force posteriorly on tooth row = 314N)(Gröning *et al.* 2013). Given the observed trend in other lizards species (see main text), it is reasonable to expect that males of *T. merianae* would have higher bite forces. I therefore, regard these estimates (SL = 70mm; bite force posteriorly on tooth row = 319N)—intermediate for bite force measurements between adult males *C. zebrata* and *T. merianae*—as reasonable. Values for females of *P. sternbergi*, especially given my interpretation of sexual dimorphism for *P. sternbergi*, would be thus lower than the value estimate above based on adult males, and should be within the range of my lower scaling factors (direct scaling and 2x scaling factor).

However, the four models studied here displayed the same patterns of stress and strain distribution for each of the three different load scaling values, indicating that any discrepancy between my bite force estimates and real values for *P. sternbergi* would not influence my results.

Soft tissues

Limitations of the CT scans meant that soft tissue sutures were not included in the model. However, other analyses show that they are expected to dampen strain values (Kupczik *et al.* 2007; Rayfield 2007). Their exclusion, therefore, results in an overestimation of strain in each bone, which is more illustrative of the changes between the models. Additionally, overall stress is likely to be greater in my model because all muscles are activated simultaneously, as occurs in most FEA studies, thus representing peak strain values during biting. The biting point was placed posteriorly on the tooth row, where the specialized cropping teeth of *P. sternbergi* are located, which provides maximum biting force (Moazen *et al.* 2008a). Finally, for a given bite force, herbivorous lizards have lower joint reaction forces when compared to omnivores and insectivores (Herrel *et al.* 1998b), and also have lighter skulls than carnivores (both with and without the influence of evolutionary history being considered), despite usually having higher bite forces (Metzger & Herrel 2005). All these indicate that bite force and overall stress conditions in my model are maximized, thus being a reasonable test to assess how stress

conditions peak during hard biting could affect the skull of *P. sternbergi*, and how the presence of a complete LTB could affect skull mechanics.

For further comments on general limitations concerning FEA in biological organisms, I refer the reader to reviews on the subject (Richmond *et al.* 2005; Rayfield 2007).

Biting mode

I tested my models using bilateral rather than unilateral biting, a model previously used by other authors (Moazen *et al.* 2009a), for a number of reasons. Despite lizards usually using one side of the jaw to process food, adductors on both sides of the skull must be activated. Applying muscle adductor forces to one side only would imply that the animal is biting with considerable force on one side, while muscles on the opposite are inert, or entirely "relaxed". This would be big a deviation of any reasonable biological assumption and modeling. Although there might exist some degree of imbalance among those forces, caused, among other factors, by asymmetries in the skull and muscle strength between both sides, testing using forces on both sides is certainly much closer to a realistic bite than applying to one side only. Assessing potential asymmetries on both sides due to skull shape was accounted by me by the usage of CT scans from a frozen extant lizard. Asymmetries in muscle load might provide even further accuracy to the model. I are unaware of current implementations of this model, however.

It is further important to consider that, depending on the size of the food particle, and the activity exerted during biting, the reaction force may actually occur on both sides. If the animal is grasping a branch or another larger plant material and pulling it, the material will be large enough to actually affect both sides of the jaws. The same applies for male-male biting for intraspecific competition, (which might actually be a likely possibility for *P. sternbergi* considering the sexual variation I observed). In fact, the information available from *P. sternbergi* suggests it did not process most of its food in its mouth, rather swallowing leaves right after cropping (see above in the subheading "Dietary habit in *Polyglyphanodon sternbergi*"). Therefore, a large proportion of the food reaction forces in the mouth was being produced by grasping branches, leaves, or other activities, such as intraspecific fighting among males (see my Sexual Dimorphism section, above). This indicates that, despite not affecting most of my stress/strain results, a bilateral bite is a meaningful replication of life situations that could be expected for *Polyglyphanodon sternbergi*.

Finally, as mentioned above, I aim to test the most stressful possible conditions to the skull, and check if the addition of a complete LTB would be functional in any way to reduce stress or strain. Applying the effects of a reaction force on both sides of the jaws replicates a more stressful condition to the skull rather than unilateral biting (as it doubles the food reaction force upon the skull), which may happen in a number of realistic situations for a lizard (see above). While I believe that some distortional effects to the skull may increase strain during unilateral biting, it is unknown how much the soft tissues could compensate for that. Having FE models that enable the testing of every soft tissue connection in the skull is a possible further development in methodology that may help in the assessment of this particular issue.

Figures and Tables

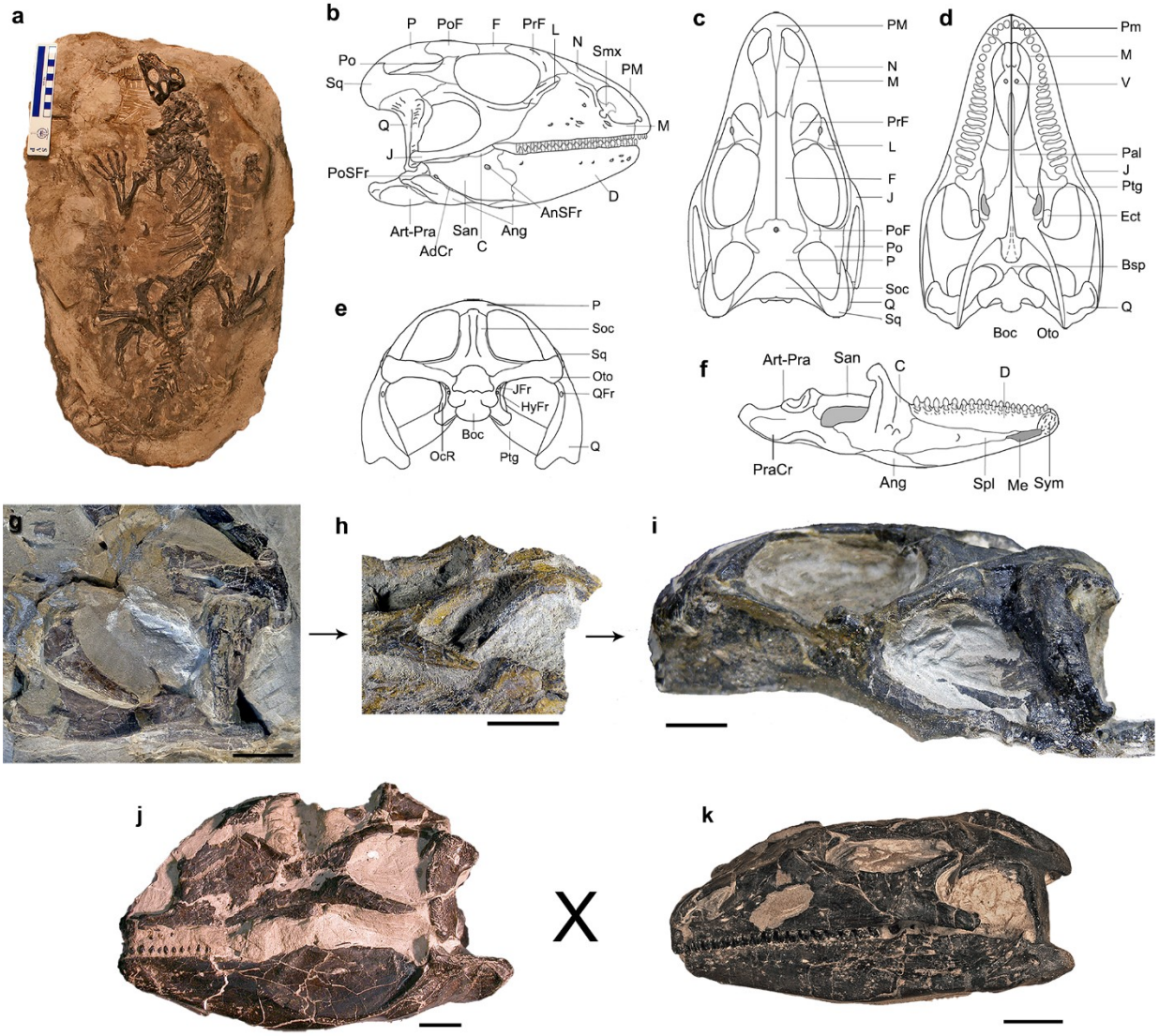

Figure 4.1. *Polyglyphanodon sternbergi*, from the Late Cretaceous of Utah (USA). (A) CM 9188 in dorsal view (image credits to Amy Henrici); (B-F), anatomy of the skull, reconstructed from all the specimens used in this study (image credits to Arthur Brum); (G-I), ontogeny of the temporal region, illustrating the relative increase in length of the LTB in *P. sternbergi*, from juvenile (G, NMNH 427672 and H, NMNH 16586) to adult (I, NMNH 15816); (J) NMNH 16587, representing the sexual morphotype A and (K) CM 9188, sexual morphotype B. Abbreviations: Art-Pra, articular+prearticular; AdCr, adductor crest of surangular; Ang, angular; AnSFr, anterior surangular foramen; Boc, basioccipital; Bsp, basipterygoid; C, coronoid; D, dentary; Ect, ectopterygoid; F, frontal; HyFr, hypoglossal foramina; J, jugal, JFr; jugular foramen; L, lacrimal; M, maxilla; Me, Meckelian canal; N, nasal; P, parietal; OcR, occipital recess; Oto, otoccipital; Pal, palatine; PM, premaxilla; Po, postorbital; PoF, postfrontal; PoSFr, posterior surangular foramen; PraCr, prearticular crest; PrF; prefrontal; Ptg, pterygoid; Q, quadrate; QFr, quadrate foramen; San, surangular; SM, septomaxilla; Soc, supraoccipital; Spl, splenial; Sq, squamosal; Sym, dentary symphysis; V, vomer. Scale bars equal to 10mm (G-K).

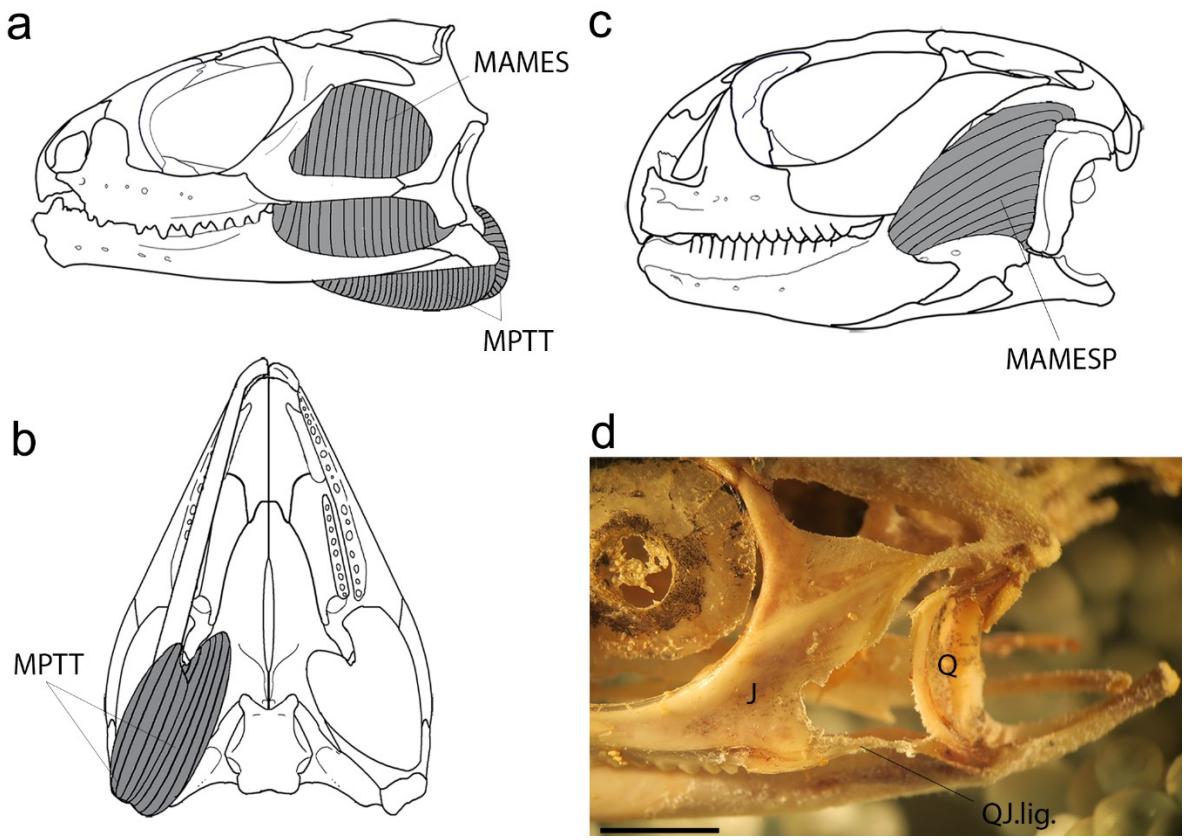

Figure 4.2. Temporal region in lepidosaurs. (A), skull of *Sphenodon punctatus* in lateral view; (B), skull of *Sphenodon punctatus* in ventral view; (C), skull of *Uromastyx aegyptius* in lateral view; (D), temporal region of *Agama agama* in lateral view. Abbreviations: MAMES, *M. adductor mandibularis externus superficialis*; MAMESP, *M. adductor mandibularis externus superficialis posterior*; MPTT, *M. pterygoideus typicus*; QJ.lig., quadratojugal ligament.

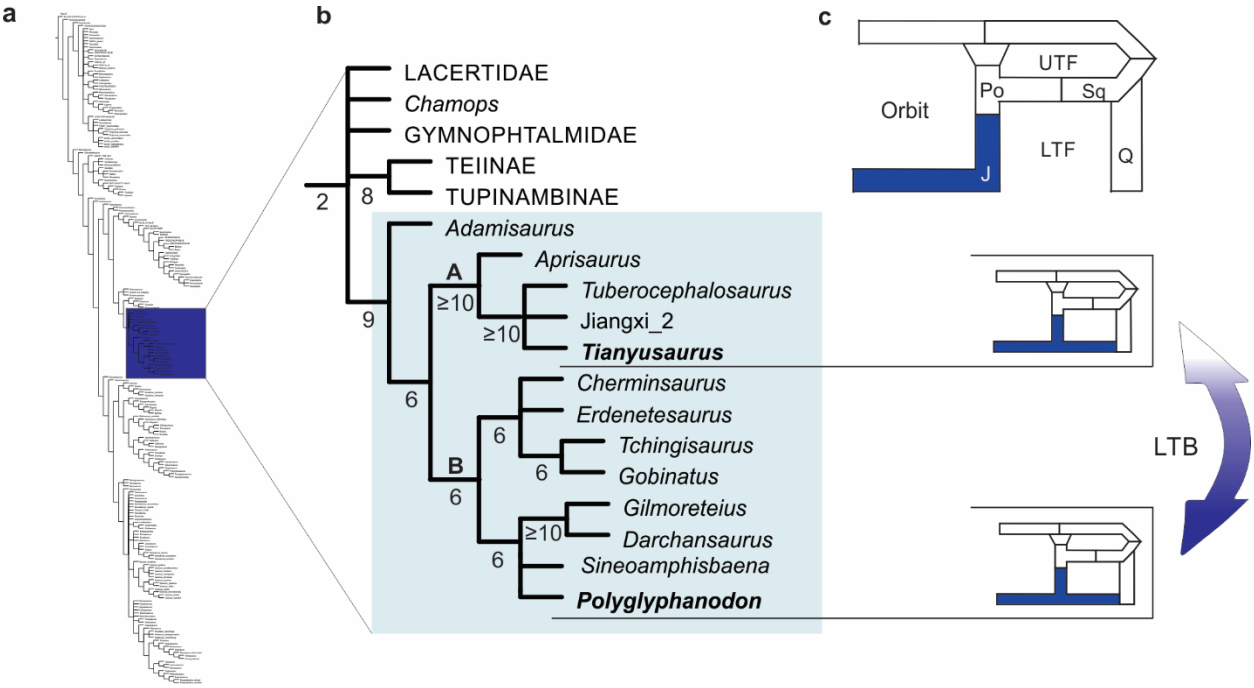

Figure 4.3. Phylogenetic position of *P. sternbergi* and *T. zhengi* amongst borioteiioid lizards. The phylogenetic position of borioteiioids within squamates was not altered in relation to previous analyses of this dataset (Conrad 2008; Mo *et al.* 2010; Simões *et al.* 2015a). (A) Abbreviated view of strict consensus tree depicting all major squamate lineages, with dark blue box highlighting the position of Lacertiformes. (B) Recovered relationships among Lacertiformes, with borioteiioids (or Polyglyophanodontidae *sensu* Conrad (2008)) highlighted by the light blue box. Strict consensus of 54,880 most parsimonious trees (consistency index = 0.1520; retention index = 0.7158) of 3,521 steps. Numbers below branches indicate absolute Bremer indices. (C) Schematic drawing of composition of the lower temporal region as observed in most lizards, depicting the independent development (connected by the arrow) of a complete LTB formed by the jugal (blue) in *P. sternbergi* and *T. zhengi*. Abbreviations: J, jugal; LTF, lower temporal fenestra, Po, postorbital; Q, quadrate; Sq, squamosal, UTF, upper temporal fenestra.

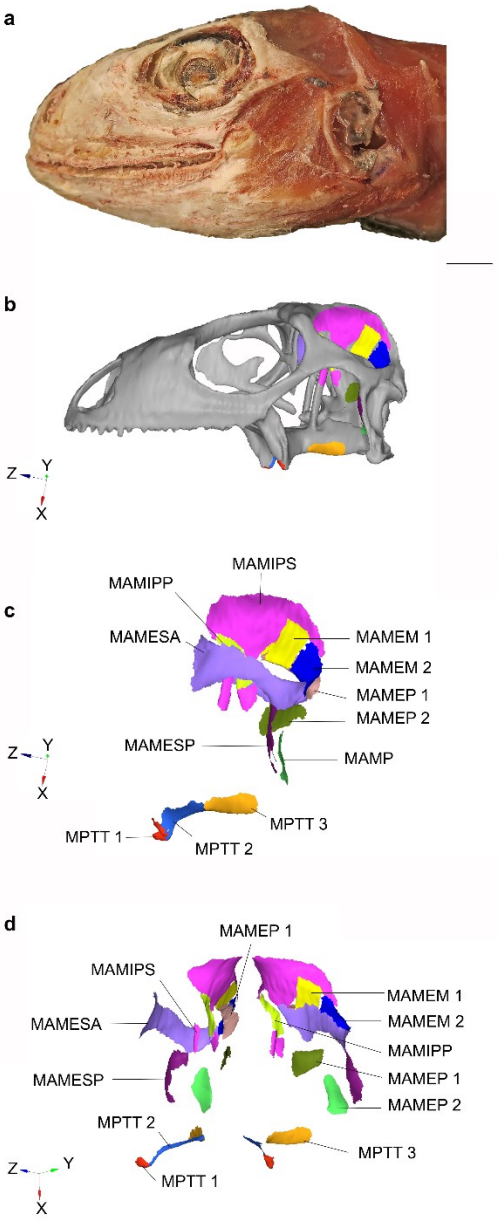

Figure 4.4. Creation of the models for the FEA. (A) specimen of *Iguana iguana* used for CT-scan and for subsequent dissection in order to model muscle origin attachment areas. (B) 3D volume mesh model of *I. iguana* used for the FEA and with muscles maps. (C) Muscle attachments in lateral aspect. (D) Muscle attachments in anterolateral aspect. Finite elements shape and number affects the shape of the borders of the muscle attachment areas, but these are minor and do not affect significantly the number of selected nodes for each muscle. Scale bar = 10mm. Abbreviations: MAMEM, *M. adductor mandibulae externus medius*; MAMEP, *M. adductor mandibulae externus profundus*; MAMESA, *M. adductor mandibulae externus superficialis anterior*; MAMESP, *M. adductor mandibulae externus superficialis posterior*; MAMIPP, *M. adductor mandibulae internus pseudotemporalis profundus*; MAMIPS, *M. adductor mandibulae internus pseudotemporalis superficialis*; MAMP, *M. adductor mandibulae* posterior; MPTT, *M. pterygoideus typicus*. Scale bar (A and B) = 10mm.

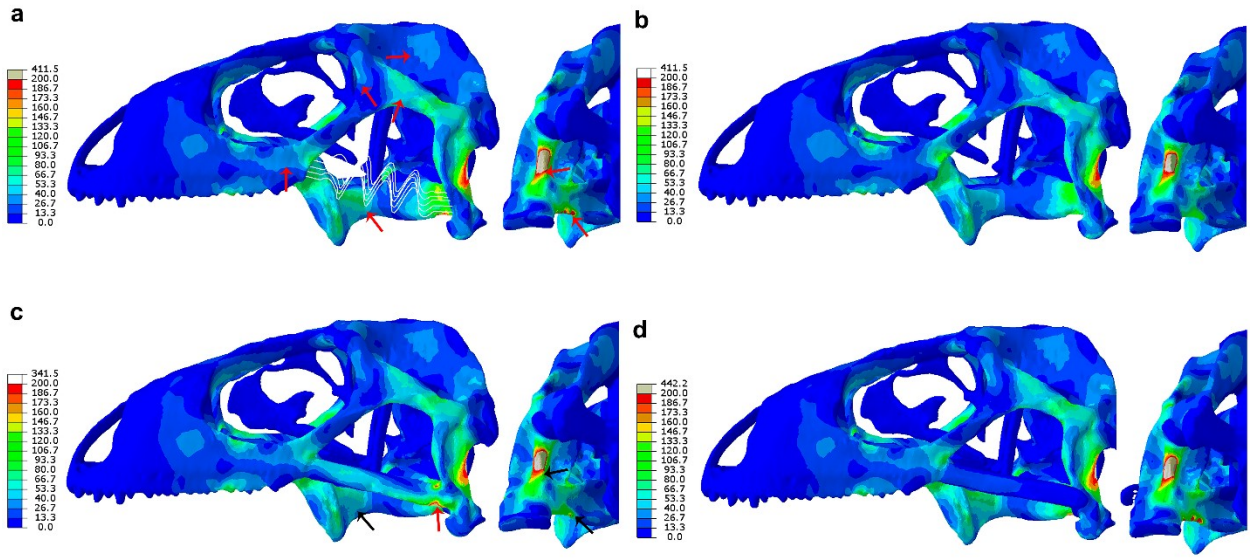

Figure 4.5. Results of the FEA of the skull of *Iguana iguana*, testing how distinct models for a LTB would affect mechanical stress during hard biting. Results are displayed as contours representing combined-axes von Mises stress. (A) model A, lizard with quadratojugal ligament; (B) model B, lizard with jugomandibular ligament; (C) model C, lizard with the addition of a complete LTB, sutured to the quadrate; (D) model D, lizard with the addition of a complete LTB, connected to the quadrate by a short quadratojugal ligament. Red arrows indicate the points in model "A" with increase of stress compared to model "B" (the ones with the least amount of increased stress regions); in model "C", red and black arrows represent areas of increased and reduces stress, respectively, compared to model "A". Model "D" had a very similar distribution of stress to model "A".

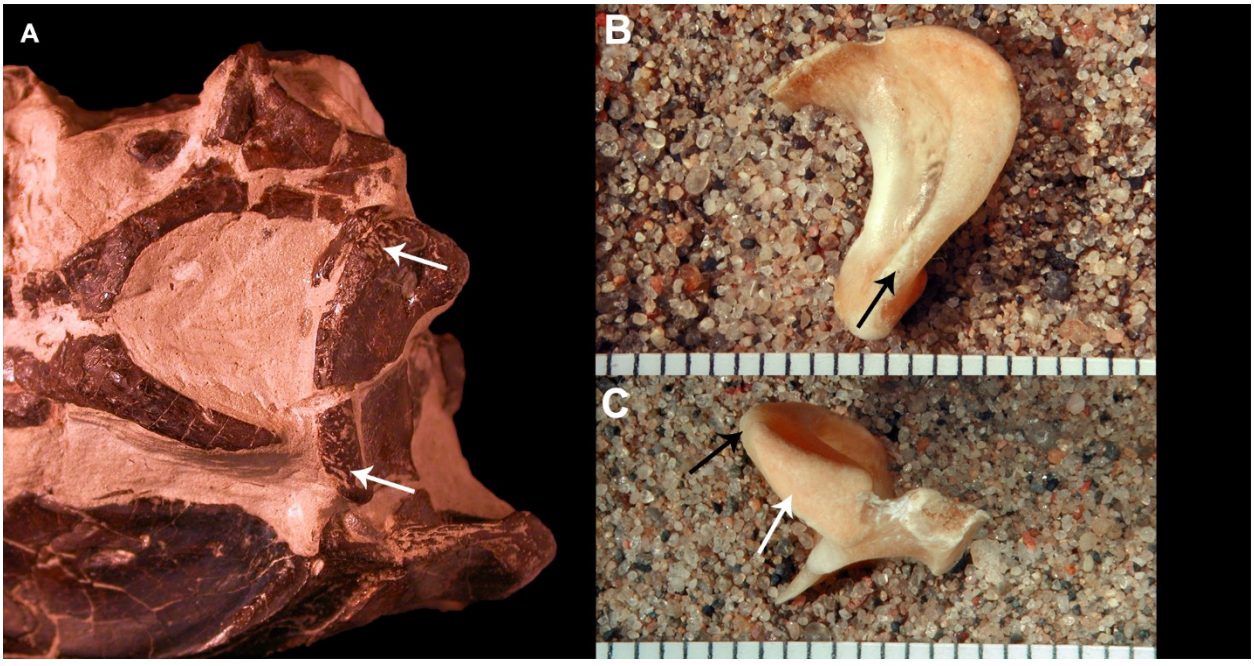

Figure 4.6. (A), quadrate of *P. sternbergi* (NMNH 16587); (B & C), quadrate of *Tupinambis teguixin* FMNH 140193. White arrows indicate regions of soft tissue contact with the quadrate (rugose texture on the surface of the bone), and black arrows indicate regions in which the quadrate is smooth. Despite the excellent preservation of the texture of the tympanic crest in NMNH 16587, the area of contact with the temporal elements is not well preserved (many parts are broken, and the most critical ones are embedded in matrix). See Fig. 4.4 for the morphology of the temporal region based on the specimen in which that region is best preserved.

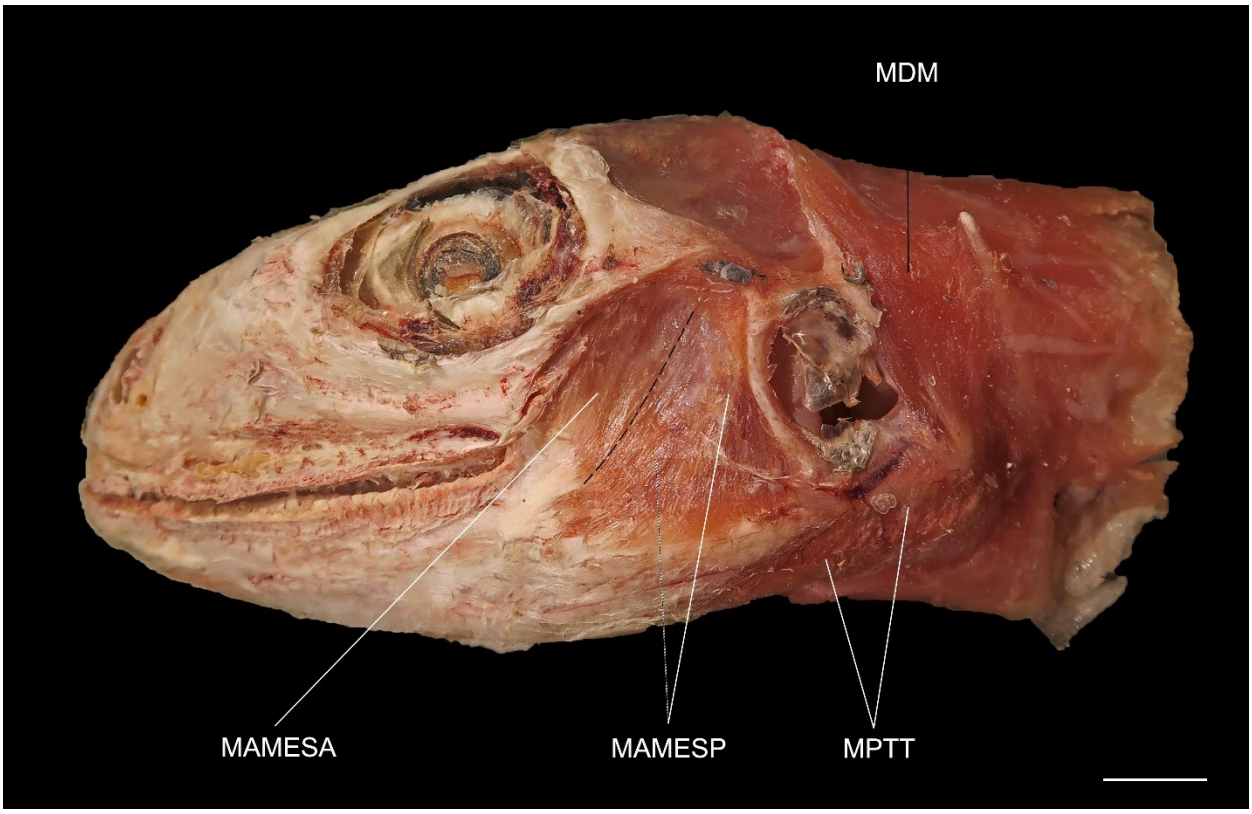

Figure 4.7. Superficial layer of skull muscles of *Iguana iguana* (UAMZ uncatalogued). The MAMESP extends laterally and over the lower jaw posteriorly, expanding the anteroposterior extent of the MAMES in comparison to *Sphenodon*(Rieppel & Gronowski 1981; Wu 2003; Jones & Lappin 2009). The anterior portion of the same muscle (MAMESA), also attaches to the lateral surface of the lower jaw, just posterior to the coronoid bone, but does not extend as far ventrally as the MAMESP. Abbreviations: MAMESA, *Musculus adductor mandibulae externus superficialis anterior*; MAMESP, *Musculus adductor mandibulae externus superficialis posterior*; MDM, *Musculus depressor mandibulae*;; MPTT, *Musculus pterygoideus typicus*. Scale bar = 10mm.

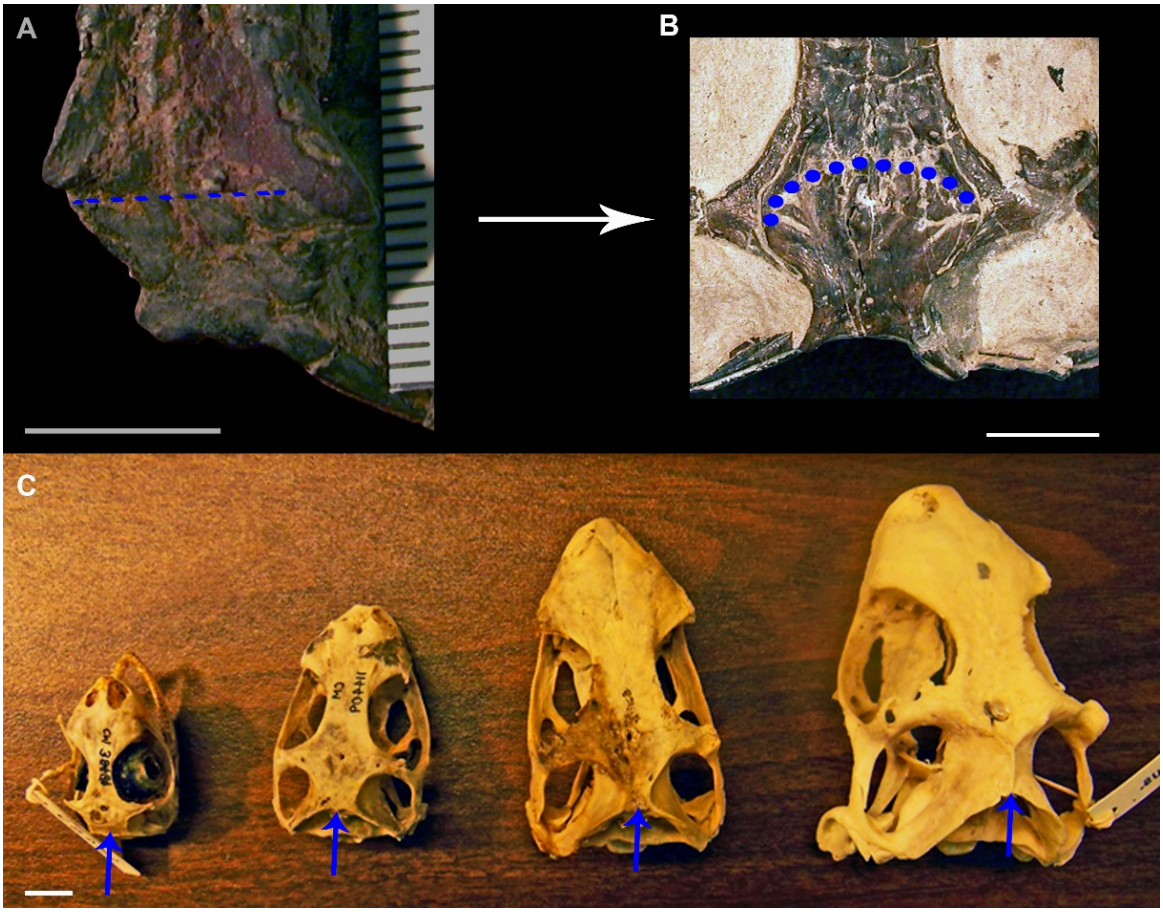

Figure 4.8. (A), the almost straight frontoparietal suture of a juvenile of *P. sternbergi* (NMNH 15568) and (B) the anteriorly curved condition in the adults (NMNH 16588). Dramatic changes in the shape of the parietal during ontogeny in the extant *Iguana iguana*. Scale bars equal to 10mm.

Figure 4.9. Temporal region of *P. sternbergi* (NMNH 15816). Note the increased area of anterodorsal contact between the quadrate, jugal and squamosal, as well as the quadrate process of the pterygoid ventrally. Abbreviations: J, jugal; J.PVP, posteroventral process of the jugal; Po, postorbital; Ptg.Q.Pr.; quadrate process of the pterygoid; Q, quadrtae; Sq, squamosal. Scale bar = 10mm.

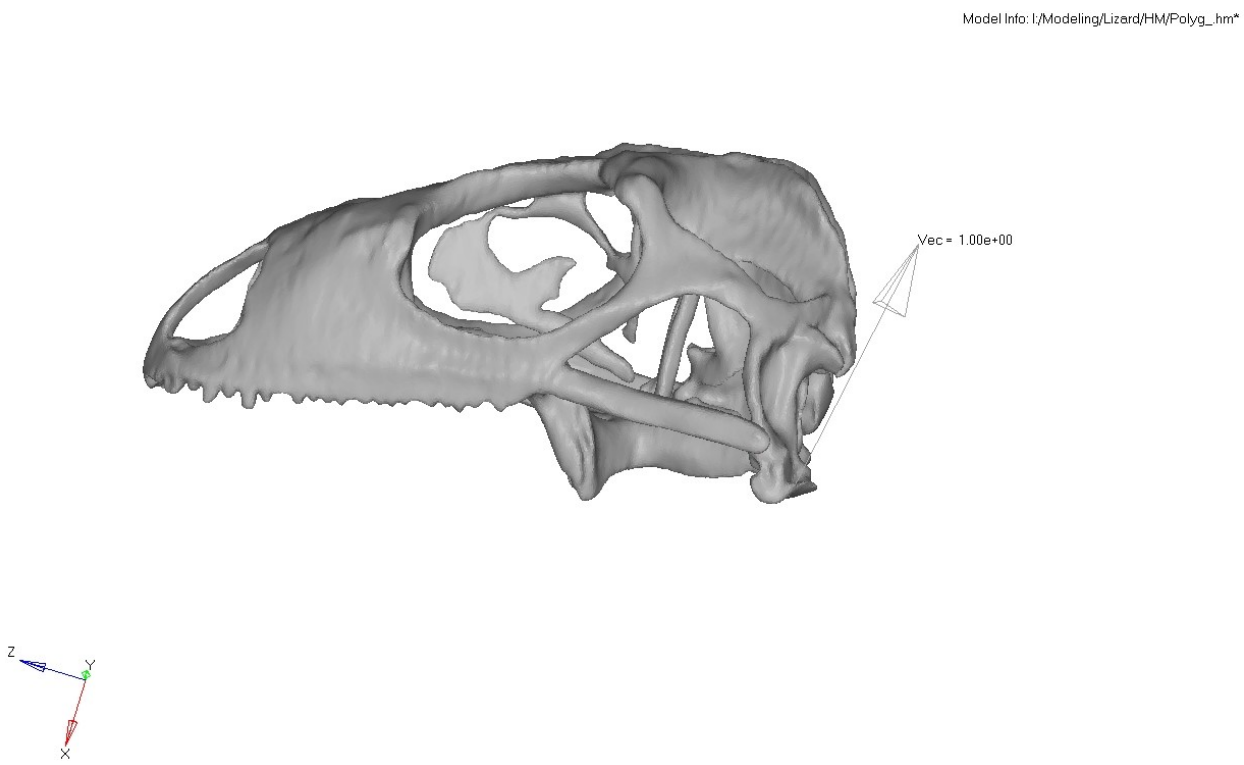

Figure 4.10. Lateral view of finite element analysis results for my hypothetical model D, indicating the direction of the resultant joint reaction force at the quadrato-mandibular joint during biting. In all models, the forces were directed posterodorsally, resulting in a tendency for the quadrate to rotate posteriorly, keeping ligaments or the LTB under tension. For specific direction and magnitudes of joint reaction force at the quadrato-mandibular joint see Table 4.5 .

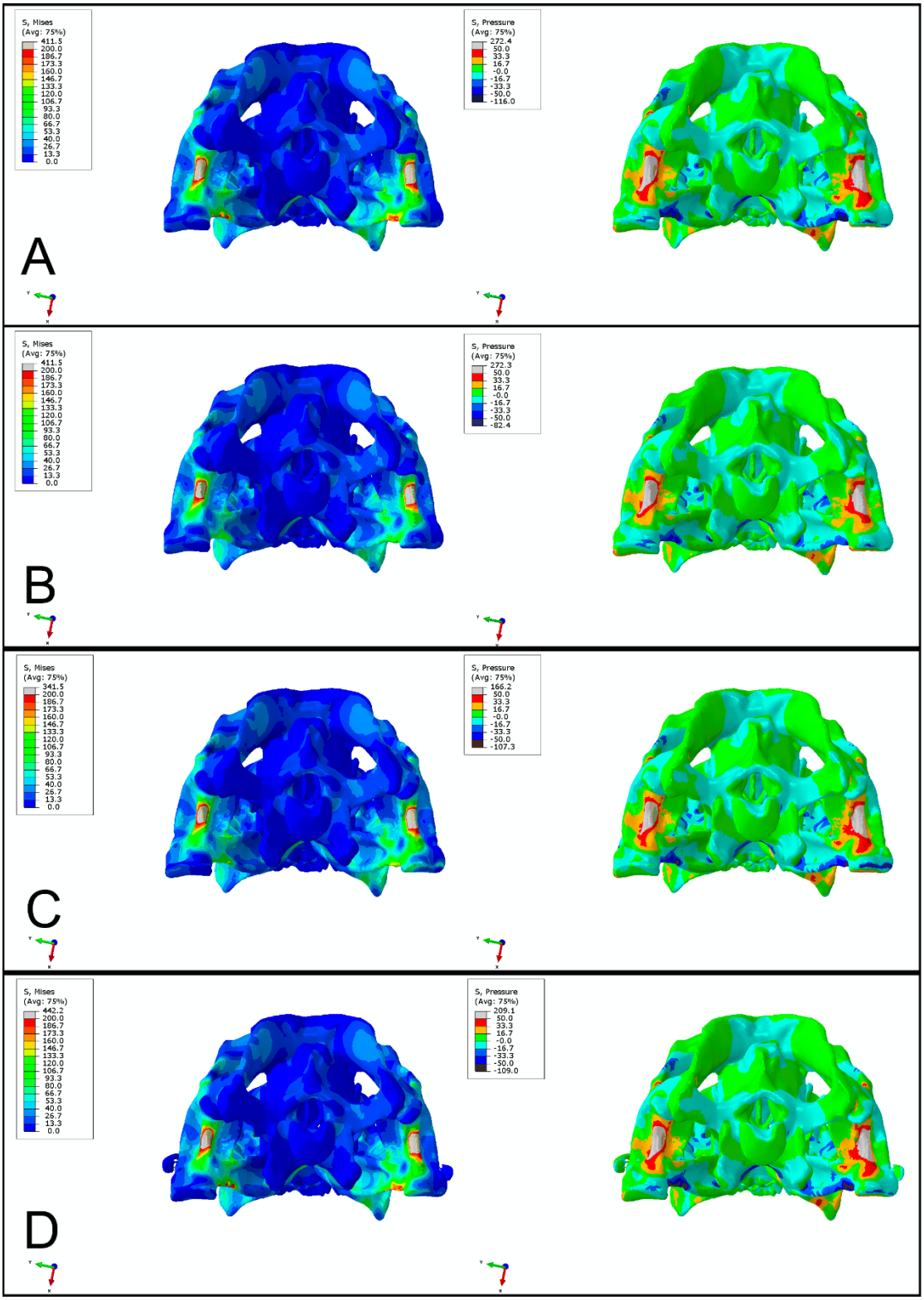

Figure 4.11. Posterior view of Finite Element analysis results for four hypothetical skull models (see main text). Contours indicate von Mises stress (warmer colours are higher stress), left, and pressure (cold colours are tension, warm colours are compression), right.

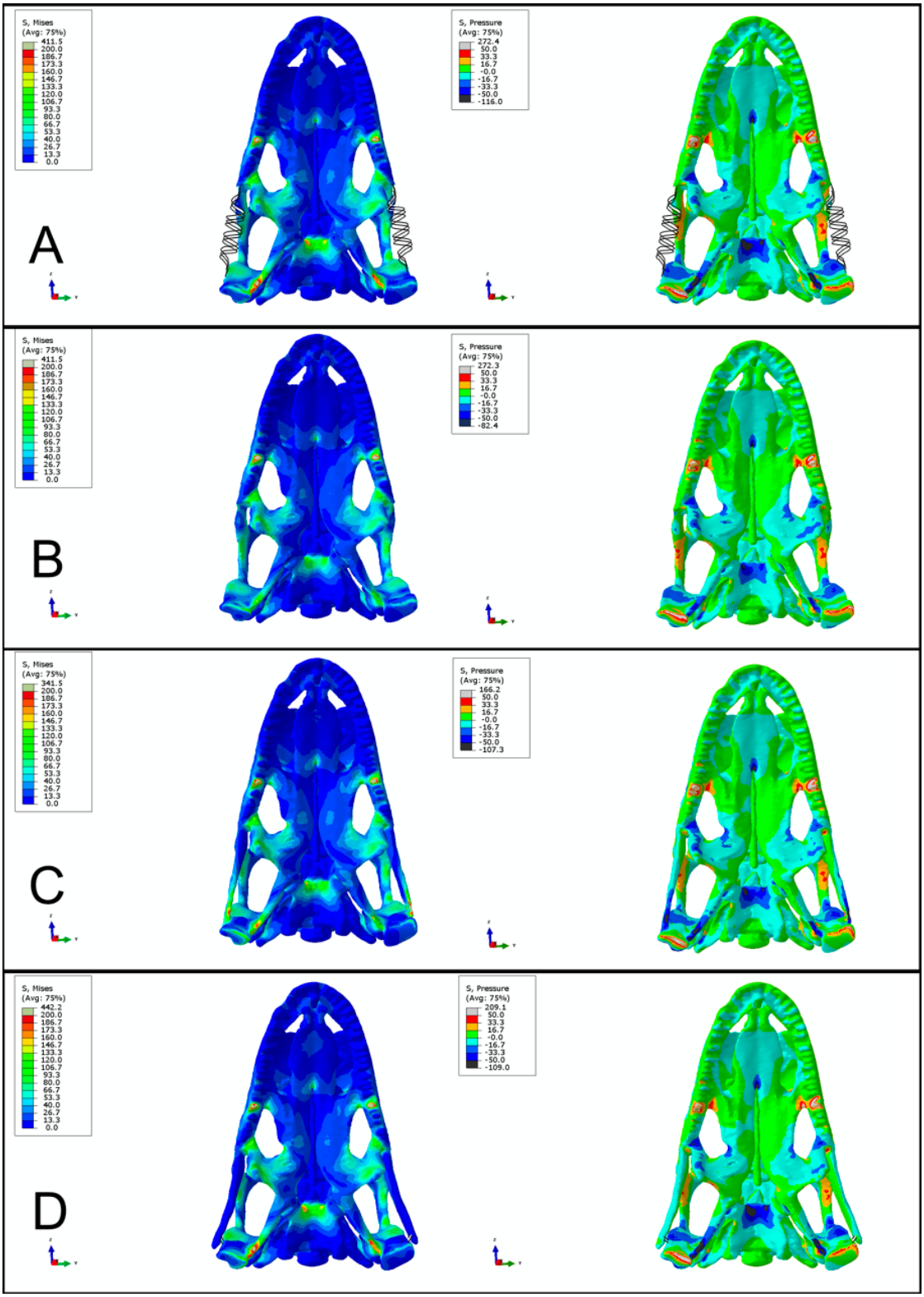

Figure 4.12. Ventral view of Finite Element analysis results for four hypothetical skull models (see main text). Contours indicate von Mises stress (warmer colours are higher stress), left, and pressure (cold colours are tension, warm colours are compression), right.

Table 4.1. Measurements obtained from different *Polyglyphanodon sternbergi* specimens. Color legend: Light green: morphotype A, dark green: morphotype B; yellow: juvenile features, orange: sub-adult/adult features; dashes, missing data. Abbreviations: FP-S, fronto-parietal suture shape; J-PP, jugal, posterior process length; PBL, parietal body length; Po-FP, postorbital, frontal process length; PW, parietal width; Q-AP, quadrate, anterior process size; SH, skull height; SL1, skull length 1; SL2, skull length 2; SW, skull width.

				CM						1547
Specimens	**15559**	**16586**	**15568**	**9188**	**16368**	**427672**	**16587**	**16588**	**15816**	**7**
Ontogeny	*juvenile*	*juvenile*	*sub-adult*	*sub-adult*	*sub-adult*	*sub-adult*	*adult*	*adult*	*adult*	*adult*
PW	11.5	-	14	14.5	15.3	1.7	?	19.7	19.7	21.3
SL1	-	-	-	58.9	-	-	?	67.2	69.1	76.7
SL2	-	-	-	65.1	-	-	80.1	?	81.4	-
SH	-	19.1	28.4	18	30.4	-	32.5	34.4	25.8	36.1
SW	-	-	-	32.6	-	-	-	43.8	41.4	50.8
SH / SL1	-	-	-	N/A	-	-	-	0.512	0.373	0.471
SH / SL2	-	-	-	0.276	-	-	0.406	-	0.317	-
SW/SL1	-	-	-	N/A	-	-	-	0.652	0.599	0.662
SW/SL2	-	-	-	0.223	-	-	-	-	0.242	-
FP-S	straight	-	straight	curved	straight	curved	-	curved	curved	curved
PBL/PW	-	-	-	0.890	0.915	-	-	0.807	0.787	-
J-PP	-	short	-	-	-	short	-	long	long	-

Table 4.2. Muscle directions and loads used in the FEA.

	Muscle Direction			Load Case 1			
Muscle Group	**X**	**Y**	**Z**	**Scaled force**	**X**	**Y**	**Z**
R MAMP	0.867	-0.342	0.363	23.405	20.293	-7.999	8.487
L MAMP	0.941	0.163	0.297	23.405	22.021	3.805	6.959
R MPTT 1	-0.095	-0.175	-0.980	31.304	-2.959	-5.474	-30.680
L MPTT 1	0.334	0.828	-0.450	31.304	10.464	25.921	-14.091
R MPTT 2	-0.009	-0.328	-0.945	29.011	-0.265	-9.519	-27.404
L MPTT 2	0.021	0.337	-0.941	29.011	0.619	9.775	-27.308
R MPTT 3	0.617	-0.761	-0.198	26.973	16.651	-20.539	-5.333
L MPTT 3	0.766	0.613	-0.193	26.973	20.669	16.533	-5.195
R MAMIPS	0.828	-0.505	0.245	4.987	4.128	-2.517	1.220
L MAMIPS	0.935	0.266	0.235	4.987	4.661	1.328	1.174
R MAMIPP	0.802	-0.596	-0.034	4.805	3.853	-2.865	-0.165
L MAMIPP	0.935	0.331	-0.123	4.805	4.495	1.592	-0.593
R MAMESA	0.961	-0.271	0.059	44.882	43.116	-12.184	2.629
L MAMESA	0.872	0.490	0.014	44.882	39.120	21.990	0.643
R MAMESP	0.890	-0.168	0.425	47.684	42.419	-8.017	20.253
L MAMESP	0.850	-0.122	0.512	47.684	40.531	-5.830	24.435
R MAMEM 1	0.829	-0.405	0.385	33.889	28.106	-13.708	13.060
L MAMEM 1	0.889	0.161	0.428	33.889	30.131	5.462	14.517
R MAMEM 2	0.835	-0.492	0.247	33.670	28.100	-16.578	8.322
L MAMEM 2	0.934	0.236	0.270	33.670	31.432	7.945	9.088
R MAMEP 1	0.789	-0.508	0.346	17.399	13.724	-8.838	6.023
L MAMEP 1	0.902	0.298	0.314	17.399	15.689	5.180	5.457
R MAMEP 2	0.703	-0.355	0.617	17.399	12.224	-6.177	10.731
L MAMEP 2	0.824	0.231	0.517	17.399	14.339	4.025	8.997
Ligament 1	0.186	-0.285	-0.940	21.076	3.924	-6.010	-19.816
Ligament 2	0.419	-0.320	-0.850	7.608	3.184	-2.433	-6.467
Bite Force	-0.981	0.146	0.126	79.573	-78.079	11.590	10.060

Table 4.3. Muscle directions and loads used in the FEA.

	Load Case 2				Load Case 3			
Muscle Group	**Scaled force**	**X**	**Y**	**Z**	**Scaled force**	**X**	**Y**	**Z**
R MAMP	46.811	40.586	-15.998	16.973	93.622	81.172	-31.996	33.946
L MAMP	46.811	44.041	7.610	13.919	93.622	88.082	15.220	27.837
R MPTT 1	62.609	-5.917	-10.949	-61.359	125.217	-11.834	-21.897	-122.718
L MPTT 1	62.609	20.928	51.843	-28.182	125.217	41.855	103.686	-56.363
R MPTT 2	58.022	-0.531	-19.038	-54.807	116.044	-1.061	-38.076	-109.615
L MPTT 2	58.022	1.238	19.549	-54.616	116.044	2.477	39.099	-109.231
R MPTT 3	53.945	33.301	-41.078	-10.665	107.891	66.603	-82.155	-21.330
L MPTT 3	53.945	41.338	33.065	-10.390	107.891	82.676	66.130	-20.780
R MAMIPS	9.974	8.257	-5.035	2.439	19.947	16.514	-10.069	4.879
L MAMIPS	9.974	9.323	2.655	2.348	19.947	18.645	5.311	4.696
R MAMIPP	9.610	7.707	-5.731	-0.330	19.219	15.414	-11.462	-0.659
L MAMIPP	9.610	8.989	3.183	-1.186	19.219	17.978	6.367	-2.372
R MAMESA	89.763	86.232	-24.367	5.259	179.527	172.465	-48.735	10.517
L MAMESA	89.763	78.241	43.979	1.287	179.527	156.482	87.958	2.574
R MAMESP	95.369	84.837	-16.034	40.507	190.738	169.674	-32.068	81.013
L MAMESP	95.369	81.062	-11.661	48.869	190.738	162.124	-23.321	97.739
R MAMEM 1	67.777	56.212	-27.417	26.121	135.555	112.425	-54.833	52.241
L MAMEM 1	67.777	60.262	10.924	29.034	135.555	120.523	21.849	58.068
R MAMEM 2	67.341	56.200	-33.155	16.644	134.681	112.401	-66.310	33.288
L MAMEM 2	67.341	62.865	15.889	18.175	134.681	125.729	31.778	36.350
R MAMEP 1	34.799	27.449	-17.676	12.045	69.597	54.897	-35.352	24.090
L MAMEP 1	34.799	31.377	10.359	10.913	69.597	62.755	20.718	21.826
R MAMEP 2	34.799	24.449	-12.353	21.462	69.597	48.897	-24.706	42.924
L MAMEP 2	34.799	28.677	8.050	17.994	69.597	57.355	16.099	35.987
Ligament 1	42.152	7.848	-12.021	-39.632	84.304	15.696	-24.042	-79.264
Ligament 2	15.216	6.368	-4.865	-12.934	30.432	12.737	-9.731	-25.869
Bite Force	159.506	-156.511	23.232	20.166	319.012	-313.023	46.464	40.332

Table 4.4. Combined joint reaction forces at quadrato-mandibular joint

Model	Fx	Fy	Fz	Magnitude (N)
A	-1150	-26.2	-205.6	1166.7
B	-1150	-26.5	-206.2	1168.6
C	-1148	-26.2	-205.6	1166.55
D	-1206	-41.1	4.09	1206.7

Force magnitudes represent the combined joint reaction forces of both sides of the skull. The component magnitude for each individual joint was approximately half of the total magnitude, with less than 2.5% variation between each side.

Table 4.5. Von Mises stress and compression values at areas of highest stress in the skull.

Model	Von Mises at Q (Mpa)	Ratio against model B (%)	Von Mises at Ptg (Mpa)	Ratio against model B (%)
A	340	+5.6	285	+43.2
B	321	0	162	0
C	341	+5.9	225	+28
D	351	+8.5	273	+40.7

Abbreviation: Q, quadrate; Ptg, pterygoid. These were the areas with highest von Mises stress and compression values other than the tooth upon which bite forces were applied. Values are of the element's centroid (integration point), which may be slightly higher than the extremes of the contour legends; the values of the contours in von Mises and pressure maps are average values of the elements in each region. The software average the values to plot a continuous contour map (color).

CHAPTER FIVE: GIANT TAXON-CHARACTER MATRICES: QUALITY OF CHARACTER CONSTRUCTIONS REMAINS CRITICAL REGARDLESS OF SIZE

[The contents of this chapter have been published in Simões, T. R., M. W. Caldwell, A. Palci and R. L. Nydam. 2017. Giant taxon-character matrices: Quality of character constructions remains critical regardless of size. Cladistics 33: 198-219.]

Introduction

There is an increasing research trend in cladistic analyses of vertebrate phylogeny using morphological data, towards the construction of extremely large datasets, comprised of large numbers of terminal taxa and extremely large numbers of characters. The outputs of these analyses are, seemingly with little criticism, dominating vertebrate systematics. This is the case for squamates (Gauthier *et al.* 2012; Conrad *et al.* 2013) for non-avian dinosaurs and birds (Godefroit *et al.* 2013), as well as for other groups such as placental mammals (O'Leary *et al.* 2013). The recent dinosaur study (Godefroit *et al.* 2013) scored 1,500 morphological characters for 101 terminal taxa of dinosaurs and birds. The placental mammal analysis of O'Leary *et al.* (2013) examined 86 fossil and extant placental mammals for character states derived from 4,541 "phenomic" characters along with nucleotide sequences from 27 nuclear genes for a total of 36,860 base pairs. While the cited squamate studies are small matrices compared to either the dinosaur or mammal matrices, it is likely only a matter of time before similar-sized matrices will be produced for squamates given the current trends—e.g., Conrad *et al.* (2013); Reeder *et al.* (2015).

There is an implicit assumption in some studies, stated explicitly in others, that gigantic datasets are more "comprehensive/extensive", thus being superior to previous datasets and their resultant hypotheses, because of their larger number of characters (Conrad 2008; Gauthier *et al.* 2012; Godefroit *et al.* 2013; O'Leary *et al.* 2013). This size property apparently suffices, or is considered to be the most important criterion, for arguing why the newest and largest dataset is inherently superior to previous smaller datasets, and thus falsifies or replaces the hypotheses derived from smaller datasets. In the absence of any obvious self-criticality, the assumption behind the method appears to be that the quantity of characters in the matrix is more important than the quality of assessment leading to the construction of characters and character states. While it may be true that such comprehensiveness/extensiveness is consistent with 'total evidence' and may be of value in some sense, it is not a logical consequence of a search for all evidence that large numbers of characters (e.g., 4,541 [O'Leary *et al*., 2013]) reflects an equivalent comprehensive effort in the construction of character concepts, e.g., primary homologs *sensu* de Pinna (1991), or conjectures of homology *sensu* Nixon & Carpenter (2012). In fact, it is fairly common in these and other morphological studies for the criteria for character

construction to be completely absent (Poe & Wiens 2000; Brazeau 2011). In other instances, these criteria are sidelined as a minor secondary concern in relation to size of the matrix, relegated to a few statements following the highlighting of the parsimony models (e.g., ordering/unordering characters).

Despite previous works criticising the indiscriminate choice of characters in phylogenetic works, such as Wilkinson (1995), Jenner (2004), Kearney & Rieppel (2006), Rieppel & Kearney (2007) and Brazeau (2011), few studies have actually tested how biased characters might be affecting the outcome of published phylogenies, and none have offered deep analyses of squamate datasets. I also agree with numerous authors, such as Farris (1983), Hawkins (2000) and Jenner (2004), that there is an explicit need for authors to be intimately familiar with the anatomy and morphology of the groups under study. It is obvious that if the authors are unable to critically evaluate morphology, diversity, and disparity within the terminal taxa under consideration for phylogenetic analysis, then the character constructions will suffer as well. Consistent with these concerns, as I agree with them philosophically and methodologically, I focus my in-depth analysis of character constructions in this study to the large morphological datasets in my collective area of expertise, the Squamata. I consider the implications of my study and critique to have broad implications in terms of character conceptualization and construction, and because of my expertise as squamate anatomists this study also addresses important issues associated with observations of squamate anatomy and morphology.

The criticisms and suggestions presented in this study arise from a philosophy expressed quite clearly by Farris (1983 – p. 14): "*Even granting that the number of potentially usable characters is large, moreover, it hardly seems accurate to describe systematic research as random sampling of unitary characters that lie waiting to be selected.*" and (p. 10) "*Usually a careful worker will have studied his characters closely before attempting to fit them into a synapomorphy scheme*…". I also hold the view that each character acts (or should act) as an independent falsifier for sister group relationships in a cladogram. As a consequence, unless the character construction and homology assessment in such studies are carefully selected, then I can only conclude that larger morphological matrices are not an improvement based merely on size as the quality of the dataset is only as good as the quality of the characters included (Kearney & Rieppel 2006). The points raised here do not relate to the discussion of relative numbers of characters per taxon in matrices, and their effects on the accuracy of phylogenies—e.g., Graybeal

(1998); Wiens (2004)—nor to criticisms that all "good" morphological characters have already been proposed (Scotland *et al.* 2003). It relates strictly to the logical basis of character construction and homology assessment, especially when these factors are treated as secondary in relation to others in cladistic studies, such as concerns for size of the matrix. I reject the argument that falsification and character analysis are meaningless (Kluge 2003) and that more characters and more taxa are inferred to be always superior samples of both diversity and character evolution. The quality of a dataset depends on the rigor and quality of its character constructions, morphological assessments, and primary homology assignments, as derived from the homolog concept at the root of the character concept (Rieppel & Kearney 2002; Jenner 2004; Kearney & Rieppel 2006; Brazeau 2011). As an example, numbers of taxa and characters are meaningless if the homolog concepts and character constructions fail the criterion, or test, of similarity (Remane 1952; Patterson 1982). Numerous authors have argued strenuously that character construction and character state coding is the key impactor of outcomes in cladistic research (Maddison 1993; Pleijel 1995; Wilkinson 1995; Hawkins *et al.* 1997; Strong & Lipscomb 1999; Sereno 2007; Brazeau 2011).

In this study I use the following terminology regarding character construction, coding and scoring. Character construction deals with the identification of primarily homologous locators (anatomical parts) in different organisms, identifying their properties, observing variation of these amongst the studied taxa, and correctly transcribing those observations into character and character statement descriptions. The term "coding" is referred to here as the specific part of character construction concerned with the process of dividing a character into its constituent character states. Both are different from "scoring", which is the process of assigning states for every taxon on every cell of the data matrix.

This study is organized as follows: 1) A brief review of tests and criteria for effective character constructions with the addition of new criteria and perspectives; 2) Identification of character types that should be avoided as they form non-meaningful conjectures/hypotheses of primary homology; 3) A list with comments on each problematic character from the character descriptions/constructions of Conrad (2008) and Gauthier *et al.* (2012) (see Supplementary Information 5.1 II-III); 4) Cladistic analyses of the modified matrices with problematic characters removed or recoded (when applicable); 5) Discussion of problematic constructions present in recent, large scale, and widely cited phylogenetic analyses of squamates, and how

these character concepts and constructions may be affecting understanding of the squamate tree of life.

Criteria for effective character constructions

Similarity: previous concepts and new insights

Operationally, the similarity test of Patterson (1982) is used by the observer as a falsifying criterion to indicate if there is enough observational evidence to support the primary hypothesis of homology between any two or more attributes of two or more species (i.e., if two or more character states belong to the same character). Only the similarity test operates at this level of empirical criticality and falsification by observation, whereas the congruence test (the cladistic analysis) delimits the most parsimonious character agreement hypothesis/hypotheses. This is especially important because the test of congruence can only test the primary homology statement of character states, but not the homology among different states of the same character. Constructing primary homologies that are plausible to reflect similarity due to recency of common ancestry (Nixon & Carpenter 2012) is intimately dependent on the test of similarity.

A similarity criterion derived from assessments of topology, connectivity, ontogeny and one-to-one relationships of the structures being compared between taxa, has been argued numerous times to be necessary to the establishment of good characters, e.g., Remane (1952); Wiley (1975); Riedl (1978); Patterson (1982); Rieppel & Kearney (2002). The reliability and applicability of each of the mentioned sub-criteria may however be variable, depending in particular on the evaluation of each character. For example, this happens with ontogeny, as homologous structures may arise from different developmental processes (Roth 1988; Wagner 1989), and one-to-one relationships may also have exceptions, as suggested by Rieppel & Kearney (2002) in their discussion of the amniote astragalus.

Connectivity is considered as an important sub-criterion of similarity, and seems to be the simplest and most clear-cut criterion—element A contacts element B, or, A does not contact B. If this state is observed, and no other tests of similarity are applied as critical assessments of the quality of that observation, then this straightforward approach to simple connectivity is referred to herein as “naïve connectivity”. I create this term in the same sense (logic and rationale) that Kuhn (1962) and Lakatos (1978) used when recognizing Popperian falsificationism (Popper

1959) as “naïve falsificationism”. As I will argue here, it is easier to construct erroneous hypotheses of primary homology than it would seem, due to the problem introduced by naïve connectivity.

As an example, I consider here the contacts between the jugal bone and the prefrontal, maxilla, and lacrimal bones of reptiles (Fig. 5.1a-d). In lepidosaurs generally, the jugal contacts the ventral part of the prefrontal (or the lacrimal) and the maxilla. These contacts help to define the *identity* of the bone as the jugal (highlighted in green in Fig. 5.1a-d), and are key to identifying similarity via connectivity in the construction of hypotheses of primary homology.

However, in squamates, exceptions to the general condition of bony connections abound, and if approached naively can result in simplistic mistakes in character state assignments, i.e., primary homology statements. For example, in *Chamaeleo laevigatus* (Fig. 5.1a) the jugal and the prefrontal are not in contact, while in *Polychrus marmoratus* (Fig. 5.1b) the anterior portion of the jugal is curved and elongated dorsally, thus contacting the prefrontal. In *Uromastyx aegyptius* (Fig. 5.1c) on the other hand, the jugal does not extend anterodorsally, but the prefrontal extends more ventrally as compared to *Polychrus*, also establishing the contact between both elements. Finally, in the non-squamate lepidosaur, *Sphenodon punctatus* (Fig. 5.1d), the prefrontal extends well ventrally as in *Uromastyx*, but the jugal is much shorter, and a contact between both elements does not occur in lateral view. It thus becomes clear that there is a significant variation in length of the jugal as well as in height of the prefrontal, and most importantly, that each element changes in length/height in distinct ways in each taxon, and that contact between both can occur as a result of changes in extension of different bones. From this simple example, it is observed that naïve connectivity would recognize two states, contact “absent” and “present”, and ignore the fact that, in each case, the contact “present” condition is formed by two very different morphologies (long anterior process of jugal versus long ventral process of prefrontal). The “presence” or “absence” of the lacrimal bone (between the jugal and prefrontal, usually preventing both elements to come into contact) also adds a third element to this nexus of contacts that is not taken into consideration when assessing primary homologies for lepidosaur-squamate datasets.

A second example concerns the contact between the vomers and the pterygoids (Fig. 5.1e-g). In most squamates these two elements never touch, being entirely separated by the palatine (e.g., *Iguana iguana*—Fig. 5.1e). However, in some groups the vomers are elongated and extend along

the medial border of the palatines (e.g. *Rhineura floridana*—Fig. 5.1f), reaching the pterygoids posteriorly. In contrast, in other taxa (e.g. *Uromastyx acanthinurus*—Fig. 5.1g), there is an extreme elongation of the pterygoids, which also results in contact with the vomers. In the latter case, the palatine process of the pterygoids (red dotted line in Fig. 5.1e-g) extends well anteriorly passing adjacent to the palatine medial border. Despite this contact between the pterygoids and vomers in both *Uromastyx* and *Rhineura,* it is clear that the contact is created differently (elongate vomers in one, and elongate pterygoids in the other), and simply coding "contact" as the same character state ignores the obvious lack of "similarity". This character, and others like it, is widely used in many squamate morphological datasets. However, there is no evidence to infer that the properties "length" or "height" of each of these distinct anatomical parts are evolutionarily integrated in such a way that the contact between them is anything more than a consequence of the independent development of the length of the vomers and pterygoids (or length of the jugal and the height of the prefrontal in the first example).

Considering that characters must be independent properties, there is no certain support that a "specific contact" can be a statement of primary homology in the instances just presented, and many others that are common in squamate phylogenies (see Character Type I A.7, below). Instead, there is an argument for the falsification of such characters as primary homologs. Therefore, despite connectivity (i.e. the complex of contacts) being useful as a way to establish the identity of the elements under comparison (such as the green element in Fig. 5.1a-c as the jugal bone), the contact itself as a character could be caused by different transformation series and the state 'contact present' does not necessarily reflect the same historical process (i.e., recency of common ancestry and thus homology).

Conjunction

The second rule available for character construction is the conjunction test, or criterion, first proposed by Patterson (1982), and used by Freudenstein (2005) to show that it is a useful way of detecting structures that belong to a single transformation series. If two structures co-exist within a single individual, they cannot belong to an evolutionary sequence of transformation. Such a condition should be distinguished from polymorphic characters, which are different character states belonging to the same transformation series, but within the same terminal taxonomic unit (e.g., species), not within an individual.

Independence of characters

The criterion of independence of characters is a fundamental one in terms of hypothesis testing, making it a pre-requisite for the congruence test to work in a falsificationist framework (Felsenstein 1982; Farris 1983; Pimentel & Riggins 1987; de Pinna 1991; Pleijel 1995; Wilkinson 1995; Hawkins *et al.* 1997; Kluge 2003; Sereno 2007). If two characters that are dependent on each other contribute to identifying a monophyletic group in an analysis, it is because their content information is the same; their congruence in a cladistic test does not arise because they support a most recent common ancestor for that grouping. Put another way, they do not reflect agreement of information on the phylogenetic history of taxa, but agreement among themselves in terms of information (Hawkins *et al.* 1997).

Differentiating characters and character states

Previous authors have stated that there is no difference between characters and character states (Platnick 1979; Patterson 1982). The general argument is that characters are organismal features, just like states, in increasing levels of generality (Platnick 1979). However, Hennig (1966) stated that character states ('characters' or 'character conditions' in his terminology), are produced by transformation. Characters are a collection of such conditions or states, the latter being comparable to each other and yet mutually exclusive. Characters themselves are not comparable to each other as they do not belong to the same transformation series, therefore being independent from each other. This view is supported by Farris *et al.* (1970), Brower & Schawaroch (1996), Hawkins *et al.* (1997), Freudenstein (2005), Sereno (2007), among others. This is an important distinction, because not accepting the difference between characters and character states may lead to coding schemes where states are coded as individual characters (such as in non-additive binary coding—see below), splitting a transformation series into multiple ones, and putting extra weight in that initial series. Not recognizing states as comparable conditions of a property, and as mutually exclusive, leads to compound characters or character states.

Character types: the case for exclusion or re-coding

Applying the philosophy and methods reviewed above as indicative of best practice in the construction of characters and character states for phylogenetic analysis using parsimony, I examine here the character constructions presented in the matrices of Conrad (2008), referred to as '(C08)', and Gauthier *et al.* (2012), referred to as '(G12)'. For a complete list of characters in each matrix that fall into each of my categories below, see the Supplementary Information 5.1 II and III—summarized in Table 1. These matrices are used as examples due to the large number of characters in each of them, and because they include numerous characters from other studies testing squamate phylogeny; they are therefore good examples of the kinds of characters usually found in datasets composed of squamate character constructions, codings and scorings. When the character is not created by these authors, but is imported from a previous matrix, a reference to the original publication of the character is provided. In order to unify the multitude of terms used for each problematic character construction, I applied the character structure nomenclature established by Sereno (2007) whenever possible.

Type I. Discrete characters not following basic principles of character formulation

Characters that do not follow the basic principles of character formulation (independent transformation series of character states) are common to most character sets and are often not recognized for what they are. In Type I characters, I make special reference to discrete data, noting that these kinds of characters should not be used if they represent:

Type I A. Character coding leading to logical dependency between characters

Logical dependency between characters (Wilkinson, 1995) creates redundancy between two separate characters in the way they are coded. Here I use the classic example of bird tails from Maddison (1993): Ch. 1- Blue tail: absent (0)/present (1); Ch. 2- Red tail: absent (0)/present (1). Type I A characters are further subdivided here into six character types, Type I A.1-A.7.

Type I A.1. Non-additive binary coding (Farris et al. 1970; Strong & Lipscomb 1999).

Example: Ch. 1- Blue tail: absent (0)/present (1)

Ch. 2- Red tail: absent (0)/present (1)

My Type 1 A.1. characters are also known as "nominal variables coding" (Pimentel & Riggins 1987; Hawkins *et al.* 1997; Hawkins 2000) or "a/p coding" (Pleijel 1995). Here, the absence of the red tail will always occur when there is presence for the blue tail, creating logical dependency and redundancy between these two characters (Hawkins *et al.* 1997; Strong & Lipscomb 1999) as a single transformation series was split into two series. This is not a common practice in parsimony studies (Kluge & Farris 1999), and is, rather, the way of coding characters for modified three-taxon-statement analysis (Carine & Scotland 1999). For cladistic investigations using parsimony, this coding should be avoided.

Example of this type of character in the examined squamate phylogenies:

(G12) "*Character 167 - Supratemporal shortens*^{N}*...(ordered)".* → It also falls into Type I (A.7), Type I (B) and Type I (C).

(G12) *"Character 168 - Supratemporal lengthens…(ordered)"*- Pregill *et al.* (1986). → The supratemporal length was divided into two characters, each representing a state (character 167—short; and character 168—long), dividing a transformation series into two different characters that are dependent on each other. It also falls into Type (A.7), Type I (B) and Type II (A).

Type I A.2. Absence coding (Strong & Lipscomb 1999)

Example: Ch.1- Tail: absent (0)/ present (1)
Ch.2- Tail length: absent (0)/short tail (1)/ long tail (2)

or

Example: Ch.1- Tail color: absent (0)/ blue tail (1)/ red tail (2)
Ch.2- Tail length: absent (0)/short tail (1)/ long tail (2)

My Type 1 A.2. characters are also known as "repeated absence" (Brazeau 2011). The absent condition of the tail is repeated in each character, creating the duplication and extra weighting of this condition (Maddison 1993; Pleijel 1995; Brazeau 2011). If there is character state agreement between both absent conditions, it is because they simply represent the same thing and bias the

congruence test: absence of tail. Another associated problem is the fact that only if the first character is scored as "present" does the following one(s) become applicable. Although the latter issue also arises in other coding formats, such as "traditional" or "contingent" codings (Strong & Lipscomb 1999; Brazeau 2011), the extra weighting over the "absent" condition is exclusive to this coding format. The best option is to score taxa with no tail in the second character as inapplicable, such as in a "traditional" or contingent coding scheme (Strong & Lipscomb 1999; Brazeau 2011), or to utilize a multistate coding option, for example:

Traditional (or contingent) coding:

Ch.1- Tail: absent (0)/ present (1)

Ch.2- Tail length: short tail (0)/ long tail (1)

Multistate coding:

Ch. 1- Tail: absent (0)/ short (1)/ long (2)

Both contingent and multistate coding may present limitations of their own in particular situations—e.g. as mentioned, contingent coding makes the second character dependent on the first. This may create spurious ancestral node optimization when inapplicable character states occur plesiomorphically in the most parsimonious solution. Discussions of the advantages and problems associated with contingent and multistate coding have been presented elsewhere and I refer the reader to such studies (Maddison 1993; Hawkins *et al.* 1997; Lee & Bryant 1999; Strong & Lipscomb 1999; Brazeau 2011). Nevertheless, absence coding performs worse than either contingent or multistate coding and should be avoided because it has not only one, but two undesirable effects on the analysis. It also includes one undesirable effect that is exclusive to this form of coding (extra weighting of the "absent" condition)—see similar conclusions regarding absence coding in Strong & Lipscomb (1999) and Brazeau (2011).

Example of this type of character in the examined squamate phylogenies:

(C08) Characters 170 + 171:

"Character 170 - Mandible, intramandibular septum (L98-116): (0) absent; (1) present...." - Lee (1998).

"Character 171 - Mandible, intramandibular septum ventral margin (M70): (0) absent; (1) posteroventral margin sutured; (2) posteroventral margin free…"—Meszoely (1970). → This character already considers the information on the absence/presence of the intramandibular septum. Thus, character 171 was kept in the modified matrix whereas character 170 was removed. This character also falls in Type I (B).

Type I A.3. Compound statement coding (new category)

Example: Ch.1- Tail: blue (0)/ red (1)/ short (2)/ long (3)

Each property (color and length) of an anatomical part (locator) under consideration (e.g., tail) belongs to a different character. The conditions in each property are comparable and mutually exclusive (blue vs. red), whereas they are not comparable among the different properties (blue vs short). Failing to recognize this leads to compound characters statements.

Example of this type of character in the examined squamate phylogenies:

(G12) "*Character 572 - Dermal skull bone ornamentation: (0) smooth (Uromastyx aegyptius, dorsal view of skull); (1) lightly rugose about frontoparietal suture (Leiocephalus barahonensis, dorsal view of skull); (2) present over dorsum (Pristidactylus torquatus, dorsal view of skull); (3)*^{N} *present on jugal postorbital bar (Shinisaurus crocodilurus, lateral view of skull)...(ordered).*"—Estes *et al.* (1988)→ States "0"and "1" relate to the ornamentation observed on the osteoderms, whereas states "2"and "3" relate to where such ornamentations are found, therefore represent not mutually exclusive states as they relate to distinct variables.

The exception to this type of problem would be properties that are logically dependent upon others in a multistate character, and which belong to the same transformation series.

Example: Ch.1- Tail: absent (0)/ red (1)/ blue (2)

Despite the absent/present conditions belonging to a different property from the color condition, color can only be scored in taxa in which tails are present, being dependent on the

absent/present property, and belonging to the same transformation series as the latter. Such multistate coding of character may be criticized for secondary reasons, such as its effect on the analysis when secondary absences occur—see Strong & Lipscomb (1999) for further details—but it is not justifiable for such character codings to be excluded from analyses because of the issues presented in my Type I A.3.

Type I A.4. Compound characters (Brazeau 2011)

Example: Ch.1- a tail with blue color, annulated scales and osteoderms: absent (0)/present (1)

This form of coding creates the same kind of dependency among different properties of the same morphological unit as indicated above in the case of "compound statements"—Type I A.3. This results from not recognizing characters as independent transformation series, unless one expects all these conditions to be always found together unconditionally. This would only be justified if these conditions are, in fact, always found together, indicating biological dependency amongst them—an assumption that cannot be confirmed if the analysis includes incompletely preserved fossil taxa lacking complete preservation of all the properties of an inferred combination. Sometimes the author may be wishing to refer to only one of these properties, and not trying to infer any biological dependency, but the extremely long and descriptive character creates lack of precision to which part (locator) or its property is being referred.

Example of this type of character in the examined squamate phylogenies:

(C08) *"Character 6 - Nares, posterior elongation invading contact between prefrontal and nasals or such that they open extensively dorsally (E-2): (0) absent (Fig. 21); (1) present (b)."*— Estes *et al.* (1988) → Both the elongation of the external nares [which by itself falls into Type I (A.7)] and the contact between the prefrontal and nasals are coded within a single character.

Type I A.5. Compound character state coding (new terminology)

Example 1: Ch.1- Tail color: blue or red (0)/ green (1)

My Type 1 A.5. characters are also known as "unifying coding" (Hawkins 2000). In this coding, a single discrete property is being considered (tail color), but more than one condition (each kind of color) is possible within the same character state. This creates artificial states in which two distinct conditions (blue and red) that are mutually exclusive are being conjectured as homologous states instead of distinct ones.

Example of this type of character in the examined squamate phylogenies:

(G12) *"Character 571- Osteoderm ornamentation: (0) vermiculate or smooth (Pseudopus apodus, dorsal view of head and neck); (1) tuberculate (Peltosaurus granulosus, dorsal view of head and neck)...*" **-** Gauthier (1982).

Type I A.6. Multiple character state variables coding (new terminology)

Example 1: Ch.1- Tail: blue and long (0)/ blue and short (1)/ red and long (2)/ red and short (3)

My Type 1 A.6. characters are also known as "A coding" (Pleijel (1995) or "composite coding" (Hawkins 2000). This type of coding also neglects independence among the different character properties (e.g., color and length, in the example above) and interprets them as a single transformation series. The homoplasies in one of the states in the transformation series (such as blue for tail color), will lead to erroneous interpretations of homoplasy in the other condition (tail length).

Example of this type of character in the examined squamate phylogenies:

(C08) "*Character 150 - Basioccipital, spheno-occipital tubercle (NG-23): (0) short and ventrally directed; (1) elongate and posterolaterally directed*"- (Norell & Gao 1997) → The direction of the tubercle is coded as dependent on the length of the same process.

Type I A.7. Unjustified composite locator coding (Wilkinson 1995)

The composite coding of Wilkinson (1995), here re-named as composite locator coding, is usually confused with composite character state coding . However, as an example of this kind of

coding, Wilkinson (1995) used the character 'eye musculature' in caecilians provided by Wake (1993), in which the muscles present in the eye (each being an anatomical part, or a locator) are treated as a character state (condition), whereas in composite character state coding different kinds of conditions (belonging to distinct properties of a part—such as color or shape) are put together under the same character state. Therefore, the present category relates to the usage of multiple anatomical parts (e.g., bones) as part of a single transformation series (see examples below). Composite locator coding often have no theoretical or observational basis to group distinct morphological units under a single character, and are likely to represent a mixture of independent transformation series, such as the ones that consider transformations of multiple bones under a single complex character:

Example 1: Ch1- Eye, musculature, composition: all muscles present (0)/ only the rectus inferior present (1)
Example 2: Ch1- Shape of the orbit: circular (0)/ oval (1)

The shape of the orbit, as well as the temporal fenestrae, external nares, and many other cranial openings, is influenced by modifications in the shape and relative size of each bone that surrounds it, as well as other neighbouring bones (Caldwell 2012). Independent shape changes in any or all elements surrounding an opening, can produce similar phenotypes (e.g., presence of a temporal fenestra), often given the same coding, even though the observable differences would strongly suggest independent origins (Nesbitt 2011; Wilberg 2012). Furthermore, characters using the entire orbit fail the "one-to-one relationship sub-criterion" of the similarity test, as the number and identity of the bones framing the orbit change from species to species [see an equivalent example of the lack of one-to-one relationship using the crista circumfenestralis in the braincase of snakes by Rieppel & Kearney (2002), p. 72]. The consequence is that similar shapes (which are being coded as the same character state) may actually be a consequence of changes in different bones, reflecting distinct evolutionary origins for the same phenotype (i.e. not being homologous). This discussion relates very closely to the arguments presented earlier for recognizing "naïve connectivity" when considering tests within the similarity criterion (a special case where the complex under investigation is represented by only two elements that seem to undergo independent changes in shape and connectivity).

The formulation of such composite locator characters could be defended on the basis that there is biological dependency (integration or correlation) among all the bones involved in such a way that they are co-evolving, and changes in one of them necessarily means a related change in the others, amongst all (or at least the majority) of the sampled taxa in the analysis. However, a wide sampling for the taxa under study would be necessary, as the number and interrelationships of the many subunits forming the skull components vary enormously among taxonomic groups (Monteiro & Abe 1997), and such deep knowledge about sampled taxa is usually absent in phylogenetic investigations.

There are only a few known examples of evolutionary correlation actually supported by empirical evidence (Goswami 2007; Kavanagh *et al.* 2013), and even fewer apply to squamates [but see a development integration study by Monteiro & Abe (1997)]. This fact, along with the principle of one-to-one relationship, indicates it is more parsimonious to assume such characters with composite locators to represent separate transformation series until such correlation is supported by evolutionary integration data. Alternatively, their conjectured dependency should at least not be contradicted by observable independent morphological variation among these parts (or morphological units as a whole) considered within such characters for the sampled taxa. These criteria should be met in order to avoid empty conjectures of homology. Such an approach has already been followed by Nesbitt (2011), who excluded complex characters under his "category 3" for character exclusion in archosaur phylogenies. This same criticism also applies to character coding Type I A.4. and Type I A.6, above.

Biological dependency is likely to occur more frequently in serially homologous characters (i.e. meristic characters—such as vertebral regions), especially because the delimitation of individual domains that are evolving independently in such characters are more difficult to identify (Nixon & Carpenter 2012). Examples include osteoderms, as indicated by Harris *et al.* (2003), by means of a correlation analysis between the characters performed in a phylogeny of aetosaurs by these authors. Such a correlation was found in another set of serial homologues, the phalanges within a single digit, by means of correlation analyses in development for different groups of tetrapods (Kavanagh *et al.* 2013). The last study was important in that the authors also pointed out there is no evidence for such an interaction between the phalanges and metapodials, indicating such dependency is localized and does not apply to the entire limb or even the entire autopodium.

Despite the phalanges constituting a morphological module as inferred from that study, there can still exist exceptions to a generalized model of dependency among its parts. One example is the elongation of the penultimate phalanx as an adaptation for grasping, where the elongation of the penultimate phalanx would have some relative degree of independence from the remaining parts. When such a support, based on biological evidence, exists for a large variety of taxa considered for a phylogenetic analysis, then it is reasonable to consider these anatomical parts as dependent morphologies forming a single character, and a composite locator coding should be more appropriate—Harris *et al.* (2003). Until such information is available for numerous taxa within Squamata, generalizations of this kind will be more likely to bias character constructions and thus the outcome of the analysis. Finally, because of the variety of methods employed to detect such morphological integration among different studies, care should be taken when comparing results from distinct studies (Klingenberg 2008).

Example of this type of character in the examined squamate phylogenies:

(C08) *"Character 2 - Skull, rostrum anterior to the bony external nares (new/extensively modified): (0) short, absent; (1) four tooth positions long or more"* → The entire rostrum is treated as a part that should have some basis for morphological integration among its constituent units (all the bones forming the rostrum). And if there is such integration, then its constituent parts (shape of the bones in the snout) are not independent and should not be treated as separate characters.

In some cases, two distinct structures that may represent independent transformation series are treated as dependent on each other without any support for this assumption. They are different from complex characters with multiple morphological units under consideration, but they are still considered under this same category because of their implicit assumption, even though without explicit basis, of biological dependency between two structures. I include in this category contact characters (as discussed in the "similarity" section above) in which the contacting structures represent independent transformations for which there is no empirical evidence for evolutionary integration:

(G12) "*Character 143- Jugal extent anteriorly with respect to tooth row*^{N}*: (0) jugal broadly overlaps level of posterior maxillary tooth row (Shinisaurus crocodilurus, lateral close-up of*

*anterior skull); (1) jugal overlaps the most posterior maxillary tooth (Heloderma suspectum, lateral close-up of anterior skull); (2) jugal just reaches base of, or stops short of, the most posterior maxillary tooth (Varanus acanthurus, lateral close-up of anterior skull) (ordered)…**There is some uncertainty on that point, however, as H. horridum has fewer maxillary teeth than any other helodermatid (Pregill et al. 1986), so it might be difficult to distinguish "reduction of the anterior extent of the jugal" from "reduction of the posterior extent of the maxillary tooth row" in that species**" [bold added]. → The statement in bold exemplifies the dependency of this character upon two properties for which there is no evidence of dependency: the length of the jugal and the length of the maxillary tooth row, as well as the length of the maxillary suborbital process.

Type I B. Character splitting (new category)

Example: Ch.1- External nares: short (0)/ elongate (1)
Ch.2- Nasal bone: short (0)/elongate (1)

Subsets of the same character (or characters split in two) create mutual logical dependency. The elongation of the external nares is a consequence of the independent elongation of the bones around it (Caldwell 2012), and in squamates most commonly results from the elongation of the nasals, premaxillary bar, maxillae, vomers, palatines, prefrontals, etc. (with an exception in mosasaurs that have lost the nasals). Even if both characters are problem free as elaborated (see above for composite locator characters and below for continuous data), their presence *together* in the matrix violates the principle of logical independence. Clearer-cut examples include series of character states, admittedly belonging to the same character, that are split into multiple characters. This differs from the non-additive binary coding character type because the states amongst the different characters are not necessarily redundant, despite belonging to the same transformation series.

Examples of this type of character in the examined squamate phylogenies:
(G12) Characters 454 – 458:

Character 454- Presacral vertebrae number reduction: (0) 24 or more presacrals; (1) 23 presacrals, Etheridge and de Queiroz (1988); (2) fewer than 23 presacrals. Estes et al. (1988) (ordered).

Character 455- Presacral vertebrae number increase I: (0) 24 or fewer; (1) 25; (2) 26; (3)^{N} 27; (4)^{N} 28 or more. Estes et al. (1988) (ordered).

Character 456- Presacral vertebrae number increase II: (0) 32 presacrals or fewer; (1) 33–39; (2) 50–55; (3) 61–84; (4)^{N} 89 or more. Lee and Scanlon (2002) (ordered).

Character 457- Presacral vertebrae number increase III: (0) less than 104; (1)^{N} 118–132 (2)^{N} 144–156; (3)^{N} 168–180; (4)^{N} 184 or more. Lee and Scanlon (2002) (ordered).

Character 458- Presacral vertebrae number increase IV: (0) less than 193; (1)^{N} 197–209; (2)^{N} more than 219. Lee and Scanlon (2002) (ordered). → The number of presacral vertebrae was split into five different characters, multiplying by five the weight of this transformation series.

Type I C. State accretion (new terminology)

Hawkins (2000) referred to subsets of other states within a single character, creating logical dependency among states, as "logically related coding", However, all characters in Type I A-C suffer the problem of being logically related, so I provide a different terminology.

Example: Ch.1- length of tail: less than 10cm (0)/ more than 10cm (1)/ more than 15cm (2)/ more than 20cm (3).

In the above example, a tail with 18cm should be scored with both states "1" and "2", and a tail with 22cm would be scored with states "1", "2" and "3".

Example of this type of character in the examined squamate phylogenies:

(C08) *"Character 1- Skull, percentage of total length made up by antorbital snout (DBC-2): (0) <30%; (1) >30%; (2) >45%; (3) >50%. The structure of this character allows that it be ordered. Logically, if a snout is 50% of the total skull length, then it is also more than 30% or 45%. The character states used for this character are somewhat arbitrarily delimited, but are*

descriptive. They largely follow the character states put forward in DeBraga and Carroll (1993).”—de Braga & Carroll (1993)→ Even though the authors tried to construct the character in order to make it an ordered one, it would have been more simply done by inputting the information into the software before the analysis. By constructing the character states as performed in this example, a taxon will be scored with two or more redundant states simultaneously. For instance, a taxon with 47% in this ratio should be scored as “1&2”, as it is both above 30 and 45 percent. However, I noticed that taxa in the C08 matrix were actually coded as in segment coding. A taxon with 47% in that matrix was scored as state “2” only, avoiding the redundancy of this coding. However, this creates another problem, which is not scoring taxa in the way the character states are actually described.

Type I D. Conjunction (Patterson 1982)

When two or more structures (locators) occur in the same individual, they cannot be interpreted as homologous.

Example of this type of character in the examined squamate phylogenies:

(G12) “*Character 228- Vomer, descending tubercle (or ridge) at vomero-palatine junction*^{N}*: (0) absent (Pogona vitticeps, oblique ventral view of palate); (1) tubercle present (Celestus enneagrammus, oblique ventral view of palate); (2) ridge/tubercle present on vomer and/or adjacent palatine (Eugongylus rufescens, oblique ventral view of palate).*” → The assumption that the tubercle on the palatine is homologous to the one on the vomer, even though both can co-exist in a single individual, fails the test of conjunction.

The problem with continuous variables

Variables with a continuous range of distribution (such as morphometric variables) have been considered problematic for cladistic analyses for a number of reasons. Among these, there is the difficulty of translating attribute states (the condition seen in each individual) into character states for phylogenetic analyses, as well difficulties of establishing an efficient way to measure such data without biases due to ontogeny or sexual dimorphism. A discussion of such methods in detail is beyond the scope of this study, but recent advances on both problems that are worth

mentioning, include the character coding method for continuous data on the software T.N.T., which can treat continuous variables as ranges and that uses Farris optimization of ancestral states (Goloboff *et al.* 2006). Before the development of that algorithm, character states representing ranges had to be converted into single values, creating biases in character state scoring and limitations towards ancestral node optimization and the treatment of polytomies. For measurement data, Catalano *et al.* (2010), Goloboff & Catalano (2011), and Catalano & Goloboff (2012) proposed a spatial optimization method that seems to be a more accurate way of measuring length variables than previously available models, even though such methods are considered to be more relevant for analyses at low taxonomic levels (Catalano *et al.* 2010).

One of the first methods proposed to code continuous data, segment gap coding, divides continuous data into intervals (e.g., state 0= 1.2–2.5; state 1 = 2.6–3.5) by dividing the total range of the data into the number of states allowed by the software (or any other criterion not related to the actual distribution of the data as seen in nature). However, this requires placement of taxa into arbitrarily delimited states, and has long been considered to be problematic (Simon 1983; Rae 1998). Any such arbitrary state delimitations allow personal biases to affect the outcome of phylogenetic analyses (Kluge & Farris 1969) and is considered here as a problematic type of character construction.

When large gaps are easily recognized for a disjoint distribution of continuous data, then character states can be constructed to represent discrete categories. In this case, particular features may be coded as, for instance, short vs. long or narrow vs. wide, even though pictures or some measurement information would be important to help other researchers in identifying what the authors mean by these discrete categories. The usefulness of discontinuous range distributions for systematics was proposed long ago (Simpson 1937). However, when continuous data is treated as discrete data (and supposedly interpreted as having a discontinuous range of distributions), but authors do not provide at least one statement that these are discontinuously distributed character states—i.e., with no intermediate conditions observed among them in the sampled taxa—then it is possible that such states were defined subjectively. If intermediate conditions exist but they are ignored during the formulation of the character, the criteria used by the author to distinguish between different states are usually arbitrary bins, such as in segment coding procedures. Furthermore, it will also be almost impossible for future workers to include more taxa in this matrix (a very common practice) without knowing how to replicate the original

author's subjective criterion for what is "narrow" or "wide", for instance, and the new taxa might be scored with a criterion different from that of the original author. This makes the replication of the results with the addition of more data difficult to achieve and thus also difficult to falsify. Moreover, the addition of taxa may introduce new intermediate categories that do not clearly fall into any of the previously defined character states.

Type II A - Data treated as continuous with arbitrary state delimitations

Data treated as continuous (referred to as proportions, counted values, length to a reference point, etc.), coded either quantitatively (with numbers) or qualitatively (with words), in which states are delimited arbitrarily or not representing the frequency range for each terminal unit (as in segment coding) should be explicitly avoided in cladistics analyses. In these cases, such arbitrary delimitations may well reflect the authors' personal and *a priori* hypotheses on the grouping of taxa.

Example 1: Ch.1- Bone "X" length (mm): 0-4.9 (0); 5.0-9.9 (1); 10-14.9 (2).

Example 2: Ch.1- Bone "X" length/width ratio: wider than long; as wide as long; longer than wide.

Examples of this type of character in the examined squamate phylogenies:

(C08) "*Character 1 - Skull, percentage of total length made up by antorbital snout (DBC-2): (0) <30%; (1) >30%; (2) >45%; (3) >50%.*" - de Braga & Carroll (1993) → this character also fall into type I (A.4).

(G12) "*Character 10- Premaxilla internasal process length: (0) less than half nasal length (Rhacodactylus auriculatus, dorsal close-up of snout); (1) more than half way to frontal between nasals (Gonatodes albogularis, dorsal close-up of snout); (2) nearly to, or articulates with, frontal (Trogonophis weigmanni, dorsal close-up of snout)…(ordered).*" - Kearney (2003a).

Type II B – Unjustified continuous data treated as discrete

Continuous data treated as discrete (and supposedly interpreted as having a discontinuous range of distributions), but for which authors do not provide at least one statement that these character states have disjoint distributions and can be coded as such.

Example: Ch.1- Bone "X" length: short/long.

Example of this type of character in the examined squamate phylogenies:

(G12) *"Character 14- Premaxilla internasal process size*^{N}*: (0) well developed (Anomochilus leonardi, anterior close-up of snout); (1) very reduced/absent (Atractaspis irregularis, anterior close-up of snout)."* → This is a highly variable trait with many intermediate conditions in terms of relative length of the internasal process, which is nevertheless treated as a discrete trait though, e.g., the continuous range in length of this process as compared between *Gekko gecko, Ophisaurus apodus, Coleonyx variegatus*, *Cordylosaurus subtesselatus* and *Varanus salvator.* A discrete coding scheme is inapplicable to this character.

Type III - Biogeographic characters

Biogeographic characters assume that geographic distributions can be treated as a form of primary homology and tested via congruence with other characters. The basic assumption is that uncertainty in the phylogenetic placement of a taxon may be resolved based on its biogeographic distribution (e.g., two similar African taxa will be placed together rather than with similar Asian taxa if their character state distributions are consistent with their close relationship). However, such assumptions are problematic because in a phylogenetic analysis a biogeographic character is not treated differently than a traditional morphological character driven by a hypothesis of primary homology. This implies that biogeography is not simply used as the final discriminator between competing phylogenetic topologies, but has an effect on the whole analysis and on the reconstruction of character state distributions. Biogeographical characters may also have a negative effect on the reconstruction of phylogenetic relationships of taxa with disjoint distributions. Furthermore, the deeper the phylogenetic analyses go into a clade evolutionary history, the less likely it will be for distinct lineages to retain their biogeographical history due to dispersal and vicariance. Depending on how deep and broad the taxon sampling is, then unlikely homologies may arise: e.g., under a biogeographically defined character for amniote

phylogenies, the South American monkey *Cebus apella* and the lizard *Teius teyou* would share a homology that is not shared with African lemurs or cordylid lizards.

Example of this type of character in the examined squamate phylogenies:

(C08) *"Character 364- Biogeography: (0) global; (1) Madagascar; (2) South America; (3) North America/ Central America; (4) Europe/western Asia; (5) sub-Saharan Africa; (6) northern Africa/Arabia; (7) India; (8) East Asia; (9) Australia".* → This character is present in the character list of Conrad (2008), although it was not actually used by the author in the original analysis of this dataset. Therefore, here I use this character only as an illustration of such a character type.

Type IV- Behavioural characters

Behavioural characters suffer a serious technical limitation as they are only measurable by the observation of the taxa *in vivo*, thus limiting the analysis of taxa represented only by specimens in museum collections or as fossils. More fundamentally, because of the influence of learning, behaviour may reflect local patterns of action by populations. Therefore, isolated populations of the same species may display different behaviours—e.g., Losos *et al.* (2004). Even among sympatric species, such differences can occur, as in the vocalization patterns of sperm whales (Rendell & Whitehead 2003). In addition, the similarity criterion for behaviour is unclear for many such characters, and it would be hard to differentiate, for instance, the burrowing habit of groundhogs and armadillos. Such a perception that these burrowing habits are not due to common ancestry may be obvious to most zoologists, but the matter remains as to how to differentiate them (and many other burrowing behaviours) in terms of the similarity criterion, thus paralleling naïve connectivity. If these were closely related clades and I could not easily distinguish them by means of morphology, the acquisition of burrowing habits would be erroneously used as a synapomorphy for an artificial burrowing clade.

Characterizing behaviour and delimiting possible states is also a complicated matter, perhaps even more so than with morphological continuous traits. One of the reasons is that it depends on the context in which it is analyzed, such as depending on a reference point (e.g., bill pointed to chest) and temporal contexts—e.g., wing-fluttering after bathing is different from after mating (Proctor 1996).

Despite the possibility that certain behaviours seen among species do have a common evolutionary origin, and thus are homologous, there are numerous operational limitations in dealing with those characters and assessing conjectures of homology. It is considered here that these problems currently prevent including behaviour as a source of characters for cladistic purposes.

Example of this type of character in the examined squamate phylogenies:

(G12) "*Character 598- Facial tongue wiping (tongue acts as an accessory eyelid): (0) absent; (1) present (Gekko gecko). Greer (1985b) All scores are pers. obs. J.A. Gauthier.*"

Type V [category 1 of Nesbitt (2011)]. Characters statements with no, little, or vague explanations

Example of this type of character in the referred squamate phylogenies:

(C08) *"Character 223- Dentition, premaxillary teeth compared to maxillary teeth (RZ-156): (0) similar (e.g., Fig. 38A); (1) markedly smaller (e.g., Fig. 38B–D); (2) absent. Note that snakes sometimes lack premaxillary teeth (state 2)."*—Rieppel & Zaher (2000) → The distinction between similar and markedly smaller is not very precise, and leaves great room for subjectivity (i.e., where do I draw the line between 'smaller' and 'markedly smaller'?).

Type VI [category 2 of Nesbitt (2011)]. Problems with the interpretation of the morphology during character construction

Example of this type of character in the examined squamate phylogenies:

(G12) "*Character 103- Parietal contribution to back of the upper temporal fenestra*^{N}*: (0) short supratemporal process, parietal only forms about half of the upper temporal fenestra posterior arch, with* ***supratemporal forming distal half*** [bold added] *(Sphenodon punctatus, dorsal view of skull); (1) long parietal supratemporal process extends distally to near the quadrate head (Sceloporus variabilis, dorsal view of skull)."* → State "0" depends on the supratemporal bone, and was used to characterize rhynchocephalians and *Huehuecuetzpalli* in this matrix. However, this bone is absent in the aforementioned taxa: *Sphenodon,* at least in the adult stage (Rieppel 1992; Jones *et al.* 2011)*, Gephyrosaurus* (Evans 1980), *Kallimodon* and

Huehuecuetzpalli (TRS, pers. obs.). Despite this being a greater issue for taxon scoring, rather than character construction, the misleading character wording affects future research on such matrices.

Type VII [category 4 of Nesbitt (2011)]. Taphonomy biased characters.

These are characters that cannot be used in phylogenetic analyses of fossil taxa. They can be used in cladistic analyses that also include recent taxa, but should be scored as inapplicable to fossil organisms.

Example of this type of character in the examined squamate phylogenies:
(G12) "*Character 79- Postorbital-squamosal suture: (0) firm, suture no wider than those among surrounding elements (Pogona vitticeps, oblique dorsal view of skull); (1) loose, sutural gap wider than that between postorbital and postfrontal, or postorbital and jugal (Uromastyx aegyptius, oblique dorsal view of skull). Arnold (1988). These bones are held together by considerable connective tissue in iguanians generally. In dried skeletal preparations, that tissue shrinks, drawing the two bones together. Nick Arnold found this kinetic joint by manipulating spiritpreserved specimens, but no one studying dried skulls appears to have noticed it. Our discovery of this apomorphy, quite independently of Arnold's insight, was an unforeseen benefit of CT-scanning wet specimens."* —Arnold (1998) → This character depends on soft tissue, and could only be coded for CT scanned wet specimens. Therefore, it should have been scored as inapplicable to fossil taxa in the Gauthier *et al.* (2012), which was not the case. All fossil taxa are here re-scored as inapplicable.

Materials and Methods

Phylogenetic Analyses

In order to detect the effects of characters with problematic constructions and/or coding in the large datasets discussed above, I first re-analysed the original matrices of Conrad (2008) and Gauthier *et al.* (2012) using the "New Technology Search" algorithms in the software T.N.T. (Goloboff *et al.* 2008b). These provide a better way to analyse datasets with a large number of

taxa, especially when combined and analysed together (Goloboff 1999). The only difference in my analysis of either dataset from the original, was that I excluded the OTUs *Parviraptor estesi* and *Parviraptor* cf. *estesi* from the original dataset of Conrad (2008), as it was recently noted that the materials attributed to these fossil squamates are chimeric compositions of distinct lizards and snakes (Caldwell *et al.* 2015). For the matrix of Gauthier *et al.* (2012), a few taxon scoring corrections were made, which have been recently presented by Simões *et al.* (2015a) and Simões *et al.* (2015b)—see also Supplementary Information 5.1 I, IV and V. I then analysed the altered version of these matrices, where all the characters falling in the categories above were removed or recoded (i.e., the states redefined). This second set of analyses using a reduced number of recoded characters are referred to as 'modified analyses', and were performed in order to provide comparative hypotheses to the original cladogram outputs, and thus to further test sister group relationships within Squamata. These modified datasets were first analysed using the original ordering of characters as used by the original authors, and then using all characters unordered (Supplementary Information 5.1 VI-IX).

The matrix of Conrad (2008) originally contained 363 characters and 223 taxa. The analysis of the original dataset, with the exclusion of *Parviraptor* OTUs (resulting in 221taxa), generated a strict consensus tree with most major clades of squamates collapsed at the base of Squamata. The "pruned trees" algorithm in T.N.T. identified three taxa that acted as wild cards in this dataset causing this collapse, and I therefore ran a second analysis without these: *Ardeosaurus*, *Scandensia* and *Slavoia*. The strict consensus of this dataset, and that of the Gauthier *et al.* (2012) dataset (610 characters and 192 taxa), closely corresponds to their original results regarding the general topology of the trees (Figs 2A, and 3A).

After a thorough analysis of both datasets, I identified a large number of characters that fall in at least one of the problematic character categories discussed above. In the matrix of Conrad (2008), 125 characters falling within the above categories were removed, and six other characters were recoded (for a total of 131 characters, or 36% of the original characters). All removed or recoded characters are listed, with comments for justification of their removal or recoding, in the Supplementary Information 5.1 II appended to this study. In both modified analyses of this dataset (as in the original dataset), some fragmentary fossil taxa, as well as a few recent taxa, acted as wild cards to the analysis. Therefore, in the modified (ordered) dataset I removed *Chamops,* FMNH polychrotid, *Igua, Becklesius* and *Necrosaurus cayluxi*. In a second modified

analysis (with all characters unordered—my preferred parsimony model), fewer taxa acted as wild cards, and only FMNH polychrotid, *Igua* and *Becklesius* had to be removed.

In the matrix of Gauthier *et al.* (2012), 243 characters fell into at least one of the problematic character types listed above and were removed from my modified dataset, with another 37 characters being recoded (total of 280 characters being affected, or 45% of the original dataset) —see Supplementary Information 5.1 III. In the modified versions of this dataset, as in the original, no particular taxon acted as a wild card, and the taxon sampling could be kept the same in all of the analyses.

Results

The results of both modified datasets of Conrad (2008)—Figs. 2B and 4A—produced topologies quite distinct from those in the original study. A major clade, Scincomorpha, was found as a paraphyletic assemblage in both ordered and unordered datasets, producing a quite distinct arrangement of the included taxa. In both cases, cordylids and scincids were more closely related to the anguimorph assemblage, a similar topology to the one found by Lee (1998), (Lee & Caldwell 2000) and Lee (2005b), forming the clade Diploglossa. However, in contrast to these studies, the Xantusiidae are at the base of the Autarchoglossa, and not associated with gekkotans. Bainguidae becomes paraphyletic, with *Bainguis* falling at the base of Platynota, along with *Parmeosaurus* (see the complete trees in Supplementary Information 5.1 X). Some other clades also become paraphyletic, such as the fossil family Polyglyphanodontidae *sensu* (Conrad 2008), as *Adamisaurus* falls outside of this group. This suggests that the scoring for this taxon should probably be verified.

In the modified analyses of the matrix of Gauthier *et al.* (2012)—Figs. 3B and 4B—the Mosasauria, a fossil clade of marine lizards of controversial relationships, was found outside of Scleroglossa and close to the base of Squamata, as observed in the original study. However, in the modified analyses, it was recovered with other autarchoglossans, forming a monophyletic group inclusive of snakes, dibamids, amphisbaenians, as well as *Feylinia, Acontias, Anniella* and *Sineoamphisbaena.* A major difference was observed between the ordered and unordered versions of the modified dataset regarding gekkotans. In the modified ordered version of

Gauthier *et al.* (2012) gekkotans are the sister group to all autarchoglossans (Fig. 5.3b), as in most published morphological squamate phylogenies. Nevertheless, in the modified unordered dataset they become paraphyletic (with pygopodids not grouping with other geckoes) and reconstruct as the basal-most members of the monophyletic group inclusive of mosasaurs, snakes and amphisbaenians as just described (Fig. 5.4b). This result was not observed by me in any previously published analysis of Squamata. However, it is somewhat similar to the strict consensus tree obtained by Caldwell (1999, Fig. 1A), where mosasaurs formed a polytomy with snakes, amphisbaenians, dibamids and also gekkotans, at the base of Scleroglossa. Also, gerrhosaurids (*Zonosaurus* and *Cordylosaurus*) and anguids (*Helodermoides, Peltosaurus, Elgaria, Celestus,* and *Pseudopus*) form paraphyletic assemblages (Fig. 5.4b). The former being found as stem taxa leading to Scincidae, whereas the latter are found as stem anguimorph taxa leading to Platynota.

Discussion

The criticisms I have raised above do not relate to specific morphological structures or their properties, but rather, strictly to the way they were coded into characters and character states. I recommend that approaches to character state assessment and character constructions, such as segment coding (utilized for a large number of characters in both matrices under evaluation, either in a quantitative or a qualitative way—see comments above) should always be avoided in morphology-based analyses. If not, such approaches risk creating subjective delimitations of transformation series into arbitrary states that are not based on the distribution of the property (or variable) of that feature (or locator), but rather risk reflecting taxonomic preconceptions of how the taxa under consideration "should" be related. For instance, Gauthier *et al.* (2012, p. 9) mention how an increase in presacral vertebral count from 24 to 26 diagnoses a major squamate clade, Scleroglossa. A preconception of a monophyletic Scleroglossa may have led to Conrad's character 236, where the proposed states are: (0) 25 or fewer; (1) 26; (2) 27 or more, despite the much greater range of variation in presacral number among squamates. This character exemplifies very well how this idea has become entrenched into the conceptualization of vertebral count numbers (and numerous other characters that imply taxonomic preconception),

thus preventing the discovery of alternative scenarios for axial skeleton evolution in squamates and other lepidosaurs.

Some characters that are clearly dependent on each other have been created via limitations of the software in assessing a large number of character states—see Gauthier *et al.* (2012, p. 9). However, splitting a transformation series, such as vertebral counts, into five different characters (Gauthier *et al.* characters 454—458) is equivalent to placing more weight on such characters (e.g., a taxon that shows body elongation will be scored for it five times). Therefore, if an analysis is to attempt to minimize its taxonomic preconceptions and *a priori* character weighting, then it is better not to include such characters, or they will be adding undesirable (and yet avoidable) noisy data into the data matrix and its results as a consequence.

It should be noted that the reduction in the number of characters did not result in an overall decrease of resolution of the strict consensus trees obtained by us. In the modified analyses of the data matrix of Gauthier *et al.* (2012), the strict consensus tree obtained from the dataset with the original ordering of character states had well resolved clades, and a slightly better resolution for Iguania (see Supplementary Information 5.1 XI). The unordered dataset had a decrease of resolution for the clade Serpentes, but the resolution within Iguania was, once again, improved. When reanalysing the original matrix of Conrad (2008) with the removal of the chimeric *Parviraptor* OTUs, the dataset became more inconsistent. In preliminary analyses, I noticed that the removal or addition of other taxa also had similar effects on the relationships of many of the individual fossil terminal taxa. Yet, these taxon additions/removals did not alter the overall configuration of the MPTs and strict consensus trees, and the major monophyletic groups retrieved in the original study were still obtained. Only the removal or recoding of problematic character types in that matrix eventually led to significant changes in the final outcome of both datasets.

Conclusions

Summary of recommendations

Not too surprisingly, as it is yet a youthful paradigm shift, modern phylogenetic systematics is still evolving to improve on the lack of precision, rigor, and objectivity it inherited from the pre-cladistic period. Furthermore, transforming a descriptive science (morphological description)

bounded by language as a means of outlining empirical observations into hopefully objectively delimited characters and character states is a difficult task; every effort to do so is to be commended, while at the same time rigorously scrutinized and improved upon. It is only possible for morphological phylogenetic analyses to move away from being a tool of subjective taxonomic and phylogenetic preconceptions if I develop, and expect others to use, a suite of powerful tools for constraining character construction, coding and scoring.

I have identified four basic operational rules for the construction of good characters, and accurate coding and scoring, but note there may well be more: (A) Utilization of as many similarity sub-criteria as possible in order to create characters that are more likely to reflect similarity due to recency of common ancestry; (B) Avoidance of logically inconsistent character construction, such as logically dependent characters, exemplified by my character type series I A; (C) Take into consideration previous studies suggesting possible biological dependency/independency among distinct morphological attributes used as characters; (D) Acknowledge that continuous variation is widespread in nature and that such data must be treated as such. In the case of phylogenetic analyses, measurement characters must not be treated as discrete when there is a continuous range of variation. When there is evidence for a disjoint distribution of data, and authors wish to treat them as discrete, a clear statement must be made supporting the disjoint nature of that data.

Final considerations and future directions

The modified versions of Conrad (2008) and Gauthier *et al.*'s (2012) matrices do not provide revised phylogenetic hypotheses that I claim to be "fixed" or "superior" versions of the same—that would also require a reanalysis of the scorings performed for all terminal taxa that are well beyond the goals of this study. In addition, these results still reflect the original authors' notions of primary homologies for many characters. My main goal was to identify general problems with character conceptualizations and constructions for morphological characters for all morphological datasets, and then to identify these problematic characters within my area of expertise, specifically studies of squamate phylogeny. The results of this study provide a different perspective of squamate relationships and indicate how specific issues with character construction may deeply affect my current notion of the squamate tree of life.

It is important to acknowledge that the majority of the characters removed or modified from the squamate matrices under consideration above (i.e., Conrad, 2008; Gauthier *et al.*, 2012) had been incorporated from characters constructed in numerous other studies. Many of these were first proposed by most of the previous analyses of Squamata and/or of major squamate clades, including some of my own: e.g. Estes *et al.* (1988), Frost & Etheridge (1989), de Braga & Carroll (1993), Evans & Chure (1998), Lee (1998), Caldwell (1999), Rieppel & Zaher (2000), among others. This indicates that the problems of character constructions as discussed here are inherent to most of my current notions of character construction methods for squamate cladistic analyses. Furthermore, the development of the first species-level squamate phylogenetic analyses, a more representative taxon sampling of a diverse number of squamate families (living and extinct), and integration with molecular data—e.g. Pyron *et al.* (2013), and Reeder *et al.* (2015)—have provided valuable contributions to better understand the squamate tree of life. Yet, some effort should be put into rethinking squamate characters, as was recently initiated for archosaur phylogenies by Nesbitt (2011) and for crocodilomorphs by Wilberg (2012). Only the recognition and identification of these issues during character construction and the positing of primary homology statements will allow a more accurate expansion of existing datasets. The analyses provided here, including the comments for every problematic character in both matrices, represents a necessary first step towards my goal of better understanding squamate relationships.

Importantly, the results obtained here urge caution during the compilation of characters for the construction of morphological datasets, especially when "giant data matrices" are the ultimate goal. The notion that morphological, or phenomic data in this case, need to be codified on a "…*scale comparable to that for genomic data*…" (O'Leary *et al.*, 2013 – p. 662) is flawed. Reasoned and logically constructed character statements and concepts, regardless of number, will always be superior to large numbers of poorly constructed characters. Some molecular datasets are already comprised of complete genomes, both nuclear and mitochondrial, thus numbering in the tens of millions of base pairs for a single taxon (dos Reis *et al.* 2012; Jarvis *et al.* 2014; Misof *et al.* 2014). It is highly unlikely that there will ever be a sensible method to reduce morphological homology statements (characters and states) to an order of magnitude even remotely similar to that of sequence data. Furthermore, it has been already shown that morphological characters, despite their relatively small number, can have a considerable effect

on the retrieved phylogeny when combined with molecular data in total evidence analyses, including in squamate analyses (Reeder *et al.* 2015). It is more likely that, in an attempt to achieve such vast numbers of morphological characters, problematic characters based on extreme fragmentation or artificial coding of morphological characters will be created.

Morphological data can help in resolving deep nodes or branching patterns in fast evolving areas of a tree (Beutel *et al.* 2011) and solve relationships that cannot be considered by genomic data. Besides, it is fundamental to analyses of large groups (e.g. Amniota, Arthropoda) composed of numerous extinct clades, as well as to the analyses of clades comprised solely of fossil taxa (e.g. non-avian dinosaurs, pterosaurs, mosasaurs). However, in order to provide a contribution to these fields of study, morphological characters must be based on solid construction and coding methods in order to obtain the best possible approach towards establishing primary homologies. I suggest that authors and editors should scrutinize criteria for morphological character constructions in both small and large datasets for problematic constructions similar to those identified herein for squamate phylogenies.

Supplementary Information 5.1

Supplementary Information 5.1 I-XI (including all individual character comments) is available online at: http://onlinelibrary.wiley.com/doi/10.1111/cla.12163/full

Figures and Tables

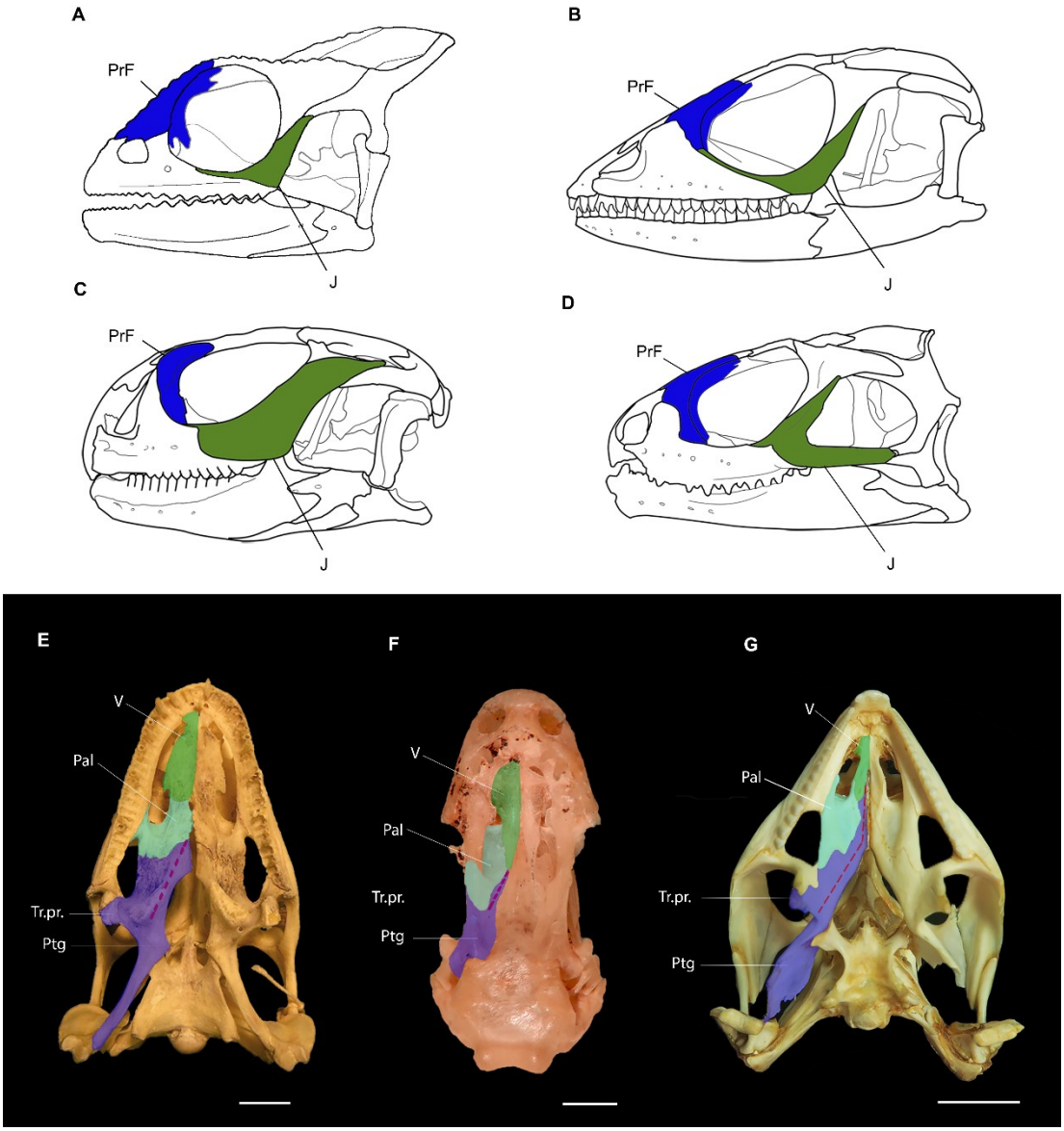

Fig 5.1. Comparisons between the different kind of contact between the jugal (green) and the prefrontal (blue) bones in some lizards. (A) *Chamaeleo laevigatus*, (B) *Polychrus marmoratus* and (C) *Uromastyx aegyptius,* (D) *Sphenodon punctatus.* Comparisons between the different bone elongations leading to the formation of the pterygoid-vomerine contact in squamates in (E) *Iguana iguana* (CM 125934), (F) *Rhineura floridana* (MCZ R-5515) and (G) *Uromastyx acanthinurus* (MCZ R-2782). Abbreviations: J, jugal; Pal, Palatine; PrF, prefrontal, Ptg, pterygoid; Tr.pr., transverse process of the pterygoid; V, vomer. Scale bars = 10mm (E and G) and 1mm (F).

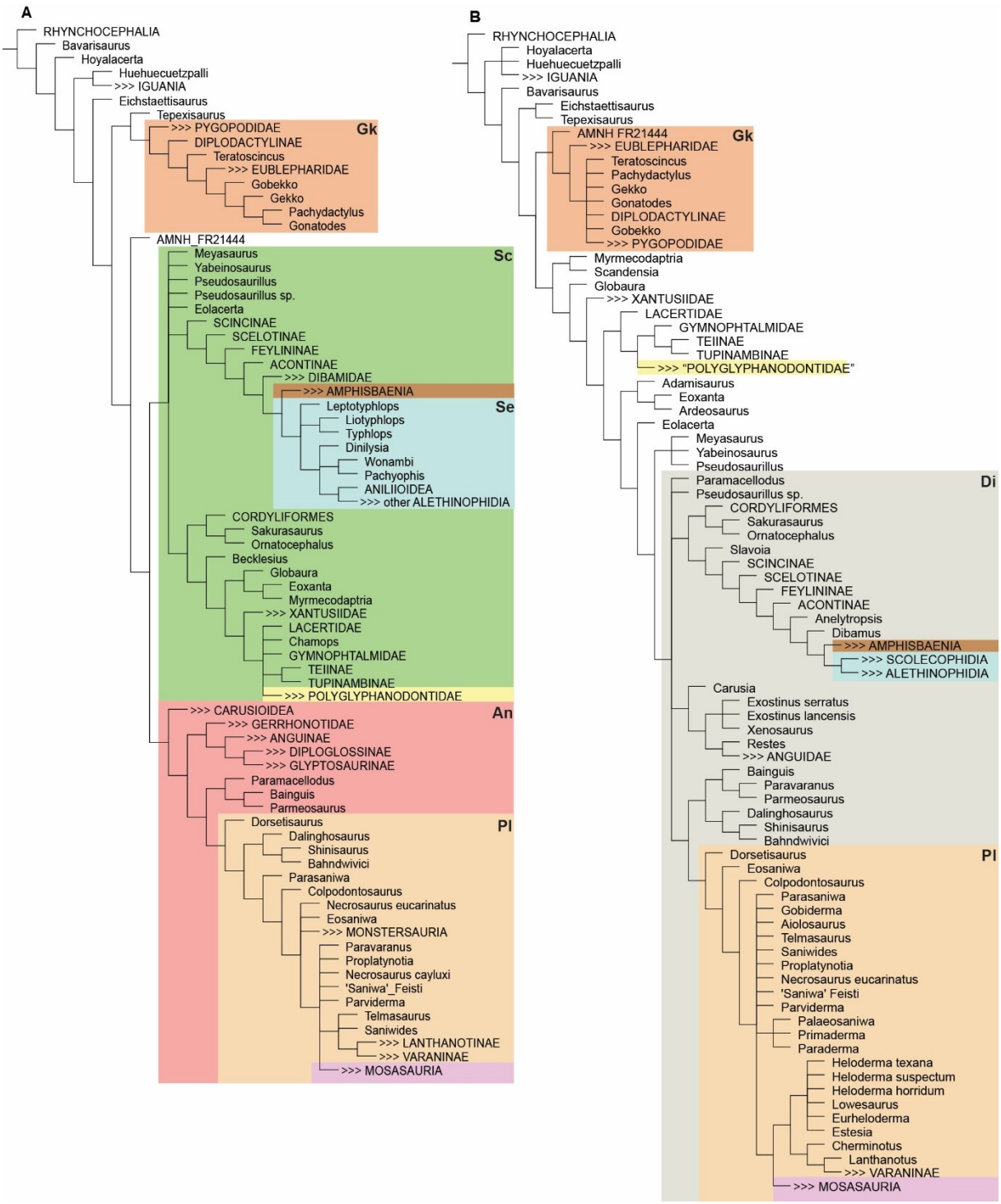

Fig 5.2. Phylogeny of the Squamata based on the matrix of Conrad (2008) utilizing (A) the original dataset (see text for details)—strict consensus tree of 52,682 MPTs of 3,199 steps each (consistency index [CI] = 0.156; retention index [RI] = 0.720); and (B) the modified version of the dataset, keeping the original ordering of character states – strict consensus tree of 78,313 MPTs of 1,726 steps each (CI = 0.146; RI = 0.702). Clades were condensed to allow for easier comparisons between results. For the entire trees, see Supplementary Information 5.1 X. The following clades are denoted: Amphisbaenia (brown); Di, Diploglossa (gray); Gk, Gekkota (light orange); Mosasauria (purple); Polyglyphanodontidae (yellow)—*sensu* Conrad (2008); Pl, Platynota (beige); Sc, Scincomorpha (green); Se, Serpentes (cyan).

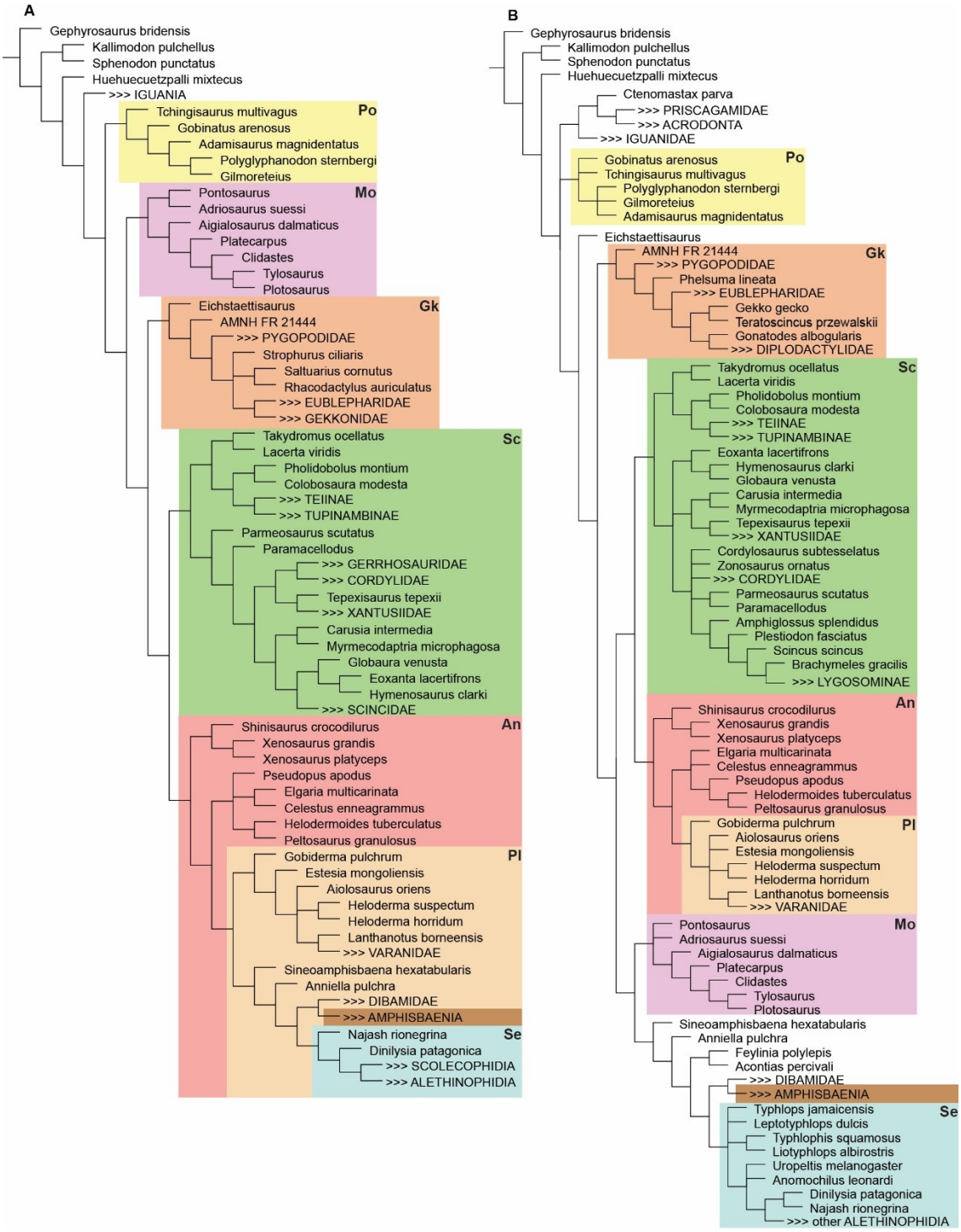

Fig 5.3. Phylogeny of the Squamata based on the matrix of Gauthier *et al.* (2012) utilizing (A) the original dataset—strict consensus tree of 142 MPTs of 5,291 steps (CI = 0.201; RI = 0.771) and (B) the modified version of the dataset, keeping the original ordering of character states – strict consensus tree of 45,170 MPTs of 2,476 steps each (CI = 0.194; RI = 0.767). Clades were condensed to allow for easier comparisons between results. For the entire trees, see Supplementary Information 5.1 XI. The following clades are denoted: Amphisbaenia (brown); Gk, Gekkota (light orange); Mo, Mosasauria (purple); Po, Polyglyphanodontia (yellow)—*sensu* Gauthier *et al.* (2012); Pl, Platynota (beige); Sc, Scincomorpha (green); Se, Serpentes (cyan).

Fig 5.4. Phylogeny of the Squamata based on the matrix of Conrad (2008) utilizing (A) the modified version of the dataset, and making all character states unordered—strict consensus tree of 77,653 MPTs of 1,713 steps each (CI = 0.146; RI = 0.702); and (B) based on the matrix of Gauthier *et al.* (2012) utilizing the modified version of the dataset, and making all character states unordered - strict consensus tree of 49,365 MPTs of 2,359 steps each (CI = 0.194; RI = 0.767). Clades were condensed to allow for easier comparisons between results. For the entire trees, see Supplementary Information 5.1 X and XI. Clades colors and abbreviations are the same as in figs. 2 and 3.

Table 5.1. Problematic types of character construction in morphological datasets

Type			Name	Description
I	A	1	Non-additive binary coding	Each state becomes a different character creating redundancy
		2	Absence coding	Extra weight for the "absent" condition creating redundancy
		3	Compound statement coding	Multiple non-dependent properties as distinct states under the same character (exception: gain/loss of the structure)
		4	Compound characters	Multiple non-dependent properties implicit in character description
		5	Compound character state coding	Alternative distinct non-dependent properties under the same state
		6	Multiple character state variables coding	Two or more non-dependent properties together under the same state
		7	Unjustified composite locator coding	Multiple anatomical elements with no evidence to be treated as having evolutionary integration under the same character
	B		Character splitting	Single transformation series broken into two or more
	C		State accretion	One state includes the other states
	D		Conjunction	Two or more structures occur in the same individuals and are treated as homologous (exception: serial homologs)
II	A		Data treated as continuous with arbitrary state delimitations	Data treated as continuous, coded either quantitatively or qualitatively, in which states are delimited arbitrarily or not representing the frequency range for each terminal unit (e.g. segment coding)
	B		Unjustified continuous data treated as discrete	Continuous data treated as discrete but with no disjoint distribution of its character states
III			Biogeographic characters	
IV			Behavioural characters	
V			Characters statements with no, little, or vague explanations	Character descriptions or character states that are ambiguous and likely to result in distinct scoring of taxa depending on the author.
VI			Problems with the interpretation of the morphology during character construction	Misinterpretation of the identity of the structure (locator) being coded
VII			Taphonomy biased characters	Characters that are easily altered during transportation or diagenesis of organic remains during the fossilization process; or may have different states when comparing a fresh specimen to a dry or fossil specimen.

CHAPTER SIX: DIAPSID PHYLOGENY AND THE ORIGIN OF SQUAMATES

[The contents of this chapter have been accepted for publication as Simões, Caldwell , Tałanda, Bernardi, Palci, Vernygora, Bernardini, Mancini & Nydam. The Origin of Squamates Revealed by a Middle Triassic Lizard from the Italian Alps. *Nature.* (publication expected on April 2018)].

Introduction

Modern squamates (lizards, snakes and amphisbaenians) are the world's most diverse group of tetrapods along with birds (Uetz & Hošek 2017) and have a long evolutionary history, with the oldest fossils known from the Middle Jurassic—168 million years (MY) ago (Nessov 1988; Fedorov & Nessov 1992; Evans 1998). The evolutionary origins of squamates is contentious because of several issues: (1) a ~70 MY fossil gap between the oldest known fossils and their estimated origin (Jones *et al.* 2013; Irisarri *et al.* 2017; Pyron 2017), (2) limited sampling of squamates in reptile phylogenies, and (3) conflicts between morphological and molecular hypotheses regarding the origin of crown squamates (Reeder *et al.* 2015; Pyron 2017; Simões *et al.* 2017b). Here, I shed light on these problems by using high resolution micro-computed tomography data from the articulated fossil reptile *Megachirella wachtleri* (Middle Triassic, Italian Alps (Renesto & Posenato 2003)). I also present the largest phylogenetic dataset ever assembled, combining fossils and extant taxa, and morphological and molecular data, analyzed under different optimality criteria to assess diapsid reptile relationships and squamate origin. My results re-shape diapsid phylogeny and present evidence that *M. wachtleri* is the oldest known stem squamate. *Megachirella* is 75 MY older than the previously known oldest squamate fossils, partially filling the fossil gap in the origin of lizards and indicates a more gradual acquisition of squamatan features in diapsid evolution than previously thought. For the first time, morphology and molecular data are in agreement regarding early squamate evolution, with geckoes as the earliest crown clade squamates (not iguanians). Divergence time estimates using relaxed morphological-molecular clocks show that lepidosaurs and most other diapsids originated before the Permian-Triassic extinction event, indicating the Triassic was a period of radiation, not origin, of several diapsid lineages.

Materials and Methods

Taxonomic sampling criteria

All taxa included in the phylogenetic analyses herein were personally observed by me for the collection of morphological data, during the period of nearly 400 days of collections visits in museums and universities around the world during the course of five years. Only one species was

assessed based on information and data personally collected by my supervisor (Michael Caldwell), namely *Pachyrhachis problematicus*.

All taxa were scored by me, and over 75% of taxa were scored in the data matrix while observing the specimens in their respective collections. In my experience, this practise increase efficiency and accuracy during data scoring by depending less on the information provided by anatomical drawings, pictures, personal notes and the availability of CT scan data.

Broad level relationships among the major groups of reptiles remain unresolved, with many conflicting hypotheses proposed during the last decades, and quite disparate proposals for the internal composition of the Lepidosauromorpha (Benton 1985; Evans 1988; Laurin 1991; Caldwell 1996; Gower 1996; Rieppel & de Braga 1996; Motani *et al.* 1998; Lee 2001; Müller 2004; Hill 2005; Scheyer *et al.* 2017; Turner *et al.* 2017). Therefore, any assumptions regarding the internal composition of the Lepidosauromorpha would be necessarily based on a preference over one of such competing hypothesis. Therefore, I sampled diapsid reptile lineages from every major group of diapsids, including at least two (usually three or more) species from each of them: Araeoscelidids, "younginiforms", coelurosauravids, turtles, ichthyopterygians, sauropterygians, saurosphargids, thalattosaurs, "protorosaurs", kuehneosaurids, archosauriforms, rhynchosaurs, besides lepidosaurs (rhynchocephalians and squamates).

Importantly, all of the diapsid datasets above mentioned suffer from the two following caveats. Firstly, squamates, which comprehend over 10,000 extant lineages and hundreds of fossil ones over the past 250 million years are usually, are almost invariably represented as a single terminal taxon (Squamata). This extreme oversimplification on the diversity of morphotypes and genotypes within squamates is likely to affect what other diapsid lineages fall closer to squamates within lepidosauromorpha, and the overall composition of lepidosauromophs too. The only exception to this case that is known to me is the study of Hill (2005), which includes some squamate taxa at the species level. However, most of the taxa used in that study are from the same clades (mostly scincids, anguids and cordylids), thus still lacking many important lineages, including the putative earliest evolving crown squamates (iguanians, geckoes and dibamids—see more below), as well as snakes and amphisbaenians.

Secondly, there is no consensus on which squamate clade represents the earliest evolving squamate lineage. Thus far, all broad level analyses of squamate relationships using only morphological data have suggested iguanians are the earliest evolving crown group squamates

[e.g. (Estes *et al.* 1988; Lee 1998; Lee & Caldwell 2000; Evans *et al.* 2005; Conrad 2008; Gauthier *et al.* 2012; Simões *et al.* 2015a)]. However, the molecular signal has always indicated geckoes and dibamids to represent the earliest evolving forms (Townsend *et al.* 2004; Vidal & Hedges 2005; Hugall *et al.* 2007; Kumazawa 2007; Vidal & Hedges 2009; Wiens *et al.* 2010; Wiens *et al.* 2012; Pyron *et al.* 2013). Combined evidence studies have also suggested the earliest squamates to be geckoes and dibamids, likely because of the overwhelming influence of molecular characters, which are usually far greater in number than morphological characters (Wiens *et al.* 2010; Reeder *et al.* 2015; Pyron 2017), apart from one study known to me (Lee 2005a), which yields a similar result to morphological data, but also has far less molecular loci than more recent combined evidence studies. Therefore, selecting a single crown group to represent the entire Squamata is also not trivial.

To address the two limitations above, I decided to include at least one taxon from every major squamate clade, including iguanians, geckoes, cordylids, scincids, lacertids, teiioids, anguids, varanoids, snakes, dibamids and amphisbaenians. I have also included numerous important fossil taxa that represent entirely extinct lineages (e.g. *Adriosaurus suessi*—dolichosaurids*, Aigialosaurus*—mosasauroids, *Gilmoreteius chulsanensis*—borioteiioids, *Priscagama gobiensis*—priscagamids)*,* and other taxa that represent some of the oldest known fossils of their clades (e.g. *Igua minuta*—iguanians, *Spathorhynchus fossorium*—crown amphisbaenians*, Najash rionegrina*—snakes), and representing some of the oldest and most complete squamates that were known up to date (e.g. *Eichstaettisaurus schroederi, Ardeosaurus brevipes, Paramacellodus oweni,* and *Huehuecuetzpalli mixtecus*).

Outgroup choice

Considering the vast representation of diapsid lineages in the current dataset, I included four early reptiles (*Protorothyris archeri* and the captorhinids *Protocaptorhinus pricei*, *Captorhinus aguti,* and *Labidosaurus hamatus*) to contribute to the polarization of characters and divergence time estimates. I chose *Protorothyris archeri* as the designated outgroup for TNT, which allows testing the placement of the other three taxa and thus the outgroup composition. In all these analyses, the four early reptiles were consistently found as outgroups to diapsids, as in all other reptile phylogenies they have been included thus far that are known to us, supporting their choice as outgroups. For Bayesian inference analyses in Mr. Bayes, I kept my ingroup monophyletic

(important for appropriate divergence time estimates and reaching stationarity in reasonable amounts of time, which is especially lengthy for clock analyses), and designated *Protorothyris archeri* as the outgroup.

Non-included, or partially included taxa

Lepidosauromorphs and other taxa from the Late Olenkian (Early Triassic), Czatkowice 1 Quarry, Kraków Region, Poland

Materials previously attributed to *Pamelina polonica*, *Sophineta cracoviensis, Czatkowiella harae* and *Osmolskina czatkowicensis,* all come from the exact same quarry, which represents an accretion deposit. The cranial elements associated to each taxon can be identified based on size and, most importantly, bone articulatory facets, which allow the reconstruction of the skull by a stepwise process of study of each cranial element. However, the same cannot be performed for the postcranial remains. The multiple vertebral and other postcranial elements found in the Czatkowice 1 quarry overlap in size, and numerous aspects of their morphology. Additionally, articulatory facets cannot be used to indicate their association with the cranial remains. Although it is clear they belong to separate taxa, attributing isolated postcranial elements to isolated cranial remains from the same quarry is problematic. Therefore, at least for the taxa that were personally observed (*Pamelina*, *Sophineta* and *Czatkowiella*), there is no sensible way of attributing postcranial remains to the cranial elements, thus only information derived from cranial elements were included in the present dataset.

Even among cranial elements associated to the taxa above, there is either some high degree of intraspecific variation, or some taxonomical mixing among those elements may occur. Yet, these variations would not affect the scorings for the characters used in the present dataset, as they are mostly variations in relative proportions. Therefore, I utilized the personally collected cranial data for from *Pamelina polonica* and *Sophineta cracoviensis*, but not their postcranial elements for the reasons just presented. Additionally, I did not include information from *Czatkowiella harae*. Even among cranial remains (e.g. dentaries), there is a considerable overlap on morphology to some other taxa from the Czatkowice fauna. I preferred to be cautious and disconsider this taxon for the present dataset.

Czatkowiella harae (Borsuk–Białynicka & Evans 2009) has some elements that seem to be unique and clearly different from other taxa from Czatkowice 1 (e.g. premaxillae, frontals and

parietals), other bones are indistinguishable from the ones attributed to other taxa, especially *Pamelina polonica*, such as the dentaries, and other bones bear only very minor detectable differences (e.g. maxillae). It is considered herein that *Czatkowiella* might be a true taxonomic unit based of some of the unique elements, but materials currently assigned to it are a composite of multiple taxa.

Lepidosauromorphs from the Late Triassic fissure sediment deposits of South West Britain

These include *Gephyrosaurus bridensis* Evans, 1980 (Pontalun and Pant quarries), *Diphyodontosaurus avonis* Whiteside, 1986 (Tytherington Quarry), *Planocephalosaurus robinsonae* Fraser, 1982 (Cromhall Quarry), and *Clevosaurus hudsoni* (Swinton, 1939) (Cromhall Quarry). Most of these taxa are comprised of dissociated materials coming from accretion deposits. Among these, *Gephyrosaurus* and *Diphyodontosaurus* come from different quarries from each other, and from the other lepidosauromorphs from South West Britain. The cranial elements personally observed for these taxa match in terms of articulatory facets and do suggest only one taxon is represented among the studied materials from the Pontalun and Pant quarries. Some specimens from this quarry also have been attributed to *C. hudsoni* (Evans & Kermack 1994), but comparisons of the studied material to articulated remains of *C. hudsoni* (see below) indicate they differ from the latter species. In Tytherington Quarry, other elements which may belong to *Planocephalosaurus* have been identified, but the vast majority of available cranial specimens belong to *Diphyodontosaurus*, and elements from both taxa could be separated in terms of discrete morphological characters and size.

The materials from Cromhall quarry, however, are more difficult to sort out into separate taxa. Each site (fissure deposit) within the quarry was filled by sediments during different periods of time, and seemingly quite fast in each event. Thus the taxonomic composition in each site of Cromhall is quite unique, showing different proportions of taxa being found (Walkden & Fraser 1993). However, faunal assemblages obtained from continuous successions (different levels) within each site are nearly identical (Fraser & Walkden 1983; Walkden & Fraser 1993; Fraser 1994), probably owing to the speed of sediment filling in each site. Additionally, the multiple taxa found in each site have undergone considerable reworking, and the individual elements have been mixed. Therefore, taxonomic assignment of the materials from Cromhall when based only on the stratigraphic position within each site of the available materials is

problematic. Although the taxonomic assignment of cranial material is facilitated by bone to bone comparison of articulatory facets, bone texture, and comparison with articulated materials from other localities (e.g. *Clevosaurus hudsoni*), the same cannot be performed for the dissociated postcranial elements. The lack of any anatomical connection between these cranial and postcranial body parts in the preserved specimens prevents any morphologically meaningful basis of comparison and thus taxonomic assignment. Additionally, the large number of similarities in the postcranial morphology of the sphenodontids found at each site (e.g. most materials from *Planocephalosaurus* occur at a site where elements attributed to *Clevosaurus* and *Diphyodontosaurus* also occur), further complicates an appropriate sorting of these postcranial elements into each taxon. Therefore, as performed for the Czatkowice quarry material from Poland, I have only considered information from the cranial remains of *Planocephalosaurus*. Regarding *Clevosaurus hudsoni*, the articulated material that includes cranium and postcranium (UMZC T1271) as well as the articulated skulls (NHMUK R604, NHMUK R605, and UMZC T1269) were used as the main basis of comparison to establish which of the isolated bones (cranial and postcranial) can be confidentially associated to *Clevosaurus hudsoni.*

Lepidosauromorphs from the Middle Jurassic of the Old Cement Works Quarry, Kirtlington, Oxfordshire, United Kingdom.

Among the taxa of interest herein, the holotype of *Marmoretta* and materials assigned to *Cteniogenys* sp. have been recovered from Kirtlington (Evans 1990; 1991a; Evans & Milner 1994). Interestingly, there is a similar faunal composition of this site to the Bathonian sites at the Isle of Skye (Waldman & Evans 1994; Evans & Waldman 1996). Despite the wealth of data from this site, the isolated and reworked nature of most preserved elements (similarly to the other faunal assemblages above) indicate caution is necessary during taxonomic assignment of the preserved materials. For instance, multiple elements displaying quite distinct dentary morphologies have been attributed to *Marmoretta* (Evans 1991a, fig. 14 A and D). Additionally, some vertebral elements that have been assigned to *Marmoretta* are in fact more similar to elements previously attributed to *Cteniogenys* sp (which also comes from the same quarry), due to the presence of a notochordal canal and a sharp midventral keel (NHMUK R12404). Although many elements can be definitely attributed to the same taxon, especially regarding tooth bearing elements and other bones that can be connected to them through articulatory facets, this is not the case for postcranial elements (see also comments for other faunal assemblages above).

Fortunately, cranial and postcranial remains of *Marmoretta* found in association from the Bathonian localities in Skye provide valuable information concerning the identity of cranial and postcranial material to this taxon.

Many elements from the Kirtlington fauna have been attributed to the choristodere *Cteniogenys*, and provide most of the available information for that genus (Evans 1989; Evans 1990; 1991b). *Cteniogenys* is only known from disarticulated and mostly dissociated elements, that span from the late Bathonian (Middle Jurassic) of Kirtlington and Isle of Skye in Britain to the mid-Campanian (Late Cretaceous) of Alberta. Additionally, numerous elements attributed to the genus, even the ones that are most easily comparable to each other (tooth bearing elements) display a variety of morphologies, such as variations in tooth shape, crown striation, and high of the lingual wall of the dentary. Such variation occurs even among elements found in the same localities, such as the Kirtlington fauna. Therefore, this genus is in great need of revision. As for the case of *Czatkowiella harae* from Poland (see above), materials attributed to this taxon are considered herein to be uninformative for a species-level phylogeny, due to the likely presence of more than one taxon among the referred specimens, with some potential mix of lepidosaurian elements into it.

Lepidosauromorphs from the Late Jurassic-Early Cretaceous Purbeck Limestones Formation in Durdlestone Bay, Swanage, Isle of Purbeck, Dorset, United Kingdom.

There is a variety of squamates from the Purbeck Limestones, including *Paramacellodus oweni, Pseudosaurillus purbeckensis, Dorsetisaurus purbeckensis, Parviraptor estesi,* and *Becklesius hoffstetteri.* However, the numerous small limestone blocks include a variety of allochtonous materials, and taxonomic assignment can be somewhat problematic. Whereas *P. oweni* is represented by a large number of specimens, including blocks with cranial and postcranial material in association and in partial articulation (suggesting they can be all be assigned to a single taxon with some confidence), that is not the case for the other taxa. The blocks containing *Parviraptor estesi* have already been demonstrated to include elements from other squamate taxa, and non-squamatan reptilians (Caldwell *et al.* 2015). This may also be the case for *Dorsetisaurus purbeckensis,* which is known from few referred specimens and for which the holotype is represented by a block containing highly disarticulated materials. These indicate the materials have been carried for some distance, and/or were under the influence of high energy fluxes which contributed to their disarticulation and mixing. Therefore, it is quite possible

materials associated to *D. purbeckensis* may include materials from more than one taxon. This is especially the case for the skull elements that have been found in isolation (e.g. frontals). For the above reasons, only *P. oweni* is considered from that faunal assemblage in the current dataset.

Microfocus X-ray computed tomography (µCT)

The holotype of *Megachirella wachtleri* was analysed by microfocus X-ray computed tomography (µCT) at the Multidisciplinary Laboratory of the "Abdus Salam" International Centre of Theoretical Physics (Trieste, Italy), using a system specifically designed for the study of paleontological and archaeological materials (Tuniz *et al.* 2013). The µCT acquisition of the complete specimen was carried out by using a sealed X-ray source (Hamamatsu L8121-03) at a voltage of 150 kV, a current of 100 µA and with a focal spot size of 20 µm. The X-ray beam was filtered by a 1.5 mm-thick aluminium absorber. A set of 2400 projections of the sample were recorded over a total scan angle of 360° by a flat panel detector (Hamamatsu C7942SK-25) with an exposure time/projection of 2.0 s. The resulting µCT slices were reconstructed in 16-bit format using the commercial software DigiXCT (DIGISENS) and an isotropic voxel size of 42.51 µm. Additionally, the proximal part of the sample was re-analysed (voltage 150 kV, current 100 µA, 1 mm copper filter, exposure time/projection 3.0 s and 1800 projections over 360°) setting an effective pixel size of 18 µm and reconstructed using the same software in order to achieve an higher spatial resolution.

Methodological criteria for character construction

The characters created herein specifically try to incorporate homology statements that support each of the morphological attributes used herein as morphological characters. In order to achieve this, my primary homology hypotheses follow the basic criteria of homology assessment for character construction presented in numerous previous studies (e.g. Patterson 1982; Hawkins *et al.* 1997; Lee & Bryant 1999; Strong & Lipscomb 1999; Forey & Kitching 2000; Rieppel & Kearney 2002; Freudenstein 2005; Kearney & Rieppel 2006; Rieppel 2006; Sereno 2007; Brazeau 2011; Simões *et al.* 2017d). These criteria have been followed herein in order to minimize character constructions that provide weak primary homology statements (i.e. character

types that fail basic criteria of character construction) as recently discussed and illustrated by Simões *et al.* (2017d). For further details, I refer the reader to the latter study.

Coding scheme and optimization criteria. In the past decades, numerous studies have discussed the pros and cons of multiple character coding schemes, as mentioned above. Of particular importance is the choice between multistate and contingently coded characters and the challenges in ordering vs. unordering multistate character states (i.e. optimization criteria), which plays a major role in the outcome of the analysis. Simões *et al.* (2017d) have recently mentioned the consequences of multiple coding schemes that violate basic criteria of character construction. However, a more detailed consideration on ordering vs. unordering characters, and the outcomes of multistate and contingently coded characters were mentioned but not discussed therein. Here, important aspects to consider before choosing between these coding schemes are discussed, and my choices for the present dataset are presented.

For morphological attributes with a non-nested relationship, multistate characters will not differ much in their assumptions and effects to the analysis from binary characters because all character states are equally distinct from each other. One example of such character is: Clavicles, position (at point of contact), in relation to anterior margin of scapula: laterally (0)/ medially (1)/ anteriorly (2) (R94, Ch. 65 – modified). In this example, all states are mutually exclusive and have a non-nested relationship to each other.

Morphological attributes representing a hierarchically nested set of features from a single transformation series represent a more challenging task towards character coding. These are much harder to be represented as independent phylogenetic characters that do not make untested or unsupported pre-assumptions of the process of evolution. For instance, for character: Squamosal absent (0)/ present without dorsal process (1)/ present with dorsal process (2). State 2 is nested within the "squamosal present" condition, because logically a process can only develop if the squamosal bone is present. However, ordering this character (i.e. making the state transformations 0<-->1<-->2) would prohibit a direct transformation from state 0 (squamosal absent) to 2 (squamosal present-with process). Therefore, ordering this transformation series would create an intrinsically higher cost for certain paths in this sequence, although no biological evidence exists to favor one path relative to others—which is also the case for most morphological characters (Forey & Kitching 2000).

Making the previous example of the squamosal bone a multistate character without ordering also creates spurious assumptions. Despite not restricting the direction of evolution (or creating unsupported assumptions on the costs of certain transformations), unordered multistate coding does not retrieve hierarchical relationships, which is an issue for characters with nested character states. For instance, all taxa grouped under state 1 (squamosal present-no process) will not be grouped with taxa bearing state 2 (squamosal present-with process) in a clade characterized by a "squamosal present" synapomorphy, because there is no character state "squamosal present" in the dataset. In essence, squamosals with and without a process are "seen" by the analysis as equally distinct and non-nested to each other as, for instance "red" and "blue" or "absent" and "present". This exemplifies how this coding scheme ignores the nested condition among its states. Consequently, it becomes possible that a clade supported by state 1 may eventually be grouped as closer to a clade without squamosals, than to a third clade supported by state 2 (which also has squamosals), because the information on the presence of the squamosal itself (and the existing hierarchy among these character states) is not retrieved by the analysis (Lee & Bryant 1999). Not considering the hierarchical relationships among nested character states has also been demonstrated to results in decreasing the resolution of cladistic analyses, contributing little or nothing to the final tree topology, which thus becomes mostly influenced by the binary characters in the dataset (Hawkins *et al.* 1997; Forey & Kitching 2000). Finally, multistate unordered coding that includes an absent state may also result in the incorrect placement of taxa due to optimized ancestral-states that should, in fact, be inapplicable to these same taxa. This happens when the most parsimonious solution recovers secondary absences of the multistate characters among some terminal taxa (Strong & Lipscomb 1999).

One proposed solution to the usage of multistate characters has been the usage of step (or Sankoff) matrices (Forey & Kitching 2000), which was more recently discussed by Brazeau (2011). These allow any state to be transformed into any other state within the same character (thus not restricting the direction of evolution), and can retrieve the hierarchical relationship among states. However, it greatly increases computational time (Kitching *et al.* 1998), which by itself may hamper finding trees representative of all local optima (Maddison 1991; Goloboff 1999). Additionally, it is theoretically challenging to determine appropriate costs of character state change (Kitching *et al.* 1998), which should be based on prior knowledge or appropriate

modeling of the probability of state transformation/substitution, as currently known for molecular data (Yang *et al.* 1994; Yang 1995);.

A third and commonly used option for characters such as the squamosal character in the example above would be splitting this character into two characters, in a contingent coding format—Ch.1. Squamosal: absent (0)/ present (1); Ch.2. Squamosal, dorsal process: absent (0)/ present (1). A contingent coding of this kind avoids restricting the direction of evolution (such as unordering a multistate character) and retrieves the hierarchical relationships between these two features being sampled, but could create problematic ancestral-state optimizations due to character 2 being inapplicable for early diverging taxa displaying the absent state for character 1 (Maddison 1993; Strong & Lipscomb 1999; Forey & Kitching 2000; Simões *et al.* 2017d)—a consequence of the logical dependency (Wilkinson 1995) among these two characters.

From the fact above it becomes clear that no specific coding scheme is free of assumptions and biases, nor provides the ideal solution for characters representing a logically or biologically nested set of features. However, contingent coding retrieves the inferred hierarchical relationship among the nested set of features, it avoids a choice for a particular direction of evolution, and its deleterious effect on taxa with inapplicable states occurs only under very specific circumstances. Therefore, this form of coding has been preferred by most previous authors (Hawkins *et al.* 1997; Strong & Lipscomb 1999; Brazeau 2011). Also, contingent coding has been preferred by other authors because it is more consistent with the primary homology statement, such as the locator and its properties being assessed separately (Lee & Bryant 1999; Sereno 2007). Therefore, this coding scheme is also used herein for characters falling into this category.

As a final consideration on character coding, in some instances in which multiple mutually exclusive and non-hierarchically nested conditions are observed for a character, a multistate coding is justifiable, because lack of hierarchical relationships will not be an issue—Example: Cephalic osteoderms, ornamentation: smooth (0)/ vermiculate (1)/ tuberculate (2). In other instances, a transformation series may include an "absent" condition, but those are not established between an anatomical part (i.e. locator) and its constituting properties (such as the ones used in contingent coding), therefore also not constituting a hierarchically nested relationship. Those multistate conditions may describe, for instance, successive discrete stages in the development of a particular feature of an anatomical part, such as: "Procoracoid, coracoid emargination: absent (0)/ anterior emargination only (1)/ anterior and posterior emarginations

(2)". In this particular character, all character states equally represent a sequence of shape variations in the coracoid (coded as states "0" to "2" herein). Unlike contingently coded characters, the "absent" or "no emargination" condition, state "0", describes a shape rather than an actual absence of a part/locator, thus being mutually exclusive to states "1" and "2". Therefore, such characters are treated as multistate, following the same logic for the osteoderms character above.

Multistate characters describing a series of shape changes, such as the procoracoid shape character above, are commonly treated as ordered in many published datasets. This treatment is usually based on the assumption that these morphological conditions are serially nested, or serially dependent, so that state "2" (e.g. two emarginations" in the procoracoid character) necessarily comes after state "1" (one emargination). However, the practise creates a pre-asssumption of character state polarity: that the anterior emargination necessarily evolved from a no emargination condition, rather than a two emargination condition. Here, it is preferred to treat the polarization of the shape character states a posteriori based on outgroup comparison during the analyses, rather than restricting the this direction a priori.

Molecular dataset alignment, model selection and partitions

Molecular dataset consists of 16 genetic markers (13 nuclear and three mitochondrial loci) for 38 extant taxa. A complete list of sampled loci and sequence lengths is provided in Table 6.1. Sequence data for the selected coding regions were obtained from GenBank. For the three ingroup taxa, *Liolaemus signifier*, *Pristidactylus scapulatus*, and *Stenocercus scapularis*, for which molecular data were not available, I used sequences of congeneric species, *L. ornatus*, *P. torquatus*, and *S. guentheri*, respectively. Sequences were aligned in MAFFT 7.245 (Katoh & Standley 2013) online server using the global alignment strategy with iterative refinement and consistency scores (G-INS-i). For the protein-coding genes, alignments were verified by translating nucleotide sequences to amino acids. The final multiple sequence alignment was concatenated and visually examined in Mesquite 3.04 (Maddison & Maddison 2015). Molecular sequences from all extant taxa were analyzed for the best partitioning scheme and model of evolution using PartitionFinder2 (Lanfear *et al.* 2016) under Akaike information criterion (AIC).

Tree search and sampling procedures

Equal weights maximum parsimony (EWMP) analysis

Analyses were conducted in TNT v. 1.1 (Goloboff *et al.* 2008b) using the New Technology Search (NTS) algorithms. The latter allows the sampling of trees from a broader spectrum of local optima than allowed by the heuristic search + Ratchet runs in PAUP* 4.0 Beta 10, especially for large datasets (Goloboff 1999; Goloboff *et al.* 2008b). Tree searches were conducted using 1,000 initial trees by random addition sequences (RAS) with 100 iterations/round for each of the four NTS algorithms: Sectorial Search, Ratchet, Drift and Tree Fusing. The output trees were used as the starting trees for subsequent runs, using 1,000 iterations/rounds of each of the NTS algorithms. The latter step was repeated once again, and the final output trees were filtered for all the most parsimonious trees (MPTs). A total of 621 MPTs were obtained with 2,268 steps each.

Implied weights maximum parsimony (IWMP) analysis

Analyses were also conducted in TNT, using the implied weighting algorithm (Goloboff *et al.* 2008a), with a K=12 and collapsing all branches with support = 0. Tree searches were conducted as performed for EWMP. Larger K values than the default (3.0) are indicated to perform better for large datasets (Goloboff *et al.* 2017). A total of five best fit trees were obtained (fit = 91.768892) and used to calculate the strict consensus tree.

Bayesian inference analyses

Analyses were conducted using Mr. Bayes v. 3.2.6 (Ronquist *et al.* 2012b) using the Cedar computer cluster made available through Compute Canada and the CIPRES Science Gateway v.3.3 (Miller *et al.* 2010). Molecular partitions were analyzed using the models of evolution obtained from PartitionFinder2 (see dataset), and the morphological partition was analyzed with the MkV model (Lewis 2001).

The distribution for rate heterogeneity was tested for best fit to the data under both gamma (GA) and lognormal (LN) distributions, as it was recently demonstrated that a lognormal distribution may better fit morphological data for a large variety of datasets (Wagner 2012; Harrison & Larsson 2015). Fit to the data was assessed using Bayes factors $[B_{10}]$ (Kass & Raftery 1995; Nylander *et al.* 2004) calculated with the marginal model likelihoods obtained

from the stepping-stone sampling (SS) method (Xie *et al.* 2011). The interpretation of the results of the model fit to the data followed Kass & Raftery (1995): when $2log_e(B_{10}) > 2$ (positive evidence against model M_0); when $2log_e(B_{10}) > 6$ (strong evidence against model M_0); when $2log_e(B_{10}) > 10$ (very strong evidence against model M_0). However, $2log_e(B_{10})$ was less than 1 between the GA and LN runs, indicating no significant difference in fit to the morphological data between both distributions. The morphological partition was thus analyzed under the GA model for all subsequent analyses.

Time-calibrated relaxed-clock Bayesian inference analyses

I implemented "total-evidence-dating" using the fossilized birth-death (FBD) tree model with sampled ancestors, under a relaxed-clock model in Mr. Bayes v.3.2.6 (Stadler 2010; Ronquist *et al.* 2012a; Zhang *et al.* 2016). The chosen relaxed-clock model is the Independent Gamma Rate (IGR) relaxed-clock model (Lepage *et al.* 2007). This is a continuous uncorrelated relaxed clock model using a gamma distribution to assess clock rate variation across lineages. The latter is compatible with the FBD tree model, unlike the compound Poisson process (CPP) relaxed-clock model (Zhang *et al.* 2016). The base of the clock rate was based on a previous non-clock analysis: the median value for tree height in substitutions from posterior trees divided by the age of the tree based on the median of the distribution for the root prior: 25.1658/325.45 = 0.0773, in natural log scale = -2.560061. Following Pyron (2017), I chose to use the exponent of the mean to provide a broad standard deviation: $e^{0.0773}$ =1.080366. Sampling strategy was set to diversity, which is more appropriate when extant taxa are sampled in a way to maximize diversity (as performed herein) and fossils are sampled randomly (Ronquist *et al.* 2012a; Zhang *et al.* 2016). Diversity sampling is very common in higher-level phylogenies, and not accounting for it has a deep effect in tree inference, pushing divergences time further back and creating unreasonably older and variable divergence times (Höhna *et al.* 2011; Zhang *et al.* 2016). This provides a considerable advantage of using Mr. Bayes for divergence time estimates over current implementations available in the software package BEAST (Bouckaert *et al.* 2014).

The wealth of fossil taxa in my dataset, including some of the oldest known taxa for some clades, provided numerous calibration points. Therefore, the vast majority of my calibrations were based on tip-dating, which accounts for the uncertainty in the placement of fossil taxa and avoids the issue of bound estimates for node based age calibrations (Ronquist *et al.* 2012a). The

fossil ages used for tip-dating correspond to the uniform prior distributions on the age range of the stratigraphic occurrence of the fossils (available in Table 6.2). However, it has recently been demonstrated that using tip-dates only can contribute to unrealistically older divergence time estimates for some clades (O'Reilly *et al.* 2015; O'Reilly & Donoghue 2016). Therefore, for the clades for which I lacked some of the oldest known fossils in my analysis, for which there is overwhelming support in the literature (and in all my other analyses) regarding their monophyletism, and for which the age of the oldest known fossil is well-established, I employed node age calibrations with a soft lower bound. Namely, these were captorhinids, choristoderes, snakes and rhynchocephalians. Combined with diversity sampling strategy, the latter dating protocol can ensure reliable divergence time estimates.

Convergence of independent runs was assessed using: average standard deviation of split frequencies (ASDSF ~ 0.01), potential scale reduction factors [PSRF ≈ 1 for all parameters (Gelman & Rubin 1992)], and effective sample size (ESS) for each parameter was greater than 200.

Calibrations used for relaxed clock analyses.

The analysis using tip-date calibration ages was based on updated information concerning the age of the stratigraphic layers from where all the fossils used herein originate from, which are all depicted in Table 6.2, and in the details in the taxonomic sampling section. Node calibrations were used for four well-supported clades (in all of my other analyses herein and by previous authors) for which I lacked some of their oldest fossils in my analyses, and therefore their divergence time estimates could be biased by unrealistically old divergence times (O'Reilly *et al.* 2015; O'Reilly & Donoghue 2016). These clades and calibrations are as follows: Serpentes: based on *Eophis underwoodi* (Bathonian, Middle Jurassic—UK) (Caldwell *et al.* 2015) → 168.3-166.1 MYA (166.1,168.3) (Ogg *et al.* 2016); Choristodera: based on *Cteniogenys* sp. (Bathonian, Middle Jurassic—UK) (Evans 1989) → 168.3-166.1 MYA (166.1,168.3) (Ogg *et al.* 2016); Rhynchocephalia: based on cf. *Diphyodontosaurus* (Ladinian, Middle Triassic—Germany) (Jones *et al.* 2013) → 241.5-237 MYA (237,241.5) (Ogg *et al.* 2016); Captorhinidae: based on *Euconcordia* (Stephanian of Europe [equivalent to the Kasimovian], Late Pennsylvanian, Carboniferous—Kansas, USA) → 307-303.7 MYA (Müller & Reisz 2005; Ogg *et al.* 2008; Ogg *et al.* 2016).

The age of the root was set with a soft lower bound, which gives a low (but non-zero) likelihood of the age being older than the lower bound value. Minimum and maximum root bounds were placed as follows: Minimum age—oldest possible age for the oldest known reptile, *Hylonomus* (from the Joggins Formation in Nova Scotia, Canada), which comes from the late Bashkirian Stage (early Pennsylvanian, Late Carboniferous) and is between 318 and 315 million years old (Ogg *et al.* 2016). Considering *Petrolacosaurus* may be as much as 307 million years old, placing the minimum age at 318 seems consistent, as the most recent common ancestor of diapsids and captorhinids must have been at least a few million years older than *Petrolacosaurus*; Maximum age—based on the maximum soft age for reptile-synapsid split (Benton *et al.* 2015): 332.9 million years ago.

Preferred phylogenetic hypotheses

I consider the trees inferred from combined evidence data under Bayesian inference analyses to be my preferred phylogenetic hypothesis (Fig. 6.7-6.10), because they consider different data types simultaneously, and Bayesian inference analyses take into consideration the different models of molecular evolution and variation in branch lengths. Statistical phylogenetic methods were found to be more accurate and efficient, especially in the analysis of molecular data (which is more prone to long branch attraction than morphological data) or when evolutionary rates vary among branches (Saitou & Imanishi 1989; Kuhner & Felsenstein 1994; Huelsenbeck & Rannala 1997; Yang & Rannala 2012). Bayesian inference has also been demonstrated to have superior performance over other statistical methods (Maximum likelihood approaches) and maximum parsimony, in the analysis of molecular, morphological, and combined evidence data (Dwivedi & Gadagkar 2009; Wright & Hillis 2014; Guillerme & Cooper 2016; O'Reilly *et al.* 2016; Puttick *et al.* 2017).

Leaf stability

Leaf stability was assessed using RogueNaRok (Aberer *et al.* 2013), which allows assessing the difference between the highest and the second highest support values for alternative resolutions of each taxon quartet/triplet in the dataset (LSdif) (Wilkinson 2006). I applied this method to the posterior trees from the Bayesian inference analysis including both morphological and molecular data. Because of the large number of taxa and large number of trees, it was

necessary to downsample the total number of posterior trees from each analysis (100,000 trees after discarding burn-in). The final sample consisted of 10,000 trees (selecting one at every 10 trees) using the Burntrees script for Perl (Nylander 2014).

Results

Osteological re-description of *Megachirella wachtleri*

Skull

One maxillary bone is preserved on the right side of the skull. It has the nasal process broken anteriorly and at least four maxillary teeth are preserved in situ. The suborbital ramus of the maxilla extends until the midorbital region and articulates with the ventral side of the jugal. The jugal forms the posteroventral margin of the orbit, and the jugal posterodorsal process extends for at least half the height of the postorbital bar. The jugal also has a short posteroventral process, thus not fully enclosing the lower temporal fenestra ventrally.

The prefrontal is relatively elongate anteroposteriorly, extending posteriorly half-way through the length of the orbit. The anteroventral margin of the prefrontal is poorly preserved and is crushed against the maxilla. Therefore, it is not possible to determine with certainty whether the lacrimal is present. The posterior opening of the lacrimal duct is not visible externally or medially on the prefrontal or maxillary border of the orbit; therefore, the posterior opening of the duct may have been fully enclosed by the lacrimal, though the latter is not preserved in the holotype.

The triradiate squamosal is preserved only on the right side of the skull. The posterior process of the squamosal fits into a groove on the cephalic condyle of the right quadrate (as observed in all squamates). The dorsal process, when in articulation with the parietal, contributed to the posterior border of the upper temporal fenestra. The anterior (postorbital) process articulated with the posterior process of the postorbitofrontal. The postorbital and the postfrontal are probably fused into a postorbitofrontal. There is no visible suture line, but it is possible that at earlier ontogenetic stages a suture between both elements would have been visible. The medial margin of the postorbitofrontal is concave, bearing two small processes: a longer frontal process anteromedially and a slightly shorter parietal process posteromedially. Its posterior (squamosal)

process is relatively elongate, and independently contributed to about one-third to one-half of the upper temporal bar anterior of its articulation with the squamosal. The posterior process of the postorbitofrontal has a tongue-and-groove articulation with the squamosal via a dorsomedial groove, such that most of the posterior process of the postorbitofrontal was hidden in lateral view. This articulation differs from the one typically found in most rhynchocephalians [including *Gephyrosaurus* (Evans 1980) and TRS pers. obs.), in which the squamosal bears a large anteriorly concave facet that is visible in lateral aspect for articulation with the postorbital. The anterolateral process of the postorbitofrontal appears to be very reduced, but the exact length is unknown as this region is poorly preserved due to the compression of the postorbitofrontal against the palatine ventrally.

The frontal is partially broken on the left side, but the CT-scans reveal that both subolfactory processes are preserved on the ventral side of the frontal (Fig. 6.3), indicating the frontals are fully fused into a single element. Fused frontals are also observed in a large number of crown squamates and some early rhynchocephalians (*Gephyrosaurus, Diphyodontosaurus* and *Planocephalosaurus*), but are absent in most later evolving rhynchocephalians and other major groups of diapsids. The frontal is constricted anteriorly, expands posteriorly, but then narrows again near the frontoparietal suture.

The parietals are also fused into a single element, as observed among almost all squamates, *Gephyrosaurus*, and possibly in *Planocephalosaurus* among rhynchocephalians. Both lateral margins of the parietal are exposed in dorsal view and project ventrally. The parietal lateral margins are slightly concave contributing to a greatly expanded adductor chamber and wide upper temporal fenestra. Posteriorly, the parietal has a pair of very elongate supratemporal processes that form part of the posterior border of the upper temporal fenestra. It is not clear if the supratemporal bones were present in *Megachirella*. It is possible that those were absent, partially fused to the parietal supratemporal process, or simply not preserved.

The quadrates are well-preserved on both sides of the skull, having a strongly developed quadrate conch and suprastapedial process. The tympanic crest is relatively well-developed on the lateral margin of the quadrate, indicating the presence of a tympanic membrane in life. Ventromedially, the quadrates have very well-developed pterygoid processes that articulate with the quadrate rami of the pterygoids. Importantly, the CT-scans show a foramen lying close to the tympanic crests of both quadrates, and a suture line emerging from those foramina and extending

dorsally and in parallel to the tympanic crest (Fig.6.3). This anatomy resembles the condition seen in some early rhynchocephalians (e.g. *Diphyodontosaurus*), which have been interpreted as consisting of a partially fused quadratojugal (Whiteside 1986). The presence of a partially fused quadratojugal in *Megachirella* indicates that the earliest squamates still retained this element. It is important to point out that due to compression of the skull both quadrates have been rotated forward, and this is evident from the fact that the ventral condyle of the left quadrate is exposed posteriorly. A consequence of this is that, contrary to previous reconstructions, the suprastapedial process in life must have been oriented posteriorly rather than posterodorsally. As such, the morphology of the quadrate in lateral view closely resembles that of many squamates.

The pterygoids are the best-preserved elements of the palate. The left pterygoid is exposed dorsally in the holotype, but CT-scans reveal an equally well-preserved right pterygoid along with many other palatal elements. The pterygoids have well-developed transverse processes that bear ventrally projecting flanges. However, the exact depth of these flanges is unclear. The anterior (palatine) process of the pterygoids extend well anteriorly and, in ventral aspect, there are three longitudinal ridges representing rows that would have supported pterygoid teeth. Although the actual pterygoid dentition is not visible given the scan resolution, I are unaware of any other palatal structure that would produce this particular morphology. Also, very similar rows of pterygoid dentition are observed in *Sophineta* (TRS pers. obs.). The ectopterygoid is preserved on the right side of the skull, it is elongated anteroposteriorly and has a semilunar shape. The portion of the ectopterygoid that articulates posteriorly with the pterygoid is expanded dorsoventrally, while the opposite portion is directed anteriorly, nearlycontacting the preserved part of the palatine. The ectopterygoid orientation (connecting the palatine and pterygoids) is similar to the condition observed among most squamates, and differs from the condition in rhynchocephalians (e.g. *Gephyrosaurus*, *Diphyodontosaurus, Planocephalosaurus, Clevosaurus* and *Sphenodon*) which have the ecytopterygoid laterally oriented, contacting the maxilla and jugal instead of the palatine [(Evans 1980; Fraser 1982; Whiteside 1986; Fraser 1988) and TRS pers. obs.].

The posterior end of the ectopterygoid also has a small ventral process that would have contributed to the formation of the attachment area of the pterygoideus muscle group along with the ventral flange of the transverse process of the pterygoid. The ventral extensions of these processes, as preserved, are shorter than those observed in rhynchocephalians and archosaurs,

thus indicating a reduced participation of the pterygoideus muscle group in the jaw adductor system when compared to those clades. Along with the greatly expanded adductor chamber on the temporal region and the loss of a complete lower temporal bar, *Megachirella* had an adductor system characterized by the expansion of the adductor externus group and reduced participation of the pterygoideus system, as also observed in crown squamates (Haas 1973; Rieppel & Gronowski 1981; Simões *et al.* 2016). The ventral flanges of the pterygoid and ectopterygoid, however, are still larger than those seen in many squamate families, approaching the degree of development of those structures as seen in iguanians and teiids.

The border between the palatine and pterygoid is not clear on either side of the skull. However, considering the placement of the ectopterygoid on the right side of the skull, I infer that the palatal elements located anteriorly to it represent remains of the palatines. One such element on the right side seems to have been displaced posteriorly and it abuts against the right ectopterygoid. The anteriormost palatal elements preserved might represent remnants of the vomers given their position just anterior to the palatine elements and medial to the anterior half of the maxilla.

The braincase is poorly exposed in the holotype, but the CT-scans reveal a large amount of information, especially for the ventral and lateral aspects. The basioccipital forms a strongly developed occipital condyle, it has a relatively flat ventral surface, and it contributes to the formation of the sphenoid tubercles. The parasphenoid seems to be fully fused to the basisphenoid, as in most reptiles. The basisphenoid has a concave ventral surface and a well-developed, thick cultriform process. Anterolaterally, the basisphenoid bears a pair of strongly developed parabasiphenoid processes for articulation with the pterygoids. An open Vidian canal is located posterior to the parabasisphenoid processes and on the ventral margin of the lateral wall of the prootics.

The prootics are preserved on both sides of the skull and the prootic crest is either reduced or absent. The anterior semicircular canal is visible in the left prootic and a well-developed alar process is located just anterior to it. The opisthotics are preserved on both sides of the skull, and the left still preserves a widely expanded paroccipital process. The base of the opisthotics have been crushed against the prootics, thus concealing most of the fenestra ovalis and possibly and the entire occipital recess. The right exoccipital can be observed dorsal to the occipital condyle, but it is not possible to determine whether it is fused to the opisthotic.

Part of the hyoid apparatus is preserved, represented by a pair of rod-like elements ventral to the braincase and palate, which might represent the first pair of ceratobranchials, which is the most common hyoid element to ossify in lepidosaurs.

Mandibles

The dentaries are elongate and relatively slender. The CT-scans enable the reconstruction of most of the dentaries, although they do not provide enough resolution to identify the individual posterior processes. However, upon personal observation of the specimen (TRS, MWC) it was possible to detect the terminal end of the coronoid process of the right dentary, located just ventrally to the dorsal process of the coronoid bone (Fig. 6.2). The CT-scans also revealed that there was no contribution of the dentary to the coronoid apex. Therefore, the coronoid process of the dentary did not expand dorsally as observed in all rhynchocephalians, and it is rather similar to the posteriorly straight condition found in most squamates and other diapsid reptiles.

The splenials are present, and are dorsoventrally deep and anteroposteriorly elongate. This also differs from the condition of all known rhynchocephalians, in which the splenials are entirely absent, even in early forms such as *Gephyrosaurus, Diphydontosaurus* and *Planocephalosaurus* [(Evans 1980; Fraser 1982; Whiteside 1986) and TRS pers. obs]. The coronoid forms the entire coronoid apex of the lower jaws, having a tall dorsal process, and a posterodorsomedial process that is visible in dorsal aspect. The medial margin of the coronoid is damaged, and it cannot be determined if the anteromedial and posteroventromedial processes are present in *Megachirella*.

The surangular is elongate, but not very deep. The posterior surangular foramen is visible on the lateral margin of the right surangular, and the anterior foramen is undeterminable. Additionally, the surangular lacks a coronoid process extending onto the posterior border of the coronoid bone and contributing to the coronoid apex, thus differing from the condition seen in all rhynchocephalians and snakes. In the CT-scan, the angular could not be distinguished from the prearticular on the ventral margin of the jaw, and a suture between the articular and prearticular appears to be absent, but this may also be an artifact of the relatively low resolution of the CT scan in this region.

The articular (possibly fused to the prearticular) forms a small medial process (angular process), as observed in iguanians, teiids, borioteiioids and cordyloids, among crown squamates.

A medial process, possibly homologous to the "angular process" in squamates, also occurs in *Gephyrosaurus* (among rhynchocephalians), and as known in other diapsid lineages in taxa such as *Euparkeria, Erythrosuchus, and Lariosaurus*. Posteriorly, the retroarticular process is very expanded and forms a dorsal fossa.

Dentition

Dentary teeth are exposed in the specimen and they can be observed both directly on the specimen and from the CT-scan images. The tooth attachment mode is pleurodont: teeth are located lingually to the labial parapet of the dentary (crista dorsalis); the labial wall is much higher than the lingual wall of the dentary, and there are no fully developed interdental ridges; also, there is no visible ankylosis of the tooth crowns to the apex of the dentary labial wall (Fig. 6.1 & 6.3). This anatomy of the dentition of *Megachirella* differs from all sphendodontians (with the exception of *Gephyrosaurus*), which possess acrodont teeth (placed on and fused to the apex of the labial parapet of the dentary) posteriorly along the marginal tooth row of the jaws. There is at least one, if not two, replacement teeth visible on the left dentary. The tooth crowns are short, roughly circular in cross section and heavily worn at their apices (possibly an artifact of preservation). Complete maxillary teeth could be observed in the CT scan images and appear to be large and conical. The exact mode of tooth implantation on the maxilla is hard to verify due to poor preservation of the medial portion of this bone.

Postcranium

Six cervicals and thirteen (three as impressions) dorsal vertebrae are preserved. The atlas neural arches are visible on either side of the anterior cervical region. A small protuberance visible on the CT-scans near the contact with the axis might represent the atlas postzygapophyses. The axis has an elongate centrum and neural spine, and the axis intercentrum is located between the axis and the 3rd cervical. Four other cervicals follow with small ribs preserved on both sides. The seventh presacral has the first elongated rib (better seen in ventral view) lying medial to the right clavicle, which could have contacted the sternal plate, and it is thus considered to be the first dorsal. Six other dorsals follow, before a gap where the carbonic impression of three additional dorsals are visible on the holotype and are followed by another three vertebrae.

The second dorsal vertebra is displaced dorsally, exhibiting the posterior cotyle, thus making clear the lack of a posterior condyle on the vertebral centrum. It also indicates the notochordal canal was fully closed, thus differing from all rhynchocephalians, which have a notochordal canal persistent into adulthood [(Hoffstetter & Gasc 1969), TRS, pers. obs]. The CT-scans also reveal the absence of anterior cotyles, indicating the amphicoelic condition of the pleurocentra. Later squamates, such as *Huehuecuetzpalli*, *Marmoretta* (TRS per obs) and basal extant squamates (geckoes) also bear this condition. The neural arches are moderately developed, and they are better exposed on the second and third dorsals, which have been slightly displaced. The third dorsal has the anterior border of the neural arch exposed, indicating the absence of accessory articulatory processes (zygosphenes)—also absent in *Huehuecutezpalli* and *Marmoretta*. The neural spines do not bear any kind of apical expansions. Intercentra are visible in the CT-scans on the cervical and dorsal region, always in an intervertebral position.

The first identifiable rib is on the second cervical (axis). All cervical ribs lack an anterior process (common in archosauriforms, protorosaurs, and some other diapsids). The dorsal ribs are significantly stouter than the cervical ribs, but not to the point that they could be considered pachyostotic, as their shafts are narrower than their heads. They decrease in robustness posteriorly, with the latest preserved dorsal ribs being much more gracile than the anterior dorsal ribs. Gastralia are visible on the left side of the specimen (a plesiomorphic condition in the context of Diapsida that is lost in crown squamates), in the gap area where the dorsals are preserved as impressions only. No traces of inscriptional ribs are visible.

The pectoral girdle preserves the right coracoid, part of the right scapula and both clavicles. The scapula is taller than wide and has a small contribution to the glenoid. A small anterior bony projection is seen anterior to the scapula, and it is part of left clavicle. The coracoid is larger than the scapula, and bears no fenestration, thus resembling more the coracoids of non-squamate diapsid reptiles. The body of the coracoid has the weakest degree of ossification and is pierced by three holes that might be the result of poor preservation. The medial margin of the coracoid is thickened and bears a narrow groove. This is indicative of a cartilaginous element attaching to the medial aspect of the coracoid, such as the epicoracoid cartilage or the presternum. A highly mineralized area of similar density to the bone is visible in the CT-scans posterior to the coracoid and may represent a calcified sternum. The right clavicle is located just medially to the scapula

and is visible in dorsal view on the holotype. The CT-scans reveal it extends ventrally and that it has a secondary curvature on the anteroposterior axis, as in most "scleroglossans" lizards.

Both forelimbs are well-preserved, with propodials and epipodials visible on both sides of the body. The autopodium is also preserved on both sides, but the right side is exquisitely preserved, and it is visible without the aid of CT-scan data. The humerus has a twist of almost 90 degrees between the humeral head and its distal end. The humeral proximal epiphysis is not yet fully ossified and fused to the humeral head, indicating secondary epiphysis ossification as seen in other lepidosaurs (including fossil taxa, such as *Homeosaurus*, *Kallimodon*, and fossil squamates such as *Tijubina pontei*—TRS pers. obs.). The distal ends are wide and carry well-developed epicondyles. In the latter, there is an ectepicondyle foramen and a fully open entepicondyle foramen. A complete entepicondylar foramen is absent in crown squamates. However, it is found in rhynchocephalians and *Huehuecuetzpalli*, making this a simplesiomorphy within Lepidosauria. The presence of these foramina in *Megachirella* and *Huehuecuetzpalli* indicate they were retained in stem squamates, but lost in the crown groups. Additionally, the humerus radial condyle (capitulum) is expanded, a feature common to squamates but poorly developed or absent in other lepidosaurs.

The radius is preserved in articulation with the humeri radial condyles on both sides, and their distal ends apparently lack a styloid process. The ulnae have well developed olecranon processes, and the right ulna has an ulnar patella preserved between the olecranon and the humerus. The ulnar patella is absent in *Sphenodon* and all other rhynchocephalians, but it is commonly observed in squamates (Regnault *et al.* 2016). The ulnar distal epiphysis is not expanded as in crown squamates, thus resembling the condition of other diapsids, as also is observed in *Huehuecuetzpalli* [(Reynoso 1998) and TRs pers. obs.].

The carpals preserve an intermedium between the radius and ulna, a small radiale (lying in articulation with the distal end of the radius) and a larger ulnare (lying in articulation with the distal end of the ulna). A wide medial centrale is located just distal to the anterodistal corner of the radius and near the proximal end of metacarpal II. A lateral centrale is located just lateral to it, and distal to the radiale (in contact with distal carpals 2 and 3). Distal carpals 2 and 3 lie in articulation with the proximal ends of metacarpals II and III. Distal carpals 4 and 5 are fused, forming a large distal carpal element in contact with metacarpals IV and V. Distal carpal 1 is missing and metacarpal 1 has an expanded head. The latter condition is also observed among

most squamate lineages, and it represents the result of the fusion between the distal carpal 1 and metacarpal 1 (Carroll 1977; Gauthier *et al.* 1988a). Since the same morphology is observed in *Megachirella*, it is considered here that the proximal expansion of metacarpal 1, and the absence of distal carpal 1, is the result of their fusion. The metacarpals increase in length from digit 1 to 4, reducing again in length in digit 5. Metacarpal IV is slightly longer than metacarpal III, as in most squamate families. The total number of phalanges in each digit is not possible to determine with certainty.

Comparative osteology and systematics

Megachirella is a lepidosaur because it has a well-developed quadrate conch, an ectepicondylar foramen in the humerus, and pleurodont dentition on both dentary and maxilla. The lepidosaur condition of *Megachirella* was recognized by Renesto & Posenato (2003) and Renesto & Bernardi (2014). Within lepidosaurs, *Megachirella* has a set of features only observed in squamates (and absent even among the earliest rhynchocephalians), such as: a triradiate squamosal (not tetraradiate as in most other diapsids, including rhynchocephalians), squamosal lacking an anteriorly concave articulatory facet for the postorbital (not contacting the maxilla and jugal as in rhynchocephalians), a well-developed alar process of the prootic, the ectoperygoids directed anteriorly (not laterally as in rhynchocephalians), a well-developed radial condyle on the humerus, presence of an ulnar patella, secondary curvature of the clavicles, and an expanded epiphysis of the first metacarpal along with absence of distal carpal 1 (suggesting the fusion of the first distal carpal to the first metacarpal, as observed in all squamates (Carroll 1977; Gauthier *et al.* 1988a) . Finally, *Megachirella* has features that are absent in all rhynchocephalians (the sister-lineage to squamates), even among the earliest forms such as *Gephyrosaurus*, including: presence of a splenial, presacral pleurocentra without a notochordal canal, and absence of a dorsal (coronoid) expansion of the surangular and dentary. Interestingly, most features that make it a squamate and not a rhynchocephalian are in the postcranium. The postcranium was also key to place *Huehuecuetzpalli* as a stem squamate (Reynoso 1998). Some plesiomorphic features (like the presence of gastralia and a quadratojugal) indicate the mosaic of conditions preserved in *Megachirella*, and the gradual acquisition of squamate features. These general diapsid characters are also retained (not exclusive to) in rhynchocephalians, and are now known to occur among the earliest known squamates.

Phylogenetic results

Major findings

The new information presented here, along with my extensive revision of diapsid and early squamate phylogeny, unambiguously resolves the placement of *Megachirella* as the oldest known squamate. As expected for a squamate that is 85 million years older than the previously oldest known articulated squamates for which the osteology is well-known—*Eichstaettisaurus* and *Ardeosaurus* from the Late Jurassic of Germany (Mateer 1982; Simões *et al.* 2017b)—*Megachirella* retains numerous plesiomorphic features. These features are observed in other diapsid reptiles, and some are retained in rhynchocephalians, but they are almost entirely lost in crown squamates. These include amphicoelic vertebrae (although present in geckoes and *Huehuecuetzpalli*), a small quadratojugal, gastralia and an entepicondylar foramen in the humerus.

Assessing the phylogenetic position of *Megachirella* and other lepidosauromorph reptiles is challenging because there has never been a phylogenetic dataset comprising a rich sampling of both non-lepidosaurian diapsid reptiles and squamates. Almost invariably, broad scale reptile phylogenies have represented the nearly 10,000 extant species and the hundreds of fossil species of squamates as a single operational taxonomic unit [e.g. (Motani *et al.* 1998; Müller 2004; Chen *et al.* 2014)—more examples in Materials and Methods]. This approach highly oversimplifies the enormous diversity of phenotypes and genotypes in squamates. On the other hand, studies focused on squamate phylogeny never include more than a few taxa outside the Squamata to serve as outgroups [e.g. (Conrad 2008; Reeder *et al.* 2015)]. Here I create the first morphological phylogenetic dataset comprising all main branches of the diapsid tree of life, inclusive of all major lineages of rhynchocephalians (e.g. tuataras) and squamates at the species level, including extant taxa and fossils (Supplementary Information 6.1-6.3). I also focused on primary data collection, personally observing numerous specimens covering nearly 100% of the taxa included in this dataset. Importantly, I performed a meticulous revision of reptile and squamate phylogenetic characters (and created new characters) to avoid issues owing to logical or biological biases in morphological characters (Simões *et al.* 2017d). Due to the rich sampling of extant squamate species, I also included molecular data from 16 loci (13 nuclear and three mitochondrial). The analyses performed include morphological and combined evidence

(morphological and molecular data) analyses of diapsid and lepidosaurian relationships, carried out under multiple phylogenetic inference methods (see Materials and Methods).

Despite the difference in datasets used (i.e. morphology vs combined evidence) and phylogenetic optimality criteria, all results converge on *Megachirella* representing a stem squamate along with *Marmoretta oxoniensis*, from the Middle Jurassic of Britain, and *Huehuecuetzpalli mixtecus*, from the Early Cretaceous of Mexico. This resolution is particularly well supported in the combined evidence analysis, in which *Megachirella* has a leaf stability above the overall mean (Figure 6.11). In analyses with maximum parsimony, *Sophineta cracoviensis* also falls within the Squamata stem, but this is not recovered in the remaining analyses. This indicates that some taxa previously proposed to be early evolving lepidosauromorphs (e.g. *Megachirella* and *Marmoretta*) (Renesto & Posenato 2003; Jones *et al.* 2013; Renesto & Bernardi 2014) actually represent the oldest known squamates, partially filling the supposed 70 MY fossil gap in the early history of the clade. Other taxa also considered to be early lepidosauromorphs by previous studies (e.g. kuehneosaurids and *Saurosternon* (Jones *et al.* 2013)) are consistently found in my results to be nested in other parts of the diapsid tree outside the Lepidosauromorpha. Additionally, all previous morphology-based and molecular-based squamate phylogenies available in the literature disagree with each other concerning the earliest evolving crown group squamates: iguanians for morphology-based analyses (Conrad 2008; Gauthier *et al.* 2012), but dibamids and gekkotans for molecular analyses (Vidal & Hedges 2005; Pyron *et al.* 2013; Irisarri *et al.* 2017) (see also Materials and Methods). The results of combined evidence analyses typically match those of the molecular data alone (Reeder *et al.* 2015; Pyron 2017), however my results show unprecedented agreement between morphological and molecular data, in placing geckoes amongst the earliest evolving squamates, instead of iguanians (Fig. 6.10, Figs 6.4-6.10). Iguanians are consistently found further crownward in the tree, either nested with anguimorphs and snakes (clade Toxicofera—Figs. 6.4, 6.7-6.10), or with teiioids (Figs 6.5). This unprecedented agreement between molecular and morphological data regarding the early evolution of squamates might be a consequence of my vast sampling of taxa outside squamates (thus affecting character polarity and branch length parameters) and strict criteria for morphological dataset construction.

Synapomorphies

Ancestral state reconstructions for key nodes at the origin of lepidosaurs and the origin of Squamata.

I report below the character state transformations that were recovered using both parsimony and likelihood ancestral state reconstructions for the relaxed clock Bayesian inference tree implementing node and tip dating.

Lepidosauromorpha

Char. 3: 1 --> 0: Premaxillae, posterodorsal process: present → absent (0.915)

Char. 61: 0 --> 1: Postfrontals, medial forking: absent → present (0.945)

Char. 167: 0 --> 1: Dentaries, anterior end, split by Meckelian canal: absent → present (0.833)

Char. 212: 2 --> 0: Posterior dentary teeth, delimitation by tooth bearing bone: by a four-sided socket → by a labial wall only (0.999)

Char. 213: 2 --> 0: Posterior maxillary teeth, delimitation by tooth bearing bone: by a four-sided socket → by a labial wall only (0.981)

Char. 232: 0 --> 1: Presacral pleurocentra, midventral crest, dorsal vertebrae: absent → present (0.761)

Char. 309: 0 --> 3: Humeri, entepicondyle foramen: absent → present, fully open (0.979)

Lepidosauria

Char. 67: 0 --> 1: Frontals, fusion to each other: absent → present (0.946)

Char. 236: 0 --> 1: Caudal vertebrae, autotomic septum: absent → present (0.877)

Char. 298: 0 --> 1: Ilia, anterior pubic process: absent → present (0.948)

Rhynchocephalia

Char. 118: 1 --> 0: Quadrate foramen: present → absent (0.889)

Char. 173: 0 --> 1: Dentary, coronoid process, dorsal expansion: absent → present (0.934)

Char. 176: 1 --> 0: Splenials: present → absent (0.993)

Char. 229: 1 --> 0: Presacral pleurocentra, notochord, persistent in adults: absent → present (0.971)

Sphenodontia

Char. 59: 2 --> 1: Postfrontals, medial margin, position, relative to parietal: lateral → dorsal (0.985)

Char. 92: 0 --> 1: Vomers, ventral surface, midline crest: absent → present (0.786)

Char. 210: 0 --> 1: Posterior dentary teeth, position, relative to dentary crista dorsalis (apex of labial wall) of dentary: lingual → apical (0.989)

Char. 211: 0 --> 1: Posterior dentary teeth, ankylosis to crista dorsalis (apex of labial wall) of dentary: absent → present (0.975)

Squamata

Char. 50: 1 --> 0: Squamosals, anteroventral process: present → absent (0.952)

Char. 114: 1 --> 0: Ectopterygoids, lateral process: present → absent (0.719)

Char. 142: 0 --> 1: Prootics, alar crest: absent → present (0.943)

Char. 287: 0 --> 1: Clavicles, secondary curvature anteroposteriorly: absent → present (0.930)

Char. 310: 1 --> 0: Humeri, developed radial condyle (= capitelum): absent → present (0.962)

Char. 324: 0 --> 1: Distal carpal 1, fusion to first metacarpal: absent → present (0.944)

Squamata -1 (-Megachirella)

Char. 38: 0 --> 1: Quadratojugals: present→ absent (0.908)

Char. 273: 0 --> 1: Mineralized poststernal inscriptional ribs: absent → present (0.829)

Char. 284: 0 --> 1: Procoracoid, coracoid emargination: absent → anterior emargination (0.813)

Char. 342: 1 --> 0: Gastralia: present→ absent (0.952)

Squamata -3 (-Megachirella, - Marmoretta, - Huehuecuetzpalli) = Crown Squamata

Char. 52: 1 --> 0: Squamosals, dorsal process: present → absent (0.993)

Char. 304: 0 --> 1: Ischia, ischiadic tuberosity: absent → present (0.989)

Char. 319: 0 --> 1: Ulnae, large (ball-like) distal epiphysis: absent → present (0.996)

Char. 330: 0 --> 1: Tibiae, distal epiphysis, notch: absent → present (0.825)

Char. 331: 0 --> 1: Astragalus and calcaneum: as totally separate elements → fused astragalocalcaneum (0.834)

Discussion

Thus far, the oldest known squamates came from the Middle Jurassic of Britain and Kyrgyzstan in central Asia. These include *Bellairsia graclis, Balnealacerta silvestris, Oxiela tenuis, Saurillodon marmorensis*, *Paramacellodus* sp., possible gekkotan vertebrae and *Eophis underwoodi* from the Bathonian of Oxfordshire (Evans & Milner 1994; Waldman & Evans 1994; Evans 1998; Caldwell *et al.* 2015) and *Changetisaurus estesi* (Callovian) and other very fragmentary remains (Bathonian) from Kyrgyzstan (Nessov 1985; 1988; Fedorov & Nessov 1992). *Bharatagama*, from the Middle Jurassic of India (Evans *et al.* 2002), is another potential Middle Jurassic squamates. However, it has recently been suggested that it may actually represent a sphenodontian (Jones *et al.* 2013). *Tikiguana*, an acrodont jaw initially published as from the Triassic of India, was eventually found to be re-worked material from recent deposits (Hutchinson *et al.* 2012). Therefore, prior to this study, the oldest unquestionable squamates were from the Middle Jurassic, ranging from the Callovian to the Bathonian (168.3 – 166.1 million years ago) (Ogg *et al.* 2016). This was already a relatively diverse assemblage (Rage 2013) that included distinct lizard morphotypes, possible geckoes, and snakes, distributed across two quite distant areas of the world.

Megachirella provides unique insights into the early acquisition of squamatan features, as it is the first unequivocal squamate from the Triassic. *Megachirella*, and also *Huehuecuetzpalli* (Reynoso 1998), show that features commonly attributed to squamates characterize crown squamates, but were not yet present in stem squamates. For instance, *Megachirella* and

Huehuecuetzpalli still retain amphicoelic vertebrae, an entepicondylar foramen, and lack a ball-like distal epiphysis of the ulna. *Megachirella* further indicates that the loss of the quadratojugal and gastralia occurred within squamates, and not at the point of divergence from rhynchocephalians. The same pattern occurs in rhynchocephalians, for which Triassic and Early Jurassic fossils were previously known (Evans 1980), and which retain plesiomorphic features (such as the pleurodont dentition) that are absent in most of the later members of that group.

Previous molecular clock estimates have placed the squamate crown divergence time between the Late Triassic and Early Jurassic (Zheng & Wiens 2016; Irisarri *et al.* 2017; Pyron 2017), and lepidosaurs originating at some point in the Triassic (Jones *et al.* 2013; Pyron 2017) or in the Middle Permian (Hugall *et al.* 2007; Irisarri *et al.* 2017). My time-calibrated Bayesian inference analyses combine information from both the molecular and morphological relaxed clocks on lepidosaurs and other diapsid lineages (Figs. 6.9 & 6.10) providing a more holistic approach to the divergence time of squamates, lepidosaurs, and other diapsids. My estimates indicate lepidosaurs originated 269 MY ago (median estimate) in the Middle Permian, and crown squamates 206 MY ago in the Late Triassic (thus agreeing with recent phylogenomic analyses (Irisarri *et al.* 2017)). Furthermore, my morphological sampling allows a more precise estimate of the origin of the squamate root by the inclusion of fossils now recognized as stem squamates, and thus setting the age of origin of all squamates at 257 MY ago, close to the Permian-Triassic Mass Extinction (PTME).

Some of the oldest known fossils for certain diapsid lineages are known from the earliest Triassic, including ichthyosaurs (Motani *et al.* 1998), sauropterygians (Jiang *et al.* 2014), and archosaurs (Butler *et al.* 2011), with more recent fossil evidence already suggesting the presence of archosauriforms in the late Permian (Bernardi *et al.* 2015), strongly suggesting their divergence preceded the PTME. In accordance, my divergence time estimates for almost all major diapsid lineages (including lepidosaurs, archosauriforms, marine reptiles, among others) are in the Permian (Figs. 6.9 & 6.10), and not in the Triassic from which their oldest known fossils are from. This corresponds to the general expectation that the oldest known fossil of a lineage is likely to be much younger than the actual divergence time for that same lineage (Ho & Phillips 2009).

The origin of lepidosaurs and other major diapsid lineages prior to the PTME contradicts previous ideas suggesting that those groups originated in the aftermath of the greatest mass

extinction in Earth history (Chen & Benton 2012). Rather, my results indicate those lineages already existed, but radiated in the Triassic. It is likely that the PTME opened new niches and opportunities to lineages previously restricted in diversity, thus enabling their radiation in the Triassic into numerous forms and sizes, occupying all major biomes on the planet.

Figures and Tables

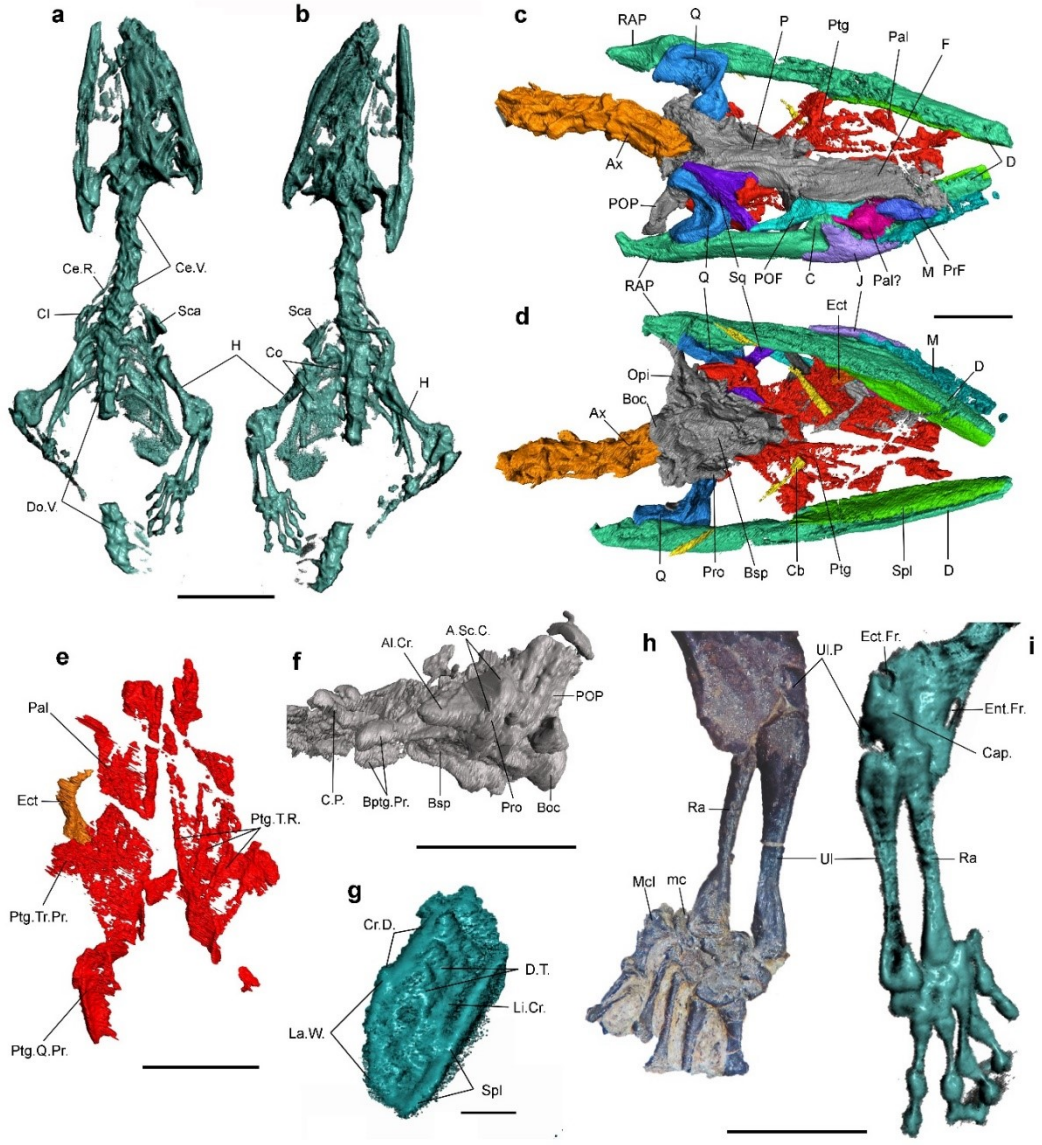

Figure 6.1. Holotype of *Megachirella wachtleri* (PZO 628). a, b, Whole skeleton dorsal and ventral views. c, d, Skull in dorsal (c) and ventral (d) views. e, Palatal region in ventral view. f, Braincase in left lateral view. g, Dentary in cross-section. h, i, Right forelimb in dorsal (h) and ventral (i) views. Abbreviations: Al.Cr., prootic alar crest; A.Sc.C., anterior semicircular canal; Ax, axis; Boc, basioccipital; Bptg.Br., basipterygoid process; Bsp, basisphenoid; C, coronoid; Cap, capitulum; Cb, ceratobranchial; Ce.R., cervical rib; Ce.V., cervical vertebrae; Cl, clavicle; Co, coracoid; C.P., cultriform process; Cr.D., crista dorsalis; D, dentary; Do.V., dorsal vertebrae; D.T., dentary teeth; Ect, ectopterygoid; Ect.Fr., ectepicondylar foramen; Ent.Fr., entepicondylar foramen; F, frontal; H, humerus; J, jugal; La.W., labial wall; Li.Cr., lingual crest; M, maxilla; mc, medial centrale; McI, metacarpal I; P, parietal; Opi, opisthotics; Pal, palatine; POF, postorbitofrontal; POP, paraoccipital process; PrF; prefrontal; Pro, prootic; Ptg, pterygoid; Ptg.T.R., pterygoid tooth rows; Ptg.Tr.Pr., pterygoid transverse process; Q, quadrate; Ra, radius; RAP, retroarticular process; Sca, scapula; Spl, splenial; Sq, squamosal; Ul, ulna; Ul.P., ulnar patella. Scale bars equal to 10mm (a and b), 5mm (c-f, h and i) and 1mm (g).

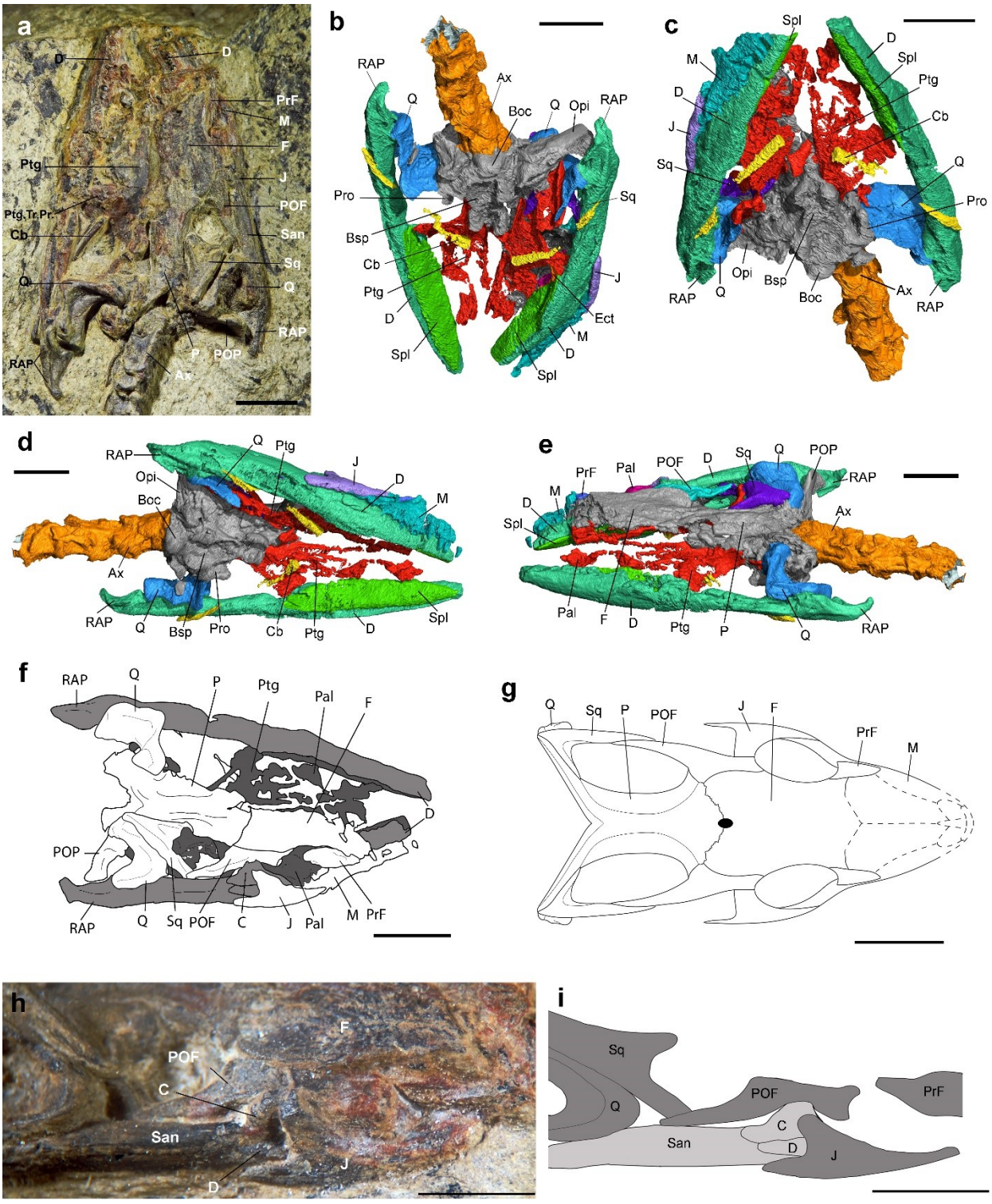

Figure 6.2. Cranial anatomy of *Megachirella wachtleri* (PZO 628) based on personal examination and μCT-scan data. a, Skull in dorsal view. b, Skull in posteroventral view. c, Skull in anteroventral view. d, Skull in right ventrolateral view. e, Skull in left dorsal lateral view. f, Line drawing of the skull in dorsal view. g, Reconstruction of the skull in dorsal view. h, Detailed view of right lateral side of the skull. i, Drawing of the view in h. Abbreviations: San, surangular. Scale bars equal to 5mm (a-g).

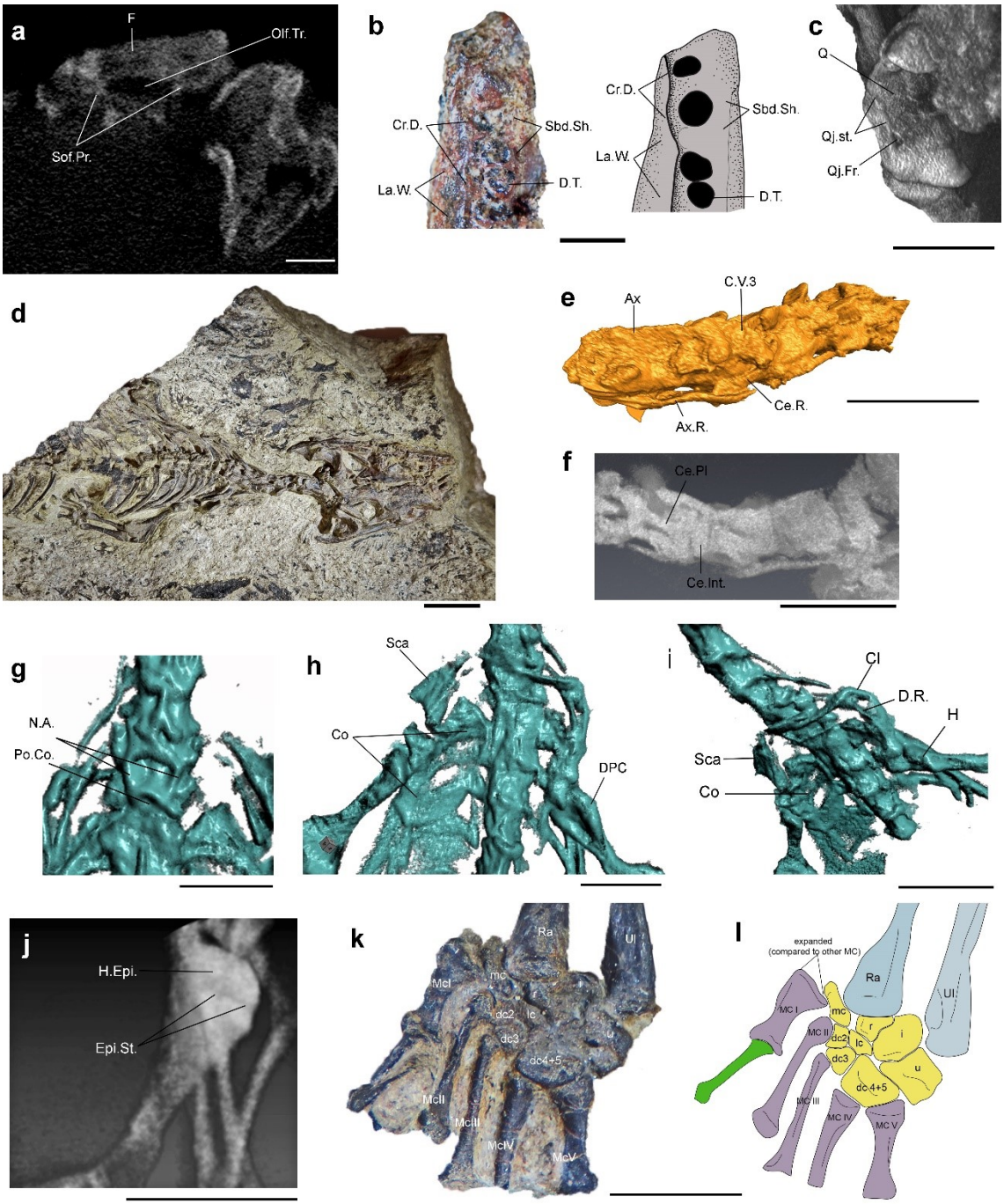

Figure 6.3. Cranial and postcranial anatomy of *Megachirella wachtleri* (PZO 628) based on personal examination and μCT-scan data. a, Cross section of the skull at the level of the frontals in anterior view. b, Details of the anterior end of the left dentary in occlusal view. c, Left quadrate. d, Whole body of the holotype as preserved in the slab (dorsal view). e, Anterior cervical vertebrae in left lateral view. f, Longitudinal section of the anterior cervicals in ventral view. g, Last cervicals and anterior dorsals in dorsal view. h, Pectoral girdle in ventral view. i, Pectoral girdle in left ventrolateral view. j, Right humerus in ventral view. k, Right manus in dorsal view. l, Line drawing of right manus in dorsal view. Abbreviations: Ax.R., axis rib; Co. cotyle; C.V.3, third cervical vertebra; dc2-5, distal carpals 2 to 5; DPC, deltopectoral crest; Epi.St., epiphysial suture; H.Epi., humeral epiphysis; i, intermedium; lc, lateral centrale; McI-V, metacarpals I to V; Olf.Tr., olfactory tract; Qj.Fr., quadratojugal foramen; Qj.St., quadratojugal suture; r, radiale; Sbd.Sh., subdentary shelf; Sof.Pr., subolfactory processes; u, ulnare. Scale bars equal to 1mm (a and b), 5mm (c, e-h, j-l), 10mm (d and i).

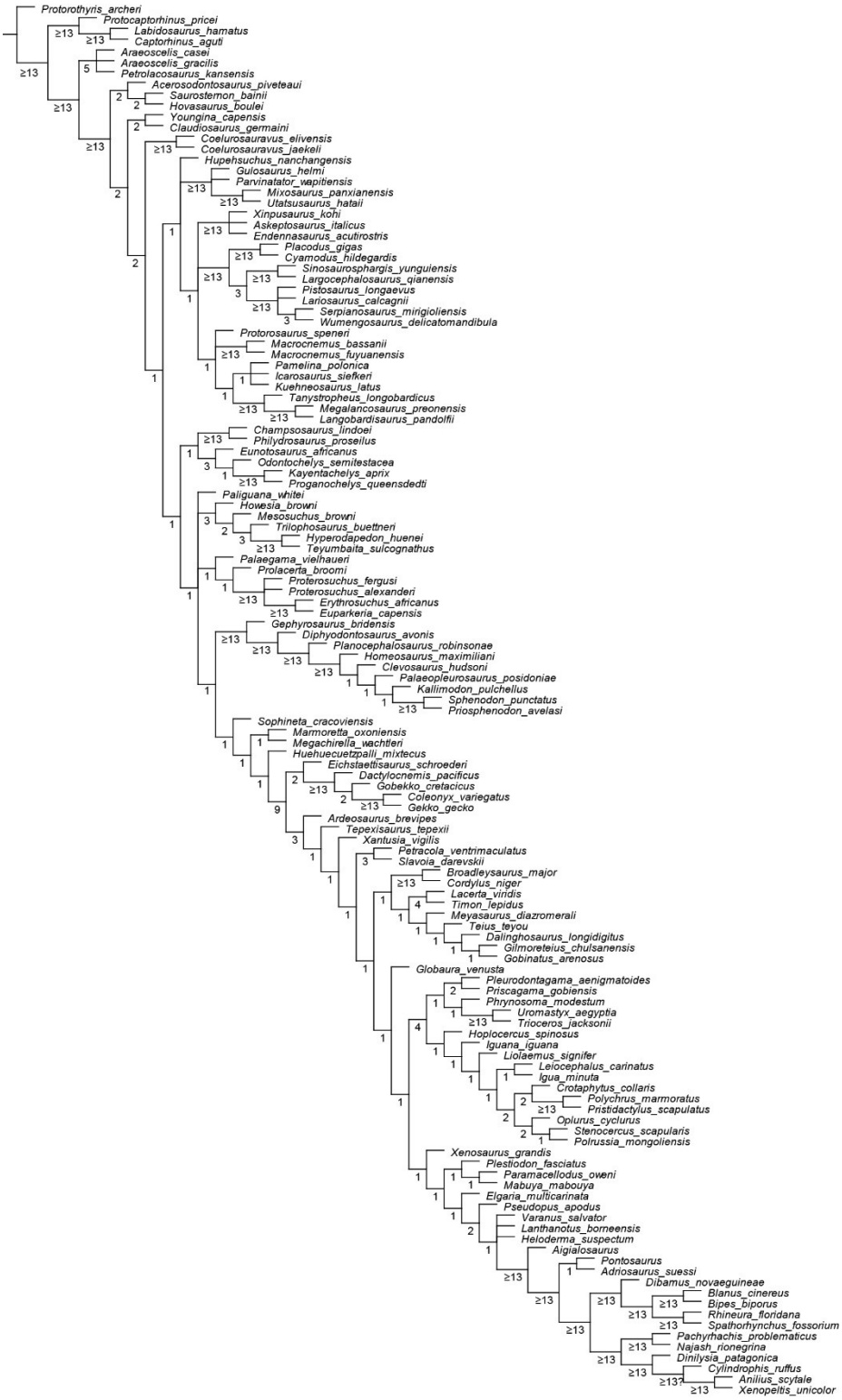

Figure 6.4. Morphological data only— equal weights maximum parsimony analysis. Strict consensus of 621 most parsimonious trees (2268 steps each). Numbers at nodes indicate Bremer indices.

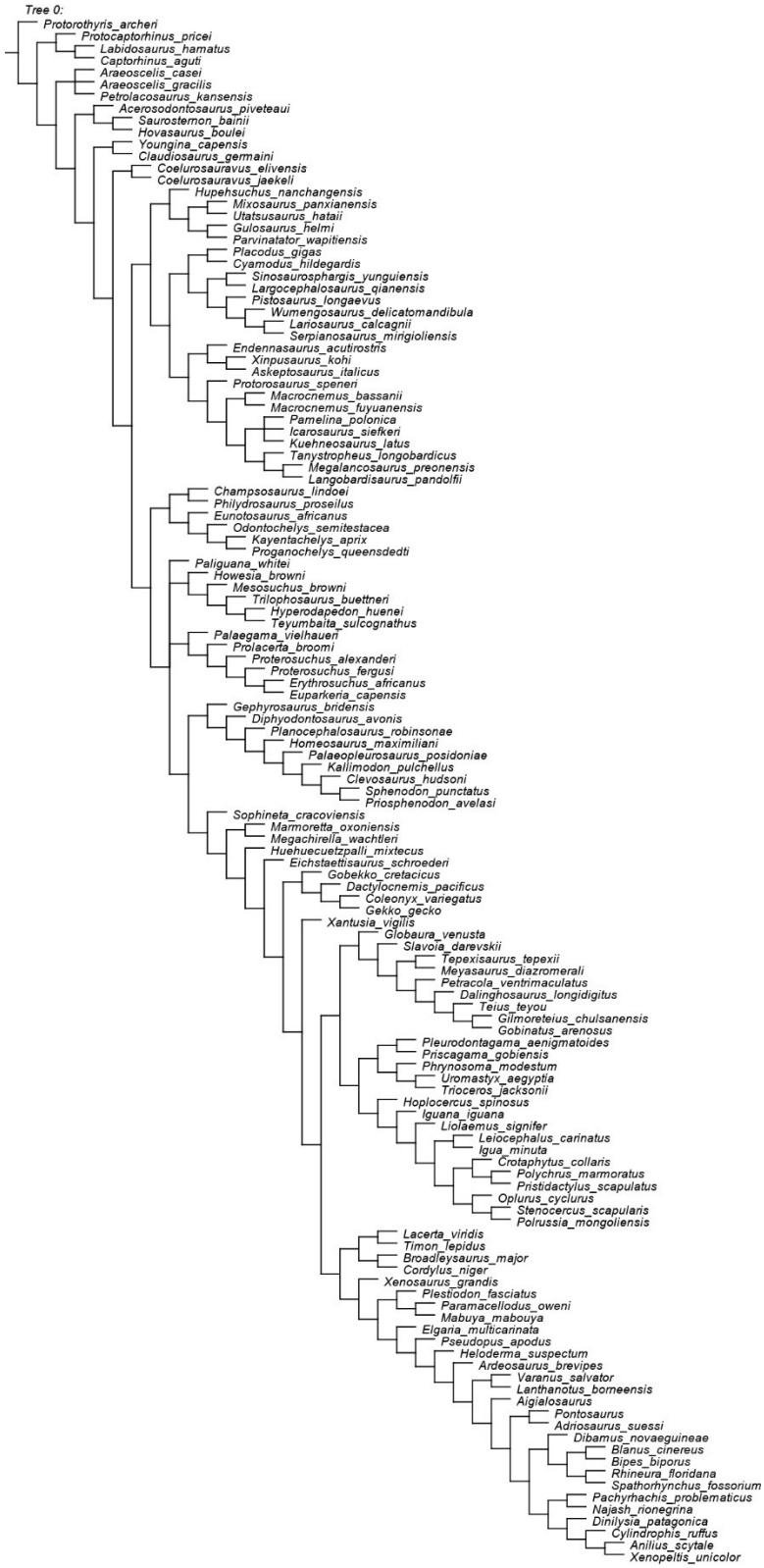

Figure 6.5. Morphological data only— implied weighting maximum parsimony analysis. Strict consensus of the five best feet trees (fit=91.768892).

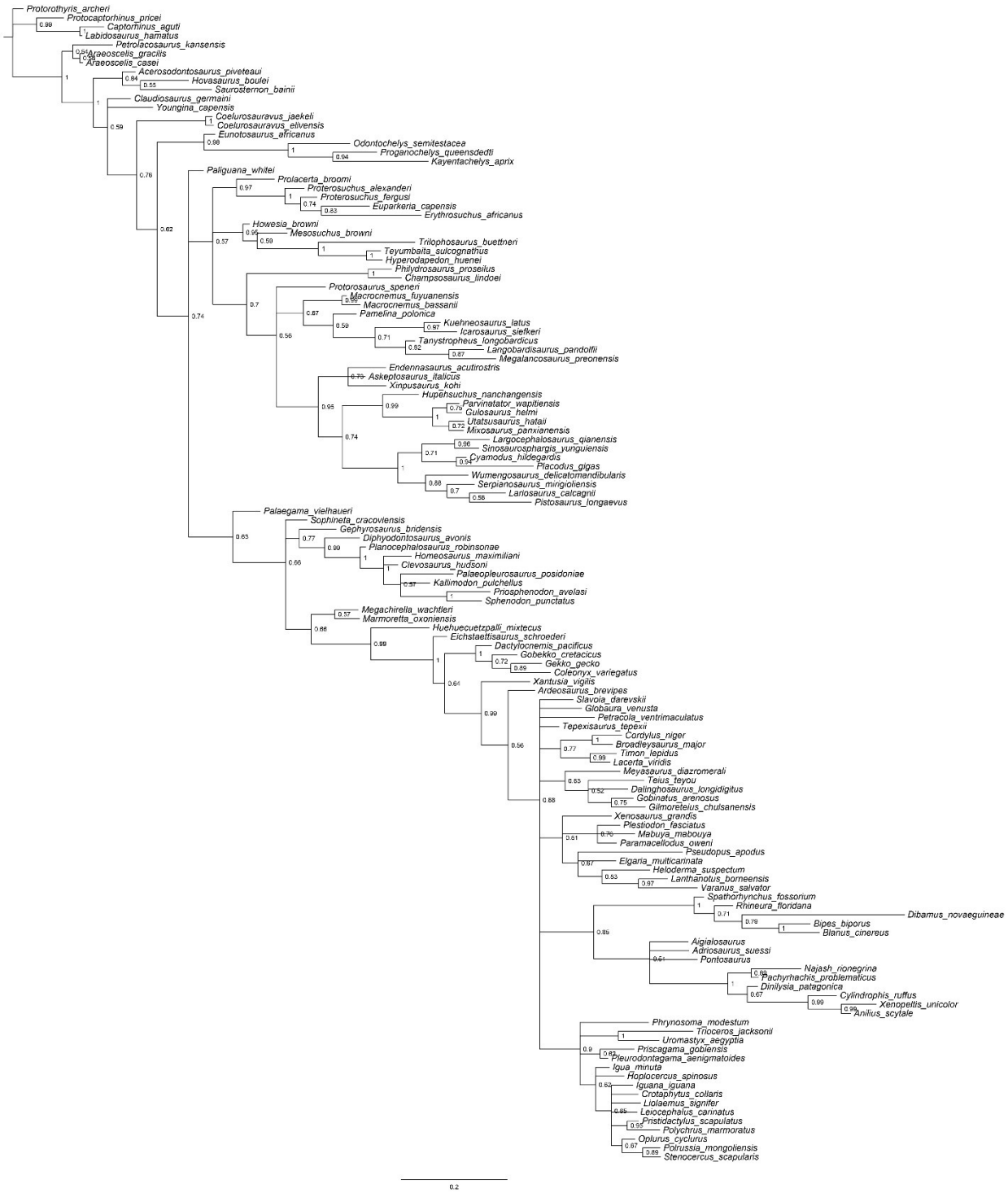

Figure 6.6. Morphological data only— Bayesian inference analysis. Bayesian majority rule consensus tree. Numbers at nodes indicate posterior probabilities.

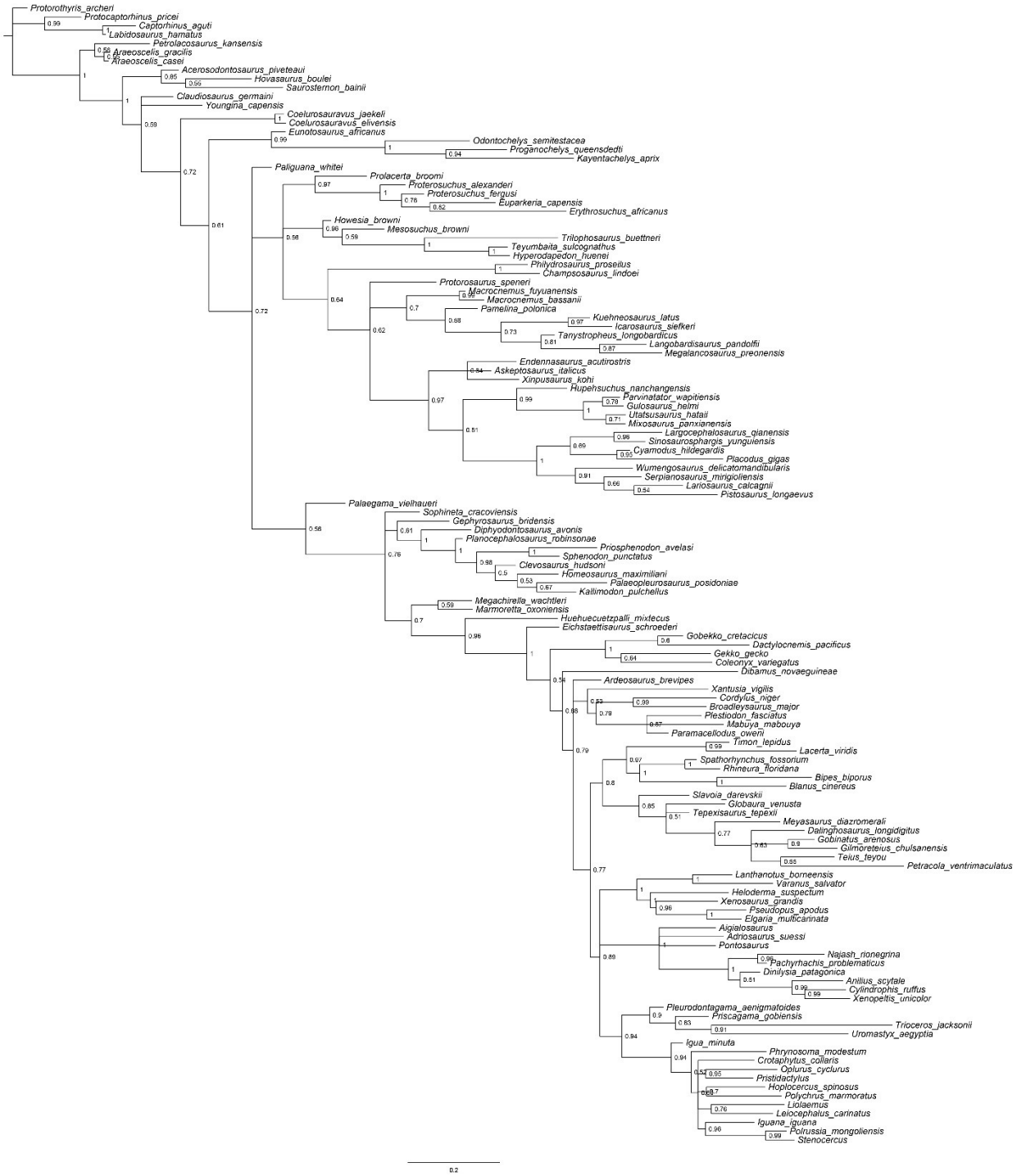

Figure 6.7. Combined morphological and molecular data— Bayesian inference analysis. Bayesian majority rule consensus tree. Numbers at nodes indicate posterior probabilities.

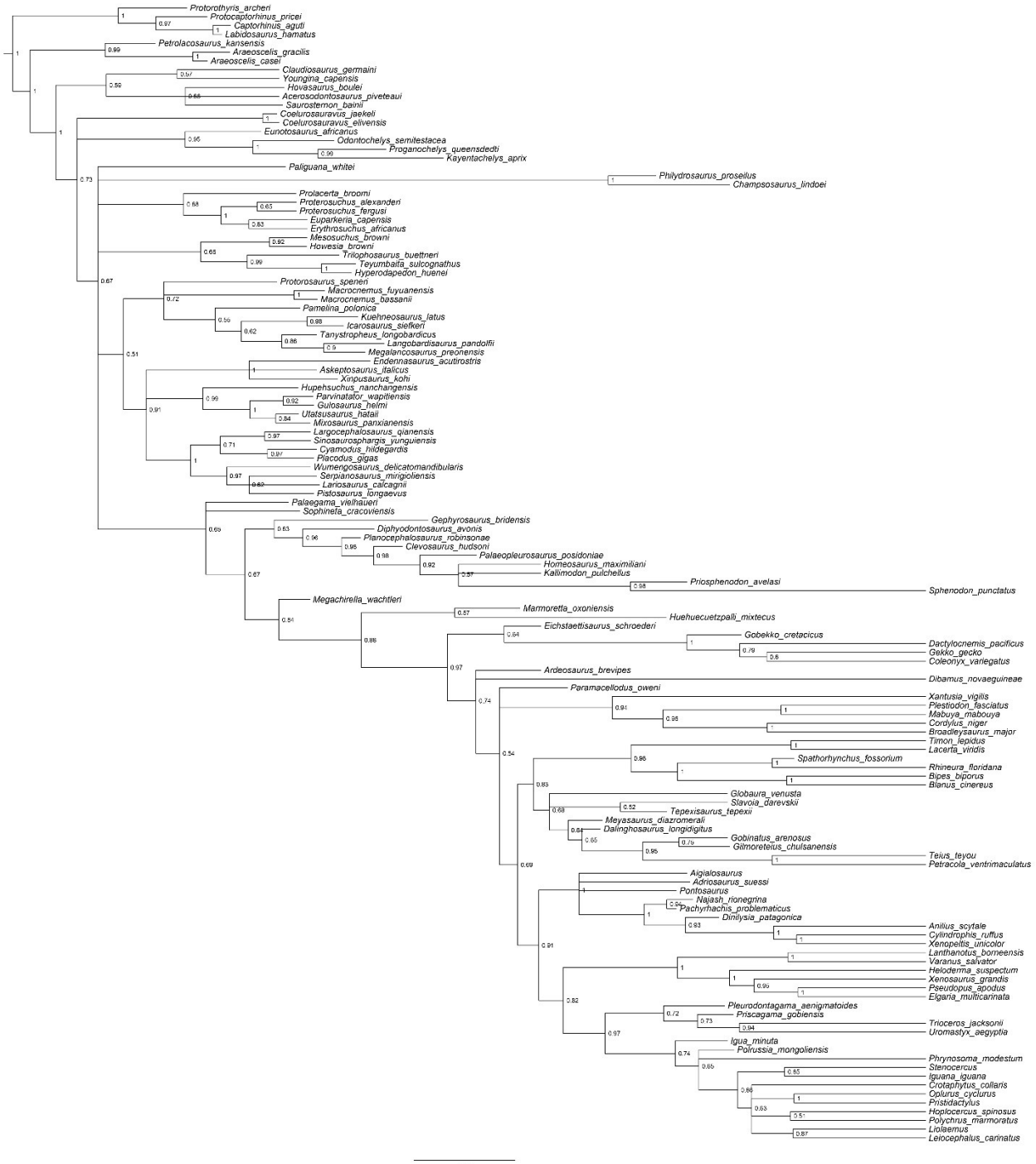

Figure 6.8. Combined morphological and molecular data—Relaxed clock Bayesian inference analysis with total evidence tip dating using the fossilized birth-death tree model. Bayesian majority rule consensus tree. Numbers at nodes indicate posterior probabilities.

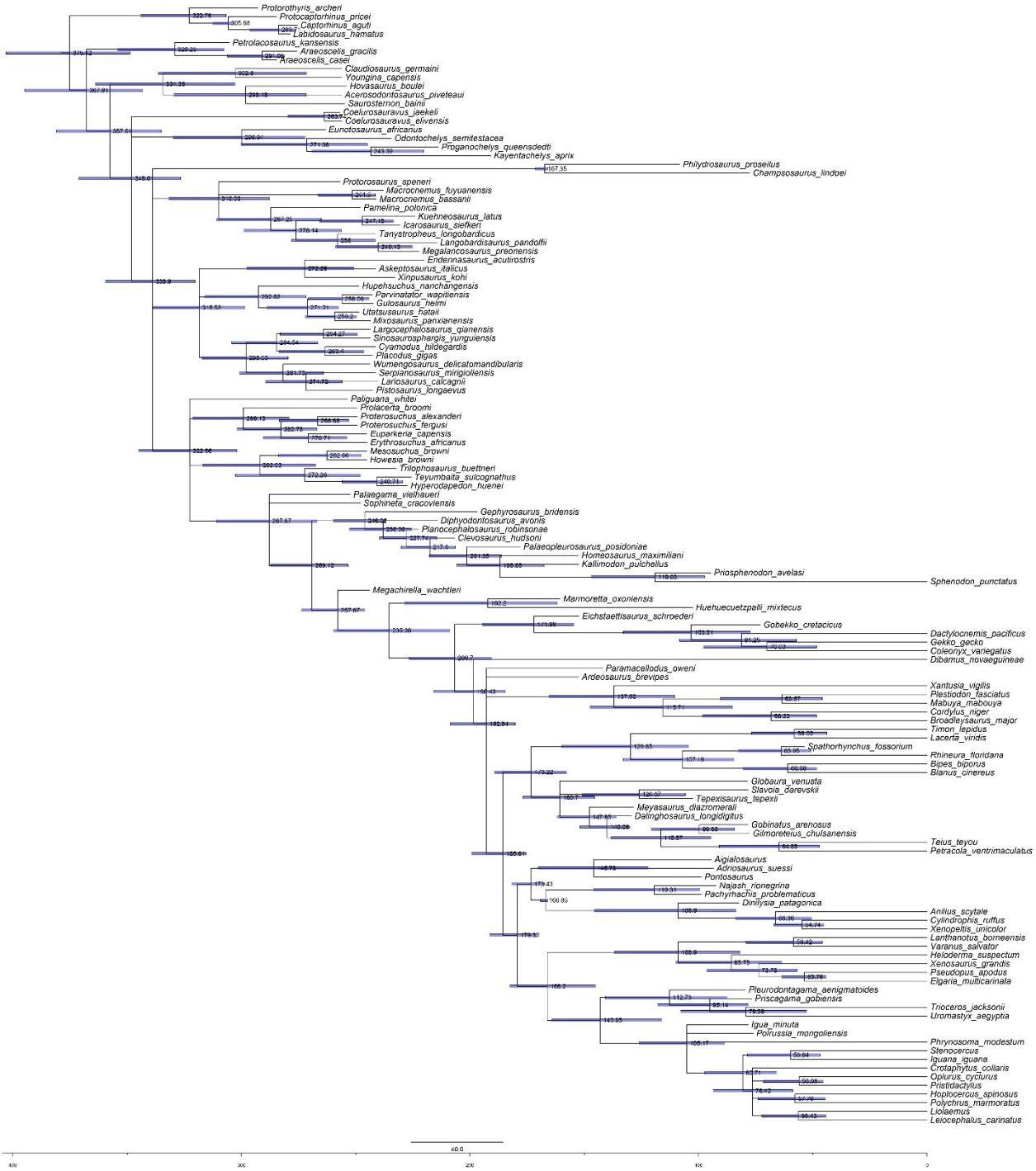

Figure 6.9. Combined morphological and molecular data—Relaxed clock Bayesian inference analysis with total evidence tip and node dating using the fossilized birth-death tree model. Bayesian majority rule consensus tree. Numbers at nodes indicate median estimates for the divergence times, and node bars indicate 95% highest posterior density for divergence times.

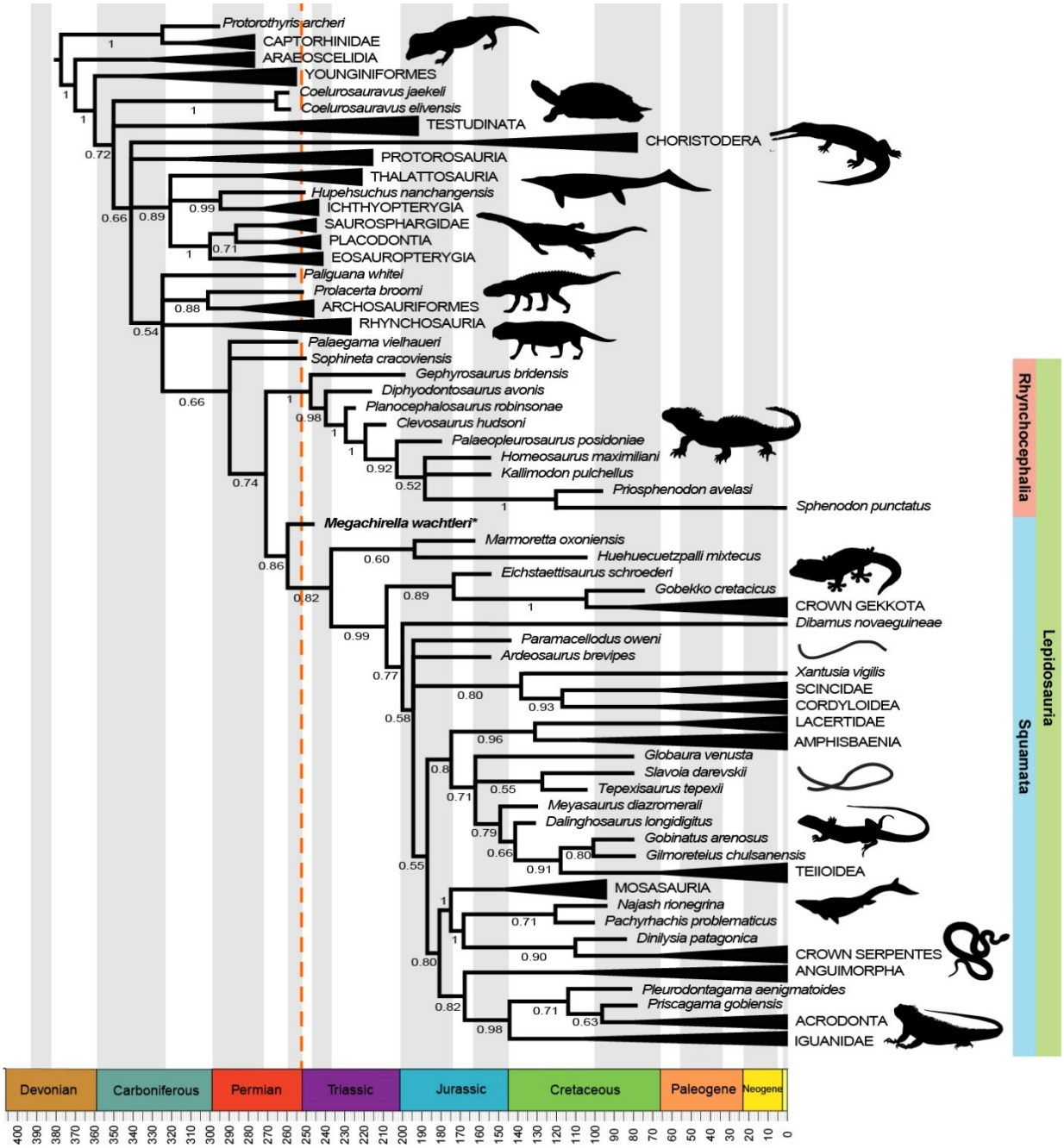

Figure 6.10. Combined evidence relaxed clock Bayesian inference analysis with total evidence tip and node dating using the fossilized birth-death tree model. Summary of the majority rule consensus tree depicting the median divergence time estimates for the major diapsid and squamates lineages against a geological time scale. Numbers at nodes indicate posterior probabilities and orange dashed line represents the Permian Triassic Mass Extinction event. For the full tree and 95% highest posterior density on divergence times see Fig. 6.9.

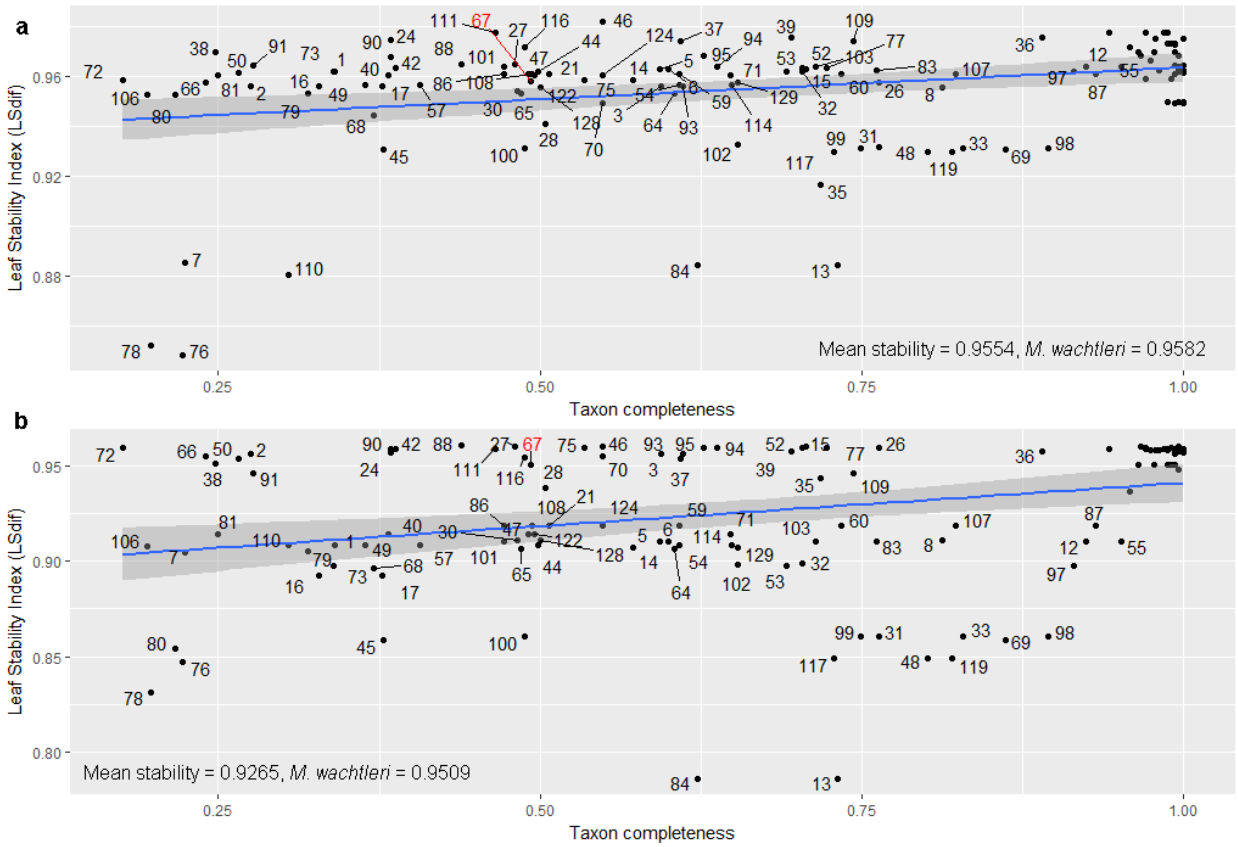

Figure 6.11. Taxon stability plotted against taxon completeness in the analysis combining both morphological and molecular data. a, Taxon stability in uncalibrated Bayesian inference analysis. b, Taxon stability in relaxed clock Bayesian inference analysis with tip dating. Taxon stability increases directly proportional to taxon completeness. *Megachirella wachtleri* (taxon 67, in red) has a stability slightly above average for uncalibrated Bayesian inference, and well above average for Bayesian inference with tip dating. All taxa are identified in Table 6.3. Regression line in blue and 95% confidence interval in grey. Labels for extant taxa (~100% completeness) are omitted for simplicity.

Table 6.1. GenBank accession numbers.

Taxon	BDNF	CAND1	C-*mos*	CXCR4
Anilius scytale	EU402625.1	GU432630.1	AF544722.1	JN702453.1
Bipes biporus	JN654794.1	JN881176.1	AF039482.1	JN702381.1
Blanus cinereus			AY444019.1	
Broadleysaurus major	HM160588.1		EU366459.1	
Coleonyx variegatus	HQ876231.1	JF818522.1	EU116676.1	JN702309.1
Cordylus niger	KT941174.1		KT941211.1	
Crotaphytus collaris	JF806021.1	JF818552.1	AY987985.1	JN702405.1
Cylindrophis ruffus	EU402635.1	JF818530.1	AF471133.1	JN702366.1
Dactylocnemis pacificus				
Dibamus novaeguineae	GU457863.1	GU432611.1	EF450999.1	JN702424.1
Elgaria multicarinata	GU457854.1	GU432602.1	AF039479.1	JN702462.1
Gekko gecko	EU402614.1	GU432614.1	EU366455.1	JN702441.1
Heloderma suspectum	GU457856.1	GU432604.1	AY487348.1	
Hoplocercus spinosus				
Iguana iguana	KR350713.1		AF148708.1	
Lacerta viridis	GU457875.1	GU432624.1	DQ097132.1	JN702397.1
Lanthanotus borneensis	GU457859.1	GU432607.1	AY662564.1	JN702444.1
Leiocephalus carinatus	AY987970.1			
*Liolaemus signifier**			JN683118.1	
Mabuya mabouya				
Oplurus cyclurus	GU457850.1	GU432597.1	EU099679.1	JN702378.1
Petracola ventrimaculatus			AY507910.1	
Phrynosoma modestum	DQ385325.1	KR360318.1		KR359901.1
Plestiodon fasciatus	HQ876228.1	JF818524.1	HQ655218.1	JN702435.1
Polychrus marmoratus	HQ876222.1	JF818569.1	AY987983.1	JN702359.1

*Pristidactylus scapulatus**	JF806025.1	JF818559.1	KT342956.1	JN702459.1
Pseudopus apodus	GU457851.1	GU432599.1		
Rhineura floridana	GU457878.1	GU432628.1	AY444021.1	JN702310.1
Sphenodon punctatus	GU457846.1	GU432592.1	AF039483.1	JN702443.1
*Stenocercus scapularis**	HQ876224.1	JF818571.1		JN702380.1
Teius teyou	JN654803.1	JN881211.1		JN702400.1
Timon lepidus			EF632290.1	
Trioceros jacksonii	KC507666.1		AF137528.1	
Uromastyx aegyptia			AF137531.1	
Varanus salvator	EU402618.1	GU432610.1	AF435017.1	JN702430.1
Xantusia vigilis	EU402620.1	JF818525.1	EU116833.1	JN702337.1
Xenopeltis unicolor	EU402668.1	GU432635.1	AF544689.1	JN702383.1
Xenosaurus grandis	GU457858.1	GU432606.1	AY662567.1	JN702341.1

Taxon	**NGFB**	**NTF3**	**PDC**	**R35**
Anilius scytale	EU437988.1	AY988055.1		HQ876355.1
Bipes biporus	JN662833.1	JN568335.1		HQ876353.1
Blanus cinereus		EU108015.1		
Broadleysaurus major		EU636222.1		HM161062.1
Coleonyx variegatus	JF818314.1	JF804539.1	EF534817.1	HQ876371.1
Cordylus niger				KT941339.1
Crotaphytus collaris	JF818338.1	JF804542.1		JF804586.1
Cylindrophis ruffus	EU437999.1	EU390915.1		JF804588.1
Dactylocnemis pacificus			GU459586.1	
Dibamus novaeguineae	GU432728.1	JF804544.1	HQ426251.1	
Elgaria multicarinata	GU432720.1	GU456010.1		HQ876338.1
Gekko gecko	EU437977.1	EU390898.1	EF534854.1	HQ876378.1

Heloderma suspectum	GU432722.1	GU456012.1	HQ426254.1	HQ876340.1
Hoplocercus spinosus				
Iguana iguana		HM352530.1		KR350699.1
Lacerta viridis	GU432740.1	GU456031.1		JF804593.1
Lanthanotus borneensis	GU432725.1	GU456015.1		
Leiocephalus carinatus		AY987999.1		KU979291.1
*Liolaemus signifier**				
Mabuya mabouya	JF498230.1			KJ574880.1
Oplurus cyclurus	GU432716.1	GU456006.1		HQ876332.1
Petracola ventrimaculatus				
Phrynosoma modestum	KR360303.1	KR360083.1		KJ124012.1
Plestiodon fasciatus	JF498300.1	JF804547.1		HQ907629.1
Polychrus marmoratus	JF818355.1	JF804564.1		HQ876335.1
*Pristidactylus scapulatus**	JF818345.1	JF804565.1		JF804601.1
Pseudopus apodus	GU432717.1	GU456007.1		JN703073.1
Rhineura floridana	GU432743.1	GU456034.1	EU293714	DQ119613.1
Sphenodon punctatus	GU432712.1	GU456002.1	HQ426257.1	HQ876320.1
*Stenocercus scapularis**	JF818357.1	JF804570.1		HQ876337.1
Teius teyou	JN662830.1	JN568323.1		JN568511.1
Timon lepidus			KX080818.1	
Trioceros jacksonii		AY988006.1		
Uromastyx aegyptia				
Varanus salvator	EU437981.1	EU390902.1		JN568500.1
Xantusia vigilis	EU437983.1	EU390904.1	HQ426258.1	HQ876351.1
Xenopeltis unicolor	EU438032.1	DQ465562.1		
Xenosaurus grandis	GU432724.1	GU456014.1		JN703069.1

Taxon	RAG1	ND2	ZEB2	FSHR
Anilius scytale	EU402834.1	NC_014343.1	EU390857.1	EU391110.1
Bipes biporus	HQ876445.1	NC_006287.1	JN568546.1	
Blanus cinereus	EU108523.1	NC_012433.1		
Broadleysaurus major		KF717422.1		
Coleonyx variegatus	HQ876448.1	NC_008774.1	JF804620.1	JF804389.1
Cordylus niger	KT941374.1	AY519699.1		
Crotaphytus collaris	JF806206.1	U82681.1	JF804623.1	JF804392.1
Cylindrophis ruffus	EU402842.1	AB179619.1	EU390866.1	EU391120.1
Dactylocnemis pacificus	GU459392.1	GU459794.1		
Dibamus novaeguineae	GU457986.1	FJ195390.1		
Elgaria multicarinata	GU457977.1	AF085620.1	GU456232.1	GU455976.1
Gekko gecko	EU402824.1	NC_007627.1	EU390847.1	EU391100.1
Heloderma suspectum	GU457979.1	NC_008776.1	GU456234.1	GU455978.1
Hoplocercus spinosus	AY662592.1	U82683.1		
Iguana iguana	KR350706.1	JF498123.1		
Lacerta viridis	GU457997.1	NC_008328.1	GU456253.1	GU455996.1
Lanthanotus borneensis	GU457982.1	AF407541.1	GU456237.1	GU455981.1
Leiocephalus carinatus	AY662598.1	AF049864.1		
*Liolaemus signifier**		AF099266.1		
Mabuya mabouya		JF498123.1		
Oplurus cyclurus	GU457973.1		GU456228.1	GU455972.1
Petracola ventrimaculatus				
Phrynosoma modestum	KR360097.1	AY297484.1	KR360287.1	KR360399.1
Plestiodon fasciatus	HQ876444.1	AY607299.1	JF804627.1	JF804396.1
Polychrus marmoratus	HQ876438.1	NC_012839.1	JF804644.1	JF804413.1
*Pristidactylus scapulatus**	JF806210.1	AF528732.1	JF804645.1	JF804414.1

Pseudopus apodus	GU457974.1	AF085623.1	GU456229.1	GU455973.1
Rhineura floridana	GU458000.1	NC_006282.1	GU456256.1	GU455999.1
Sphenodon punctatus	GU457969.1	KP996625.1	GU456224.1	GU455968.1
*Stenocercus scapularis**	HQ876440.1	DQ080223.1	JF804650.1	JF804419.1
Teius teyou	JN654865.1	JN700172.1	JN568560.1	JN568475.1
Timon lepidus	EF110996.1	DQ902256.1		
Trioceros jacksonii	JQ073211.1	AF448753.1		
Uromastyx aegyptia		AB619817.1		
Varanus salvator	EU402828.1	NC_010974.1	EU390851.1	EU391104.1
Xantusia vigilis	EU402830.1	EU130279.1	EU390853.1	EU391106.1
Xenopeltis unicolor	EU402870.1	NC_007402.1	EU390897.1	EU391152.1
Xenosaurus grandis	GU457981.1	U71333.2	GU456236.1	GU455980.1

Taxon	**TRAF6**	**FSTL5**	**12S**	**16S**
Anilius scytale	EU391058.1	EU402785.1	NC_014343.1	NC_014343.1
Bipes biporus	JN568459.1	JN654834.1	NC_006287.1	NC_006287.1
Blanus cinereus			NC_012433.1	NC_012433.1
Broadleysaurus major			AJ416921.1	AJ416922.1
Coleonyx variegatus	JF804342.1	JF806108.1	NC_008774.1	NC_008774.1
Cordylus niger			HQ167106.1	HQ167217.1
Crotaphytus collaris	JF804345.1	JF806134.1	L40439.1	L41443.1
Cylindrophis ruffus	EU391069.1	EU402795.1	AB179619.1	AB179619.1
Dactylocnemis pacificus				GU459993.1
Dibamus novaeguineae			FJ195390.1	FJ195390.1
Elgaria multicarinata	GU456155.1	GU457947.1	AY649110.1.1	
Gekko gecko	EU391048.1	EU402775.1	NC_007627.1	NC_007627.1
Heloderma suspectum	GU456157.1	GU457948.1	NC_008776.1	NC_008776.1

Hoplocercus spinosus				
Iguana iguana			NC_002793.1	NC_002793.1
Lacerta viridis	GU456176.1	GU457964.1	NC_008328.1	NC_008328.1
Lanthanotus borneensis	GU456160.1	GU457951.1		
Leiocephalus carinatus				
*Liolaemus signifier**			KF969090.1	
Mabuya mabouya			JF497871.1	AY070357.1
Oplurus cyclurus	GU456151.1	GU457943.1	U39585.1	
Petracola ventrimaculatus			KJ948193.1	KJ948144.1
Phrynosoma modestum	KR360111.1	KR360139.1	DQ385397.1	L41455.1
Plestiodon fasciatus	JF804349.1	JF806110.1	AY315505.1	AY308199.1
Polychrus marmoratus	JF804366.1	JF806144.1	NC_012839.1	NC_012839.1
*Pristidactylus scapulatus**	JF804367.1	JF806145.1	KT342931.1	
Pseudopus apodus	GU456152.1	GU457944.1	AF380955.1	JX987420.1
Rhineura floridana	GU456179.1	GU457967.1	NC_006282.1	NC_006282.1
Sphenodon punctatus	GU456147.1	GU457940.1	KP996625.1	KP996625.1
*Stenocercus scapularis**	JF804372.1	JF806148.1		L41481.1
Teius teyou	JN568447.1	JN654844.1	AY046461.1	AY046503.1
Timon lepidus			GQ142071.1	AF378949.1
Trioceros jacksonii			DQ397240.1	JN165401.1
Uromastyx aegyptia			FJ639656.1	FJ639621.1
Varanus salvator	EU391052.1	JF806113.1	NC_010974.1	NC_010974.1
Xantusia vigilis	EU391054.1	EU402781.1	AY218042.1	KC621482.1
Xenopeltis unicolor	EU391099.1	EU402823.1	NC_007402.1	NC_007402.1
Xenosaurus grandis	GU456159.1	GU457950.1		

Table 6.2. List of fossil taxa and updated ages used for tip-calibrations.

Fossil Taxa	**Chronostratigraphy**	**Age**	**Age references**
EARLY REPTILES			
Protorothyris archeri	Sakmarian, Cisuralian, Lower Permian	295-290.1	Clark & Carroll (1973); Lucas (2006); Ogg et al (2016)
Protocaptorhinus pricei	late Artinskian, Cisuralian, Lower Permian	286-283.5	Clark & Carroll (1973); Lucas (2006); Ogg et al (2016)
Captorhinus aguti	Early to Late Cisuralian, Lower Permian	298.9-272.3	Fox & Bowman (1966); Cisneros et al. (2015); Ogg et al (2016)
Labidosaurus hamatus	Kungurian, Cisuralian, Lower Permian	282-272.3	Lucas (2006); Ogg et al (2016)
Eunotosaurus africanus	middle Capitanian to Capitanian/Wuchiapingian boundary, Late Permian	265.8-260.4	Day et al. (2013)
Proganochelys queensdedti	Late Norian, Late Triassic	218-210	Menning et al. (2011); Ogg et al. (2016)
Odontochelys semitestacea	Lower Carnian, Late Triassic	237-232	Li et al. (2008); Ogg et al (2016)
Kayentachelys aprix	Sinemurian-Pliensbachian, Lower Jurassic	199.4-183.7	Padian (1989); Ogg et al (2016)
Petrolacosaurus kansensis	Stephanian of Europe [equivalent to the Kasimovian, Late Pennsylvanian, Carboniferous	307-303.7	Peabody (1952); Ogg et al. (2008); Ogg et al (2016)
Araeoscelis gracilis	Late Kungurian, Cisuralian, Lower Permian	278-272.3	Lucas (2006); Ogg et al (2016)
Araeoscelis casei	Artinskian and lower Kungurian, Cisuralian, Lower Permian	290.1-280	Lucas (2006); Ogg et al (2016)
Claudiosaurus germaini	Lopingian, Late Permian	257-255.2	Lucas (2006); Smith et al. (2012); Rubidge et al. (2013)
Youngina capensis	Lopingian, Late Permian	257-255.2	Smith et al. (2012); Rubidge et al. (2013)
Hovasaurus boulei	Lopingian, Late Permian to Induan, Early Triassic	257-251.2	Lucas (2006); Smith et al. (2012); Rubidge et al. (2013); Ketchum & Barret (2004)
Acerosodontosaurus piveteaui	Lopingian, Late Permian	257-255.2	Lucas (2006); Smith et al. (2012); Rubidge et al. (2013)
Coelurosauravus jaekeli	Middle Wuchiapingian, Lopingian, Late Permian	258-256	Menning et al. (2011)
Coelurosauravus elivensis	Lopingian, Late Permian	257-255.2	Lucas (2006); Smith et al. (2012); Rubidge et al. (2013)
Hupehsuchus nanchangensis	Spathian, late Olenkian, Lower Triassic	250-247.2	Carroll & Zhi-Ming (1991); Chen et al. (2014)
Parvinatator wapitiensis	Spathian, late Olenekian, Lower Triassic - latest Ladinian, Middle Triassic	248.4-237	McGowan & Motani (2003); Ogg et al (2016)
Gulosaurus helmi	Spathian, late Olenekian, Lower Triassic-latest Ladinian, Middle Triassic	248.4-237	Brinkman, Zhao & Nicholls (1992); McGowan & Motani (2003); Ogg et al (2016)

Utatsusaurus hataii	Spathian, late Olenkian, Lower Triassic	250-247.2	Motani et al. (1998)
Mixosaurus panxianensis	late Pelsonian, Anisian, Middle Triassic	244-243.5	Benton et al. (2013); Ogg et al (2016)
Protorosaurus speneri	Middle Wuchiapingian, Lopingian, Late Permian	258-256	Menning et al. (2011)
Prolacerta broomi	Induan-Olenekian, Early Triassic	251.9-246.8	Smith et al. (2012)
Macrocnemus bassanii	Late Anisian to early Ladinian, Middle Triassic	243.5-239	Rieppel (1993); Furrer (1995); Ogg et al. (2016)
Macrocnemus fuyuanensis	Longobardian, late Ladinian, Middle Triassic	239-237	Li et al. (2007); Benton (2013); Ogg et al. (2016)
Langobardisaurus tonelloi	Late Alaunian-early Sevatian, late Norian, Late Triassic	217-212	Saller, renesto & Dalla Vechia (2013); Ogg et al. (2016)
Tanystropheus longobardicus	Late Anisian to early Ladinian, Middle Triassic	243.5-239	Rieppel (1993); Furrer (1995); Ogg et al. (2016)
Megalancosaurus preonensis	Middle Norian, Late Triassic	228-218	Renesto et al. (2010); Ogg et al. (2016)
Endennasaurus acutirostris	Middle-late Norian, Late Triassic	223-217	Tintori (1995); Gaetani et al. (1998); Ogg et al. (2016)
Askeptosaurus italicus	Late Anisian to early Ladinian, Middle Triassic	243.5-239	Rieppel (1993); Furrer (1995); Ogg et al. (2016)
Xinpusaurus kohi	Carnian, Late Triassic	237.5-228.5	Jiang et al. (2005); Ogg et al. (2016)
Champsosaurus lindoei	Mid-Campania, Late Cretaceous	79-76	Gao & Brinkman (2005); Ogg et al. (2016)
Phylidrosaurus proseilus	Albian, Early Cretaceous	113.1-100.5	Gao & Fox (2005); Ogg et al. (2016)
Trilophosaurus buettneri	Middle Otischalkian, lower Carnian, Late Triassic to late Adamanian, latest Carnian, Late Triassic	237-228.5	Spielmann et al. (2008); Ogg et al. (2016)
Mesosuchus browni	Earliest to middle/late Anisian, Middle Triassic	246.8-243.5	Dilkes (1998); Smith et al. (2012)
Howesia browni	Earliest to middle/late Anisian, Middle Triassic	246.8-243.5	Dilkes (1995); Smith (2012)
Teyumbaita sulcognathus	Early Norian, Late Triassic	228.5-223	Langer et al. (2007); Montefeltro, Langer & Schultz (2010); Ogg et al. (2016)
Hyperodapedon huenei	Latest Carnian-earliest Norian, Late Triassic	230-225	Langer et al. (2007); Ogg et al. (2016)
Proterosuchus fergusi	Induan-Olenekian, Early Triassic	251.9-246.8	Smith et al. (2012)
Proterosuchus alexanderi	Induan-Olenekian, Early Triassic	251.9-246.8	Smith et al. (2012)
Erythrosuchus africanus	Earliest to middle/late Anisian, Middle Triassic	246.8-243.5	Dilkes (1995); Smith (2012)
Euparkeria capensis	Earliest to middle/late Anisian, Middle Triassic	246.8-243.5	Dilkes (1995); Smith (2012)

Placodus gigas	Early Anisian to early Ladinian, Middle Triassic	246-240	Menning et al. (2011); Ogg et al. (2016)
Cyamodus hildegardis	Late Anisian to early Ladinian, Middle Triassic	243.5-239	Rieppel (1993); Furrer (1995); Ogg et al. (2016)
Largocephalosaurus qianensis	Late Pelsonian, Anisian, Middle Triassic	244-243.5	Benton et al. (2013); Ogg et al. (2016)
Sinosaurosphargis yunguiensis	Late Pelsonian, Anisian, Middle Triassic	244-243.5	Benton et al. (2013); Ogg et al. (2016)
Serpianosaurus mirigioliensis	Late Anisian to early Ladinian, Middle Triassic	243.5-239	Rieppel (1993); Furrer (1995); Ogg et al. (2016)
Wumengosaurus delicatomandibularis	late Pelsonian, Anisian, Middle Triassic	244-243.5	Benton et al. (2013); Ogg et al (2016)
Lariosaurus calcagnii	Lower Ladinian, Middle Triassic	241.5-239	Furrer (1995); Ogg et al. (2016)
Pistosaurus longaevus	Illyrium, late Anisian, Middle Triassic	243.5-241.5	Menning et al. (2011); Ogg et al. (2016)
Palaegama vielhaueri	Middle Lopingian, Late Permian-middle Olenekian, Early Triassic	258-247.5	Smith et al. (2012)
Paliguana whitei	Middle Lopingian, Late Permian-middle Olenekian, Early Triassic	258-247.5	Smith et al. (2012)
Saurosternon bainii	Middle Wuchiapigian-latest Changhsingian, Lapingian, Late Permian	258-251.9	Smith et al. (2012)
Pamelina polonica	Early late Olenekian, Early Triassic	248.5-247.5	Shishkin & Sulej (2009)
Sophineta cracoviensis	Early late Olenekian, Early Triassic	248.5-247.5	Shishkin & Sulej (2009)
Megachirella wachtleri	Pelsonian, Anisian, Middle Triassic	244.5-243.5	Renesto & Bernardi (2014)
Kuehneosaurus latus	Carnian-Rhaetian, Late Triassic	237-201.4	Fraser (1994); Evans & Jones (2010)
Icarosaurus siefkeri	Tuvalian, Carnian, Late Triassic	233-228.5	Lucas (1998); Ogg et al. (2016)
Marmoretta oxoniensis	Late Bathonian, Middle Jurassic to Kimmeridgian, Late Jurassic	167-152.1	Evans & Kermack (1994); Ogg et al (2016)
Gephyrosaurus bridensis	Haettagian or Sinemurian, Lower Jurassic	201.4-191.4	Evans & Kermack (1994); Evans & Jones (2010); Ogg et al (2016)
Diphyodontosaurus avonis	Carnian-Rhaetian, Late Triassic	237-201.4	Fraser (1994); Evans & Jones (2010)
Planocephalosaurus robinsonae	Carnian-Rhaetian, Late Triassic	237-201.4	Fraser (1994); Evans & Jones (2010)
Clevosaurus hudsoni	Carnian-Rhaetian, Late Triassic	237-201.4	Fraser (1994); Evans & Jones (2010)
Palaeopleurosaurus posidoniae	Toarcian, Early Jurassic	183.7-174.2	Carroll (1985); Ogg et al. (2016)
Homeosaurus maximiliani	Latest Kimmeridgian-early Tithonian, Late Jurassic	155-150	Schweigert (2007); Ogg et al (2016)
Kallimodon pulchellus	Latest Kimmeridgian-early Tithonian, Late Jurassic	155-150	Schweigert (2007); Ogg et al (2016)

Priosphenodon avelasi	Cenomanian-Turonian, Late Cretaceous	100.5-89.8	Apesteguía & Novas (2003); Ogg et al (2016)
Sphenodon punctatus			
Eichstaettisaurus schroederi	Latest Kimmeridgian-early Tithonian, Late Jurassic	155-150	Schweigert (2007); Ogg et al (2016)
Ardeosaurus brevipes	Latest Kimmeridgian-early Tithonian, Late Jurassic	155-150	Schweigert (2007); Ogg et al (2016)
Paramacellodus oweni	Berriasian, Early Cretaceous	145-139.4	Evans 2003; Ogg et al (2016)
Huehuecuetzpalli mixtecus	Late Albian, Early Cretaceous	105-100	Benammi et al. (2006)
Tepexisaurus tepexi	Late Albian, Early Cretaceous	105-100	Benammi et al. (2006)
Priscagama gobiensis	Campanian-earliest Maastrichtian, Late Cretaceous	84.2-71	Jerzykiewicz et al. (1993); Dashzeveg et al. (2005); Dingus et al. (2008); Ogg et al (2016)
Pleurodontagama aenigmatoides	Campanian, Late Cretaceous	84.2-72.1	Eberth (1993); Jerzykiewicz et al. (1993); Dingus et al. (2008); Ogg et al (2016)
Igua minuta	Campanian, Late Cretaceous	84.2-72.1	Jerzykiewicz et al. (1993); Dingus et al. (2008); Ogg et al (2016)
Polrussia mongoliensis	Campanian, Late Cretaceous	84.2-72.1	Jerzykiewicz et al. (1993); Dingus et al. (2008); Ogg et al (2016)
Gilmoreteius chulsanensis	Campanian, Late Cretaceous	84.2-72.1	Dingus et al. (2008); Ogg et al (2016)
Gobinatus arenosus	Campanian, Late Cretaceous	84.2-72.1	Jerzykiewicz et al. (1993); Dingus et al. (2008); Ogg et al (2016)
Gobekko cretacicus	Late Campanian-earliest Maastrichtian, Late Cretaceous	75-71	Dashzeveg et al. (2005)
Meyasaurus diazromerali	Barremian, Early Cretaceous	130.8-126.3	Buscalioni & Fregenal-Martínez (2010); Ogg et al (2016)
Globaura venusta	Campanian-earliest Maastrichtian, Late Cretaceous	84.2-71	Dashzeveg et al. (2005); Dingus et al. (2008); Ogg et al (2016)
Slavoia darevskii	Campanian, Late Cretaceous	84.2-71	Dashzeveg et al. (2005); Dingus et al. (2008); Ogg et al (2016)
Dalinghosaurus longidigitus	Earliest Hautuverian-Barremian/Aptian, Early Cretaceous	134.7 to 126.3	Sha (2007); Ogg et al. (2016)
Dinilysia patagonica	Santonian to early/middle Campanian, Late Cretaceous	86.3-77	Leanza & Hugo (2001); Scanferla & Canale (2007); Filippi & Garrido (2012); Ogg et al. (2016)
Najash rionegrina	Cenomanian-Turonian, Late Cretaceous	95-89.8	Corbella et al. (2004); Zaher et al. (2009); Ogg et al. (2016)
Pachyrhachis problematicus	lower Cenomanian, Late Cretaceous	100.5-97	Lee & Caldwell (1998); Ogg et al. (2016)
Spathorhynchus fossorium	Early to Middle Eocene, Paleogene	56-45	Berman (1977); Ogg et al. (2016)
Aigialosaurus	Late Cenomanian-Early Turonian, Late Cretaceous	97-92	Gušić & Jelaska (1993); Ogg et al. (2016)

Adriosaurus suessi	late Cenomanian- late Turonian, Late Cretaceous	97-90	Gušić & Jelaska (1993); Lee & Caldwell (2000); Ogg et al. (2016)
Pontosaurus	Early-middle Cenomanian , Late Cretaceous (oldest record of the genus)	100.5-97	Dal Sasso & Pinna (1997); Ogg et al. (2016)

Table 6.3. List of taxa for leaf stability index analysis depicted in Figure 6.11.

Number	Taxon	Completeness	Comb_Bayes	Comb_Bayes_Cal_Tip
1	Acerosodontosaurus piveteaui	0.34017595	0.962152	0.908309
2	Adriosaurus suessi	0.2748538	0.956248	0.956339
3	Aigialosaurus	0.5945122	0.956237	0.956328
4	Anilius scytale	0.97119342	0.958804	0.959452
5	Araeoscelis casei	0.59292035	0.962772	0.910641
6	Araeoscelis gracilis	0.59940653	0.962787	0.910641
7	Ardeosaurus brevipes	0.22418879	0.885262	0.904393
8	Askeptosaurus italicus	0.81268882	0.955652	0.911004
9	Bipes biporus	0.98513011	0.977336	0.958663
10	Blanus cinereus	0.94262295	0.977336	0.958663
11	Broadleysaurus major	0.99402985	0.973275	0.950836
12	Captorhinus aguti	0.9244713	0.963932	0.910634
13	Champsosaurus lindoei	0.73111782	0.884349	0.78622
14	Claudiosaurus germaini	0.57227139	0.95841	0.907198
15	Clevosaurus hudsoni	0.70694864	0.962838	0.960308
16	Coelurosauravus elivensis	0.32835821	0.956084	0.892316
17	Coelurosauravus jaekeli	0.37724551	0.956084	0.892316
18	Coleonyx variegatus	0.97749196	0.969812	0.950728
19	Cordylus niger	0.98802395	0.973275	0.950836
20	Crotaphytus collaris	1	0.961666	0.956926
21	Cyamodus hildegardis	0.5074184	0.960744	0.918726
22	Cylindrophis ruffus	0.97119342	0.958806	0.959452
23	Dactylocnemis pacificus	0.96485623	0.969719	0.95063
24	Dalinghosaurus longidigitus	0.38392857	0.974663	0.957222
25	Dibamus novaeguineae	0.95867769	0.97163	0.93664
26	Dinilysia patagonica	0.76383764	0.957702	0.959312
27	Diphyodontosaurus avonis	0.48071217	0.964906	0.960323
28	Eichstaettisaurus schroederi	0.50453172	0.94097	0.938666
29	Elgaria multicarinata	1	0.949526	0.957921
30	Endennasaurus acutirostris	0.48203593	0.954134	0.910997
31	Erythrosuchus africanus	0.76331361	0.931479	0.860712
32	Eunotosaurus africanus	0.70414201	0.962036	0.898578
33	Euparkeria capensis	0.82890855	0.931471	0.860721
34	Gekko gecko	0.99361022	0.969801	0.95074
35	Gephyrosaurus bridensis	0.71856287	0.916428	0.943606
36	Gilmoreteius chulsanensis	0.8902439	0.975325	0.957829
37	Globaura venusta	0.60895522	0.974063	0.953875
38	Gobekko cretacicus	0.24776119	0.969772	0.950881
39	Gobinatus arenosus	0.69552239	0.975317	0.957828
40	Gulosaurus helmi	0.38235294	0.96053	0.91411
41	Heloderma suspectum	0.99384615	0.949491	0.957887

42	Homeosaurus maximiliani	0.3880597	0.963147	0.959109
43	Hoplocercus spinosus	0.9939577	0.960882	0.956013
44	Hovasaurus boulei	0.49853372	0.962139	0.908218
45	Howesia browni	0.37790698	0.930622	0.858453
46	Huehuecuetzpalli mixtecus	0.54848485	0.981662	0.959917
47	Hupehsuchus nanchangensis	0.49122807	0.96086	0.91413
48	Hyperodapedon huenei	0.80120482	0.930009	0.849181
49	Icarosaurus siefkeri	0.36390533	0.956633	0.908467
50	Igua minuta	0.26530612	0.96126	0.953559
51	Iguana iguana	1	0.964159	0.958863
52	Kallimodon pulchellus	0.70392749	0.963542	0.959193
53	Kayentachelys aprix	0.69180328	0.961909	0.897687
54	Kuehneosaurus latus	0.60843373	0.956634	0.908468
55	Labidosaurus hamatus	0.95180723	0.963932	0.910634
56	Lacerta viridis	0.98776758	0.977283	0.958607
57	Langobardisaurus pandolfii	0.40672783	0.956627	0.908707
58	Lanthanotus borneensis	1	0.949554	0.957956
59	Largocephalosaurus qianensis	0.60843373	0.96075	0.918735
60	Lariosaurus calcagnii	0.73413897	0.960835	0.918792
61	Leiocephalus carinatus	0.99698795	0.96217	0.957885
62	Liolaemus signifer	1	0.962401	0.957932
63	Mabuya mabouya	0.99079755	0.973021	0.950835
64	Macrocnemus bassanii	0.60486322	0.95301	0.906555
65	Macrocnemus fuyuanensis	0.48502994	0.95301	0.906555
66	Marmoretta oxoniensis	0.23976608	0.957512	0.955068
67	Megachirella wachtleri	0.49253731	0.958161	0.950858
68	Megalancosaurus preonensis	0.37091988	0.94443	0.896143
69	Mesosuchus browni	0.86176471	0.930657	0.858454
70	Meyasaurus diazromerali	0.54896142	0.949009	0.955181
71	Mixosaurus panxianensis	0.64776119	0.960479	0.914062
72	Najash rionegrina	0.17589577	0.95845	0.959302
73	Odontochelys semitestacea	0.33923304	0.961909	0.897684
74	Oplurus cyclurus	0.98159509	0.962528	0.958215
75	Pachyrhachis problematicus	0.53405018	0.95849	0.959302
76	Palaegama vielhaueri	0.22222222	0.848587	0.847395
77	Palaeopleurosaurus posidoniae	0.72256098	0.963552	0.959554
78	Paliguana whitei	0.19710145	0.852412	0.831552
79	Pamelina polonica	0.31952663	0.953214	0.905014
80	Paramacellodus oweni	0.21613833	0.952589	0.85434
81	Parvinatator wapitiensis	0.24927536	0.960528	0.914108
82	Petracola ventrimaculatus	0.97859327	0.975089	0.957983
83	Petrolacosaurus kansensis	0.76190476	0.962309	0.910619
84	Philydrosaurus proseilus	0.62275449	0.884349	0.78622

85	Phrynosoma modestum	0.975	0.966252	0.95824
86	Pistosaurus longaevus	0.47239264	0.960759	0.918688
87	Placodus gigas	0.93209877	0.960729	0.918704
88	Planocephalosaurus robinsonae	0.43843844	0.965075	0.96045
89	Plestiodon fasciatus	0.99384615	0.973024	0.950835
90	Pleurodontagama aenigmatoides	0.38392857	0.967595	0.959013
91	Polrussia mongoliensis	0.27728614	0.964168	0.945868
92	Polychrus marmoratus	0.99695122	0.961863	0.957326
93	Pontosaurus	0.61111111	0.956117	0.956021
94	Priosphenodon avelasi	0.6375	0.963713	0.959748
95	Priscagama gobiensis	0.62732919	0.968126	0.959592
96	Pristidactylus scapulatus	0.99697885	0.962528	0.958215
97	Proganochelys queensdedti	0.91515152	0.961909	0.897687
98	Prolacerta broomi	0.89552239	0.931275	0.86065
99	Proterosuchus alexanderi	0.74926254	0.93141	0.860698
100	Proterosuchus fergusi	0.48823529	0.931351	0.86065
101	Protocaptorhinus pricei	0.47181009	0.963928	0.910614
102	Protorosaurus speneri	0.65373134	0.932596	0.898021
103	Protorothyris archeri	0.71428571	0.963928	0.910614
104	Pseudopus apodus	0.99652778	0.949526	0.957921
105	Rhineura floridana	0.97083333	0.977335	0.958663
106	Saurosternon bainii	0.19476744	0.952625	0.907698
107	Serpianosaurus mirigioliensis	0.82317073	0.96076	0.918732
108	Sinosaurosphargis yunguiensis	0.49386503	0.960748	0.918734
109	Slavoia darevskii	0.74404762	0.973912	0.945952
110	Sophineta cracoviensis	0.30409357	0.880758	0.908308
111	Spathorhynchus fossorium	0.46540881	0.977335	0.958663
112	Sphenodon punctatus	0.99691358	0.963714	0.948019
113	Stenocercus scapularis	0.99390244	0.964182	0.958857
114	Tanystropheus longobardicus	0.64939024	0.956559	0.908655
115	Teius teyou	1	0.975072	0.957983
116	Tepexisaurus tepexii	0.48816568	0.971429	0.95435
117	Teyumbaita sulcognathus	0.72891566	0.930009	0.849181
118	Timon lepidus	0.98791541	0.977283	0.958607
119	Trilophosaurus buettneri	0.82066869	0.929982	0.849137
120	Trioceros jacksonii	0.96763754	0.968248	0.959907
121	Uromastyx aegyptia	0.99692308	0.968246	0.959905
122	Utatsusaurus hataii	0.49552239	0.960481	0.914064
123	Varanus salvator	0.98784195	0.949554	0.957956
124	Wumengosaurus delicatomandibularis	0.54896142	0.960528	0.918775
125	Xantusia vigilis	0.99369085	0.972481	0.950663
126	Xenopeltis unicolor	0.99126638	0.958806	0.959452

127	Xenosaurus grandis	1	0.949494	0.957887
128	Xinpusaurus kohi	0.5	0.955476	0.910996
129	Youngina capensis	0.65384615	0.957561	0.907039

CHAPTER SEVEN: GENERAL CONCLUSIONS

In the present thesis, I have tried to provide insights on the early history of squamate evolution in general, and the origin of the major lizard groups in different continents more specifically, utilizing information from extant taxa and the fossil record, based on both morphological and molecular data. Most importantly, I have tried to combine this massive data collection with the most recent advances in the field of phylogenetics, in order to provide the most technically sound analysis of early squamates evolution available thus far. In this chapter, I try to summarize some of the major findings and overall conclusions on the early history of lizards that I have drawn during the last five and a half years.

The early evolution of teiioids

As a continuation of the work developed during my MSc research (Simões 2012; Simões *et al.* 2015a), the initial stages of my PhD thesis aimed towards shedding some light on the early evolution of squamates in South America, by assessing the taxonomy, phylogeny and biogeography of the oldest known lizards in that continent. Undoubtedly, one of the greatest challenges in answering those questions is related to the origin of teiioids (Simões *et al.* 2017a), which is one of the most conspicuous lizard clades of that continent. The origin of teiioids has once been linked to the origin of borioteiioids and champosids (possibly related clades) from North America. The most common classification of borioteiioids and champosiids as a subgroup of teiioids (Estes 1969; 1983b; Gao & Fox 1996; Gao & Norell 2000), or their sister clade (Nydam *et al.* 2007), contributed to the hypothesis that South American teiioids were later surviving members of a Cretaceous teiioid migration from North into South America (Presch 1974; Estes 1983a; Estes & Báez 1985; Nydam *et al.* 2007). However, a recent drawback to this hypothesis was the attribution of borioteiioids, or Polyglyphanodontia sensu Gauthier *et al.* (2012), as the sister clade to Mosasauria+Scleroglossa, or to iguanians (Reeder *et al.* 2015), which means that they could not be teiioids nor their sister clade (Gauthier *et al.* 2012). In all of my phylogenetic results derived from my own dataset (see Chapter 6), however, I provide support to the most common hypothesis that borioteiioids are closely related to modern teiioids, specifically as their sister clade. Importantly, several fossil lizards from other regions of the world, such as *Meyasaurus* (Early Cretaceous of Spain), *Dalinghosaurus* (Early Cretaceous of China), and *Slavoia* (Late Cretaceous of Mongolia), seem to be early members of the lineage

leading up to borioteiioids and teiioids. This indicates that some fossil lizards of hitherto controversial phylogenetic affinities may actually be the earliest members of the teiioid lineage, or actually be part of an entirely extinct lineages of their own, but which does share the most recent common ancestor with borioteiioids and teiioids. It also indicates that the origin of South American teiioids could well be in other continents.

Finding Cretaceous teiioids in South America could provide important clues to that origin, as it could indicate, for instance, if the first teiioids in South America are actually well nested within borioteiioids and teiioids, or if they are part of this "early-teiioid" fauna, in which *Meyasaurus* and other Early Cretaceous taxa seem to be part of. Thus far, the only Cretaceous South American lizard that may provide answers to this question is *Calanguban alamoi* from the Early Cretaceous of the Crato Formation, in northeastern Brazil (Simões *et al.* 2015a; Simões *et al.* 2017e). *Calanguban* preserves features that it shares in common with teiioids and this "early-teiioid" fauna of the Early Cretaceous, especially *Meyasaurus*, such as a fused postorbitofrontal and a dorsal process of the squamosal. However, this feature is also present in other squamates groups, most notably mosasauroids. Also, important details of the skull and vertebral anatomy are not preserved in *Calanguban.* Whether *Calanguban* represents a link to a possible Cretaceous teiioid fauna in South America, is still unclear, but further fieldwork in Cretaceous outcrops in South America may provide important new insights into the early history of teiioids.

The early evolution of acrodontan and non-acrodontan iguanians

Among iguanians, *Gueragama sulamericana* (see Chapter 2) provides new information on the biogeographic history of acrodontans. Some authors had considered that the radiation of acrodontans followed an origin in Eastern Laurasia, with subsequent dispersal events, mostly in Asia and Africa (Honda *et al.* 2000). Others, however, suggested an initial dispersal of the group, followed by vicariant events after the break-up of Gondwana, giving origin to most of the modern clades, and their subsequent dispersal during the Cenozoic (Moody 1980; Macey *et al.* 2000). *Gueragama* supports the latter hypothesis, as it provides evidence for an early broad distribution of acrodontans. However, their occurrence in the Cretaceous of South America indicates this early distribution was geographically much broader than previously thought, reaching parts of the world they never occurred again during the Cenozoic (given our current

knowledge). The available evidence from Mesozoic (presented herein) and Cenozoic lizards (Estes 1983b; Albino & Brizuela 2014) in South America indicates only non-acrodontans and scincomorphs passed through the Cretaceous-Paleogene (K-Pg) boundary. This raises the possibility that the K-Pg extinction might have influenced the eventual demise of acrodontans in South America, and the subsequent radiation of non-acrodontan families. An alternative hypothesis is a competitive exclusion of acrodontans by pleurodont iguanians. Competition between both groups has been previously suggested to explain the complementary distribution of both groups (Diamond 1975), but the current fossil record does not provide enough information to test this idea (Augé 2007a). At least regarding the replacement of iguanids by lacertids in Europe, where competitive exclusion had also been postulated, has been falsified (Augé 2007b).

Iguanians, both acrodontans and non-acrodontans, were globally distributed by the Late Cretaceous, occurring in North (Gao & Fox 1996; Demar *et al.* 2015) and South America (Estes & Price 1973; Nava & Martinelli 2011; Simões *et al.* 2015b; Simões *et al.* 2017e), Africa (Apesteguía *et al.* 2016), Europe (Sigé *et al.* 1997; Rage 1999; Blanco *et al.* 2016) and throughout Asia: Mongolia [e.g. Borsuk-Białynicka & Moody (1984) and Gao & Norell (2000)], China (Gao & Hou 1995; Li *et al.* 2007b), Myanmar (Daza *et al.* 2016), and Uzbekistan (Nessov 1988; Gao & Nessov 1998). One further North American taxon, *Pariguana lancensis*, has been described from the Late Maastrichtian of Lance Formation as an iguanid. However, the tooth morphology (labiolingually expanded), a widely open Meckelian canal, and an anteriorly elongate splenial make this taxon quite similar to the teiid fauna (e.g. *Sphenosiagon*) from western Canada (Gao & Fox 1996). Therefore, I consider this only a tentative assignment to Iguania, pending revision of the holotype. The identification if the gliding lizard *Xianglong* as an acrodontan is also problematic, given the poor preservation of its cranial characters (Evans & Manabe 2009). *Bharatagama rebbanensis*, from the Early-Middle Jurassic of India, initially considered the oldest known acrodontan (Evans *et al.* 2002; Jones *et al.* 2013), has also been recently is considered as likely to be a sphenodontian (Jones *et al.* 2013; Conrad 2017), a position that I personally find plausible, although I have not personally observed this specimen.

Despite the limitation of the fossil record, the presently known pattern indicates iguanian global distribution during the Cretaceous was even larger than their extant one. It is yet unclear whether this Cretaceous distribution represents the first radiation of iguanians. However, it is

very likely that they reached such geographically distant parts of the world before the final break-up of Laurasia and Gondwana during the Cretaceous.

The early evolution of geckoes

As outlined in Chapter 3, some of the oldest known articulated lizards in the world that come from the Late Jurassic of Solnhofen, Germany, containing some of the oldest known geckoes. The placement of *Ardeosaurus* remains somewhat contentious, given the poor preservation of diagnostic characters of *Ardeosaurus digitatellus*, but which still placed it within Gekkota in the analysis performed in Chapter 3, using updates on the dataset of Gauthier *et al.* (2012). The better preserved *Ardeosaurus brevipes* is phylogenetically close to *Eichstaettisaurus* and geckoes, but was not placed within Gekkota in the analyses using my own dataset. However, the placement of *Eichstaettisaurus* as the earliest Gekkota is supported by several anatomical features, the analysis performed in Chapter 3, and by the analyses with my own dataset under equal weights maximum parsimony and time calibrated Bayesian inference analysis combining morphological and molecular data, which is the preferred hypothesis herein.

The significance of finding that some of the oldest articulated fossil lizards in the world represent early members of what both the morphological and molecular data indicate as the earliest evolving crown squamates clade cannot be overstated. This indicates that the fossil record supports previous hypothesis provided by molecular studies and my own morphological data—that geckoes represent the earliest evolving lineages among crown squamates. Although current knowledge of squamate evolution based on the fossil record remains limited because of the extremely scarce record during the Triassic and most of the Jurassic, I expect that further findings from Jurassic squamates will further support the ancestry of geckoes.

Functional morphology and biomechanics

The autopodial morphology of both *Eichstaettisaurus* and *Ardeosaurus* indicate those taxa had adaptations to scansoriality that were previously unrecognized. Some of those morphologies include relatively elongate penultimate phalanges; claws tall at their bases, providing a greater lever arm moment for the flexor tendon (increasing grasping capacity); and the overall depressed

shape of the body, bringing the centre of gravity closer to the substrate. The autopodial features used to infer scansorial adaptations in those Late Jurassic species have been supported by previous studies based on quantitative analysis of extant taxa, which found a significant correlation even when taking the phylogenetic signal under consideration [e.g. (Tulli *et al.* 2009)]. Importantly, the hand symmetry of *Eichstaettisaurus* not only indicates a remarkable similarity to the hand symmetry that is only observed in geckoes, among crown squamates, but implies that hand symmetry, and scansoriality, evolved in geckoes at least as far back as the Late Jurassic.

As indicated in Chapter 4, squamate reptiles had long been characterized by the absence of a lower temporal bar in the skull. This had previously been indicated as an adaptation to increase the cross-section area of the external adductor muscle mass (in particular, the adductor superficialis), which leads to greater biting force in squamates compared to other reptiles that possess a complete lower temporal bar (Rieppel & Gronowski 1981). Therefore, the discovery that some Late Cretaceous borioteiioids had independently broken this character canalization and redeveloped a complete lower temporal bar is not only unexpected, but also triggers important biomechanical questions.

In the analyses performed in Chapter 4, replicating individual muscle load values on reconstructed skulls and assessing stress and distortion using infinite elements analysis, it was detected that the most common configuration of the lizard skull (without a lower temporal bar and with a jugomandibular ligament) is the best suited and most efficient configuration for hard biting, explaining why this is a conspicuous feature of herbivorous lizards. This configuration of the temporal ligament is therefore more adapted for hard biting (and, therefore, herbivory) than other temporal configurations that are found in squamates, such as the one in which the temporal ligament connects the jugal to the quadrate bone (a quadratojugal ligament). Interestingly, the replacement of the temporal ligament by a bony lower temporal bar connecting the main body of the jugal to the quadrate bone (by means of an elongate posteroventral process of the jugal), and fusing to the quadrate, seems to improve performance compared to skulls with quadratojugal ligaments. This suggests that the reacquisition of the lower temporal bar, with complete fusion of the jugal to the quadrate, as observed in *Tyaniusaurus*, is functionally advantageous for hard biting (Moazen *et al.* 2009a; Mo *et al.* 2010) and improves performance in a similar way that the jugomandibular does. However, when the lower temporal bar is not fused to the quadrate, as in

Polyglyphanodon, then it does not provide any functional advantage for hard biting and herbivory compared to the more common ligamentous connections between the jugal and the quadrate or between the jugal and the mandible. In fact, it performs worse than some of the later conditions. The lower temporal bar in *Polyglyphanodon* can also excluded as an adaptation to stabilize the quadrate because of the highly akinetic configuration of the skull in this taxon, which includes a strong contact between the quadrate and the pterygoid ventrally, and between the quadrate and the squamosal dorsally. Finally, juveniles do not yet have the jugal contacting the quadrate, indicating the jugal is not fundamental to stabilize the quadrate during biting for most of the ontogeny in *Polyglyphanodon*.

In the absence of any reasonable functional explanation, I propose that the reacquisition of the lower temporal bar in *Polyglyphanodon* is an example of non-functional/non-adaptive evolution, but merely the result of constraint release. It also suggests that the genetic background for the redevelopment of a full bony lower temporal bar was widespread among borioteiioids, given the independent reacquisition of this feature in taxa that are phylogenetically and geographically distant from each other in the borioteiioids tree.

Diapsid phylogeny and the origin of squamates

The results of Chapter 6 significantly alter previous notions of lepidosauromorph composition and the early evolution of squamates based on the morphological record. Among its most significant findings, it becomes clear that some taxonomic groups previously considered to be early lepidosauromorphs by previous authors, such as *Paliguana*, kuehneosaurids, younginiforms and sauropterygians, are found widespread across different sectors of the diapsid tree, but not within the Lepidosauromorpha. Additionally, some other taxa previously considered to be early lepidosauromorphs, or early lepidosaurs (but outside the Squamata and Rhynchocephalia), actually represent early evolving squamates. This indicates that the squamate-sphenodontian split is phylogenetically very close to the split between lepidosaurs and other diapsid reptiles, such as archosauromorphs. These also indicates that the time of origin of the two major lepidosaurian clades must be considerably older than usually assumed, which was subsequently confirmed by my time calibrated analysis.

Specifically, younginiforms are found as paraphyletic in most trees, although there is a short phylogenetic distance between the so-called younginiform taxa. On the other hand, the time calibrated Bayesian inference analysis indicates a monophyletic younginiform clade. The later result is certainly influenced by the tree prior, because of the very similar calibration times for all younginiforms. Whether this is a "better" phylogenetic representation than uncalibrated Bayesian inferences is debatable, given that uncalibrated Bayesian inference analysis are more precise, whereas time calibrated analyses can be more accurate at the cost of precision (Wertheim *et al.* 2010). Additionally, *Saurosternon* was consistently found among younginiform taxa in all of the trees of Chapter 6. This is unsurprising, given the numerous similarities between *Saurosternon* and younginiforms, such as the ossified sternal plate, combined with autopodial elements that are more similar to the ones in early diapsids than in lepidosauromorphs (such as the absence of a hook-shaped fifth metatarsal).

Kuehneosaurids are found within protorosaurus in all of the resulting trees. Although kuehneosaurids have traditionally been placed within lepidosauromorphs because of their pleurodont dentition and absence of a lower temporal bar (Evans & Jones 2010), both features can also be observed in other reptile taxa other than lepidosauromorphs. For instance, kuehneosaurids have postcranial features that are unobserved in squamates and rhynchocephalians, but which are present in protorosaurs, such as the apical expansion of the neural spine, especially on the dorsal vertebrae. They also share with protorosaurs and marine reptiles, a semi-lunate shaped postfrontal, which is absent in rhynchocephalians and early squamates.

Paliguana and *Palaegama* are both highly unstable taxa, shifting in position and creating lack of resolution in all of the resulting trees from my analysis, also being recovered among the most unstable taxa under the leaf stability analysis. This is probably because of the poor preservation of the only specimens of both taxa. *Paliguana* is only known from a skull, which has sutures that are very hard to observe, making the limits between bones of dubious interpretation. In my analysis, I tried to score only the characters that I could interpret without ambiguity, but the preservation of this specimen is likely to create ambiguity among different morphological datasets. While *Paliguna* seems to be of extreme relevance to diapsid analyses, additional specimens are certainly needed to unambiguously place *Paliguana* in the diapsid tree. *Palaegama* has both the skull and postcranium preserved, but the cranial features are not

extensively preserved, and it is also known from a single specimen. Given its potential placement as either an early lepidosauromorph, or an early archosauromorph among my results, I consider its placement as still contentious. As with *Paliguana*, this situation may only be overcome by the discovery of new specimens.

The placement of *Sophineta* is also ambiguous. Whereas in the maximum parsimony analyses it is found as an early squamate, Bayesian inference analyses indicate that *Sophineta* is either an early lepidosauromorph, or it falls in a polytomy with squamates and rhynchocephalians. I consider this as another result of problematic preservation of the specimens associated with this taxon. In this instance, however, this is not caused by poor preservation, but of the fragmentary and disarticulated nature of those specimens. As indicated in the taxon sampling criteria of Chapter 6, *Sophineta* is preserved as several isolated and fragmentary elements that needed to be assembled together. Because of lack of anatomical connections between some of those elements, I specifically excluded those unconnected elements from the list of specimens I utilized to score *Sophineta* in my dataset. Therefore, *Sophineta* and *Pamelina* (which come from the same locality) are represented by a significant amount of missing data. I consider that only by the discovery of articulated specimens, as it was the case for *Clevosaurus hudsoni*, that a precise knowledge of the anatomy of those very important taxa will be gained, which will make them significantly more informative for the purposes of assessing diapsid phylogenetic relationships.

Megachirella and *Marmoretta* were consistently found as early evolving squamates, contrary to previous hypothesis regarding their phylogenetic relationships, and closely related to the other early evolving fossil squamate *Huhuecuetzpalli*. This finding indicates that poor taxon sampling of squamates in previous diapsid phylogenies probably prevented the accurate placement of those taxa. It also bridges what was previously thought as a fossil gap between the oldest known fossil squamates from the Middle Jurassic of Britain, Morocco and Central Asia, and the estimated time for the origin of squamates based on the molecular clock. Importantly, the relatively well-preserved and articulated nature of *Megachirella* allows it to provide fundamental insights into the early acquisition of squamate features, such as: changes in the mode of articulation between the suspensorium and the quadrate; the development of the alar process of the prootic; the development of the squamate palate; and changes in the appendicular skeleton,

including the acquisition of the anteroposteriorly curved clavicles, and fusion of the medial centrale to the head of the first metacarpal.

Finally, the results of my analyses indicate that there is a morphological signal for the placement of Gekkota as the earliest evolving squamate crown clade. This result indicates that features observed in geckoes that are common to other diapsid reptiles, but absent in all other squamates, are not independent reacquisitions, but actually plesiomorphic traits. These features include the presence of amphicoelic vertebrae, the persistence of a notochordal canal in adults, a perforated stapes, the metotic fenestra undivided externally (although divided medially), and the presence of paired premaxillae. Some of those features are also shared with xantusiids and dibamids. This provides the first ever agreement between morphological and molecular hypothesis concerning the early evolution of crown squamates. Additionally, the relaxed clock Bayesian inference analyses indicate divergence time estimates for the major groups of diapsids, including squamates, to be in the Permian, thus prior to the Permian-Triassic extinction event. This indicates that the time of origin of those clades is somewhat older than their oldest known fossils (which is not unexpected), thus contradicting previous ideas that the origin of the modern reptile fauna dates back to the Triassic. From my results, it is clear that the origin of the major reptile clades is in the Permian, but those lineages underwent considerable diversification in the Triassic, which explains the pattern currently observed in the fossil record.

Concluding remarks

For at least 15 years, the conflict between morphological and molecular data concerning broad level relationships among squamates have been a source of debate and wondering (Losos *et al.* 2012). Most often, the morphological data has been blamed for not being as precise and objective as molecular data, although some studies have tried to find potential biases in the molecular signal too (McMahan *et al.* 2015). From the work that I carried out in the various chapters of my thesis, especially in chapters 5 and 6, there is an indication that the source of conflict, especially regarding the early evolution of squamates, does lie in the morphological data. However, this is not because morphological data is a problem in itself, as argued by some authors (Scotland *et al.* 2003), but mostly because of lack of attention and care to the way that morphological datasets are constructed.

Morphological characters utilized in phylogenetic datasets do not represent raw biological data, as argued by some authors, especially those who defend the indiscriminate collection of characters from the literature, or the creation of characters without concern for primary homologies (Kluge 2003). Phylogenetic characters represent a translation of observable raw biological data from individual specimens into characters statements that should accurately reflect the variation under consideration (Nixon & Carpenter 2013; Simões *et al.* 2017c). Errors in this process of extraction and translation may be caused by numerous factors, including: taxonomic preconceptions, logical dependencies among characters, or failure to pass basic tests of primary homology (similarity and conjunction) [de Pinna (1991); Pleijel (1995); Rae (1998); Rieppel & Kearney (2002); Kearney & Rieppel (2006); Sereno (2007); Brazeau (2011); Simões *et al.* (2017d)].

Importantly, there is a growing trend of new phylogenetic datasets based on morphological data of being mostly extracted from information from the literature only [e.g. (Baron *et al.* 2017)], which unavoidably leads to incorrect taxon scorings, and profound changes to the subsequent results (Langer *et al.* 2017). This, I consider the second significant contribution of my thesis concerning morphological dataset construction. I have extracted information based on personal observations on nearly all of the taxa included in my dataset. I also scored the majority of the cells in the present dataset while observing the referred specimens in their respective collections, which made the process of data scoring more efficient, thus being less prone to errors.

In conclusion, I attribute the significant changes of my results concerning the early evolution of squamates as compared to previous studies, and its agreement with molecular hypothesis, based on the explicit and careful consideration of the basic criteria of primary homology assessment and character construction proposed by me (Simões *et al.* 2017d) and others before me (see above) along with my effort towards primary data collection. It is only by careful dataset construction that phylogenetic analyses will have any meaning, something already recognized for molecular data (Philippe & Roure 2011; Roure & Philippe 2011), but still fought against when it comes to morphological data (Kluge 2003; Laing *et al.* 2017). I hope that these findings will promote further attention to morphological data construction not only in squamates, but also in other taxonomic groups in the tree of life.

Supplementary Information 6.1

The complete morphological and molecular datasets, along with the Mr. Bayes data blocks are available online with the paper "The Origin of Squamates Revealed by a Middle Triassic Lizard from the Italian Alps" at: https://www.nature.com/nature (DOI: 10.1038/s41586-018-0093-3).

Supplementary Information 6.2

Taxonomic sampling for phylogenetic analyses

A detailed list with information on each taxonomic unit used herein is provided. General remarks on the age, stratigraphic horizon and locality, holotype number (and if this was personally observed), additional materials that have been personally observed, and main references on the taxonomy and anatomy of each species are also provided. Mere references to the species without anatomical/taxonomic discussions, their mention or inclusion in phylogenetic datasets without further discussion on the taxon, and information from unpublished PhD theses are omitted. References to other species from the same genus that are not included herein are also not included. Although the reference list is not an exhaustive compilation of all studies mentioning or figuring the referred taxa, they comprehend what is considered herein the most relevant published studies on each referenced taxon, especially regarding their taxonomy and anatomy.

Fossil Taxa

Protorothyris archeri Price, 1937

Age. Sakmarian, Cisuralian, Lower Permian (Clark & Carroll 1973; Lucas 2006)

Horizon/Locality. Moran Formation, Wichita Group—Cottonwood Creek, Archer County, Texas, USA (Clark & Carroll 1973).

Holotype. MCZ 1532 (observed)

Observed referred materials. MCZ 2148, MCZ 2149, MCZ 4204, MCZ 4416, and NMNH 392180.

Main bibliography. Price (1937); Huene (1944b); Carroll (1969a); Clark & Carroll (1973).

Protocaptorhinus pricei Clark & Carroll, 1973

Age. Late Artinskian, Cisuralian, Lower Permian (Clark & Carroll 1973; Lucas 2006).

Horizon/Locality. Uppermost Admiral Formation, Wichita Group—Rattlesnake Canyon, Archer County, Texas, USA (Clark & Carroll 1973).

Holotype. MCZ 1478 (observed)

Main bibliography. Clark & Carroll (1973); Gaffney & McKenna (1979); Olson (1984); Heaton & Reisz (1986).

Captorhinus aguti (Cope, 1882)

Age. Early to late Cisuralian, Lower Permian (Fox & Bowman 1966; Cisneros *et al.* 2015)..

Horizon/Locality. Admiral, Belle Plains and Clyde formations, Wichita group—Texas, USA; Arroyo, Vale (?) and Choza formations, Clear Fork Group—Texas, USA; Abo Formation—New Mexico, USA; Arroyo (?) Formation, Clear Fork Group—Oklahoma, USA; Lower Pedra de Fogo Formation, Parnaíba Basin— Nazária Municipality, Piauí State, Brazil (Fox & Bowman 1966; Cisneros *et al.* 2015).

Holotype. AMNH 4333 (observed)

Observed referred materials. AMNH 4332, AMNH 4338**,** AMNH 4339, AMNH 4340, AMNH 4434, KU 9978, KU 106458**,** FMNH UC 383, FMNH 386, FMNH UC 491, FMNH UC 1699, FMNH PR 913.

Main bibliography. Cope (1882); Cope (1896a); Case (1911); Price (1935); Price (1940); Romer (1946); Peabody (1951); Romer (1956); Fox & Bowman (1966); Bolt & DeMar (1975); Holmes (1977); de Ricqlès & Bolt (1983); Heaton & Reisz (1986); Modesto (1998); Holmes (2003); Cisneros *et al.* (2015).

Labidosaurus hamatus (Cope, 1895)

Age. Kungurian, Cisuralian, Lower Permian (Lucas 2006)

Horizon/Locality. Lowermost Arroyo Formation, Clear Folk Group—Baylor County, Texas, USA (Modesto *et al.* 2007).

Holotype. AMNH 4341

Observed referred materials. FMNH P 12758 FMNH UC 634, FMNH UR 161, FMNH UR 273, FMNH UR 634, FMNH UR 643, FMNH UR 696, FMNH UR 727, FMNH UR1198, FMNH UC 1543.

Main bibliography. Cope (1895); Cope (1896b); Case (1911); Williston (1910b); Williston (1917); Olson (1937); Parrington (1937); Olson (1984); Sumida (1987); Sumida (1989); Sumida (1991); Modesto *et al.* (2007).

Remarks. Modesto *et al.* (2007) indicated the age of *L. hamatus* as being "Leonardian (= Artinskian)". However, the Leonardian has been indicated to correspond to the Kugurian by Lucas (2006). Data on the morphology of the autopodium in *Labidosaurus* has been obtained from Sumida (1989).

Eunotosaurus africanus Seeley, 1892

Age. middle Capitanian to Capitanian/Wuchiapingian boundary, Late Permian (Day *et al.* 2013).

Horizon/Locality. *Tapinocephalus* and *Pristerognathus* zones of the Abrahamskaal Formation, upper part of the Koonap Formation, and lowermost Middleton Formation, Beaufort Group, Karoo Supergroup—multiple localities in the Western Cape, Northern Cape, Free State and Eastern Cape provinces, South Africa [for details see Day *et al.* (2013)].

Holotype. NHMUK R1968 (observed)

Observed referred materials. NHMUK R4949, NHMUK R49424, SAM-PK-K7909.

Main bibliography. Seeley (1892); Cox (1969); Gow (1997); Gow & de Klerk (1997); Lyson *et al.* (2010); Lyson & Joyce (2012); Carroll (2013); Day *et al.* (2013); Lee (2013a); Lee (2013b); Lyson *et al.* (2013a); Lyson *et al.* (2014); Bever *et al.* (2015b); Joyce (2015); Nagashima *et al.* (2015); Lyson *et al.* (2016).

Remarks. Additional and well informative data on the skull of *Eunotosaurus* was obtained from published 3D CT scans of the adult skull of CM 777 (Bever *et al.* 2015b; a), and additional details on the pedal morphology from Gow & de Klerk (1997).

Eunotosaurus is a key taxon towards understanding diapsid relationships that has also called more recent attention towards understanding the early evolution of turtles (Lee 2013a; Lyson *et al.* 2013a; Bever *et al.* 2015b; Joyce 2015; Lyson *et al.* 2016). Similarity between *Eunotosaurus* and turtles is best represented by the postcranial morphology, especially the anteroposteriorly expanded presacral ribs, which might have contributed to form the turtle shell (Lyson *et al.*

2013a; Lyson *et al.* 2016). Important similarities in the cranial morphology also occur between *Eunotosaurus* and *Proganochelys*, such as the presence of teeth on the pterygoids, palatines and vomers, the presence of a lateral process of the ectopterygoid, the supratemporal expanded anteriorly—covering the upper temporal fenestra in adults of *Eunotosaurus* (Bever *et al.* 2015a; b). The relatively expanded temporal bones in adults *Eunotosaurus*, such as the postorbital and squamosal, also confer a more similar shape to the same elements in turtles, especially *Proganochelys* among the observed taxa herein, with the consequent reduction of the processes in these bones and the closure of the temporal fenestrae. The quadrate in *Eunotosaurus* differs from most turtles in not having a well-developed posterior emargination and tympanic conch, such as in *Odontochelys*, *Kayentachelys*, and in later forms. However, *Proganochelys* has a posterior emargination while lacking a tympanic conch, indicating the latter feature was acquired later in turtle evolution, and thus explaining the condition in *Eunotosaurus*. A laterosphenoid has also been suggested for *Eunotosaurus* (Bever *et al.* 2015b), but its homology to the one in *Proganochelys* (Bhullar & Bever 2009) is uncertain.

Proganochelys queensdedti Baur, 1887

Age. Late Norian, Late Triassic (Gaffney 1990).

Horizon/Locality. Upper Stubensandstein, Keuper Group, Germanic Basin—Halberstadt, Tübingen and Trossingen, Germany [(Gaffney 1990) and SMNS specimen labels].

Holotype. uncatalogued material in Tubingen [see Gaffney (1990)].

Observed referred materials. SMNS 16980, SMNS 15759

Main bibliography. Baur (1887); Quenstedt (1888); Fraas (1899); Jaekel (1914); Jaekel (1918); Parsons & Williams (1961); Gaffney & Meeker (1983); Gaffney (1985); Gaffney (1990); Müller (2004); Bhullar & Bever (2009); Lyson *et al.* (2010); Carroll (2013); Lyson *et al.* (2013a); Lyson *et al.* (2013b); Nagashima *et al.* (2015); Joyce (2015); Lyson *et al.* (2016).

Remarks. A relevant difference in our interpretation of the anatomy of *Proganochelys* to that of Gaffney (1990) is the presence of a postfrontal that is not fused to the postorbital. A similar characterization of *Pappochelys* (Schoch & Sues 2015) and *Eunotosaurus* (Bever *et al.* 2015b), both inferred to lie more rootward relative to *Proganochelys,* indicates both elements were

separate during early turtle evolution, thus becoming fully fused in later evolving forms, such as *Kayentachelys.*

Odontochelys semitestacea Li et al. 2008

Age. Lower Carnian, Late Triassic (Li *et al.* 2008b)

Horizon/Locality. Wayao Member, Falang Formation—Guanling, Guizhou Province, southwestern China (Li *et al.* 2008b).

Holotype. IVPP V 15639

Paratype: IVPP V 13240 (observed).

Observed referred materials. IVPP V 15653.

Main bibliography. Li *et al.* (2008b); Lyson *et al.* (2010); Lyson & Joyce (2012) ;Carroll (2013); Lyson *et al.* (2013a); Lyson *et al.* (2014); Hirasawa *et al.* (2015); Nagashima *et al.* (2015); Joyce (2015); Lyson *et al.* (2016).

Kayentachelys aprix Gaffney et al., 1987

Age. Sinemurian—Pliensbachian, Lower Jurassic (Padian 1989)

Horizon/Locality. Silty facies of the Kayenta Formation—Gold Springs and Willow Springs, Adeii Eechii Cliffs, Coconino County, Arizona, USA (Gaffney *et al.* 1987).

Holotype. MNA V1558 (also catalogued as MCZ 8913)

Observed referred materials. MCZ 8914, MCZ 8915, MCZ 8916, MCZ 8917, MCZ 8983, MCZ 8999, TMM 43647−1, TMM 43669−2, TMM 43670−2.

Main bibliography. Gaffney *et al.* (1987); Sterli & Joyce (2007); Gaffney & Jenkins (2010); Lyson *et al.* (2013b)

Petrolacosaurus kansensis Lane, 1945

Age. Stephanian of Europe [equivalent to the Kasimovian (Ogg *et al.* 2008)], Late Pennsylvanian, Carboniferous.

Horizon/Locality. Stanton Formation, Lansing Group—Garnett, Kansas, USA (Peabody 1952; Reisz 1977).

Holotype. KUVP 1424 (observed)

Observed referred materials. KUVP 1423, KUVP 1426, KUVP 1427**,** KUVP 8351, KUVP 9940, KUVP 9951 A, B & C, KUVP 9952, KUVP 9955, ROM 29900, ROM 29907, ROM 55098, ROM uncatalogued.

Main bibliography. Lane (1945); Peabody (1952); Kuhn (1969); Reisz (1975); Reisz (1977); Reisz (1981); Benton (1985); Müller (2004).

Remarks. The presence and configuration of the supratemporal and tabular are preserved only on the left side of KUVP 9952 (Reisz 1981). However, the left side of this specimen is now covered in resin, and our scorings on these elements follows Reisz (1981). Contrary to the interpretation provided by Reisz (1981), the ankle of the holotype (KUVP 1424) includes both the medial and lateral centralia.

Araeoscelis gracilis Williston, 1910a

Age. Late Kungurian, Cisuralian, Lower Permian (Vaughn 1955; Lucas 2006).

Horizon/Locality. Arroyo Formation, Clear Fork Group—Craddock bonebed, near Seymour, Baylor County, Texas, USA [(Vaughn 1955) and FMNH specimen labels].

Holotype. FMNH UR 341 (observed).

Lectotype series. FMNH UC 659, FMNH UC 660, FMNH UC 661, FMNH UC 662 (all observed).

Observed referred materials: FMNH UC 1708, FMNH UC 2415, FMNH UC 2416, FMNH UC 2417, FMNH UC 2418, FMNH UC 2419.

Main bibliography. Williston (1910a); Williston (1913); Williston (1914); Broom (1931); Parrington (1937); Huene (1944a); Huene (1944b); Romer (1946); Romer (1947); Vaughn (1955); Kuhn (1969).

Araeoscelis casei (Broom, 1913c)

Age. Artinskian and lower Kungurian, Cisuralian, Lower Permian (Vaughn 1955; Lucas 2006).

Horizon/Locality. Admiral Formation, Wichita Group—Godwin Creek, Archer County, Texas, USA; Belle Plains Formation, Wichita Group—Turbeville Pasture, Baylor County, Texas [(Vaughn 1955) and MCZ specimen labels].

Holotype. AMNH 4685 (observed)

Observed referred materials. MCZ 4380, MCZ 8828

Main bibliography. Case (1907); Broom (1913c); Williston (1914); Broom (1931); Romer (1946); Romer (1947); Vaughn (1955); Kuhn (1969); Reisz *et al.* (1984).

Hupehsuchus nanchangensis Young & Dong, 1972

Age. Spathian, late Olenekian, Lower Triassic (Li *et al.* 2008a; Chen *et al.* 2014)

Horizon/Locality. Upper Jialingjian Formation— Mingfeng Town, Yuanan County and Xunjian Commune, Nanzhang County, both in Hubei Province, China (Carroll & Zhi-Ming 1991; Li *et al.* 2008a; Chen *et al.* 2014).

Holotype. IVPP V3232 (observed)

Paratype. IVPP V4608

Main bibliography. Young & Dong (1972); Carroll & Zhi-Ming (1991); Li *et al.* (2008a); Wu *et al.* (2016).

Remarks. Additional information from *Hupehsuchus nanchangensis* concerning the temporal region and parts of the pectoral girdle have been obtained by new specimens and good quality pictures published by Wu *et al.* (2016).

Utatsusaurus hataii Shikama, Kamei, and Murata, 1978

Age. Spathian, late Olenekian, Lower Triassic (Motani *et al.* 1998)

Horizon/Locality. Middle-Upper Osawa Formation, Inai Group—Utatsu and Miyagi, Japan (Shikama *et al.* 1978; Motani *et al.* 1998)

Holotype. IGPS 95941

Observed referred materials. NSM-VP-20028, UHR 30691

Main bibliography. Shikama *et al.* (1978); Mazin (1986); Nicholls & Brinkman (1993); Minoura (1994); Motani (1997); Motani *et al.* (1998); Motani (1999b); Maisch & Matzke (2000); Sander (2000); McGowan & Motani (2003); Müller (2004); Cuthbertson *et al.* (2013b); Cuthbertson *et al.* (2014).

Parvinatator wapitiensis Nicholls & Brinkman, 1995

Age. Spathian, late Olenekian, Lower Triassic-latest Ladinian, Middle Triassic (McGowan & Motani 2003)

Horizon/Locality. Unknown specific horizon, Sulphur Mountain Formation—Wapiti Lake, east-central British Columbia, Canada (Maisch & Matzke 2000; McGowan & Motani 2003).
Holotype. TMP 1989.127.0008 (observed)
Main bibliography. Nicholls & Brinkman (1995); Motani (1999b); Maisch & Matzke (2000); Sander (2000); McGowan & Motani (2003).

Gulosaurus helmi Cuthbertson, Russell & Anderson, 2013
Age. Spathian, late Olenekian, Lower Triassic-latest Ladinian, Middle Triassic (Brinkman *et al.* 1992; McGowan & Motani 2003)
Horizon/Locality. Vega-Phroso Siltstone Member, Sulphur Mountain Formation—south-east of Wapiti Lake, east-central British Columbia, Canada (Brinkman *et al.* 1992).
Holotype. TMP 1989.127.0003 (observed)
Main bibliography. Brinkman *et al.* (1992); Cuthbertson *et al.* (2013a); Kelley *et al.* (2016); Ji *et al.* (2016).

Mixosaurus panxianensis Jiang et al., 2006
Age. Late Pelsonian, Anisian, Middle Triassic (Jiang *et al.* 2006; Sun *et al.* 2006; Benton *et al.* 2013).
Horizon/Locality. Upper Member, Guanling Formation—Yangjuan Village, Xinmin District, Panxian County, Guizhou Province, China (Jiang *et al.* 2006).
Holotype. GMPKU-P-1033 (observed)
Observed referred materials. GMPKU-P-1031, GMPKU-P-1038, GMPKU-P-1039, IVPP uncatalogued.
Main bibliography. Jiang *et al.* (2006); Li *et al.* (2008a); Benton *et al.* (2013); Ji *et al.* (2016).

Youngina capensis Broom, 1914
Age. Lopingian, Late Permian (Smith *et al.* 2012; Rubidge *et al.* 2013).
Horizon/Locality. *Daptocephalus* zone [= late Cistecephalus and Dicynodon Zones], Beaufort Group, Karoo Supergroup—New Bethesda, Eastern Cape Province and Doornplaat, North-West Province, South Africa [(Gow 1974), SAM and BPI databases].
Holotype. AMNH 5561 (observed)

Observed referred materials. BPI/1/70, BPI/1/2459, BPI/1/2871, BPI/1/3859, NHMUK 5481, SAM-PK-K7578, SAM-PK-K8565.

Main bibliography. Broom (1914); Kuhn (1969); Broom (1937); Parrington (1937); Huene (1944b); Romer (1946); Young (1948); Wild (1973); Kuhn-Schnyder (1974); Gow (1974); Currie (1981b); Estes (1983b); Evans (1984); Benton (1985); Evans (1987); Gardner *et al.* (2010).

Remarks. Information from the braincase of *Y. capensis* was complemented using the CT scan data published by Gardner *et al.* (2010). Specimen TM 3603, used by Gow (1974) in his description of *Y. capensis* is damaged and broken into separate pieces. TM 3603, along with TM 200 and TM 4095 are regarded herein as cf. *Youngina* due to their fragmentary condition. The same applies to TM 1490, initially described as *Younginopsis*, but synonymized with *Y. capensis* by Gow (1974). SAM-PK-K8565 can be assigned to *Y. capensis* on the basis skull morphology, and it is represented by a juvenile. However, this specimen is not used in order to avoid biases due to ontogeny. Specimens SAM-PK-K5836, SAM-PK-K10651, SAM-PK-K10681, SAM-PK-K10777 and SAM-PK-K10818 are very poorly preserved and are only referred herein as cf. *Youngina*. Specimen SAM-PK-K7710, which consists of at least four juvenile individuals in a single block, differs from *Y. capensis* by having ventral midline crests on its cervical and dorsal vertebrae, and by its dorsal neural spines lacking the lateral expansion seen in *Y. capensis*. Additionally, the pubis seems to lack an obturator foramen, although the degree of preservation may affect this assessment. This specimen may represent a separate species o the genus *Youngina*.

Hovasaurus boulei Pivetau, 1926

Age. Early Lopingian, Late Permian (Lucas 2006; Smith *et al.* 2012; Rubidge *et al.* 2013) to Induan, Early Triassic (Wescott & Diggens 1998; Ketchum & Barrett 2004).

Horizon/Locality. Lower Sakamena Formation, Sakamena Group, Karoo Supergroup— near Mount Eliva, Sakamena River Valley, southwestern Magadascar (Currie 1981a; Lucas 2006); "Couches à Claraia et Poissons" or the overlying "Couches à Poissons et Ammonites" [equivalent to the Middle Sakamena Formation], Diego Basin—northwestern Madagascar (Wescott & Diggens 1998; Ketchum & Barrett 2004).

Lectotype series. MNHN 1908-21-2 and MNHN 1908-21-7 (observed)

Observed referred materials. MNHN 1925-5-34, MNHN 1925-5-30, MNHN 1908-21-14b.
Main bibliography. Piveteau (1926); Haughton (1929); Kuhn (1969); Currie (1981a); Benton (1985); Carroll (1985a); Carroll (1988); Carroll & Currie (1991); Caldwell (1995); Caldwell (2002); Ketchum & Barrett (2004).

Acerosodontosaurus piveteaui Currie, 1980
Age. Lower Lopingian, Late Permian (Lucas 2006; Smith *et al.* 2012; Rubidge *et al.* 2013).
Horizon/Locality. Lower Sakamena Formation, Sakamena Group, Karoo Supergroup —exact locality unknown, Sakamena River Valley, southwestern Magadascar (Currie 1980; Lucas 2006).
Holotype. MNHN 1908-32-57a,b (observed)
Observed referred materials. UALVP 45621 (cast of holotype)
Main bibliography. Currie (1980); Carroll (1988); Bickelmann *et al.* (2009).
Remarks. Currie (1980) indicated the presence of a quadratojugal in *A. piveteaui*, which was later contested by Bickelmann *et al.* (2009). The latter authors suggested the element identified as the quadratojugal is, in fact, a rib head. It is agreed herein that the element in question is most likely to represent a rib head, as suggested by Bickelmann *et al.* (2009). However, an additional element distinct from the quadrate and articulating laterally to it in the skull of the holotype (and not mentioned by previous authors) is suggested herein to represent the quadratojugal. It bears an anterior process, but its anteriormost end is broken, and the total extension of it is unknown.

Claudiosaurus germaini Carroll, 1981
Age. Lopingian, Late Permian (Lucas 2006; Smith *et al.* 2012; Rubidge *et al.* 2013).
Horizon/Locality. Upper portion of the Lower Sakamena Formation, Sakamena Group, Karoo Supergroup —near the village of Leoposa, southwestern Magadascar (Carroll 1981).
Holotype. MNHN 1978-6-1 (observed)
Observed referred materials. MNHN 1978-6-2, MNHN 1910-33-1a, MNHN 1925-5-90, SAM-PK-K8265, SAM-PK-K8580.
Main bibliography. Carroll (1981); de Buffrénil & Mazin (1989); Caldwell (1995); Müller (2004).
Remarks. Many of the specimens used by Carroll (1981) in the description of *Claudiosaurus* were in a private collection that could not be located. Additionally, some of the specimens

housed at the MNHN could not be found (MNHN 1911-18, MNHN 1909-3-21, MNHN 1909-3-22, MNHN 1909-3-25, MNHN 1909-3-26, MNHN 1909-3-37, MNHN 1909-34-3). This limitation prevented a better assessment of the skull morphology of *Claudiosaurus.* Nevertheless, new specimens at the SAM provided some additional details on the postcranial morphology of *Claudiosaurus.*

Coelurosauravus jaekeli (Weigelt, 1930)

Age. Middle Wuchiapingian, lower Lopingian, Late Permian (Menning *et al.* 2011).

Horizon/Locality. Kupferschiefer Formation, Zechstein Group—Ellrich (Thuringia), Richelsdorf (Hesse), Mansfeld, (Sachsen/Anhalt), Germany; and Marl Slate— Eppleton Quarry, Tyne and Wear, United Kingdom (Schaumberg 1976; Evans & Haubold 1987; Frey *et al.* 1997; Schaumberg *et al.* 2007).

Holotype. SSWG 113/7 (observed)

Main bibliography. Weigelt (1930a); Weigelt (1930b); Kuhn (1939); Kuhn (1969); Schaumberg (1976); Evans (1982); Evans & Haubold (1987); Frey *et al.* (1997); Schaumberg *et al.* (2007); Bulanov & Sennikov (2010)**.**

Remarks. Here I follow the assignment of *Gracilisaurus* Weigelt, 1930a and *Weigeltisaurus* Wigelt, 1930b as a junior synonyms of *Coelurosauravus* by Evans & Haubold (1987).

Coelurosauravus elivensis Piveteau, 1926

Age. Wuchiapingian, lower Lopingian, Late Permian (Lucas 2006; Smith *et al.* 2012; Rubidge *et al.* 2013)

Horizon/Locality. Upper portion of the Lower Sakamena Formation, Sakamena Group, Karoo Supergroup—near Mount Eliva, Sakamena River Valley, southewstern Magadascar (Carroll 1978).

Holotype. MNHN IP 1908-11-21a (observed)

Observed referred materials. MNHN IP 1908-11-22a, MNHN IP 1908-11-23a, MNHN IP 1908-5-2 (previous holotype of *Daedalosaurus madagascariensis*)

Main bibliography.(Piveteau 1926) ;Kuhn (1969); Carroll (1978); Evans (1982); Evans & Haubold (1987); Bulanov & Sennikov (2015b).

Remarks. Here I follow the assignment of *Daedalosaurus* Carroll, 1981 as a junior synonyms of *Coelurosauravus* by Evans & Haubold (1987).

Protorosaurus speneri Meyer, 1832

Age. Middle Wuchiapingian, lower Lopingian, Late Permian (Menning *et al.* 2011).

Horizon/Locality. Kupferschiefer Formation, Zechstein Group—Heilderberg, Suhl, Gliicksbrunn, Kupfersuhl, Rothenburg (Thuringia), Richelsdorf (Hesse), Near Ibbenbiihren (North Rhine-Westphalia), and mining pits in Richelsdorfer Gebirge, Germany (Gottmann-Quesada & Sander 2009); Marl Slate—Quarrington Quarry, near Durham, England, United Kindom (Evans & King 1993).

Lectotype. NHMW 194314

Observed referred materials. NMOK S 180, NMOK SSch 185, NMOK SSch 186 a-b-c, NMOK SSch 187, NMOK cast (SIMON-BARTHOLOMAUS specimen), SMNS 59790 (cast), WMsN 47361

Main bibliography. Meyer (1832); Fitzinger (1843); Hancock & Howse (1870); Seeley (1887); Huene (1944a); Romer (1947); Kuhn (1969); Benton (1985); Haubold & Schaumberg (1985); Carroll (1988); Carroll & Currie (1991); Evans & King (1993); Gottmann-Quesada & Sander (2009). For a more comprehensive bibliographic list on *P. speneri* see Gottmann-Quesada & Sander (2009), p. 135.

Prolacerta broomi Parrington, 1935

Age. Induan-Olenekian, Early Triassic (Smith *et al.* 2012).

Horizon/Locality. *Lystrosaurus* zone, Beaufort Group, Karoo Supergroup—Harrismith District (Free State Province), Hueningkrans (Burgersdorp District, Eastern Cape Province), Fairydale and Tweefontein (Bethulie District, Free State Province), Rietport (Dewetsdorp District, Free State Province), Big Bank, Queen's Hill and Old Brickfield's Donga (Harrismith District, Free State Province), Barendskraal (Middleburg District, Eastern Cape Province) South Africa [(Gow 1974; Modesto & Sues 2004) and individual specimen labels]; possibly from Fremow Formation—Transantarctic Mountains, Antarctica (Colbert 1987).

Holotype. UMZC 2003.40 (high resolution pictures provided by F. Costa)

Observed referred materials. BPI/1/471, BPI/1/2675, BPI/1/2676, BPI/1/4504a &b, BP/1/5066, BPI/1/5375, BPI/1/5880

Main bibliography. Parrington (1935); Huene (1944b); Camp (1945); Broom & Robinson (1948); Young (1948); Robinson (1967a); Kuhn (1969); Wild (1973); Kuhn-Schnyder (1974); Gow (1974); Wild (1980a); Evans (1984); Evans (1986); Colbert (1987); Modesto & Sues (2004); Müller (2004); Botha-Brink & Smith (2011).

Remarks. I follow here the designation of *Pricea longipes* Broom & Robinson, 1948 as a junior synonym of *Prolacerta broomi* (Gow 1974; Modesto & Sues 2004).

Macrocnemus bassanii (Nopcsa, 1930)

Age. Late Anisian to early Ladinian, Middle Triassic (Kuhn-Schnyder 1962; Rieppel 1993a; Furrer 1995).

Horizon/Locality. *Grenzbitumen* Horizon (Besano Formation)—Monte San Giorgio, Switzerland-Italy, and Besano, Italy (Kuhn-Schnyder 1962; Rieppel 1989a).

Holotype. Destroyed during World War II (Rieppel 1989a).

Observed referred materials. PIMUZ T2472, PIMUZ T2477, PIMUZ T4355, PIMUZ T5753, MSNM 15863 V457, MSNM BES SC 111.

Main bibliography. Nopcsa (1930); Peyer (1931c); Peyer (1937); Huene (1944a); Huene (1944b); Kuhn-Schnyder (1962); Kuhn-Schnyder (1964); Kuhn (1969); Wild (1973); Kuhn-Schnyder (1974); Wild (1980a); Rieppel & Gronowski (1981); Benton (1985); Rieppel (1989a); Renesto & Avanzini (2002); Müller (2004); Fraser & Furrer (2013).

Macrocnemus fuyuanensis Li et al., 2007

Age. Longobardian, late Ladinian, Middle Triassic (Benton *et al.* 2013).

Horizon/Locality. Zhuganpo Formation—Huabi of Fuyuan, Yunnan Province, southwestern China (Li *et al.* 2007a; Benton *et al.* 2013).

Holotype. IVPP V15001

Observed referred materials. GMPKU-P-3001

Main bibliography. Li *et al.* (2007a); Jiang *et al.* (2011).

Langobardisaurus pandolfii Renesto, 1994

Age. Late Alaunian-early Sevatian, late Norian, Late Triassic (Saller *et al.* 2013).

Horizon/Locality. Dolomia di Forni Formation—Seazza Creek, near the village of Preone, Udine, Friuli, Italy, and Rovadia Creek, Venezia, Italy; Zorzino Limestone Formation—Cene, Lombardy, Italy; Seefeld Formation—Seefeld, Tyrol, Austria (Renesto & Dalla Vecchia 2000; Saller *et al.* 2013).

Holotype. MBSN 2883

Observed referred materials. MFSN 1921

Main bibliography. Renesto (1994b); Muscio (1996); Renesto & Dalla Vecchia (2000); Renesto *et al.* (2002); Saller *et al.* (2013).

Remarks. Saller *et al.* (2013) revised the genus *Langobardisaurus*, re-assigning the specimen studied herein (MFSN 1921, previously, the holotype of *L. tonelloi*) to *L. pandolfii*.

Tanystropheus longobardicus (Bassani, 1886)

Age. Late Anisian to early Ladinian, Middle Triassic (Kuhn-Schnyder 1962; Rieppel 1993a; Furrer 1995).

Horizon/Locality. *Grenzbitumen* Horizon (Besano Formation) and Meride Formation—northern Italy and Monte San Giorgio, Switzerland-Italy (Nosotti 2007)

Neotype. PIMUZ T2791

Observed referred materials. PIMUZ T2817, PIMUZ T2818, PIMUZ T2819, PIMUZ T2793, MSNM BES SC 1018, MSNM BES SC 265

Main bibliography. Bassani (1886); Nopcsa (1923b); Wild (1973); Kuhn-Schnyder (1959); Kuhn (1969); Kuhn-Schnyder (1974); Wild (1980a); Wild (1980b); Benton (1985); Tschanz (1985); Wild (1987); Tschanz (1988); Renesto (2005a); Nosotti (2007); Rieppel *et al.* (2010)

Remarks. Among the studied specimens, some considerable morphological variation was observed. Therefore, only specimens MSNM BES SC 1018, MSNM BES SC 265 and PIMUZ T2818 (some of the most complete specimens that seem to constitute a single morphospecies) have been used for scoring this taxon.

Megalancosaurus preonensis Calzavara, Muscio & Wild, 1980

Age. Middle Norian, Late Triassic (Renesto 2000).

Horizon/Locality. Dolomia di forni (Friuli) and Zorzino Limestone (Bergamo), Italy (Renesto 2000; Renesto *et al.* 2010).

Holotype. MFSN 1769 a&b (observed)

Observed referred materials. MFSN 1801, MFSN 18443 a&b, MBSN 25, MBSN 26.

Main bibliography. Calzavara *et al.* (1980); Feduccia & Wild (1993); Renesto (1994a); Renesto (2000); Renesto & Dalla Vecchia (2005); Spielmann *et al.* (2006); Renesto *et al.* (2010); Castiello *et al.* (2015).

Remarks. The structure of the fibula and the pedal unguals differ between specimens MBSN 25 and MPUM 8437. In MBSN 25 the fibula is curved and the unguals have a deeper basis for articulation with the penultimate phalanx, whereas MPUM 8437 has a straight fibula and shallower bases of the pedal unguals (Renesto *et al.* 2010). Renesto *et al.* (2010) and Castiello *et al.* (2015) further indicated a difference in the first pedal digit, mentioning the presence of a modified pedal digit 1, with an opposable, clawless hallux. These differences were first attributed to sexual dimorphism (Renesto 2000), but later were re-interpreted as a taxonomical difference, and a new species was named, *Megalancosaurus endennae* (holotype: MBSN 25; referred specimen: MBSN 26). However, personal observations indicate the presence of an ungual element in MBSN 25, lying ventral to the penultimate phalanx and oriented on the same direction of the other pedal phalanges, thus differing from the interpretation by Renesto *et al.* (2010). This observation is also consistent with the morphology of other scansorial reptiles, in which the deep unguals are an important adaptation towards climbing (Zani 2000; Tulli *et al.* 2009). Therefore, the supposed absence of an ungual on pedal digit one (especially if that was an opposed hallux) would also prevent an efficient grasping capacity for the feet in *M. endennae*. Finally, the holotype of *M. preonensis* (MFSN 1769 a&b) lacks its hindlimbs, thus preventing a direct comparisons between the type materials of these two putative species—this limitation was also mentioned by Renesto *et al.* (2010). Therefore, it is considered herein that even if the two remaining differences between MBSN 25 and MPUM 8437 mentioned by Renesto *et al.* (2010); (shape of fibula, and height of the pedal unguals) are indeed taxonomically significant (and not intraspecific variation), it cannot be assessed with enough precision which of these correspond to the condition in the holotype of *M. preonensis*. For the above reasons, the validity of *M. endennae* is questioned herein. Additionally, for the purposes of the present analysis, scoring either MBSN 25, or MPUM 8437, or both as belonging to *M. preonensis*, would also not affect

any of the scorings performed, as none of the characters herein relate to any of the only two differences observed between these specimens. Therefore, I score all the specimens of *Megalancosaurus* under the OTU *M. preonensis*.

Askeptosaurus italicus Nopcsa, 1925

Age. Late Anisian to early Ladinian, Middle Triassic (Kuhn-Schnyder 1962; Rieppel 1993a; Furrer 1995).

Horizon/Locality. *Grenzbitumen* Horizon (Besano Formation)—Monte San Giorgio, Switzerland-Italy (Müller 2005).

Holotype. MSNM V3550

Observed referred materials. MSNM V456, PIMUZ T 4831, PIMUZ T 4832, PIMUZ T 4846.

Main bibliography. Nopcsa (1925); Kuhn (1952); Kuhn-Schnyder (1960); Kuhn-Schnyder (1964); Kuhn (1969); Kuhn-Schnyder (1971); Kuhn-Schnyder (1974); Carroll (1985a); Kuhn-Schnyder (1988); Carroll & Currie (1991); Müller (2004); Müller (2005).

Endennasaurus acutirostris Renesto, 1984

Age. Middle-late Norian, Late Triassic (Tintori 1995; Gaetani *et al.* 1998).

Horizon/Locality. Upper levels of the Zorzino Limestone Formation—Endenna quarry, Zogno region of the Lombardian pre-alps, Italy (Müller *et al.* 2005).

Holotype. MBSN 5170 (observed)

Observed referred materials. MBSN 27

Main bibliography. Renesto (1984); Renesto (1991); Müller *et al.* (2005); Renesto (2005b).

Xinpusaurus kohi Jiang et al., 2004

Age. Carnian, Late Triassic (Jiang *et al.* 2005)

Horizon/Locality. Wayao Member, Falang Formation— Xinpu village, Guizhou Province, China (Jiang *et al.* 2004).

Holotype. GMPKU- 2000/005 (observed)

Main bibliography. Jiang *et al.* (2004); Jiang *et al.* (2005); Rieppel & Jun (2006); Liu (2013); Maisch (2014); Li *et al.* (2016).

Remarks. There is an existing debate on the validity of *X. kohi*, regarded as a junior synonym of *X. bamaolinensis* by Rieppel & Jun (2006), as a junior synonym of *X. suni* (Liu 2013), and once again as a valid taxon by Maisch (2014). The latter author considered, however, that a re-description of *X. bamaolinensis* is necessary before decisive conclusions regarding the status of *X. kohi*. Therefore, only data personally collected from the holotype of *X. kohi* has been utilized herein (pending revision to determine whether this also represents *X. bamaolinensis*).

Champsosaurus lindoei Gao & Fox, 1998

Age. Mid-Campania, Late Cretaceous (Gao & Brinkman 2005).

Horizon/Locality. Dinosaur Park Formation—Dinosaur Provincial Park, Alberta, Canada (Gao & Brinkman 2005).

Holotype. UALVP 931 (observed).

Observed referred materials. UALVP 33928; TMP 1987.036.0041; TMP 1994.163.0001.

Main bibliography. Fox (1968); (Gao & Fox 1998); Gao & Brinkman (2005); Matsumoto & Evans (2016).

Philydrosaurus proseilus Gao & Fox, 2005

Age. Albian, Early Cretaceous (Gao & Fox 2005).

Horizon/Locality. Jiufotang Formation, Jehol Group - near the city of Chaoyang, Liaoning Province, China (Gao & Fox 2005).

Holotype. PKU V2001 (observed)

Main bibliography. Gao & Fox (2005); Gao *et al.* (2007); Gao *et al.* (2013).

Remarks. Additional information on the braincase and palate obtained from pictures in Gao *et al.* (2007).

Trilophosaurus buettneri Case, 1928a

Age. Middle Otischalkian, lower Carnian, Late Triassic to late Adamanian, latest Carnian, Late Triassic (Spielmann *et al.* 2008).

Horizon/Locality. Colorado City Formation, Chinle Group and Tecovas Formation, Dockum Group—Texas, USA; Blue Mesa Member, Petrified Forest Formation, Chinle Group—Arizona,

USA; Bluewater Creek Formation, Chinle Group—New Mexico, USA (Lucas 1998; Spielmann *et al.* 2008).

Holotype. MNA V3192

Observed referred materials. TMM 31025-4, TMM 31025-5, TMM 31025-68, TMM 31025-73, TMM 31025-74, TMM 31025-80, TMM 31025-116, TMM 31025-125, TMM 31025-140, TMM 31025-142, TMM 31025-143, TMM 31025-144, TMM 31025-154-164, TMM 31025-207, TMM 31025-208, TMM 31025-210, TMM 31025-225, TMM 31025-233, TMM 31025-239, TMM 31025-248, TMM 31025-357, TMM 31025-366, TMM 31025-394.

Main bibliography. Case (1928a); Case (1928b); Gregory (1945); Robinson (1957); Kuhn (1969); Parks (1969); Demar & Bolt (1981); Murry (1986); Elder (1987); Murry (1987);Carroll & Currie (1991); Spielmann *et al.* (2005); Heckert *et al.* (2006); Spielmann *et al.* (2008); Nesbitt *et al.* (2015). Additional literature on the genus *Trilophosaurus* has been discussed in detail by (Spielmann *et al.* 2008).

Mesosuchus browni Watson, 1912

Age. Earliest to middle/late Anisian, Middle Triassic (Dilkes 1998; Smith *et al.* 2012).

Horizon/Locality. *Cynognathus* Zone B, Bugersdrop Formation, Tarkastad Sub-group, Beaufort Group, Karoo Supergroup—near Aliwal North, Eastern Cape Province, South Africa [SAM database and Dilkes (1998)].

Holotype. SAM-PK-5882 (observed)

Observed referred materials. SAM-PK-6046, SAM-PK-6536, SAM-PK-7416.

Main bibliography. Watson (1912); Broom (1913a); Broom (1913b); Haughton (1922); Haughton (1924); Broom (1925); Romer (1946); Hoffstetter (1955a); Romer (1956); Malan (1963); Robinson (1967a); Kuhn (1969); Carroll (1976); Dilkes (1998); Müller (2004); Ezcurra *et al.* (2016); Ezcurra (2016).

Remarks. Two additional specimens, SAM-PK-6546 and SAM-PK-7701 are morphological similar to *M. browni*, but because of the limited amount of information preserved they are only tentatively assigned to that species (cf. *Mesosuchus browni*). Important similarities were observed between *Mesosuchus* and protorosaurs, such as the squamosal having distinct anteroventral and posterior processes; the squamosal anterior process forked to receive the postorbital (also observed in later rhynchosaurs); the quadratojugal without an anterior extension

contacting the jugal, the shape of the scapula, coracoid, and the presence of a hooked fifth metatarsal (also present in later rhynchosaurs). It is also remarkable the presence in intercentra between the dorsal vertebrae (also occurring in *Howesia* and *Trilophosaurus*) and teeth on the vomers, palatines and pterygoids, common features of early diapsids such as *Youngina* and non-diapsid reptiles. Importantly, postparietals are present in SAM-PK-6535, contrary to previous observations—e.g. Dilkes (1998) and Nesbitt (2011). Both elements of the postparietals are clearly distinct from the parietals at their anterior margin, and their sutures quite symmetrical on both lateral sides, but the suture becomes obliterated posteriorly on the left side, which may have induced previous authors to consider it as absent in this taxon. The presence of postparietals further indicates the similarity between this taxon with earlier diapsids and with early archosauriforms such as *Proterosuchus* and *Euparkeria.*

Howesia browni Broom, 1905

Age. Earliest to middle/late Anisian, Middle Triassic (Dilkes 1995; Smith *et al.* 2012).

Horizon/Locality. *Cynognathus* Zone B, Bugersdrop Formation, Tarkastad Sub-group, Beaufort Group, Karoo Supergroup—near Aliwal North, Eastern Cape Province, South Africa (SAM database).

Holotype: SAM 5884 (observed)

Observed referred materials. SAM 5885, SAM 5886.

Main bibliography. Broom (1905b); Broom (1906b); Haughton (1924); Hoffstetter (1955a); Malan (1963); Kuhn (1969); Carroll (1976); Benton (1985); Dilkes (1995); Ezcurra *et al.* (2016); Ezcurra (2016).

Remarks. The only difference suggested by Dilkes (1998) between *Mesosuchus* and *Howesia* is the depth of the pockets on the neural arches above the transverse processes of the posterior dorsals, the orientation of the caudal neural spines, and the presence of a groove on the ventral side of the second sacral and first two anterior caudals. The neural spines are slightly inclined posteriorly in *Mesosuchus* and steeply inclined in *Howesia*, however, the degree in depth of the pockets on the lateral sides of the neural arches on the posteriormost dorsal vertebrae is quite similar between *Mesosuchus* (SAM-PK-6046) and *Howesia* (SAM-PK-5886). One of the few significant difference between both taxa is that mentioned by Ezcurra (2016), which relates to the number of maxillary tooth rows. Details of the supratemporal, squamosal and postorbital of

SAM-PK-5885 are not visible as the specimen is now placed on a gypsum bed, thus concealing the dorsal view of the skull bones. Inormation on those elements was obtained from Dilkes (1995).

Teyumbaita sulcognathus Azevedo & Schultz, 1987.
Age. Early Norian, Late Triassic (Langer *et al.* 2007; Montefeltro *et al.* 2010).
Horizon/Locality. Lower part of the Caturrita Formation, Paraná Basin—outcrops between the cities of Santa Maria and Candelária, Central areas of Rio Grande do Sul, Brazil (Montefeltro *et al.* 2010).
Holotype. UFRGS-PV-0232T (observed)
Main bibliography. Azevedo & Schultz (1987); Montefeltro *et al.* (2010); Montefeltro *et al.* (2013); Ezcurra *et al.* (2016).

Hyperodapedon huenei Langer & Schutlz, 2000
Age. Latest Carnian-earliest Norian, Late Triassic (Langer *et al.* 2007).
Horizon/Locality. Santa Maria Formation, Paraná Basin—Inhamandá outcrop, east of São Pedro do Sul, Rio Grande do Sul, BrazilRio Grande do Sul, Brazil (Langer & Schultz 2000).
Holotype. UFRGS-PV-0132T
Observed referred materials. UFRGS-PV-0309T, UFRGS-PV-0408T
Main bibliography. Langer & Schultz (2000); (Langer *et al.* 2000);Ezcurra *et al.* (2016).

Proterosuchus fergusi Broom, 1903
Age. Induan-Olenekian, Early Triassic (Smith *et al.* 2012).
Horizon/Locality. *Lystrosaurus* Zone, Katberg Formation, Beaufort Group, Karoo Supergroup—Farm Wheatlands, Tarkastad, Chris Hani District, Eastern Cape Province, South Africa (Broom 1903a; Ezcurra 2016).
Holotype. SAM-PK-591 (observed)
Neotype. RC 846 (Ezcurra & Butler 2015b).
Observed referred materials. BPI/1/3993, BPI/1/4016, TM 201, SAM-PK-11208.
Main bibliography. Broom (1903a); Hughes (1963); Charig & Reig (1970); Cruickshank (1972); Charig & Sues (1976); Benton & Clark (1988);Carroll (1988); Carroll & Currie (1991);

Clark *et al.* (1993); Welman (1998); Klembara & Welman (2009); Botha-Brink & Smith (2011); Ezcurra & Butler (2015a); Ezcurra & Butler (2015b); Ezcurra (2016).

Remarks. All South African proterosuchids have been synonymized by Welman (1998) under *P. fergusi*, namely: *Chasmatosaurus vanhoepeni*, *C. alexanderi*, and *Elaphrosuchus rubidgei*. However, Ezcurra & Butler (2015b) split the specimens that had been attributed by Welman (1998) as a single species into distinct taxa, thus resurrecting *Proterosuchus* (=*Chasmatosaurus*) *alexanderi* based on NMQR 1484/C.3016, and erecting a new taxon, *Proterosuchus goweri* based on a complete skull (NMQR 880/C.500). **I** follow the taxonomy of Ezcurra & Butler (2015b) herein. Regarding the morphology of *P. fergusi*, Cruickshank (1972) misinterpreted the partially broken anteroventral process of the squamosal in BPI/1/4016 as being a suture between the squamosal and the quadratojugal. Instead, the quadratojugal is a very reduced element, with its dorsal margin being located more ventrally relative to the point illustrated by Cruickshank (1972). Additionally, the quadratojugal does not have an anterior extension as observed in later archosaurs, thus having the lower temporal bar formed entirely by the jugal posterior process. This condition is similar to the one seen in *Prolacerta*, in which the jugal has an elongate posterior process (although not reaching the quadratojugal), and the quadratojugal does not have an anterior extension. The observed specimens all have the retroarticular process directed posteriorly (BPI/1/3993, BPI/1/4016). This is also illustrated by Welman (1998) in his fig. 3. The interpretation of a dorsally oriented retroarticular process is usually based on the specimen RC 96 (not observed herein). Whether this is an artefact or intraspecific variation cannot be determined by us, and may be addressed in further detail the future.

Proterosuchus alexanderi (Hoffman, 1965)

Age. Induan-Olenekian, Early Triassic (Smith *et al.* 2012).

Horizon/Locality. *Lystrosaurus* Zone, Balfour Formation or Katberg Formation, Beaufort Group, Karoo Supergroup— Farm Zeekoegat, four miles from Venterstad, Joe Gqabi District, Eastern Cape Province, South Africa (Hoffman 1965; Ezcurra 2016)

Holotype. NMQR 1484/C.3016 (observed).

Main bibliography. Hoffman (1965)**;** Charig & Reig (1970); Cruickshank (1972)**;** Charig & Sues (1976); Clark *et al.* (1993);**;**Welman (1998); Ezcurra & Butler (2015b); Ezcurra (2016).

Erythrosuchus africanus Broom, 1905

Age. Earliest to middle/late Anisian, Middle Triassic (Dilkes 1995; Smith *et al.* 2012).

Horizon/Locality. *Cynognathus* Zone B, Bugersdrop Formation, Tarkastad Sub-group, Beaufort Group, Karoo Supergroup—Oorlogsfontein (type locality), Lemoenfontein, and other sites near Aliwal North, Eastern Cape Province, South Africa; Burgersdorp and Rouxville, Free State Province, South Africa (Gower 2003; Botha-Brink & Smith 2011; Smith *et al.* 2012).

Holotype. SAM-PK-905 (observed)

Observed referred materials. BPI/1/5207, BPI/1/4680, BPI/13893, SAM 905, NM QS1473, NHMUK R3592, NHMUK R2790, NHMUK 3762a.

Main bibliography. Broom (1905a); Broom (1906a); Huene (1911);Williston (1911); Brink (1955); Hughes (1963); Cruickshank (1978); Benton (1985); Benton & Clark (1988); Parrish (1992); Gower (1996); Gower (1997); Gower (2001); Gower (2003); O'Connor (2006); Botha-Brink & Smith (2011).

Euparkeria capensis Broom, 1913a

Age. Earliest to middle/late Anisian, Middle Triassic (Dilkes 1995; Smith *et al.* 2012).

Horizon/Locality. *Cynognathus* Zone B, Bugersdrop Formation, Tarkastad Sub-group, Beaufort Group, Karoo Supergroup—different quarries near Aliwal North, Eastern Cape Province, South Africa [SAM database; Smith *et al.* (2012); Sookias & Butler (2013)].

Holotype. SAM-PK-5867 (observed)

Observed referred materials. AMNH 2239, AMNH 5548, SAM-PK-6047A&B, SAM-PK-6050, SAM-PK-7699-7710, SAM-PK-7696, SAM-PK-13665, SAM-PK-13666.

Main bibliography. Broom (1913a); Broom (1913b); Haughton (1922); Romer (1946); Ewer (1965); Gow (1970); Benton (1985); Benton & Clark (1988); Sereno & Arcucci (1990); Carroll & Currie (1991); Sereno (1991); Welman (1995); Gower & Weber (1998); Senter (2003); Müller (2004); Botha-Brink & Smith (2011); Sookias & Butler (2013); Sobral *et al.* (2016).

Remarks. The atlas intercentrum described by Ewer (1965) in SAM-PK-6047A could not be located. Intercentra are presented between cervicals and dorsals, a feature also observed in *Mesosuchus*, and earlier diapsids (e.g. *Youngina*). This feature could not be assessed with confidence either species of *Proterosuchus*, but it suggests intercentra between dorsals may be a plesiomorphic feature among archosauriforms, and shared with early rhynchosaurs. No cleithra

are preserved, but a facet on the posterodorsal margin of the scapular blade in SAM-PK-13665 suggests it could have been present.

Largocephalosaurus qianensis Li et al., 2014

Age. Late Pelsonian, Anisian, Middle Triassic (Benton *et al.* 2013).

Horizon/Locality. Member 2, Guanling Formation—Xinmin District, Panxian County, southwest-most Guizhou Province, China (Benton *et al.* 2013; Li *et al.* 2014)

Holotype. IVPP V 15638.

Observed referred materials. GMPKU-P-1532-A, GMPKU-P-1532-B .

Main bibliography. Benton *et al.* (2013); Li *et al.* (2014)**.**

Remarks. Information from the palate of the holotype was obtained from Li *et al.* (2014)**.**

Sinosaurosphargis yunguiensis Li et al., 2011

Age. Late Pelsonian, Anisian, Middle Triassic (Benton *et al.* 2013).

Horizon/Locality. Member 2, Guanling Formation—Xinmin District, Panxian County, southwest-most Guizhou Province, China (Li *et al.* 2011; Benton *et al.* 2013).

Holotype. IVPP V 17040 (observed).

Main bibliography. Li *et al.* (2011)**;** Benton *et al.* (2013)**.**

Remarks. Information on the ventral aspect of the axial skeleton was obtained from Li *et al.* (2011).

Placodus gigas Agassiz, 1833

Age. Early Anisian to early Ladinian, Middle Triassic (Rieppel 2000; Menning *et al.* 2011).

Horizon/Locality. Jena Formation to Warburg Formation, Muschelkalk Group, Germanic Basin—central and southern Europe (Rieppel 2000; Neenan & Scheyer 2012).

Holotype. BSPG AS VII 1208 (observed).

Observed referred materials. BSPG I 76, BSPG 1968 I 75, UMO BT 13, UMO BT uncatalogued, SMNS 54437, SMNS 54558, SMNS 54567, SMNS 54571, SMNS 59824, SMF R 1035.

Main bibliography. A thorough review of the literature concerning *Placodus gigas* has been provided by Rieppel (2000). Subsequent literature includes: Rieppel (2001); Nosotti & Rieppel

(2002); Scheyer (2007); Diedrich (2010); Diedrich (2011a); Neenan & Scheyer (2012); Diedrich (2013c); Neenan *et al.* (2014).

Cyamodus hildegardis Peyer, 1931

Age. Late Anisian to early Ladinian, Middle Triassic (Kuhn-Schnyder 1962; Rieppel 1993a; Furrer 1995).

Horizon/Locality. *Grenzbitumen* Horizon (Besano Formation)— Monte San Giorgio, Southern Alps, Europe (Rieppel 2000; Scheyer 2010).

Holotype. PIMUZ T 4763 (observed).

Observed referred materials. PIMUZ T58, PIMUZ T 4768, PIMUZ T 4771, PIMUZ T 2796, PIMUZ T A/III 729 (cast of MSNM V458).

Main bibliography. A thorough review of the literature concerning *Cyamodus hildegardis* has been provided by Rieppel (2000). Subsequent literature includes: Scheyer (2010); Diedrich (2011b); Scheyer *et al.* (2012); Klein *et al.* (2015).

Serpianosaurus mirigioliensis Rieppel, 1989

Age. Late Anisian to early Ladinian, Middle Triassic (Kuhn-Schnyder 1962; Rieppel 1993a; Furrer 1995).

Horizon/Locality. *Grenzbitumen* Horizon (Besano Formation)—Monte San Giorgio, Southern Alps, Europe (Rieppel 1989c).

Holotype. PIMUZ T3931 (observed).

Observed referred materials. PIMUZ T132, PIMUZ T951, PIMUZ T3678, PIMUZ T3681, PIMUZ T3685, PIMUZ T3709, PIMUZ T3771, MSNM MSC SC1280.

Main bibliography. A thorough review of the literature concerning *Serpianosaurus mirigioliensis* has been provided by Rieppel (2000). Subsequent literature includes: Caldwell (2002); Hugi *et al.* (2011); Beardmore *et al.* (2012); Diedrich (2013a); Renesto *et al.* (2014).

Wumengosaurus delicatomandibularis Jiang et al., 2008

Age. Late Pelsonian, Anisian, Middle Triassic (Benton *et al.* 2013).

Horizon/Locality. Upper Member, Guanling Formation—Yangjuan Village, Xinmin District, Panxian County, Guizhou Province, China (Jiang *et al.* 2008).

Holotype. GMPKU-P-1210 (observed).

Observed referred materials. GMPKU-P-1209.

Main bibliography. Jiang *et al.* (2008); Wu *et al.* (2011); Benton *et al.* (2013).

Lariosaurus calcagnii (Peyer, 1931b)

Age. Lower Ladinian, Middle Triassic (Furrer 1995).

Horizon/Locality. Cava Inferiore beds, lower Meride Limestones—Near Serpiano, Monte San Giorgio, Southern Alps, Europe (Rieppel 2000).

Holotype. PIMUZ T 2460 (observed).

Observed referred materials. PIMUZ T 2461, PIMUZ T 2435, PIMUZ T 4914.

Main bibliography. A thorough review of the literature concerning *Cyamodus hildegardis* has been provided by Rieppel (2000). Subsequent literature includes: Caldwell (2002); Hugi (2011); Araújo & Correia (2015).

Remarks. Originally classified under the genus *Ceresiosaurus* by Peyer (1931b), but reassigned to *Lariosaurus* by Rieppel (1998).

Pistosaurus longaevus Meyer, 1839

Age. Illyrium, late Anisian, Middle Triassic (Menning *et al.* 2011).

Horizon/Locality. Trochitenkalk or lower Meissner Formation, Upper Muschelkalk Group, Germanic Basin—Bavaria, Southern Germany (Rieppel 2000).

Holotype. UMO BT, uncatalogued (observed)

Observed referred materials. SMF 4041, SMF R 870, SMF R 75

Main bibliography. A thorough review of the literature concerning *Cyamodus hildegardis* has been provided by Rieppel (2000). Subsequent literature includes: Rieppel *et al.* (2002); Diedrich (2013b); Krahl *et al.* (2013).

Remarks. Sues (1987) and Rieppel (2000) have considered *P. grandaevus*, *P. strunzi*, and *P. typus* as junior synonyms of *P. longaevus*, with which I concur and follow herein.

Palaegama vielhaueri Broom, 1926

Age. Middle Lopingian, Late Permian-middle Olenekian, Early Triassic (Smith *et al.* 2012).

Horizon/Locality. Top of *Daptocephalus* zone [= late *Cistecephalus* and *Dicynodon* Zones], or *Lystrosaurus* Zone, Beaufort Group, Karoo Supergroup—Kinira, Mount Frere District, Eastern Cape Province, South Africa (Broom 1926; Carroll 1975).

Holotype. MGM 3707 (observed).

Main bibliography. Broom (1926); Haughton (1929); Kuhn (1969); Carroll (1975); Carroll (1977); Estes (1983b); Evans (1984); Carroll (1988); Carroll & Currie (1991).

Remarks. The identification of the squamosal and quadrate by Carroll (1975) are dubious, and thus considered to be only tentative. Additionally, the suture between the lacrimal and prefrontal is difficult to distinguish and could be merely a crack. Nevertheless, the shape of the postfrontal, postorbital and jugal are considered to be just as provided by Carroll (1975).

Paliguana whitei Broom, 1903

Age. Middle Lopingian, Late Permian-middle Olenekian, Early Triassic (Smith *et al.* 2012).

Horizon/Locality. *Daptocephalus* zone [= late *Cistecephalus* and *Dicynodon* Zones], or *Lystrosaurus* Zone, Beaufort Group, Karoo Supergroup —Donnybrook, KwaZulu-Natal Province, South Africa (Carroll 1975; Estes 1983b).

Holotype. AM 3585 (observed).

Main bibliography. Broom (1903b); Nopcsa (1908); Broom (1925); Huene (1944b); Kuhn (1969); Carroll (1975); Carroll (1977); Estes (1983b); Evans (1984); Benton (1985); Carroll (1988); Carroll & Currie (1991).

Remarks. The shape of the lacrimal is different from that suggested by Carroll (1975; 1977). The lacrimal is much deeper than in his reconstruction, and is limited anteriorly by the nasal process of the maxilla, as in nearly all other diapsid reptiles. Additionally, Carroll (1975) indicated the opening between the quadrate and the quadratojugal to be an artefact. However, the internal margins of the opening are smoothly rounded and do not indicate breakage. The shape of the entire structure is very similar to the condition see in *Sphenodon*, in which a large quadratojugal foramen separates the quadrate and the quadratojugal. Therefore, this opening is considered to be a quadratojugal foramen, as also indicated by Broom (1925). Nevertheless, there is no evidence for an anterior extension of the quadratojugal contacting the jugal, as proposed by Broom. The shape of the squamosal, postorbital, postfrontal and jugal are interpreted here in agreement with the description provided by Carroll (1975; 1977).

Saurosternon bainii Huxley, 1868

Age. Middle Wuchiapigian-latest Changhsingian, Lapingian, Late Permian (Smith *et al.* 2012)

Horizon/Locality. *Daptocephalus* zone [= late *Cistecephalus* and *Dicynodon* Zones], Beaufort Group, Karoo Supergroup—Krantz, Sneeuwberg, Eastern Cape Province, South Africa (Carroll 1975; Estes 1983b).

Holotype. NHMUK R1234 (observed).

Observed referred materials. SAM-PK-919.

Main bibliography. Huxley (1868); Haughton (1929)**;** Kuhn (1969); Carroll (1975); Carroll (1977); Evans (1984); Benton (1985); Carroll (1988); Carroll & Currie (1991).

Pamelina polonica Evans, 2009

Age. Early late Olenekian, Early Triassic (Shishkin & Sulej 2009),

Horizon/Locality. Czatkowice 1 Quarry, Kraków Region, Poland (Evans 2009).

Holotype. ZPAL RV/1036 (observed)

Observed referred materials. ZPAL RV/142, ZPAL RV/143, ZPAL RV/144, ZPAL RV/149, ZPAL RV/151, ZPAL RV/153, ZPAL RV/154, ZPAL RV/155, ZPAL RV/ 384, ZPAL RV/537, ZPAL RV/555, ZPAL RV/975, ZPAL RV/977, ZPAL RV/978, ZPAL RV/979, ZPAL RV/1003, ZPAL RV/1004, ZPAL RV/1005, ZPAL RV/1008, ZPAL RV/1009, ZPAL RV/1011, ZPAL RV/1012, ZPAL RV/1029, ZPAL RV/1036, ZPAL RV/1046, ZPAL RV/1047, ZPAL RV/1048, ZPAL RV/1049 ZPAL RV/1050, 1066, ZPAL RV/1067, ZPAL RV/1073, ZPAL RV/1074, ZPAL RV/1077, ZPAL RV/1094, ZPAL RV/1097, ZPAL RV/1098, ZPAL RV/1202, ZPAL RV/1205, ZPAL RV/1206, ZPAL RV/1209, ZPAL RV/1210, ZPAL RV/1211, ZPAL RV/1212, ZPAL RV/1214.

Main bibliography. Evans (2009)

Remarks. The remains of this taxon are composed of isolated bones only. Upon personal observation, it could be detected that most of the skull elements fit into each other, thus demonstrating an anatomical connectivity between the referred specimens. The dental morphology also matches between the lower and upper jaws. However, the absence of anatomical connections between the preserved skull elements and the postcranium make the

attribution of the postcranial material previously assigned to *P. polonica* only tentative. For this reason, I chose to be conservative and only include data from the skull remains of this taxon.

Sophineta cracoviensis Evans & Borsuk-Bialynicka, 2009

Age. Early late Olenekian, Early Triassic (Shishkin & Sulej 2009),

Horizon/Locality. Czatkowice 1 Quarry, Kraków Region, Poland (Evans & Borsuk-Białynicka 2009).

Holotype. ZPAL RV/175 (observed)

Observed referred materials. ZPAL RV/10, ZPAL RV/13, ZPAL RV/226, ZPAL RV/227, ZPAL RV/228, ZPAL RV/232, ZPAL RV/233, ZPAL RV/234, ZPAL RV/431, ZPAL RV/236, ZPAL RV/246-247, ZPAL RV/248-249, ZPAL RV/506, ZPAL RV/746, ZPAL RV/747, ZPAL RV/748, ZPAL RV/749, ZPAL RV/974, ZPAL RV/1053, ZPAL RV/1054, ZPAL RV/1061, ZPAL RV/1089, ZPAL RV/1094, ZPAL RV/1101, ZPAL RV/1142, ZPAL RV/1145, ZPAL, ZPAL RV/1584, ZPAL RV/1121.

Main bibliography. Evans & Borsuk-Białynicka (2009)

Remarks. Remarks. The remains of this taxon are composed of isolated bones only. Upon personal observation, it could be detected that most of the skull elements fit into each other, thus demonstrating an anatomical connectivity between the referred specimens. The dental morphology also matches between the lower and upper jaws. However, the absence of anatomical connections between the preserved skull elements and the postcranium make the attribution of the postcranial material previously assigned to *S. cracoviensis* only tentative. For this reason, I chose to be conservative and only include data from the skull remains of this taxon.

Megachirella wachtleri Renesto & Posenato, 2003

Age. Pelsonian, Anisian, Middle Triassic (Renesto & Bernardi 2014)

Horizon/Locality. Dont Formation, Braies Group—Monte Prà della Vacca, Braies/Prags Dolomites, Bolzano, Italy (Renesto & Posenato 2003).

Holotype. PZO628 (observed)

Main bibliography. Renesto & Posenato (2003); Renesto & Bernardi (2014).

Kuehneosaurus latus Robinson, 1962

Age. Carnian-Rhaetian, Late Triassic (Fraser 1994; Evans & Jones 2010).

Horizon/Locality. Emborough, Cromhall and Pant quarries, southwest England and Wales, United Kindgom (Evans & Kermack 1994).

Holotype. NHMUK R8172 (observed).

Observed referred materials. NHMUK R5968- NHMUK R5985, NHMUK R5987-NHMUK R5994, NHMUK R5998, NHMUK R5999, NHMUK R6006-NHMUK R6037, NHMUK R6050, NHMUK R6059-NHMUK R6061, NHMUK R6063-NHMUK R6066, NHMUK R6068-NHMUK R6090, NHMUK R6092, NHMUK R6096-NHMUK R6098, NHMUK R6116-NHMUK R6124, NHMUK R6126-NHMUK R6215.

Main bibliography. Robinson (1962); Robinson (1967a); Robinson (1967b); Wild (1973); Estes (1983b); Evans (1984); Benton (1985); Evans & Kermack (1994); Fraser (1994); Müller (2004); Stein *et al.* (2008); Evans & Jones (2010).

Icarosaurus siefkeri Colbert, 1966

Age. Tuvalian, Carnian, Late Triassic (Lucas 1998).

Horizon/Locality. Lockatong Formation, Newark Group [Conewagian assemblage, a correlate of the Adamanian assemblage from the Chinle Group (Lucas 1998)]—Granton Quarry, New Jersey, USA (Colbert 1966).

Holotype. AMNH 2101 (observed)

Main bibliography. Colbert (1966); Colbert (1970); Wild (1973); Estes (1983b); Benton (1985); Fraser *et al.* (2007).

Marmoretta oxoniensis Evans, 1991

Age. Late Bathonian, Middle Jurassic to Kimmeridgian, Late Jurassic (Evans & Kermack 1994)

Horizon/Locality. Kirtlington Mammal Bed, near the base of Forest Mable Formation (late Bathonian)—Old Cement Works Quarry, Kirtlington, Oxfordshire, United Kingdom; Kilmaluag Formation (Bathonian)—north side of Glen Scaladel (Cladach a'Ghlinne), Isle of Skye, Scotland, United Kingdom; Guimarota lignite mine, Leira, Portugal (Kimmeridgian) (Evans 1991a; Evans & Kermack 1994; Waldman & Evans 1994).

Holotype. NHMUK R.12020.

Paratypes. NHMUK R.12025, NHMUK R.12026, NHMUK R.12027, NHMUK R.12028.

Observed referred materials. NHMUK 12400-12406, NMS G 1992.47.1, NMS G 1992.47.4, NMS G 1992.47.5.

Main bibliography. Evans (1991a); Evans & Milner (1994); Waldman & Evans (1994); Benton & Spencer (1995); Evans & Waldman (1996).

Remarks. Semi-articulated and associated cranial and postcranial remains of *Marmoretta* from the Bathonian of the Isle of Skye, Scotland, have been used as means of anatomical comparison and attribution of some isolated remains to this taxon.

Gephyrosaurus bridensis Evans, 1980

Age. Haettagian or Sinemurian, Lower Jurassic (Evans & Kermack 1994; Evans & Jones 2010).

Horizon/Locality. Pontalun and Pant quarries, and St. Bride's Island, South Glamorgan, Wales, United Kingdom (Evans 1980; Evans & Kermack 1994).

Holotype. NHMUK T.1503 (observed)

Observed referred materials. NHMUK T.722, NHMUK T.748, NHMUK T.752, NHMUK T.753, NHMUK T.755, NHMUK T.766, NHMUK T.769, NHMUK T.772, NHMUK T.782, NHMUK T.791, NHMUK T.856, NHMUK T.860, NHMUK T.865, NHMUK T.901, NHMUK T.907-910, NHMUK T.913-917, NHMUK T.937, NHMUK T.938, NHMUK T.940, NHMUK T.945-948, NHMUK T.950, NHMUK T.955-959, NHMUK T.1001, NHMUK T.1015, NHMUK T.1055, NHMUK T.1177, NHMUK T.1238-1264, NHMUK T.1428, NHMUK T.1450, NHMUK T.1454, NHMUK T.1481, NHMUK T.1509, NHMUK T.1512, NHMUK T.1515, NHMUK T.1522, NHMUK T.1528, NHMUK T.1543, NHMUK T.1553, NHMUK T.1554, NHMUK T.1618, NHMUK T.1633, NHMUK T.1693, NHMUK T.1751, NHMUK T.1814, NHMUK T.1815, NHMUK T.1818-1833, NHMUK T.1845, NHMUK T.1847, NHMUK T.1849, NHMUK T.1853, NHMUK T.1855, NHMUK T.1863-1866, NHMUK T.1874, NHMUK T.1875, NHMUK T.1880, NHMUK T.1881, NHMUK T.1942, NHMUK T.1951, NHMUK T.1993, NHMUK T.1994, NHMUK T.2044, NHMUK T.2046, NHMUK T.2047, NHMUK T.2054, NHMUK T.2055, NHMUK T.2065, NHMUK T.2066, NHMUK T.2070, NHMUK T.2086, NHMUK T.2093, NHMUK T.2098, NHMUK T.2111, NHMUK T.2135, NHMUK T.2143, NHMUK T.2154, NHMUK T.2175, NHMUK T.2196, NHMUK T.2216,

NHMUK T.2225, NHMUK T.2227, NHMUK T.2231, NHMUK T.2301, NHMUK T.2311, NHMUK T.2313, NHMUK T.2319, NHMUK T.2320, NHMUK T.2323, NHMUK T.2325, NHMUK T.2335, NHMUK T.2336, NHMUK T.2337, NHMUK T.2346-2352, NHMUK T.2357-2361, NHMUK T.232, NHMUK T.2639-2642, NHMUK T.3017-3022, NHMUK T.3113-3117, NHMUK T.3223

Main bibliography. Evans (1980); Evans (1981); Estes (1983b); Evans (1984); Benton (1985); Evans (1985); Fraser & Benton (1989); Evans & Kermack (1994); Borsuk-Białynicka (1996); Wu (2003); Jones (2008); Evans & Jones (2010); Simões *et al.* (2016 [Suppl. Mat.]).

Remarks. Although no articulated specimens of *G. bridensis* are known, personal observation of the referred specimens indicates that most of the skull elements fit into each other, thus demonstrating an anatomical connectivity between the referred specimens. The dental morphology also matches between the lower and upper jaws. Furthermore, all cranial material studied herein from Pontalun and Pant quarries could be assigned to *G. bridensis*, and thus the associated postcranial material (Evans 1981) was also treated as part of this same taxon.

Diphyodontosaurus avonis Whiteside, 1986

Age. Carnian-Rhaetian, Late Triassic (Fraser 1994; Evans & Jones 2010).

Horizon/Locality. Tytherington and Cromhall quarries, South Gloucestershire, United Kingdom (Whiteside 1986).

Holotype. BU 23760 (observed).

Paratypes. BU 23763, BU 23764, BU 23842, BU 23787, BU 23789, BU 23785, BU 23781, BU 23790, BU 23780, BU 23782, BU 23783, BU 23784, BU 23772, 23776, BU 23768 BU 23774, BU 23986, BU 23778, BU 23777, BU 23761, BU 23762 (all observed).

Main bibliography. Whiteside (1986); Fraser & Benton (1989); Evans & Kermack (1994); Fraser (1994)**;** Borsuk-Białynicka (1996); Wu (2003); Jones (2008); Evans & Jones (2010); Simões *et al.* (2016 [Suppl. Mat.]).

Remarks. The remains of this taxon are composed of isolated bones only. Upon personal observation, it could be detected that most of the skull elements fit into each other, thus demonstrating an anatomical connectivity between the referred specimens. The dental morphology also matches between the lower and upper jaws. However, the absence of anatomical connections between the preserved skull elements and the postcranium make the

attribution of the postcranial material previously assigned to *D. avonis* only tentative. For this reason, I chose to be conservative and only include data from the skull remains of this taxon.

Planocephalosaurus robinsonae Fraser, 1982

Age. Carnian-Rhaetian, Late Triassic (Fraser 1994; Evans & Jones 2010).

Horizon/Locality. Cromhall (old Slickstones) and Tytherington quarries, South Gloucestershire, United Kingdom (Fraser 1982; Evans & Kermack 1994).

Holotype. AUP 11061 (observed).

Observed referred materials AUP 11062-AUP 11081, AUP 11170-AUP 11185, NHMUK R9953-NHMUK R9976.

Main bibliography. Fraser (1982); Fraser & Walkden (1984); Fraser & Benton (1989); Evans & Kermack (1994); Fraser (1994)**;** Wu (2003); Jones (2008); Evans & Jones (2010); Simões *et al.* (2016 [Suppl. Mat.]).

Remarks. The remains of this taxon are composed of isolated bones only. Upon personal observation, it could be detected that most of the skull elements fit into each other, thus demonstrating an anatomical connectivity between the referred specimens. The dental morphology also matches between the lower and upper jaws. However, the absence of anatomical connections between the preserved skull elements and the postcranium make the attribution of the postcranial material previously assigned to *P. robinsonae* only tentative. For this reason, I chose to be conservative and only include data from the skull remains of this taxon.

Clevosaurus hudsoni (Swinton, 1939)

Age. Carnian-Rhaetian, Late Triassic (Fraser 1994; Evans & Jones 2010).

Horizon/Locality. Cromhall (old Slickstones) Quarry, South Gloucestershire, United Kingdom (Fraser 1988); same genus (possibly the same speies) from Tytherington, Emborough, and Pant quarries, southwest England and Wales, United Kingdom (Fraser 1988; Evans & Kermack 1994).

Holotype. NHMUK R5939 (syntypes).

Observed referred materials. NHMUK R604, NHMUK R605 (a,b,c), NHMUK R9249, UMZC T1264, UMZC T1265, UMZC T1266, UMZC T1267, UMZC T1268, UMZC T1269, UMZC

T1270, UMZC T1271, UMCZ T 1272, UMCZ T 1273, UMCZ T 1274, UMCZ T 1275, UMCZ T 1276, UMCZ T 1277, UMCZ T 1279.

Main bibliography. Swinton (1939); Robinson (1973); Fraser (1988); Fraser & Benton (1989); Evans & Kermack (1994); Fraser (1994); Wu (2003); Jones (2008); Evans & Jones (2010); Simões *et al.* (2016 [Suppl. Mat.]).

Remarks. The articulated material that includes cranium and postcranium (UMZC T1271) as well as the articulated skulls (NHMUK R604, NHMUK R605, and UMZC T1269) was used as the main basis of comparison to establish which of the isolated bones can be confidentially associated to *Clevosaurus hudsoni*. See also comments for the Late Triassic-Early Jurassic British faunas in the taxonomic sampling criteria above.

Palaeopleurosaurus posidoniae Carroll, 1985b

Age. Toarcian, Early Jurassic (Carroll 1985b).

Horizon/Locality. Posidonienschiefer, Schwarzjura, Lias Epsilon II1and2—P. Kirchmann Quarry, in Staatswald Ohmden, near Holzmaden, Germany (Carroll 1985b)

Holotype. SMN 50722 (observed)

Paratype. SMN 50721

Observed referred materials.

Main bibliography. Carroll (1985b)**;** Carroll & Wild (1994); Dupret (2004)**;** Jones (2008); Evans & Jones (2010).

Homeosaurus maximiliani Meyer, 1847

Age. Latest Kimmeridgian-early Tithonian, Late Jurassic (Schweigert 2007)

Horizon/Locality. Solnhofen Plattenkalk—Kelheim and Wintershof, Bavaria, Germany [specimen identification labels and Cocude-Michel (1963b)].

Holotype. lost in 1944 in Munich—see Cocude-Michel (1963b).

Neotype: BSPG 1887 VI 502 (observed).

Observed referred materials. BSPG 1937-1-40.

Main bibliography. Meyer (1847); Wagner (1852); Meyer (1860a); Meyer (1866); Boulenger (1891); Broili (1925); Barbour & Stetson (1929); Cocude-Michel (1963b); Kuhn (1969).

Remarks. The genus *Homeosaurus* is in need of revision, therefore only the neotype of *H. maximiliani* and another specimen housed at the BSPG collection (BSPG 1937-1-40.) that could be attributed to the same species are included herein as *H. maximialiani*. The localities provided herein are the ones where the specimens referred above come from.

Kallimodon pulchellus Zittel, 1887

Age. Latest Kimmeridgian-early Tithonian, Late Jurassic (Schweigert 2007).

Horizon/Locality. Solnhofen Plattenkalk—Kelheim and Kupferberg, Bavaria, Germany [specimen identification labels and Cocude-Michel (1963b)].

Holotype. BSPG 1887 VI 1 (observed).

Observed referred materials. MB.R. 1008.1 (previously Berlin Rhy 2), MB.R. 1009.1-2 (previously Berlin Rhy 3), BSPG 1887 VI 2, BSPG 1922 I 15.

Main bibliography. Zittel (1887); Broili (1925); Cocude-Michel (1959); Cocude-Michel (1963b); Kuhn (1969); Fabre *et al.* (1982); Fraser & Benton (1989).

Remarks. As with *Homeosaurus*, the genus *Kallimodon* also needs revision as numerous specimens attributed to *K. pulchellus* display significant differences to the holotype, mostly based on the postcranium morphology. Additionally, specimens labeled as belonging to other taxa show no significant differences to the holotype of *K. pulchellus.* Only studied specimens that show no observable differences to the holotype are included herein as *K. pulchellus*, but a revision and re-characterization of the genus might reveal additional specimens of *K. pulchellus* that were not studied herein. The localities provided herein are the ones where the specimens referred above come from.

Priosphenodon avelasi Apesteguia & Novas, 2003.

Age. Cenomanian-Turonian, Late Cretaceous (Apesteguia & Novas 2003).

Horizon/Locality. Candeleros Formation, Neuquén Group—La Buitreta Quarry, Río Negro Province, Argentina (Leanza & Hugo 2001; Apesteguia & Novas 2003).

Holotype. MPCA 300 (observed).

Observed referred materials. MPCA 275, MPCA 293, MPCA 303, MPCA 304, MPCA 305, MPCA 316, MPCA 374.

Main bibliography. Apesteguia & Novas (2003); Simón & Kellner (2003); Jones (2008); Evans & Jones (2010); Apesteguia & Carballido (2014).

Remarks. *P. avelasi* and *Kaikaifilusaurus calvoi* are synonynoum taxa considering the published accounts on both taxa. Although *K. calvoi* has priority due to an earlier publication, this taxon has been considered as a nomen dubium by Apesteguia & Carballido (2014). For an account in the taxonomic dispute between *Kaikaifilusaurus calvoi* and *Priosphenodon avelasi*, see Apesteguia & Carballido (2014).

Eichstaettisaurus schroederi (Broili, 1938)

Age. Latest Kimmeridgian-early Tithonian, Late Jurassic (Schweigert 2007).

Horizon/Locality. Solnhofen Plattenkalk— Wintershof (near Eichstätt), Bavaria, Germany (Broili 1938).

Holotype. BSPG 1937 I 1 (observed)

Main bibliography. (Broili 1938); Young (1948); Hoffstetter (1953); Kuhn (1958); Cocude-Michel (1961); Cocude-Michel (1963b); Hoffstetter (1964); Hoffstetter (1966); Estes (1983b); Evans (1993); Rieppel (1994a); Evans *et al.* (2000); Evans *et al.* (2004); Daza *et al.* (2014); Simões *et al.* (2017b).

Remarks. For a detailed recent account on the taxonomy, systematics, and re-assessment of the osteology of *E. schroederi* see Simões *et al.* (2017b).

Ardeosaurus brevipes (Meyer, 1855)

Age. Latest Kimmeridgian-early Tithonian, Late Jurassic (Schweigert 2007).

Horizon/Locality. Solnhofen Plattenkalk—Eichstätt, Bavaria, Germany (Mateer 1982).

Holotype. Collection Hetzell, now lost (Mateer 1982; Estes 1983b). Cast of holotype: NHMUK 38006 (observed).

Observed referred materials. BSPG 1923. I. 501.

Main bibliography. Meyer (1855); Meyer (1860a); Zittel (1887); Nopcsa (1908); Camp (1923); Broili (1925); Hoffstetter (1953); Hoffstetter (1955b); Cocude-Michel (1963b); Hoffstetter (1964); Hoffstetter (1966); Estes (1983b); Evans (1993); (Simões *et al.* 2017b).

Remarks. After the loss of the holotype of *A. brevipes*, a new specimen (PMU.R58) was discovered an described by Mateer (1982). However, PMU.R58 is currently lost as well (B.

Kear, personal communication). Another specimen, previously assigned as *Ardeosaurus* cf. *digitatellus* (BSPG 1923. I. 501), displays several features that allow its assignment to *A. brevipes*. These include: impressions of skull roof osteoderms, a wider posterior margin of the parietals between the supratemporal processes (compared to the holotype of *A. digitatellus*), separate postorbital and posfrontal, and only three phalanges on the fifth pedal digit. Although preserved mostly as impressions, the level of detail preserved in the soft matrix allows the identification of individual bones and sutures, which highly contribute to increase the amount of information to be scored for this taxon in the present dataset.

Paramacellodus oweni Hoffstetter, 1967

Age. Bathonian, Middle Jurassic (?); Berriasian, Early Cretaceous (Evans 2003a).

Horizon/Locality. Purbeck Limestone Formation (Berriasian)—Durdlestone Bay, Swanage, Isle of Purbeck, Dorset, United Kingdom; possibly from Kilmaluag Formation (Bathonian)—north side of Glen Scaladel (Cladach a'Ghlinne), Isle of Skye, Scotland, United Kingdom (Hoffstetter 1967; Estes 1983b).

Holotype. NHMUK R8131-8132 (observed).

Observed referred materials. NHMUK R8082, NHMUK R8085, NHMUK R8104, NHMUK R8115, NHMUK R8117a, NHMUK R8118, NHMUK R8130, NHMUK R8208, NHMUK R8209, NHMUK R8210.

Main bibliography. Hoffstetter (1967); Estes (1983b); Waldman & Evans (1994); Rieppel (1994a); Evans & Chure (1998); Evans & Searle (2002).

Huehuecuetzpalli mixtecus Reynoso, 1998

Age. Late Albian, Early Cretaceous (Benammi *et al.* 2006).

Horizon/Locality. Middle portion of the Tlayúa Formation—south of Tepexi de Rodríguez, State of Puebla, Mexico (Reynoso & Cruz 2014).

Holotype. IGM 7389 (observed).

Paratype. IGM 4185**.**

Main bibliography. Reynoso (1998); Reynoso & Cruz (2014).

Remarks. Personal observation of the holotype and paratype indicate a few differences to the description provided by Reynoso (1998). Among these, vertebrae on the pelvic region of the

holotype are somewhat disarticulated and the anteriormost portion of their neural arches exposed with no clear indication of a zygosphene-zygantra system. On the skull, the left side of the parietal includes an elongate supratemporal process contacting the left squamosal, which is slightly displaced anteriorly. Between the squamosal and the supratemporal process of the parietal, a third distinct element is present, sutured to the parietal and elongate in shape. This corresponds to the supratemporal, which also occupies this same position and has this same overall shape in most squamates bearing those three elements. The supratemporal is less distinct on right side of the skull, but under UV light a partial suture is observed between it and the parietal. This suggests a partial fusion of the right element took place. Additionally, the presence of dorsal intercentra could not be confirmed. The holotype is preserved in dorsal view, preventing an assessment of the later condition, whereas the paratype shows the posterior dorsals in lateral view. Reynoso (1998) mentioned the presence of intercentra in the last presacrals (an inference that might have been made based on the paratype), but no clear structures between the dorsal centra could be established as intercentra. Therefore, this particular feature is treated herein as missing data.

Tepexisaurus tepexii Reynoso & Callison, 2000
Age. Late Albian, Early Cretaceous (Benammi *et al.* 2006).
Horizon/Locality. Middle portion of the Tlayúa Formation—south of Tepexi de Rodríguez, State of Puebla, Mexico (Reynoso & Cruz 2014).
Holotype. IGM 7466 (observed).
Main bibliography. Reynoso & Callison (2000); Reynoso & Cruz (2014).

Priscagama gobiensis Borsuk-Bialynicka & Moody, 1984
Age. Campanian-earliest Maastrichtian (Jerzykiewicz *et al.* 1993; Dashzeveg *et al.* 2005; Dingus *et al.* 2008).
Horizon/Locality. Barun Goyot (Khermeen Tsav and Khulsan) and Djadochta Formation (Bayn Dzak and Ukhaa Tolgod), Nemegt Basin—Gobi Desert, Mongolia; Djadokhta Formation, Nemegt Basin—Bayan Mandahu redbeds, Inner Mongolia, China (Gao & Norell 2000).
Holotype. ZPAL MgR/III-32 (observed).

Observed referred materials. ZPAL MgR/III-31, ZPAL MgR/III-72, ZPAL MgR/III-33, ZPAL MgR/III-83, ZPAL MgR/lI-77, ZPAL MgR/II-101, IVPP V 10038.
Main bibliography. Borsuk-Białynicka & Moody (1984); Alifanov (1989); Rieppel (1994a); Dashzeveg *et al.* (1995); Alifanov (1996); Borsuk-Białynicka (1996); Gao & Hou (1996); Alifanov (2000a); Gao & Norell (2000); Conrad & Norell (2007); Wang & Li (2008).
Remarks. The age of the Djadokhta Formation is usually restricted to the latest Campanian-early Maastrichtian (between 75 and 71 MYA) such as inferred from more recent datings for the Bayn Dzak Member (Dashzeveg *et al.* 2005). The age of the overlying Tugrugeen Shireh (or Tugrugyin Shireh) is therefore supposed to be earliest Maastrichtian. However, a more precise dating for other localities is lacking, and these are often referred to only as Campanian, such a Ukhaa Tolgod and the Bayan Mandahu redbeds in Inner Mongolia (China) (Eberth 1993; Jerzykiewicz *et al.* 1993; Dingus *et al.* 2008). Therefore, *Priscagama* and other taxa that occur in Bayn Dzak and Tugrugeen Shireh certainly occur in the late Campanian and earliest Maastrichtian. However, when such taxa also occur in other localities (e.g. Barun Goyot) then their stratigraphic range may be higher, and thus a less restrictive age range is provided herein (e.g. Campanian or Campanian-earliest Maastrichtian).

Pleurodontagama aenigmatoides Borsuk-Bialynicka & Moody, 1984
Age. Campanian (Jerzykiewicz *et al.* 1993; Dingus *et al.* 2008).
Horizon/Locality. Barun Goyot (Khermeen Tsav) Formation—Gobi Desert, Mongolia; Djadokhta Formation, Nemegt Basin—Bayan Mandahu redbeds, Inner Mongolia, China (Borsuk-Białynicka 1996).
Holotype. ZPAL MgR-III/35 (observed).
Main bibliography. Borsuk-Białynicka & Moody (1984); Rieppel (1994a); Alifanov (1996); Borsuk-Białynicka (1996); Gao & Hou (1996); Gao & Norell (2000); Wang & Li (2008).

Igua minuta Borsuk-Bialynicka & Alifanov, 1991
Age. Campanian, Late Cretaceous (Jerzykiewicz *et al.* 1993; Dingus *et al.* 2008).
Horizon/Locality. Barun Goyot Formation (Khulsan)—Gobi Desert, Mongolia (Gao & Norell 2000).
Holotype. ZPAL MgR-I/60 (observed).

Main bibliography. Borsuk-Białynicka & Alifanov (1991).

Remarks. The holotype constitutes a juvenile [already noticed by Borsuk-Białynicka & Alifanov (1991)], lacking fusion between the exoccipitals and opisthotics (and among any other braincase elements), and bearing a squared parietal with an enlarged parietal foramen, forming a parietal fontanelle. A squared parietal in many lizards, including iguanians such as *Stenocercus* and *Iguana*, is common among juveniles (Barahona & Barbadillo 1998; Bell *et al.* 2003; Torres-Carvajal 2003; Simões *et al.* 2016). Additionally, a parietal fontanelle is observed in the early development of the pineal foramen (Torres-Carvajal 2003). For those reasons, the juvenile condition of the holotype of *Igua minuta* is confirmed herein. Therefore, characters prone to ontogenetic variation in squamates are treated as uninformative herein (with "?") herein. This is the case of characters related to the parietal table shape and ornamentation, and fusion of braincase elements.

Polrussia mongoliensis Borsuk-Bialynicka & Alifanov, 1991

Age. Campanian, Late Cretaceous (Jerzykiewicz *et al.* 1993; Dingus *et al.* 2008).

Horizon/Locality. Barun Goyot Formation (Khulsan)—Gobi Desert, Mongolia (Gao & Norell 2000).

Holotype. ZPAL MgR-I/119 (observed).

Main bibliography. Borsuk-Białynicka & Alifanov (1991); Alifanov (2000a); Gao & Norell (2000).

Remarks. Gao & Norell (2000) stated the squared shape of the parietal in *Polrussia* as a feature that the latter has in common with *Igua minuta*. However, as noted above, this particular feature is a result of ontogeny in *Igua*, and possibly also the case of the two known specimens of *Polrussia*. Although the dentition of *Polrussia* has been described as unicuspid, most tooth apices are broken or not observable. On the right maxilla, although some teeth seem unicuspid, the fourth (front to back) tooth in situ has incicipient mesiodistally places cusps. It is possible that *Polrussia* has at least some unicuspid teeth, but the state of preservation combined with potential tooth wear creates an apparent unicuspidity in the holotype. The second reported specimen of *Polrussia* [IGM3/73—Gao & Norell (2000)] has been reported to bear unicuspid teeth, but given some differences between it and the holotype (e.g. presence of pterygoid teeth, which are absent in the holotype) it may actually not belong to *Polrussia*.

Gilmoreteius chulsanensis (Sulimski, 1975)

Age. Campanian, Late Cretaceous (Dingus *et al.* 2008).

Horizon/Locality. Barun Goyot Formation (Khulsan and Monadnocks), Nemegt Basin—Gobi Desert, Mongolia (Gao & Norell 2000).

Holotype. ZPAL MgR-I/14 (observed).

Observed referred materials. ZPAL MgR-I/18, ZPAL MgR-I/20, ZPAL MgR-I/21, ZPAL MgR-I/22, ZPAL MgR-I/23, ZPAL MgR-I/24, ZPAL MgR-I/5.

Main bibliography. Gilmore (1943); Sulimski (1975); Langer (1998); Alifanov (2000b); Gao & Norell (2000).

Gobinatus arenosus Alifanov, 1993

Age. Campanian, Late Cretaceous (Jerzykiewicz *et al.* 1993; Dingus *et al.* 2008).

Horizon/Locality. Barun Goyot (Khermeen Tsav and Khulsan) and Djadokhta Formation (Ukhaa Tolgod)—Gobi Desert, Mongolia (Gao & Norell 2000).

Holotype. PIN No. 3142/308.

Observed referred materials. ZPAL MgR-I/77, ZPAL MgR-II/1 (duplicated No), ZPAL MgR-II/8, ZPAL MgR-II/56, ZPAL MgR-III/44.

Main bibliography. Alifanov (1993a); Alifanov (2000b); Gao & Norell (2000).

Gobekko cretacicus Borsuk-Bialynicka, 1990

Age. Late Campanian-earliest Maastrichtian, Late Cretaceous (Dashzeveg *et al.* 2005).

Horizon/Locality. Djadokhta Formation (Bayn Dzak), Nemegt Basin—Gobi Desert, Mongolia (Borsuk-Białynicka 1990).

Holotype. ZPAL MgR-II/4 (observed).

Observed referred materials. ZPAL MgR-II/43, ZPAL MgR-II/47.

Main bibliography. Borsuk-Białynicka (1990); Conrad & Norell (2006); Daza *et al.* (2013); Daza *et al.* (2014); Conrad & Daza (2015).

Meyasaurus diazromerali Evans & Barbadillo, 1997

Age. Barremian, Early Cretaceous (Buscalioni & Fregenal-Martínez 2010).
Horizon/Locality. La Huérguina Limestone Formation—Las Hoyas fossil site, Serranía de Cuenca, Cuenca Province, Castilla-La Mancha, Spain (Evans & Barbadillo 1997).
Holotype. LH 370 (observed).
Observed referred materials. LH 33, LH 372, LH 13510, LH 6026, LH 143175.
Main bibliography. Evans & Barbadillo (1997); Bolet & Evans (2010); Bolet & Evans (2012); Venczel & Codrea (2016).

Globaura venusta Borsuk-Bialynicka, 1988
Age. Campanian-earliest Maastrichtian, Late Cretaceous (Dashzeveg *et al.* 2005; Dingus *et al.* 2008).
Horizon/Locality. Barun Goyot (Khermeen Tsav and Khulsan) and Djadochta Formation (Bayn Dzak and Ukhaa Tolgod), Nemegt Basin—Gobi Desert, Mongolia (Gao & Norell 2000).
Holotype. ZPAL MgR-III/40 (observed).
Observed referred materials. ZPAL MgR-I/45, ZPAL MgR-I/46, ZPAL MgR-I/47, ZPAL MgR-I/48, ZPAL MgR-I/49, ZPAL MgR-I/50, ZPAL MgR-I/51, ZPAL MgR-I/53, ZPAL MgR-I/71, ZPAL MgR-I/118, ZPAL MgR-II/26, ZPAL MgR-II/42, ZPAL MgR-II/53, ZPAL MgR-II/55, ZPAL MgR-III/36, ZPAL MgR-III/41, ZPAL MgR-III/43.
Main bibliography. Borsuk-Białynicka (1988); Alifanov (2000a); Gao & Norell (2000).

Slavoia darevskii Sulimski, 1984
Age. Campanian, Late Cretaceous (Dashzeveg *et al.* 2005; Dingus *et al.* 2008).
Horizon/Locality. Barun Goyot (Khermeen Tsav and Khulsan) and Djadochta Formation (Ukhaa Tolgod), Nemegt Basin—Gobi Desert, Mongolia (Gao & Norell 2000).
Holotype. ZPAL MgR-I/8 (observed).
Observed referred materials. ZPAL MgR-I/2, ZPAL MgR-I/9, ZPAL MgR-I/77, ZPAL MgR-I/85, ZPAL MgR-I/93, ZPAL MgR-I/94, ZPAL MgR-I/95, ZPAL MgR-I/96, ZPAL MgR-I/97, ZPAL MgR-I/98, ZPAL MgR-I/99, ZPAL MgR-I/100, ZPAL MgR-I/101, ZPAL MgR-I/102, ZPAL MgR-I/103, ZPAL MgR-I/104, ZPAL MgR-I/105, ZPAL MgR-I/106, ZPAL MgR-I/107, ZPAL MgR-I/108, ZPAL MgR-I/112, ZPAL MgR-III/76, ZPAL MgR-III/81.

Main bibliography. Sulimski (1984); Rieppel (1994a); Alifanov (2000a); Gao & Norell (2000); Tałanda (2016); Tałanda (2017).

Remarks. The genus *Slavoia* has been suggested to occur in the Late Cretaceous of Kazakhstan (Kordikova *et al.* 2001), but the referred material has been recently re-assigned as Scincomorpha indet. (Averianov *et al.* 2016). Alifanov (1993b) and Alifanov (2000a) also lists *Slavoia* in the Early Cretaceous, but does not provide further details on this potential occurrence. Therefore, the stratigraphic distribution of the genus is here restricted to the Late Cretaceous.

Dalinghosaurus longidigitus Ji, 1998

Age. Earliest Hautuverian-Barremian/Aptian, Early Cretaceous (Sha 2007).

Horizon/Locality. Lujiatun, Jianshangou and Dawangzhangzi beds, Yixian Formation, Jehol Group—Beipiao and Lingyuan, Liaoning Province, China (Evans & Wang 2005; Wang & Li 2008).

Holotype. GMV2127.

Observed referred materials. IVPP V12345 A&B, IVPP V12586, IVPP V13282, IVPP V14342.

Main bibliography. Ji (1998); Ji (2004); Ji & Ji (2004); Evans & Wang (2005); Evans & Wang (2007); Evans *et al.* (2007); Wang *et al.* (2010).

Dinilysia patagonica Woodward, 1901

Age. Santonian to early/middle Campanian, Late Cretaceous (Leanza & Hugo 2001; Scanferla & Canale 2007; Filippi & Garrido 2012)

Horizon/Locality. Bajo de la Carpa Formation, Rio Colorado Subgroup, Neuquén Group—City of Neuquén, Boca del Sapo, Aca Mahuida, Barreales Norte and Tripailao Farm localities (Neuquén Province), Paso Córdova (Rio Negro Province), Argentina; Anacleto Formation, Rio Colorado Subgroup, Neuquén Group— Aguada Toledo, south of Mari Menuco Lake and Puesto La Rinconada (Neuquén Province), Argentina (Caldwell & Albino 2002; Scanferla & Canale 2007; Filippi & Garrido 2012; Triviño & Albino 2015).

Holotype. MLP 26-410 (observed)

Observed referred materials. MACN-N 26, MACN-N 27, MACN-N 115, MACN-RN 976, MACN-RN 1013, MACN-RN 1014, MACN-RN 1015, MACN-RN 1016, MACN-RN 1017, MLP 79-11-27-2, MLP 79-11-27-8.

Main bibliography. Woodward (1901); Estes *et al.* (1970); Frazzetta (1970); Rage (1977); Hecht (1982); Rage & Albino (1989); Caldwell & Albino (2001); Caldwell & Albino (2002); Albino & Caldwell (2003); Budney *et al.* (2006); Caldwell & Calvo (2008); Filippi & Garrido (2012); Zaher & Scanferla (2012); Palci & Caldwell (2014); Scanferla & Bhullar (2014); Triviño & Albino (2015).

Najash rionegrina Apesteguía & Zaher, 2006

Age. Cenomanian-Turonian, Late Cretaceous (Corbella *et al.* 2004; Zaher *et al.* 2009)

Horizon/Locality. mid to upper levels of the Candeleros Formation, Neuquén Group—La Buitrera Quarry, Río Negro, Argentina (Apesteguía & Zaher 2006; Zaher *et al.* 2009).

Holotype. MPCA 390-398, 400 (observed).

Observed referred materials. MPCA 380, MPCA 381, MPCA 382, MPCA 383, MPCA 385, MPCA 386, MPCA 388, MPCA 417, MPCA 418, MPCA 419, MPCA 480, MPCA 500.

Main bibliography. Apesteguía & Zaher (2006); Zaher *et al.* (2009); Palci *et al.* (2013a).

Remarks. Due to the possible presence of more than one taxa among the type specimens of *Najash rionegrina* [Palci *et al.* (2013a), TRS personal observations] only the specimens from the holotype were utilized herein for the scorings of *Najash*. The latter includes the holotype lower jaw, which was found in close association to the postcranial elements of the holotype (F. Garberoglio, personal communication).

Pachyrhachis problematicus Haas, 1979

Age. lower Cenomanian, Late Cretaceous (Lee & Caldwell 1998)

Horizon/Locality. Bed-Meir Formation—Ein Jabrud, near Ramallah, Israel (Caldwell & Lee 1997; Lee & Caldwell 1998)

Holotype. HUJ-PAL 3659 (observed)

Observed referred materials. HUJ-PAL 3775

Main bibliography. Haas (1979); Caldwell & Lee (1997); Lee & Caldwell (1998); Zaher (1998); Scanlon *et al.* (1999); Zaher & Rieppel (1999); Caldwell (2000); Coates & Ruta (2000);

Rieppel & Zaher (2000); Caldwell & Albino (2001); Rieppel & Zaher (2001); Zaher & Rieppel (2002); Rage & Escuillié (2003); Polcyn *et al.* (2005); Palci & Caldwell (2013); Palci *et al.* (2013b).

Spathorhynchus fossorium Berman, 1973

Age. Early to Middle Eocene, Paleogene (Berman 1977).

Horizon/Locality. Bridger and Wind River formations—Sweetwater County, Wyoming, USA (Berman 1973; 1977).

Holotype. NMNH 26317.

Paratype. NMNH26318.

Observed referred materials. AMNH 25556.

Main bibliography. Berman (1973); Berman (1977); Müller *et al.* (2016).

Aigialosaurus Kramberger, 1892

Age. Late Cenomanian-Early Turonian, Late Cretaceous (Gušić & Jelaska 1993)

Horizon/Locality. Island of Hvar, Croatia (Caldwell & Dutchak 2006).

Holotype. BSPG 1902II501 (observed)

Main bibliography. Kramberger (1892); Williston (1904); Nopcsa (1903); Nopcsa (1908); Carroll (1985a); Carroll & de Braga (1992); de Braga & Carroll (1993); Dutchak (2005); Caldwell & Dutchak (2006).

Adriosaurus suessi Seeley, 1881

Age. late Cenomanian- late Turonian, Late Cretaceous (Gušić & Jelaska 1993; Lee & Caldwell 2000).

Horizon/Locality. Komen Platey Limestone—Near Komen, Slovenia; Island of Hvar, Croatia (Lee & Caldwell 2000).

Holotype. NHMW unumbered

Observed referred materials. NHMUK R2867

Main bibliography. Seeley (1881); Nopcsa (1908); Nopcsa (1923a); Lee & Caldwell (2000)

Pontosaurus Kramberger, 1892

Age. Early-middle Cenomanian (*P. kornhuberi*) to Late Cenomanian-Early Turonian (*P. lesinensis*), Late Cretaceous (Gušić & Jelaska 1993; Dal Sasso & Pinna 1997).
Horizon/Locality. Quarry in the Valley of Al Gabour near Al Nammoura, 10 km southeast of Hadjula, Lebanon (Caldwell 2006); Island of Hvar, Croatia.
Holotype. MSNM V3662 (observed).
Main bibliography. Kornhuber (1873); Kramberger (1892); Caldwell & Sasso (2004); Pierce & Caldwell (2004); Caldwell (2006).

Extant taxa

Rhynchocephalia

Sphenodon punctatus: MCZ R4702, FMNH 11113, FMNH 197942, FMNH 207433.

Squamata

Iguania

Trioceros jacksonii*:** AMNH R-84559, AMNH R-99984, AMNH R-141099, FMNH 206753, ***Uromastyx aegyptia*:** AMNH R-73160, FMNH 63961, FMNH 31030, ***Hoplocercus spinosus*:** AMNH R-89398, AMNH R-90384, AMNH R-90658, ***Iguana iguana*:** AMNH R-43302, AMNH R-81871, AMNH R-82125, ***Polychrus marmoratus*:** AMNH R-141084, AMNH R-148543, AMNH R-148544, AMNH R-141130, ***Pristidactylus scapulatus*:** AMNH R-148535, AMNH R-148534, AMNH R-148536, ***Crotaphytus collaris*:** AMNH R-75090, AMNH R-82297, AMNH R-84489, AMNH R-85381, ***Liolaemus signifer: AMNH R-80140, AMNH R-81801, AMNH R-80139, AMNH R-154846, ***Leiocephalus carinatus*:** AMNH R-70575, AMNH R-59988, AMNH R-57461, ***Oplurus cyclurus*:** FMNH 75620, FMNH 72640, ***Stenocercus scapularis*:** FMNH 40612, ***Phrynosoma modestum*:** TMP1997.030.0318, TMP1997.030.0321, TMP1997.030.0324, TMP1990.007.0161.

Gekkota

Coleonyx variegatus*:** AMNH R-74613, AMNH R-89271, AMNH R-73763, AMNH R-73762, ***Dactylocnemis pacificus: MCZ R-141790, MCZ R-141791, MCZ R-141793, MCZ R-141794, MCZ R-141796*,* ***Gecko gekko***: TMP 1990.007.0021, 1997.030.0333, TMP 1997.030.0327.

"Scincomorpha"

Xantusia vigilis*:** AMNH R-150167, AMNH R-150164, R-150165, FMNH 22329; ***Cordylus niger*:** AMNH R-81809, AMNH R-82396, AMNH R-81885, ***Broadleysaurus major*:** AMNH R-173621, MCZ R-147438, ***Timon lepidus*:** FMNH 22267, FMNH 22098, FMNH 229612, ***Lacerta viridis: UAMZ uncatalogued; ***Plestiodon fasciatus*:** AMNH R-92742, AMNH R-155177, AMNH R-155179, AMNH R-155181, ***Mabuya mabouya*:** AMNH R-141128, ***Teius teyou*:** FMNH 170853, FMNH 10407**;** ***Petracola ventrimaculatus*:** CJB 571.

Anguimorpha

***Xenosaurus grandis*:** AMNH R-103212, AMNH R-98122, AMNH R-91487, AMNH R-19380, FMNH 117105, ***Elgaria multicarinata*:** AMNH R-154694, AMNH R-154693, AMNH R-154692, ***Pseudopus apodus*:** AMNH R-57958, AMNH R-75481, AMNH R-73228, ***Heloderma suspectum*:** AMNH R-72646, AMNH R-71864, AMNH R-73771, ***Lanthanotus borneensis*:** FMNH 134771, FMNH 130981, ***Varanus salvator*:** TMP 1990.007.0036, TMP 1990.007.0037, TMP 1990.007.0270.

Amphisbaenia

***Rhineura floridana*:** AMNH R-92989, AMNH R-147916, FMNH 263913, ***Bipes biporus*:** AMNH R-92758, AMNH R-154703, FMNH 266420, ***Blanus cinereus*:** AMNH 95942*,* FMNH 265151.

Serpentes

Anilius scytale: MCZ R-19537, MCZ R-17645, MCZ R-2984, ***Xenopeltis unicolor*:** MCZ-R5483, MCZ-R188759, MCZ-R188760, MCZ-R3114, FMNH 287277, ***Cylindrophis ruffus*** FMNH 297456.

Dibamidae

***Dibamus novaeguineae*:** NMNH 305914; NMNH 305916

Supplementary Information 6.3

Characters list

Character references indicate the first usage of such characters in any of the data matrices compiled by us. They do not refer to when the character was first mentioned in the literature, only to its actual first usage for a cladistic purpose.

AN03 (Apesteguia & Novas 2003); B85 (Benton 1985); C99 (Caldwell 1999); Ch14 (Chen *et al.* 2014); CoN06 (Conrad & Norell 2006); Co08 (Conrad 2008); D98 (Dilkes 1998); DBC93 (de Braga & Carroll 1993); DBR96 (de Braga & Reisz 1996); DBR97 (de Braga & Rieppel 1997); E88 (Estes *et al.* 1988); Ev88 (Evans 1988); Ev90 (Evans 1990); G88a (Gauthier *et al.* 1988b); G88b (Gauthier *et al.* 1988a); G12 (Gauthier *et al.* 2012); GN98 (Gao & Norell 1998); GS96 (Gower & Sennikov 1996); J94 (Juul 1994); K03 (Kearney 2003b); LC00 (Lee & Caldwell 2000); LS02 (Lee & Scanlon 2002); Lee 93 (Lee 1993); Lee97 (Lee 1997b); Lee98 (Lee 1998); Lee01 (Lee 2001); Lo12 (Longrich *et al.* 2012); LR95 (Laurin & Reisz 1995); Ly13 (Lyson *et al.* 2013a); M80 (Moody 1980); Mo99 (Motani 1999b); MS04 (Modesto & Sues 2004); N11 (Nesbitt 2011); P86 (Pregill *et al.* 1986); PR88 (Presch 1988); R94 (Rieppel 1994b); R99 (Rieppel *et al.* 1999); RZ00 (Rieppel & Zaher 2000); RD03 (Reisz & Dilkes 2003); S09 (Smith 2009).

Cranium

Premaxillae

1. Premaxillae, fusion: unfused (0)/ fused (1) (B85, Ch. Y1).

2. Premaxillae, nasal process: present (0)/ absent (1) (B85, Ch. Y1).

Remarks: The nasal (or dorsal) process of the premaxilla occurs in most reptiles, contributing to the division of the external nares. It is absent in taxa such as kuehneosaurids, *Pamelina, Palaegama*, and rhynchosaurs. When the nasal process is absent, there is usually a single aperture of the external naris.

3. Premaxillae, posterodorsal process: absent (0)/ present (1) (Ev88, Ch. G1—modified).
Remarks: Posterodorsal process extending on top of the dorsal surface of the premaxillary process of the maxilla. It is observed in many diapsids, including sphenodontians, rhynchosaurs, *Euparkeria* and other archosauriforms.

4. Premaxillae, dentition: present (0)/ absent medially only (1)/ entirely absent (2) (DBR97, Ch. 3—modified).
Remarks: In some snakes (e.g. *Anilius*) and dolichosaurids (e.g. *Pontosaurus*) the premaxillary teeth are present, but they are absent medially (state "1"), thus splitting the dentigerous region of the premaxilla in two. However, other reptile groups lose their premaxillary dentition entirely, such as some snakes (e.g. *Cylindrophis* and scolecophidians), and most turtles.

5. Premaxillae, dentigerous beak: absent (0) / present (1) (NEW).
Remarks: A dentigerous beak is present in *Sphenodon* and other sphenodontians. It is formed by enlarged premaxillary teeth with secondarily grown bony tissue in between them (Carroll 1985b; Fraser 1988). In some sphenodontians, the secondary bone growth is extensive (e.g. *Kallimodon pulchellus*). This differs from the condition seen in rhynchosaurs, in which the premaxillae form a beak-like structure but the dentition is not an integral part of it, even when teeth are present on the premaxillae (as in *Mesosuchus browni*). Therefore, the ventral projection (beak-like structure) of rhynchosaurs is treated here as a non-primary homolog to the ventral projection observed in sphenodontians. When premaxillary teeth are absent, the present character must be treated as inapplicable.

6. Premaxillae, ventral bony beak: absent (0)/ present (1) (D98, Ch. 6 – modified). D*

Remarks: Beak-like structure in which the dentition is not an integral part of its composition, such as observed in rhynchosaurs (see further explanation above for character 5), captorhinids, proterosuchids, and later evolving thalattosaurs such as *Thalattosaurus* (Nicholls 1999).

7. Premaxillae, incisive process: absent (0)/ present (1) (Co08, Ch. 14—modified).

8. Premaxillae, ventral surface, premaxillary foramina: absent (0)/ present (1) (G12m Ch. 8—modified).
Remarks: The locator or part under consideration here are the openings for the exit of the terminal branches of the maxillary artery that pierces the premaxillae ventrally (Bahl 1937; Oelrich 1956).

9. Premaxillae, vomerine medial flange: absent (0)/ present (1) (Pr88, Ch. 40—modified).
Remarks: The vomerine medial flange is a process located on the ventral surface of the premaxilla, which is located posteriorly to the incisive process (when the latter is present), and extends in the direction of the vomers, occasionally contacting them.

Septomaxillae

10. Septomaxillae: present (0)/ absent (1) (D98, Ch. 14).

11. Septomaxillae, position: on narial margin (0)/ within nasal capsule (1) (G88a, Ch.3).
Remarks: In the vast majority of reptiles, the septomaxillae is within the nasal capsule. However, in a few reptiles the septomaxillae is on the surface of the snout. In *Captorhinus aguti*, for instance, each septomaxilla contacts the external surface of the maxilla, nasal and lacrimal.

12. Septomaxillae, shape, anteriorly: flat (0)/ convex dorsally (1)/ convex ventrally (2)/ laterally compressed (3) (E88, Ch. 41 – modified).
Remarks: When convex dorsally (e.g. *Xenopeltis*), the septomaxilla roofs the vomeronasal organ.

13. Septomaxillae, midline crest, dorsal projection: absent (0)/ present (1) (E88, Ch. 40; Fig. in G12, Ch. 205).
Remarks: A midline crest formed by both septomaxillae is observed within certain clades of squamates, including some scincids, teiids, amphisbaenians and scolecophidian snakes. This crest may extend ventrally to the point of contact between both septomaxillae (see G12, Fig. 202), or dorsally to where both septomaxilla meet. I scored only for the midline crest that forms a dorsal projection because it is considered herein that the ventral and dorsal projections are non-primary homologs, deserving to be coded as separate characters. In this character list, I coded only for the dorsal projection because it can be scored for numerous extant and fossil taxa without the aid of CT scan data.

Maxillae

14. Maxillae, contact, with premaxilla: syndesmotic (0)/ sutural (1) (Lee97, Ch. 7; Fig. in G12, Ch. 9).
Remarks: When there is a syndesmotic contact between the maxilla and the premaxilla, the maxilla has a premaxillary process that is convex and smoothly blunt surface anteriorly, such as observed mostly among snakes, but also in *Pontosaurus kornhuberi* and *Eichstaettisaurus schroederi*. This character is based on osteology, so I score state "0" based on the absence of sutural articulation between the maxilla and the premaxilla.

15. Maxilla-premaxilla fenestra, ventrally: absent (0)/ present (1) (G12, Ch. 5, Fig. Ch. 5 therein).
Remarks: This fenestra may occur on the ventral side of the skull in specimens in which it is not visible dorsally, such as when this fenestra is covered dorsally by the premaxillary process of the maxilla (e.g. some amphisbaenians). Therefore, this character has been scored based only on skulls in which the ventral side of the maxilla can be observed.

16. Maxillae, anterior superior alveolar foramen: absent (0)/ present (1) (LR95, Ch. 21).
Remarks: This foramen serves for the passage of the anterior superior alveolar nerve and the terminal branch of the maxillary artery in lizards (Oelrich 1956). A similarly located foramen for

the passage of the same soft tissues occurs in rhynchosaurs (Benton 1983) and turtles (Gaffney 1972). The maxillary anterior narial foramen of procolophonids and pareiasaurs (Laurin & Reisz 1995) lies in the same position, likely giving passage to the same nerve and artery. The location of the ASAF can be quite variable, such as on the external surface of the maxilla, the internal border of the external nares (as in many lepidosaurs), or well posteriorly on the internal surface of the maxilla (e.g. *Trilophosaurus*).

17. Maxillae, nasal process: absent (0)/ present (1) (LR95, Ch. 19).
Remarks: Diapsid reptiles almost invariably have a nasal (or facial) process of the maxilla, which establishes a contact with the nasals and isolates the lacrimals posteriorly from the external naris. This process is reduced in many snakes, dolichosaurids and mosasauroids.

18. Maxillae, posterior emargination, between nasal and orbital processes: absent (0)/ present (1) (NEW).
Remarks: The antorbital fenestra in archosauriform reptiles is characterized by an emargination of the maxilla posteriorly that is usually seen in conjunction with an anteriorly curved lacrimal—e.g. *Euparkeria, Proterosuchus, Erythrosuchus*, and most of the later evolving archosaurian lineages (Romer 1956; Ewer 1965; Witmer 1997; Gower 2003). The observed modifications in the maxillae and lacrimals, however, vary differently in each lineage. For instance, in the crocodylomorph *Pelagosaurus typus*, the maxilla emargination is regressed, but the lacrimal still curves forward (Witmer 1997), producing a reduced antorbital fenestra. In later evolving crocodylomorphs and many hadrosaurs, regression of both the maxillary emargination and lacrimal curvature reduces or entirely closes the antorbital fenestra. Finally, in some birds (*e.g. Aquila chrysaetos*) and in some other archosaurs, including *Lesothosaurus diagnosticus* and *Scleromochlus taylori* (Witmer 1997; Benton 1999) the fenestra is fully open due to the maxillary posterior emargination, but the lacrimal is not curved. These differences are illustrative of the many distinct morphological transformations leading up to superficially similar "absences" and "presences" of the antorbital fenestra. Nevertheless, upon a more detailed consideration of the morphological changes leading up to the development or loss of the antorbital fenestra, it is clear that these "absent" and "present" conditions fail the criteria of similarity. Different morphological changes in the history of archosauriforms have led to

multiple independent acquisitions and loss of the antorbital fenestra, and only detecting the individual changes in the anatomical parts composing the fenestra those changes can be appropriately assessed phylogenetically. Therefore, the maxillary emargination and lacrimal curvature are treated separately in here, allowing the detection of different "kinds" of antorbital fenestra that would, otherwise, be mistakenly coded as primary homologs. This approach follows the discussions on "complex characters" (Nesbitt 2011), or "composite locator coding" (Wilkinson 1995; Simões *et al.* 2017d) that affects most characters associated with skull fenestration.

19. Maxillae, antorbital fossa: absent (0)/ present (1) (G88a, Ch.32).

20. Maxillae, premaxillary process: present (0)/ absent (1) (NEW).
Remarks: the premaxillary process of the maxilla projects medially from the anterior margin of the maxilla and ventrally to the external naris, and it is seen in most squamates and other lepidosaurs.

21. Maxillae, premaxillary process, groove, on dorsal surface: absent (0)/ present (1) (S09, Ch. 7; Fig. in G12, Ch. 112).
Remarks: A groove for the passage of the internal ramus of the subnarial artery (Gauthier *et al.* 2012) is observed in some squamates, most specially among iguanians, and it occurs on the premaxillary process of the maxilla.

Nasals

22. Nasals, fusion: paired (0)/ fused (1) (P86, Ch. 1).

23. Nasals, ventrolateral process: absent (0)/ present (1) (G12, Ch. 22, Fig. Ch. 22 therein).

24. Nasals, ventrolateral process, position, relative to maxillary nasal process: posteriorly (0)/ anteriorly (1)/ dorsally (2) (NEW).

Remarks: When a ventrolateral process of the nasal occurs in reptiles it is almost always in contact with the nasal process of the maxilla (especially among diapsids). Exceptions occur in a few instances in which the nasal process of the maxilla is absent in diapsids (e.g. some dolichosaurids and snakes, among squamates), and among non-diapsid forms (e.g. captorhinids). When a ventrolateral process of the nasals is present, but the maxillary nasal process is absent, this character is inapplicable. However, the conservative relationship of the contact between nasals and maxilla in the vast majority of diapsids allows the position of the ventrolateral process of the nasal relative to the maxillary nasal process to be comparable across a broad range of reptiles.

25. Nasals, foramina: absent (0)/ present (1) (NEW).

26. Nasals, ventromedial crest: absent (0)/ present (1) (G12, Ch. 21, Fig. Ch. 21 therein).
Remarks: Present as a small crest in taxa such as in *Xantusia vigilis* and *Elgaria multicarinata*, becoming much deeper in amphisbaenians and dividing the olfactory tract anteriorly. In some snakes (e.g. scolecophidians), a deep single medial pillar is present as a result of the fusion of the nasals (and their medial crests).

Lacrimals

27. Lacrimals: present (0)/ absent (1) (E88, Ch. 28)

28. Lacrimals, position, relative to prefrontal lateral margin: ventral (0)/ anterior (1)/ posterior (2) (B85, Ch. B1).
Remarks: In most reptiles, the prefrontals extend ventrally contacting the palatines and the medial margin of the maxilla, but the lateral margin of the prefrontals remains restricted dorsally to the lacrimals not contacting the maxilla in lateral view. In *Kuehneosaurus* and *Icarosaurus*, however, the lateral margin of the prefrontal extends ventrally contacting the maxilla, and the lacrimal is positioned anterior to this extension. The conservative relationship of contact between the lacrimals and prefrontals across a wide range of reptiles and sampled taxa herein justifies the codification of the position of the lacrimal using the prefrontal as a referential landmark.

The lacrimals are not visible in many rhynchocephalians, being detectable externally only in *Gephyrosaurus* (Evans 1980). Additionally, there is no sign of fusion between the lacrimal and the prefrontal during ontogeny nor phylogeny (Howes & Swinnerton 1901; Whiteside 1986), thus current evidence indicates the element is lost in sphenodontians. Wu *et al.* (1996) considered the position of the lacrimal duct (posteriorly or laterally on the skull) as a proxy to evaluate whether the lacrimal bone was present, but fused to the prefrontal (when the lacrimal duct was facing posteriorly), or if it is absent altogether (when the lacrimal duct facing laterally). However, this conflicts with the observational and literature evidence gathered herein regarding the fusion of the lacrimal to the prefrontal. Additionally, even if fusion indeed occurs in some specimens, expanding the assumption of fusion to all sphenodontians in a dataset would be a major overreach in taxon scoring practise. Therefore, I keep the absence/presence of the lacrimal as a separate character in relation to the position of the lacrimal duct.

29. Lacrimal duct, foramen, division: single (0)/ double (1) (P86, Ch. 22—modified).
Remarks: The lacrimal duct can be single, or divided in two, passing through two distinct foramina, such as in *Varanus* (Bellairs 1949) and in some rhynchosaurs.

30. Lacrimal duct, posterior opening on skull surface, position: posteriorly (0)/ laterally (1) (RD03, Ch. 19 - modified).
Remarks: When the lacrimal duct passes to the snout region through an opening that lies between the prefrontal and the maxilla, the lacrimal foramen is located laterally on the skull.

31. Lacrimals, shape, curved anteriorly: absent (0)/ present (1) (NEW).
Remarks: See above (character 18). This anterior curvature usually occurs in taxa with an antorbital fenestra, in which the lacrimal has a "Γ" shape in lateral view.

Prefrontals

32. Prefrontals, ornamentation on external surface: absent (0)/ rugosities (1)/ tubercles (2)/ pits (3) (L98, Ch. 17 - modified).

Remarks: The different types of ornamentation are seen as distinct from each other as they are from absence of ornamentation (not hierarchically nested and being mutually exclusive). Therefore, these conditions are all included as part of the same character instead of being split into contingent characters.

33. Prefrontal crest: absent (0)/ present (1) (G12, Ch. 130, Fig. Ch. 130 therein).
Remarks: Thickening of the dorsal margin of the prefrontal, just above the anterodorsal margin of the orbit, forming a crest.

Supraorbital (palpebral) bones

34. Supraorbital bones: absent (0)/ present (1) (E88, Ch. 36).

Jugals

35. Jugals: present (0)/ absent (1) (Lee98, Ch. 12).

36. Jugals, posteroventral process: absent (0)/ present (1) (Ev88, Ch. O5).
Remarks: Most diapsids have a posteroventral process of the jugal forming a lower temporal bar that delimits the lower temporal fenestra. In most squamates, however, a posteroventral process of the jugal is entirely absent, and the jugal smoothly curves posterodorsally. The development of the posteroventral process of the jugal and a complete lower temporal bar seem to be evolutionary constrained in squamates, but has been -de-canalized and evolved at least twice independently in borioteiioids (Simões *et al.* 2016). The length of the posteroventral process of the jugal exhibits ontogenetic variation in stem rhynchocephalians, sometimes forming a complete lower temporal bar in old individuals of some taxa, such as: *Planocephalosaurus*, *Clevosaurus*, and *Diphyodontosaurus* (Fraser 1982; Whiteside 1986; Fraser 1988). Ontogenetic variation in this feature was also present in *Polyglyphanodon sternbergi*, a squamate from the Late Cretaceous of North America (Simões *et al.* 2016). Among early reptiles a similar ontogenetic variation also seems to be present, such as in the development of a third posterior process that forms the tetraradiate jugal of the parareptile *Delorhynchus* (Haridy *et al.* 2016).

Due to intraindividual variation and the continuous nature of this feature, I do not consider the presence or absence of a complete lower temporal bar as a valid discrete character. Therefore, only the overall presence or absence of the jugal posteroventral process is considered.

37. Jugals, posteroventral process, shape: separate from dorsal process (0)/ connected to dorsal process by bony flange (1) (NEW). D*
Remarks: In early reptiles, such as *Protorothyris archeri* and *Protocaptorhinus pricei*, the jugal bears a posterior process contacting the quadratojugal that is connected via a bony flange to the dorsal (= orbital) process of the jugal (which, in turn, contacts the postorbital bone). In many diapsids, the jugal has a posteroventral process that is separated from the dorsal process (lacking a bony flange connection), acquiring a forked aspect posteriorly.

Quadratojugals

38. Quadratojugals: present (0)/ absent (1)/ (G88b, Ch. 12).

39. Quadratojugals, anterior extension: present (0)/ absent (1) (G88b, Ch. 9). D*
Remarks: In lepidosaurs, when the quadratojugal is present, the main body of the quadratojugal contacts the quadrate, but its anterior extension (such as the one observed in many archosauriforms) is absent.

40. Quadratojugals, ventral margin, medially inflected flange: absent (0)/ present (1) (NEW).
Remarks: In choristoderes, the quadratojugal has a medially inflected flange that is visible on the ventral side of the skull.

41. Quadratojugals, ornamentation, on external surface: absent (0)/ pits (1)/ rugosities (2)/ striations (3)/ tubercles (4) (DBR97, Ch. 43 - modified). D*
Remarks: The different types of ornamentation are seen as distinct from each other as they are from absence of ornamentation (not hierarchically nested and being mutually exclusive). Therefore, these conditions are all included as part of the same character instead of being split into contingent characters.

42. Quadratojugal foramen: absent (0)/ present (1) (Re-conceptualized).
Remarks: The quadratojugal foramen of many reptiles is a space in between the quadrate and the quadratojugal through which the mandibular and internal mandibular veins pass, such as in *Sphenodon* (O'Donoghue 1920, plate 7, fig. 2). In some previous publications (e.g., Gauthier *et al.* 1988a) this opening was homologized to the quadrate foramen of squamates. However, in extant squamates (where a quadratojugal is absent), the quadrate foramen carries the anterior tympanic vein, and a branch of the posterior condylar artery (Oelrich 1956). Furthermore, the quadratojugal foramen and the quadrate foramen may occur in conjunction, such as observed in *Sphenodon punctatus* (MCZ R4702, TRS pers. obs.). These observations preclude the treatment of both structures as homologs, and they are treated as separate characters in the present dataset.

Postorbitals

43. Postorbitals: present (0)/ absent (1) (G88a, Ch. 12).

44. Postorbitals, fusion to postfrontal: unfused (0)/ fused (1) (E88, Ch. 14).
Remarks: The postfrontal is fused to the postorbital in some lizards, such as in some teiids (although this can vary intraspecifically), some scincids, *Xantusia*, some anguimorphs, and mosasauroids. The fusion between both elements is also observed in other diapsids, such as within turtles and thalattosaurs.

45. Postorbitals, dorsal margin, position relative to postfrontal: laterally (0)/ posteriorly (1)/ anteriorly (2) (NEW).
Remarks: The contact between the postorbital and the postfrontal occurs in most, if not all, reptiles [including snakes in which both elements are present—see Palci & Caldwell (2013) for a recent review on the topic]. Therefore, the conservative relationship of the contact between the postorbital and postfrontal across a wide range of clades and sampled taxa allows the codification of the position of the postorbital using the postfrontal as a referential landmark. In most reptiles, the postorbital contacts the postfrontal posteriorly. However, in some instances the postorbital is positioned anteriorly to the postfrontal (e.g. *Eichstaettisaurus schroederi*), or

laterally to the lateral margin of the postfrontal (e.g. *Sphenodon punctatus*, and borioteiioid squamates).

46. Postorbitals, dorsal process: absent (0)/ present (1) (NEW).

Remarks: The main body of the postorbital contacts the squamosal posteriorly in most reptiles by means of a posterior process. I use this conservative landmark as a reference point to detect if a distinct dorsal process (usually contacting the postfrontal) is absent or present. This character is inapplicable when the postorbital is completely fused with the postfrontal, as its dorsal process is undistinguishable from the distal process of the postfrontal. In non-diapsids, as well as a few modified diapsids with a reduced upper temporal fenestra, a distinct dorsal process is absent. In most diapsids this process contributes to the formation of the upper temporal fenestra. However, in most ichthyosaurs and hupehsuchids this process is absent, and the upper temporal fenestra is bordered anteriorly by an elongate distal (or postorbital) process of the postfrontal. In some instances, where the parietals acquire a lateral extension (see more details below), the upper temporal fenestra becomes reduced or entirely closed despite the presence of the dorsal process of the postorbital, such as in the saurosphargid *Sinosaurophargis yunguiensis* (and also in cordyloid squamates). The present character, as well as others linked to the bones that frame the temporal fenestrae (see below), is useful to identify subsequent non-homologous modifications in the structure of temporal fenestration in reptiles. See also discussion for character 18, above, and (Simões *et al.* 2017d).

47. Postorbitals, ventral process: absent (0)/ present (1) (NEW).

Remarks: Using the contact between the main body of the postorbital with the squamosal as a reference landmark (see above), a distinct ventral process of the postorbital (usually contacting the jugal) can be distinguished in most diapsids. This process is defined as a process extending ventrally towards the jugal (usually contacting it when the latter is present), and distinct from the posterior contact of the postorbital with the squamosal This process contributes to the formation of a lower temporal fenestra of most reptiles when the latter is present, but not in most choristoderes, such as *Phylidrosaurus* and *Champsosaurus*. This character is useful to distinguish between the different kinds of lower temporal fenestration in reptiles, and to track putative independent developments of that structure in phylogenetic reconstructions. In some

squamates, such as *Globaura venusta*, this process becomes highly reduced, but it is still present ventral to the jugal. In taxa with fused postorbitals and postfrontals, the process is still distinct projecting towards the jugal anteroventrally, as in *Aigialosaurus dalmaticus* and *Pontosaurus kornhuberi*. In xenosaurids, this process is reduced and projects anteriorly.

48. Postorbitals, dorsal concavity: absent (0)/ present (1) (AN03, Ch. 13).
Remarks: Observed within sphenodontians.

Squamosals

49. Squamosals: present (0)/ absent (1) (E88, Ch. 33)
Remarks: Absent in snakes, most amphisbaenians, *Dibamus*, *Anniella* and some geckoes (Estes *et al.* 1988).

50. Squamosals, anteroventral process: absent (0)/ present (1) (Ev88, Ch. L4 - modified).
Remarks: The squamosal of diapsids can be tetraradiate in many early diapsids and rhynchocephalians (Benton 1985). One of the processes creating the tetraradiate condition is the anteroventrally directed process, which braces the quadrate (and the quadratojugal, when present) anteriorly, as seen in most rhynchocephalians.

51. Squamosals, posterior process: absent (0)/ present (1) (NEW).
Remarks: The posterior process is distinct from the main body of the squamosal that contacts the postorbital bone, and it usually extends posteroventrally to contact the quadrate. It inserts into a squamosal notch on the cephalic condyle of the quadrate in most squamates, or it covers the quadrate in lateral aspect as in saurosphargids. Many rhynchocephalians (e.g. *Gephyrosaurus, Homeosaurus,* and *Palaeopleurosaurus*) have a posterior process that, along with the anterovetral process, make the ventral margin of the squamosal to become U-shaped, into which the quadrate-quadratojugal complex attach to in lateral view.

52. Squamosals, dorsal process: absent (0)/ present (1) (E88, Ch. 34 - modified).

Remarks: Occurs in a variety of diapsid reptiles, but is absent in many squamates (although present in stem squamates, many iguanians, teiioids, borioteiioids and mosasauroids).

53. Squamosals, occipital flange: present (0)/ absent (1) (LR95, Ch. 27).
Remarks: The absence of the occipital flange exposes the quadrate laterally and posterolaterally in many reptiles (e.g. *Claudiosaurus* compared to *Youngina*). The lateral exposure of the quadrate is thus biologically dependent on the absence or presence of the occipital flange, and it this feature is not treated separately from the present character.

54. Squamosals, ventral margin, medial inflection: absent (0)/ present (1) (NEW).
Remarks: The squamosal in choristoderes has a medial flange that forms the internal aspect of the posterolateral margin of the upper temporal fenestra. Within the upper temporal fenestra, this flange also projects medially, forming a temporal terrace.

55. Squamosals, anterior margin, bifid facet for postorbital: absent (0)/ present (1) (NEW).
Remarks: This facet occurs on the region where the squamosal articulates with the postorbital, and it is observed in rhynchocephalians, as well as in many protorosaurians and rhynchosaurs (e.g. *Mesosuchus* and *Howesia*).

Postfrontals

56. Postfrontals: present (0)/ absent (1) (B85, Ch. Y2—modified).

57. Postfrontals, distal process: present (0)/ absent (1) (NEW).

58. Postfrontals, distal process, division: single (0)/ double (1) (G12, Ch. 64).

59. Postfrontals, medial margin, position, relative to parietal: ventral (0)/ dorsal (1)/ lateral (2)/ anterior (3) (G12, Ch. 65 – modified).

Remarks: The conservative relationship of contact between the parietal and postfrontal across a wide range of clades and sampled taxa justifies the codification of the position of the postfrontal using the parietal as a referential landmark.

60. Postfrontals, parietal process: absent (0)/ present (1) (E88, Ch. 13—modified).
Remarks: When the postfrontal parietal process is absent, the postfrontal acquires a lunate-like appearance, such as in kuehneosaurids, protorosaurs, *Prolacerta. Palaegama, Pamelina*, and iguanians.

61. Postfrontals, medial forking: absent (0)/ present (1) (E88, Ch. 13).
Remarks: When the parietal process of the postfrontal is absent (character 60), the present character is inapplicable.

Supratemporals

62. Supratemporals: absent (0)/ present (1) (B85, Ch. J3).

63. Supratemporals, temporal process: absent (0)/ present (1) (NEW).
Remarks: A temporal process of the supratemporal, extending laterally on the temporal region, is observed in most ichthyosaurs.

Tabulars

64. Tabulars: present (0)/ absent (1) (B85, Ch. C4).

Postparietals

65. Postparietals: present (0)/ absent (1) (G88b, Ch. 5). D*

66. Postparietals, number: single (0)/ paired (1) (Ev88, Ch. D3).

Frontals

67. Frontals, fusion to each other: unfused (0)/ fused (1) (B85, Ch. Y1).

68. Frontals, parietal tabs: absent (0)/ present (1) (E88, Ch. 10).
Remarks: Among some early diapsids and rhynchocephalians, each frontal possesses a process overlying the parietal laterally.

69. Frontals, subolfactory processes: absent (0)/ present (1) (G12, Ch. 38—modified, Fig. Ch. 38 therein).

70. Frontals, subolfactory processes, fusion to each other: absent (0)/ present (1) (P86, Ch. 7 – modified).

71. Frontals, orbitonasal projection: absent (0)/ present (1) (NEW).
Remarks: This projection is absent in most reptiles and iguanian squamates, but it occurs among most other squamates. These constitute anterior projections of the frontals that border the orbitonasal fenestra laterally and adjacent to the main body of the prefrontal medially. This structure is not part of the transformation series related to the ventral expansion of the subolfactory process, because some taxa (e.g. *Coleonyx*) have strongly developed suborbital processes (forming a tube), but lack the orbitonasal projection. Furthermore, among taxa with weakly developed subolfactory processes, there are species with (*Lacerta viridis*) and without (*Sphenodon punctatus*) orbitonasal projections. Such variation indicates the subolfactory process and the orbitonasal projection are better treated as separate characters.

Parietals

72. Parietals, fusion: unfused (0)/ fused (1) (B85, Ch. Y1).

73. Pineal foramen: present (0)/ absent (1) (B85, Ch. K2).

74. Parietals, supratemporal process: absent (0)/ present (1) (LC00, Ch. 46—modified).

75. Parietals, supratemporal process, distal end, division: single (0)/ bifid (1) (NEW).
Remarks: Early reptiles have the supratemporal process of the parietal bifid distally to receive the supratemporal, such as in *Hovasaurus* and *Araeoscelis.*

76. Parietals, ornamentation: absent (0)/ rugosities (1)/ tubercles (2)/ pits (3) (LR95, Ch. 38—modified).
Remarks: It is rather difficult to determine if the sculpturing in all dermal ossifications are primarily homologous or not. Nevertheless, because the parietal is usually one of the most common bones to present sculpturing, the parietal sculpturing is used here as a character to represent skull roof ornamentation. A single bone (parietal) is chosen for this character to make sure the skull roof ornamentations are comparable across taxa. The different types of ornamentation are seen as distinct from each other as they are from absence of ornamentation (not hierarchically nested and being mutually exclusive). Therefore, these conditions are all included as part of the same character instead of being split into contingent characters.

77. Parietals, lateral frill: absent (0)/ present (1) (NEW).
Remarks: In weigeltisaurids, the parietals possess laterally projecting frills (depressed spikes). This condition is seen in *Coelurosauravus* [(Evans 1982; Evans & Haubold 1987) and TRS pers. obs.], and also in *Rautiana* (Bulanov & Sennikov 2006), but are somewhat reduced in *Glaurung* (Bulanov & Sennikov 2015a) .

78. Parietals, frontal tabs of parietal: absent (0)/ present (1) (E88, Ch. 22).
Remarks: Parietal projection inserting ventrally on the frontals of some lepidosaurs, such as *Marmoretta, Gephyrosaurus, Planocephalosaurus*, and also within squamates (Lee 1998).

79. Parietals, nuchal fossa: absent (0)/ present (1) (G12, Ch. 94—modified, Fig. Ch. 94 therein).
Remarks: The parietal nuchal fossa is a thin bony plate projecting posteriorly from the parietal posterior margin, and which is distinct from the main body of the parietal.

80. Parietals, nuchal fossa, roofing by parietal posterior flange: unroofed (0)/ roofed (1) (CoN06, Ch. 47; Fig. in G12, Ch. 94(1 and 2)).
Remarks: When present, the nuchal fossa may be covered by a posterior growth of the parietal main table (the parietal flange), as seen in *Gekko gecko* for instance.

81. Parietals, ventral side, parietal fossa: present (0)/ absent (1) (CoN06, Ch. 46; Fig. 33 in Co08).

82. Parietals, ventral side, parietal fossa, posterior margin: open (crests extend posterolaterally) (0)/ closed (crests meet at midline) (1) (CoN06, Ch. 46—modified).

83. Parietals, posteromedial (= postparietal) process: absent (0)/ present (1) (G12, Ch. 95, Fig. Ch. 95 therein).

84. Parietals, posteromedial (= postparietal) process, division: single (0)/ bifid (1) (G12, Ch. 97-modified, Fig. Ch. 97 therein).

85. Parietals, parietal table, shape: margins ventrally directed, sagittal crest present (0)/ margins ventrally directed, without sagittal crest (1)/ margins laterally directed (2) (Lee98, Ch. 35 and G88a, Ch.19).
Remarks: Many reptiles, including numerous squamates, have ventrally directed lateral margins of the parietal(s), to which the epipterygoid attaches to. In such instances, some adductor muscles (*M. adductor mandibulae externus medialis* and the *M. adductor mandibulae internus pseudotemporalis superficialis* in squamates) attach to the dorsal side of the parietal. In many rhynchocephalians, among other reptilian groups, this condition is further developed by the formation of a sagittal crest dorsally on the parietal. The sagittal crest only occurs in ventrally directed lateral margins, and due to this conservative relationship among the studied taxa, the sagittal crest is considered herein to be part of the transformation series of the parietal table shape and not an independent variable. In other reptiles, the lateral margin of the parietal extends laterally, partially closing the supratemporal fossa (e.g. *Cordylus*). In the latter case, the

epipterygoid attaches to the crista cranii parietalis [or ventrolateral crest of Evans (2008)] on the ventral side of the parietal (e.g. *Xantusia*) and the aforementioned adductor muscles also attach to the ventral side of the parietal. This suggests that the origin of the temporal muscles [character #54 of Estes *et al.* (1988)] and the orientation of the parietal(s) lateral margins are dependent features—the adductors cannot attach dorsally when the supratemporal fenestra is reduced or closed. Because the actual site of attachment of the adductors cannot be always determined for most fossil taxa, this transformation series is scored based on the orientation of the lateral margin of the parietal.

86. Parietals, dorsal surface, parasagittal crests: absent (0)/ present (1) (NEW).
Remarks: In some reptiles, parasagittal crests occur on the lateral margins of the parietal(s), such as in choristoderes and *Placodus*. The development of these crests might reflect a greater development of the adductor musculature rather than the position of the adductor musculature and the overall shape of the parietal lateral margins (accounted for in the previous character).

87. Parietals, crista cranii parietalis, epipterygoid process: absent (0)/ present (1) (E88, Ch. 23 – modified; Fig. in G12, Ch. 108).

Palate

Vomers

88. Vomers, fusion: unfused (0)/ fused (1) (G88a, Ch.43 – modified).

89. Vomers, teeth: absent (0)/ present (1) (G88a, Ch. 120).

90. Vomers, anterior premaxillary process: absent (0)/ present (1) (NEW).
Remarks: When present, the vomerine premaxillary process partially divides the incisive foramen between the vomer and the premaxilla.

91. Vomers, lateral expansion: absent (0)/ present (1) (Ev90, Ch. 8; Fig. in G12, Ch. 214).
Remarks: When present, the lateral processes may contribute to a neochoanate condition separating the vomeronasal fenestra from the fenestra exochoanalis.

92. Vomers, ventral surface, midline crest (=longitudinal ridge): absent (0)/ present (1) (G12, Ch. 222 – modified; Fig. in Ch. 222 therein).
Remarks: Among squamates, this is observed in some teiids, for instance. These crests lie adjacent and butt against each other on the midline, sometimes diverging anteriorly.

93. Vomers, ventral surface, lateral crest (=longitudinal ridge): absent (0)/ present (1) (G12, Ch. 222 – modified; Fig. in Ch. 222 therein).
Remarks: Observed in many squamates, this crest is generally observed on the anterior half of the vomers. They are parallel and curve inwards anteriorly, occasionally touching each other. Both a lateral and medial crest are observed in *Varanus*, and due to the criterion of conjunction they are treated as separate characters.

94. Vomers, ventral foramina, in each vomerine element: present (0)/ absent (1) (G12, Ch. 229—modified, Fig. in Ch. 229 therein).

95. Vomers, shape in cross-section: flat (0)/ convex ventrally (1) (NEW).

96. Vomers, posteroventral process (=descending tubercle): absent (0)/ present (1) (G12, Ch. 228—modified, Fig. in Ch. 228 therein).
Remarks: A posteroventrally directed process from the vomer that overlaps with the anterior margin of the palatine, as observed in *Acontias plumbeus* and other scincids, anguids, pygopodids, *Xantusia vigilis*, among others.

Palatines

97. Palatines, teeth: absent (0)/ present (1) (E88, Ch. 82).

98. Palatines, ascending process: absent (0)/ present (1) (G88a, Ch. 45).

99. Palatines, dorsomedially directed process: absent (0)/ present (1) (Lee97, Ch. 59).

100. Palatines, ventral surface, sulcus choanalis: absent (0)/ present (1) (G88b, Ch. 60 – modified).

101. Palatines, infraorbital foramen: present (0)/ absent (1) (NEW).

102. Palatine foramen: absent (0)/ present (1) (G12, Ch. 246, Fig. in Ch. 246 therein).
Remarks: Present dorsomedially to the infraorbital foramen, occurring in most iguanins.

103. Palatines, maxillary process, ventral aspect: absent (0)/ present (1) (G12, Ch. 239, Fig. in Ch. 239 therein).

104. Palatines, subchoanal shelf: absent (0)/ present (1) (G12, Ch. 251—modified, Fig. in Ch. 251 therein).

Pterygoids

105. Pterygoids, teeth: absent (0)/ present (1) (E88, Ch. 83).

106. Pterygoids, anteromedial processes, anterior end division: single (0)/ bifurcate (1) (Wu96, Ch. 93—modified).
Remarks: Present in some squamates (e.g. borioteiioids, *Varanus*). Wu *et al.* (1996) originally designated this character as another process of the pterygoid (a lateral process of the palatine ramus). However, no difference is observed between the condition described by the authors and the anterior bifurcation of the palatine ramus as proposed by Gao & Norell (1998).

107. Pterygoids, transverse processes: absent (0)/ present (1) (NEW).

108. Pterygoids, transverse processes, flange: absent (0)/ present (1) (G12, Ch. 266, Fig. in Ch. 266 therein).
Remarks: The acquisition of the pterygoid flange on its transverse process has been considered as one of the distinguishing feature of reptiles (Carroll 1969b).

109. Pterygoids, transverse process, teeth: absent (0)/ present (1) (G88a, Ch. 123).

110. Pterygoids, main body, concave in ventral aspect: absent (0)/ present (1) (NEW).
Remarks: The main body is considered the portion of the pterygoid from which the transverse process and the anteromedial process originate. This area is usually flat in reptiles, but in many squamates this area is concave in ventral view and it is bordered by the lateral margins of the pterygoid.

111. Pterygoids, arcuate flange: absent (0)/ present (1) (LR95, Ch. 42).
Remarks: A large number of reptiles, such as captorhinids, early turtles, early diapsids, rhynchosaurs, and some sphenodontians developed a posteromedially directed flange at the level of the transverse process of the pterygoid, and close to the point of contact with the basipterygoid process of the basisphenoid.

112. Pterygoids, quadrate rami, posterolateral excavation: absent (0)/ present (1) (DBR96, Ch. 29).

Ectopterygoids

113. Ectopterygoids: absent (0)/ present (1) (G88a, Ch. 55).

114. Ectopterygoids, lateral process: absent (0)/ present (1) (G12, Ch. 283—modified, Fig. in Ch. 283 therein).

Palatoquadrate

Epipterygoid (= alisphenoid): processus ascedens of the palatoquadrate that gives origin to the ala temporalis. This process ossifies endochondrally into the epipterygoid bone in lepidosaurs and turtles and the alisphenoid bone in mammals (Gauthier et al. 1988b).

115. Epipterygoid: present (0)/ absent (1) (E88, Ch. 47).
Remarks: The epipterygoid is absent in most snakes, amphisbaenians [except *Blanus* (Montero & Gans 2008) and *Trogonophis* (Kearney 2003b)], and also absent *Dibamus*, but present in *Anelytropsis* (Rieppel 1984a; Greer 1985b).

116. Epipterygoid, base shape: base flared out (0)/ base columnar (1) (G88b, Ch. 28; Fig. in G12, Ch. 295).
Remarks: Most reptiles have a flared base of the epipterygoid attaching to the pterygoid dorsally. However, most squamates that bear an epipterygoid have a straight shaft of the latter element without any flaring or widening of its base, thus having a continuous width throughout its entire extension. Although some variation may exist on the degrees of width of the flared bases of the epipterygoid in non-squamatan reptiles, here I assess only the qualitative difference on the absence or presence of this structure.

Quadrates

117. Quadrates, articulating surface: flat (0)/ with condyles (1) (LR95, Ch. 65—modified).

118. Quadrate foramen: present (0)/ absent (1) (G88b, Ch. 21).
Remarks: The quadrate foramen is considered to be solely the small foramen piercing the quadrate bone itself, usually near the base of the quadrate posterior pillar. This is not to be confounded with the opening between the quadrate and the quadratojugal—see also character 42 (quadratojugal foramen).

119. Quadrates, pterygoid process: present (0)/ absent (1) (G88b, Ch. 27—modified).

120. Quadrates, posterior emargination: absent (0)/ present (1) (B85, Ch. B6).

121. Quadrates, quadrate conch: absent (0)/ present (1) (B85, Ch. Y11).
Remarks: The tympanic membrane attachment to the quadratojugal (or the quadrate when the quadratojugal is lost) creates a reinforced attachment site (the tympanic crest) that always occurs in conjunction with thinner and medially projecting bony flange that forms by the quadrate conch. Therefore, the absence/presence of a quadrate conch, and the absence/presence of a tympanic crest are dependent characters among the studied taxa herein, and the quadrate conch is scored in this dataset to avoid redundancy. Another important consideration is that the tympanic crest of most squamates is positioned on the lateral margin of the quadrate, whereas in most rhynchocephalians this crest actually belongs to the fused quadratojugal. This topological difference seems to be a consequence of the loss of the quadratojugal in squamates, transferring the attachment site of the tympanum from the qudratojugal to the quadrate. Therefore, this topological difference on the composition of the tympanic crest is dependent upon the loss of the quadratojugal itself (already considered under character 38), and thus, it is not a separate and independent character. Accordingly, I do not treat the composition of the tympanic crest as a distinct character herein to avoid redundancy.

122. Quadrates, suprastapedial process: absent (0)/ present (1) (DBC93, Ch. 40).
Remarks: A posteroventral extension of the cephalic condyle of the quadrate, which is most commonly present in mosasauroids and dolichosaurids, but also occurs in some teiids (e.g. *Dracaena*) and some early snakes (*Dinilysia patagonica*). This process is only considered to be present if it is ventrally directed. This ventral deflection of the expanded cephalic condyle provides a better assessment on the absent/present state of the suprastapedial process than a more subjective assessment of the degree of expansion of the cephalic condyle. The vast majority of mosasauroids and other lizards that are considered to possess a suprastapedial process have this ventral deflection of the process [e.g. Bell (1997), fig. 7].

123. Quadrates, cephalic condyle, notch for the squamosal: absent (0)/ present (1) (Ev88, Ch. L9 – modified).

Braincase

The fusion of braincase elements is especially important in the evolution of many groups of squamates that have special adaptations for burrowing, such as amphisbaenians and burrowing snakes. Despite the fact many distinct groups of squamates present "braincase fusion", burrowing squamates show great variation in their degrees and particular modes of braincase fusion. Individual braincase components are fused differently across these taxa, and assessing these differences should provide a better indication of their phylogenetic histories than an overall assessment of "braincase fusion". For instance, the fusion of the basioccipital to the basisphenoid occurs in some taxa (e.g. *Bipes, Blanus,* and *Priscagama*) regardless of the fusion of the basioccipital to other elements, such as the exoccipitals. Also, fusion of the basioccipital to the exoccipitals (but not to the basisphenoid) occurs in xantusiids. The opposite is also true, as some taxa (e.g. *Slavoia darevskii*) have fused the basioccipital to the basisphenoid, but there is no detectable fusion to the exoccipitals. Therefore, fusion of distinct braincase elements are coded under separate characters. It is expected that this more detailed analysis of braincase fusion may provide better ways to detect homoplasies in this set of processes that are so widely distributed among squamates and that may affect inferences of their phylogenetic relationships.

Nerves and vessels

124. Carotid foramina, entrance in braincase, position: lateral wall of braincase (0)/ ventral surface of braincase (1) (D98, Ch. 45).
Remarks: The entrance of the canal or groove for the internal carotid artery in the braincase can be either laterally, as in *Captorhinus aguti* and squamates, or ventrally, as in *Gephyrosaurus* and *Mesosuchus*.

Supraoccipital

125. Supraoccipital, lateral ascending processes: absent (0)/ present (1) (NEW).

Remarks: This character refers to dorsolateral processes on the supraoocipital that extend onto the dorsal surface of the braincase. In early reptiles, this process may be enlarged and partially cover the post-temporal fenestra, such as in captorhinids. I use this character to replace Gauthier *et al.* (1988b) character on the closure of the post-temporal fenestra, since that character did not make specific reference to an anatomical part that could be referenced as the homolog under consideration. Also, the presence of this processs does not necessarily close the post-temporal fenestra.

126. Supraoccipital, medial ascending process: absent (0)/ present (1) (RZ00, Ch. 232; Fig. in G12, Ch. 297).
Remarks: Usually referred to as the processus ascendens of the synotic tectum in squamates (Oelrich 1956), this character reflects the ossification of this medially placed and dorsally ascending process that, in many squamates, contacts the parietal ventrally.

127. Supraoccipital, fusion to exoccipitals: unfused (0)/ fused (1) (NEW).
Remarks: The fusion between the supraoccipital to the adjacent exoccipitals may occur later during the ontogeny (e.g. *Coleonyx variegatus*). In such cases, the medial contact between the exoccipitals (see below) can be determined from individuals that still have partially separate supraoccipital and exoccipitals. The fusion of the supraoccipitals to the exoccipitals (or otoccipitals) may vary during post-embryonic ontogeny in many squamates (Maisano 2002), which may also occur in other reptiles, and thus only adults specimens are scored for his character.

128. Supraoccipital, sagittal crest: absent (0)/ present (1) (LR95, Ch. 55).

129. Supraoccipital, lateral nuchal crest: absent (0)/ present (1) (G12, Ch. 300, Fig. in Ch. 300 therein).
Remarks: Posteroventrally directed crests that are more commonly observed in snakes. In *Hoplodactylus* and other squamates with diminutive size and reduced degree of ossification of the skull, the posterior semi-circular canals pathways become visible externally, and thus form a

"crest" on the supraoccipital (Simões *et al.* 2017b). This feature might also be the case of other small-sized reptiles. This is not homologous to the external crests referred to in this character.

Basioccipital

130. Basioccipital/basisphenoid, sphenoid tubercles: absent (0)/ present (1) (LR95, Ch. 63).
Remarks: In amphisbaenians, despite the presence of the sphenooccipital epiphyses (element "X") in many species, a distinct sphenoid tubercle is commonly absent. Considering the sphenooccipital epiphyses may occur in taxa with (e.g. *Uromastyx*) or without (amphisbaenians) sphenoid tubercles, I treat both atributes under separate characters.

131. Sphenooccipital epiphyses: absent (0)/ present (1) (K03, Ch. 102; Fig. in G12, Ch. 340).
Remarks: The "element X" of amphisbaenians has been widely regarded to represent the sphenooccipital epiphyses observed in many other squamates (e.g. *Uromastyx* and *Oplurus*, *Heloderma, Elgaria, Xenosaurus* and *Scincus*) [(Rieppel 1981; Montero *et al.* 1999; Kearney 2003b) and TRS personal observation].

132. Basioccipital, fusion, to exoccipital: unfused (0)/ fused (1) (NEW).
Remarks: See comments and examples above in the introduction of the "Braincase" section. The fusion of the basioccipital to the exoccipitals (or otoccipitals) may vary during post-embryonic ontogeny in many squamates (Maisano 2002), which may also occur in other reptiles. Therefore, only adults specimens are scored for this character.

133. Basioccipital, fusion to basisphenoid: unfused (0)/ fused (1) (Lee93, Ch. A5).
Remarks: See comments and examples above in the introduction of the "Braincase" section. The fusion of the basioccipital to the exoccipitals (or otoccipitals) may vary during post-embryonic ontogeny in many squamates (Maisano 2002), which may also occur in other reptiles, and thus only adults specimens are scored for his character.

134. Basioccipital, ventral aspect, shape, concavity: single (0)/ divided (1)/ absent (2) (NEW).

Remarks: This concavity the for axial musculature can be either single or divided. Since both conditions are seen as distinct from each other as they are from the absent condition (not hierarchically nested and being mutually exclusive) they are all included as part of the same character instead of being split into contingent characters.

Basisphenoid

135. Basisphenoid, Vidian canal: open (0)/ fully enclosed (1) (B85, Ch. Y14).
Remarks: The palatine ramus of the facial nerve (VII) and carotid artery pass laterally to the braincase (in a groove) in most reptiles, but they are enclosed by the basisphenoid in the form of a canal in most squamates. In some scolecophidian snakes and early deriving alethinophidian snakes the Vidian canal is open, but in other snakes and dibamids the Vidian canal is partially or entirely closed by the parabasisphenoid. Additionally, polymorphisms may occur, with some individuals presenting both an open or partially closed canal, such as in *Liotyphlops albirostris* (Rieppel *et al.* 2009). Here, I consider the closure of the canal only when it is closed by the basisphenoid itself (or parabasisphenoid, when fusion between the basisphenoid and parasphenoid occurs). I do not consider this closure primarily homologous (by the criterion of similarity) to the one caused by an extreme ventral projection of the parietal, which may occasionally contribute to the closure of the Vidian canal, as observed in *Anilius*.

136. Basisphenoid, basipterygoid processes: present (0)/ absent (1) (G12, Ch. 332—modified, Fig. in Ch. 332 therein).
Remarks: The basispterygoid processes are absent in some snakes, such as *Xenopeltis unicolor*.

137. Basisphenoid, dorsum sellae: absent (0)/ present (1) (Ev88, Ch. J14).
Remarks: The dorsum sellae is absent in dibamids and in some snakes [e.g. *Liotypholps albirsotris* (Rieppel *et al.* 2009)].

138. Basisphenoid (or fused parabasisphenoid), ventral aspect, shape, concavity: single (0)/ divided (1)/ absent (2) (LR95, Ch. 50).

Remarks: In a variety of reptiles the basisphenoid possesses a ventral concavity—or pocket Laurin & Reisz (1995)—that is delimited laterally by the cristae ventrolaterales.

139. Basisphenoid, lateral depression: absent (0)/ present (1) (NEW). D*
Remarks: Small depression located ventrolaterally on the basisphenoid, and usually lying dorsal or posterodorsal to the level of the basipterygoid process within archosauriforms. This recess has been recently considered to be homologous to the anterior tympanic recess observed in later archosauriforms, such as *Silesaurus* and dinosaurs (Sobral et al. 2016).

Prootics

140. Prootics, prootic crest: absent (0)/ present (1) (LC00, Ch. 78—modified).
Remarks: A prootic crest is common among squamates, although absent in *Dibamus* (Evans 2008).

141. Prootics, prootic crest, shape: crest (0)/ curved flange (1) (LC00, Ch. 78—modified; Fig. in G12, Ch. 310).
Remarks: Expansion of the prootic crest into a posteriorly curved bony flange (state "1") occurs in macrostomatan snakes (e.g. *Xenopeltis, unicolor* and *Cylindrophis rufus*), and contributes to the formation of the crista circumfenestralis of most snakes. Expansion of the prootic crest, along with an expansion of the crista interfenestralis, contributes to the formation of a distinct kind of crista circumfenestralis in later evolving mosasauroid reptiles (Rieppel & Kearney 2002).

142. Prootics, alar crest: absent (0)/ present (1) (E88, Ch. 49—modified; Fig. in G12, Ch. 305).
Remarks: The alar crest is a thin bony flange projecting anteriorly on prootics, located just anterior to the anterior semicircular canals (Oelrich 1956; Rieppel 1984a). The alar crest is absent in most iguanians, but it is common among other squamate lineages. It is very elongated in some taxa, such as *Varanus* and mosasauoirds, occasionally contacting the parietal, as in some mosasauroids.

143. Prootics, supratrigeminal process: absent (0)/ present (1) (E88, Ch. 5; Fig. in G12, Ch. 306).

144. Prootics, anterior inferior process: present (0)/ absent (1)/ (D98, Ch. 48).

145. Prootics, lateral wall, facial foramen: absent (0)/ present (1) (L98, Ch. 68; Fig. in G12, ch. 313).
Remarks: Opening for the exit of the facial nerve (VII) on the lateral wall of the braincase.

146. Prootics, lateral wall, facial foramen, division: single (0)/ double (1) (Lee97, Ch. 42; Fig. in G12, Ch. 313).
Remarks: The facial nerve (VII) leaves the braincase through a single opening on the lateral wall of the prootics and then branches off into its hyomandibular (Vidian nerve) and palatine branches in *Ctenosaura* (Oelrich 1956). However, this division may occur inside the braincase, with each branch exiting through separate openings (state "2" herein). In the latter case, there is usually an anteroventrally located opening for the hyomandibular branch and a more ventral opening for the palatine branch, which then passes anteriorly through the Vidian groove or canal.

Parasphenoid

147. Parasphenoid, teeth: absent (0)/ present (1) (B85, Ch. B9).

148. Parasphenoid, orbitosphenoid processes: absent (0)/ present (1) (NEW).
Remarks: The orbitosphenoid processes of the parabasisphenoid in contact the orbitosphenoid in amphisbaenians.

Opisthotics

149. Opisthotics, crista interfenestralis: present (0)/ absent (1) (G12, Ch. 311, Fig. in Ch. 311 therein).

Remarks: The crista or processus interfenestralis separates the fenestra ovalis and the lateral aperture of recessus scale tympani (LARST). The crista is absent in amphisbaenians and *Anniella pulchra* among squamates. In *Acontias,* separate openings for the fenestra ovalis, LARST and vagus foramen are present, despite the LARST being reduced by a close apposition between the crista interfenestralis and the crista tuberalis.

Exoccipitals

150. Exoccipitals, lateral flange: absent (0)/ present (1) (Lee93, Ch. A4).
Remarks: This character is inapplicable when the exoccipitals are fused to the opisthotics. Observed within pareiasaurs, turtles and rhynchosaurs.

151. Exoccipitals, fusion: unfused (0)/ to opisthotics only (1)/ to opisthotics and prootics (2) (G88a, Ch. 80 - modified).
Remarks: The exoccipitals become fused to the opisthotics (forming otoccipitals) in squamates. In some snakes, the otoccipitals are also fused to the prootics (state "2"). Fusion of the exoccipitals to the basioccipital may also occurs in some taxa (character 132). However, they are treated as separate characters because the distribution of these sequences of fusion among the observed taxa suggests both belong to independent transformation series. For instance, in all taxa studied herein, the fusion of the exoccipitals to the prootics only takes place when they are also fused to the opisthotics. However, fusion of the exoccipitals (or otoccipitals) to the basioccipital may occur regardless of its fusion to the prootics (e.g. *Cordylus niger*). The fusion of the otoccipitals to the prootics may vary during post-embryonic ontogeny in many squamates (Maisano 2002), which may also occur in other reptiles, and thus only adults specimens are scored for his character.

152. Exoccipitals, occipital condyle process: absent (0)/ present (1) (G88a, Ch. 81 - modified).
Remarks: The exoccipitals usually contribute to the formation of the single occipital condyle of reptiles by means of two processes abutting each lateral side of the basioccipital occipital condyle. However, many taxa do not have such processes, and the occipital condyle is thus

formed solely by the basioccipital. This character is inapplicable when the exoccipitals and basioccipitals are fused.

153. Exoccipitals, crista tuberalis: absent (0)/ present (1) (G12, Ch.312—modified, Fig. in Ch. 311 therein).

Remarks: The fissura metotica (Rieppel 1985) can be undivided (foramen metoticum) as in most reptiles, or divided by a crista tuberalis (from the exoccipitals) as in squamates. The formation of the crista tuberalis creates two separate openings on the external wall of the braincase: the jugular or vagus foramen for nerves X and XI, and the lateral aperture of the recessus scalae tympani (LARST) (=foramen rotundum), through which the glossopharyngeal nerve (IX) exits the braincase. This division of the braincase also occurs on the medial wall of the braincase in squamates, where the medial aperture of the recessus scalae tympani is separated from the jugular foramen. However, in some squamates the external division of the fissure metotica by the crista tuberalisis is absent (although the medial wall remains divided), such as in *Xantusia vigilis*, *Coleonyx variegatus*, and *Acontias plumbeus*, where the exit for the nerve IX is confluent with the exit of the vagus nerve.

Among other reptiles, in some turtles (e.g. *Chelonia*) the glossopharyngeal nerve exits laterally though a separate opening from the vagus nerve, the foramen externum nervi glossopharyngei (Gaffney 1972). However, the latter foramen is enclosed within the processus (= crista) interfenestralis. This condition is quite distinct from the condition seen in squamates, because the separation between both nerve openings is not due to a division of the LARST by a bony process from the exoccipitals. In some other turtles (e.g. *Chelydra*), a bony flange from the exoccipital and opisthtotics forms a lateral division between the LARST and the posterior opening for the vagus nerve, similar to what is observed in squamates. The latter condition is probably a derived condition within Testudinata (not sampled herein), because the earliest fossil turtles (e.g. *Proganochelysi*) show a condition more similar to *Chelonia,* without this external division by the exoccipitals/opistothics (Rieppel 1985).

154. Exoccipitals (or otoccipitals), contact to each other, medially: absent (0)/ present (1) (G12, Ch. 353, Fig. in Ch. 353 therein).

Remarks: the otoccipitals expand and contact each other medially above the foramen magnum within snakes. The condition in amphisbaenians (where a fused occipital complex occurs) is indeterminate.

Stapes (= columella)

155. Stapes, dorsal process: present (0)/ absent (1) (G88a, Ch. 69 - modified).
Remarks: The stapes bears a dorsal process in early reptiles (e.g. captorhinids).

156. Stapes, stapedial foramen: present (0)/ absent (1) (B85, Ch. C5).
Remarks: The stapes is perforated by a stapedial foramen in early reptiles (e.g. captorhinids and *Youngina*). In squamates, only some gekkotans (e.g. *Coleonyx*) and dibamids possess a stapedial foramen (Rieppel 1984b; Rieppel 1984a; Evans 2008). Even among gekkotans, the stapedial foramen is absent in pygopodids (when the stapes is ossified), *Gekko*, among others (Underwood 1957; Rieppel 1984b; Evans 2008).

Laterosphenoid (= pleurosphenoid): endochondral ossification of the pila antotica (Gauthier et al. 1988b).

157. Laterosphenoids: absent (0)/ present (1) (B85, Ch. L4).
Remarks: Positioned anteriorly to the trigeminal notch on the prootic, forming a trigeminal foramen with the latter element.

Orbitosphenoid (= postoptic Cope 1892**)**: Endochondral ossification of the bulk of the pila metoptica and part of the taenia parietalis, forming the posterior margin of the optic foramen. (Oelrich 1956).

158. Orbitosphenoids: absent (0)/ present (1) (Wu96, Ch. 86).
The orbitosphenoid is ossified in squamates, becoming enlarged and fused medially in most amphisbaenians.

159. Orbitosphenoids, fusion to each other: unfused (0)/ fused medially (1) (G12, Ch. 318, Fig. in Ch. 318 therein).

Sphenethmoid: Ossified anterior extension of the interorbital septum. It can be Y or V shaped. When Y shaped, its ventral projection forms the interorbital septum. The sphenethmoid therefore has similar developmental origins to the pleurosphenoid, and it may enclose cranial nerves II if expanded ventrally, and a concavity or foramina for nerves III and IV when expanded posteriorly (Romer 1956, p. 68; Holmes 1984). Oelrich (1956) calls the sphenethmoid bone an ossification of the interorbital septum, but I attain here to the nomenclature present in Romer (1956).

160. Ossified sphenethmoid: present (0)/ absent (1) (DBR97, Ch. 70—modified).

161. Ossified sphenethmoid, shape: without orbital septum (0)/ with orbital septum also ossified (1) / only orbital septum (2) (DBR97, Ch. 70—modified).
Occurrence: An ossification of the sphenethmoid occurs within lepidosaurs, especially revealed by CT-scan data (e.g. Digimorph repository). However, the shape of the ossified element can be quite variable, including the absence (“V” shaped) or presence (“Y” shaped) of an orbital septum, or with only the orbital septum being ossified (“I” shaped).

Mandibles:

162. Anterior mylohyoidal foramen: absent (0)/ present (1) (G12, Ch. 379, Fig. in Ch. 353 therein).
Remarks: Located within the splenial in most reptiles. This foramen serves for passage of the anteromedial branch of the inferior alveolar nerve (mylohyoideus nerve) in lizards (Oelrich 1956), turtles [where it is termed foramen intermandiularis oralis (Gaffney 1972)], and rhynchosaurs [where it is termed anterior meckelian foramen (Benton 1983)].

163. Posterior mylohyoidal foramen: absent (0)/ present (1) (CoN06, Ch. 112).
Remarks: Usually located within the angular in squamates. This foramen serves for passage of the posteromedial branch of the inferior alveolar nerve in lizards (Oelrich 1956), turtles [where it

is termed foramen intermandiularis caudalis (Gaffney 1972)], and rhynchosaurs [where it is termed posterior meckelian foramen (Benton 1983)].

164. Anterior inferior alveolar foramen: absent (0)/ present (1) (NEW)
Remarks: Usually located on the splenial, or between the splenial and dentary in squamates. Serves for the passage of the inferior alveolar nerve and a medial branch of the internal mandibular artery in lizards (Oelrich 1956).

Dentaries

165. Dentaries, symphyses, fusion to each other: unfused (0)/ fused (1) (NEW).
Remarks: The mandibular symphysis may become fused in some sauropterygians, some turtles and *Trilophosaurus*.

166. Dentaries, symphysial area, shape: flat (0)/ convex (1) (Lee 1998, Ch. 110, Fig. in G12, Ch. 355).
Remarks: The mandibular symphysis may have a distinct flat area in lizards, a rounded surface (resulting into a movable symphysial articulatory surface) as in snakes.

167. Dentaries, anterior end, split by Meckelian canal: absent (0)/ present (1) (NEW).
Remarks: Most reptiles have the Meckelian canal open medially. However, even in cases where the Meckelian canal is open throughout most of the extension of the dentary, the anterior tip of the dentary is still formed by a contact between its dorsal and ventral margins (that frame the Meckelian canal), as seen in most squamates. In some reptiles, however, this anterior end is split (or indented) by the Meckelian canal, which becomes open anteriorly. When the Meckelian canal is closed by the dentary (e.g. geckoes, xantusiids, and *Rhineura*), this character is inapplicable.

168. Dentaries, anterior end, symphysial articulatory facet, position: on dorsal margin only (0)/ on dorsal and ventral margins (1)/ on ventral margin only (2) (Lo12, Ch. 612).

Remarks: The articulatory facet of the dentary symphysis is usually located dorsally to the Meckelian canal, on the subdental crest/ridge. However, in some taxa (e.g. many amphisbaenians, rhynchocephalians, turtles, captorhinids, among others) it is also located ventrally on the anterior tip of the dentary, on a medial projection of the dentary ventral margin. When the symphysial facet occurs both dorsally and ventrally, these facets can either be separated (e.g. most squamates), or connected, forming a single and dorsoventrally deep symphysial facet, as occurring in some sphenodontians (e.g. *Sphenodon, Priosphenodon*) and amphisbaenians among lepidosaurs, and captorhinids and turtles among other diapsid reptiles. However, in taxa such as *Iguana iguana* and some acrodontans, a deep symphysis is present, but the symphysial facet is located only dorsally (on the anterior tip of the subdental shelf, or subdental ridge), thus indicating this character can be assessed independently of symphysial depth, and these conditions are nor primarily homologous to state "1' herein. Furthermore, an elongate symphysis may also occur in earlier diverging amniotes and non-amniotes, including *Limnoscelis*, caseid synapsids, and placodonts. In such cases, the symphysial process of the splenial forms the ventral part of the elongate symphysis, also making the condition in these taxa not primarily homologous to the condition represented by state "1". When the ventral surface of the dentary is fused to the subdental shelf and the dentary tapers anteriorly (such as in geckoes), this character is indeterminate, and it is thus scored as inapplicable.

169. Dentaries, subdental shelf: present (0)/ absent (1) (E88, Ch. 59).

Remarks: This refers to the lingual bony projection supporting the dentary teeth (Rage & Augé 2010). The absence and presence of a subdental shelf is mostly considered a lepidosaurian character, as it becomes reduced or absent in certain clades, including platynotans (McDowell & Bogert 1954), in which the teeth attach directly to the lingual side of the lateral wall of the dentary. The subdental shelf is also reduced in taxa bearing acrodont dentition, including acrodontans (Cooper *et al.* 1970; Cooper & Poole 1973; Simões *et al.* 2015b), priscagamids (Borsuk-Białynicka & Moody 1984; Borsuk-Białynicka 1996) and most sphenodontids (Evans 2008), in which mandibular teeth are placed apically on the lateral wall of the dentary. In non-lepidosaurian reptiles, however, this character is also informative. A shelf is present in a large number of reptiles, including forms with teeth set in sockets (the sockets themselves being placed on the shelf). In edentulous taxa, however, the scoring of this character can be

problematic. Also, in rhynchosaurs the teeth are placed apically on the dentary, but it is uncertain whether this condition is a result of the loss of the subdental shelf as in lepidosaurs with acrodont dentition. In such instances, I leave this character unscored (?) because of the lack of a reasonable indication on the absence or presence of a subdental shelf. In others, a reasonable estimate can be made. In turtles, for instance, *Proganochelys* displays small tooth alveoli in a dental sulcus, enclosed by labial and lingual walls. This indicates a subdental shelf was present among stem turtles.

170. Dentaries, dorsal margin, contact, with ventral margin in medial view: absent (0)/ present (1) (E88, Ch. 55—modified).
Remarks: The degree of contact between both margins along the length of the dentary is a variable with a continuous range of variation, which I do not attempt to code herein. Only the absence/presence of that contact is considered for this character. Because the contact between both margins results mostly from a ventral expansion of the subdental crest of the dentary in all of the observed taxa, I consider this feature to be primarily homologous among the sampled species.

171. Dentaries, dorsal margin, fusion, with ventral margin in medial view: absent (0)/ present (1) (E88, Ch. 55—modified).

172. Dentaries, coronoid process: absent (0)/ present (1) (E88, Ch. 60—modified)..
Remarks: The coronoid process is the edentulous posteriorly projecting area of the dentary bone. Some taxa lack this process entirely, whereas in others the coronoid process may be extremely reduced and it is hard to be noticed in lateral aspect, but it is still present if observed in dorsal view (e.g. *Pristidactylus scapulatus* and *Polychrus marmoratus*). In taxa with edentulous dentaries (e.g. most turtles) this character is impossible to determine with confidence.

173. Dentaries, coronoid process, dorsal expansion: absent (0)/ present (1) (E88, Ch. 60—modified).

Remarks: A dorsal expansion of the coronoid process is observed within lepidosaurs, butting against the lateral margin of the dorsal process of the coronoid bone (e,g, sphenodontians) or the anterior margin of the same (e.g. cordylids and scincids).

174. Dentaries, coronoid process, division: single (0)/ double (1) (NEW).
Remarks: In sphenodontians and some acrodontan lizards, the coronoid process is posteriorly divided, with one process extending posteriorly and another one dorsally (covering the coronoid bone laterally) (Simões *et al.* 2015b).

175. Dentaries, posteroventral process: absent (0)/ present (1) (G88b, Ch. 66—modified).
Remarks: In most reptiles, only the coronoid (posterodorsal) process of the dentary is present. In lepidosaurs (mostly squamates), a posteroventral process occurs (as in *Huehuecuetzpalli*, acrodontans, xantusiids, among others) below the level of the anterior surangular foramen.

Splenials

176. Splenials: absent (0)/ present (1) (B85, Ch. Z12).

177. Splenials, fusion to dentary: unfused (0)/ fused (1) (G12, Ch. 374—modified, Fig. in Ch. 374 therein).
Remarks: According to Estes *et al.* (1988), the splenial becomes fused to the dentary in xantusiids (also, TRS pers. obs.). The fusion of the splenial to the dentary in xantusiids does not seem to belong to the same transformation sequence of the fusion of the post-dentary elements that results in the compound bone of snakes and amphisbaenians. In all of the studied taxa, fusion of the articular to the prearticular, surangular, and angular, always precedes fusion to the splenial. However, in xantusiids, splenial fusion to the dentary occurs without fusion of the splenial to other lower jaw elements. Therefore, I treat fusion of the splenial to the dentary under a separate character in relation to the sequence of fusions that leads to the formation of the compound bone in some taxa (see below).

178. Splenials, symphysial process: absent (0) / present (1) (LR95, Ch. 80).

179. Splenials, anterior border, shape: rounded (0)/ notched (1)/ flat (2)/ tapering (3) (Lee93, Ch. D6 - modified).

Angulars

180. Angulars: present (0)/ absent (1) (E88, Ch. 72).
Remarks: According to Estes *et al.* (1988), the angular is absent in many gekkotans, and it is a separate distinct element in adult eublepharids (Evans 2008). However, there is a suture separating the angular from the prearticular in some of the observed specimens of *Coleonyx variegatus* and *Gekko gecko*. Therefore, it seems that the angular undergoes fusion with the prearticular in geckoes where a distinct angular is not visible. Developmental evidence would help to assess if the supposed absence of angular in some geckoes actually represents fusion, or only an elongation of the prearticular. In *Xantusia vigilis*, the angular may occur in some posthatchlings (Estes *et al.* 1988). In adults, however, this suture disappears and both elements are fused, with the the fused prearticular+angular extending well anteriorly, contacting the fused dentary+splenial.

181. Angulars, anterior end, medial view, position relative to splenial: lateral (0)/ dorsal (1)/ ventral (2)/ posterior (3) (L97, Ch. 70—modified)
Remarks: The splenial is in contact with the angular in the vast majority of studied taxa. Additionally, despite a considerable variation in shape of the splenial, the posteroventral end of the splenial is almost invariably in contact with the ventral margin of the dentary. Therefore, this region becomes a useful landmark to assess the position of the angular in the lower jaw. In most cases, the angular is always positioned dorsally to the splenial in medial view. In some taxa (e.g. *Tanystropheus*), however, it is placed ventrally to it. This occurs regardless of the relative lengths of each of these elements. Finally, the angular may butt against the splenial posteriorly, as in mosasauroids and snakes.

Surangulars

182. Surangulars, coronoid process: absent (0)/ present (1) (G88b, Ch. 69, Fig. in G12, Ch. 400).
Remarks: The surangular may have a dorsal contribution to the coronoid eminence of the mandible, with variable degrees of contribution of the coronoid dorsal process.

183. Surangulars, lateral adductor crest: absent (0)/ present (1) (LR95, Ch. 73—modified, Fig. in G12, Ch. 399).
Remarks: The adductor crest, defining a lateral adductor fossa, is considered herein primarily homologous to the "lateral shelf" on the surangular described by Laurin & Reisz (1995), since both represent attachment areas for the external adductors, most likely the *M. adductor mandibularis externus superficialis* of extant reptiles (Oelrich 1956; Haas 1973). A distinct adductor crest/fossa system is absent in most early reptiles, but it is common within diapsids.

184. Surangulars, anterior surangular foramen: absent (0)/ present (1) (MS04, Ch.145).
Remarks: Located anterodorsally on the lateral side of the surangular, usually ventral to the suture with the coronoid process of the dentary (Simões *et al.* 2015b). This foramen serves as passage for the posterior cutaneous branch of the inferior alveolar nerve (Oelrich 1956).

185. Surangulars, posterior surangular foramen: absent (0)/ present (1) (MS04, Ch.146).
Remarks: Located posterodorsally on the lateral side of the surangular, close to the glenoid. This foramen serves as passage for the posterior cutaneous branch of the inferior alveolar nerve (Oelrich 1956) [termed foramen nervi auricolotemporalis in turtles (Gaffney 1972)].

186. Surangulars, mandibular fenestra: absent (0)/ present (1) (D98, Ch. 76).
Remarks: Large fenestra enclosed by the surangular, with some occasional contribution of the dentary to its anterior margin. Occurrence within archosauriforms.

Articular

187. Articulars, lateral shelf: absent (0)/ present (1) (LR95, Ch. 78).

Remarks: Lateral expansion of the dorsal surface of the articular, both in the glenoid and retroarticular areas, likely serving as an expanded area of attachment for the pterigoideal adductor system. Occurs in taxa such as pareiasaurians (Laurin & Reisz 1995), *Proganochelys*, *Trilophosaurus*, and within archosauriforms (e.g. *Erythrosuchus*, *Prestosuchus*).

188. Articulars, fusion: unfused (0)/ to prearticular only (1)/ to prearticular + surangular only (2)/ to prearticular + surangular + angular only (3)/ to prearticular + surangular + angular + splenial (4) (B85, Ch. Y16).
Remarks: This character assesses the fusion of the post-dentary elements. The articular and prearticular are fused in most, if not all, adult squamates, and may become further fused to other post-dentary elements in what, as assessed herein, seems to follow a particular sequence of events: fusion of the articular+prearticular to the angular, and then to the surangular too, and eventually to also include the splenial in some amphisbaenians.

189. Articulars, foramen chorda tympani: absent (0)/ present (1) (NEW).

190. Articulars, retroarticular process: absent (0)/ present (1) (LR95, Ch. 76—modified).

191. Articulars, retroarticular process, dorsal fossa: absent (0)/ present (1) (E88, Ch. 74).

192. Articulars, retroarticular process, lateral notch: absent (0)/ present (1) (E88, Ch. 77, Fig. in G12, Ch. 409).

193. Articulars and prearticulars, medial process: absent (0)/ present (1) (E88, Ch. 73, modified as in Co08, Ch. 209) .
Remarks: A medial process on the posterior end of the lower jaw is observed in a variety of reptilian groups for the attachment of the pterygoideus adductor complex (Haas 1973). This medial process may be formed by the articular or the articular and prearticular, and in squamates it is usually termed angular process. Relative to the longitudinal axis of the lower jaw, the medial process is usually located medial to the glenoid cavity for the articulation with the quadrate, but may also be entirely medial to the retroarticular process.

194. Articulars and prearticulars, medial process, prearticular crest: absent (0)/ present (1) (E88, Ch. 73—modified).
Remarks: Commonly observed in teiioids and some borioteiioids, this crest in located on the dorsal surface of the medial (angular) process of the articular and prearticular.

Prearticular

195. Prearticulars, retroarticular process: absent (0)/ present (1) (LR95, Ch. 77 – modified).
Remarks: This character refers only to the prearticular contribution to the retroarticular process. This process of the prearticular may or may not occur in conjunction with the retroarticular process of the articular when both bones are not fused, thus indicating they should be treated as separate chatacters.

196. Prearticulars, mandibular fossa: present (0)/ absent (1) (L97, Ch. 80—modified).
Remarks: The prearticular bears a posteriomedial concavity that contributes to the formation of the mandibular fossa.

Coronoid:

197. Coronoids, dorsal process: absent (0)/ present (1) (B85, Ch. J7—modified, Fig. in G12, Ch. 386).

198. Coronoids, anterolateral (=labial) process: absent (0)/ present (1) (E88, Ch. 68—modified).

199. Coronoids, anteromedial process: present (0)/ absent (1) (LC00, Ch. 138, Fig. in G12, Ch. 391).

200. Coronoids, posterodorsomedial process: present (0)/ absent (1) (NEW)

201. Coronoid, posteroventromedial process: present (0)/ absent (1) (G12, Ch. 393, Fig. in Ch. 393 therein).

Dentition

202. Dentition, crown apical striations, labial side: absent (0)/ present (1) (Co08, Ch. 219).

203. Dentition, mesiodistal serration: absent (0)/ present (1) (D98, Ch. 57).
Remarks: Occurrence within archosauriformes and varanids.

204. Posterior dentition, accessory cusps, mesiodistally oriented: absent (0)/ present (1) (NEW).
Remarks: Accessory cusps may be distributed mesiodistally on the tooth crown, as in some iguanians and lacertids among squamates. Mesiodistally distributed accessory cusps were also observed in tanystropheids and *Langobardisaurus*. Due to their topological difference, these cusps are primarily non-homologous to labiolingually arranged accessory cusps (e.g. as in *Trilophosaurus*).

205. Posterior dentition, accessory cusps, labiolingually oriented: absent (0)/ present (1) (Lo12, Ch. 620).
Remarks: see comments for character 204 above.

206. Posterior dentition, replacement teeth: absent (0)/ present (1) (P86, Ch. 26—modified).

207. Posterior dentition, resorption pits: present (0)/ absent (1) (E88, Ch. 85, Fig. in G12, Ch. 431).
Remarks: Among squamates, snakes, varanids, lanthanotids, helodermatids, and some anguids have tooth replacement, but lack resorption pits (Edmund 1960; 1969; Lee 1997a). Rhynchosaurs have multiple rows of dentary and maxillary teeth positioned mostly apically and ankylosed to the jaws. Differently from the condition in most acrodontan lizards and sphenodontians, however, at least in *Hyperodapedon gordoni* and *Stenaulorhynchus stockleyi*, tooth replacement

with resorption pits is present (Benton 1984). In *Captorhinus aguti*, in which multiple tooth rows also occur, resorption pits have been documented, although replacement was certainly slow, and was likely to be very similar to the replacement pattern in rhynchosaurs (Fox & Bowman 1966; de Ricqlès & Bolt 1983; Benton 1984). Therefore, the previously reported pattern of tooth replacement without resorption pits appears to be conspicuous to some squamates only.

208. Posterior dentition, replacement teeth, position in relation to functional teeth: lingual (0)/ posterolingual (1) (P86, Ch. 26 – modified).

209. Posterior dentition, tooth shape, concave anteriorly: absent (0)/ present (1) (NEW).
Remarks: observed in some rhynchocephalians.

210. Posterior dentary teeth, position, relative to dentary crista dorsalis (apex of labial wall) of dentary: lingual (0)/ apical (1)/ apicolingual (2) (G88, Ch. 75 – modified).
Remarks: The classical categories of "tooth attachment", such as acrodonty, pleurodonty and thecodonty usually mix a combination of distinct features, such as tooth position on the jaws, ankylosis, and mode of replacement. However, tooth ankylosis to its surrounding tissue of attachment may occur in reptiles in combination with different kinds of tooth topologies, and replacement modes. For instance, teeth set in four-sided sockets may or may not be ankylosed to alveolar bone, suggesting both are independent characters. Therefore, here I divide the classical tooth attachment classifications into its different properties that seem to vary independently in at least part of the sampled taxa: tooth position on the jaw bone (relative to the jaws labial wall apical margins), tooth ankylosis, tooth delimitation (e.g. three-sided vs four-sided sockets), and presence or absence of replacement. In the present character, tooth position can be defined as: lingual to the dentary/maxillary labial wall; apically on the labial wall (sitting entirely on the crest forming the apex of the labial wall of the tooth bearing bones), such as in chamaeleonids, some priscagamids (e.g. *Mimeosaurus crassus*), and most sphenodontians (e.g. *Kallimodon, Pleurosaurus* and *Sphenodon*); or apicolingually, in which part of the tooth base lies apically to the dorsal crest, but they also extend lingually to it, such as in many agamids and priscagamids (Borsuk-Białynicka & Moody 1984; Borsuk-Białynicka 1996; Evans *et al.* 2002; Simões *et al.*

2015b), a condition previously described as “pleuroacrodonty” (Evans *et al.* 2002; Simões *et al.* 2015b).

Importantly, dental position (or topography) and tooth delimitation (see below) characters refer to position and enclosure of the dental tissues by jaw bone only. Therefore, conditions in which alveolar bone or cementum create an apparent apical placement of teeth on the jaw, such as seen in *Dracaena* and *Tupinambis*, are not considered as apically placed teeth, as the dental tissues in these cases are still placed lingually to the labial wall of the jaw bone. In some instances, the scoring for these conditions follows the literature on the subject (e.g. Edmund 1960; de Ricqlès & Bolt 1983; Budney 2004; Budney *et al.* 2006), but in others (especially fossils) an external morphological differentiation between dental tissue and jaw bone is readily visible and enhanced by the differential degree of mineralization of those tissues in fossils. This approach towards considering the distinct histological locators (or homologs) provides a better approach towards the coding of dental characters.

211. Posterior dentary teeth, ankylosis to crista dorsalis (apex of labial wall) of dentary: absent (0)/ present (1) (NEW).
Remarks: See comments above for character 210. Most acrodontan species with teeth placed at the apex or apicolingually on the jaws also have their teeth ankylosed to the labial wall of the jaw. This is also the case in most sphenodontians, rhynchosaurs and *Captorhinus*. This character refers to the externally observable fusion of the dentition to the jaw bone. Although many squamates fuse their tooth bases to the labial wall of the jaw bone, the apical margin of the bone is still distinct from the tooth crown. However, in most acrodontan lizards and sphenodontians the tooth crowns are fused to the apical margin of the jaw bone.

212. Posterior dentary teeth, delimitation by tooth bearing bone: by a labial wall only (0)/ by a three-sided socket (1)/ by a four-sided socket (2)/ by a lingual and labial wall only (3) (NEW).
Remarks: See comments above for character 210. The three-sided socket condition occurs when interdental ridges are present connecting to the labial wall of the jaws. The four-sided socket condition occurs when the teeth are fully enclosed inside a socket or alveolus on the jaws. When teeth are at the apex of the labial wall, instead of medially to it, this character is scored as inapplicable.

213. Posterior maxillary teeth, delimitation by tooth bearing bone: by a labial wall only (0)/ by a three-sided socket (1)/ by a four-sided socket (2)/ by a lingual and labial wall only (3) (NEW). Remarks: See comments above for character 210. Due to differences in jaw bone morphology when the dentaries and maxillae are compared, tooth delimitation by the jaw bone is treated separately for dentaries and maxillae in the present dataset.

214. Posterior dentary dentition, lingual and labial carinae: absent (0)/ present (1) (L97, Ch. 87).

215. Anterior dentary teeth: present (0)/ absent (1). (NEW).

216. Anterior dentary teeth, position relative to the jaw apical margin (dentary dorsal crest or maxillary ventral crest): lingual (0)/ apical (1)/ apicolingual (2) (G88b, Ch. 75 – modified). Remarks: : See comments above for character 210. The distinction on the placement between the anterior and posterior teeth series is observed in acrodontans lizards and a few rhynchocephalians among lepidosaurs. It also observed in other reptiles, such as some captorhinids.

217. Posterior maxillary teeth, posteromedial ridge: absent (0)/ present (1) (Ev88, Ch. K6). Remarks: occurrence within sphenodontians (e.g. *Kallimodon pulchellus*)

218. Anterior maxillary teeth, alternating teeth series: absent (0)/ present (1) (NEW). Remarks: In *Sphenodon* there are five generations of teeth, the first three ones occurring in the embryo. The fourth and fifth generations occur after hatching and are termed successional teeth (or replacement teeth). Each of these successional teeth replace two or more of the teeth from the preceding generation (Harrison 1901), but some of the hatchling dentition is kept with the larger successional teeth on the maxilla, creating a pattern of alternating teeth. This alternating teeth pattern is also observed in adults of fossil sphenodontians, such as *Diphyodontosaurus* (Whiteside 1986).

Postcranium

Axial skeleton

Atlas and axis

219. Atlas, pleurocentrum, fusion to axis: unfused (0)/ fused (1) (G88a, Ch. 133).
Remarks: Within Reptilia, the atlas centrum fuses to the axis in birds and lepidosaurs, forming the odontoid process of the axis. Fusion is absent, however, in some squamates, such as uropeltid snakes (Hoffstetter & Gasc 1969).

220. Atlas, neural arches: separate (0)/ sutured to each other (1)/ sutured to axis neural spine (2) (NEW).
Remarks: The neural arches are separate in most reptiles, but they may become sutured to each other in many lizards. In some taxa, such as *Polychrus marmoratus* and *Leiocephalus carinatus*, the axis neural spine extends anteriorly between the atlas neural arches, and becoming sutured to the latter. Considering the medial fusion of the atlas neural arches is dependent on the presence of the neural spine of the axis intervening between them, these three variables are coded under the same character. In some squamates, the neural arches are fused medially (e.g. *Bipes biporus*). However, this condition seems to be exteremly plastic and I do not make a distinction between sutured unfused neural arches to fused ones.

221. Atlas, neural arches, postzygapophyses: absent (0)/ present (1) (Lee97, Ch. 106).

222. Atlas, ribs: present (0)/ absent (1) (DBR97, Ch. 102).

223. Axis, pleurocentrum, fusion to neural arch: unfused (0)/ fused (1) (NEW).

224. Axis, intercentrum: present (0)/ absent (1) (NEW; Fig. 35 (Hoffstetter & Gasc 1969)).

225. Axis, connectivity to intercentra: to intercentra 2 only (0)/ to intercentra 2 and 3 (1) (NEW).
Remarks: Anguimorphs, amphisbaenians, snakes and mosasaurs have intercentra 2 and 3 on the axis (Russell 1967; Hoffstetter & Gasc 1969).

226. Axis, intercentrum, fusion to axial pleurocentrum: unfused (0)/ fused (1) (G88a, Ch. 131).

227. Axis, ribs: present (0)/ absent (1) (NEW).

Postaxial vertebrae: Presacral/precloacal pleurocentra

Most reptiles have a clearly discernable sacral region. This vertebral domain (as well as the cloacal domain in limbless forms), separates two other domains that usually have very distinct morphologies and represent serial homologs: the presacral and the caudal regions. The presacral region further comprises the cervical and dorsal (or trunk) domains, but their distinction is rather difficult for a number of taxa. A cervical region is defined as comprising all vertebrae anterior to the first vertebra bearing ribs contacting the sternal plate in lepidosaurs, for instance (Hoffstetter & Gasc 1969). However, this is can be hardly discerned in limbless squamates, which usually lose part or all of the pectoral girdle elements. In non-squamate fossil diapsids it also can be hard to identify distinct domains in the presacral region with precision because of lack of articulation between the ribs and other skeletal elements. For these reasons, I avoided the usage of the cervical and dorsal (trunk) domains for many characters, aiming for characters that are more easily identifiable (and less prone to erroneous scoring) throughout the entire presacral region. For some characters, clear differences between the cervical and dorsal regions are easily discernable—e.g. some features that occur only in the cervical region (or the anteriormost presacrals of limbless taxa). In such cases, I included these features among my characters. Whenever a particular feature could not be confidently attributed to either a cervical or a dorsal region when these domains were used, taxa were scored with missing data.

228. Presacral pleurocentra, orientation of centrum: amphicoelous (0)/ procoelous (1)/ opistocoelous (2)/ platycoelous (3)/ amphyplatyan (4) (G88b, Ch.84—modified).
Remarks: *Trilophosaurus* displays procoely among its cervicals and most of its dorsals, but it has amphicoelous dorsals close to the sacral region. Contrary to scorings in previous datasets (de Braga & Rieppel 1997; Müller 2004), choristoderes have amphyplatyan centra [(Brown 1905; Gao & Fox 2005; Katsura 2007) and TRS personal observation]. Defining distinct domains within serial homologues, such as vertebrae, can be problematic (as discussed above), especially when unusual variations occur (e.g. variation in centrum orientation in the presacral region). Polymorphic scoring is not justifiable under the circumstances observed in *Trilophosaurus*, as polymorphism applies to different individuals within a species displaying different states (not distinct regions within the same individual). Additionally, because the distinct centrum conditions may belong to distinct vertebral domains, the conjunction criterion of similarity (Patterson 1982) is also not applicable to justify the creation of a new character state. Therefore, in such instances, I score the most frequently observed condition within the vertebral sequence of *Trilophosaurus* (procoely).

229. Presacral pleurocentra, notochord, persistent in adults: present (0)/ absent (1) [B85, Ch. C6; Fig. 34 in (Hoffstetter & Gasc 1969)].
Remarks: Although persistent notochords are most commonly seen in taxa with amphicoelic vertebrae, this character undergoes variation independent of the orientation of the pleurocentra. For instance, most geckoes have amphicoelic vertebrae with notochordal canals, but geckoes with procoelic vertebrae, such as *Sphaerodactylus parkeri*, also have a persistent notochord (Holder 1960).

230. Presacral parapophyses: present (0)/ absent (1) (LR97, Ch. 116—modified).
Remarks: When the parapophyses are absent, the vertebral connection to the ribs is established by the diapophyses only.

231. Presacral pleurocentra, midventral crest, cervical vertebrae: absent (0)/ present (1) [G88a, Ch. 139; Fig. 37 in (Hoffstetter & Gasc 1969)].

Remarks: A midventral crest connecting to the hypapophyses occurs in *Blanus* among other amphisbaenians, but it is indeterminate in rhineurids. Despite snakes not having a clear difference between the cervical and dorsal regions, the anteriormost precloacal vertebrae of most observed taxa lack a midventral crest, and therefore they could be safely scored as "0" in such instances. *Xenopeltis unicolor*, on the other hand, has a ventral keel throughout the entire column, and was thus coded with state "1".

232. Presacral pleurocentra, midventral crest, posterior dorsal vertebrae: absent (0)/ present (1) [Ev88, Ch. B2; Fig. 34 (Hoffstetter & Gasc 1969)].
Remarks: Despite snakes not having a clear difference between the cervical and dorsal regions, even the posteriormost precloacal vertebrae of most observed taxa lacked a midventral crest, and therefore they were scored as "0" in such instances. *Xenopeltis unicolor*, on the other hand, has a ventral keel throughout the entire column, and was thus coded with state "1".

233. Posterior presacral pleurocentra, precondylar constriction: absent (0)/ present (1) (E88, Ch. 94).
Remarks: Precondylar constriction usually occurs in most presacral vertebrae of platynotan lizards. However, it is more clearly discernable in the posteriormost presacral vertebrae. Therefore, I use that particular region as the vertebral domain (locator) under comparison. This character is inapplicable for taxa without a condyle (e.g. with amphicoelic vertebrae).

234. Posterior presacral pleurocentra, dorsal vertebrae, margo ventralis (= ventrolateral crest): absent (0)/ present (1) [NEW; Fig. 69 in (Hoffstetter & Gasc 1969)].
Remarks: This crest, also named posterior centrosynapophyseal lamina crest (Tschopp 2016) connects the parapophyses (or fused synapophyses) to the vertebral condyle (Hoffstetter & Gasc 1969). This feature is most commonly observed in squamates, including snakes, teiids, *Crotaphytus*, among others. When present, the margo ventralis usually occurs in most presacral vertebrae. However, it is more clearly discernable in the posteriormost presacral vertebrae of squamates.

Sacral vertebrae

235. Sacral vertebrae, number: zero (0)/ one (1)/ two (2)/ three (3)/ four (4) (G88a, Ch. 141 - modified).
Remarks: Squamates with body elongation and limb reduction usually have a defined cloacal region that bears distally forked ribs (Hoffstetter & Gasc 1969). However, it is not possible to determine if all these cloacal ribs are modifications from sacrals, or if they include some of the anterior caudal vertebrae too. For this reason, only clearly defined sacrals (bearing distally expanded ribs attaching to the ilium) are considered herein.

Caudal vertebrae

236. Caudal vertebrae, autotomic septum: absent (0)/ present (1) (P86, Ch. 52; Fig. 52 (Hoffstetter & Gasc 1969))
Remarks: There is only one autotomic vertebra in some taxa, such as *Bipes biporus.* However, the vast majority of squamates bear vertebrae with autotomic septum past the first 10 or 15 caudals. An autotomic septum has also been identified in the captorhinids *Captorhinus* and *Labidosaurus* (Price 1940).

Intercentra

237. Intercentra, on cervical vertebrae: absent (0)/ present (1) (G88a, Ch. 129).

238. Intercentra, on cervical vertebrae, position: intervertebral (0)/ on preceding centrum body (1)/ on following centrum body (2) [E88, Ch. 97 and 98—modified; Fig. 44 in (Hoffstetter & Gasc 1969)].

239. Intercentra, on dorsal vertebrae: absent (0)/ present (1) (B85, Ch. L5).

240. Intercentra, on anteriormost caudal: absent (0)/ present (1) (NEW).
Remarks: The anteriormost caudal region (pygals) usually have intercentra that differ from the more posteriorly located intercentra (haemal arches) in both their presence and shape.

241. Intercentra, on anteriormost caudal, shape: wedge-like elements (0)/ modified into chevron elements (1) (NEW).
Remarks: The anteriormost caudals that bear intercentra may have intercentra that differ in shape from the more posteriorly located intercentra, suggesting this region corresponds to a different domain in the caudal series. If any variation in the anterior caudal series occurs, this should be observed in the first caudal. Therefore, I score the condition for the anterior caudal intercentra based on the anteriormost caudal. Such variation is observed, for instance, in *Sphenodon,* which has wedge-like intercentra in the anteriormost caudals followed posteriorly by the intercentra forming chevron elements (forming the haemal arches).

242. Intercentra, on posterior caudals (chevron bones): present (0)/ absent (1) (NEW).

243. Chevron bones, articulation: between pleurocentra (0)/ with pleurocentrum, on articulatory facets (1)/ with pleurocentrum, on haemapophyses (=pedicles) (2) (P86, Ch. 54—modified).
Remarks: The condition when the chevrons articulate with the vertebral condyle is considered as either states “1” or” 2”, depending on the kind of articulation. State “0” occurs when the chevrons do not articulate directly with the pleurocentrum, but between them. These conditions are mutually exclusive, justifying their coding under the same character.

244. Chevron bones, fusion to pleurocentrum: unfused (0)/ fused (1) (Lee98, Ch. 184).
Remarks: When the chevrons lay in between the pleurocentra, then the present character is considered to be inapplicable.

245. Chevron bones, distal fusion: separate elements (0)/ “V” shaped (1) / “Y” shaped (2)/ eliptically shaped (3) (NEW).
Remarks: The chevrons may fuse distally into a V-shaped condition, or may have a ventrally directed spine, thus becoming Y-shaped. *Megalancosaurus* has a peculiar elliptically shaped haemal arch, with the two halves being fused proximally and distally (“3”).

Neural arch and neural spine

246. Neural arches, dorsal vertebrae, ventral bridge, posterior borders of neural arches: absent (0)/ present (1) (Lee93, Ch. D9). D*
Remarks: A bony lamella may occur on the posterior border of the neural arches, connecting its two halves ventrally and bridging the gap between them. This condition is observed in captorhinids and in some sauropterygians.

247. Neural arches, prezygapophyses, presacral vertebrae, processes ventrolaterally on prezygapophyses: absent (0)/ present (1) (LS02, Ch. 200).
Remarks: Observed in many snakes, amphisbaenians and dibamids.

248. Neural arches, presacral vertebrae, zygosphenes: absent (0)/ present (1) [LC00, Ch. 186; Fig. 41 in (Hoffstetter & Gasc 1969)].

249. Neural arches, presacral vertebrae, zygosphenes orientation: facing dorsolaterally (0)/ facing ventrolaterally (1) [LC00, Ch. 187; Fig. 41 in (Hoffstetter & Gasc 1969)].
Remarks: The zygosphenes in neural arches with a zygosphene/zygantra articulation system, can be facing dorsolaterally, as in *Lacerta, Cordylus* and *Zonosaurus* and some iguanians (e.g. *Hoplocercus*), or ventrolaterally, as in *Iguana iguana*, snakes and mosasauroids (Hoffstetter & Gasc 1969; Rieppel & Zaher 2000).

250. Neural arches and pleurocentrum, diapophysis, anterior dorsal vertebrae, fusion to parapophysis: absent (0)/ present (1) (NEW).
Remarks: This character refers to the fusion of the para- and diapophyses only, regardless of the number of rib heads (in many instances the two apophyses are confluent, although the ribs still have two separate heads). The degree of fusion between the para- and diapophyses throughout the dorsal region may vary within individuals among some reptiles, usually fusing on the posterior dorsals and decreasing in the degree of fusion further anteriorly. This is very evident in ichthyosaurs (McGowan & Motani 2003), for instance. For this reason, I scored taxa based on

the anterior dorsals, as they are the most conservative region on the dorsals regarding this character. Most taxa without a clear dorsal region (e.g. snakes and amphisbaenians) have the same condition visible throughout all, or almost all of their postaxial vertebrae, thus being able to be scored for this particular character.

Kuehneosaurus has three cervical rib attachment surfaces: two in the neural arch (what apparently is a double diapophyses) and one on the anterior border of the pleurocentrum (the true parapophysis)—see also Robinson (1962) and Colbert (1970). The anterior dorsals bear double diapophyses, but the parapophysis is absent. Further posteriorly, on the mid-dorsal region, the number of lateral apophyses is reduced and the vertebrae bear only a single elongated transverse processes. Therefore, it is considered herein that the transverse processes of *Kuehneosaurus* (and which also seems to be the case in *Icarosaurus*), represents only the fusion of the double diapophyses (due to the apparent loss of the parapophyses on the anterior dorsals), instead of a being a true synapophysis by the definition of Hoffstetter & Gasc (1969).

251. Neural arches, margo lateralis, posterior presacral vertebrae: absent (0)/ present (1) [NEW; Fig. 69 (Hoffstetter & Gasc 1969)].
Remarks: Crest joining pre- and postzygapophyses (Hoffstetter & Gasc 1969).

252. Neural spine, cervical vertebrae, posterior notch: absent (0)/ present (1) (NEW).
Remarks: In some squamates (e.g. anguids) a posterior notch occurs on the apex of the cervical neural spines.

253. Neural spine, cervical vertebrae, apically, lateral expansion: absent (0)/ present (1) (N11, Ch. 191—modified).
Remarks: Occurrence in *Prolacerta*, *Youngina, Icarosaurus* [see also Colbert (1970)], *Kuehneosaurus* and within archosauriforms. In these taxa, the neural spine has a flat apical surface with short laterally projecting apical borders, conferring a "T" shaped neural spine in cross section.

254. Dermal neural spine, dorsal vertebrae: absent (0)/ present (1) (NEW).

Remarks: This additional segment of the neural spine has been suggested to have a different embryological origin from the endochondral ossification leading to the formation of the neural spine of most vertebrates. It has been proposed to be of dermal origin and positioned above the endochondral neural spines (Carroll & Zhi-Ming 1991). This additional segment of the neural spine has been observed in *Hupehsuchus* (Carroll & Zhi-Ming 1991) *Nanchangosaurus* (Chen *et al.* 2014), and, within ichthyosaurs, *Stenopterygius* (McGowan 1992) and *Utatsusaurus* (TRS, pers. obs).

255. Neural spine, dorsal vertebrae: present (0)/ absent (1) (LS02, Ch. 190—modified).
Remaarks: Loss of the neural spine occurs within amphisbaenians, some snakes (mostly burrowing forms), and the dolichosaurid *Pontosaurus*.

256. Neural spine, dorsal vertebrae, anterior midline process: absent (0)/ present (1)/ (B85, Ch. R2).
Remarks: The anterior (accessory) midline process of the neural spine fits into paired posterior pits at the base of the neural spines of the vertebrae immediately anterior to it. This condition is observed in taxa such as *Hovasaurus*, *Youngina* [see also Currie (1981a) and Currie (1981b)] and the sauropterygians *Neusticurus*, *Serpianosaurus* and *Lariosaurus*. Much reduced midline processes and posterior pits occur in the cervicals and anteriormost dorsals of *Kuehneosaurus*. These anterior projections are considered to be non-primary homologous to the zygosphene-zygantra system (of the neural arches) observed within lepidosaurs, because the midline processes occur at the base of the neural arches (Rieppel 1989c).

257. Neural spine, dorsal vertebrae, mammillary process: absent (0)/ present (1) (Ev88, Ch. B3 – modified).
Remarks: These are accessory processes located on either side of the neural arches and occur in *Hovasaurus* and *Protorosaurus.*

258. Neural spine, dorsal vertebrae, apically, lateral expansion: absent (0)/ present (1) (N11, Ch. 197).

Remarks: The morphology of this attribute is similar to the neural spine expansion located on the cervical region. Occurrence within archosauromorphs, such as *Prolacerta* and *Prestosuchus*. A similar structure is also observed in the anteriormost dorsals of *Pleurosaurus goldfussi* (BSPG 1978 I 7) and kuehneosaurids. Some taxa bearing the lateral expansion on the cervical region lack it on the dorsal region (e.g. *Youngina*) or vice-versa (e.g. *Proterosuchus alexanderi*), suggesting these distinct vertebral domains have some degree of independent variation that is visible across disparate lineages.

Presacral ribs

259. Presacral ribs, anteroposterior crests: absent (0)/ present (1) (Ly13, Ch. 2).
Remarks: The development of anteroposterior crests on the dorsal ribs creates the T-shaped ribs observed in turtles (e.g.as early as in the stem turtles *Eunotosaurus, Odontochelys* and *Proganochelys*) as well as in *Sinosaurophargis*.

260. Presacral ribs, cervical ribs: present (0)/ absent (1) (NEW).
Remarks: Some protorosaurians lose their cervical ribs, such as observed in *Langobardisaurus* and *Megalancosaurus*.

261. Presacral ribs, cervical ribs, anterior process: absent (0)/ present (1) (G88a, Ch. 143 - modified).
Remarks: Anterior extensions of the rib shafts, as present on the cervical ribs of archosauriforms, rhynchosaurs, some sauropterygians, thallatosaurs and many protorosaurs.

262. Presacral ribs, uncinate processes, anterior dorsals: absent (0)/ present (1) (G88a, Ch. L17).
Remarks: Neomorph cartilages that calcify in *Sphenodon* and crocodiles, and ossify in birds (Gauthier et al. 1988b), as well as within some marine reptiles.

263. Presacral ribs, anteroventral process at rib head (= pseudotuberculum): absent (0)/ present (1) [Lee98, Ch. 187, Fig. 43 in (Hoffstetter & Gasc 1969)].

Remarks: The posterodorsal process and the anterodorsal process may occur in conjunction or separately within squamates, justifying their placement as distinct characters.

264. Presacral ribs, posterodorsal process at rib head (= pseudotuberculum): absent (0)/ present (1) [Lee98, Ch. 188, Fig. 43 in (Hoffstetter & Gasc 1969)].

265. Posteriormost presacral vertebra, ribs: present (0)/ absent (1) (NEW).
Remarks: Some lizards may lack rib attachment in the last presacrals, forming a "lumbar" region (Hoffstetter & Gasc 1969).

266. Posteriormost presacral vertebra, ribs articulation: ribs unfused (0)/ ribs fused (1) D98, Ch. 137).

267. Sacral ribs, distal forking: absent (0)/ on first sacral rib only (1)/ on first and second sacral ribs (2)/ on second sacral rib only (3) (Lee98, Ch. 189 - modified).
Remarks: Because of the uncertain homology of the sacral elements in squamates with reduced pelvic elements or reduced number of sacrals, this character is inapplicable in such cases (e.g. snakes and amphisbaenians). The forking on distinct sacral vertebrae are treated under the same character because the sacral region is a quite distinct domain and can be considered as a serial homolog in the vertebral column of most tetrapods.

268. Sacral/Cloacal ribs, fusion to pleurocentra: unfused (0)/ fused (1) (G88b, Ch. 87 - modified).

269. Anterior caudal ribs: absent (0)/ present (1) (NEW).
Remarks: Caudal ribs are present in the vast majority of reptiles, but are seemingly absent in *Protorosaurus speneri*, in which only short transverse processes are present (Gottmann-Quesada & Sander 2009) and *Coelurosauravus elivensis* (MNHN MAP 327b—old MNHN 1908-5-2b).

270. Anterior caudal ribs, fusion to pleurocentra: unfused (0)/ fused (1) (G88b, Ch. 87 - modified).

Remarks: The fusion of the anterior caudals to the pleurocentra forms the pleurapophyses observed in captorhinomorphs, in lepidosaurs (Gauthier *et al.* 1988a) as well as *Saurosternon*, squamates and sphenodontids (Carroll 1975). The interpretation of the anterior caudals "transverse processes" in lizards as fused caudal ribs is further supported by personal observation of juveniles of *Liolaemus signifier* (AMNH R80140) that still bear these anterior caudal ribs unfused, and attaching distally to the true transverse processes.

Presternum (=sternum of most reptiles). Squamates have a presternum, a mesosternum and a xiphisternum. The main sternal plate, homologous to other reptile sterna, is formed by the presternum (Russell & Bauer 2008).

271. Presternum, mineralized: absent (0)/ present (1) (B85, Ch. R5; Fig. 1.2 (Russell & Bauer 2008)).
Remarks: A mineralized presternum occurs among most lepidosaurs, but is also observed in "younginiforms" (e.g. *Hovasaurus* and *Thadeosaurus*), and *Saurosternon*.

Xiphisternum

272. Xiphisternum: absent (0)/ present (1) (G88b, Ch. 90—modified; Fig. 1.2 (Russell & Bauer 2008)).

Poststernal inscriptional ribs

273. Mineralized poststernal inscriptional ribs: absent (0)/ present (1) (E88, Ch. 110; Fig. 2 (Etheridge 1965)).
Remarks: Also termed postxiphisternal ribs, these are present posterior to the last presternal ribs and connected distally to the dorsal ribs in many instances. Alternatively, inscriptional ribs may occurs as "free" ribs, when not attaching to the dorsal ribs, such as in *Chalarodon* (Etheridge 1965). The latter condition is observed in many squamates and within rhynchocephalians (e.g. *Sphenodon punctatus* and *Kallimodon* pulchellus, but absent in observed specimens of pleurosaurs and *Clevosaurus hudsoni*). I only scored for mineralized inscriptional ribs, since

cartilaginous ones may be incorrectly scored as absent in fossils. Also, as for other characters in this dataset, reduced but still present inscriptional ribs (e.g. as in *Uromastyx*) are scored with the present state. Within squamates, inscriptional ribs are absent or remain cartilaginous in some burrowing forms, and also in some non-burrowing taxa like *Lanthanotus borneensis*.

274. Distal ribs: absent (0)/ present (1) (NEW).
Remarks: In weigeltisaurids [e.g. *Coelurosauravus*—for the taxonomic status of the family, see Bulanov & Sennikov (2010)], there is a secondary set of ribs articulating distally to the proximal (or primary) set, and which is straight and directed laterally. This distal set of ribs is considered non-homologous to the laterally elongate ribs seen in other gliders, such as *Icarosaurus, Kuehneosaurus, Kuehneosuchus* and *Draco*. In the latter instances, the laterally elongate ribs are attaching to expanded transverse processes of the dorsal vertebrae, and are thus considered homologous to the ribs of other reptiles (or the proximal set of dorsal ribs of weigeltisaurids). The distal set of ribs of weigeltisaurids is also non-homologous to the inscriptional ribs, such as the ones present in most squamates. Despite both the distal ribs and inscriptional ribs attaching distally to the primary set of ribs, they are morphologically distinct in terms of shape and degree of mineralization.

Apendicular skeleton

Pectoral girdle

Scapula

275. Scapula, supraglenoid foramen: absent (0)/ present (1) (LR95, Ch. 97).
Remarks: This foramen is observed just above the glenoid, and it is more laterally placed in early reptiles. In some iguanian squamates, a supraglenoidal foramen is also observed, but placed more posteriorly on the scapula, as in *Crotaphytus collaris* and *Polychrus marmoratus*.

276. Scapula, supraglenoid buttress: absent (0)/ present (1) (G88a, Ch. 147).

277. Scapula, scapula ray: absent (0)/ present (1) (E88, Ch. 111 – modified; Fig. 1.2 (Russell & Bauer 2008)).

278. Scapula, dorsal acromion process: absent (0)/ present (1) (NEW).
Remarks: This character refers to the dorsalmost region of the scapular blade (and part of the suprascapular) that might be expanded anterodorsally, as observed in many squamate clades.

279. Scapula, supracoracoidal acromion process: absent (0)/ present (1).
Remarks: The present structure is located on the anteroventral margin of the scapula, as seen in *Proganochelys* and other turtles, and is not homologous to the structure of similar name seen in squamates, and which is located anterodorsally.

280. Scapula, posterior emargination: absent (0)/ present (1) (NEW).
Remarks: Observed among many sauropterygians and protorosaurs.

281. Scapula, anterior emargination: absent (0)/ present (1) (E88, Ch. 111).
Remarks: In squamates, the anterior margin is not truly emarginated. In most squamates the anterior margin is relatively straight or convex. Iguanians may bear a scapular ray (see above), but the margin to which it connects to is straight too. Some rhynchocephalians have a true emargination, with the anterior margin being concave anteriorly, and which is not homologous to the scapular "emargination" or fenestra to which the scapular ray contributes to delimit in some squamates.

Procoracoid. The squamate coracoid is homologous to the procoracoid (= anterior coracoid) of early deriving amniotes (Russell & Bauer 2008, p. 84) which bears the supracoracoid foramen.

282. Procoracoid, supracoracoid foramen: absent (0)/ notch (1)/ complete foramen (2) (R94, Ch. 71-modified; Fig. 1.2 (Russell & Bauer 2008)).
Remarks: In *Placodus gigas* and *Neusticosaurus (= Pachypleurosaurus) edwardsi* the supracoracoid foramen is actually a notch on the proximal margin of the coracoid.

283. Procoracoid, angulation medially: absent (0)/ present (1) (NEW).
Remarks: Observed within sauropterygians.

284. Procoracoid, coracoid emargination: absent (0)/ anterior emargination (1)/ anterior and posterior emarginations (2) (P86, Ch. 56 and 57; Fig. 1.2, 1.3 and 1.5 (Russell & Bauer 2008)).
Remarks: The anterior coracoid emargination is separated from the scapulocoracoid emargination dorsally by the first (anterior) coracoid ray and the posterior coracoid emargination is separated from an anterior coracoid emargination by the second (posterior) coracoid ray. The posterior emargination only occurs if the anterior one is also present; thus they are part of the same transformation series and logically nested. Therefore, this character is treated as ordered.

Posterior coracoid

285. Posterior coracoid: absent (0)/ present (1) [G88a, Ch. 148; Fig. 142 and 143 in (Romer 1956)].
Remarks: The posterior coracoid occurs in early amniotes, such as early synapsids and reptiles. Whereas the anterior coracoid (procoracoid) is homologous with the single coracoid of most reptiles, the posterior coracoid in homologous to the mammalian coracoid (Romer 1922; Romer 1956; Russell & Bauer 2008).

286. Epicoracoids: absent (0)/ present (1) [NEW; Fig. 1.2 in (Russell & Bauer 2008)].
Remarks: Present as a calcified cartilage within lepidosaurs.

Clavicles. Considered homologous to the epiplastron of turtles (Gaffney 1990; Lyson *et al.* 2013a; Rice *et al.* 2015; Rice *et al.* 2016).

287. Clavicles, secondary curvature anteroposteriorly: absent (0)/ present (1) (E88, Ch. 116; Fig. in G12, Ch. 502).
Remarks: In some squamate taxa, the clavicle is curved posterolaterally, and then anteromedially on its most dorsal portion, such as in *Lacerta viridis*.

288. Clavicles, proximoventral fenestration: absent (0)/ present (1) (LC00, Ch. 218—modified; Fig. in G12, Ch. 500).
Remarks: In the present character, the absent condition may include ventrally emarginated or hook-shaped clavicles that do not constitute fully fenestrated clavicles.

289. Clavicles, posterior process: absent (0)/ present (1) (NEW).
Remarks: Observed in scleroglossans lizards, such as some anguids, scincids and cordylids.

290. Clavicles, dorsolateral flange: absent (0)/ present (1) (NEW).
Remarks: Observed within sauropterygians and saurospharids.
291. Clavicles, position (at point of contact), in relation to anterior margin of scapula: laterally (0)/ medially (1)/ anteriorly (2) (R94, Ch. 65 – modified).
Remarks: Whereas in most reptiles the clavicles are positioned laterally or anteriorly to the anterior edge of the scapula, in sauropterygians the clavicles are positioned medially to the scapula.

292. Clavicles, position (at point of contact), in relation to anterior margin of the interclavicle: ventrally (0)/ dorsally (1)/ anteriorly (2) (R94, Ch. 62 and DBR96, Ch. 54).
Remarks: The clavicles are positioned ventrally to the anterior margin of the interclavicle in most reptiles, but in many sauropterygians the clavicles are positioned dorsally. The clavicles are positioned anteriorly in procolophonians (de Braga & Reisz 1996), captorhinids, some early diapsids, and in various groups of squamates.

Interclavicle: considered homologous to the entoplastron of turtles (Gaffney 1990; Lyson *et al.* 2013a; Rice *et al.* 2015; Rice *et al.* 2016).

293. Interclavicle, anterior process: absent (0)/ present (1) (P86, Ch. 59).
Remarks: A distinct anterior process of the interclavicle is absent in the earliest amniotes, which had a polygonal shaped interclavicle. However, an anterior process becomes distinct and present

when a cruciform interclavicle is acquired in later forms. The anterior process is absent or reduced in some diapsid taxa, including sauropterygians and some rhynchocephalians.

294. Interclavicle, posterior process: present (0)/ absent (1) (G88a, Ch. 156).
Remarks: The posterior process of the interclavicle is present in most reptiles, with the exception of sauropterygians.

Cleithra: considered homologous to the turtle nuchal bone (Lyson *et al.* 2013b).

295. Cleithra: present (0)/ absent (1) (B85, Ch. C8).

Pelvic girdle

Ilia

296. Ilia, posterodorsal notch, on acetabular margin: absent (0)/ present (1) (NEW).
Remarks: This notch occurs on the posterodorsal margin of the acetabulum of most reptiles, but is absent within sauropterygians.

297. Ilia, supraacetabular buttress: absent (0)/ present (1) (G88a, Ch. 179).
Remarks: There may also exist some contribution from the pubis for the formation of the supraacetabular buttress.

298. Ilia, anterior pubic process: absent (0)/ present (1) (B85, Ch. J12).
Remarks: The anterior extension of the ilium dorsally to the pubis is present in some early reptiles (e.g. *Hovasaurus* and *Acerosodontosaurus*) and most squamates, but this process is absent in many reptilian lineages, such as *Youngina*, *Prolacerta*, rhynchosaurs, and early archosauriformes, such as *Erythrosuchus, Proterosuchus* and *Euparkeria*.

299. Ilia, anterior (=preacetabular) process: absent (0)/ present (1) (Lee97, Ch. 132; Fig. 1.14 (Russell & Bauer 2008)).

Remarks: Process located on the iliac blade or the anterior extension of the ilium (character #).

Pubes

300. Pubes, obturator foramen: absent (0)/ complete foramen (1)/ notch (2) (NEW).
Remarks: The obturator foramen becomes incorporated into a thyroid fenestra in extant turtles (Romer 1956) and some ichthyosaurs (McGowan & Motani 2003) . A notch on the lateral margin of the pubes is seen in some sauropterygians and saurophargids (e.g. *Largocephalosaurus*).

301. Pubes, pubic tubercle: absent (0)/ present (1) (B85, Ch. J11; Fig. 1.14 (Russell & Bauer 2008)).

Ischia

302. Ischia, fusion to pubes: absent (0)/ present (1) (NEW).
Remarks: In some captorhinids (e.g. *Captorhinus aguti* and *Labidosauru hamatus*), the pubes and ischia are fused into a single bony plate.

303. Ischia, anterior border, emargination: absent (0)/ present (1) (NEW).
Remarks: The thyroid fenestra is usually formed by an anteromedial emargination on the ischium and another emargination on the posterior border of the pubis. In some taxa, however, the thyroid fenestra is formed only by the anterior concavity of the isquia (e.g. *Utatsusaurus hataii*). The present character construction avoids scoring taxa with different kinds of thyroid fenestra under the same character state by coding the actual bone morphology that results in the formation of the fenestra. When the ischium and pubes are fused (e.g. *Captorhinus aguti* and *Labidosauru hamatus*), then the shape of the anterior border cannot be assessed.

304. Ischia, ischiadic tuberosity: absent (0)/ present (1) (J94, Ch. 10—modified; Fig. 1.14 (Russell & Bauer 2008)).

305. Ischia, isquiadic neck: absent (0)/ present (1) (NEW).
Remarks: Thick “neck-like”region observed on the dorsal surface of the ischium, extending from the acetabular region to the symphysial margin of the ischium.

306. Ischia, facet, for hypoisquium: absent (0)/ present (1) (NEW; Fig. 1.14 (Russell & Bauer 2008)).
Remarks: Rather than coding for the absence or presence of the hypoisquium, coding the facet for it allows its scoring for fossil forms with less ambiguity and missing data.

Anterior propodial (= stylopodial)

Humeri

307. Humeri, ectepicondyle foramen: absent (0)/ groove (1)/ notch (2)/ complete foramen (3) (G88a, Ch. 162 and 163—modified).
Remarks: When the ectepicondyle foramen is incomplete and forms a notch, then a supinator process becomes evident, such as observed in *Paleothyris*. When this foramen is complete, such as in *Protorothyris*, then the supinator process is absent. For this reason, I consider the character presence or absence of the supinator process as part of the transformation series of the ectepicondyle foramen. In some taxa, only a groove with no foramen or notch is present, such as in *Placodus gigas*. Considering that an ectepicondylar groove may occur even in the absence of a distinct epicondyle (as it can be located on the humeral shaft), this character is scored even in the absence of the epicondyles.

308. Humeri, epicondyles: present (0)/ absent (1) (R94, Ch. 75).
Remarks: In all observed taxa, when one of the epicondyles is absent, the other is missing too, thus I code both epicondyles together to avoid overweighting these variables.

309. Humeri, entepicondyle foramen: absent (0)/ opening dorsally only (1)/ opening ventrally only (2)/ fully open ventrally and dorsally (3) (B85, Ch. C9 - modified).

Remarks: Most reptiles with an entepicondylar foramen display it on the dorsal surface of the distal end of the humerus, state “1”. However, some sphenodontians develop this foramen ventrally only, and in sauropterygians and early reptiles there is a full opening connecting the dorsal and ventral sides of the humerus. The character states herein do not occur in conjunction, thus being mutually exclusive and being better coded as different character states within a single character instead of split into contingently coded characters.

310. Humeri, expanded radial condyle (= capitelum): present (0)/ absent (1) (NEW).

311. Humeri, pectoral process: present (0)/ absent (1) [DBC93, Ch. 107—modified; Fig. 163-165 in (Romer 1956)].
Remarks: In some early reptiles, the pectoral process is a distinct element, separate from the humeral head. When the pectoral and deltoid processes are connected to the humeral head, a deltopectoral crest is formed.

312. Humeri, pectoral process, connection to humeral head: separate (0)/ connected (1) [DBC93, Ch. 107—modified; Fig. 166 and 167 in (Romer 1956)].

313. Humeri, shaft angulation: straight (0)/ angulate posteriorly (1) (R94, Ch. 74).
Remarks: Humeral shaft posteriorly angulated within sauropterygians and in some “younginiforms”.

314. Humeri, secondary ossification of epiphyses: absent (0)/ present (1) (B85, Ch. X1—modified).
Remarks: Observed in squamates and rhynchocephalians.

315. Humeri, anterior flange: absent (0)/ present (1) (Ch14, Ch. 209; Fig. 2 (Motani 1999a)).
Remarks: Present on the humerus of ichthyosaurs.

Anterior epipodials (= zeugopodials)

Radia

316. Radia, distal epiphysis, styloid process: absent (0)/ present (1) (G88b, Ch. 99; Fig. 9 in G88b).
Remarks: Observable in ventral and medial aspect in articulation with the radiale. This feature may not be seen in fossil taxa with the epiphyses not preserved (in which case they are scored as missing data).

317. Radia, anteroproximal process: absent (0)/ present (1) (NEW; Fig. 6b (Motani 1999a)).
Remarks: Similar in shape in lateral aspect (dorsal aspect in the forefin plane of orientation) to the olecranon process of the ulna. Present in the radius of early ichthyosaurs.

Ulnae

318. Ulnae, ossified olecranon process: present (0)/ absent (1) (B85, Ch. B11).

319. Ulnae, distal epiphysis, expansion: absent (0)/ present (1) (B85, Ch. X3; Fig. 9 in G88b).
Remarks: A distally expanded or "ball-like" distal epiphysis of the ulna is observed within squamates. The presence of a proximal concavity on the ulnare of lizards is dependent upon the presence of a distal ball-like distal epiphysis of the ulna and the formation of a ball-socket articulation. Therefore, a character on the proximal concavity on the ulnare is not included in the present dataset.

Anterior mesopodials (= carpals)

320. Perforating foramen, manus: absent (0)/ between ulnare and intermedium (1)/ between radiale and intermedium (2) (B85, Ch. C10 and DBR97, Ch. 131).
Remarks: The perforating foramen is usually present between the ulnare and intermedium, such as in *Hovasaurus* (Currie 1981a), but may also occur between the radiale and intermedium, such as in *Trilophosaurus* (Gregory 1945). This character refers to the mutually exclusive positions of

the perforating artery. Therefore, character state “0” is mutually exclusive to states “1”, “2” and “3” herein, and does not justify its splitting into two contingent characters.

Intermedium

321. Intermedium: present (0)/ absent (1) (Ev88, Ch. E8).

Pisiform

322. Pisiform: absent (0)/ present (1) (Mo99, Ch. 67).
Remarks: Postaxial element, positioned ventrally to the ulnare in squamates and other reptiles.

Palmar sesamoid

323. Palmar sesamoid: absent (0)/ present (1) (G12, Ch. 539, Fig. 539).

Distal carpal 1:

324. Distal carpal 1: present (0)/ absent (1) (G88b, Ch. 103; Fig. 4c and d in G88b).
Remarks: The element that partially occupies the position of the first distal carpal in lizards represents the medial centrale(Russell & Bauer 2008) [lateral central *sensu* Romer (1956) resulting from the fusion of the first carpal to the first metacarpal, and a slight shift in position of the medial centrale (Carroll 1977; Gauthier *et al.* 1988a). This fusion usually results in an enlarged epiphysis of the first metacarpal (which also occupies part of the position of the first carpal) followed by a reduced number of anterior carpal elements. Because the underlying developmental process of fusion cannot be assessed in the vast majority of sampled taxa, the wording of the present character reflects the absence of DC1 only. Nevertheless, among all taxa studied herein the absence of a distinct DC1 always seemed to reflect the fusion of the latter to the first metacarpal (by possessing an expanded proximal epiphysis on MC I). Therefore, all taxa scored with the absent condition herein are primarily homologous based on similarity, likely all due to the fusion of the DC1 to the first metacarpal.

Distal carpal 5

325. Distal carpal 5: present (0)/ absent (1) (NEW).
Remarks: Absent in a variety of taxa, including *Hupehsuchus,* ichthyosaurs, *Askeptosaurus*, at least some sauropterygians, *Protorosaurus* and *Mesosuchus*.

Anterior metapodials (metacarpals)

Femora

326. Femora: present (0)/ absent (1) (G12, Ch. 548).

327. Femora, internal trochanter: present (0)/ absent (1) (G12, Ch. 550; Fig. 1.35 in (Russell & Bauer 2008)).
Remarks: The minor trochanter of turtles is considered to be primarily homologous with the internal trochanter of other reptiles, whereas the greater trochanter is unique to them and distinct from the mammalian one (Romer 1956). Despite the femur being present in some amphisbaenians and snakes, its highly reduced morphology makes the scoring of this character (and subsequent ones) inapplicable.

328. Femora, fourth trochanter: absent (0)/ present (1) (B85, Ch. I4).

329. Femora, intertrochanteric fossa: present (0)/ absent (1) (G88a, Ch. 184—modified; Fig. 1.35 in (Russell & Bauer 2008)).

Tibiae

330. Tibiae, distal epiphysis, notch: absent (0)/ present (1) (E88, Ch. 123—modified; Fig. 555 in G12).
Remarks: When the distal epiphysis notch is present it creates the saddle-shaped joint between the tibia and the astragalocalcaneum observed in some lizards. This feature is observable in ventral and dorsal aspects, but may not be seen in fossil taxa with the epiphyses not preserved (in which case they are scored as missing data).

Posterior mesopodials (= tarsals)

Astragalus

331. Astragalus and calcaneum: as totally separate elements (0)/ fused (1) (B85, Ch. X10).

332. Astragalus, shape, concave laterally: absent (0)/ present (1) (B85, Ch. C12-modified).
Remarks: This character refers to the lateral concavity of the astragalus that serves for the reception of the calcaneum in some archosauromorphs.

Calcaneum

333. Calcaneum, lateral tuber (or process) of the calcaneum: present (0)/ absent (1) (G88a, Ch. 198; Fig. 1.18 (Russell & Bauer 2008)).
Remarks: The lateral flange of the calcaneum is present in many reptiles but is most commonly observed among lepidosaurs.

334. Calcaneum, foramen for perforating artery, position: absent (0)/ between astragalus and cacaneum (1)/ between proximal ends of tibia and fibula (R94, Ch. 87).
Remarks: A notch on both the astragalus and calcaneum characterizes the opening between both for the perforating artery (Romer 1956, p. 392). The opening for the artery is displaced proximally in lepidosaurs and turtles (between the distal heads of the tibia and fibula), to allow for the formation of an active joint between the astragalus and calcaneum (Rieppel 1993b; O'Keefe *et al.* 2006). A similar active joint between the astragalus and calcaneum is seen in

captorhinids, but the perforating artery is, instead, displaced distally (Holmes 2003; O'Keefe *et al.* 2005; O'Keefe *et al.* 2006). This character refers to the mutually exclusive positions of the perforating artery. Therefore, character state "0" is consideres to be mutually exclusive to states "1" and "2" herein, and does not justify its splitting into two contingent characters.

Lateral centrale

335. Pedal lateral centrale: absent (0)/ present (1) (B85, Ch. X11; Fig. 8 in G88b).
Occurrence: The pedal lateral central is absent in lepidosaurs.

Distal tarsal 1 (Dt1)

336. Distal tarsal 1: present (0)/ absent (1) (B85, Ch. X12).

Distal tarsal 2 (Dt2)

337. Distal tarsal 2: present (0)/ absent (1) (Ev88, Ch. L20).
Remarks: Absent in squamates, and some rhynchocephalians, protorosaurs, and sauropterygians.

Distal tarsal 4 (Dt4)

338. Distal tarsal 4, proximal peg: present (0)/ absent (1) (Ev88, Ch. J1; Fig. 1.20 (Russell & Bauer 2008)).
Remarks: This proximal peg is better observed in ventral aspect of the tarsus of lizards, in articulation with the astragalocalcaneum. The proximal peg is responsible for the mesotarsal articulation in lizards, and is also observed in other reptilian groups. The presence of a distomesial articulatory surface on the astragalocalcaneum that articulates with this proximal peg is dependent upon this character, and therefore it is not included as a character here to avoid redundancy.

Distal tarsal 5 (Dt5):

339. Distal tarsal 5: present (0)/ absent (1) (R99, Ch. 114).
Remarks: The absence of the distal tarsal 5 may be due to its fusion to the metatarsal V, forming a hooked fifth metatarsal. However, numerous taxa that lack distal tarsal 5 do not have a hooked fifth metatarsal (e.g. sauropterygians, thalattosaurs, *Protorosaurus,* ichthyosaurs and *Odontochelys*). Therefore, I coded both features as separate characters herein.

Posterior metapodials (metatarsals)

Metatarsal 5 (Mt5)

340. Metatarsal 5, hooked: absent (0)/ present (1) (B85, Ch. C14; Fig. 1.20 (Russell & Bauer 2008)).
Remarks: Benton (1985) described this character originally as a non-lepidosaur type of hooked fifth metatarsal, such as lacking the plantar tubercle observed in lepidosaurs. However, the latter feature is placed herein as a distinct character.

341. Metatarsal 5, plantar tubercle: absent (0)/ present (1) (DBR97, Ch. 156; Fig. 1.20 (Russell & Bauer 2008)).

Other ossifications

342. Gastralia: absent (0)/ present (1) (G88b, Ch. 136).
Remarks: These are dermal ossifications that should not be confused with the inscriptional ribs (of endochondral ossification) structure present in lizards, sometimes erroneously referred to as "abdominal ribs", "gastralia", "parasternal chevrons" or "parasternal ribs" (Etheridge 1965).

343. Dorsal trunk osteoderms: absent (0)/ present (1) (B85, Ch. K9).

344. Dorsal trunk osteoderms, imbrication: not imbricated (1)/ imbricated (2) (G12, Ch. 570).

345. Plastron plate: absent (0)/ present (1) (Ly13, Ch. 11).
Remarks: The gastral plates in the plastron of turtles are considered a derivative from the ventral ribs (gastralia) of most other reptiles (Scheyer *et al.* 2008; Lyson *et al.* 2013b; Rice *et al.* 2016). Because I adopted a contingent coding scheme here, the plastron condition is scored as a distinct character, instead of forming an ordered multistate character related to the gastralia.

346. Neural plates: absent (0)/ present (1) (Ly13, Ch. 8).
Remarks: The homology of the neural and costal plates of turtles has long been debate, but more recent data suggests they are periosteal derivatives of the axial skeleton, thus not being independent centres of ossification (Scheyer *et al.* 2008). Yet, their distinct morphology, topology and connectivity indicate that (even if connected to the vertebrae and ribs), the neural and costal plates can be characterized as a distinct locator, and thus an independent character of its own. The same occurs for the distal ribs seen in kuehneosaurids and the inscriptional ribs of many squamates.

347. Costal plates: absent (0)/ present (1) (NEW).
Remarks: see character 346, above.

Synonyms between some of the anatomical terms used herein and terms used by other authors.

Meckel's (or Meckelian) canal (Oelrich 1956) = mandibular canal (Lee *et al.* 2001); Internal mental canal (Gauthier 1982) = intramandibular canal (Gauthier *et al.* 2012); Posterior surangular foramen (Oelrich 1956) = foramen nervi auriculotemporalis (Gaffney 1972); Posterior mylohyoidal foramen (Oelrich 1956) = foramen intermandiularis caudalis (Gaffney 1972) = posterior mekelian foramen (Benton 1983); Anterior mylohyoidal foramen (Oelrich 1956) =

foramen intermandiularis oralis (Gaffney 1972) = anterior mekelian foramen (Benton 1983); Suborbital fenestra = suborbital foramen = inferior orbital foramen (Oelrich 1956) = palatine fontanelle (Jollie 1960); Infraorbital foramen (Oelrich 1956; Kluge 1962) = maxillopalatine foramen = infraorbital canal (Jollie 1960) = foramen alveolare superior (Gaffney 1972); Trigeminal notch (McDowell & Bogert 1954) = prootic incisures (Romer 1956) = Incisura prootica; Supratemporal process of parietal (Oelrich 1956) = Postparietal process (Evans 2008); Quadrate conch (Jollie 1960) = tympanic recess (Clark & Hernández 1994); Adductor fossa (Romer 1956) = mandibular foramen (Oelrich 1956) = Mandibular fossa (Jollie 1960); Atlas zygapophyseal articulation (Hoffstetter & Gasc 1969) = Atlas postzygapohysis (used herein) = posterodorsal process (Čerňanský *et al.* 2014; Čerňanský 2016); Margo ventralis (Hoffstetter & Gasc 1969) = subcentral ridge (Auffenberg 1963) = posterior centrosynapophyseal lamina (Tschopp 2016); Margo lateralis (Hoffstetter & Gasc 1969) = interzygapophyseal ridge (Auffenberg 1963) = postzygoprezygapophyseal lamina (Tschopp 2016).

References

Aberer, A. J., Krompass, D. & Stamatakis, A. 2013. Pruning Rogue Taxa Improves Phylogenetic Accuracy: An Efficient Algorithm and Webservice. *Systematic Biology*, **62**(1), 162-166.

Agassiz, L. 1833-1845. Recherches sur les poissons fossiles. *Petipierre, Neuchatel*, 1-188.

Albino, A. M. & Brizuela, S. 2014. An Overview of the South American Fossil Squamates. *The Anatomical Record*, **297**(3), 349-368.

Albino, A. M. & Caldwell, M. W. 2003. Hábitos de vida de la serpiente cretácica *Dinilysia patagonica* Woodward. *Ameghiniana*, **40**(3), 407-414.

Alifanov, V. R. 1989. New Priscagamida (Lacertilia) from the Upper Cretaceous of Mongolia and their systematic position among Iguania. *Paleontological Journal*, **4**, 68-80.

Alifanov, V. R. 1993a. New lizards of the family Macrocephalosauridae (Sauria) from the Upper Cretaceous of Mongolia, critical remarks on the systematics of the Teiidae (sensu Estes, 1983). *Paleontological Journal*, **27**, 70-90.

Alifanov, V. R. 1993b. Some peculiarities of the Cretaceous and Palaeogene lizard faunas of the Mongolian People's Republic. *Kaupia*, **3**, 9-13.

Alifanov, V. R. 1996. Lizard families Priscagamidae and Hoplocercidae (Sauria, Iguania): Phylogenetic position and new representatives from the Late Cretaceous of Mongolia. *Paleontological Journal*, **3**, 100-118.

Alifanov, V. R. 2000a. The fossil record of Cretaceous lizards from Mongolia. Pp. 368-389 in M.J. Benton, M.A. Shishkin, D.M. Unwin & E.N. Kurochkin (eds) *The age of dinosaurs in Russia and Mongolia*. Cambridge University Press, Cambridge.

Alifanov, V. R. 2000b. *Macrocephalosaurs* and the early evolution of lizards of Central Asia [in Russian]. *Trudy Paleontologicheskogo Instituta*, **272**, 3–126.

Alifanov, V. R. 2009. New acrodont lizards (Lacertilia) from the Middle Eocene of southern Mongolia. *Paleontological Journal*, **43**(6), 675-685.

Apesteguia, S. & Carballido, J. L. 2014. A new eilenodontine (Lepidosauria, Sphenodontidae) from the Lower Cretaceous of central Patagonia. *Journal of Vertebrate Paleontology*, **34**(2), 303-317.

Apesteguía, S., Daza, J. D., Simões, T. R. & Rage, J. C. 2016. The first iguanian lizard from the Mesozoic of Africa. *Royal Society Open Science*, **3**(9), 160462.

Apesteguia, S. & Novas, F. E. 2003. Large Cretaceous sphenodontian from Patagonia provides insight into lepidosaur evolution in Gondwana. *Nature*, **425**(6958), 609-612.

Apesteguía, S. & Zaher, H. 2006. A Cretaceous terrestrial snake with robust hindlimbs and a sacrum. *Nature*, **440**(7087), 1037-1040.

Araújo, R. & Correia, F. 2015. Plesiosaur pectoral myology. *Palaeontologia Electronica*, **18**(1), 1-32.

Arnold, E. N. 1973. Relationships of the Palaearctic lizards assigned to the genera *Lacerta*, *Algyroides* and *Psammodromus* (Reptilia: Lacertidae). *Bulletin of the British Museum (Natural History), Zoology Series*, **25**, 291-366.

Arnold, E. N. 1998. Cranial Kinesis in Lizards: variations, uses, and origins. Pp. 323-357 in P. Eggleton & R.I. Vane-Wright (eds) *Phylogeny and Ecology*. Academic Press, London.

Auffenberg, W. 1963. The fossil snakes of Florida. *Tulane Studies in Zoology*, **10**(3), 131-216.

Augé, M. 2007a. Past and present distribution of iguanid lizards. *Arquivos do Museu Nacional, Rio de Janeiro*, **65**(4), 403-416.

Augé, M. 2007b. Past and present distribution of iguanid lizards. *Arquivos do Museu Nacional*, **65**(4), 403-416.

Averianov, A. O., Danilov, I. G., Skutschas, P. P., Kuzmin, I. T., Sues, H.-D. & Dyke, G. 2016. The Late Cretaceous vertebrate assemblages of western Kazakhstan. *New Mexico Museum of Natural History and Science Bulletin*, **71**, 5-17.

Azevedo, S. A. K. & Schultz, C. L. 1987. *Scaphonyx sulcognathus* (sp. nov.) um novo rincossaurídeo do Neotriássico do Rio Grande do Sul, Brasil. *Congresso Brasileiro Paleontologia*, 10, 99-113.

Bahl, K. 1937. Skull of *Varanus monitor*. *Records of the Indian Museum*, **39**, 133-174.

Barahona, F. & Barbadillo, L. J. 1998. Inter- and intraspecific variation in the post-natal skull of some lacertid lizards. *Journal of Zoology*, **245**(04), 393-405.

Barbour, T. & Stetson, H. C. 1929. The squamation of *Homoeosaurus*. *Bulletin of the Museum of Comparative Zoology*, **69**(4), 97-104.

Baron, M. G., Norman, D. B. & Barrett, P. M. 2017. A new hypothesis of dinosaur relationships and early dinosaur evolution. *Nature*, **543**(7646), 501-506.

Barthel, K. W., Swinburne, N. H. M. & Morris, S. C. 1990. *Solnhofen*. CUP Archive.

Bassani, F. 1886. Sui fossili e sull'eta degli schisti bituminosi triasici di Besano in Lombardia. *Atti Societa Italiana di Scienze Naturali*, **29**, 15-72.

Baur, G. 1887. Ueber den Ursprung der Extremitäten der Ichthyopterygia. *Oberrheinischer Geologischer Verein*, **20**, 17-20.

Beardmore, S. R., Orr, P. J., Manzocchi, T., Furrer, H. & Johnson, C. 2012. Death, decay and disarticulation: Modelling the skeletal taphonomy of marine reptiles demonstrated using *Serpianosaurus* (Reptilia; Sauropterygia). *Palaeogeography, Palaeoclimatology, Palaeoecology*, **337–338**, 1-13.

Bell, C. J., Evans, S. E. & Maisano, J. A. 2003. The skull of the gymnophthalmid lizard *Neusticurus ecpleopus* (Reptilia: Squamata). *Zoological Journal of the Linnean Society*, **139**(2), 283-304.

Bell, G. L. 1997. A phylogenetic revision of North American and Adriatic Mosasauroidea. Pp. 293-332 in J.M. Callaway & E.L. Nicholls (eds) *Ancient Marine Reptiles*. San Diego Academic Press, San Diego.

Bellairs, A. A. 1949. Observations on the snout of *Varanus*, and a comparison with that of other lizards and snakes. *Journal of Anatomy*, **83**(Pt 2), 116.

Benammi, M., Alvarado-Ortega, J. & Urrutia-Fucugauchi, J. 2006. Magnetostratigraphy of the lower cretaceous strata in Tlayúa Quarry, Tepexi de Rodriguez, state of Puebla, Mexico. *Earth, planets and space*, **58**(10), 1295-1302.

Benton, M. J. 1983. The Triassic Reptile *Hyperodapedon* from Elgin: Functional Morphology and Relationships. *Philosophical Transactions of the Royal Society of London. B, Biological Sciences*, **302**(1112), 605-718.

Benton, M. J. 1984. Tooth form, growth, and function in Triassic rhynchosaurs (Reptilia, Diapsida). *Palaeontology*, **27**(4), 737-776.

Benton, M. J. 1985. Classification and phylogeny of the diapsid reptiles. *Zoological Journal of the Linnean Society*, **84**(2), 97-164.

Benton, M. J. 1999. *Scleromochlus taylori* and the origin of dinosaurs and pterosaurs. *Philosophical Transactions of the Royal Society of London B: Biological Sciences*, **354**(1388), 1423-1446.

Benton, M. J. 2005. *Vertebrate Paleontology*. Blackwell, 455 pp.

Benton, M. J. & Clark, J. M. 1988. Archosaur phylogeny and the relationships of the Crocodylia. Pp. 295-338 in M.J. Benton (ed) *The Phylogeny and Classification of the Tetrapods, Volume 1: Amphibians, Reptiles, Birds*. Clarendon Press, Oxford.

Benton, M. J., Donoghue, P. C., Asher, R. J., Friedman, M., Near, T. J. & Vinther, J. 2015. Constraints on the timescale of animal evolutionary history. *Palaeontologia Electronica*, **18**(1), 1-106.

Benton, M. J. & Spencer, P. S. 1995. *Fossil Reptiles of Great Britain*. Springer Science & Business Media.

Benton, M. J., Zhang, Q., Hu, S., Chen, Z.-Q., Wen, W., Liu, J., Huang, J., Zhou, C., Xie, T., Tong, J. & Choo, B. 2013. Exceptional vertebrate biotas from the Triassic of China, and the expansion of marine ecosystems after the Permo-Triassic mass extinction. *Earth-Science Reviews*, **125**, 199-243.

Berman, D. S. 1973. *Spathorhynchus fossorium*, a Middle Eocene Amphisbaenian (Reptilia) from Wyoming. *Copeia*, **1973**(4), 704-721.

Berman, D. S. 1977. *Spathorhynchus natronicus,* a New Species of Rhineurid Amphisbaenian (Reptilia) from the Early Oligocene of Wyoming. *Journal of Paleontology*, **51**(5), 986-991.

Bernardi, M., Klein, H., Petti, F. M. & Ezcurra, M. D. 2015. The origin and early radiation of archosauriforms: integrating the skeletal and footprint record. *PLoS ONE*, **10**(6), e0128449.

Beutel, R. G., Friedrich, F., Hörnschemeyer, T., Pohl, H., Hünefeld, F., Beckmann, F., Meier, R., Misof, B., Whiting, M. F. & Vilhelmsen, L. 2011. Morphological and molecular evidence converge upon a robust phylogeny of the megadiverse Holometabola. *Cladistics*, **27**(4), 341-355.

Bever, G. S., Lyson, T. R., Field, D. J. & Bhullar, B.-A. S. 2015a. "*Eunotosaurus africanus*" (On-line), Digital Morphology.

Bever, G. S., Lyson, T. R., Field, D. J. & Bhullar, B.-A. S. 2015b. Evolutionary origin of the turtle skull. *Nature*, **525**, 239-242.

Bhullar, B.-A. S. & Bever, G. S. 2009. An archosaur-like laterosphenoid in early turtles (Reptilia: Pantestudines). *Breviora*, 1-11.

Bickelmann, C., Müller, J. & Reisz, R. R. 2009. The enigmatic diapsid *Acerosodontosaurus piveteaui* (Reptilia: Neodiapsida) from the Upper Permian of Madagascar and the paraphyly of "younginiform" reptiles. *Canadian Journal of Earth Sciences*, **46**(9), 651-661.

Blanco, A., Bolet, A., Blain, H.-A., Fondevilla, V. & Marmi, J. 2016. Late Cretaceous (Maastrichtian) amphibians and squamates from northeastern Iberia. *Cretaceous Research*, **57**, 624-638.

Blob, R. W. 1998. Evaluation of Vent Position from Lizard Skeletons for Estimation of Snout: Vent Length and Body Mass. *Copeia*, **1998**(3), 792-801.

Bolet, A. & Evans, S. E. 2010. A new lizard from the Early Cretaceous of Catalonia (Spain), and the Mesozoic lizards of the Iberian Peninsula. *Cretaceous Research*, **31**(4), 447-457.

Bolet, A. & Evans, S. E. 2011. New material of the enigmatic *Scandensia*, an Early Cretaceous lizard from the Iberian Peninsula. *Special Papers in Palaeontology*, **86**, 99-108.

Bolet, A. & Evans, S. E. 2012. A tiny lizard (Lepidosauria, Squamata) from the Lower Cretaceous of Spain. *Palaeontology*, **55**(3), 491-500.

Bolt, J. R. & DeMar, R. 1975. An explanatory model of the evolution of multiple rows of teeth in *Captorhinus aguti*. *Journal of Paleontology*, **49**(5), 814-832.

Borsuk-Białynicka, M. 1988. *Globaura venusta* gen. et sp. n. and *Eoxanta lacertifrons* gen. et sp. n.—non-Teiid Lacertoids from the Late Cretaceous of Mongolia. *Acta Palaeontologica Polonica*, **33**(3), 211-248.

Borsuk-Białynicka, M. 1990. *Gobekko cretacicus* gen. et sp. n., a new gekkonid lizard from the Cretaceous of the Gobi Desert. *Acta Palaeontologica Polonica*, **35**(1-2), 67-76.

Borsuk-Białynicka, M. 1996. The Late Cretaceous lizard *Pleurodontagama* and the origin of tooth permanency in Lepidosauria. *Acta Palaeontologica Polonica*, **41**, 231-252.

Borsuk-Białynicka, M. & Alifanov, V. R. 1991. First Asiatic 'iguanid' lizards in the Late Cretaceous of Mongolia. *Acta Palaeontologica Polonica*, **36**(3), 325-342.

Borsuk-Białynicka, M. & Moody, S. M. 1984. Priscagaminae. A new subfamily of the Agamidae (Sauria) from the Late Cretaceous of the Gobi Desert. *Acta Palaeontologica Polonica*, **29**(1-2), 51-81.

Borsuk–Białynicka, M. & Evans, S. E. 2009. A long-necked archosauromorph from the Early Triassic of Poland. *Palaeontol Polonica*, **65**, 203-234.

Botha-Brink, J. & Smith, R. M. H. 2011. Osteohistology of the Triassic archosauromorphs *Prolacerta*, *Proterosuchus*, *Euparkeria*, and *Erythrosuchus* from the Karoo Basin of South Africa. *Journal of Vertebrate Paleontology*, **31**(6), 1238-1254.

Bouckaert, R., Heled, J., Kühnert, D., Vaughan, T., Wu, C.-H., Xie, D., Suchard, M. A., Rambaut, A. & Drummond, A. J. 2014. BEAST 2: A Software Platform for Bayesian Evolutionary Analysis. *PLoS Comput Biol*, **10**(4), e1003537.

Boulenger, G. A. 1891. On British Remains of *Homœosaurus*, with Remarks on the Classification of the Rhynchocephalia. *Proceedings of the Zoological Society of London*, **59**(1), 167-172.

Brazeau, M. D. 2011. Problematic character coding methods in morphology and their effects. *Biological Journal of the Linnean Society*, **104**(3), 489-498.

Brink, A. S. 1955. Notes on some thecodonts. *Navorsinge van die Nasionale Museum: Researches of the National Museum*, **1**(6), 141-148.

Brinkman, B., Zhao, X. & Nicholls, E. 1992. A primitive ichthyosaurfrom the Lower Triassic of British Columbia, Canada. *Palaeontology*, **35**(Part 2), 465-474.

Brinkman, D. 1980. Structural correlates of tarsal and metatarsal functioning in *Iguana* (Lacertilia; Iguanidae) and other lizards. *Canadian Journal of Zoology*, **58**(2), 277-289.

Brizuela, S. & Albino, A. M. 2011. A Scincomorph lizard from the Campanian of Patagonia. *Cretaceous Research*, **32**, 781-785.

Broili, F. 1925. Beobachtungen an der Gattung *Homeosaurus* H. v. Meyer. *Sitzungsberichte Bayerische Akademie der Wissenschaften zu München Mathematisch-Naturwissenschaftliche Abteilung*, **1925**, 81-121.

Broili, F. 1938. Ein neuer Fund von ? *Ardeosaurus* H. v. Meyer. *Sitzungsberichte Bayerische Akademie der Wissenschaften zu München Mathematisch-Naturwissenschaftliche Abteilung*, **1938**, 97-114.

Broom, R. 1903a. On a new reptile (*Proterosuchus fergusi*) from the Karoo beds of Tarkastad, South Africa. *Annals of the South African Museum*, **4**, 159-164.

Broom, R. 1903b. On the skull of a true lizard (*Paliguana whitei*) from the Triassic beds of South Africa. *Records of the Albany Museum*, **1**(1), 1-3.

Broom, R. 1905a. Notice of some new fossil reptiles from the Karroo beds of South Africa. *Records of the Albany Museum*, **1**, 331-337.

Broom, R. 1905b. Preliminary notice of some new fossil reptiles collected by Mr. Alfred Brown at Aliwal North, South Africa. *Records of the Albany Museum*, **1**, 269-275.

Broom, R. 1906a. On the remains of *Erythrosuchus africanus*. *Annals of the South African Museum*, **5**, 187-196.

Broom, R. 1906b. On the South African diaptosaurian reptile *Howesia*. *Proceedings of the Zoological Society of London*, **1906**, 591-600.

Broom, R. 1913a. Note on *Mesosuchus browni*, Watson, and on a new South African Triassic pseudosuchian (*Euparkeria capensis*). *Records of the Albany Museum*, **2**, 394-396.

Broom, R. 1913b. On the South-African Pseudosuchian *Euparkeria* and Allied Genera. *Proceedings of the Zoological Society of London*, **83**(3), 619-633.

Broom, R. 1913c. On the structure and affinities of *Bolosaurus*. *Bulletin of the American Museum of Natural History*, **32**(33), 509-516.

Broom, R. 1914. A new thecodont reptile. *Proceedings of the Zoological Society of London*, 1072-1077.

Broom, R. 1925. On the Origin of Lizards. *Proceedings of the Zoological Society of London*, **95**(1), 1-16.

Broom, R. 1926. On a nearly complete skeleton of a new eosuchian reptile (*Palaeagama vielhaueri*, gen. et sp. nov.). *Proceedings of the Zoological Society of London*, **96**(2), 487-492.

Broom, R. 1931. On the skull of the primitive reptile *Araeoscelis*. *Proceedings of the Zoological Society of London*, 741-744.

Broom, R. 1937. A Further Contribution to our Knowledge of the Fossil Reptiles of the Karroo. *Proceedings of the Zoological Society of London*, **B107**(3), 299-318.

Broom, R. & Robinson, J. T. 1948. Some Now Fossil Reptiles from the Karoo Beds of South Africa. *Proceedings of the Zoological Society of London*, **118**(2), 392-407.

Brower, A. V. Z. & Schawaroch, V. 1996. Three steps of homology assessment. *Cladistics*, **12**(3), 265-272.

Brown, B. 1905. The osteology of *Champsosaurus* Cope. *Memoirs of the American Museum of Natural History*, **9**, 1-26.

Budney, L. A. 2004. *A survey of tooth attachment histology in Squamata: The evaluation of tooth attachment classifications and characters*. Unpublished PhD thesis, University of Alberta, 299 pp.

Budney, L. A., Caldwell, M. W. & Albino, A. M. 2006. Tooth socket histology in the Cretaceous snake *Dinilysia*, with a review of amniote dental attachment tissues. *Journal of Vertebrate Paleontology*, **26**(1), 138-145.

Bulanov, V. V. & Sennikov, A. G. 2006. The first gliding reptiles from the upper Permian of Russia. *Paleontological Journal*, **40**(5), S567-S570.

Bulanov, V. V. & Sennikov, A. G. 2010. New data on the morphology of permian gliding weigeltisaurid reptiles of Eastern Europe. *Paleontological Journal*, **44**(6), 682-694.

Bulanov, V. V. & Sennikov, A. G. 2015a. *Glaurung schneideri* gen. et sp. nov., a new weigeltisaurid (Reptilia) from the Kupfershiefer (Upper Permian) of Germany. *Paleontological Journal*, **49**(12), 1353-1364.

Bulanov, V. V. & Sennikov, A. G. 2015b. New data on the morphology of the Late Permian gliding reptile *Coelurosauravus elivensis* Piveteau. *Paleontological Journal*, **49**(4), 413-423.

Buscalioni, A. D. & Fregenal-Martínez, M. A. 2010. A holistic approach to the palaeoecology of Las Hoyas Konservat-Lagerstätte (La Huérguina Formation, Lower Cretaceous, Iberian Ranges, Spain). *Journal of Iberian Geology*, **36**(2), 297-326.

Butler, M. A. & Losos, J. B. 2002. Multivariate sexual dimorphism, sexual selection, and adaptation in Greater Antillean *Anolis* lizards. *Ecological Monographs*, **72**(4), 541-559.

Butler, R. J., Brusatte, S. L., Reich, M., Nesbitt, S. J., Schoch, R. R. & Hornung, J. J. 2011. The sail-backed reptile *Ctenosauriscus* from the latest Early Triassic of Germany and the timing and biogeography of the early archosaur radiation. *PLoS ONE*, **6**(10), e25693.

Caldwell, M. W. 1995. Developmental Constraints and Limb Evolution in Permian and Extant Lepidosauromorph Diapsids. *Journal of Vertebrate Paleontology*, **14**(4), 459-471.

Caldwell, M. W. 1996. Ichthyosauria: a preliminary phylogenetic analysis of diapsid affinities. *Neues Jahrbuch für Geologie und Paläontologie - Abhandlungen*, **200**(3), 361 - 386.

Caldwell, M. W. 1999. Squamate phylogeny and the relationships of snakes and mosasauroids. *Zoological Journal of the Linnean Society*, **125**, 115-147.

Caldwell, M. W. 2000. On the Phylogenetic Relationships of *Pachyrhachis* within Snakes: A Response to Zaher (1998). *Journal of Vertebrate Paleontology*, **20**(1), 187-190.

Caldwell, M. W. 2002. From fins to limbs to fins: Limb evolution in fossil marine reptiles. *American Journal of Medical Genetics*, **112**(3), 236-249.

Caldwell, M. W. 2006. A new species of *Pontosaurus* (Squamata, Pythonomorpha) from the Upper Cretaceous of Lebanon and a phylogenetic analysis of Pythonomorpha. *Memorie della Società italiana di scienze naturali e Museo civico di storia naturale di Milano*, **34**(3), 1-43.

Caldwell, M. W. 2012. A challenge to categories: "What, if anything, is a mosasaur?". *Bulletin de la Societe Geologique de France*, **183**(1), 7-34.

Caldwell, M. W. & Albino, A. M. 2001. Palaeoenvironment and palaeoecology of three Cretaceous snakes: *Pachyophis*, *Pachyrhachis*, and *Dinilysia*. *Acta Palaeontologica Polonica*, **46**(2), 203-218.

Caldwell, M. W. & Albino, A. M. 2002. Exceptionally Preserved Skeletons of the Cretaceous Snake *Dinilysia patagonica* Woodward, 1901. *Journal of Vertebrate Paleontology*, **22**(4), 861-866.

Caldwell, M. W. & Calvo, J. 2008. Details of a new skull and articulated cervical column of *Dinilysia patagonica* Woodward, 1901. *Journal of Vertebrate Paleontology*, **28**(2), 349-362.

Caldwell, M. W. & Dutchak, A. R. 2006. Redescription of *Aigialosaurus dalmaticus* Kramberger, 1892, a Cenomanian mosasauroid lizard from Hvar Island, Croatia. *Canadian Journal of Earth Sciences*, **43**(12), 1821-1834.

Caldwell, M. W. & Lee, M. S. Y. 1997. A snake with legs from the marine Cretaceous of the Middle East. *Nature*, **386**(6626), 705-709.

Caldwell, M. W., Nydam, R. L., Palci, A. & Apesteguía, S. 2015. The oldest known snakes from the Middle Jurassic-Lower Cretaceous provide insights on snake evolution. *Nature Communications*, **6**, 5996.

Caldwell, M. W. & Sasso, C. D. 2004. Soft-Tissue Preservation in a 95 Million Year Old Marine Lizard: Form, Function, and Aquatic Adaptation. *Journal of Vertebrate Paleontology*, **24**(4), 980-985.

Calzavara, M., Muscio, G. & Wild, R. 1980. *Megalancosaurus preonensis* n.gn. sp., a new reptile from the Norian of Friuli. *Gortania*, **2**, 59-64.

Camp, C. 1923. Classification of the lizards. *Bulletin of the American Museum of Natural History*, **48**, 289-481.

Camp, C. 1945. *Prolacerta* and the protorosaurian reptiles. *American Journal of Science*, **243**(1), 17-32.

Carine, M. A. & Scotland, R. W. 1999. Taxic and Transformational Homology: Different Ways of Seeing. *Cladistics*, **15**(2), 121-129.

Carothers, J. H. 1984. Sexual Selection and Sexual Dimorphism in Some Herbivorous Lizards. *The American Naturalist*, **124**(2), 244-254.

Carroll, R. L. 1969a. The Origin of Reptiles. Pp. 1-44 in C. Gans, A.d.A. Bellairs & T.S. Parsons (eds) *Biology of the Reptilia*. Academic Press, London and New York.

Carroll, R. L. 1969b. Problems of the origin of reptiles. *Biological Reviews*, **44**(3), 393-431.

Carroll, R. L. 1975. Permo-Triassic 'lizards' from the Karroo. *Palaeontologia Africana*, **18**, 71-87.

Carroll, R. L. 1976. *Noteosuchus*, the oldest known rhynchosaur. *Annals of the South African Museum*, **72**, 37-57.

Carroll, R. L. 1977. The origin of lizards. Pp. 1-28 in S.M. Andrews, R.S. Miles & A.D. Walker (eds) *Problems in Vertebrate Evolution*. Academic Press, London and New York.

Carroll, R. L. 1978. Permo-triassic" lizards" from the Karoo System. Part II: A gliding reptile from the upper Permian of Madagascar. *Palaeontologia Africana*, **21**, 143-159.

Carroll, R. L. 1981. Plesiosaur Ancestors from the Upper Permian of Madagascar. *Philosophical Transactions of the Royal Society of London. Series B, Biological Sciences*, **293**(1066), 315-383.

Carroll, R. L. 1985a. Evolutionary constraints in aquatic diapsid reptiles. *Special Papers in Palaeontology*, **33**, 145-155.

Carroll, R. L. 1985b. A pleurosaur from the Lower Jurassic and the taxonomic position of the Sphenodontida. *Palaeontographica Abteilung A*, **189**(1-3), 1-28.

Carroll, R. L. 1988. Late Paleozoic and early Mesozoic lepidosauromorphs and their relation to lizard ancestry. Pp. 99-118 in R. Estes & G. Pregill (eds) *The phylogenetic relationships of the lizard families*. Stanford University Press, Stanford.

Carroll, R. L. 2013. Problems of the ancestry of turtles. Pp. 19-36 in D. Brinkman, P.A. Holroyd & J.D. Gardner (eds) *Morphology and Evolution of Turtles*. Springer, Dordrecht.

Carroll, R. L. & Currie, P. J. 1991. The early radiation of diapsid reptiles. Pp. 354-424 in H.-P. Schultze & L. Trueb (eds) *Origins of the higher groups of tetrapods: controversy and consensus*. Cornstock Publishing Associates, Ithaca and London.

Carroll, R. L. & de Braga, M. 1992. Aigialosaurs: Mid-Cretaceous Varanoid Lizards. *Journal of Vertebrate Paleontology*, **12**(1), 66-86.

Carroll, R. L. & Wild, R. 1994. Marine members of the Sphenodontia. Pp. 70-83 in N.C. Fraser & H.D. Sues (eds) *In the shadow of the dinosaurs: early Mesozoic tetrapods*. Cambridge University Press, New York.

Carroll, R. L. & Zhi-Ming, D. 1991. *Hupehsuchus*, an Enigmatic Aquatic Reptile from the Triassic of China, and the Problem of Establishing Relationships. *Philosophical Transactions: Biological Sciences*, **331**(1260), 131-153.

Cartmill, M. 1985. Climbing. Pp. 73-88 in M. Hildebrand, D.M. Bramble, K.F. Liem & D. Wake (eds) *Functional Vertebrate Morphology*. Belknap Press of Harvard University Press, Cambridge, MA.

Case, E. C. 1907. Description of the skull of *Bolosaurus striatus* Cope. *Bulletin of the American Museum of Natural History*, **23**, 653-658.

Case, E. C. 1911. A revision of the Cotylosauria of North America. *Carnegie Institute of Washington Publication*, **145**, 1-122.

Case, E. C. 1928a. A cotylosaur from the Upper Triassic of western Texas. *Journal of the Washington Academy of Sciences*, **18**(7), 177-178.

Case, E. C. 1928b. Indications of a Cotylosaur and of a New Form of Fish from the Triassic Beds of Texas: With Remarks on the Shinarump Conglomerate. *Contributions from the Museum of Paleontology: University of Michigan*, **3**(1), 1-14.

Castiello, M., Renesto, S. & Bennett, S. C. 2015. The role of the forelimb in prey capture in the Late Triassic reptile *Megalancosaurus* (Diapsida, Drepanosauromorpha). *Historical Biology*, **Ahead of print**, 1-11.

Catalano, S. A. & Goloboff, P. A. 2012. Simultaneously Mapping and Superimposing Landmark Configurations with Parsimony as Optimality Criterion. *Systematic Biology*, **61**(3), 392-400.

Catalano, S. A., Goloboff, P. A. & Giannini, N. P. 2010. Phylogenetic morphometrics (I): the use of landmark data in a phylogenetic framework. *Cladistics*, **26**(5), 539-549.

Čerňanský, A. 2016. From lizard body form to serpentiform morphology: The atlas–axis complex in African cordyliformes and their relatives. *Journal of Morphology*, **277**(4), 512-536.

Čerňanský, A., Boistel, R., Fernandez, V., Tafforeau, P., Nicolas, L. N. & Herrel, A. 2014. The Atlas-Axis Complex in Chamaeleonids (Squamata: Chamaeleonidae), with Description of a New Anatomical Structure of the Skull. *The Anatomical Record*, n/a-n/a.

Chan, Y. F., Marks, M. E., Jones, F. C., Villarreal, G., Shapiro, M. D., Brady, S. D., Southwick, A. M., Absher, D. M., Grimwood, J., Schmutz, J., Myers, R. M., Petrov, D., Jónsson, B., Schluter, D., Bell, M. A. & Kingsley, D. M. 2010. Adaptive Evolution of Pelvic Reduction in Sticklebacks by Recurrent Deletion of a Pitx1 Enhancer. *Science*, **327**(5963), 302-305.

Charig, A. J. & Reig, O. A. 1970. The classification of the Proterosuchia. *Biological Journal of the Linnean Society*, **2**(2), 125-171.

Charig, A. J. & Sues, H.-D. 1976. *Handbuch der Paläoherpetologie: Thecodontia-Part 13*. Gustav Fischer Verlag, Stuttgart.

Chen, X.-h., Motani, R., Cheng, L., Jiang, D.-Y. & Rieppel, O. 2014. The Enigmatic Marine Reptile *Nanchangosaurus* from the Lower Triassic of Hubei, China and the Phylogenetic Affinities of Hupehsuchia. *PLoS ONE*, **9**(7), e102361.

Chen, Z.-Q. & Benton, M. J. 2012. The timing and pattern of biotic recovery following the end-Permian mass extinction. *Nature Geosciences*, **5**(6), 375-383.

Christian, A. & Garland, T. 1996. Scaling of limb proportions in monitor lizards (Squamata: Varanidae). *Journal of Herpetology*, **30**(2), 219-230.

Cisneros, J. C., Marsicano, C., Angielczyk, K. D., Smith, R. M. H., Richter, M., Frobisch, J., Kammerer, C. F. & Sadleir, R. W. 2015. New Permian fauna from tropical Gondwana. *Nature Communications*, **6**.

Clark, J. & Carroll, R. L. 1973. Romeriid reptiles from the Lower Permian. *Bulletin of the Museum of Comparative Zoology*, **144**(5), 353-407.

Clark, J. M. & Hernández, R. 1994. A New Burrowing Diapsid from the Jurassic La Boca Formation of Tamaulipas, Mexico. *Journal of Vertebrate Paleontology*, **14**(2), 180-195.

Clark, J. M., Welman, J., Gauthier, J. A. & Parrish, J. M. 1993. The laterosphenoid bone of early archosauriforms. *Journal of Vertebrate Paleontology*, **13**(1), 48-57.

Coates, M. & Ruta, M. 2000. Nice snake, shame about the legs. *Trends in Ecology & Evolution*, **15**(12), 503-507.

Cocude-Michel, M. 1959. Le carpe de *Homeosaurus,* sphenodontide Jurassique. *Bulletin de la Societe Geologique de France*, **7**(3), 230-232.

Cocude-Michel, M. 1961. Les Sauriens des calcaires lithographiques de Bavière, d'âge portlandien inferieur. *Bulletin de la Societe Geologique de France*, **7**(6), 707-710.

Cocude-Michel, M. 1963a. Les Rhynchocephales et les Sauriens des calcaires lithographiques (Jurassique Superieur) d'Europe occidentale. *Nouvelles archives du Muséum d'Histoire Naturelle de Lyon*, **7**, 1-187.

Cocude-Michel, M. 1963b. *Les Rhynchocephales et les Sauriens des calcaires lithographiques (Jurassique Superieur) d'Europe occidentale*. Unpublished PhD thesis, Nouvelles archives du Muséum d'Histoire Naturelle de Lyon, 187 pp.

Colbert, E. H. 1966. A gliding reptile from the Triassic of New Jersey. *American Museum Novitates*, **2246**, 1-23.

Colbert, E. H. 1970. The Triassic gliding reptile *Icarosaurus*. *Bulletin of the American Museum of Natural History*, **143**(2), 85-142.

Colbert, E. H. 1987. The Triassic reptile *Prolacerta* in Antarctica. *American Museum Novitates*, **2882**, 1-19.

Colosimo, P. F., Hosemann, K. E., Balabhadra, S., Jr, G. V., Dickson, M., Grimwood, J., Schmutz, J., Myers, R. M., Schluter, D. & Kingsley, D. M. 2005. Widespread Parallel Evolution in Sticklebacks by Repeated Fixation of Ectodysplasin Alleles. *Science*, **307**(5717), 1928-1933.

Conrad, J. L. 2008. Phylogeny and systematics of Squamata (Reptilia) based on morphology. *Bulletin of the American Museum of Natural History*, **310**, 1-182.

Conrad, J. L. 2017. A new lizard (Squamata) was the last meal of *Compsognathus* (Theropoda: Dinosauria) and is a holotype in a holotype. *Zoological Journal of the Linnean Society*, **Online first**, DOI: 10.1093/zoolinnean/zlx1055.

Conrad, J. L. & Daza, J. D. 2015. Naming and rediagnosing the Cretaceous gekkonomorph (Reptilia, Squamata) from Öösh (Övörkhangai, Mongolia). *Journal of Vertebrate Paleontology*, e980891.

Conrad, J. L. & Norell, M. A. 2006. High-resolution X-ray computed tomography of an Early Cretaceous gekkonomorph (Squamata) from Öösh (Övörkhangai; Mongolia). *Historical Biology*, **18**(4), 405-431.

Conrad, J. L. & Norell, M. A. 2007. A complete Late Cretaceous Iguanian (Squamata, Reptilia) from the Gobi and identification of a new Iguanian clade. *American Museum Novitates*, **3584**, 1 - 47.

Conrad, J. L., Wang, Y., Xu, X., Pyron, A. & Clark, J. 2013. Skeleton of a Heavily Armored and Long Legged Middle Jurassic Lizard (Squamata, Reptilia). *72nd Annual Meeting - Society of Vertebrate Paleontology*, Journal of Vertebrate Paleontology, SVP Program and Abstracts Book, 108.

Cooper, J. S. & Poole, D. F. G. 1973. The dentition and dental tissues of the agamid lizard, *Uromastyx*. *Journal of Zoology*, **169**(1), 85-100.

Cooper, J. S., Poole, D. F. G. & Lawson, R. 1970. The dentition of agamid lizards with special reference to tooth replacement. *Journal of Zoology*, **162**(1), 85-98.

Cope, E. D. 1882. Third contribution to the history of the Vertebrata of the Permian formation of Texas. *Proceedings of the American Philosophical Society*, **20**(112), 447-461.

Cope, E. D. 1895. The Reptilian Order Cotylosauria. *Proceedings of the American Philosophical Society*, **34**(149), 436-457.

Cope, E. D. 1896a. The reptilian order Cotylosauria. *Proceedings of the American Philosophical Society*, **34**(149), 436-457.

Cope, E. D. 1896b. Second Contribution to the History of the Cotylosauria. *Proceedings of the American Philosophical Society*, **35**(151), 122-139.

Corbella, H., Novas, F., Apesteguía, S. & Leanza, H. 2004. First fission-track age for the dinosaur-bearing Neuquén Group (Upper Cretaceous), Neuquén basin, Argentina. *Revista del Museo Argentino de Ciencias Naturales nueva serie*, **6**(2), 227-232.

Cox, C. B. 1969. The problematic Permian reptile *Eunotosaurus*. *Bulletin of the British Museum (Natural History), Geology*, **18**(5), 165-196.

Crandell, K. E., Herrel, A., Sasa, M., Losos, J. B. & Autumn, K. 2014. Stick or grip? Co-evolution of adhesive toepads and claws in *Anolis* lizards. *Zoology*, **117**(6), 363-369.

Cruickshank, A. R. I. 1972. The proterosuchian thecodonts. Pp. 89-119 in K.A. Joysey & T.S. Kemp (eds) *Studies in vertebrate evolution*. Oliver and Boyd, Edinburgh.

Cruickshank, A. R. I. 1978. The pes of *Erythrosuchus africanus* Broom. *Zoological Journal of the Linnean Society*, **62**(2), 161-177.

Currie, A. M. 2012. Convergence, contingency & morphospace. *Biology & Philosophy*, **27**(4), 583-593.

Currie, A. M. 2013. Convergence as Evidence. *The British Journal for the Philosophy of Science*, **64**(4), 763-786.

Currie, P. J. 1980. A new younginid (Reptilia: Eosuchia) from the Upper Permian of Madagascar. *Canadian Journal of Earth Sciences*, **17**(4), 500-511.

Currie, P. J. 1981a. *Hovasaurus boulei*, an aquatic eosuchian from the Upper Permian of Madagascar. *Palaeontologia Africana*, **24**, 99-168.

Currie, P. J. 1981b. The vertebrae of *Youngina* (Reptilia: Eosuchia). *Canadian Journal of Earth Sciences*, **18**(4), 815-818.

Curtis, N., Jones, M. E. H., Lappin, A. K., O'Higgins, P., Evans, S. E. & Fagan, M. J. 2010. Comparison between *in vivo* and theoretical bite performance: Using multi-body modelling to predict muscle and bite forces in a reptile skull. *Journal of Biomechanics*, **43**(14), 2804-2809.

Cuthbertson, R. S., Russell, A. P. & Anderson, J. S. 2013a. Cranial morphology and relationships of a new grippidian (Ichthyopterygia) from the Vega-Phroso Siltstone Member (Lower Triassic) of British Columbia, Canada. *Journal of Vertebrate Paleontology*, **33**(4), 831-847.

Cuthbertson, R. S., Russell, A. P. & Anderson, J. S. 2013b. Reinterpretation of the cranial morphology of *Utatsusaurus hataii* (Ichthyopterygia) (Osawa Formation, Lower Triassic, Miyagi, Japan) and its systematic implications. *Journal of Vertebrate Paleontology*, **33**(4), 817-830.

Cuthbertson, R. S., Russell, A. P. & Anderson, J. S. 2014. The first substantive evidence of *Utatsusaurus* (Ichthyopterygia) from the Sulphur Mountain Formation (Lower–Middle Triassic) of British Columbia, Canada: a skull roof description in comparison with other early taxa. *Canadian Journal of Earth Sciences*, **51**(2), 180-185.

Dal Sasso, C. & Pinna, G. 1997. *Aphanizocnemus libanensis* n. gen. n. sp, a new dolichosaur (Reptilia, Varanoidea) from the Upper Cretaceous of Lebanon. *Paleontologia Lombarda, Milano, Nuova serie*, **7**, 3-31.

Dashzeveg, D., Dingus, L., Loope, D. B., Swisher, C. C., Dulam, T. & Sweeney, M. R. 2005. New Stratigraphic Subdivision, Depositional Environment, and Age Estimate for the Upper

Cretaceous Djadokhta Formation, Southern Ulan Nur Basin, Mongolia. *American Museum Novitates*, 1-31.

Dashzeveg, D., Novacek, M. J., Norell, M. A., Clark, J. M., Chiappe, L. M., Davidson, A., McKenna, M. C., Dingus, L., Swisher, C. & Altangerel, P. 1995. Extraordinary preservation in a new vertebrate assemblage from the Late Cretaceous of Mongolia. *Nature*, **374**(6521), 446-449.

Day, M., Rubidge, B., Almond, J. & Jirah, S. 2013. Biostratigraphic correlation in the Karoo: The case of the Middle Permian parareptile *Eunotosaurus*. *South African Journal of Science*, **109**, 1-4.

Daza, J. D., Abdala, V., Thomas, R. & Bauer, A. M. 2008. Skull anatomy of the miniaturized gecko *Sphaerodactylus roosevelti* (Squamata: Gekkota). *Journal of Morphology*, **269**(11), 1340-1364.

Daza, J. D., Bauer, A. M. & Snively, E. 2013. *Gobekko cretacicus* (Reptilia: Squamata) and its bearing on the interpretation of gekkotan affinities. *Zoological Journal of the Linnean Society*, **167**(3), 430-448.

Daza, J. D., Bauer, A. M. & Snively, E. D. 2014. On the Fossil Record of the Gekkota. *The Anatomical Record*, **297**(3), 433-462.

Daza, J. D., Stanley, E. L., Wagner, P., Bauer, A. M. & Grimaldi, D. A. 2016. Mid-Cretaceous amber fossils illuminate the past diversity of tropical lizards. *Science advances*, **2**(3), e1501080.

de Braga, M. & Carroll, R. L. 1993. The origin of mosasaurs as a model of macroevolutionary patterns and processes. *Evolutionary Biology*, **27**, 245-322.

de Braga, M. & Reisz, R. R. 1996. The Early Permian Reptile *Acleistorhinus pteroticus* and Its Phylogenetic Position. *Journal of Vertebrate Paleontology*, **16**(3), 384-395.

de Braga, M. & Rieppel, O. 1997. Reptile phylogeny and the interrelationships of turtles. *Zoological Journal of the Linnean Society*, **120**, 281 - 354.

de Buffrénil, V. & Mazin, J. M. 1989. Bone histology of *Claudiosaurus germaini* (Reptilia, Claudiosauridae) and the problem of pachyostosis in aquatic tetrapods. *Historical Biology*, **2**(4), 311-322.

de Pinna, M. C. C. 1991. Concepts and tests of homology in the cladistic paradigm. *Cladistics*, **7**(4), 367-394.

de Ricqlès, A. & Bolt, J. R. 1983. Jaw growth and tooth replacement in *Captorhinus aguti* (Reptilia: Captorhinomorpha): a morphological and histological analysis. *Journal of Vertebrate Paleontology*, **3**(1), 7-24.

Demar, J. D. G., Conrad, J. L., Head, J. J., Varricchio, D. D. & WIlson, G. P. 2015. Phylogenetics and paleobiology of a late cretaceous stem iguanian from Montana. *Journal of Vertebrate Paleontology*, **35**(Supplement), 115.

Demar, R. & Bolt, J. R. 1981. Dentitional Organization and Function in a Triassic Reptile. *Journal of Paleontology*, **55**(5), 967-984.

Diamond, J. M. 1975. Assembly of species communities. Pp. 342-344 in M.L. Cody & J.M. Diamond (eds) *Ecology and evolution of communities*. Belknap Press Cambridge.

Diedrich, C. G. 2010. Palaeoecology of *Placodus gigas* (Reptilia) and other placodontids — Middle Triassic macroalgae feeders in the Germanic Basin of central Europe — and evidence for convergent evolution with Sirenia. *Palaeogeography, Palaeoclimatology, Palaeoecology*, **285**(3–4), 287-306.

Diedrich, C. G. 2011a. Fossil middle triassic "sea cows"–placodont reptiles as macroalgae feeders along the north-western Tethys coastline with pangaea and in the Germanic basin. *Natural Science*, **3**(1), 9-27.

Diedrich, C. G. 2011b. The shallow marine placodont *Cyamodus* of the central European Germanic Basin: its evolution, paleobiogeography and paleoecology. *Historical Biology*, **23**(4), 391-409.

Diedrich, C. G. 2013a. The marine pachypleurosaur *Serpianosaurus germanicus* nov. spec.–skeleton and isolated bone remains from the Pelsonian (Middle Triassic) of the european Germanic basin carbonate intertidals and its paleobiology and taphonomy. Pp. 159-168 in L.H. Tanner, J.A. Spielmann & S.G. Lucas (eds) *The Triassic System: New Developments in Stratigraphy and Paleontology*.

Diedrich, C. G. 2013b. The oldest "subaquatic flying" reptile in the world—*Pistosaurus longaevus* Meyer, 1839 (Sauropterygia) from the Middle Triassic of Europe. Pp. 169-215 in L.H. Tanner, J.A. Spielmann & S.G. Lucas (eds) *The Triassic System: New Developments in Stratigraphy and Paleontology*. New Mexico Museum of Natural History and Science, Albuquerque.

Diedrich, C. G. 2013c. Review of the Middle Triassic "sea cow" *Placodus gigas* (Reptilia) in Pangea's shallow marine macroalgae meadows of Europe. Pp. 104-131 in L.H. Tanner, J.A. Spielmann & S.G. Lucas (eds) *The Triassic System: New Developments in Stratigraphy and Paleontology*. New Mexico Museum of Natural History and Science, Albuquerque.

Dilkes, D. W. 1995. The rhynchosaur *Howesia browni* from the Lower Triassic of South Africa. *Palaeontology*, **38**(3), 665-686.

Dilkes, D. W. 1998. The early Triassic rhynchosaur *Mesosuchus browni* and the interrelationships of basal archosauromorph reptiles. *Philosophical Transactions of the Royal Society of London. Series B: Biological Sciences*, **353**(1368), 501-541.

Dingus, L., Loope, D. B., Dashzeveg, D., Swisher, C. C., Minjin, C., Novacek, M. J. & Norell, M. A. 2008. The Geology of Ukhaa Tolgod (Djadokhta Formation, Upper Cretaceous, Nemegt Basin, Mongolia). *American Museum Novitates*, 1-40.

dos Reis, M., Inoue, J., Hasegawa, M., Asher, R. J., Donoghue, P. C. J. & Yang, Z. 2012. Phylogenomic datasets provide both precision and accuracy in estimating the timescale of placental mammal phylogeny. *Proceedings of the Royal Society of London B: Biological Sciences*, **279**(1742), 3491-3500.

Dupret, V. 2004. The pleurosaurs: anatomy and phylogeny. *Revue de Paléobiologie, Genève*, **9**, 61-80.

Dutchak, A. R. 2005. A review of the taxonomy and systematics of aigialosaurs. *Netherlands Journal of Geosciences - Geologie en Mijnbouw*, **84**(3), 221-229.

Dwivedi, B. & Gadagkar, S. R. 2009. Phylogenetic inference under varying proportions of indel-induced alignment gaps. *BMC Evolutionary Biology*, **9**(1), 211.

Eberth, D. A. 1993. Depositional environments and fades transitions of dinosaur-bearing Upper Cretaceous redbeds at Bayan Mandahu (Inner Mongolia, People's Republic of China). *Canadian Journal of Earth Sciences*, **30**(10), 2196-2213.

Edmund, A. G. 1960. Tooth replacement phenomena in the lower vertebrates. *Contributions of the Royal Ontario Museum, Life Sciences Division*, **52**, 1-190.

Edmund, A. G. 1969. Dentition. Pp. 117-200 in C. Gans, A.d.A. Bellairs & T.S. Parsons (eds) *Biology of the Reptilia*. Academic Press, London and New York.

Elder, R. L. 1987. Taphonomy and Paleoecology of the Dockum Group, Howard County, Texas. *Journal of the Arizona-Nevada Academy of Science*, **22**(1), 85-94.

Erickson, G. M., Lappin, A. K. & Vliet, K. A. 2003. The ontogeny of bite-force performance in American alligator (*Alligator mississippiensis*). *Journal of Zoology*, **260**(3), 317-327.

Estes, R. 1969. Relationships of two cretaceous lizards (Sauria, Teiidae). *Breviora*, **317**, 1-8.

Estes, R. 1983a. The fossil record and early distribution of lizards. Pp. 365-398 in A. Rhodin & K. Miyata (eds) *Studies in Herpetology and Evolutionary Biology. Essays in Honor of Ernest Edward Williams.* Museum of Comparative Zoology, Harvard University, Cambridge, MA.

Estes, R. 1983b. *Handbuch der Paläoherpetologie: Sauria terrestria, Amphisbaenia, part 10A*. Gustav Fischer Verlag, Munich, 249 pp.

Estes, R. & Báez, A. M. 1985. Herpetofaunas of North and South America during the Late Cretaceous and Cenozoic: evidence for interchange? Pp. 139-197 in F. Stehli, G. & D.S. Webb (eds) *The Great American Biotic Interchange*. Plenum Press, New York and London.

Estes, R., de Queiroz, K. & Gauthier, J. A. 1988. Phylogenetic relationships within Squamata. Pp. 119-281 in R. Estes & G. Pregill (eds) *Phylogenetic relationships of the lizard families*. Stanford University Press, Stanford.

Estes, R., Frazzetta, T. H. & Williams, E. E. 1970. Studies on the fossil snake *Dinilysia patagonica* Woodward. *Bulletin of the Museum of Comparative Zoology*, **140**(2), 25-73.

Estes, R. & Price, L. I. 1973. Iguanid lizard from the Upper Cretaceous of Brazil. *Science*, **180**, 748-751.

Etheridge, R. 1965. The Abdominal Skeleton of Lizards in the Family Iguanidae. *Herpetologica*, **21**(3), 161-168.

Etheridge, R. & de Queiroz, K. 1988. A phylogeny of the Iguanidae. Pp. 283 - 367 in R. Estes & G. Pregill (eds) *Phylogenetic relationships of the lizard families*. Stanford University Press, Stanford.

Evans, S. E. 1980. The skull of a new eosuchian reptile from the Lower Jurassic of South Wales. *Zoological Journal of the Linnean Society*, **70**(3), 203-264.

Evans, S. E. 1981. The postcranial skeleton of the Lower Jurassic eosuchian *Gephyrosaurus bridensis*. *Zoological Journal of the Linnean Society*, **73**(1), 81-116.

Evans, S. E. 1982. The gliding reptiles of the Upper Permian. *Zoological Journal of the Linnean Society*, **76**(2), 97-123.

Evans, S. E. 1984. The classification of the Lepidosauria. *Zoological Journal of the Linnean Society*, **82**(1-2), 87-100.

Evans, S. E. 1985. Tooth replacement in the Lower Jurassic lepidosaur *Gephyrosaurus bridensis* *Neues Jahrbuch für Geologie und Paläontologie - Monatshefte*, **7**, 411-420.

Evans, S. E. 1986. The braincase of *Prolacerta broomi* (Reptilia, Triassic). *Neues Jahrbuch für Geologie und Paläontologie - Abhandlungen*, **173**, 181-200.

Evans, S. E. 1987. The braincase of *Youngina capensis* (Reptilia: Diapsida; Permian). *Neues Jahrbuch fur Geologie und Palaontologie Monatshefte*, **1987**, 181-200.

Evans, S. E. 1988. The early history and relationships of the Diapsida. Pp. 221-260 in M.J. Benton (ed) *The phylogeny and classification of the tetrapods*. Clarendon Press, Oxford.

Evans, S. E. 1989. New material of *Cteniogenys* (Reptilia: Diapsida; Jurassic) and a reassessment of the phylogenetic position of the genus. *Neues Jahrbuch für Geologie und Paläontologie Monatschefte*, **1989**, 577-589.

Evans, S. E. 1990. The skull of *Cteniogenys*, a choristodere (Reptilia: Archosauromorpha) from the Middle Jurassic of Oxfordshire. *Zoological Journal of the Linnean Society*, **99**(3), 205-237.

Evans, S. E. 1991a. A new lizard-like reptile (Diapsida: Lepidosauromorpha) from the Middle Jurassic of England. *Zoological Journal of the Linnean Society*, **103**(4), 391-412.

Evans, S. E. 1991b. The postcranial skeleton of the choristodere *Cteniogenys* (Reptilia: Diapsida) from the Middle Jurassic of England. *Geobios*, **24**(2), 187-199.

Evans, S. E. 1993. Jurassic lizard assemblages. *Revue de Paléobiologie*, **7**, 55-65.

Evans, S. E. 1994a. A new anguimorph lizard from the Jurassic and Lower Cretaceous of England. *Palaeontology*, **37**, 33-49.

Evans, S. E. 1994b. The Solnhofen (Jurassic: Tithonian) genus *Bavarisaurus*: new material and a new interpretation. *Neues Jahrbuch fur Geologie und Palaontologie. Abhandlungen*, **192**(1), 37-52.

Evans, S. E. 1998. Crown group lizards from the Middle Jurassic of Britain. *Palaeontographica Abteilung A Palaeozoologie-Stratigraphie*, **250**, 123-154.

Evans, S. E. 2003a. At the feet of the dinosaurs: the early history and radiation of lizards. *Biological Reviews*, **78**, 513-551.

Evans, S. E. 2003b. "*Nephrurus levis*" (On-line), Digital Morphology. .

Evans, S. E. 2008. The Skull of Lizards and Tuatara. Pp. 1 - 347 in C. Gans, A. Gaunt & K. Adler (eds) *Biology of the Reptilia*. Academic Press, Ithaca.

Evans, S. E. 2009. An early kuehneosaurid reptile from the Early Triassic of Poland. *Palaeontologica Polonica*, **65**, 145-178.

Evans, S. E. & Barbadillo, J. 1997. Early Cretaceous lizards from Las Hoyas, Spain. *Zoological Journal of the Linnean Society*, **119**(1), 23-49.

Evans, S. E. & Barbadillo, L. J. 1998. An unusual lizard (Reptilia: Squamata) from the Early Cretaceous of Las Hoyas, Spain. *Zoological Journal of the Linnean Society*, **124**(3), 235-265.

Evans, S. E. & Barbadillo, L. J. 1999. A short-limbed lizard from the Lower Cretaceous of Spain. *Special Papers in Palaeontology*, **60**, 73-85.

Evans, S. E. & Borsuk-Białynicka, M. 2009. A small lepidosauromorph reptile from the Early Triassic of Poland. *Palaeontologica Polonica*, **65**, 179-202.

Evans, S. E. & Chure, D. C. 1998. Paramacellodid lizard skulls from the Jurassic Morrison Formation at Dinosaur National Monument, Utah. *Journal of Vertebrate Paleontology*, **18**(1), 99-114.

Evans, S. E. & Haubold, H. 1987. A review of the Upper Permian genera *Coelurosauravus*, *Weigeltisaurus* and *Gracilisaurus* (Reptilia: Diapsida). *Zoological Journal of the Linnean Society*, **90**(3), 275-303.

Evans, S. E. & Jones, M. E. H. 2010. The Origin, Early History and Diversification of Lepidosauromorph Reptiles. Pp. 27-44 in S. Bandyopadhyay (ed) *New Aspects of Mesozoic Biodiversity*. Springer Berlin Heidelberg.

Evans, S. E. & Kermack, K. A. 1994. Assemblages of small tetrapods from the Early Jurassic of Britain. Pp. 271-283 in N.C. Fraser & H.-D. Sues (eds) *In the shadow of the dinosaurs: early Mesozoic tetrapods*. Cambridge University Press, New York.

Evans, S. E. & King, M. S. 1993. A new specimen of *Protorosaurus* (Reptilia: Diapsida) from the Marl Slate (late Permian) of Britain. *Proceedings of the Yorkshire Geological and Polytechnic Society*, **49**(3), 229-234.

Evans, S. E. & Manabe, M. 2009. The Early Cretaceous lizards of eastern Asia: new material of Sakurasaurus from Japan. *Special Papers in Palaeontology*, **81**, 43-59.

Evans, S. E. & Milner, A. R. 1994. Middle Jurassic microvertebrate assemblages from the British Isles. Pp. 303-321 in N.C. Fraser & H.-D. Sues (eds) *In the shadow of the dinosaurs: early Mesozoic tetrapods*. Cambridge University Press, New York.

Evans, S. E., Prasad, G. V. R. & Manhas, B. K. 2002. Fossil lizards from the Jurassic Kota Formation of India. *Journal of Vertebrate Paleontology*, **22**(2), 299-312.

Evans, S. E., Raia, P. & Barbera, C. 2004. New lizards and rhynchocephalians from the Lower Cretaceous of southern Italy. *Acta Palaeontologica Polonica*, **49**(3), 393-408.

Evans, S. E., Ruiz, A. L. & Rey, J. 2000. A lizard from the Early Cretaceous (Berriasian-Valanginian) of Montsec, Catalonia, Spain. *Neues Jahrbuch fur Geologie und Palaontologie. Abhandlungen*, **215**(1), 1-15.

Evans, S. E. & Searle, B. 2002. Lepidosaurian reptiles from the Purbeck limestone Group of Dorset, southern England. *Special Papers in Palaeontology*, **68**, 145–159.

Evans, S. E. & Waldman, M. 1996. Small reptiles and amphibians from the Middle Jurassic of Skye, Scotland. *Museum of Northern Arizona Bulletin*, **60**, 219-226.

Evans, S. E. & Wang, Y. 2005. The Early Cretaceous lizard *Dalinghosaurus* from China. *Acta Palaeontologica Polonica*, **50**(4), 725-742.

Evans, S. E. & Wang, Y. 2007. A juvenile lizard specimen with well-preserved skin impressions from the Upper Jurassic/Lower Cretaceous of Daohugou, Inner Mongolia, China. *Naturwissenschaften*, **94**(6), 431-439.

Evans, S. E., Wang, Y. & Jones, M. E. H. 2007. An aggregation of lizard skeletons from the Lower Cretaceous of China. *Senckenbergiana Lethaea*, **87**(1), 109-118.

Evans, S. E., Wang, Y. & Li, C. 2005. The Early Cretaceous lizard genus *Yabeinosaurus* from China: resolving an enigma. *Journal of Systematic Palaeontology*, **3**(4), 319-335.

Ewer, R. F. 1965. The Anatomy of the Thecodont Reptile *Euparkeria capensis* Broom. *Philosophical Transactions of the Royal Society of London B: Biological Sciences*, **248**(751), 379-435.

Ezcurra, M. D. 2016. The phylogenetic relationships of basal archosauromorphs, with an emphasis on the systematics of proterosuchian archosauriforms. *PeerJ*, **4**, e1778.

Ezcurra, M. D. & Butler, R. J. 2015a. Post-hatchling cranial ontogeny in the Early Triassic diapsid reptile *Proterosuchus fergusi*. *Journal of Anatomy*, **226**(5), 387-402.

Ezcurra, M. D. & Butler, R. J. 2015b. Taxonomy of the proterosuchid archosauriforms (Diapsida: Archosauromorpha) from the earliest Triassic of South Africa, and implications for the early archosauriform radiation. *Palaeontology*, **58**(1), 141-170.

Ezcurra, M. D., Montefeltro, F. & Butler, R. J. 2016. The Early Evolution of Rhynchosaurs. *Frontiers in Ecology and Evolution*, **3**(142).

Fabre, J., Broni, F. d., Ginsburg, L. & Wenz, S. 1982. Les vertébrés du Berriasiende Canjuers (Var, France) et leur environnement. *Geobios*, **15**(6), 891-923.

Farris, J. S. 1983. The logical basis of phylogenetic analysis. Pp. 7-36 in N. Platnick & V. Funk (eds) *Advances in cladistics*. Columbia University Press, New York.

Farris, J. S., Kluge, A. G. & Eckardt, M. J. 1970. A Numerical Approach to Phylogenetic Systematics. *Systematic Zoology*, **19**(2), 172-189.

Fedorov, P. & Nessov, L. 1992. A lizard from the boundary of the Middle and Late Jurassic of north-east Fergana. *Bulletin of the St Petersburg University, Geology, Geography*, **3**, 9-14.

Feduccia, A. & Wild, R. 1993. Birdlike characters in the Triassic archosaur *Megalancosaurus*. *Naturwissenschaften*, **80**(12), 564-566.

Felsenstein, J. 1982. Numerical Methods for Inferring Evolutionary Trees. *The Quarterly Review of Biology*, **57**(4), 379-404.

Fernandes, L., Sedor, F., Silva, R., Silva, L., Azevedo, A. & Siqueira, A. 2009. Icnofósseis da Usina Porto Primavera, SP-Rastros de dinossauros e de mamíferos em rochas do deserto neocretáceo Caiuá in M. Winge (ed) *Sítios Geológicos e Paleontológicos do Brasil*. CPRM, Brasília.

Filippi, L. S. & Garrido, A. C. 2012. Nuevo registro del género *Dinilysia* (Squamata, Serpentes) para la Formación Anacleto (Campaniano Inferior-Medio), Rincón de Los Sauces, Neuquén, Argentina. *Ameghiniana*, **49**(1), 132-136.

Fitzinger, L. 1843. *Systema Reptilium*. Braumüller et Seidel, Vienna, 106 pp.

Forey, P. L. & Kitching, I. 2000. Experiments in coding multistate characters. Pp. 54-80 in R.W. Scotland & R.T. Pennington (eds) *Homology and systematics : coding characters for phylogenetic analysis*. Taylor & Francis, London & New York.

Fox, R. C. 1968. Studies of Late Cretaceous Vertebrates I. The Braincase of *Champsosaurus* Cope (Reptilia: Eosuchia). *Copeia*, **1968**(1), 100-109.

Fox, R. C. & Bowman, M. C. 1966. Osteology and relationships of *Captorhinus aguti* (Cope)(Reptilia: Captorhinomorpha). *The University of Kansas - Paleontological Contributions*, **Article 11**, 1-79.

Fraas, E. 1899. *Proganochelys quenstedti* Baur (Psamobates keuperina Qu.) Ein neuer Fund der Keuperschildkrote aus dem Stubensandstein. *Jahreshberg Verein Vaterl Naturk Württemberg*, **60**, 401-424.

Fraser, N. C. 1982. A new rhynchocephalian from the British Upper Trias. *Palaeontology*, **25**(4), 709-725.

Fraser, N. C. 1988. The Osteology and Relationships of *Clevosaurus* (Reptilia: Sphenodontida). *Philosophical Transactions of the Royal Society of London, Series B: Biological Sciences*, **321**(1204), 125-178.

Fraser, N. C. 1994. Assemblages of small tetrapods from British Late Triassic fissure deposits. Pp. 214-226 in N.C. Fraser & H.D. Sues (eds) *In the shadow of the dinosaurs: early Mesozoic tetrapods*. Cambridge University Press, New York.

Fraser, N. C. & Benton, M. J. 1989. The Triassic reptiles *Brachyrhinodon* and *Polysphenodon* and the relationships of the sphenodontids. *Zoological Journal of the Linnean Society*, **96**(4), 413-445.

Fraser, N. C. & Furrer, H. 2013. A new species of *Macrocnemus* from the Middle Triassic of the eastern Swiss Alps. *Swiss Journal of Geosciences*, **106**(2), 199-206.

Fraser, N. C., Olsen, P. E., Dooley, A. C. & Ryan, T. R. 2007. A new gliding tetrapod (Diapsida: ?Archosauromorpha) from the Upper Triassic (Carnian) of Virginia. *Journal of Vertebrate Paleontology*, **27**(2), 261-265.

Fraser, N. C. & Walkden, G. M. 1983. The ecology of a Late Triassic reptile assemblage from Gloucestershire, England. *Palaeogeography, Palaeoclimatology, Palaeoecology*, **42**(3-4), 341-365.

Fraser, N. C. & Walkden, G. M. 1984. The postcranial skeleton of the Upper Triassic sphenodontid *Planocephalosaurus robinsonae*. *Palaeontology*, **27**(3), 575-595.

Frazzetta, T. H. 1962. A functional consideration of cranial kinesis in lizards. *Journal of Morphology*, **111**(3), 287-319.

Frazzetta, T. H. 1970. Studies on the fossil snake *Dinilysia patagonica* Woodward Part II. Jaw machinery in the earliest snakes. *Forma et Functio*, **3**, 205-221.

Freudenstein, J. V. 2005. Characters, States and Homology. *Systematic Biology*, **54**(6), 965-973.

Frey, E., Sues, H.-D. & Munk, W. 1997. Gliding Mechanism in the Late Permian Reptile *Coelurosauravus*. *Science*, **275**(5305), 1450-1452.

Friedman, M. 2012. Parallel evolutionary trajectories underlie the origin of giant suspension-feeding whales and bony fishes. *Proceedings of the Royal Society B: Biological Sciences*, **279**(1730), 944-951.

Frost, D. R. & Etheridge, R. 1989. A phylogenetic analysis and taxonomy of iguanian lizards (Reptilia: Squamata). *University of Kansas Natural History Museum Miscellaneous Publication*, **81**, 1-65.

Fürbringer, M. 1900. Beitrag zur Systematik und Genealogie der Reptilien. *Jenaischen Zeitschrift für Naturwissenschaften*, **34**, 596-682.

Furrer, H. 1995. The Kalkschieferzone (Upper Meride Limestone; Ladinian) near Meride (Canton Ticino, Southern Switzerland) and the evolution of a Middle Triassic intraplatform basin. *Eclogae Geologicae Helvetiae*, **88**(3), 827-852.

Gaetani, M., Gnaccolini, M., Jadoul, F. & Garzanti, E. 1998. Multiorder sequence stratigraphy in the Triassic system of the western Southern Alps. Mesozoic and Cenozoic sequence stratigraphy of European Basins. *SPecial Publication SEPM*, **60**, 701-717.

Gaffney, E. S. 1972. An illustrated glossary of turtle skull nomenclature. *American Museum Novitates*, **2486**, 1-33.

Gaffney, E. S. 1985. The shell morphology of the Triassic turtle *Proganochelys*. *Neues Jahrbuch für Geologie und Paläontologie - Abhandlungen*, **170**(1), 1-26.

Gaffney, E. S. 1990. The comparative osteology of the Triassic turtle *Proganochelys Bulletin of the American Museum of Natural History*, **194**, 1-263.

Gaffney, E. S., Hutchison, J. H., Jenkins, F. A. & Meeker, L. J. 1987. Modern Turtle Origins: The Oldest Known Cryptodire. *Science*, **237**(4812), 289-291.

Gaffney, E. S. & Jenkins, F. A. 2010. The cranial morphology of *Kayentachelys*, an Early Jurassic cryptodire, and the early history of turtles. *Acta Zoologica*, **91**(3), 335-368.

Gaffney, E. S. & McKenna, M. M. 1979. A late Permian captorhinid from Rhodesia. *American Museum Novitates*, **2688**, 1-15.

Gaffney, E. S. & Meeker, L. J. 1983. Skull morphology of the oldest turtles: a preliminary description of *Proganochelys quenstedti*. *Journal of Vertebrate Paleontology*, **3**(1), 25-28.

Gao, K.-Q. & Brinkman, D. B. 2005. Choristoderes from the Park and Its Vicinity. Pp. 221-234 in P.J. Currie & E.B. Koppelhus (eds) *Dinosaur Provincial Park: a spectacular ancient ecosystem revealed*. Indiana University Press, Bloomington and Indianapolis.

Gao, K.-Q. & Fox, R. C. 1996. Taxonomy and evolution of Late Cretaceous lizards (Reptilia: Squamata) from western Canada. *Bulletin of the Carnegie Museum of Natural History*, **33**, 1-107.

Gao, K.-Q. & Fox, R. C. 1998. New choristoderes (Reptilia: Diapsida) from the Upper Cretaceous and Palaeocene, Alberta and Saskatchewan, Canada, and phylogenetic relationships of Choristodera. *Zoological Journal of the Linnean Society*, **124**(4), 303-353.

Gao, K.-Q. & Fox, R. C. 2005. A new choristodere (Reptilia: Diapsida) from the Lower Cretaceous of western Liaoning Province, China, and phylogenetic relationships of Monjurosuchidae. *Zoological Journal of the Linnean Society*, **145**(3), 427-444.

Gao, K.-Q. & Hou, L. 1995. Iguanians from the Upper Cretaceous Djadochta Formation, Gobi Desert, China. *Journal of Vertebrate Paleontology*, **15**(1), 57-78.

Gao, K.-Q. & Hou, L. 1996. Systematics and taxonomic diversity of squamates from the Upper Cretaceous Djadochta Formation, Bayan Mandahu, Gobi Desert, People's Republic of China. *Canadian Journal of Earth Sciences*, **33**(4), 578-598.

Gao, K.-Q., Ksepka, D., Lianhai, H., Ye, D. & Dongyu, H. 2007. Cranial morphology of an Early Cretaceous Monjurosuchid (Reptilia: Diapsida) from Liaoning Province of China and evolution of the choristoderan palate. *Historical Biology*, **19**(3), 215-224.

Gao, K.-Q. & Norell, M. 1998. Taxonomic revision of *Carusia* (Reptilia, Squamata) from the Late Cretaceous of the Gobi Desert and phylogenetic relationships of anguimorphan lizards. *American Museum Novitates*, **3230**, 1-51.

Gao, K.-Q. & Norell, M. A. 2000. Taxonomic composition and systematics of Late Cretaceous lizard assemblages from Ukhaa Tolgod and adjacent localities, Mongolian Gobi Desert. *Bulletin of the American Museum of Natural History*, **249**, 1-118.

Gao, K.-Q., Zhou, C.-F., Hou, L. & Fox, R. C. 2013. Osteology and ontogeny of Early Cretaceous *Philydrosaurus* (Diapsida: Choristodera) based on new specimens from Liaoning Province, China. *Cretaceous Research*, **45**(0), 91-102.

Gao, K. & Nessov, L. 1998. Early Cretaceous squamates from the Kyzylkum Desert, Uzbekistan. *Neues Jahrbuch für Geologie und Paläontologie - Abhandlungen*, **207**, 289-309.

Gardner, N. M., Holliday, C. M. & O´Keefe, F. R. 2010. The braincase of *Youngina capensis* (Reptilia, Diapsida): New insights from high-resolution CT scanning of the holotype. *Palaeontologia Electronica*, **13**(3), 19A(16p).

Gauthier, J. A. 1982. Fossil xenosaurid and anguid lizards from the early Eocene Wasatch Formation, Southeast Wyoming, and a revision of the Anguioidea. *Rocky Mountain Geology*, **21**(1), 7-54.

Gauthier, J. A., Estes, R. & de Queiroz, K. 1988a. A phylogenetic analysis of Lepidosauromorpha. Pp. 15-98 in R. Estes & G. Pregill (eds) *Phylogenetic relationships of the lizard families*. Stanford University Press, Stanford.

Gauthier, J. A., Kearney, M., Maisano, J. A., Rieppel, O. & Behlke, A. D. B. 2012. Assembling the Squamate Tree of Life: Perspectives from the Phenotype and the Fossil Record. *Bulletin of the Peabody Museum of Natural History*, **53**(1), 3-308.

Gauthier, J. A., Kluge, A. G. & Rowe, T. 1988b. Amniote Phylogeny and the Importance of Fossils. *Cladistics*, **4**(2), 105-209.

Gelman, A. & Rubin, D. B. 1992. Inference from Iterative Simulation Using Multiple Sequences. *Statistical Science*, **7**(4), 457-472.

Geyer, O. F. 1969. The ammonite genus Sutneria in the Upper Jurassic of Europe. *Lethaia*, **2**(1), 63-72.

Gilmore, C. W. 1943. Fossil lizards of Mongolia. *Bulletin of the American Museum of Natural History*, **81**, 361-384.

Godefroit, P., Cau, A., Dong-Yu, H., Escuillié, F., Wenhao, W. & Dyke, G. 2013. A Jurassic avialan dinosaur from China resolves the early phylogenetic history of birds. *Nature*, **498**, 359–362.

Goloboff, P. A. 1999. Analyzing large datasets in reasonable times: solutions for composite optima. *Cladistics*, **15**(4), 415-428.

Goloboff, P. A., Carpenter, J. M., Arias, J. S. & Esquivel, D. R. M. 2008a. Weighting against homoplasy improves phylogenetic analysis of morphological datasets. *Cladistics*, **24**(5), 758-773.

Goloboff, P. A. & Catalano, S. A. 2011. Phylogenetic morphometrics (II): algorithms for landmark optimization. *Cladistics*, **27**(1), 42-51.

Goloboff, P. A., Farris, J. S. & Nixon, K. C. 2008b. TNT, a free program for phylogenetic analysis. *Cladistics*, **24**(5), 774-786.

Goloboff, P. A., Mattoni, C. I. & Quinteros, A. S. 2006. Continuous characters analyzed as such. *Cladistics*, **22**(6), 589-601.

Goloboff, P. A., Torres, A. & Arias, J. S. 2017. Weighted parsimony outperforms other methods of phylogenetic inference under models appropriate for morphology. *Cladistics*, Online first: 10.1111/cla.12205.

Goswami, A. 2007. Phylogeny, Diet, and Cranial Integration in Australodelphian Marsupials. *PLoS ONE*, **2**(10), e995.

Gottmann-Quesada, A. & Sander, P. M. 2009. A redescription of the early archosauromorph *Protorosaurus speneri* MEYER, 1832, and its phylogenetic relationships. *Palaeontographica Abteilung A*, **287**, 123-220.

Gould, S. J. 1989. *Wonderful Life: The Burgess Shale and the Nature of History*. Norton, New York, 347 pp.

Gould, S. J. 2002. *The Structure of Evolutionary Theory*. Harvard University Press, Cambridge, MA & London, 1433 pp.

Gould, S. J. & Lewontin, R. C. 1979. The spandrels of San Marco and the Panglossian paradigm: a critique of the adaptationist programme. *Proceedings of the Royal Society of London B: Biological Sciences*, **205**(1161), 581-598.

Gow, C. E. 1970. The anterior of the palate in *Euparkeria*. *Palaeontologia Africana*, **13**, 61-62.

Gow, C. E. 1974. *The morphology and relationships of Youngina capensis Broom and Prolacerta broomi Parrington*. Unpublished PhD thesis, University of the Witwatersrand, Johannesburg.

Gow, C. E. 1997. A reassessment of *Eunotosaurus africanus* Seeley (Amniota: Parareptilia). *Palaeontologia Africana*, **34**, 33-42.

Gow, C. E. & de Klerk, B. 1997. First record of *Eunotosaurus* (Amniota: Parareptilia) from the Eastern Cape. *Palaeontologia Africana*, **34**, 27-31.

Gower, D. J. 1996. The tarsus of erythrosuchid archosaurs, and implications for early diapsid phylogeny. *Zoological Journal of the Linnean Society*, **116**(4), 347-375.

Gower, D. J. 1997. The braincase of the early archosaurian reptile *Erythrosuchus africanus*. *Journal of Zoology*, **242**(3), 557-576.

Gower, D. J. 2001. Possible postcranial pneumaticity in the last common ancestor of birds and crocodilians: evidence from *Erythrosuchus* and other Mesozoic archosaurs. *Naturwissenschaften*, **88**(3), 119-122.

Gower, D. J. 2003. Osteology of the early archosaurian reptile *Erythrosuchus africanus*, Broom. *Annals of the South African Museum*, **110**(1), 1-88.

Gower, D. J. & Sennikov, A. G. 1996. Morphology and phylogenetic informativeness of early archosaur braincases. *Palaeontology*, **39**(Part 4), 883-906.

Gower, D. J. & Weber, E. 1998. The braincase of *Euparkeria*, and the evolutionary relationships of birds and crocodilians. *Biological Reviews*, **73**(4), 367-411.

Graybeal, A. 1998. Is It Better to Add Taxa or Characters to a Difficult Phylogenetic Problem? *Systematic Biology*, **47**(1), 9-17.

Greer, A. E. 1985a. Facial tongue-wiping in xantusiid lizards: its systematic implications. *Journal of Herpetology*, **19**(1), 174-175.

Greer, A. E. 1985b. The Relationships of the Lizard Genera *Anelytropsis* and *Dibamus*. *Journal of Herpetology*, **19**(1), 116-156.

Gregory, J. 1945. Osteology and relationships of *Trilophosaurus*. *University of Texas Publication*, **4401**, 273-359.

Grier, N. M. 1914. A new Rhynchocephalian from the Jura of Solenhofen. *Annals of the Carnegie Museum*, **9**, 86-90.

Gröning, F., Jones, M. E. H., Curtis, N., Herrel, A., O'Higgins, P., Evans, S. E. & Fagan, M. J. 2013. The importance of accurate muscle modelling for biomechanical analyses: a case study with a lizard skull. *Journal of The Royal Society Interface*, **10**(84).

Guillerme, T. & Cooper, N. 2016. Effects of missing data on topological inference using a total evidence approach. *Molecular Phylogenetics and Evolution*, **94**, 146-158.

Gušić, I. & Jelaska, V. 1993. Upper Cenomanian-lower Turonian sea-level rise and its consequences on the Adriatic-Dinaric carbonate platform. *Geologische Rundschau*, **82**(4), 676-686.

Haas, G. 1973. Muscles of the jaws and associated structures in the Rhynchocephalia and Squamata. Pp. 285-490 in C. Gans & T.S. Parsons (eds) *Biology of the Reptilia*. Academic Press, London and New York.

Haas, G. 1979. On a new snakelike reptile from the Lower Cenomanian of Ein Jabrud, near Jerusalem. *Bulletin du Muséum National d'Histoire Naturelle de Paris Ser. 4*, **1**, 51-64.

Haddoumi, H., Allain, R., Meslouh, S., Metais, G., Monbaron, M., Pons, D., Rage, J.-C., Vullo, R., Zouhri, S. & Gheerbrant, E. 2016. Guelb el Ahmar (Bathonian, Anoual Syncline, eastern Morocco): first continental flora and fauna including mammals from the Middle Jurassic of Africa. *Gondwana Research*, **29**(1), 290-319.

Haeckel, E. H. P. A. 1866. *Generelle Morphologie der Organismen: allgemeine Grundzüge der organischen Formen-Wissenschaft, mechanisch begründet durch die von Charles Darwin reformirte Descendenz-Theorie*. Georg Reimer, Berlin, 574 pp.

Hall, B. & Hallgrimson, B. 2008. *Strickberger's Evolution*. Jones & Bartlett Publishers, Sudbury, 760 pp.

Hancock, A. & Howse, R. 1870. On *Proterosaurus speneri*, von Meyer, and a new species, *Proterosaurus huxleyi*, from the Marl-slate of Midderidge, Durham. *Quarterly Journal of the Geological Society*, **26**(1-2), 565-572.

Haridy, Y., Macdougall, M. J., Scott, D. & Reisz, R. R. 2016. Ontogenetic Change in the Temporal Region of the Early Permian Parareptile *Delorhynchus cifellii* and the Implications for Closure of the Temporal Fenestra in Amniotes. *PLoS ONE*, **11**(12), e0166819.

Harris, S. R., Gower, D. J. & Wilkinson, M. 2003. Intraorganismal Homology, Character Construction, and the Phylogeny of Aetosaurian Archosaurs (Reptilia, Diapsida). *Systematic Biology*, **52**(2), 239-252.

Harrison, H. S. 1901. The development and succession of teeth in *Hatteria punctata*. *Quarterly Journal of Microscopical Science*, **44**, 161-213.

Harrison, L. B. & Larsson, H. C. 2015. Among-character rate variation distributions in phylogenetic analysis of discrete morphological characters. *Systematic Biology*, **64**(2), 307-324.

Haubold, H. & Schaumberg, G. 1985. *Die Fossilien des Kupferschiefers*. A. Ziemsen Verlag, Wittenberg, 223 pp.

Haughton, S. H. 1922. On the reptilian genera *Euparkeria* Broom, and *Mesosuchus* Watson. *Transactions of the Royal Society of South Africa*, **10**(1), 81-88.

Haughton, S. H. 1924. On a skull and partial skeleton of *Mesosuchus browni* Watson. *Transactions of the Royal Society of South Africa*, **12**(1), 17-26.

Haughton, S. H. 1929. Notes on the Karroo Reptilia from Madagascar. *Transactions of the Royal Society of South Africa*, **18**(2), 125-136.

Hawkins, J. A. 2000. A survey of primary homology assessment: different botanists perceive and define characters in different ways. Pp. 22-53 in R.W. Scotland & R.T. Pennington (eds) *Homology and systematics: coding characters for phylogenetic analysis*. The Systematics Association, London and New York.

Hawkins, J. A., Hughes, C. E. & Scotland, R. W. 1997. Primary Homology Assessment, Characters and Character States. *Cladistics*, **13**(3), 275-283.

Heaton, M. J. & Reisz, R. R. 1986. Phylogenetic relationships of captorhinomorph reptiles. *Canadian Journal of Earth Sciences*, **23**(3), 402-418.

Hecht, M. 1982. The vertebral morphology of the Cretaceous snake, *Dinilysia patagonica* Woodward. *Neues Jahrbuch für Geologie und Paläontologie, Monatshefte*, **1982**, 523-532.

Hecht, M. K. & Hecht, B. M. 1984. A new lizard from Jurassic deposits of Middle Asia. *Paleontological Journal*, **18**, 133-136.

Heckert, A. B., Lucas, S. G., Rinehart, L. F., Spielmann, J. A., Hunt, A. P. & Kahle, R. 2006. Revision of the archosauromorph reptile *Trilophosaurus*, with a description of the first skull of *Trilophosaurus jacobsi*, from the Upper Triassic Chinle Group, West Texas, USA. *Palaeontology*, **49**(3), 621-640.

Hennig, W. 1966. *Phylogenetic Systematics*. The University of Illinois Press, Urbana, Chicago and London, 263 pp.

Herrel, A. 2007. Herbivory and foraging mode in lizards. Pp. 209-236 in S. Reilly, L. McBrayer & D. Miles (eds) *Lizard ecology: the evolutionary consequences of foraging mode*. Cambridge University Press, New York.

Herrel, A., Aerts, P. & De Vree, D. 1998a. Static biting in lizards: functional morphology of the temporal ligaments. *Journal of Zoology*, **244**(1), 135-143.

Herrel, A., Aerts, P. & De Vree, F. 1998b. Ecomorphology of the Lizard Feeding Apparatus: a Modelling Approach. *Netherlands Journal of Zoology*, **48**(1), 1-25.

Herrel, A., Castilla, A. M., Al-Sulaiti, M. K. & Wessels, J. J. 2014. Does large body size relax constraints on bite-force generation in lizards of the genus *Uromastyx*? *Journal of Zoology*, **292**(3), 170-174.

Herrel, A., Spithoven, L., Van Damme, R. & De Vree, F. 1999. Sexual dimorphism of head size in *Gallotia galloti*: testing the niche divergence hypothesis by functional analyses. *Functional Ecology*, **13**(3), 289-297.

Herrel, A., Van Wassenbergh, S. & Aerts, P. 2012. Biomechanical studies of food and diet selection. Pp. 1-9*Encyclopedia of Life Sciences* John Wiley & Sons, Chichester.

Herrel, A. & Vree, F. D. 1999. Kinematics of intraoral transport and swallowing in the herbivorous lizard *Uromastix acanthinurus*. *Journal of Experimental Biology*, **202**(9), 1127-1137.

Hill, R. V. 2005. Integration of Morphological Datasets for Phylogenetic Analysis of Amniota: The Importance of Integumentary Characters and Increased Taxonomic Sampling. *Systematic Biology*, **54**(4), 530-547.

Hirasawa, T., Pascual-Anaya, J., Kamezaki, N., Taniguchi, M., Mine, K. & Kuratani, S. 2015. The evolutionary origin of the turtle shell and its dependence on the axial arrest of the embryonic rib cage. *Journal of Experimental Zoology Part B: Molecular and Developmental Evolution*, **324**(3), 194-207.

Ho, S. Y. & Phillips, M. J. 2009. Accounting for calibration uncertainty in phylogenetic estimation of evolutionary divergence times. *Systematic Biology*, syp035.

Hoffman, A. C. 1965. On the discovery of a new thecodont from the Middle Beaufort Beds. *Navorsinge van die Nasionale Museum Bloemfontein*, **2**, 33-40.

Hoffstetter, R. 1953. Les Sauriens anté crétacés. *Bulletin du Museum National d'Histoire Naturelle*, **25**(3), 345-352.

Hoffstetter, R. 1955a. Rhynchocéphales. Pp. 556–576 in J. Piveteau (ed) *Traité de paléontologie*. Masson et Cie, Paris.

Hoffstetter, R. 1955b. Squamates de type moderne. *Traité de paléontologie*, **5**, 606-662.

Hoffstetter, R. 1964. Les Sauria du Jurassique supérieur et specialement les Gekkota de Bavière et de Mandchourie. *Senckenberger Biologisches*, **45**, 281-324.

Hoffstetter, R. 1966. A propos des genres *Ardeosaurus* et *Eichstaettisaurus* (Reptilia, Sauria, Gekkonoidea) du Jurassique Supérieur de Franconie. *Bulletin de la Societe Geologique de France*, **7**, 592-595.

Hoffstetter, R. 1967. Coup d'oeil sur les Sauriens (Lacertiliens) des couches de Purbeck (Jurassique supérieur d'Angleterre). *Colloques Internationaux du Centre National de la Recherche Scientifique*, **163**, 349-371.

Hoffstetter, R. & Gasc, J.-P. 1969. Vertebrae and ribs of modern reptiles. Pp. 201-310 in C. Gans, A.d.A. Bellairs & T.S. Parsons (eds) *Biology of the Reptilia*. Academic Press, London and New York.

Höhna, S., Stadler, T., Ronquist, F. & Britton, T. 2011. Inferring Speciation and Extinction Rates under Different Sampling Schemes. *Molecular Biology and Evolution*, **28**(9), 2577-2589.

Holder, L. A. 1960. The comparative morphology of the axial skeleton in the Australian Gekkonidae. *Journal of the Linnean Society of London, Zoology*, **44**(297), 300-335.

Holmes, R. B. 1977. The osteology and musculature of the pectoral limb of small captorhinids. *Journal of Morphology*, **152**(1), 101-140.

Holmes, R. B. 1984. The Carboniferous Amphibian *Proterogyrinus scheelei* Romer, and the Early Evolution of Tetrapods. *Philosophical Transactions of the Royal Society of London. Series B, Biological Sciences*, **306**(1130), 431-524.

Holmes, R. B. 2003. The hind limb of *Captorhinus aguti* and the step cycle of basal amniotes. *Canadian Journal of Earth Sciences*, **40**(4), 515-526.

Holmes, R. B., Murray, A. M., Chatrath, P., Attia, Y. S. & Simons, E. L. 2010. Agamid lizard (Agamidae: Uromastycinae) from the lower Oligocene of Egypt. *Historical Biology*, **22**(1-3), 215-223.

Honda, M., Ota, H., Kobayashi, M., Nabhitabhata, J., Yong, H.-S., Sengoku, S. & Hikida, T. 2000. Phylogenetic Relationships of the Family Agamidae (Reptilia: Iguania) Inferred from Mitochondrial DNA Sequences. *Zoological Science*, **17**(4), 527-537.

Howes, G. B. & Swinnerton, H. H. 1901. On the development of the skeleton of the tuatara, S*phenodon punctatus*; with remarks on the egg, on the hatching, and on the hatched young. *The Transactions of the Zoological Society of London*, **16**(1), 1-84.

Hsiou, A. S., Albino, A. M., Medeiros, M. A. & Santos, R. A. B. 2014. The oldest Brazilian Snakes from the Cenomanian (Early Late Cretaceous). *Acta Palaeontologica Polonica*, **59**(3), 635-642.

Huelsenbeck, J. P. & Rannala, B. 1997. Phylogenetic methods come of age: testing hypotheses in an evolutionary context. *Science*, **276**(5310), 227-232.

Huene, F. v. 1911. Über *Erythrosuchus* Vertreter der neuen Reptil-Ordnung Pelycosima. *Geologische und Paläontologische Abhandlungen.*, **10**, 1-58.

Huene, F. v. 1944a. Beitrage zur kenntnis der Protorosaurier. *Neues Jahrbuch für Mineralogie, Geologie und Paläontologie, Monatshefte, Abteilung B*, **Jahrg. 1944**(Heft 5), 120-131.

Huene, F. v. 1944b. Die Zweiteilung des Reptilstammes. *Neues Jahrbuch für Mineralogie, Geologie und Paläontologie*, **88**, 427-440.

Hugall, A. F., Foster, R. & Lee, M. S. Y. 2007. Calibration Choice, Rate Smoothing, and the Pattern of Tetrapod Diversification According to the Long Nuclear Gene RAG-1. *Systematic Biology*, **56**(4), 543-563.

Hughes, B. 1963. The earliest archosaurian reptiles. *South African Journal of Science*, **59**, 221-241.

Hugi, J. 2011. The long bone histology of *Ceresiosaurus* (Sauropterygia, Reptilia) in comparison to other eosauropterygians from the Middle Triassic of Monte San Giorgio (Switzerland/Italy). *Swiss Journal of Palaeontology*, **130**(2), 297.

Hugi, J., Scheyer, T. M., Sander, P. M., Klein, N. & Sánchez-Villagra, M. R. 2011. Long bone microstructure gives new insights into the life of pachypleurosaurids from the Middle Triassic of Monte San Giorgio, Switzerland/Italy. *Comptes Rendus Palevol*, **10**(5), 413-426.

Hutchinson, M. N., Skinner, A. & Lee, M. S. Y. 2012. *Tikiguania* and the antiquity of squamate reptiles (lizards and snakes). *Biology Letters*, **8**(4), 665-669.

Huxley, T. H. 1868. I.—On *Saurosternon bainii*, and *Pristerodon mckayi*, Two New Fossil Lacertilian Reptiles from South Africa. *Geological Magazine*, **5**(47), 201-205.

Iordansky, N. N. 1990. Evolution of cranial kinesis in lower tetrapods. *Netherlands Journal of Zoology*, **40**(1-2), 32-54.

Irisarri, I., Baurain, D., Brinkmann, H., Delsuc, F., Sire, J.-Y., Kupfer, A., Petersen, J., Jarek, M., Meyer, A., Vences, M. & Philippe, H. 2017. Phylotranscriptomic consolidation of the jawed vertebrate timetree. *Nature Ecology & Evolution*.

Irschick, D. J. & Jayne, B. C. 1999. Comparative three-dimensional kinematics of the hindlimb for high-speed bipedal and quadrupedal locomotion of lizards. *Journal of Experimental Biology*, **202**(9), 1047-1065.

Jaekel, O. 1914. Über die Wirbeltierfunde in der oberen Trias von Halberstadt. *Paläontologische Zeitschrift*, **1**(1), 155-215.

Jaekel, O. 1918. Die Wirbeltierfunde aus dem Keuper von Halberstadt. Serie II. Testudinata. Teil 1 *Stegochelys dux*, n.g., m.sp. *Paläontologische Zeitschrift*, **2**(1), 88-214.

Jarvis, E. D., Mirarab, S., Aberer, A. J., Li, B., Houde, P., Li, C., Ho, S. Y. W., Faircloth, B. C., Nabholz, B., Howard, J. T., Suh, A., Weber, C. C., da Fonseca, R. R., Li, J., Zhang, F., Li, H., Zhou, L., Narula, N., Liu, L., Ganapathy, G., Boussau, B., Bayzid, M. S., Zavidovych, V., Subramanian, S., Gabaldón, T., Capella-Gutiérrez, S., Huerta-Cepas, J., Rekepalli, B., Munch, K., Schierup, M., Lindow, B., Warren, W. C., Ray, D., Green, R. E., Bruford, M. W., Zhan, X., Dixon, A., Li, S., Li, N., Huang, Y., Derryberry, E. P., Bertelsen, M. F., Sheldon, F. H., Brumfield, R. T., Mello, C. V., Lovell, P. V., Wirthlin, M., Schneider, M. P. C., Prosdocimi, F., Samaniego, J. A., Velazquez, A. M. V., Alfaro-Núñez, A., Campos, P. F., Petersen, B., Sicheritz-Ponten, T., Pas, A., Bailey, T., Scofield, P., Bunce, M., Lambert, D. M., Zhou, Q., Perelman, P., Driskell, A. C., Shapiro, B., Xiong, Z., Zeng, Y., Liu, S., Li, Z., Liu, B., Wu, K., Xiao, J., Yinqi, X., Zheng, Q., Zhang, Y., Yang, H., Wang, J., Smeds, L., Rheindt, F. E., Braun, M., Fjeldsa, J., Orlando, L., Barker, F. K., Jønsson, K. A., Johnson, W., Koepfli, K.-P., O'Brien, S., Haussler, D., Ryder, O. A., Rahbek, C., Willerslev, E., Graves, G. R., Glenn, T. C., McCormack, J., Burt, D., Ellegren, H., Alström, P., Edwards, S. V., Stamatakis, A., Mindell, D. P., Cracraft, J., Braun, E. L., Warnow, T., Jun, W., Gilbert, M. T. P. & Zhang, G. 2014. Whole-genome analyses resolve early branches in the tree of life of modern birds. *Science*, **346**(6215), 1320-1331.

Jenner, R. A. 2004. The scientific status of metazoan cladistics: why current research practice must change. *Zoologica Scripta*, **33**(4), 293-310.

Jerzykiewicz, T., Currie, P. J., Eberth, D. A., Johnston, P. A., Koster, E. H. & Zheng, J.-J. 1993. Djadokhta Formation correlative strata in Chinese Inner Mongolia: an overview of the stratigraphy, sedimentary geology, and paleontology and comparisons with the type locality in the pre-Altai Gobi. *Canadian Journal of Earth Sciences*, **30**(10), 2180-2195.

Ji, C., Jiang, D.-Y., Motani, R., Rieppel, O., Hao, W.-C. & Sun, Z.-Y. 2016. Phylogeny of the Ichthyopterygia incorporating recent discoveries from South China. *Journal of Vertebrate Paleontology*, **36**(1), e1025956.

Ji, S. A. 1998. A new long-tailed lizard from the Upper Jurassic of Liaoning, China. *International Symposium on Geological Science, Peking University.*, 496-505.

Ji, S. A. 2004. Late Mesozoic fossil lizards (Reptilia: Squamata) from western Liaoning and northern Hebei, China. *Science Technology and Engineering*, **4**(9), 756-759.

Ji, S. A. & Ji, Q. 2004. Postcranial Anatomy of the Mesozoic *Dalinghosaurus* (Squamata): Evidence from a New Specimen of Western Liaoning. *Acta Geologica Sinica - English Edition*, **78**(4), 897-905.

Jiang, D.-Y., Maisch, M. W., Sun, Y.-L., Matzke, A. T. & Hao, W.-C. 2004. A new species of *Xinpusaurus* (thalattosauria) from the Upper Triassic of China. *Journal of Vertebrate Paleontology*, **24**(1), 80-88.

Jiang, D.-Y., Motani, R., Li, C., Hao, W., Sun, Y., Sun, Z. & Schmitz, L. 2005. Guanling Biota: A Marker of Triassic Biotic Recovery from the end-Permian Extinction in the Ancient Guizhou Sea. *Acta Geologica Sinica (English Edition)*, **79**(6), 729-738.

Jiang, D.-Y., Motani, R., Tintori, A., Rieppel, O., Chen, G.-B., Huang, J.-D., Zhang, R., Sun, Z.-Y. & Ji, C. 2014. The Early Triassic Eosauropterygian *Majiashanosaurus discocoracoidis*, gen. et sp. nov. (Reptilia, Sauropterygia), from Chaohu, Anhui Province, People's Republic of China. *Journal of Vertebrate Paleontology*, **34**(5), 1044-1052.

Jiang, D.-Y., Rieppel, O., Fraser, N. C., Motani, R., Hao, W.-C., Tintori, A., Sun, Y.-L. & Sun, Z.-Y. 2011. New information on the protorosaurian reptile *Macrocnemus fuyuanensis* Li et al., 2007, from the Middle/Upper Triassic of Yunnan, China. *Journal of Vertebrate Paleontology*, **31**(6), 1230-1237.

Jiang, D.-Y., Rieppel, O., Motani, R., Hao, W.-C., Sun, Y.-L., Schmitz, L. & Sun, Z.-Y. 2008. A new Middle Triassic Eosauropterygian (Reptilia, Sauropterygia) from southwestern China. *Journal of Vertebrate Paleontology*, **28**(4), 1055-1062.

Jiang, D.-Y., Schmitz, L., Hao, W.-C. & Sun, Y.-L. 2006. A new mixosaurid ichthyosaur from the Middle Triassic of China. *Journal of Vertebrate Paleontology*, **26**(1), 60-69.

Jollie, M. T. 1960. The head Skeleton of the Lizard. *Acta Zoologica*, **41**(1-2), 1-64.

Jones, M. E. H. 2008. Skull shape and feeding strategy in *Sphenodon* and other Rhynchocephalia (Diapsida: Lepidosauria). *Journal of Morphology*, **269**(8), 945-966.

Jones, M. E. H., Anderson, C. L., Hipsley, C. A., Müller, J., Evans, S. E. & Schoch, R. R. 2013. Integration of molecules and new fossils supports a Triassic origin for Lepidosauria (lizards, snakes, and tuatara). *BMC Evolutionary Biology*, **13**(208), Available online: 10.1186/1471-2148-1113-1208.

Jones, M. E. H., Curtis, N., Fagan, M. J., O'Higgins, P. & Evans, S. E. 2011. Hard tissue anatomy of the cranial joints in *Sphenodon* (Rhynchocephalia): sutures, kinesis, and skull mechanics. *Palaeontologia Electronica*, **14**(2), 17A:92p.

Jones, M. E. H. & Lappin, A. K. 2009. Bite-force performance of the last rhynchocephalian (Lepidosauria: Sphenodon). *Journal of the Royal Society of New Zealand*, **39**(2-3), 71-83.

Joyce, W. G. 2015. The origin of turtles: A paleontological perspective. *Journal of Experimental Zoology Part B: Molecular and Developmental Evolution*, **324**(3), 181-193.

Juul, L. 1994. The phylogeny of basal archosaurs. *Palaeontologia Africana*, **31**, 1-38.

Kaliontzopoulou, A., Carretero, M. A. & Llorente, G. A. 2007. Multivariate and geometric morphometrics in the analysis of sexual dimorphism variation in *Podarcis* lizards. *Journal of Morphology*, **268**(2), 152-165.

Kass, R. E. & Raftery, A. E. 1995. Bayes factors. *Journal of the American Statistical Association*, **90**(430), 773-795.

Katoh, K. & Standley, D. M. 2013. MAFFT Multiple Sequence Alignment Software Version 7: Improvements in Performance and Usability. *Molecular Biology and Evolution*, **30**(4), 772-780.

Katsura, Y. 2007. Fusion of sacrals and anatomy in *Champsosaurus* (Diapsida, Choristodera). *Historical Biology*, **19**(3), 263-271.

Kavanagh, K. D., Shoval, O., Winslow, B. B., Alon, U., Leary, B. P., Kan, A. & Tabin, C. J. 2013. Developmental bias in the evolution of phalanges. *Proceedings of the National Academy of Sciences*, **110**(45), 18190-18195.

Kearney, M. 2002. Fragmentary Taxa, Missing Data, and Ambiguity: Mistaken Assumptions and Conclusions. *Systematic Biology*, **51**(2), 369-381.

Kearney, M. 2003a. The phylogenetic position of *Sineoamphisbaena hexatabularis* reexamined. *Journal of Vertebrate Paleontology*, **23**(2), 394-403.

Kearney, M. 2003b. Systematics of the Amphisbaenia (Lepidosauria:Squamata) based on morphological evidence from recent and fossil forms. *Herpetological Monographs*, **17**(1), 1-74.

Kearney, M. & Rieppel, O. 2006. Rejecting "the given" in systematics. *Cladistics*, **22**(4), 369-377.

Kelley, N. P., Motani, R., Embree, P. & Orchard, M. J. 2016. A new Lower Triassic ichthyopterygian assemblage from Fossil Hill, Nevada. *PeerJ*, **4**, e1626.

Ketchum, H. F. & Barrett, P. M. 2004. New reptile material from the Lower Triassic of Madagascar: implications for the Permian–Triassic extinction event. *Canadian Journal of Earth Sciences*, **41**(1), 1-8.

Kitching, I. J., Forey, P. L., Humphries, C. J. & William, D. D. 1998. *Cladistics: the theory and practise of parsimony analysis (2nd edition)*. Oxford University Press, Oxford, New York & Tokyo.

Klein, N., Houssaye, A., Neenan, J. M. & Scheyer, T. M. 2015. Long bone histology and microanatomy of Placodontia (Diapsida: Sauropterygia). *Contributions to Zoology*, **84**(1), 59-84.

Klembara, J., Böhme, M. & Rummel, M. 2010. Revision of the anguine lizard *Pseudopus laurillardi* (Squamata, Anguidae) from the Miocene of Europe, with comments on paleoecology. *Journal of Paleontology*, **84**(2), 159-196.

Klembara, J. & Welman, J. 2009. The anatomy of the palatoquadrate in the Lower Triassic *Proterosuchus fergusi* (Reptilia, Archosauromorpha) and its morphological transformation within the archosauriform clade. *Acta Zoologica*, **90**(3), 275-284.

Klingenberg, C. P. 2008. Morphological Integration and Developmental Modularity. *Annual Review of Ecology, Evolution, and Systematics*, **39**(1), 115-132.

Kluge, A. G. 1962. Comparative osteology of the eublepharid lizard genus *Coleonyx* Gray. *Journal of Morphology*, **110**(3), 299-332.

Kluge, A. G. 2003. The repugnant and the mature in phylogenetic inference: atemporal similarity and historical identity. *Cladistics*, **19**(4), 356-368.

Kluge, A. G. & Farris, J. S. 1969. Quantitative Phyletics and the Evolution of Anurans. *Systematic Biology*, **18**(1), 1-32.

Kluge, A. G. & Farris, J. S. 1999. Taxic Homology = Overall Similarity. *Cladistics*, **15**(2), 205-212.

Kordikova, E. G., Polly, P. D., Alifanov, V. A., Roček, Z., Gunnell, G. F. & Averianov, A. O. 2001. Small vertebrates from the Late Cretaceous and Early Tertiary of the northeastern Aral Sea Region, Kazakhstan. *Journal of Paleontology*, **75**(2), 390-400.

Kornhuber, G. A. 1873. Über einen neuen fossilen Saurier aus Lesina. *Herausgegeben von der k. k. geologischen Reichsanstalt, Wien*, **5**(4), 75-90.

Krahl, A., Klein, N. & Sander, P. M. 2013. Evolutionary implications of the divergent long bone histologies of *Nothosaurus* and *Pistosaurus* (Sauropterygia, Triassic). *BMC Evolutionary Biology*, **13**(1), 123.

Kramberger, K. G. 1892. *Aigialosaurus*, eine neue Eidechse aus den Kreideschiefern der Insel Lesina mit Rücksicht auf die bereits beschriebenen Lacertiden von Comen und Lesina. *Glasnik huvatskoga naravolosovnoga derstva (Societas historico-matulis croatica) u Zagrebu*, **7**, 74-106.

Kratochvíl, L. & Frynta, D. 2002. Body size, male combat and the evolution of sexual dimorphism in eublepharid geckoes (Squamata: Eublepharidae). *Biological Journal of the Linnean Society*, **76**(2), 303-314.

Kuhn-Schnyder, E. 1959. Hand und Fuss von *Tanystropheus longobardicus* (Bassani). *Eclogae Geologicae Helvetiae*, **52**, 921-941.

Kuhn-Schnyder, E. 1960. Über einen Schultergürtel von *Askeptosaurus italicus* Nopcsa aus der anisischen Stufe der Trias des Monte San Giorgio (Kt. Tessin, Schweiz). *Eclogae Geologicae Helvetiae*, **53**, 805-810.

Kuhn-Schnyder, E. 1962. Ein weiterer Schädel von *Macrocnemus bassanii* Nopcsa aus der anisischen Stufe der Trias des Monte San Giorgio (Kt. Tessin, Schweiz). *Paläontologische Zeitschrift*, **36**(1), 110-133.

Kuhn-Schnyder, E. 1964. Die Wirbeltierfauna der Trias der Tessiner Kalkalpen. *Geologische Rundschau*, **53**(1), 393-412.

Kuhn-Schnyder, E. 1971. Über einen Schädel von *Askeptosaurus italicus* Nopcsa aus der Mittleren Trias des Monte San Giorgio (Kt. Tessin, Schweiz). *Abhandlungen des Hessischen Landesamts für Bodenforschung*, **60**, 89-98.

Kuhn-Schnyder, E. 1974. Die Triasfauna der Tessiner Kalkalpen. *Neujahrsblätter - Naturforschende Gesellschaft in Zürich*, **1974**, 1-119.

Kuhn-Schnyder, E. 1988. Bemerkungen zur Ordnung der Thalattosauria (Reptilia). *Eclogae Geologicae Helvetiae*, **81**(3), 879-886.

Kuhn, E. 1952. Die Triasfauna der Tessiner Kalkalpen. XVII: *Askeptosaurus italicus* Nopsca. *Schweizer Paläontologische Abhandlungen*, **69**, 1-73.

Kuhn, O. 1939. Schädelbau und systematische Stellung von *Weigeltisaurus*. *Palaeontologische Zeitschrift*, **21**(3), 163-167.

Kuhn, O. 1958. Ein neuer Lacertilier aus dem fränkischen Lithographieschiefer. *Neues Jahrbuch für Geologie und Paläontologie, Monatshefte*, **1958**, 380-382.

Kuhn, O. 1969. *Handbuch der Paläoherpetologie-Part 9: Proganosauria, Bolosauria, Placodontia, Araeoscelidia, Trilophosauria, Weigeltisauria, Millerosauria, Rhynchocephalia, Protorosauria*. Verlag Dr. Friedrich Pfeil, Stuttgart.

Kuhn, T. S. 1962. *The Structure of Scientific Revolutions (1st Ed.)*. University of Chicago Press, Chicago, 172 pp.

Kuhner, M. K. & Felsenstein, J. 1994. A simulation comparison of phylogeny algorithms under equal and unequal evolutionary rates. *Molecular Biology and Evolution*, **11**(3), 459-468.

Kumazawa, Y. 2007. Mitochondrial genomes from major lizard families suggest their phylogenetic relationships and ancient radiations. *Gene*, **388**(1–2), 19-26.

Kupczik, K., Dobson, C., Fagan, M., Crompton, R., Oxnard, C. & O'Higgins, P. 2007. Assessing mechanical function of the zygomatic region in macaques: validation and sensitivity testing of finite element models. *Journal of Anatomy*, **210**(1), 41-53.

Laing, A. M., Doyle, S., Gold, M. E. L., Nesbitt, S. J., O'Leary, M. A., Turner, A. H., Wilberg, E. W. & Poole, K. E. 2017. Giant taxon-character matrices: the future of morphological systematics. *Cladistics*, ahead of print (10.1111/cla.12197).

Lakatos, I. 1978. *The Methodology of Scientific Research Programmes: Philosophical Papers Volume 1.* Cambridge University Press, Cambridge, 260 pp.

Landsmeer, J. M. F. 1981. Digital morphology in *Varanus* and *Iguana*. *Journal of Morphology*, **168**(3), 289-295.

Lane, H. H. 1945. New mid-Pennsylvanian reptiles from Kansas. *Transactions of the Kansas Academy of Science*, **47**(3), 381-390.

Lanfear, R., Frandsen, P. B., Wright, A. M., Senfeld, T. & Calcott, B. 2016. PartitionFinder 2: New Methods for Selecting Partitioned Models of Evolution for Molecular and Morphological Phylogenetic Analyses. *Molecular Biology and Evolution*.

Langer, M. C. 1998. Gilmoreteiidae new family and *Gilmoreteius* new genus (Squamata, Scincomorpha): replacement names for Macrocephalosauridae Sulimski, 1975 and *Macrocephalosaurus* Gilmore, 1943. *Comunicações do Museu de Ciências da PUCRS. Série Zoologia*, **11**, 13-18.

Langer, M. C., Ezcurra, M. D., Rauhut, O. W., Benton, M. J., Knoll, F., McPhee, B. W., Novas, F. E., Pol, D. & Brusatte, S. L. 2017. Untangling the dinosaur family tree. *Nature*, **551**(7678), E1.

Langer, M. C., Ferigolo, J. & Schultz, C. L. 2000. Heterochrony and tooth evolution in hyperodapedontine rhynchosaurs (Reptilia, Diapsida). *Lethaia*, **33**(2), 119-128.

Langer, M. C., Ribeiro, A. M., Schultz, C. L. & Ferigolo, J. 2007. The continental tetrapod-bearing Triassic of south Brazil. Pp. 201-218 in S.G. Lucas & J.A. Spielmann (eds) *The Global Triassic*. New Mexico Museum of Natural History, Albuquerque.

Langer, M. C. & Schultz, C. L. 2000. A new species of the Late Triassic rhynchosaur *Hyperodapedon* from the Santa Maria Formation of South Brazil. *Palaeontology*, **43**(4), 633-652.

Lappin, A. K., Hamilton, P. S. & Sullivan, B. K. 2006. Bite-force performance and head shape in a sexually dimorphic crevice-dwelling lizard, the common chuckwalla [*Sauromalus ater* (= *obesus*)]. *Biological Journal of the Linnean Society*, **88**(2), 215-222.

Laurin, M. 1991. The osteology of a Lower Permian eosuchian from Texas and a review of diapsid phylogeny. *Zoological Journal of the Linnean Society*, **101**(1), 59-95.

Laurin, M. & Reisz, R. R. 1995. A reevaluation of early amniote phylogeny. *Zoological Journal of the Linnean Society*, **113**(2), 165-223.

Leanza, H. A. & Hugo, C. A. 2001. Cretaceous red beds from southern Neuquén Basin (Argentina): age, distribution and stratigraphic discontinuities. *Asociación Paleontológica Argentina, Publicación Especial*, **7**, 117-122.

Lee, D.-C. & Bryant, H. N. 1999. A reconsideration of the coding of inapplicable characters: assumptions and problems. *Cladistics*, **15**(4), 373-378.

Lee, M. S. Y. 1993. The Origin of the Turtle Body Plan: Bridging a Famous Morphological Gap. *Science*, **261**(5129), 1716-1720.

Lee, M. S. Y. 1997a. On snake-like dentition in mosasaurian lizards. *Journal of Natural History*, **31**(2), 303-314.

Lee, M. S. Y. 1997b. The phylogeny of varanoid lizards and the affinities of snakes. *Philosophical Transactions of the Royal Society of London, Series B: Biological Sciences*, **352**(1349), 53-91.

Lee, M. S. Y. 1998. Convergent evolution and character correlation in burrowing reptiles: towards a resolution of squamate relationships. *Biological Journal of the Linnean Society*, **65**(4), 369-453.

Lee, M. S. Y. 2001. Molecules, morphology, and the monophyly of diapsid reptiels. *Contributions to Zoology*, **70**(1), 1-22.

Lee, M. S. Y. 2005a. Molecular evidence and marine snake origins. *Biology Letters*, **1**(2), 227-230.

Lee, M. S. Y. 2005b. Squamate phylogeny, taxon sampling, and data congruence *Organisms Diversity & Evolution*, **5**(1), 25-45.

Lee, M. S. Y. 2013a. Palaeontology: Turtles in Transition. *Current Biology*, **23**(12), R513-R515.

Lee, M. S. Y. 2013b. Turtle origins: insights from phylogenetic retrofitting and molecular scaffolds. *Journal of Evolutionary Biology*, **Online only**, DOI: 10.1111/jeb.12268.

Lee, M. S. Y. & Caldwell, M. W. 1998. Anatomy and relationships of *Pachyrhachis problematicus*, a primitive snake with hindlimbs. *Philosophical Transactions of the Royal Society of London, Series B: Biological Sciences*, **353**(1375), 1521-1552.

Lee, M. S. Y. & Caldwell, M. W. 2000. *Adriosaurus* and the affinities of mosasaurs, dolichosaurs and snakes. *Journal of Paleontology*, **74**(5), 915-937.

Lee, M. S. Y. & Scanlon, J. D. 2002. Snake phylogeny based on osteology, soft anatomy and ecology. *Biological Reviews of the Cambridge Philosophical Society*, **77**(03), 333-401.

Lee, M. S. Y., Scanlon, J. D. & Price, A. H. 2001. On the lower jaw and intramandibular septum in snakes and anguimorph lizards. *Copeia*, **2001**(2), 531-535.

Lepage, D. 2017. Avibase-the world bird database.

Lepage, T., Bryant, D., Philippe, H. & Lartillot, N. 2007. A general comparison of relaxed molecular clock models. *Molecular Biology and Evolution*, **24**(12), 2669-2680.

Lewis, P. O. 2001. A Likelihood Approach to Estimating Phylogeny from Discrete Morphological Character Data. *Systematic Biology*, **50**(6), 913-925.

Li, C., Jiang, D.-Y., Cheng, L., Wu, X.-C. & Rieppel, O. 2014. A new species of *Largocephalosaurus* (Diapsida: Saurosphargidae), with implications for the morphological diversity and phylogeny of the group. *Geological Magazine*, **151**(1), 100-120.

Li, C., Liu, J. & Dong, Z. 2008a. Marine diapsids. Pp. 139-165 in J. Li, X. Wu & F. Zhang (eds) *The Chinese Fossil Reptiles and Their Kin*. Science Press Beijing.

Li, C., Rieppel, O., Wu, X.-C., Zhao, L.-J. & Wang, L.-T. 2011. A New Triassic Marine Reptile from Southwestern China. *Journal of Vertebrate Paleontology*, **31**(2), 303-312.

Li, C., Wu, X.-C., Rieppel, O., Wang, L.-T. & Zhao, L.-J. 2008b. An ancestral turtle from the Late Triassic of southwestern China. *Nature*, **456**(7221), 497-501.

Li, C., Zhao, L. & Wang, L. 2007a. A new species of *Macrocnemus* (Reptilia: Protorosauria) from the Middle Triassic of southwestern China and its palaeogeographical implication. *Science in China Series D: Earth Sciences*, **50**(11), 1601-1605.

Li, P.-P., Gao, K.-Q., Hou, L.-H. & Xu, X. 2007b. A gliding lizard from the Early Cretaceous of China. *Proceedings of the National Academy of Sciences*, **104**(13), 5507-5509.

Li, Z.-G., Jiang, D.-Y., Rieppel, O., Motani, R., Tintori, A., Sun, Z.-Y. & Ji, C. 2016. A new species of *Xinpusaurus* (Reptilia, Thalattosauria) from the Ladinian (Middle Triassic) of Xingyi, Guizhou, southwestern China. *Journal of Vertebrate Paleontology*, e1218340.

Liu, J. 2013. On the taxonomy of *Xinpusaurus* (Reptilia: Thalattosauria). *Vertebrata PalAsiatica*, **51**(1), 17-23.

Ljubisavljević, K., Polović, L. & Ivanović, A. 2008. Sexual differences in size and shape of the Mosor rock lizard [*Dinarolacerta mosorensis* (Kolombatović, 1886)] (Squamata: Lacertidae): a case study of the Lovćen mountain population (Montenegro). *Archives of Biological Sciences*, **60**(2), 279-288.

Longrich, N. R., Bhullar, B.-A. S. & Gauthier, J. A. 2012. Mass extinction of lizards and snakes at the Cretaceous–Paleogene boundary. *Proceedings of the National Academy of Sciences*.

Losos, J. B., Hillis, D. M. & Greene, H. W. 2012. Who speaks with a forked tongue? *Science*, **338**(6113), 1428-1429.

Losos, J. B., Jackman, T. R., Larson, A., Queiroz, K. d. & Rodríguez-Schettino, L. 1998. Contingency and Determinism in Replicated Adaptive Radiations of Island Lizards. *Science*, **279**(5359), 2115-2118.

Losos, J. B., Schoener, T. W. & Spiller, D. A. 2004. Predator-induced behaviour shifts and natural selection in field-experimental lizard populations. *Nature*, **432**(7016), 505-508.

Lü, J.-c., Ji, S.-a., Dong, Z.-m. & Wu, X.-c. 2008. An Upper Cretaceous lizard with a lower temporal arcade. *Naturwissenschaften*, **95**(7), 663-669.

Lucas, S. G. 1998. Global Triassic tetrapod biostratigraphy and biochronology. *Palaeogeography, Palaeoclimatology, Palaeoecology*, **143**(4), 347-384.

Lucas, S. G. 2006. Global Permian tetrapod biostratigraphy and biochronology. *Geological Society, London, Special Publications*, **265**(1), 65-93.

Lyson, T. R., Bever, G. S., Bhullar, B. A. S., Joyce, W. G. & Gauthier, J. A. 2010. Transitional fossils and the origin of turtles. *Biology Letters*, **6**(6), 830-833.

Lyson, Tyler R., Bever, Gabe S., Scheyer, Torsten M., Hsiang, Allison Y. & Gauthier, Jacques A. 2013a. Evolutionary Origin of the Turtle Shell. *Current Biology*, **23**(12), 1113-1119.

Lyson, T. R., Bhullar, B. A. S., Bever, G. S., Joyce, W. G., de Queiroz, K., Abzhanov, A. & Gauthier, J. A. 2013b. Homology of the enigmatic nuchal bone reveals novel reorganization of the shoulder girdle in the evolution of the turtle shell. *Evolution & Development*, **15**(5), 317-325.

Lyson, T. R. & Joyce, W. G. 2012. Evolution of the turtle bauplan: the topological relationship of the scapula relative to the ribcage. *Biology Letters*, **8**(6), 1028-1031.

Lyson, T. R., Rubidge, B. S., Scheyer, T. M., de Queiroz, K., Schachner, E. R., Smith, Roger M. H., Botha-Brink, J. & Bever, G. S. 2016. Fossorial Origin of the Turtle Shell. *Current Biology*, **26**(14), 1887-1894.

Lyson, T. R., Schachner, E. R., Botha-Brink, J., Scheyer, T. M., Lambertz, M., Bever, G. S., Rubidge, B. S. & de Queiroz, K. 2014. Origin of the unique ventilatory apparatus of turtles. *Nature Communications*, **5**, 6211.

Macey, J. R., Schulte, J. A., Larson, A., Ananjeva, N. B., Wang, Y., Pethiyagoda, R., Rastegar-Pouyani, N. & Papenfuss, T. J. 2000. Evaluating Trans-Tethys Migration: An Example Using Acrodont Lizard Phylogenetics. *Systematic Biology*, **49**(2), 233-256.

Maddison, D. R. 1991. The Discovery and Importance of Multiple Islands of Most-Parsimonious Trees. *Systematic Biology*, **40**(3), 315-328.

Maddison, W. P. 1993. Missing Data Versus Missing Characters in Phylogenetic Analysis. *Systematic Biology*, **42**(4), 576-581.

Maddison, W. P. & Maddison, D. R. 2015. Mesquite: a modular system for evolutionary analysis. Version 3.04 (http://mesquiteproject.org).

Maisano, J. A. 2002. Terminal fusions of skeletal elements as indicators of maturity in squamates. *Journal of Vertebrate Paleontology*, **22**(2), 268-275.

Maisch, M. W. 2014. On the morphoplogy and taxonomic status of *Xinpusaurus kohi* Jiang et al., 2004 (Diapsida: Thalattosauria) from the Upper Triassic of China. *Palaeodiversity*, **7**, 47-59.

Maisch, M. W. & Matzke, A. T. 2000. The Ichthyosauria. *Stuttgarter Beiträge zur Naturkunde*, **298**, 1 - 159.

Malan, M. E. 1963. The dentitions of the South African Rhynchocephalia and their bearing on the origin of the rhynchosaurs. *South African Journal of Science*, **59**, 214-220.

Manzig, P. C., Kellner, A. W. A., Weinschütz, L. C., Fragoso, C. E., Vega, C. S., Guimarães, G. B., Godoy, L. C., Liccardo, A., Ricetti, J. H. Z. & de Moura, C. C. 2014. Discovery of a Rare Pterosaur Bone Bed in a Cretaceous Desert with Insights on Ontogeny and Behavior of Flying Reptiles. *PLoS ONE*, **9**(8), e100005.

Mateer, N. 1982. Osteology of the Jurassic lizard *Ardeosaurus brevipes* (Meyer). *Palaeontology*, **25**(3), 461-469.

Matsumoto, R. & Evans, S. E. 2016. Morphology and function of the palatal dentition in Choristodera. *Journal of Anatomy*, **228**(3), 414-429.

Mazin, J. M. 1986. A new interpretation of the fore-fin of *Utatsusaurus hataii* (reptilia, ichthyopterygia). *Paläontologische Zeitschrift*, **60**(3), 313-318.

McDowell, S. B. & Bogert, C. M. 1954. The systematic position of *Lanthanotus* and the affinities of the anguinomorphan lizards. *Bulletin of the American Museum of Natural History*, **105**(1-142).

McGowan, C. 1992. Unusual extensions of the neural spines in two ichthyosaurs from the Lower Jurassic of Holzmaden. *Canadian Journal of Earth Sciences*, **29**(2), 380-383.

McGowan, C. & Motani, R. 2003. *Handbook of Paleoherpetology. Part 8 - Ichthyopterygia*. Verlag Dr. Friedrich Pfeil, München, 175 pp.

McMahan, C. D., Freeborn, L. R., Wheeler, W. C. & Crother, B. I. 2015. Forked Tongues Revisited: Molecular Apomorphies Support Morphological Hypotheses of Squamate Evolution. *Copeia*, **103**(3), 525-529.

Menning, M., Schröder, B., Plein, E., Simon, T., Lepper, J., Röhling, H.-G., Heunisch, C., Stapf, K., Lützner, H., Käding, K.-C., Paul, J., Horn, M., Hagdorn, H., Beutler, G. & Nitsch, E. 2011. Beschlüsse der Deutschen Stratigraphischen Kommission 1991–2010 zu Perm und Trias von Mitteleuropa *Zeitschrift der Deutschen Gesellschaft für Geowissenschaften*, **162**(1), 1-18.

Meszoely, C. A. 1970. North American fossil anguid lizards. *Bulletin of the Museum of Comparative Zoology*, **139**, 87-150.

Metzger, K. A. & Herrel, A. 2005. Correlations between lizard cranial shape and diet: a quantitative, phylogenetically informed analysis. *Biological Journal of the Linnean Society*, **86**(4), 433-466.

Meyer, H. v. 1832. *Palaeologica zur Geschichte der Erde und ihrer Geschöpfe*. Verlag Siegmund Schmerber, Frankfurt.

Meyer, H. v. 1839. Mittheilung. *Neues Jahrbuch für Mineralogie, Geognosie, Geologie und Petrefaktenkunde*, **1839**, 699-701.

Meyer, H. v. 1847. *Homoeosaurus maximiliani und Rhamphorhynchus (Pterodactylus) longicaudus: zwei fossile reptilien aus dem kalkschiefer von Solenhofen im Naturalienkabinet seiner baiserlich hoheit des Herzogs Maximilian von Leuchtenberg zu Eichstaedt*. Verlag der S. Schmerber'schen buchhandlung, Frankfurt.

Meyer, H. v. 1855. Briefliche Mitteilung an Prof. Bronn. *Neues Jahrbuch für Mineralogie, Geognosie, Geologie und Petrefaktenkunde*, **1855**, 326-337.

Meyer, H. v. 1860a. *Zur Fauna der Vorwelt. Reptilien aus dem lithographischen Schiefer des Jura in Deutschland und Frankreich*. Verlag der S. Schmerbersche Buchhandlung, Frankfurt.

Meyer, H. v. 1860b. *Zur Fauna tier Vaupelt, Reptilien sue dern lithographischen Schiefer des Jura in Deutechland und Frankreich*, Frankfurt.

Meyer, H. v. 1866. *Homoeosaurus maximiliani* aus dem lithographischen Schiefer von Kelheim. *Palaeontographica*, **15**(2), 49-65.

Miller, M. A., Pfeiffer, W. & Schwartz, T. 2010. Creating the CIPRES Science Gateway for inference of large phylogenetic trees. *Gateway Computing Environments Workshop (GCE), 2010*, 1-8.

Minoura, N. 1994. Evolution and paleobiogeography of the Early Triassic ichthyosaurs. Pp. 65-68 in Anonymous (ed) *From Paleoasian Ocean to Paleo-Pacific Ocean*. Hokkaido University, Sapporo.

Misof, B., Liu, S., Meusemann, K., Peters, R. S., Donath, A., Mayer, C., Frandsen, P. B., Ware, J., Flouri, T., Beutel, R. G., Niehuis, O., Petersen, M., Izquierdo-Carrasco, F., Wappler, T., Rust, J., Aberer, A. J., Aspöck, U., Aspöck, H., Bartel, D., Blanke, A., Berger, S., Böhm, A., Buckley, T. R., Calcott, B., Chen, J., Friedrich, F., Fukui, M., Fujita, M.,

Greve, C., Grobe, P., Gu, S., Huang, Y., Jermiin, L. S., Kawahara, A. Y., Krogmann, L., Kubiak, M., Lanfear, R., Letsch, H., Li, Y., Li, Z., Li, J., Lu, H., Machida, R., Mashimo, Y., Kapli, P., McKenna, D. D., Meng, G., Nakagaki, Y., Navarrete-Heredia, J. L., Ott, M., Ou, Y., Pass, G., Podsiadlowski, L., Pohl, H., von Reumont, B. M., Schütte, K., Sekiya, K., Shimizu, S., Slipinski, A., Stamatakis, A., Song, W., Su, X., Szucsich, N. U., Tan, M., Tan, X., Tang, M., Tang, J., Timelthaler, G., Tomizuka, S., Trautwein, M., Tong, X., Uchifune, T., Walzl, M. G., Wiegmann, B. M., Wilbrandt, J., Wipfler, B., Wong, T. K. F., Wu, Q., Wu, G., Xie, Y., Yang, S., Yang, Q., Yeates, D. K., Yoshizawa, K., Zhang, Q., Zhang, R., Zhang, W., Zhang, Y., Zhao, J., Zhou, C., Zhou, L., Ziesmann, T., Zou, S., Li, Y., Xu, X., Zhang, Y., Yang, H., Wang, J., Wang, J., Kjer, K. M. & Zhou, X. 2014. Phylogenomics resolves the timing and pattern of insect evolution. *Science*, **346**(6210), 763-767.

Mo, J.-Y., Xu, X. & Evans, S. E. 2010. The evolution of the lepidosaurian lower temporal bar: new perspectives from the Late Cretaceous of South China. *Proceedings of the Royal Society B: Biological Sciences*, **277**(1679), 331-336.

Moazen, M., Curtis, N., Evans, S. E., O'Higgins, P. & Fagan, M. J. 2008a. Combined finite element and multibody dynamics analysis of biting in a Uromastyx hardwickii lizard skull. *Journal of Anatomy*, **213**(5), 499-508.

Moazen, M., Curtis, N., Evans, S. E., O'Higgins, P. & Fagan, M. J. 2008b. Rigid-body analysis of a lizard skull: Modelling the skull of *Uromastyx hardwickii*. *Journal of Biomechanics*, **41**(6), 1274-1280.

Moazen, M., Curtis, N., O'Higgins, P., Evans, S. E. & Fagan, M. J. 2009a. Biomechanical assessment of evolutionary changes in the lepidosaurian skull. *Proceedings of the National Academy of Sciences*, **106**(20), 8273-8277.

Moazen, M., Curtis, N., O'Higgins, P., Jones, M. E. H., Evans, S. E. & Fagan, M. J. 2009b. Assessment of the role of sutures in a lizard skull: a computer modelling study. *Proceedings of the Royal Society B: Biological Sciences*, **276**(1654), 39-46.

Modesto, S. P. 1998. New information on the skull of the Early Permian reptile *Captorhinus aguti*. *PaleoBios*, **18**(2-3), 21-35.

Modesto, S. P., Scott, D. M., Berman, D. S., MÜLler, J. & Reisz, R. R. 2007. The skull and the palaeoecological significance of *Labidosaurus hamatus*, a captorhinid reptile from the Lower Permian of Texas. *Zoological Journal of the Linnean Society*, **149**(2), 237-262.

Modesto, S. P. & Sues, H.-D. 2004. The skull of the Early Triassic archosauromorph reptile *Prolacerta broomi* and its phylogenetic significance. *Zoological Journal of the Linnean Society*, **140**(3), 335-351.

Montefeltro, F. C., Bittencourt, J. S., Langer, M. C. & Schultz, C. L. 2013. Postcranial anatomy of the hyperodapedontine rhynchosaur *Teyumbaita sulcognathus* (Azevedo and Schultz, 1987) from the Late Triassic of Southern Brazil. *Journal of Vertebrate Paleontology*, **33**(1), 67-84.

Montefeltro, F. C., Langer, M. C. & Schultz, C. L. 2010. Cranial anatomy of a new genus of hyperodapedontine rhynchosaur (Diapsida, Archosauromorpha) from the Upper Triassic of southern Brazil. *Earth and Environmental Science Transactions of the Royal Society of Edinburgh*, **101**(1), 27-52.

Monteiro, L. R. & Abe, A. S. 1997. Allometry and morphological integration in the skull of *Tupinambis merianae* (Lacertilia: Teiidae). *Amphibia-Reptilia*, **18**(4), 397-405.

Montero, R., Gans, C. & Luisa Lions, M. 1999. Embryonic development of the skeleton of *Amphisbaena darwini heterozonata* (Squamata: Amphisbaenidae). *Journal of Morphology*, **239**(1), 1-25.

Moody, S. M. 1980. *Phylogenetic and Historical Biogeographical Relationships of the Genera in the Family Agamidae (Reptilia: Lacertilia)*. Unpublished PhD thesis, University of Michigan.

Motani, R. 1997. New data on the forefin of *Utatsusaurus hataii* (Ichthyosauria). *Journal of Paleontology*, **71**(3), 475 - 479.

Motani, R. 1999a. On the evolution and homology of ichthyosaurian forefins. *Journal of Vertebrate Paleontology*, **19**, 42 - 49.

Motani, R. 1999b. Phylogeny of the Ichthyopterygia. *Journal of Vertebrate Paleontology*, **19**, 473 - 496.

Motani, R. 2005. Evolution of fish-shaped reptiles (Reptilia: Ichthyopterygia) in their physical environments and constraints. *Annual Review of Earth & Planetary Sciences*, **33**, 395-420.

Motani, R., Minoura, N. & Ando, T. 1998. Ichthyosaurian relationships illuminated by new primitive skeletons from Japan. *Nature*, **393**, 255 - 257.

Mulcahy, D. G., Noonan, B. P., Moss, T., Townsend, T. M., Reeder, T. W., Sites Jr, J. W. & Wiens, J. J. 2012. Estimating divergence dates and evaluating dating methods using

phylogenomic and mitochondrial data in squamate reptiles. *Molecular Phylogenetics and Evolution*, **65**(3), 974-991.

Müller, J. 2004. The relationships among diapsid reptiles and the influence of taxon selection. Pp. 379-408 in G. Arratia, M.V.H. Wilson & R. Cloutier (eds) *Recent advances in the origin and early radiation of vertebrates*. Verlag Dr. Friedrich Pfeil, Munich.

Müller, J. 2005. The anatomy of *Askeptosaurus italicus* from the Middle Triassic of Monte San Giorgio and the interrelationships of thalattosaurs (Reptilia, Diapsida). *Canadian Journal of Earth Sciences*, **42**(7), 1347-1367.

Müller, J., Hipsley, C. A. & Maisano, J. A. 2016. Skull osteology of the Eocene amphisbaenian *Spathorhynchus fossorium* (Reptilia, Squamata) suggests convergent evolution and reversals of fossorial adaptations in worm lizards. *Journal of Anatomy*, **229**(5), 615-630.

Müller, J. & Reisz, R. R. 2005. An Early Captorhinid Reptile (Amniota, Eureptilia) from the Upper Carboniferous of Hamilton, Kansas. *Journal of Vertebrate Paleontology*, **25**(3), 561-568.

Müller, J., Renesto, S. & Evans, S. E. 2005. The marine diapsid reptile *Endennasaurus* from the Upper Triassic of Italy. *Palaeontology*, **48**(1), 15-30.

Murry, P. A. 1986. Vertebrate paleontology of the Dockum Group, western Texas and eastern New Mexico. Pp. 109-137 in K. Padian (ed) *The beginning of the age of dinosaurs*. Cambridge University Press, Cambridge.

Murry, P. A. 1987. New reptiles from the Upper Triassic Chinle Formation of Arizona. *Journal of Paleontology*, **61**(4), 773-786.

Muscio, G. 1996. Preliminary note on a specimen of Prolacertiformes (Reptilia) from the Norian (Late Triassic) of Preone (Udine, north-eastern Italy). *Gortania*, **18**, 33-40.

Nagashima, H., Sugahara, F., Takechi, M., Sato, N. & Kuratani, S. 2015. On the homology of the shoulder girdle in turtles. *Journal of Experimental Zoology Part B: Molecular and Developmental Evolution*, **324**(3), 244-254.

Nava, W. R. & Martinelli, A. G. 2011. A new squamate lizard from the Upper Cretaceous Adamantina Formation (Bauru Group), São Paulo State, Brazil. *Anais da Academia Brasileira de Ciencias*, **83**, 291-299.

Neenan, J. M., Li, C., Rieppel, O., Bernardini, F., Tuniz, C., Muscio, G. & Scheyer, T. M. 2014. Unique method of tooth replacement in durophagous placodont marine reptiles, with new data on the dentition of Chinese taxa. *Journal of Anatomy*, **224**(5), 603-613.

Neenan, J. M. & Scheyer, T. M. 2012. The braincase and inner ear of *Placodus gigas* (Sauropterygia, Placodontia)—a new reconstruction based on micro-computed tomographic data. *Journal of Vertebrate Paleontology*, **32**(6), 1350-1357.

Nesbitt, S. J. 2011. The Early Evolution of Archosaurs: Relationships and the Origin of Major Clades. *Bulletin of the American Museum of Natural History*, **352**, 1-292.

Nesbitt, S. J., Flynn, J. J., Pritchard, A. C., Parrish, J. M., Ranivoharimanana, L. & Wyss, A. R. 2015. Postcranial Osteology of *Azendohsaurus madagaskarensis* (?Middle to Upper Triassic, Isalo Group, Madagascar) and its Systematic Position Among Stem Archosaur Reptiles. *Bulletin of the American Museum of Natural History*, 1-126.

Nessov, L. 1985. Rare bony fishes, terrestrial lizards and mammals from the lagoonal zone of the littoral lowlands of the Cretaceous of the Kyzylkumy. *Yearbook of the All-Union Palaeontological Society, Leningrad*, **28**, 199-219.

Nessov, L. 1988. Late mesozoic amphibians and lizards of Soviet Middle Asia. *Acta Zoologica Cracoviensia*, **31**(14), 475-486.

Nicholls, E. & Brinkman, D. 1995. A new ichthyosaur from the Triassic Sulphur Mountain formation of British Columbia. Pp. 521-535 in W.S. Sarjeant (ed) *Vertebrate Fossils and the Evolution of Scientific Concepts.* . Gordon and Breach, London.

Nicholls, E. L. 1999. A reexamination of *Thalattosaurus* and *Nectosaurus* and the relationships of the Thalattosauria (Reptilia: Diapsida). *PaleoBios*, **19**(1), 1-29.

Nicholls, E. L. & Brinkman, D. 1993. A new specimen of *Utatsusaurus* (Reptilia: Ichthyosauria) from the Lower Triassic Sulphur Mountain Formation of British Columbia. *Canadian Journal of Earth Sciences*, **30**(3), 486-490.

Nixon, K. C. & Carpenter, J. M. 2012. On homology. *Cladistics*, **28**(2), 160-169.

Nixon, K. C. & Carpenter, J. M. 2013. More on Absences. *Cladistics*, **29**(1), 1-6.

Nopcsa, F. v. 1903. V.—On the Origin of the Mosasaurs. *Geological Magazine (Decade IV)*, **10**(03), 119-121.

Nopcsa, F. v. 1908. Zur kenntnis der fossilen Eidechsen. *Beiträge zur Paläontologie Österreich-Ungarns und des Orients.*, **21**, 33-62.

Nopcsa, F. v. 1923a. *Eidolosaurus* und *Pachyophis*: Zwei neue Neocom-Reptilien von Franz Baron Nopcsa. . *Palaeontographica*, **65**, 99–154.

Nopcsa, F. v. 1923b. Neubeschreibung des Trias-Pterosauriers *Tribelesodon*. *Palaeontologische Zeitschrift*, **5**(3), 161-181.

Nopcsa, F. v. 1925. *Askeptosaurus*, ein neues Reptil aus der Trias von Besano. *Centralblätter für Mineralogie, Geologie und Paläontologie*, **1925B**, 265-267.

Nopcsa, F. v. 1930. Notizen iiber *Macrochemus Bassanii* nov. gen. et spec. *Centralblatt für Mineralogie, Geologie und Paläontologie B*, **1930**, 252-255.

Norell, M. A. & Gao, K.-Q. 1997. Braincase and phylogenetic relationships of Estesia mongoliensis from the late Cretaceous of the Gobi Desert and the recognition of a new clade of lizards. *American Museum Novitates*, **3211**, 1-25.

Nosotti, S. 2007. *Tanystropheus Longobardicus* (Reptilia, Protorosauria): Re-interpretations of the Anatomy Based on New Specimens from the Middle Triassic of Besano (Lombardy, Northern Italy). *Memoir della Società Italiana di Scienze Naturali e Museo Civico di Storia Naturale di Milano*, **35**(3), 1-88.

Nosotti, S. & Rieppel, O. 2002. The Braincase of *Placodus* Agassiz, 1833 (Reptilia, Placodontia). *Memorie della Società Italiana di Scienze Naturali e del Museo Civico di Storia Naturale di Milano*, **31**(1), 1-18.

Nydam, R. L. & Cifelli, R. L. 2005. New data on the dentition of the scincomorphan lizard *Polyglyphanodon sternbergi*. *Acta Palaeontologica Polonica*, **50**(1), 73-78.

Nydam, R. L., Eaton, J. G. & Sankey, J. 2007. New taxa of transversely-toothed lizards (Squamata: Scincomorpha) and new information on the evolutionary history of 'Teiids'. *Journal of Paleontology*, **81**(3), 538-549.

Nylander, J. A. A. 2014. Burntrees.

Nylander, J. A. A., Ronquist, F., Huelsenbeck, J. P. & Nieves-Aldrey, J. 2004. Bayesian Phylogenetic Analysis of Combined Data. *Systematic Biology*, **53**(1), 47-67.

O'Connor, P. M. 2006. Postcranial pneumaticity: An evaluation of soft-tissue influences on the postcranial skeleton and the reconstruction of pulmonary anatomy in archosaurs. *Journal of Morphology*, **267**(10), 1199-1226.

O'Donoghue, C. H. 1920. The Blood Vascular System of the Tuatara, *Sphenodon punctatus*. *Philosophical Transactions of the Royal Society of London. Series B, Biological Sciences*, **210**, 175-252.

O'Keefe, F. R., Sidor, C. A., Larsson, H. C. E., Maga, A. & Ide, O. 2005. The vertebrate fauna of the Upper Permian of Niger—III, morphology and ontogeny of the hindlimb of Moradisaurus grandis (Reptilia, Captorhinidae). *Journal of Vertebrate Paleontology*, **25**(2), 309-319.

O'Keefe, F. R., Sidor, C. A., Larsson, H. C. E., Maga, A. & Ide, O. 2006. Evolution and homology of the astragalus in early amniotes: New fossils, new perspectives. *Journal of Morphology*, **267**(4), 415-425.

O'Leary, M. A., Bloch, J. I., Flynn, J. J., Gaudin, T. J., Giallombardo, A., Giannini, N. P., Goldberg, S. L., Kraatz, B. P., Luo, Z.-X., Meng, J., Ni, X., Novacek, M. J., Perini, F. A., Randall, Z. S., Rougier, G. W., Sargis, E. J., Silcox, M. T., Simmons, N. B., Spaulding, M., Velazco, P. M., Weksler, M., Wible, J. R. & Cirranello, A. L. 2013. The Placental Mammal Ancestor and the Post–K-Pg Radiation of Placentals. *Science*, **339**(6120), 662-667.

O'Reilly, J. E. & Donoghue, P. C. 2016. Tips and nodes are complementary not competing approaches to the calibration of molecular clocks. *Biology Letters*, **12**(4), 20150975.

O'Reilly, J. E., Puttick, M. N., Parry, L., Tanner, A. R., Tarver, J. E., Fleming, J., Pisani, D. & Donoghue, P. C. J. 2016. Bayesian methods outperform parsimony but at the expense of precision in the estimation of phylogeny from discrete morphological data. *Biology Letters*, **12**(4).

O'Reilly, J. E., dos Reis, M. & Donoghue, P. C. 2015. Dating tips for divergence-time estimation. *Trends in Genetics*, **31**(11), 637-650.

Oelrich, T. M. 1956. The anatomy of the head of *Ctenosaura pectinata* (Iguanidae). *Miscellaneous Publications - Museum of Zoology, University of Michigan*, **94**, 1-122.

Ogg, J. G., Ogg, G. & Gradstein, F. 2008. *The Concise Geologic Time Scale*. Cambridge University Press, Cambridge, 177 pp.

Ogg, J. G., Ogg, G. & Gradstein, F. M. 2016. *A Concise Geologic Time Scale*. Elsevier, Amsterdam, 234 pp.

Olson, E. C. 1937. A Mounted Skeleton of *Labidosaurus* Cope. *The Journal of Geology*, **45**(1), 95-100.

Olson, E. C. 1984. The Taxonomic Status and Morphology of *Pleuristion brachycoelus* Case; Referred to *Protocaptorhinus pricei* Clark and Carroll (Reptilia: Captorhinomorpha). *Journal of Paleontology*, **58**(5), 1282-1295.

Olsson, M., Shine, R., Wapstra, E., Ujvari, B. & Madsen, T. 2002. Sexual Dimorphism in Lizard Body Shape: The Roles of Sexual Selection and Fecundity Selection. *Evolution*, **56**(7), 1538-1542.

Oppel, M. 1811. *Die ordnungen, familien und gattungen der reptilien als prodrom einer naturgeschichte derselben*. Joseph Lindauer, Münich, 77 pp.

Padian, K. 1989. Presence of the dinosaur *Scelidosaurus* indicates Jurassic age for the Kayenta Formation (Glen Canyon Group, northern Arizona). *Geology*, **17**(5), 438-441.

Palci, A. & Caldwell, M. W. 2013. Primary homologies of the circumorbital bones of snakes. *Journal of Morphology*, **274**(9), 973-986.

Palci, A. & Caldwell, M. W. 2014. The upper cretaceous snake *Dinilysia patagonica* Smith-Woodward, 1901, and the crista circumfenestralis of snakes. *Journal of Morphology*, **275**(10), 1187-1200.

Palci, A., Caldwell, M. W. & Albino, A. M. 2013a. Emended diagnosis and phylogenetic relationships of the Upper Cretaceous fossil snake *Najash rionegrina* Apesteguía and Zaher, 2006. *Journal of Vertebrate Paleontology*, **33**(1), 131-140.

Palci, A., Caldwell, M. W. & Nydam, R. L. 2013b. Reevaluation of the anatomy of the Cenomanian (Upper Cretaceous) hind-limbed marine fossil snakes *Pachyrhachis*, *Haasiophis*, and *Eupodophis*. *Journal of Vertebrate Paleontology*, **33**(6), 1328-1342.

Parks, P. 1969. *Cranial anatomy and mastication of the Triassic reptile Trilophosaurus*. Unpublished PhD thesis, University of Texas, 100 pp.

Parrington, F. R. 1935. XVI.—On *Prolacerta broomi*, gen. et sp. n., and the origin of lizards. *Journal of Natural History Series 10*, **16**(92), 197-205.

Parrington, F. R. 1937. A note on the supratemporal and tabular bones in reptiles. *Annals and Magazine of Natural History*, **20**(115), 69-76.

Parrish, J. M. 1992. Phylogeny of the Erythrosuchidae (Reptilia: Archosauriformes). *Journal of Vertebrate Paleontology*, **12**(1), 93-102.

Parsons, T. S. & Williams, E. E. 1961. Two Jurassic turtle skulls: a morphological study. *Bulletin of the Museum of Comparative Zoology*, **125**, 43-107.

Patterson, C. 1982. Morphological characters and homology. Pp. 21-74 in K.A. Joysey & A.E. Friday (eds) *Systematics Association Special Volume: "Problems of phylogenetic reconstruction"*. Academic Press, London and New York.

Peabody, F. E. 1951. The Origin of the Astragalus of Reptiles. *Evolution*, **5**(4), 339-344.

Peabody, F. E. 1952. *Petrolacosaurus kansensis* Lane, a Pennsylvanian reptile from Kansas. *The University of Kansas - Paleontological Contributions*, **Article 1**, 1-41.

Peyer, B. 1931a. Die Triasfauna der Tessiner Kalkalpen III. Placodontia. *Abhandlungen der Schweizerischen Paläontologischen Gesellschaft*, **51**, 1-25.

Peyer, B. 1931b. Die Triasfauna der Tessiner Kalkalpen IV. *Ceresiosaurus calcagnii* nov. gen. nov. spec. *Abhandlungen der Schweizerischen Paläontologischen Gesellschaft*, **51**, 1-68.

Peyer, B. 1931c. *Macrocnemus*, nicht *Macrochemus*. *Centralblatt für Mineralogie, Geologie und Paläontologie B*, **1931**, 190-192.

Peyer, B. 1937. Die Triasfauna der Tessiner Kalkalpen XII. *Macrocnemus Bassanii* Nopcsa. *Schweizerische Paläontologische Abhandlungen*, **59**, 1-140.

Philippe, H. & Roure, B. 2011. Difficult phylogenetic questions: more data, maybe; better methods, certainly. *BMC Biology*, **9**(1), 91.

Pianka, E. R. & Vitt, L. J. 2003. *Lizards: Windows to the Evolution of Diversity*. University of California Press, 333 pp.

Pierce, S. E. & Caldwell, M. W. 2004. Redescription and phylogenetic position of the Adriatic (Upper Cretaceous; Cenomanian) dolichosaur *Pontosaurus lesinensis* (Kornhuber, 1873). *Journal of Vertebrate Paleontology*, **24**(2), 373-386.

Pimentel, R. A. & Riggins, R. 1987. The nature of cladistic data. *Cladistics*, **3**(3), 201-209.

Pincheira-Donoso, D., Bauer, A. M., Meiri, S. & Uetz, P. 2013. Global taxonomic diversity of living reptiles. *PLoS ONE*, **8**(3), e59741.

Piveteau, J. 1926. Paléontologie de Madagascar XIII, Amphibiens et Reptiles permiens. *Annales de Paleontologie*, **15**(2-4), 55-180.

Platnick, N. I. 1979. Philosophy and the Transformation of Cladistics. *Systematic Biology*, **28**(4), 537-546.

Pleijel, F. 1995. On Character Coding for Phylogeny Reconstruction. *Cladistics*, **11**(3), 309-315.

Poe, S. & Wiens, J. J. 2000. Character selection and the methodology of morphological phylogenetics. Pp. 20-36 in J.J. Wiens (ed) *Phylogenetic analysis of morphological data*. Smithsonian Institution Press, Washington, D.C.

Polcyn, M. J., Jacobs, L. L. & Haber, A. 2005. A morphological model and CT assessment of the skull of *Pachyrhachis problematicus* (Squamata, Serpentes), a 98 million year old snake with legs from the Middle East. *Palaeontologia Electronica*, **8**(1), 1-24.

Popper, K. 1959. *The Logic of Scientific Discovery*. Hutchinson and Company, London, 545 pp.

Pregill, G. K., Gauthier, J. A. & Greene, H. W. 1986. The evolution of helodermatid squamates with description of a new taxon and an overview of Varanoidea. *Transactions of the San Diego Society of Natural History*, **21**, 167-202.

Presch, W. 1974. Evolutionary relationshiops and biogeography of macroteiid lizards (Family Teiidae, Subfamily Teiinae). *Bulletin of the Southern California Academy of Sciences*, **73**, 23-32.

Presch, W. 1988. Phylogenetic relationships of the Scincomorpha. Pp. 471-492 in R. Estes & G. Pregill (eds) *Phylogenetic relationships of the lizard families*. Stanford University Press, Stanford.

Price, L. I. 1935. Notes on the brain case of *Captorhinus*. *Proceedings of the Boston Society of Natural History*, **40**, 377-386.

Price, L. I. 1937. Two new cotylosaurs from the Permian of Texas. *Proceedings of the New England Zoological Club*, **16**, 97-102.

Price, L. I. 1940. Autotomy of the Tail in Permian Reptiles. *Copeia*, **1940**(2), 119-120.

Proctor, H. C. 1996. Behavioral characters and homoplasy: perception versus practice. Pp. 131-149 in M.J. Sanderson & L. Hufford (eds) *Homoplasy: The Recurrence of Similarity in Evolution (MJ Sanderson & L. Hufford, eds)*. Academic Press, San Diego.

Puttick, M. N., O'Reilly, J. E., Oakley, D., Tanner, A. R., Fleming, J. F., Clark, J., Holloway, L., Lozano-Fernandez, J., Parry, L. A., Tarver, J. E., Pisani, D. & Donoghue, P. C. J. 2017. Parsimony and maximum-likelihood phylogenetic analyses of morphology do not generally integrate uncertainty in inferring evolutionary history: a response to Brown *et al.* *Proceedings of the Royal Society B: Biological Sciences*, **284**(1864).

Pyron, R. A. 2017. Novel Approaches for Phylogenetic Inference from Morphological Data and Total-Evidence Dating in Squamate Reptiles (Lizards, Snakes, and Amphisbaenians). *Systematic Biology*, **66**(1), 38-56.

Pyron, R. A. & Burbrink, F. T. 2014. Early origin of viviparity and multiple reversions to oviparity in squamate reptiles. *Ecology Letters*, **17**(1), 13-21.

Pyron, R. A., Burbrink, F. T. & Wiens, J. J. 2013. A phylogeny and revised classification of Squamata, including 4161 species of lizards and snakes. *BMC Evolutionary Biology*, **13**(93), Available online: 10.1186/1471-2148-1113-1193.

Quenstedt, F. A. 1888. *Psammochelys keuperina*. *Jahreshefte des Vereins für vaterländische Naturkunde in Württemberg*, 120-130.

Rae, T. C. 1998. The Logical Basis for the use of Continuous Characters in Phylogenetic Systematics. *Cladistics*, **14**(3), 221-228.

Rage, J. C. 1977. La position phylétique de *Dinilysia patagonica,* serpent du Cretacé supérieur. *Comptes Rendus de l'Académie des Sciences de Paris*, **284**, 1765-1768.

Rage, J. C. 1999. Squamates (Reptilia) from the Upper Cretaceous of Laño (Basque Country, Spain). Pp. 121-133 in H. Astibia, J.C. Corral, X. Murelaga, X. Orue-Etxebarria & X. Pereda Suberbiola (eds) *Geology and Paleontology of the Upper Cretaceous Vertebrate-Bearing Beds of the Laño Quarry*. Museo de Ciencias Naturales de Álava, Álava.

Rage, J. C. 2013. Mesozoic and Cenozoic squamates of Europe. *Palaeobiodiversity and Palaeoenvironments*, **93**(4), 517-534.

Rage, J. C. & Albino, A. M. 1989. *Dinilysia patagonica* (Reptilia, Serpentes): matériel vertébral additionnel du Crétacé supérieur d'Argentine. Étude complémentaire des vertèbres, variations intraspécifiques et intracolumnaires. *Neues Jahrbuch für Geologie und Paläontologie, Monatshefte*, **1989**, 433-447.

Rage, J. C. & Augé, M. 2010. Squamate reptiles from the middle Eocene of Lissieu (France). A landmark in the middle Eocene of Europe. *Geobios*, **43**, 253-268.

Rage, J. C. & Escuillié, F. 2003. The Cenomanian: stage of hindlimbed snakes. *Carnets de Geologie*, **CG2003**(A01-en), 1-11.

Raxworthy, C. J., Forstner, M. R. J. & Nussbaum, R. A. 2002. Chameleon radiation by oceanic dispersal. *Nature*, **415**(6873), 784-787.

Rayfield, E. J. 2007. Finite element analysis and understanding the biomechanics and evolution of living and fossil organisms. *Annual Review of Earth & Planetary Sciences*, **35**, 541-576.

Rayfield, E. J., Norman, D. B., Horner, C. C., Horner, J. R., Smith, P. M., Thomason, J. J. & Upchurch, P. 2001. Cranial design and function in a large theropod dinosaur. *Nature*, **409**(6823), 1033-1037.

Reeder, T. W., Townsend, T. M., Mulcahy, D. G., Noonan, B. P., Wood, P. L., Jr., Sites, J. W., Jr. & Wiens, J. J. 2015. Integrated Analyses Resolve Conflicts over Squamate Reptile Phylogeny and Reveal Unexpected Placements for Fossil Taxa. *PLoS ONE*, **10**(3), e0118199.

Regnault, S., Hutchinson, J. R. & Jones, M. E. H. 2016. Sesamoid bones in tuatara (*Sphenodon punctatus*) investigated with X-ray microtomography, and implications for sesamoid evolution in Lepidosauria. *Journal of Morphology*, n/a-n/a.

Reilly, D. T. & Burstein, A. H. 1975. The elastic and ultimate properties of compact bone tissue. *Journal of Biomechanics*, **8**(6), 393-405.

Reisz, R. R. 1975. *Petrolacosaurus kansensis Lane: the oldest known diapsid reptile*. Unpublished PhD thesis, Thesis (Ph. D.)--McGill University.

Reisz, R. R. 1977. *Petrolacosaurus*, the oldest known diapsid reptile. *Science*, **196**(4294), 1091-1093.

Reisz, R. R. 1981. A diapsid reptile from the Pennsylvanian of Kansas. *University of Kansas Museum of Natural History Special Publication*, **7**, 1-74.

Reisz, R. R., Berman, D. S. & Scott, D. 1984. The Anatomy and Relationships of the Lower Permian Reptile *Araeoscelis*. *Journal of Vertebrate Paleontology*, **4**(1), 57-67.

Reisz, R. R. & Dilkes, D. W. 2003. *Archaeovenator hamiltonensis*, a new varanopid (Synapsida: Eupelycosauria) from the Upper Carboniferous of Kansas. *Canadian Journal of Earth Sciences*, **40**(4), 667-678.

Remane, A. 1952. Die Grundlagen des Natürlichen Systems der Vergleichenden Anatomie und der Phylogenetik*Theoretische Morphologie und Systematik* Akad. Verlag-Ges. Geest & Portig, Leipzig.

Rendell, L. E. & Whitehead, H. 2003. Vocal clans in sperm whales (*Physeter macrocephalus*). *Proceedings of the Royal Society of London. Series B: Biological Sciences*, **270**(1512), 225-231.

Renesto, S. 1984. A new lepidosaur (Reptilia) from the Norian beds of the Bergamo Prealps. Preliminary note. *Rivista Italiana di Paleontologia e Stratigrafia*, **90**, 165-176.

Renesto, S. 1991. The anatomy and relationships of *Endennasaurus acutirostris* (Reptilia, Neodiapsida), from the Norian (Late Triassic) of Lombardy. *Rivista Italiana di Paleontologia e Stratigrafia*, **97**(3-4), 409-430.

Renesto, S. 1994a. *Megalancosaurus*, a Possibly Arboreal Archosauromorph (Reptilia) from the Upper Triassic of Northern Italy. *Journal of Vertebrate Paleontology*, **14**(1), 38-52.

Renesto, S. 1994b. A new prolacertiform reptile from the Late Triassic of Northern Italy. *Rivista Italiana di Paleontologia e Stratigrafia*, **100**(2), 285-306.
Renesto, S. 2000. Bird-like head on a chameleon body: new specimens of the enigmatic diapsid reptile *Megalancosaurus* from the Late Triassic of Northern Italy, con 4 tav. e 14 fig. *Rivista Italiana di Paleontologia e Stratigrafia*, **106**(2), 157-180.
Renesto, S. 2005a. A new specimen of *Tanystropheus* (Reptilia Protorosauria) from the Middle Triassic of Switzerland and the ecology of the genus. *Rivista Italiana di Paleontologia e Stratigrafia*, **111**(3), 377-394.
Renesto, S. 2005b. A possible find of *Endennasaurus* (Reptilia Thalattosauria), with a comparison between *Endennasaurus* and *Pachystropheus*. *Neues Jahrbuch fur Geologie und Palaontologie-Monatshefte*, **2005**(2), 118-128.
Renesto, S. & Avanzini, M. 2002. Skin remains in a juvenile *Macrocnemus bassanii* NOPCSA (Reptilia, Prolacertiformes) from the Middle Triassic of northern Italy. *Neues Jahrbuch für Geologie und Paläontologie-Abhandlungen*, **224**, 31-48.
Renesto, S. & Bernardi, M. 2014. Redescription and phylogenetic relationships of *Megachirella wachtleri* Renesto et Posenato, 2003 (Reptilia, Diapsida). *Paläontologische Zeitschrift*, **88**(2), 197-210.
Renesto, S., Binelli, G. & Hagdorn, H. 2014. A new pachypleurosaur from the Middle Triassic Besano Formation of Northern Italy. *Neues Jahrbuch für Geologie und Paläontologie-Abhandlungen*, **271**(2), 151-168.
Renesto, S. & Dalla Vecchia, F. M. 2000. The unusual dentition and feeding habits of the prolacertiform reptile *Langobardisaurus* (Late Triassic, northern Italy). *Journal of Vertebrate Paleontology*, **20**(3), 622-627.
Renesto, S. & Dalla Vecchia, F. M. 2005. The skull and lower jaw of the holotype of *Megalancosaurus preonensis* (Diapsida, Drepanosauridae) from the Upper Triassic of Northern Italy. *Rivista Italiana di Paleontologia e Stratigrafia (Research In Paleontology and Stratigraphy)*, **111**(2), 247-257.
Renesto, S., Dalla Vecchia, F. M. & Peters, D. 2002. Morphological evidence for bipedalism in the Late Triassic prolacertiform reptile *Langobardisaurus*. *Senckenbergiana Lethaea*, **82**(1), 94-106.

Renesto, S. & Posenato, R. 2003. A new lepidosauromorph reptile from the Middle Triassic of the Dolomites (Northern Italy). *Rivista Italiana di Paleontologia e Stratigrafia*, **109**(3), 463-474.

Renesto, S., Spielmann, J. A., Lucas, S. G. & Spagnoli, G. T. 2010. The taxonomy and paleobiology of the Late Triassic (Carnian-Norian: Adamanian-Apachean) drepanosaurs (Diapsida: Archosauromorpha: Drepanosauromorpha). *New Mexico Museum of Natural History and Science*, **46**, 1-81.

Rewcastle, S. C. 1983. Fundamental Adaptations in the Lacertilian Hind Limb: A Partial Analysis of the Sprawling Limb Posture and Gait. *Copeia*, **1983**(2), 476-487.

Reynoso, V.-H. 1998. *Huehuecuetzpalli mixtecus* gen. et sp. nov: a basal squamate (Reptilia) from the Early Cretaceous of Tepexi de Rodríguez, Central México. *Philosophical Transactions of the Royal Society of London B: Biological Sciences*, **353**(1367), 477-500.

Reynoso, V.-H. & Callison, G. 2000. A new scincomorph lizard from the Early Cretaceous of Puebla, Mexico. *Zoological Journal of the Linnean Society*, **130**(2), 183-212.

Reynoso, V.-H. & Cruz, J. A. 2014. Mesozoic Lepidosauromorphs of Mexico: a review and discussion of taxonomic assignments. Pp. 44-78 in H.E. Rivera-Sylva, K. Carpenter & E. Frey (eds) *Dinosaurs and Other Reptiles from the Mesozoic of Mexico*. Indiana University Press, Bloomington and Indianapolis.

Rice, R., Kallonen, A., Cebra-Thomas, J. & Gilbert, S. F. 2016. Development of the turtle plastron, the order-defining skeletal structure. *Proceedings of the National Academy of Sciences*, **113**(19), 5317-5322.

Rice, R., Riccio, P., Gilbert, S. F. & Cebra-Thomas, J. 2015. Emerging from the rib: resolving the turtle controversies. *Journal of Experimental Zoology Part B: Molecular and Developmental Evolution*, **324**(3), 208-220.

Richmond, B. G., Wright, B. W., Grosse, I., Dechow, P. C., Ross, C. F., Spencer, M. A. & Strait, D. S. 2005. Finite element analysis in functional morphology. *The Anatomical Record Part A*, **283**(2), 259-274.

Riedl, R. 1978. *Order in living organisms: a systems analysis of evolution*. John Wiley & Sons, New York, 334 pp.

Rieppel, O. 1981. The skull and the jaw adductor musculature in some burrowing scincomorph lizards of the genera *Acontias*, *Typhlosaurus* and *Feylinia*. *Journal of Zoology*, **195**(4), 493-528.

Rieppel, O. 1984a. The cranial morphology of the fossorial lizard genus *Dibamus* with a consideration of its phylogenetic relationships. *Journal of Zoology*, **204**(3), 289-327.
Rieppel, O. 1984b. The structure of the skull and jaw adductor musculature in the Gekkota, with comments on the phylogenetic relationships of the Xantusiidae (Reptilia: Lacertilia). *Zoological Journal of the Linnean Society*, **82**(3), 291-318.
Rieppel, O. 1985. The Recessus Scalae Tympani and Its Bearing on the Classification of Reptiles. *Journal of Herpetology*, **19**(3), 373-384.
Rieppel, O. 1989a. The hind limb of *Macrocnemus bassanii* (Nopcsa) (Reptilia, Diapsida): development and functional anatomy. *Journal of Vertebrate Paleontology*, **9**(4), 373-387.
Rieppel, O. 1989b. *A New Pachypleurosaur (Reptilia: Sauropterygia) from the Middle Triassic of Monte San Giorgio, Switzerland*, 1-73 pp.
Rieppel, O. 1989c. A New Pachypleurosaur (Reptilia: Sauropterygia) from the Middle Triassic of Monte San Giorgio, Switzerland. *Philosophical Transactions of the Royal Society of London*, **323**(1212), 1-73.
Rieppel, O. 1992. The Skull in a Hatchling of *Sphenodon punctatus*. *Journal of Herpetology*, **26**(1), 80-84.
Rieppel, O. 1993a. Middle Triassic reptiles from Monte San Giorgio: recent results and future potential of analysis. *Paleontologia Lombarda*, **2**, 131-144.
Rieppel, O. 1993b. Studies on Skeletion Formation in Reptiles. IV. The Homology of the Reptilian (Amniote) Astragalus Revisited. *Journal of Vertebrate Paleontology*, **13**(1), 31-47.
Rieppel, O. 1994a. The Lepidosauromorpha: an overview with special emphasis on the Squamata. Pp. 23-37 in N.C. Fraser & H.D. Sues (eds) *In the shadow of the dinosaurs: early Mesozoic tetrapods*. Cambridge University Press, New York.
Rieppel, O. 1994b. Osteology of *Simosaurus gaillardoti* and the relationships of stem-group Sauropterygia *Fieldiana (Geology)*, **28**, 1-85.
Rieppel, O. 1994c. Studies on skeleton formation in reptiles. Patterns of ossification in the skeleton of *Lacerta agilis exigua* Eichwald (Reptilia, Squamata). *Journal of Herpetology*, **28**(2), 145-153.
Rieppel, O. 1998. The status of the sauropterygian reptile genera *Ceresiosaurus*, *Lariosaurus*, and *Silvestrosaurus* from the Middle Triassic of Europe. *Fieldiana (Geology - New Series)*, **38**, 1-46.

Rieppel, O. 2000. *Handbook of Paleoherpetology: Teil 12A. Sauropterygia I. Placodontia, Pachypleurosauria, Nothosauria, Pistosauria.* . Friedrich Pfeil-Verlag, München, 134 pp.

Rieppel, O. 2001. Tooth implantation and replacement in Sauropterygia. *Paläontologische Zeitschrift*, **75**(2), 207.

Rieppel, O. 2006. The merits of similarity reconsidered. *Systematics and biodiversity*, **4**(2), 137-147.

Rieppel, O. & de Braga, M. 1996. Turtles as diapsid reptiles. *Nature*, **384**, 453-455.

Rieppel, O. & Gronowski, R. W. 1981. The loss of the lower temporal arcade in diapsid reptiles. *Zoological Journal of the Linnean Society*, **72**(3), 203-217.

Rieppel, O., Jiang, D.-Y., Fraser, N. C., Hao, W.-C., Motani, R., Sun, Y.-L. & Sun, Z.-Y. 2010. *Tanystropheus* cf. *T. longobardicus* from the early Late Triassic of Guizhou Province, southwestern China. *Journal of Vertebrate Paleontology*, **30**(4), 1082-1089.

Rieppel, O. & Jun, L. I. U. 2006. On *Xinpusaurus* (Reptilia: Thalattosauria). *Journal of Vertebrate Paleontology*, **26**(1), 200-204.

Rieppel, O. & Kearney, M. 2002. Similarity. *Biological Journal of the Linnean Society*, **75**(1), 59-82.

Rieppel, O. & Kearney, M. 2007. The Poverty of Taxonomic Characters. *Biology & Philosophy*, **22**(1), 95-113.

Rieppel, O., Kley, N. J. & Maisano, J. A. 2009. Morphology of the skull of the white-nosed blindsnake, *Liotyphlops albirostris* (Scolecophidia: Anomalepididae). *Journal of Morphology*, **270**(5), 536-557.

Rieppel, O., Mazin, J.-M. & Tchernov, E. 1999. Sauropterygia from the Middle Triassic of Makhtesh Ramon, Negev, Israel. *Fieldiana (Geology - New Series)*, **40**, 1-85.

Rieppel, O., Sander, P. M. & Storrs, G. W. 2002. The skull of the pistosaur "*Augustasaurus*" from the Middle Triassic of Northwestern Nevada. *Journal of Vertebrate Paleontology*, **22**(3), 577-592.

Rieppel, O. & Zaher, H. 2000. The intramandibular joint in squamates: and the phylogenetic relationships of the fossil snake *Pachyrhachis problematicus* Haas. *Fieldiana (Geology - New Series)*, **43**, 1-69.

Rieppel, O. & Zaher, H. 2001. Re-building the bridge between mosasaurs and snakes. *Neues Jahrbuch für Geologie und Paläontologie-Abhandlungen*, 111-132.

Robinson, P. L. 1957. An unusual sauropsid dentition. *Journal of the Linnean Society of London, Zoology*, **43**(291), 283-293.

Robinson, P. L. 1962. Gliding lizards from the Upper Keuper of Great Britain. *Proceedings of the Geological Society of London*, **1601**, 137-146.

Robinson, P. L. 1967a. The evolution of the Lacertilia. *Colloques Internationaux Centre national de la Recherche Scientifique (CNRS)*, **163**, 395-407.

Robinson, P. L. 1967b. Triassic vertebrates from lowland and upland. *Science and Culture*, **33**, 169-173.

Robinson, P. L. 1973. A problematic reptile from the British Upper Trias. *Journal of the Geological Society*, **129**(5), 457-479.

Robinson, P. L. 1975. The functions of the hooked fifth metatarsal in lepidosaurian reptiles. *Colloques Internationaux Centre national de la Recherche Scientifique (CNRS)*, **218**, 461-483.

Robinson, P. L. 1976. How *Sphenodon* and *Uromastyx* grow their teeth and use them. Pp. 43-64 in A.d.A. Bellairs & C.B. Cox (eds) *Morphology and biology of reptiles*. Academic Press, London and New York.

Romer, A. S. 1922. The comparison of mammalian and reptilian coracoids. *The Anatomical Record*, **24**(2), 38-47.

Romer, A. S. 1946. The primitive reptile *Limnoscelis* restudied. *American Journal of Science*, **244**(3), 149-188.

Romer, A. S. 1947. The relationships of the Permian reptile *Protosaurus*. *American Journal of Science*, **245**(1), 19-30.

Romer, A. S. 1956. *Osteology of the Reptiles*. University of Chicago Press, Chicago, 772 pp.

Ronquist, F., Klopfstein, S., Vilhelmsen, L., Schulmeister, S., Murray, D. L. & Rasnitsyn, A. P. 2012a. A total-evidence approach to dating with fossils, applied to the early radiation of the Hymenoptera. *Systematic Biology*, **61**(6), 973-999.

Ronquist, F., Teslenko, M., van der Mark, P., Ayres, D. L., Darling, A., Höhna, S., Larget, B., Liu, L., Suchard, M. A. & Huelsenbeck, J. P. 2012b. MrBayes 3.2: efficient Bayesian phylogenetic inference and model choice across a large model space. *Systematic Biology*, **61**(3), 539-542.

Roth, V. L. 1988. The Biological Basis of Homology. Pp. 1-26 in C.J. Humphries (ed) *Ontogeny and systematics*. Columbia University Press, New York.

Roure, B. & Philippe, H. 2011. Site-specific time heterogeneity of the substitution process and its impact on phylogenetic inference. *BMC Evolutionary Biology*, **11**.

Rubidge, B. S., Erwin, D. H., Ramezani, J., Bowring, S. A. & de Klerk, W. J. 2013. High-precision temporal calibration of Late Permian vertebrate biostratigraphy: U-Pb zircon constraints from the Karoo Supergroup, South Africa. *Geology*, **41**(3), 363-366.

Russell, A. P. 1975. A contribution to the functional analysis of the foot of the Tokay, *Gekko gecko* (Reptilia: Gekkonidae). *Journal of Zoology*, **176**(4), 437-476.

Russell, A. P. 1986. The morphological basis of weight-bearing in the scansors of the tokay gecko (Reptilia: Sauria). *Canadian Journal of Zoology*, **64**(4), 948-955.

Russell, A. P. 2002. Integrative Functional Morphology of the Gekkotan Adhesive System (Reptilia: Gekkota). *Integrative and Comparative Biology*, **42**(6), 1154-1163.

Russell, A. P. & Bauer, A. M. 2008. The appendicular locomotor apparatus of *Sphenodon* and normal-limbed squamates. Pp. 1-465 in C. Gans, A. Gaunt & K. Adler (eds) *Biology of the Reptilia*. Society for the Study of Amphibians and Reptiles, Ithaca, NY.

Russell, A. P., Bauer, A. M. & Laroiya, R. 1997. Morphological correlates of the secondarily symmetrical pes of gekkotan lizards. *Journal of Zoology*, **241**(4), 767-790.

Russell, A. P. & Bels, V. 2001. Digital Hyperextension in *Anolis sagrei*. *Herpetologica*, **57**(1), 58-65.

Russell, A. P. & Oetelaar, G. S. 2015. Limb and digit orientation during vertical clinging in Bibron's gecko, *Chondrodactylus bibronii* (A. Smith, 1846) and its bearing on the adhesive capabilities of geckoes. *Acta Zoologica*, DOI: 10.1111/azo.12128 (ahead of print).

Saitou, N. & Imanishi, T. 1989. Relative efficiencies of the Fitch-Margoliash, maximum-parsimony, maximum-likelihood, minimum-evolution, and neighbor-joining methods of phylogenetic tree construction in obtaining the correct tree. *Mol. Biol. Evol*, **6**(5), 514-525.

Saller, F., Renesto, S. & Dalla Vecchia, F. M. 2013. First record of *Langobardisaurus* (Diapsida, Protorosauria) from the Norian (Late Triassic) of Austria, and a revision of the genus. *Neues Jahrbuch für Geologie und Paläontologie - Abhandlungen*, **268**(1), 83-95.

Sander, P. M. 2000. Ichthyosauria: their diversity, distribution, and phylogeny. *Paläontologische Zeitschrift*, **74**(1), 1-35.

Scanferla, A. & Bhullar, B.-A. S. 2014. Postnatal development of the skull of *Dinilysia patagonica* (Squamata-Stem Serpentes). *The Anatomical Record*, **297**(3), 560-573.

Scanferla, C. A. & Canale, J. I. 2007. The youngest record of the Cretaceous snake genus *Dinilysia* (Squamata, Serpentes). *South American Journal of Herpetology*, **2**(1), 76-81.

Scanlon, J. D., Lee, M. S. Y., Caldwell, M. W. & Shine, R. 1999. The palaeoecology of the primitive snake *Pachyrhachis*. *Historical Biology*, **13**(2-3), 127-152.

Schaerlaeken, V., Herrel, A., Aerts, P. & Ross, C. F. 2008. The functional significance of the lower temporal bar in *Sphenodon punctatus*. *Journal of Experimental Biology*, **211**(24), 3908-3914.

Schaumberg, G. 1976. Zwei Reptilneufunde (*Weigeltisaurus* Kuhn?, Lepidosauria?, Reptilia) aus dem Kupferschiefer von Richelsdorf (Perm, Hessen). *Philippia*, **3**(1), 3-8.

Schaumberg, G., Unwin, D. M. & Brandt, S. 2007. New information on the anatomy of the Late Permian gliding reptile *Coelurosauravus*. *Paläontologische Zeitschrift*, **81**(2), 160-173.

Scheyer, T. M. 2007. Skeletal histology of the dermal armor of Placodontia: the occurrence of 'postcranial fibro-cartilaginous bone' and its developmental implications. *Journal of Anatomy*, **211**(6), 737-753.

Scheyer, T. M. 2010. New interpretation of the postcranial skeleton and overall body shape of the placodont *Cyamodus hildegardis* Peyer, 1931 (Reptilia, Sauropterygia). *Palaeontologia Electronica*, **13**(2), Online only (http://palaeo-electronica.org/2010_2012/2232/index.html).

Scheyer, T. M., Bruellmann, B. & Sánchez-Villagra, M. R. 2008. The ontogeny of the shell in side-necked turtles, with emphasis on the homologies of costal and neural bones. *Journal of Morphology*, **269**(8), 1008-1021.

Scheyer, T. M., Neenan, J. M., Bodogan, T., Furrer, H., Obrist, C. & Plamondon, M. 2017. A new, exceptionally preserved juvenile specimen of *Eusaurosphargis dalsassoi* (Diapsida) and implications for Mesozoic marine diapsid phylogeny. *Scientific Reports*, **7**(1), 4406.

Scheyer, T. M., Neenan, J. M., Renesto, S., Saller, F., Hagdorn, H., Furrer, H., Rieppel, O. & Tintori, A. 2012. Revised paleoecology of placodonts – with a comment on 'The shallow marine placodont *Cyamodus* of the central European Germanic Basin: its evolution, paleobiogeography and paleoecology. *Historical Biology*, **24**(3), 257-267.

Schmid, D. U., Leinfelder, R. R. & Schweigert, G. 2005. Stratigraphy and palaeoenvironments of the Upper Jurassic of Southern Germany–a review. *Zitteliana, Series B*, **B26**, 31-41.

Schoch, R. R. & Sues, H.-D. 2015. A Middle Triassic stem-turtle and the evolution of the turtle body plan. *Nature*, **523**, 584-587.

Schwarzkopf, L. 2005. Sexual dimorphism in body shape without sexual dimorphism in body size in water skinks (*Eulamprus quoyii*). *Herpetologica*, **61**(2), 116-123.

Schweigert, G. 2007. Ammonite biostratigraphy as a tool for dating Upper Jurassic lithographic limestones from South Germany–first results and open questions. *Neues Jahrbuch für Geologie und Paläontologie-Abhandlungen*, **245**(1), 117-125.

Scotland, R. W., Olmstead, R. G. & Bennett, J. R. 2003. Phylogeny reconstruction: the role of morphology. *Systematic Biology*, **52**(4), 539-548.

Seeley, H. G. 1881. On Remains of a small Lizard from the Neocomian Rocks of Comén, near Trieste preserved in the Geological Museum of the University of Vienna. *Quarterly Journal of the Geological Society*, **37**(1-4), 52-56,NP.

Seeley, H. G. 1887. Researches on the Structure, Organization, and Classification of the Fossil Reptilia.-- I. On *Protorosaurus Speneri* (von Meyer). *Philosophical Transactions of the Royal Society of London. B*, **178**, 187-213.

Seeley, H. G. 1892. On a New Reptile from Welte Vreden (Beaufort West), *Eunotosaurus africanus* (Seeley). *Quarterly Journal of the Geological Society*, **48**(1-4), 583-585.

Senter, P. 2003. New information on cranial and dental features of the Triassic archosauriform reptile *Euparkeria capensis*. *Palaeontology*, **46**(3), 613-621.

Sereno, P. C. 1991. Basal Archosaurs: Phylogenetic Relationships and Functional Implications. *Journal of Vertebrate Paleontology*, **11**(sup004), 1-53.

Sereno, P. C. 2007. Logical basis for morphological characters in phylogenetics. *Cladistics*, **23**(6), 565-587.

Sereno, P. C. & Arcucci, A. B. 1990. The monophyly of crurotarsal archosaurs and the origin of bird and crocodile ankle joints. *Neues Jahrbuch für Geologie und Paläontologie, Abhandlungen*, **180**(1), 21-52.

Sha, J. 2007. Cretaceous stratigraphy of northeast China: non-marine and marine correlation. *Cretaceous Research*, **28**(2), 146-170.

Shikama, T., Kamei, T. & Murata, M. 1978. Early Triassic ichthyosaurus, *Utatsusaurus hataii* gen. et sp. nov., from the Kitakami Massif, Northeast Japan. *Tohoku University Science Report, 2nd Series (Geology)*, **48**(2), 77-97.

Shishkin, M. A. & Sulej, T. 2009. The Early Triassic temnospondyls of the Czatkowice 1 tetrapod assemblage. *Palaeontologia Polonica*, **65**(3), 77.

Sigé, B., Buscalioni, A. D., Duffaud, S., Gayet, M., Orth, B., Rage, J. & Sanz, J. 1997. Etat des données sur le gisement crétacé supérieur continental de Champ-Garimond (Gard, Sud de la France). *Münchner Geowissenschaftliche Abhandlungen*, **34**, 111-130.

Simões, T. R. 2012. Redescription of *Tijubina pontei*, an Early Cretaceous lizard (Reptilia; Squamata) from the Crato Formation of Brazil. *Anais da Academia Brasileira de Ciencias*, **84**(1), 79-93.

Simões, T. R., Apesteguía, S., Hsiou, A. S. & Daza, J. D. 2017a. Lepidosaurs from Gondwana: An Introduction. *Journal of Herpetology*, **51**(3), 297-299.

Simões, T. R., Caldwell, M. W. & Kellner, A. W. A. 2015a. A new Early Cretaceous lizard species from Brazil, and the phylogenetic position of the oldest known South American squamates. *Journal of Systematic Palaeontology*, **13**(5-8), 601-614.

Simões, T. R., Caldwell, M. W., Nydam, R. L. & Jiménez-Huidobro, P. 2017b. Osteology, phylogeny, and functional morphology of two Jurassic lizard species and the early evolution of scansoriality in geckoes. *Zoological Journal of the Linnean Society*, **180**(1), 216-241.

Simões, T. R., Caldwell, M. W., Palci, A. & Nydam, R. L. 2017c. Giant taxon-character matrices II: a response to Laing et al. (2017). *Cladistics*, **online first**, DOI: 10.1111/cla.12231.

Simões, T. R., Caldwell, M. W., Palci, A. & Nydam, R. L. 2017d. Giant taxon-character matrices: quality of character constructions remains critical regardless of size. *Cladistics*, **33**(2), 198-219.

Simões, T. R., Caldwell, M. W., Weinschütz, L. C., Wilner, E. & Kellner, A. W. A. 2017e. Mesozoic Lizards from Brazil and Their Role in Early Squamate Evolution in South America. *Journal of Herpetology*, **51**(3), 307-315.

Simões, T. R., Funston, G. F., Vafaeian, B., Nydam, R. L., Doschak, M. R. & Caldwell, M. W. 2016. Reacquisition of the lower temporal bar in sexually dimorphic fossil lizards provides a rare case of convergent evolution. *Scientific Reports*, **6**, 24087.

Simões, T. R., Wilner, E., Caldwell, M. W., Weinschütz, L. C. & Kellner, A. W. A. 2015b. A stem acrodontan lizard in the Cretaceous of Brazil revises early lizard evolution in Gondwana. *Nature Communications*, **6**(8149), 9149.

Simon, C. 1983. A new coding procedure for morphometric data with an example from periodical cicada wing veins. Pp. 378-382 in J. Felsenstein (ed) *Numerical taxonomy*. Springer-Verlag, New York.

Simón, M. E. & Kellner, A. W. A. 2003. New Sphenodontid (Lepidosauria, Rhynchocephalia, Eilenodontinae) from the Candeleros Formation, Cenomanian of Patagonia, Argentina:(with 12 Figures). *Boletim do Museu Nacional, Nova série, Geologia*, **68**, 1-12.

Simpson, G. G. 1937. The Fort Union of the Crazy Mountain field, Montana and its mammalian faunas. *Bulletin United States National Museum*, **169**, 1-287.

Smith, K. T. 2009. Eocene Lizards of the Clade *Geiseltaliellus* from Messel and Geiseltal, Germany, and the Early Radiation of Iguanidae (Reptilia: Squamata). *Bulletin of the Peabody Museum of Natural History*, **50**(2), 219-306.

Smith, R., Rubidge, B., Van der Walt, M. & Chinsamy-Turan, A. 2012. Therapsid biodiversity patterns and paleoenvironments of the Karoo Basin, South Africa. Pp. 30-62*Forerunners of Mammals: Radiation, Histology, Biology*. Indiana University Press, Indianapolis.

Sobral, G., Sookias, R. B., Bhullar, B. A. S., Smith, R., Butler, R. J. & Müller, J. 2016. New information on the braincase and inner ear of *Euparkeria capensis* Broom: implications for diapsid and archosaur evolution. *Royal Society Open Science*, **3**, 160072.

Sookias, R. B. & Butler, R. J. 2013. Euparkeriidae. *Geological Society, London, Special Publications*, **379**(1), 35-48.

Spielmann, J. A., Heckert, A. B. & Lucas, S. G. 2005. The Late Triassic archosauromorph *Trilophosaurus* as an arboreal climber. *Rivista Italiana di Paleontologia e Stratigrafia*, **111**(3), 395-412.

Spielmann, J. A., Lucas, S. G., Rhinehart, L. F. & Heckert, A. B. 2008. The Late Triassic Archosauromorph *Trilophosaurus Bulletin of the New Mexico Museum of Natural History and Science*, **43**, 1-177.

Spielmann, J. A., Renesto, S. & Lucas, S. G. 2006. The utility of claw curavture in assessing the arboreality of fossil reptiles. *New Mexico Museum of Natural History and Science Bulletin*, **37**, 365-368.

Stadler, T. 2010. Sampling-through-time in birth–death trees. *Journal of Theoretical Biology*, **267**(3), 396-404.

Stein, K., Palmer, C., Gill, P. G. & Benton, M. J. 2008. The aerodynamics of the British Late Triassic Kuehneosauridae. *Palaeontology*, **51**(4), 967-981.

Sterli, J. & Joyce, W. G. 2007. The cranial anatomy of the Early Jurassic turtle *Kayentachelys aprix*. *Acta Palaeontologica Polonica*, **52**(4), 675.

Strong, E. E. & Lipscomb, D. 1999. Character Coding and Inapplicable Data. *Cladistics*, **15**(4), 363-371.

Sues, H. D. 1987. Postcranial skeleton of *Pistosaurus* and interrelationships of the Sauropterygia (Diapsida). *Zoological Journal of the Linnean Society*, **90**(2), 109-131.

Sulimski, A. 1975. Macrocephalosauridae and Polyglyphanodontidae (Sauria) from the late Cretaceous of Mongolia. *Palaeontologia Polonica*, **33**, 25-102.

Sulimski, A. 1984. A new Cretaceous scincomorph lizard from Mongolia. *Acta Palaeontologica Polonica*, **46**, 143-155.

Sumida, S. S. 1987. Two different vertebral forms in the axial column of *Labidosaurus* (Captorhinomorpha: Captorhinidae). *Journal of Paleontology*, **61**(01), 155-167.

Sumida, S. S. 1989. The appendicular skeleton of the Early Permian genus *Labidosaurus* (Reptilia, Captorhinomorpha, Captorhinidae) and the hind limb musculature of captorhinid reptiles. *Journal of Vertebrate Paleontology*, **9**(3), 295-313.

Sumida, S. S. 1991. Vertebral morphology, alternation of neural spine height, and structure in Permo-Carboniferous tetrapods, and a reappraisal of primitive modes of terrestrial locomotion. *Berkeley: University Of California Publications in Zoology*, **122**, 1-133.

Sun, Z., Sun, Y., Hao, W. & Jiang, D.-Y. 2006. Conodont Evidence for the Age of the Panxian Fauna, Guizhou, China. *Acta Geologica Sinica - English Edition*, **80**(5), 621-630.

Swinton, W. E. 1939. LI.—A new Triassic Rhynchocephalian from Gloucestershire. *Journal of Natural History*, **4**(24), 591-594.

Tałanda, M. 2016. Cretaceous roots of the amphisbaenian lizards. *Zoologica Scripta*, **45**(1), 1-8.

Tałanda, M. 2017. Evolution of postcranial skeleton in worm lizards inferred from its status in the Cretaceous stem-amphisbaenian *Slavoia darevskii*. *Acta Palaeontologica Polonica*, **62**(1), 9-23.

Throckmorton, G. Y. S. 1976. Oral food processing in two herbivorous lizards, *Iguana iguana* (Iguanidae) and *Uromastix aegyptius* (Agamidae). *Journal of Morphology*, **148**(3), 363-390.

Tintori, A. 1995. The Norian (Late Triassic) Calcare di Zorzino fauna from Lombardy (northern Italy): the state of the art. *II International Symposium on Lithographic Limestones.*, 139-142.

Tischlinger, H. & Wild, R. 2009. Den Schwanz verloren—das Leben gerettet! *Fossilien*, **26**(4), 203-209.

Torres-Carvajal, O. 2003. Cranial osteology of the andean lizard *Stenocercus guentheri* (Squamata: Tropiduridae) and its postembryonic development. *Journal of Morphology*, **255**(1), 94-113.

Townsend, T., Larson, A., Louis, E. & Macey, R. J. 2004. Molecular phylogenetics of Squamata: the position of snakes, amphisbaenians, and dibamids, and the root of the squamate tree. *Systematic Biology*, **53**(5), 735-757.

Triviño, L. N. & Albino, A. M. 2015. Hallazgo de restos de la serpiente *Dinilysia patagonica* Smith-Woodward 1901 en una nueva localidad del Santoniano de Patagonia, Argentina. *Estudios Geológicos*, **71**(2), 1-9.

Tschanz, K. 1985. *Tanystropheus*—an unusual reptilian construction. *Konstruktionsprinzipien lebender und ausgestorbener Reptilien*, **230**(4), 169-177.

Tschanz, K. 1988. Allometry and heterochrony in the growth of the neck of Triassic prolacertiform reptiles. *Palaeontology*, **31**(4), 997-1011.

Tschopp, E. 2016. Nomenclature of Vertebral Laminae in Lizards, with Comments on Ontogenetic and Serial Variation in Lacertini (Squamata, Lacertidae). *PLoS ONE*, **11**(2), e0149445.

Tulli, M. J., Cruz, F. B., Herrel, A., Vanhooydonck, B. & Abdala, V. 2009. The interplay between claw morphology and microhabitat use in neotropical iguanian lizards. *Zoology*, **112**(5), 379-392.

Tuniz, C., Bernardini, F., Cicuttin, A., Crespo, M. L., Dreossi, D., Gianoncelli, A., Mancini, L., Mendoza Cuevas, A., Sodini, N., Tromba, G., Zanini, F. & Zanolli, C. 2013. The ICTP-Elettra X-ray laboratory for cultural heritage and archaeology. *Nuclear Instruments and Methods in Physics Research Section A: Accelerators, Spectrometers, Detectors and Associated Equipment*, **711**, 106-110.

Turner, A. H., Pritchard, A. C. & Matzke, N. J. 2017. Empirical and Bayesian approaches to fossil-only divergence times: A study across three reptile clades. *PLoS ONE*, **12**(2), e0169885.

Uetz, P. & Hošek, J. 2016. The Reptile Database.

Uetz, P. & Hošek, J. 2017. The Reptile Database.

Underwood, G. 1957. On lizards of the family pygopodidae. A contribution to the morphology and phylogeny of the squamata. *Journal of Morphology*, **100**(2), 207-268.

van Ruijven, L. J. & Weijs, W. A. 1990. A new model for calculating muscle forces from electromyograms. *European Journal of Applied Physiology and Occupational Physiology*, **61**(5-6), 479-485.

Vanhooydonck, B. & Van Damme, R. 1999. Evolutionary relationships between body shape and habitat use in lacertid lizards. *Evolutionary Ecology Research*, **1**(7), 785-805.

Vaughn, P. P. 1955. The Permian reptile *Araeoscelis* restudied. *Bulletin of the Museum of Comparative Zoology*, **113**(467-514).

Venczel, M. & Codrea, V. A. 2016. A new teiid lizard from the Late Cretaceous of the Haţeg Basin, Romania and its phylogenetic and palaeobiogeographical relationships. *Journal of Systematic Palaeontology*, **14**(3), 219-237.

Vidal, N. & Hedges, B. S. 2005. The phylogeny of squamate reptiles (lizards, snakes, and amphisbaenians) inferred from nine nuclear protein-coding genes. *Comptes Rendus Biologies*, **328**, 1000-1008.

Vidal, N. & Hedges, S. B. 2009. The molecular evolutionary tree of lizards, snakes, and amphisbaenians. *Comptes Rendus Biologies*, **332**(2–3), 129-139.

Vitt, L. J. 1982. Sexual Dimorphism and Reproduction in the Microteiid Lizard, *Gymnophthalmus multiscutatus*. *Journal of Herpetology*, **16**(3), 325-329.

Vitt, L. J. 1983. Reproduction and Sexual Dimorphism in the Tropical Teiid Lizard *Cnemidophorus ocellifer*. *Copeia*, **1983**(2), 359-366.

Vitt, L. J. & Zani, P. A. 1996. Ecology of the elusive tropical lizard *Tropidurus* [= *Uracentron*] *flaviceps* (Tropiduridae) in lowland rain forest of Ecuador. *Herpetologica*, **51**(2), 121-132.

Waddington, C. H. 1942. Canalization of development and the inheritance of acquired characters. *Nature*, **150**(3811), 563-565.

Wagner, A. 1852. Neu-aufgefundene Saurier, Überreste aus dem lithographischen Schiefern und dem obern Jurakalke. *Abhandlungen Bayerische Akademie der Wissenschaften zu München Mathematisch-Physikalischen Klasse*, **3**(6), 661-710.

Wagner, G. P. 1989. The Biological Homology Concept. *Annual Review of Ecology and Systematics*, **20**, 51-69.

Wagner, P. J. 2012. Modelling rate distributions using character compatibility: implications for morphological evolution among fossil invertebrates. *Biology Letters*, **8**(1), 143-146.

Wake, D. B. 1991. Homoplasy: The Result of Natural Selection, or Evidence of Design Limitations? *The American Naturalist*, **138**(3), 543-567.

Wake, D. B., Wake, M. H. & Specht, C. D. 2011. Homoplasy: From Detecting Pattern to Determining Process and Mechanism of Evolution. *Science*, **331**, 1032-1035.

Wake, M. H. 1993. Non-Traditional Characters in the Assessment of Caecilian Phylogenetic Relationships. *Herpetological Monographs*, **7**, 42-55.

Waldman, M. & Evans, S. E. 1994. Lepidosauromorph reptiles from the Middle Jurassic of Skye. *Zoological Journal of the Linnean Society*, **112**, 135-150.

Walkden, G. M. & Fraser, N. C. 1993. Late Triassic fissure sediments and vertebrate faunas: environmental change and faunal succession at Cromhall, South West Britain. *Modern Geology*, **18**, 511-535.

Wang, Y., Dong, L. & Evans, S. E. 2010. Jurassic-Cretaceous herpetofaunas from the Jehol associated strata in NE China: evolutionary and ecological implications. *Bulletin of the Chinese Academy of Sciences*, **24**, 76-79.

Wang, Y. & Li, J. 2008. Order Squamata. Pp. 115-137 in J. Li, X. Wu & F. Zhang (eds) *The Chinese Fossil Reptiles and Their Kin*. Science Press, Beijing.

Watson, D. M. S. 1912. *Mesosuchus browni*, gen. et spec. nov. *Records of the Albany Museum*, **2**, 298-299.

Weigelt, J. 1930a. *Gracilisaurus ottoi* n.g.n.sp. *Leopoldina*, **6**, 269-280.

Weigelt, J. 1930b. *Palaeochamaeleo jaekeli* nov. gen. nov. sp., ein neuer Rhynchocephale aus dem Mansfelder Kupferschiefer. *Leopoldina*, **6**, 625-642.

Welman, J. 1995. *Euparkeria* and the origin of birds. *South African Journal of Science*, **91**(10), 533-537.

Welman, J. 1998. The taxonomy of the South African proterosuchids (Reptilia, Archosauromorpha). *Journal of Vertebrate Paleontology*, **18**(2), 340-347.

Wertheim, J. O., Sanderson, M. J., Worobey, M. & Bjork, A. 2010. Relaxed Molecular Clocks, the Bias–Variance Trade-off, and the Quality of Phylogenetic Inference. *Systematic Biology*, **59**(1), 1-8.

Wescott, W. A. & Diggens, J. N. 1998. Depositional history and stratigraphical evolution of the Sakamena group (Middle Karoo Supergroup) in the southern Morondava Basin, Madagascar. *Journal of African Earth Sciences*, **27**(3), 461-479.

Whiteside, D. I. 1986. The Head Skeleton of the Rhaetian Sphenodontid *Diphydontosaurus avonis* gen. et sp. nov. and the Modernizing of a Living Fossil. *Philosophical Transactions of the Royal Society of London, Series B: Biological Sciences*, **312**(1156), 379-430.

Wiens, J. J. 2003. Missing Data, Incomplete Taxa, and Phylogenetic Accuracy. *Systematic Biology*, **52**(4), 528-538.

Wiens, J. J. 2004. The role of morphological data in phylogeny reconstruction. *Systematic Biology*, **53**(4), 653-661.

Wiens, J. J. 2006. Missing data and the design of phylogenetic analyses. *Journal of Biomedical Informatics*, **39**(1), 34-42.

Wiens, J. J., Hutter, C. R., Mulcahy, D. G., Noonan, B. P., Townsend, T. M., Sites, J. W. & Reeder, T. W. 2012. Resolving the phylogeny of lizards and snakes (Squamata) with extensive sampling of genes and species. *Biology Letters*, **8**(6), 1043-1046.

Wiens, J. J., Kuczynski, C. A., Townsend, T., Reeder, T. W., Mulcahy, D. G. & Sites, J. W. 2010. Combining phylogenomics and fossils in higher-level squamate reptile phylogeny: molecular data change the placement of fossil taxa. *Systematic Biology*, **59**(6), 674-688.

Wilberg, E. W. 2012. *Phylogenetic and morphometric assessment of the evolution of the longirostrine crocodylomorphs*. Unpublished PhD thesis, University of Iowa, 250 pp.

Wild, R. 1973. Die Triasfauna der Tessiner Kalkalpen XXIII *Tanystropheus longobardicus* (Bassani)(Neue Ergebnisse). *Schweizerische Paläontologische Abhandlungen*, **95**, 1-162.

Wild, R. 1980a. Die Triasfauna der Tessiner Kalkalpen. XXIV. Neue Funde von *Tanystropheus* (Reptilia, Squamata). *Schweizerischen Paläontologischen Abhandlungen*, **102**, 1-31.

Wild, R. 1980b. *Tanystropheus* (Reptilia: Squamata) and its importance for stratigraphy. *Mémoires de la Société Géologique de France NS*, **139**, 201-206.

Wild, R. 1987. An example of biological reasons for extinction: *Tanystropheus* (Reptilia, Squamata). *Mémoires de la Société Géologique de France, NS*, **150**, 37-44.

Wiley, E. O. 1975. Karl R. Popper, Systematics, and Classification: A Reply to Walter Bock and Other Evolutionary Taxonomists. *Systematic Zoology*, **24**(2), 233-243.

Wilkinson, M. 1995. A Comparison of Two Methods of Character Construction. *Cladistics*, **11**(3), 297-308.

Wilkinson, M. 2006. Identifying stable reference taxa for phylogenetic nomenclature. *Zoologica Scripta*, **35**(1), 109-112.

Williston, S. W. 1904. The Relationships and Habits of the Mosasaurs. *The Journal of Geology*, **12**(1), 43-51.

Williston, S. W. 1910a. New Permian Reptiles: Rhachitomous Vertebrae. *The Journal of Geology*, **18**(7), 585-600.

Williston, S. W. 1910b. The skull of *Labidosaurus*. *American Journal of Anatomy*, **10**(1), 69-84.

Williston, S. W. 1911. Ueber *Erythrosuchus*, Vertreter der neuen Reptilordnung Pelycosimia. F. von Huene. *The Journal of Geology*, **19**(7), 661-664.

Williston, S. W. 1913. The Skulls of *Araeoscelis* and *Casea*, Permian Reptiles. *The Journal of Geology*, **21**(8), 743-747.

Williston, S. W. 1914. The Osteology of Some American Permian Vertebrates. *The Journal of Geology*, **22**(4), 364-419.

Williston, S. W. 1917. *Labidosaurus* Cope, a Lower Permian Cotylosaur Reptile from Texas. *The Journal of Geology*, **25**(4), 309-321.

Witmer, L. M. 1997. The Evolution of the Antorbital Cavity of Archosaurs: A Study in Soft-Tissue Reconstruction in the Fossil Record with an Analysis of the Function of Pneumaticity. *Memoir (Society of Vertebrate Paleontology)*, **3**, 1-73.

Woodward, A. S. 1901. On some Extinct Reptiles from Patagonia, of the Genera *Miolania*, *Dinilysia*, and *Genyodectes*. *Proceedings of the Zoological Society of London*, **70**(2), 169-184.

Wright, A. M. & Hillis, D. M. 2014. Bayesian Analysis Using a Simple Likelihood Model Outperforms Parsimony for Estimation of Phylogeny from Discrete Morphological Data. *PLoS ONE*, **9**(10), e109210.

Wu, X.-C. 2003. Functional morphology of the temporal region in the Rhynchocephalia. *Canadian Journal of Earth Sciences*, **40**(4), 589-607.

Wu, X.-C., Brinkman, D. B. & Russell, A. P. 1996. *Sineoamphisbaena hexatabularis*, an amphisbaenian (Diapsida: Squamata) from the Upper Cretaceous redbeds at Bayan Mandahu (Inner Mongolia, People's Republic of China), and comments on the phylogenetic relationships of the Amphisbaenia. *Canadian Journal of Earth Sciences*, **33**(4), 541-577.

Wu, X.-C., Cheng, Y.-N., Li, C., Zhao, L.-J. & Sato, T. 2011. New Information on *Wumengosaurus delicatomandibularis* Jiang et al., 2008 (Diapsida: Sauropterygia), with a Revision of the Osteology and Phylogeny of the Taxon. *Journal of Vertebrate Paleontology*, **31**(1), 70-83.

Wu, X.-C., Zhao, L.-J., Sato, T., Gu, S.-X. & Jin, X.-S. 2016. A new specimen of *Hupehsuchus nanchangensis* Young, 1972 (Diapsida, Hupehsuchia) from the Triassic of Hubei, China. *Historical Biology*, **28**(1-2), 43-52.

Xie, W., Lewis, P. O., Fan, Y., Kuo, L. & Chen, M.-H. 2011. Improving marginal likelihood estimation for Bayesian phylogenetic model selection. *Systematic Biology*, **60**, 150-160.

Yang, Z. 1995. A space-time process model for the evolution of DNA sequences. *Genetics*, **139**(2), 993-1005.

Yang, Z., Goldman, N. & Friday, A. 1994. Comparison of models for nucleotide substitution used in maximum-likelihood phylogenetic estimation. *Molecular Biology and Evolution*, **11**(2), 316-324.

Yang, Z. & Rannala, B. 2012. Molecular phylogenetics: principles and practice. *Nature Reviews Genetics*, **13**(5), 303-314.

Young, C.-C. & Dong, Z. 1972. On the Triassic aquatic reptiles of China. *IVPP, Chinese Academy of Science, Memoir*, **9**, 1-34.

Young, C. C. 1948. A review of Lepidosauria from China. *American Journal of Science*, **246**(11), 711-719.

Zaaf, A. & Van Damme, R. 2001. Limb proportions in climbing and ground-dwelling geckoes (Lepidosauria, Gekkonidae): a phylogenetically informed analysis. *Zoomorphology*, **121**, 45-53.

Zaher, H. 1998. The Phylogenetic Position of *Pachyrhachis* within Snakes (Squamata, Lepidosauria). *Journal of Vertebrate Paleontology*, **18**(1), 1-3.

Zaher, H., Apesteguía, S. & Scanferla, C. A. 2009. The anatomy of the upper cretaceous snake *Najash rionegrina* Apesteguía & Zaher, 2006, and the evolution of limblessness in snakes. *Zoological Journal of the Linnean Society*, **156**(4), 801-826.

Zaher, H. & Rieppel, O. 1999. The phylogenetic relationships of *Pachyrhachis problematicus*, and the evolution of limblessness in snakes (Lepidosauria, Squamata). *Comptes rendus de l'Académie des sciences, Sciences de la Terre et des planètes*, **329**, 831-837.

Zaher, H. & Rieppel, O. 2002. On the phylogenetic relationships of the Cretaceous snakes with legs, with special reference to *Pachyrhachis problematicus* (Squamata, Serpentes). *Journal of Vertebrate Paleontology*, **22**(1), 104-109.

Zaher, H. & Scanferla, C. A. 2012. The skull of the Upper Cretaceous snake *Dinilysia patagonica* Smith-Woodward, 1901, and its phylogenetic position revisited. *Zoological Journal of the Linnean Society*, **164**(1), 194-238.

Zani, P. A. 2000. The comparative evolution of lizard claw and toe morphology and clinging performance. *Journal of Evolutionary Biology*, **13**(2), 316-325.

Zeiss, A. 1968. Untersuchungen zur Paläontologie der Cephalopoden des Unter-Tithon der Südlichen Frankenalb. *Bayerische Akademie der Wissenschaften zu München Math.-Naturw. Abt., neue Folge*, **132**, 1-190.

Zhang, C., Stadler, T., Klopfstein, S., Heath, T. A. & Ronquist, F. 2016. Total-Evidence Dating under the Fossilized Birth–Death Process. *Systematic Biology*, **65**(2), 228-249.

Zheng, Y. & Wiens, J. J. 2016. Combining phylogenomic and supermatrix approaches, and a time-calibrated phylogeny for squamate reptiles (lizards and snakes) based on 52 genes and 4162 species. *Molecular Phylogenetics and Evolution*, **94**(B), 537-547.

Zittel, K. 1887. Handbuch der Palaeontologie I. Abtheilung, Palaeozoologie III. Band., Pisces, Amphibia, Reptilia, Aves. Druck und Verlag Von R. Oldenbourg.